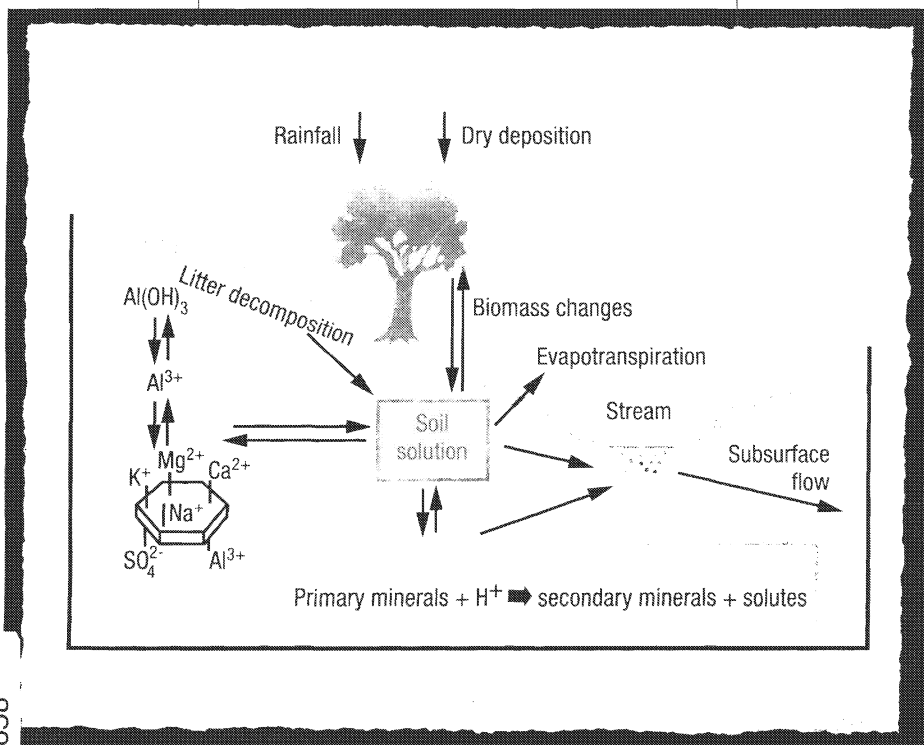


# THE GEOCHEMISTRY OF NATURAL WATERS

Surface and Groundwater Environments

THIRD EDITION



AMES I. DREVER



**The Geochemistry of Natural Waters**  
**Surface and Groundwater Environments**

Third Edition

**James I. Drever**  
University of Wyoming

**Prentice Hall**  
**Upper Saddle River, NJ 07458**

**Library of Congress Cataloging-in-Publication Data**

Drever, James I.

The geochemistry of natural waters: surface and groundwater environments / James I. Drever. — 3rd ed.

p. cm.

Includes bibliographical references and index.

ISBN 0-13-272790-0

1. Water chemistry. 2. Hydrogeology. I. Title.

GB855.D73 1997

551.48—dc21

96-51617

CIP

Executive Editor: Robert A. McConnin  
Production Coordinator: Custom Editorial Productions, Inc.  
Manufacturing Manager: Trudy Piscioti  
Buyer: Ben Smith  
Cover Designer: Bruce Kenselaar

© 1997, 1988, 1982 by Prentice-Hall, Inc.

Upper Saddle River, New Jersey 07458

All rights reserved. No part of this book may be reproduced, in any form or by any means, without permission in writing from the publisher.

Printed in the United States of America

10 9 8 7 6 5 4

ISBN: 0-13-272790-0

Prentice-Hall International (UK) Limited, *London*

Prentice-Hall of Australia Pty. Limited, *Sydney*

Prentice-Hall Canada Inc., *Toronto*

Prentice-Hall Hispanoamericana, S. A., *Mexico*

Prentice-Hall of India Private Limited, *New Delhi*

Prentice-Hall of Japan, Inc., *Tokyo*

Editora Prentice-Hall do Brasil, Ltda., *Rio de Janeiro*

# Contents

## **Preface xi**

## **1 The Hydrologic Cycle 1**

- Composition of Rainwater 3
- Hydrology 6
  - Groundwater 9
  - Groundwater as a Resource and Groundwater Contamination 11
- Nonmeteoric Types of Water 12
- Chemical Terms in Hydrology 13
- Suggested Reading 13

## **2 Chemical Background 15**

- Units and Terminology 15
- Equilibrium Thermodynamics 17
  - Equilibrium Constant 19
  - Measurements of Disequilibrium 24
- Activity-Concentration Relationships 26
  - Activities of Ionic Species 27
  - Complex Formation 34
  - Apparent Equilibrium Constants 35
- Computer Codes 36
- Review Questions 37
- Suggested Reading 40

## **3 The Carbonate System and pH Control 41**

- Carbonic Acid System 41
- Alkalinity and Titration Curves 45
  - Alkalinity Titration 47
  - Gran Plots 50

Calcium Carbonate Solubility	52
Dolomite	58
High-Magnesium Calcite	59
Ground and Surface Waters in Carbonate Terrains	60
Review Questions	67
Suggested Reading	68

## **4 Clay Minerals and Cation Exchange 69**

Mineralogy and Composition	69
Brucite $[\text{Mg}(\text{OH})_2]$ and Gibbsite $[\text{Al}(\text{OH})_3]$	69
Kaolinite and Related Minerals	71
2:1 Clay Minerals	74
Chlorite	77
Mixed-Layer Clays	78
Sepiolite and Palygorskite	79
Colloid Properties	79
The Double Layer	80
Membrane Filtration	81
Ion Exchange	82
Review Questions	85
Suggested Reading	86

## **5 Adsorption 87**

Empirical Equations	87
Linear Distribution Coefficient	88
Freundlich Isotherm	89
Langmuir Isotherm	89
Surface Complexation	90
Acid-Base Equilibria	92
Adsorption of Metal Cations	97
Adsorption of Anions	98
The Electric Double Layer	99
Modeling Adsorption with MINTEQA2	102
Review Questions	104
Suggested Reading	105

## **6 Organic Compounds in Natural Waters 107**

Natural Organic Matter	107
Structure of Natural Organic Solutes	108
Functional Groups	109
Humic Substances	113
Dissolved Organic Carbon (DOC) in Natural Environments	118

Organic Pollutants	119
Solubility and Related Properties	121
Adsorption	122
Biodegradation and Bioremediation	125
Review Questions	126
Suggested Reading	127

## **7 Redox Equilibria 129**

The Standard Hydrogen Electrode and Thermodynamic Conventions	130
Use of Eh as a Variable	133
Use of pe as a Variable	134
Definition of pe and Eh by Redox Pairs	135
Measurement of Eh	136
Redox Calculations Using WATEQ4F	136
pe–pH and Eh–pH Diagrams	137
System Fe–O–H <sub>2</sub> O	137
System Fe–O–H <sub>2</sub> O–CO <sub>2</sub>	144
System Fe–O–H <sub>2</sub> O–S	148
Eh–pH Diagrams	152
Partial Pressure or Fugacity-Fugacity Diagrams	154
Review Questions	156
Suggested Reading	157

## **8 Redox Conditions in Natural Waters 159**

Photosynthesis	159
Respiration and Decay	160
Redox Buffering	162
Lakes	166
The Ocean	169
Groundwater	171
Summary	174
Review Questions	174
Suggested Reading	174

## **9 Heavy Metals and Metalloids 175**

Sources of Heavy Metals	175
Speciation	177
Organic Matter and Complex Formation	177
Equilibrium Solubility Control	179
Solubility in Redox Reactions	180
pe–pH and Eh–pH Diagrams	182
Roll-Front Uranium Deposits	184

Adsorption and Coprecipitation Controls	185
Adsorption by Hydrous Iron and Manganese Oxides	186
Adsorption by Silicates and Carbonates	188
Adsorption by Solid Organic Matter	188
Uptake by Living Organisms	188
Behavior of Specific Elements	189
Copper, Zinc, Cadmium, and Lead	189
Arsenic and Selenium	192
Chromium	194
Mercury	195
Summary	195
Review Questions	196
Suggested Reading	196

## **10 Stability Relationships and Silicate Equilibria 197**

Solubility Equilibria (Congruent Solution)	197
Solubility of Magnesium Silicates	199
Solubility of Gibbsite	200
Solubility of Aluminosilicates	203
Incongruent Solution and Stability Diagrams	204
Uncertainty in Mineral Stability Diagrams	210
Review Questions	213
Suggested Reading	213

## **11 Kinetics 215**

Nucleation	217
Dissolution and Growth	218
Surface Reaction Mechanisms	220
Diffusion Control	220
Dissolution of Calcite in Seawater	221
Growth of Calcite and Aragonite in Seawater	223
Dissolution of Silicates	225
Effect of Solution Composition on Dissolution Rates	228
Relative Dissolution Rates of Different Minerals	232
Comparisons Between Laboratory and Field Dissolution Rates	232
Review Questions	233
Suggested Reading	234

## **12 Weathering and Water Chemistry 235**

Soil Formation	235
The Mass-Balance Approach to Catchment Processes and Mineral Weathering Reactions	236
Catchment Processes	236
Mineral Weathering Reactions	240
Mass-Balance Calculations in Groundwater Systems	245



The Thermodynamic Approach to Mineral Weathering Reactions	246
The Statistical Approach	251
Case Studies	255
Mackenzie River System, Canada	255
Amazon and Orinoco River Systems	257
Absaroka Mountains, Wyoming	262
Mattole River, California	269
Cascade Mountains, Washington; Loch Vale, Colorado	269
Adirondack Mountains, New York	275
Waters from Ultramafic Rocks	279
Rhine River	280
Summary	282
Thermodynamic Controls on Clay Mineral Formation	282
Environmental Factors and Water Chemistry	283
Review Questions	287
Suggested Reading	288

### **13 Acid Water 289**

Acidity and Alkalinity	289
Solubility of Aluminum Hydroxide	291
Acid Deposition	292
Cation Exchange	293
Anion Mobility and Anion Exchange	295
Processes Affecting Sulfate Mobility	296
Biological Processes	297
Chemical Weathering	299
Integrated Models	301
Environmental Effects	305
Acid Mine Drainage	306
Prediction of Acid Generation	308
Prevention of Acid Generation	308
Review Questions	309
Suggested Reading	309

### **14 Isotopes 311**

Stable Isotopes	311
Fractionation Processes	312
$^{18}\text{O}/^{16}\text{O}$ and D/H	314
$^{13}\text{C}/^{12}\text{C}$	320
$^{34}\text{S}/^{32}\text{S}$	321
$^{15}\text{N}/^{14}\text{N}$	321
Radioactive Isotopes	322
Tritium	322
$^{14}\text{C}$	322

Chlorine-36	323
Radon 222	323
Radiogenic Isotopes: Strontium-87	324
Review Questions	325
Suggested Reading	325

## **15 Evaporation and Saline Waters 327**

Evaporation of Sierra Nevada Spring Water	327
Chemical Divides and the Hardie-Eugster Model	329
Modifications of the Hardie-Eugster Model	332
Magnesium Carbonate Formation	332
Sulfate Reduction and Sulfide Oxidation	334
Ion Exchange and Adsorption	334
Cyclic Wetting and Drying	335
Examples	336
Lake Magadi Basin, Kenya	336
Teels Marsh, Nevada	340
Evaporation of Seawater	343
Persian Gulf Sabkhas	345
Saline Formation Waters	348
Summary	350
Review Questions	351
Suggested Reading	351

## **16 Transport and Reaction Modeling 353**

The Advection-Diffusion Equation	353
Advection	356
Diffusion and Dispersion	356
Chemical Reaction and Retardation	364
Reaction Path Modeling	368
Application to Contaminant Transport in Groundwater	374
Chemical Evolution of Groundwater	377
Review Questions	378
Suggested Reading	379

## **References 381**

## **Glossary of Geological Terms 403**

## **Appendix I Piper and Stiff Diagrams 409**

## **Appendix II Standard-State Thermodynamic Data for Some Common Species 413**

**Appendix III Equilibrium Constants at 25°C and Enthalpies  
of Reaction for Selected Reactions 419**

**Answers to Problems 423**

**Author Index 426**

**Subject Index 431**

# Preface

*The Geochemistry of Natural Waters: Surface and Groundwater Environments* is a textbook for advanced undergraduate and beginning graduate classes in aqueous geochemistry, environmental geochemistry, and groundwater chemistry. The overall purpose of the book is to give the reader an understanding of the processes that control the chemical composition of surface and ground waters, both natural and polluted. The approach is to combine background theory with numerous case studies from the literature. I believe the balance between theory and examples gives the reader real insight into the way natural systems behave.

In the sixteen years since the first edition of this book appeared, the focus of aqueous geochemistry has changed. One change has been a greatly increased awareness of and interest in pollution of ground and surface waters. A second change has been the enormous expansion in the use of computer codes to perform geochemical calculations. Environmental permitting procedures require predictions of contaminant migration far into the future; such predictions require both an understanding of underlying fundamental processes and the ability to use computer codes. There has also been renewed interest in rock weathering from the perspective of its influence on the global carbon cycle and, hence, global climate.

In revising this book I have attempted to respond to these changes. A completely new chapter on adsorption has been added (Chapter 5), a section on organic contaminants has been added to Chapter 6, and the chapter on trace elements (Chapter 9) has been greatly expanded. The use of the computer codes WATEQ4F, MINTEQA2, and NETPATH is illustrated and incorporated into the chapters and the problem sets at the end of the chapters. There is a greatly expanded chapter on contaminant transport modeling (Chapter 16), and many additional end-of-chapter problems. An appendix explaining Piper and Stiff diagrams, widely used by hydrogeologists, has been added, and the appendices with thermodynamic data and equilibrium constants have been completely revised; they are now largely consistent with the databases of the WATEQ4F and MINTEQA2 codes.

I have retained the basic theory of carbonate and silicate equilibria more or less unchanged, as it remains fundamental to understanding aqueous geochemistry. I have also retained the “case-study” approach to build the bridge between theory and reality in the field. The order of chapters has been changed to introduce redox equilibria earlier (Chapter 7),

which leads to a more logical presentation in the subsequent chapters. As with the previous edition, groups of chapters are more or less self-contained, so the instructor can present the material in the order that he or she prefers. To allow room for the additional material on surface and ground waters, the chapter on the oceans has been eliminated, and discussions of processes in the ocean have been reduced in other chapters. Marine chemistry is such a complex subject that I felt it was unrealistic to try to cover it in one chapter. The book as a whole is now more tightly focused on freshwater environments.

Many friends and colleagues have contributed to this book in many ways. In addition to those acknowledged in previous editions, I would like to thank Lisa Stillings (University of Wyoming) and Simon Poulson (University of Wyoming), who read the entire book, and Don Langmuir (Golden, CO), Diane McKnight (U.S. Geological Survey), J. Barry Maynard (University of Cincinnati), Eugene Perry (Northern Illinois University), Richard Yuretich (University of Massachusetts at Amherst), Robert A. Berner (Yale University), W. C. Fetter, Jr. (University of Wisconsin, Oshkosh), and Luis A. Gonzalez (University of Iowa), who reviewed individual chapters. They made many excellent suggestions and caught at least some of my errors.

Much of the revision for this edition was written while I was a sabbatical guest at the Centre de Géochimie de la Surface, CNRS, Strasbourg, France. I thank Bertrand Fritz and his colleagues for their hospitality and support.

J. I. D.

# 1

## The Hydrologic Cycle

Approximately 96 percent of the water at the earth's surface is in the oceans, 3 percent is in the form of ice, 1 percent is groundwater, 0.01 percent is in streams and lakes, and only about 0.001 percent is in the atmosphere (Berner and Berner, 1996). Although rivers and lakes make up only a small fraction of the hydrosphere, the rate of water circulation through them is quite rapid. The amount of water discharging from rivers to the sea each year is about equal to the total amount of water present in rivers and lakes. The hydrologic cycle is a description of the way water moves through these various environments (Fig. 1-1).

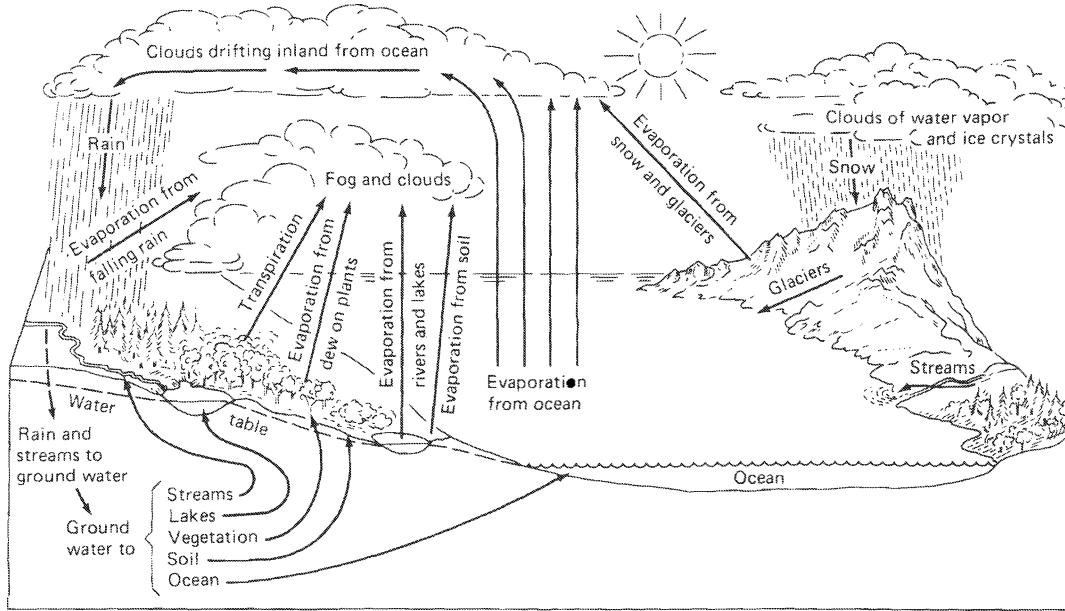
Fig. 1-1 can be drawn in a more abstract way to illustrate some of the terms used in describing geochemical cycles (Fig. 1-2). Each box represents a *reservoir*, an arbitrarily defined space containing a certain mass of the substance of interest, and the arrows represent the transfer or *flux* of material into and out of the reservoirs. The number of reservoirs used to describe a particular cycle is somewhat arbitrary (compare Fig. 1-2 with Fig. 1-3), depending on the particular problem being studied. The *residence time* of a substance (in this example, water) in a reservoir is obtained by dividing the amount of the substance in the reservoir by the flux of that substance into (or out of) the reservoir. Thus the residence time of water in the ocean is (from Fig. 1-2)

$$\frac{13,700 \times 10^{20} \text{ g}}{(0.36 + 3.5) \times 10^{20} \text{ g/y}} = 3550\text{y}$$

and the residence time of water in the atmosphere is

$$\frac{0.13 \times 10^{20} \text{ g}}{(3.8 + 0.63) \times 10^{20} \text{ g/y}} = 0.03\text{y} = 11 \text{ days}$$

If the amount of the substance in a reservoir is not changing with time (i.e., the reservoir is in a *steady state*), the residence time represents the average time a molecule of the substance spends in the reservoir between the time it arrives and the time it leaves. If the reservoir is not in a steady state, the term *residence time* is not really appropriate, although it is widely used in the literature. The term *response time* is preferable. If, for example, the output from a reservoir

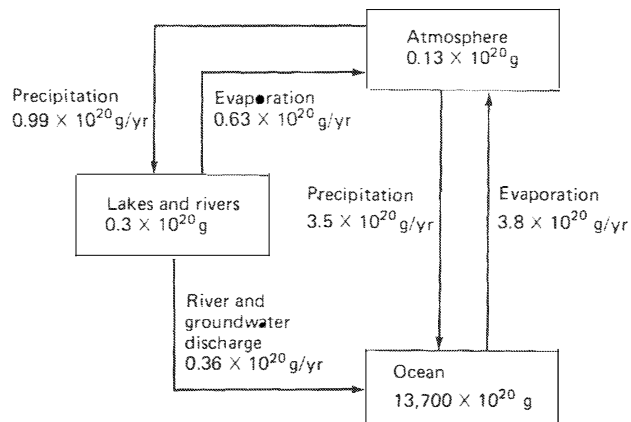


**FIGURE 1-1** The hydrologic cycle. (From *Principles of Geology*, 4th ed., by James Gilluly, Aaron C. Walters, and A. O. Woodford. W. H. Freeman and Company. Copyright © 1975.)

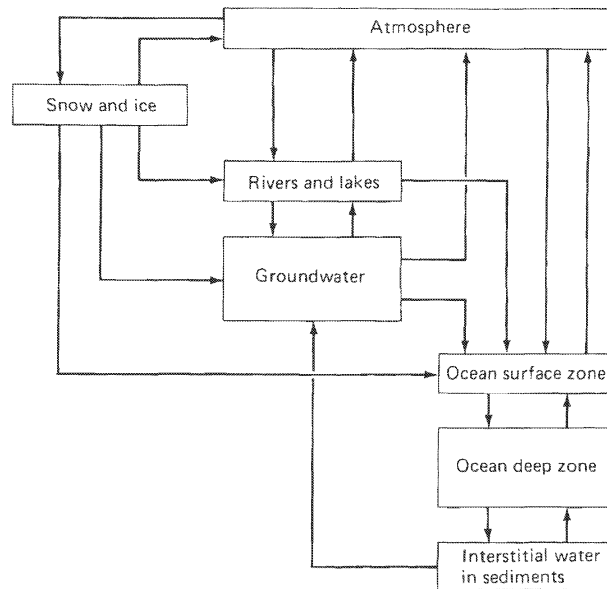
ceased completely and the input continued, the response time would represent the time required for the amount of the substance in the reservoir to double. The response time indicates the time scale on which the amount of a substance in a reservoir will change in response to a change in the rate of input or output.

The simple box model illustrated here has been used to budget the cycles of many substances in nature and for predicting the consequences of human inputs into natural systems (see, e.g., Garrels et al., 1975). In general, if the anthropogenic (human-caused) flux of a substance is comparable in magnitude to the natural flux, significant changes in the natural system

**FIGURE 1-2** Simple schematic diagram (box model) for the hydrologic cycle. (Numbers are from Garrels and Mackenzie, 1971).



**FIGURE 1-3** Outline of a more complex box model of the hydrologic cycle.



are to be expected. An example is the injection of carbon dioxide into the atmosphere from the burning of fossil fuels. The anthropogenic flux of  $\text{CO}_2$  into the atmosphere is a significant fraction of the natural flux, and as a consequence the concentration of  $\text{CO}_2$  in the atmosphere is steadily increasing.

The atmosphere derives its water from evaporation of the ocean and, to a lesser extent, from evaporation of water at the surface of the continents. When moisture-laden air is cooled, the water vapor in the air condenses to form clouds; if the water (or ice) droplets in the clouds grow sufficiently large, rain or snow (or, in general, *precipitation*) will start to fall. The atmospheric cooling that results in precipitation is usually caused by adiabatic expansion as air rises. Air may rise because of atmospheric circulation patterns (as, for example, in the equatorial belt), or because air is forced to rise over a mountain belt. When moist air from the oceans blows over a coastal mountain range, there is usually heavy precipitation on the windward side of the mountains (e.g., the mountains of Oregon, Washington, and British Columbia in North America, and the mountains of Norway and Scotland in Europe) and relatively little precipitation beyond the mountains.

## COMPOSITION OF RAINWATER

Rain is not pure  $\text{H}_2\text{O}$ , but instead contains a wide range of dissolved substances. Over the oceans and near coasts, the main source of dissolved material is sea salt. When waves break, fine droplets of seawater are injected into the atmosphere. The water evaporates, leaving a solid aerosol particle, which is transported by winds until it is dissolved by rain. The concentrations of sodium and chloride in rainwater in the United States (Fig. 1-4) show the input of sea salts near the coast and lesser input farther inland.



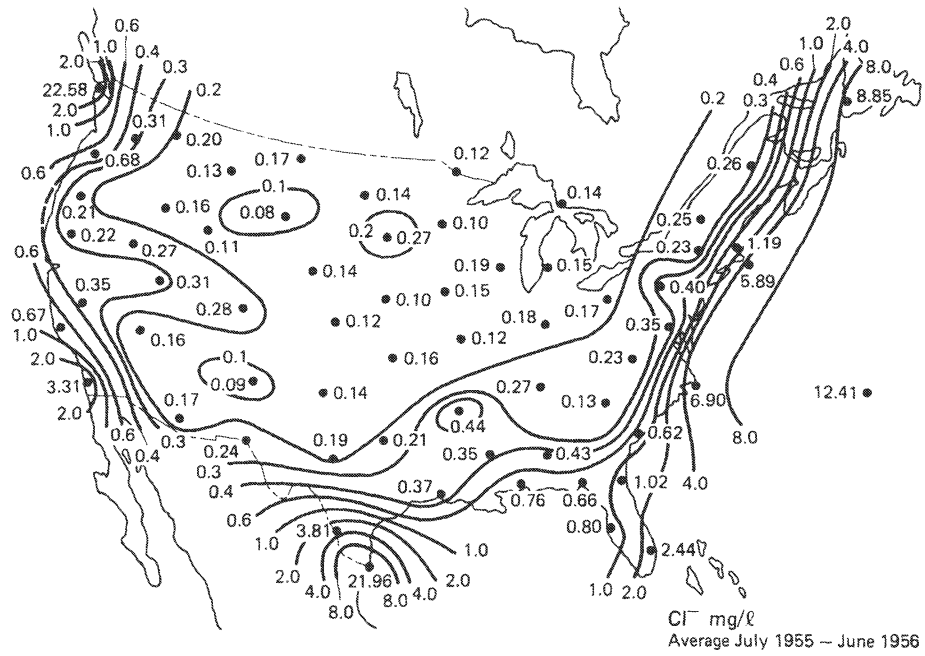
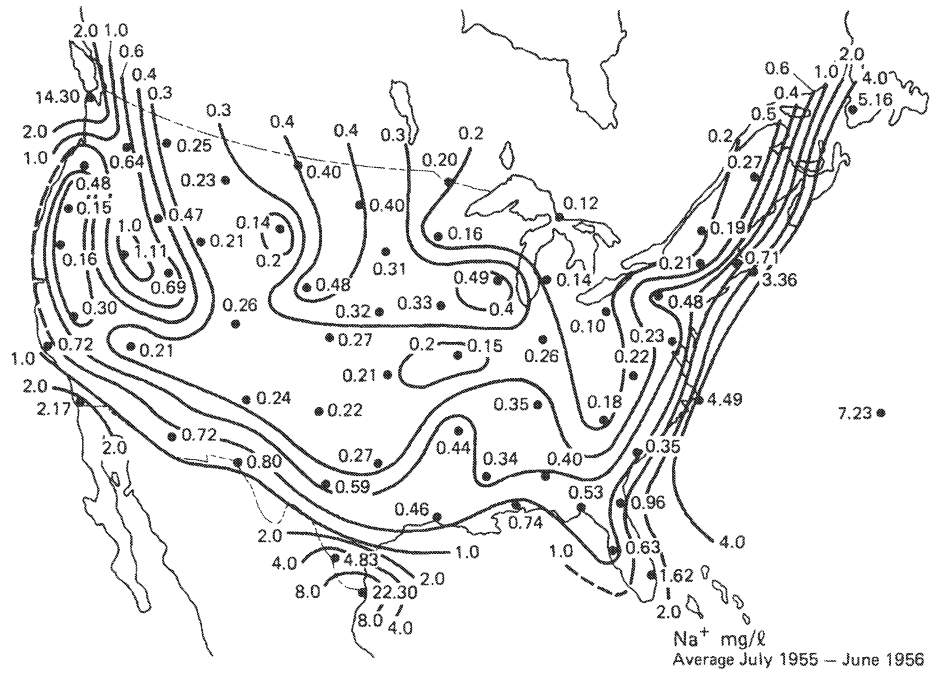
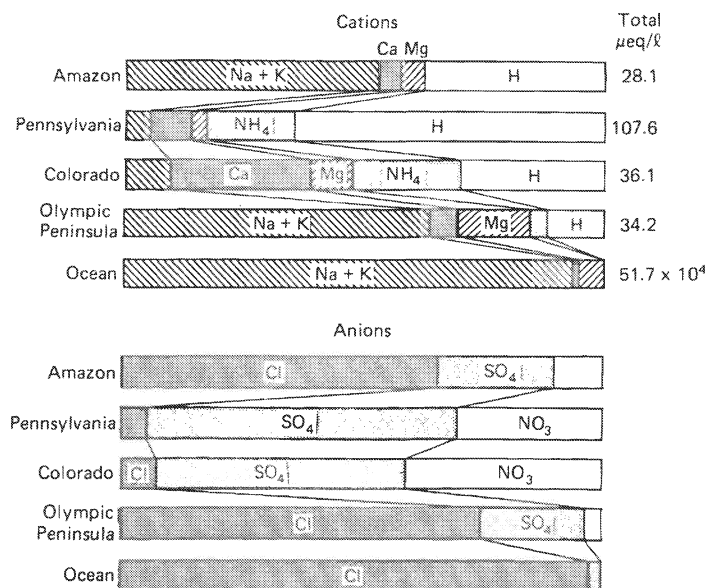


FIGURE 1-4 Average sodium and chloride concentrations in precipitation over the United States (Junge and Werby, 1958).

Sea salt is only one source of solutes in precipitation, and the ratios of the various solutes in rain differ to varying extents from the ratios in sea water (Fig. 1-5). The ionic ratios in rainfall on the Olympic Peninsula in Washington State, adjacent to the Pacific Ocean, are similar to those in sea water, but there is an addition of  $\text{SO}_4^{2-}$ ,  $\text{H}^+$ ,  $\text{NH}_4^+$ , and  $\text{NO}_3^-$ . Rainfall over the Amazon is similar, but the additions are larger. The additional sulfuric acid appears to come from oxidation of dimethyl sulfide and hydrogen sulfide produced by biological processes in the ocean (Bonsang et al., 1980). The  $\text{NH}_4^+$  and  $\text{NO}_3^-$  probably result from gaseous nitrogen species released by terrestrial vegetation (Stallard and Edmond, 1981). It is interesting that these essentially unpolluted rain samples are naturally "acid" (Chapter 13), although much less so than samples from industrial areas. The total concentration of solutes in Colorado rainfall is similar to that of the Olympic Peninsula, but the ionic ratios are very different. The input of sea salt is much less, as one would expect in view of the distance from the ocean. In Colorado, the most important ions are calcium and sulfate. Calcium is presumably derived from dust in the atmosphere. There is some argument as to whether calcium sulfate dust is derived from the land surface or whether calcium carbonate dust reacts with sulfuric acid in the atmosphere. Both processes may be important. There is likewise disagreement as to how much of the sulfate is a result of the burning of fossil fuels and how much is natural. Again, both are probably important.

The nitrogen species ( $\text{NH}_4^+$  and  $\text{NO}_3^-$ ) are derived from plants, agriculture, and automobile exhausts. Animal wastes and fertilizers are sources of both ammonium and nitrate, and there is some input of nitrate from nitrogen oxides in automobile exhausts from the Denver metropolitan area to the southeast.



**FIGURE 1-5** Relative concentrations (in equivalents) of ions in the ocean and in rainfall from the Amazon basin (average from Stallard and Edmond, 1981) and from National Acid Deposition Program sites in Central Pennsylvania, Rocky Mountain National Park in Colorado, and the Olympic Peninsula in Washington State (NADP, 1985). "Total" represents the total concentration of cations in microequivalents per liter.

Rainfall from the Pennsylvania site illustrates the effect of industrial pollution. The total concentration is about three times as high as those of the “natural” sampling stations, and the dominant solutes are sulfuric and nitric acids. Burning of sulfur-containing fossil fuel (mostly coal) injects sulfur dioxide ( $\text{SO}_2$ ) into the atmosphere. Slow oxidation and hydration of  $\text{SO}_2$  in the atmosphere produces  $\text{H}_2\text{SO}_4$ . Washout of  $\text{H}_2\text{SO}_4$  in precipitation is the principal cause of acid rain (see Chapter 13). Various combustion processes, including the internal combustion engine, cause oxidation of atmospheric nitrogen to a range of oxides referred to collectively as  $\text{NO}_x$ . Oxidation and hydration of  $\text{NO}_x$  produces nitric acid, which is the other important source of acidity in rainfall.  $\text{NH}_4^+$  concentrations are also generally high in precipitation in areas affected by atmospheric pollution; the source seems to be largely agricultural, particularly volatilization from animal wastes.

Rainfall also contains a variety of organic acids, notably formic and acetic (Keene and Galloway, 1984). These decompose rapidly unless the rain sample is immediately preserved. Most of the low-molecular-weight organic acids result from photodecomposition of larger organic molecules in the atmosphere.

The composition of rain at any one location may vary greatly with time. The first drops of rain at the beginning of a storm may contain most of the soluble material available in the atmosphere; rain toward the end of a storm is relatively dilute. Also, when snow first melts at the end of winter, most of the accumulated salts from atmospheric deposition over winter are flushed out with the initial meltwater. In areas subject to acid deposition, this causes an *acid pulse*, which can be very harmful to aquatic organisms.

Solutes are also transferred from the atmosphere to the earth's surface and hence surface waters by what is called *dry deposition* or *occult deposition*. Conceptually, dry deposition can be regarded as (1) uptake of gases and very small aerosol particles by vegetation and wet surfaces, and (2) sedimentation and impaction of larger aerosol particles. *Occult deposition* is a slightly more general term that includes deposition from mist and fog. It has proved exceedingly difficult to measure occult deposition quantitatively (e.g., Fowler, 1980). The concentration of gases and particles in the atmosphere can be measured fairly readily, but not the rate at which they are removed from the atmosphere. An alternative approach (summarized in Drever and Clow, 1995) is to measure *throughfall*, which is water collected under the forest canopy, and assume that the solutes represent precipitation plus occult deposition plus elements cycled through the trees. If the elements cycled through the trees can be estimated independently, occult deposition can be calculated. There is a general consensus that in areas where the atmosphere is affected by industrial pollution occult deposition is at least as important a source of acidity to surface waters as rainfall is.

## HYDROLOGY

When rain falls on land, the water can follow several pathways (Fig. 1-6). Some of the water will remain as droplets on vegetation or remain close to the top of the soil and evaporate soon after the rainfall ends. Some of it will be taken up by the roots of plants and evaporated through leaves, a process termed *transpiration*. The term *evapotranspiration* is used for the combined processes of evaporation and transpiration. Some of the water may infiltrate into the soil, where it migrates laterally toward a stream, a process called *interflow*, or it may percolate downward to the permanent groundwater system. When a rainfall is too heavy or pro-

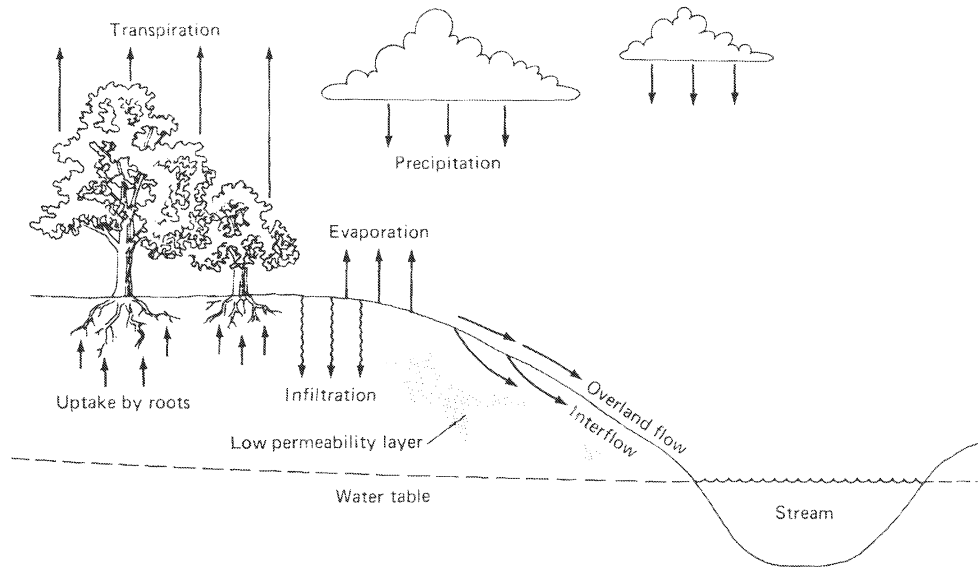


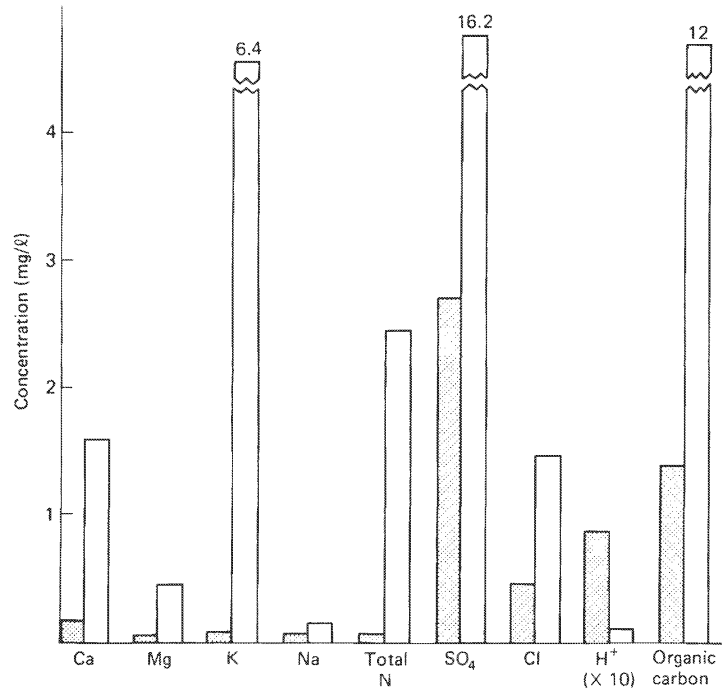
FIGURE 1-6 Near-surface hydrologic processes.

longed for infiltration to accommodate the water, water will flow on the surface of the ground as *overland flow*.

The chemistry of rainwater undergoes drastic changes as it comes in contact with the earth's surface. Even before it reaches the ground, rain may pick up solutes from plants (Fig. 1-7), and much of its acidity may be neutralized. As water passes through the soil zone, it acquires solutes from dissolution or partial dissolution of minerals, and some solutes (notably nitrogen compounds and phosphate) are extracted from the water by plants. The organisms of the soil release soluble organic compounds to the water, and these compounds may accelerate the breakdown of minerals. When rain is not falling, evapotranspiration removes essentially pure water from the soil, so that any solutes in the water, either brought in by rain or dissolved from soil minerals, tend to build up in concentration and may even precipitate as solid phases.

As water leaves the soil zone and passes through the groundwater system, the concentration of organic matter greatly decreases (through either bacterial decay or adsorption), the concentration of elements that are in the form of organic complexes (notably iron and aluminum) decreases, and the concentrations of the common major ions generally increase as a result of reaction between the water and the enclosing rock. Stream waters generally reflect the composition of near-surface groundwater; an example of the difference between soil water and ground- or surface water is shown in Table 1-1.

The water in streams and rivers is derived from several sources. When it is not raining and has not rained for some time, the water in the stream (its *base flow*) is derived from the permanent groundwater system. During and immediately after a rainstorm, the base flow will be augmented by contributions from interflow, overland flow, and, of course, rain falling directly on the stream channel. As a stream rises, water often flows from the channel into porous alluvium that forms its banks, a process termed *bank storage*. As the stream recedes, water flows back from bank storage into the channel. Stream water constantly exchanges with water in the pores



**FIGURE 1-7** Comparison of the chemistry of incident precipitation (shaded bars) and precipitation collected under the forest canopy (throughfall) in a deciduous forest in northeastern United States (data from Likens et al., 1977).

of its bed and banks. The term *hyporheic zone* is used for the zone that experiences exchange with the stream on a reasonably short time scale. The term *runoff* is generally used for the total amount of water leaving an area in streams or rivers. The ratio of runoff to precipitation varies greatly from region to region, depending on climate, geology, and vegetation.

The natural changes in the chemistry of a mass of water as it flows down a river, apart from the effects of mixing, are generally relatively small compared to changes that take place in the soil zone or in an aquifer. This is because the residence time of water in a river is relatively short and

**TABLE 1-1** Chemical Composition (mg/l) of (A) Soil Water (from Antweiler and Drever, 1983) and (B) River Water (from Miller and Drever, 1977a) from Areas Underlain by Volcanic Rocks in Northwest Wyoming

	A	B		A	B
Ca <sup>2+</sup>	2.5	6	HCO <sub>3</sub> <sup>-</sup>	<5	40
Mg <sup>2+</sup>	0.7	1.7	DOC <sup>a</sup>	120	<2
Na <sup>+</sup>	3	6.3	Al <sub>total</sub>	2	<0.005
K <sup>+</sup>	3	0.5	Fe <sub>total</sub>	1.5	<0.01
SiO <sub>2</sub>	40	17	pH	5.2	7.5

<sup>a</sup>DOC is dissolved organic carbon in mg carbon/l. It is a measure of the total amount of organic compounds dissolved in the water. In the soil water, organic anions are the major anionic species.

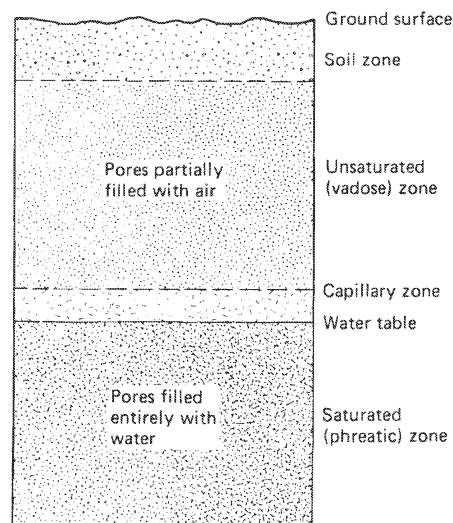
because there is relatively little contact between the water and solid phases. Such changes as do occur are generally caused by biological processes and affect primarily the nutrient elements (nitrogen, phosphorus, and potassium), silica (microscopic plants, *diatoms*, extract silica from the water to form their skeletons), and certain trace elements. The chemistry of many rivers today is strongly influenced by inputs of domestic and industrial wastes. Such wastes are often modified by oxidation and precipitation within the river and adsorption on the river bottom. Pollution may upset the natural balance of a river by destroying the indigenous biota either through the direct effects of toxic materials or because oxygen is depleted by decomposition of organic matter.

### Groundwater

At some depth below the earth's surface everywhere, any pores, voids, or open cracks in the rocks are filled with water. The *water table* is the surface that divides rocks in which the pores are completely filled with water from those in which the pores are partially filled with air (Fig. 1-8). The water table refers strictly to a system in which the pores are connected to the atmosphere and sufficiently large for capillary effects to be insignificant; capillary action in fine-grained rocks will cause water to rise a short distance above the true water table, causing a *capillary fringe*. The region below the water table is called the *phreatic* or *saturated* zone; the region above the water table is the *vadose* or *unsaturated* zone. Often the soil and the water in it are considered as a separate system because the water content and water chemistry in the soil zone fluctuate rapidly, whereas those of the deeper zones are relatively stable.

The behavior of groundwater systems is generally controlled by the porosity and permeability of the rocks involved. *Porosity* is the fraction (or percent) of the total rock that is void space; *permeability* is a measure of the ability of a rock to transmit fluids. A coarse, uncemented sandstone will typically have a high porosity and a high permeability because the pores are large and interconnected. A shale may have a high porosity, but its permeability is likely to be small because the pores are so small that water can flow through them only very

**FIGURE 1-8** Terminology of some subsurface features in permeable rock.



slowly. Limestones often have quite low porosities but very high permeabilities because the “pores” are large solution channels or fractures. Even igneous rocks such as granite may have significant permeability resulting from fractures and joints in the rock. An *aquifer* is a water-saturated rock with sufficient porosity and permeability to be a usable source of water for wells. An *aquitard* is a rock whose permeability is too low to allow significant passage of water on the time scales considered in water-supply development. On a geological time scale, however, rocks designated aquitards may transmit large volumes of water.

In the simple case of a uniform, permeable rock type in a humid climate, the water table will be a subdued version of the topography (Fig. 1-9). Streams, lakes, springs, and swamps represent places where the water table intersects the ground surface. The *recharge area* (the area in which the aquifer receives water) for such a system would be the entire area away from the stream channel. The *discharge area* (the area where the aquifer loses water) would be the stream channel, where water might discharge directly, and the area near the stream where plants might have roots below the water table and remove water by transpiration. Streams may also be a source of aquifer recharge over part of their length, particularly in arid regions. The level of the water table will fluctuate as the recharge rate (controlled by precipitation) fluctuates.

Whenever the water table is not horizontal, water will flow from areas where the water table has a higher elevation to areas where its elevation is lower. Flow rates are determined by the gradient of the water table and by the permeability of the rock. Groundwater flow rates are often very slow; for example, the flow rate in the main aquifer in central Florida is 2 to 8 m/y (Back and Hanshaw, 1971).

Where permeable and impermeable rocks alternate, the situation becomes more complicated (Fig. 1-10). A *perched* water table may occur where saturated permeable rocks are separated from unsaturated rocks below by an impermeable barrier. A *confined* or *artesian* aquifer occurs when the upper boundary of the groundwater is in contact with an impermeable rock unit rather than with unsaturated permeable rock. If a well is drilled into a confined aquifer, the water in the well will rise to a level above the top of the aquifer. The level to which the water would rise in a series of such wells is the *piezometric surface*. If the piezometric surface is above ground level (Fig. 1-11), water will flow from the well without pumping. Artesian water is now extensively used for irrigation in many parts of the world. If the discharge from wells is greater than the natural recharge, the water in the aquifer will be depleted and the piezometric surface will be progressively lowered.

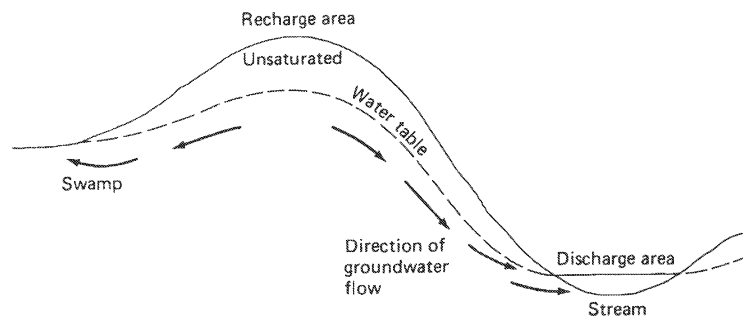


FIGURE 1-9 Groundwater system in a uniform, permeable rock.

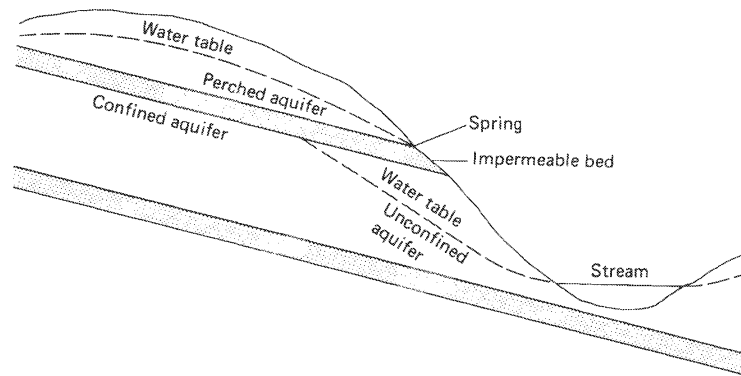


FIGURE 1-10 Perched and confined aquifers.

### Groundwater as a Resource and Groundwater Contamination

Groundwater is widely used as a source of water for various purposes (Table 1-2). In the United States, approximately 40 percent of the water used for public water supplies is drawn from groundwater. Contamination of groundwater has become a major concern in recent years, both because so many people depend on it as a source of potable water and because once an aquifer is contaminated, it is generally extremely difficult to clean it up and restore the purity of its water. Groundwater contamination has many sources. Common examples are leakage from landfills and other waste-disposal sites; leakage from agricultural activities, including animal wastes, fertilizers, and pesticides; leakage from underground storage tanks for petroleum products and various solvents; and even deliberate discharge from septic tanks. Septic-tank systems were designed to minimize bacterial contamination of surface waters, but the design results in remarkably efficient transfer of nitrate (from decomposition of organic nitrogen compounds) to groundwater.

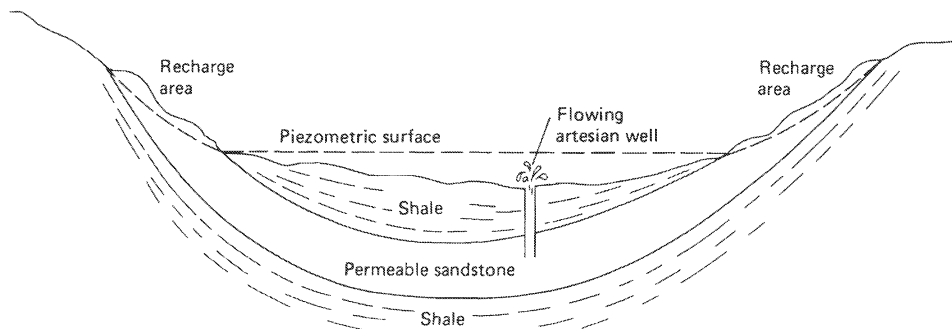


FIGURE 1-11 A simple artesian system in a syncline. The piezometric surface will become depressed if significant amounts of water are withdrawn from the aquifer.



**TABLE 1-2 Major Water Uses (Excluding Electricity Generation) in the United States** (from Solley et al., 1988). Units Are Millions of Gallons Per Day.

	<i>Surface Water</i> 134,885 (65%)	<i>Groundwater</i> 73,300 (35%)	
<i>Usage</i>			% from groundwater
Agriculture	92,750	48,671	34
Public water supplies	21,995	14,660	40
Industrial & mining	19,610	5,267	21
Direct domestic & commercial	565	3,989	88

## NONMETEORIC TYPES OF WATER

Most of the water we observe on the continents is meteoric in origin, that is, it has been derived from the atmosphere as rain or snow in relatively recent geologic times. Other types of water do exist and, although they have an insignificant impact on the chemistry of surface waters at any instant in time, their cumulative effects in transporting solutes may be important over geological time.

When a sediment is deposited, water is trapped between the grains. If the sediment is then buried, the water trapped in it would be called *connate*. In practice, it is generally impossible to tell whether the water in the pores of an ancient sediment is really the same water as was incorporated when the sediment was deposited, so use of the term *connate* is not recommended. The term *formation water* is used for a water, often a saline water, occurring in the pores of a deeply buried sedimentary rock. Use of the term *formation water* avoids a specific genetic connotation.

When rock undergoes chemical weathering, clay minerals are formed that contain water chemically combined in the mineral structure. The sediments containing these clay minerals become sedimentary rocks, and these rocks may be subjected to heat and pressure, which converts them into metamorphic rocks. During metamorphism, the hydrous clay minerals are converted into less hydrous phases, and water is expelled from the rock. This water is called *metamorphic water*. It appears that as metamorphic water migrates toward the earth's surface, it generally mixes with meteoric waters and becomes difficult to recognize. It is probable that some of California's carbon-dioxide-rich springs contain a significant component of metamorphic water (Barnes, 1970).

The earth's mantle contains chemically combined water that is gradually being transferred to the earth's surface by volcanism. It is probable that the volcanic gases in basaltic eruptions contain this *juvenile* water, but the fact is difficult to document because volcanic magma generally becomes contaminated with water from other sources as it comes up through the crust.

A final type of water that might appear different in origin is that in hot springs and geysers. In fact, these almost invariably turn out to be meteoric water that has been heated by contact with hot rock (Ellis and Mahon, 1977). Hot springs also occur under the oceans, particularly at spreading centers. The water in these springs is seawater that has been heated and chemically altered by contact with hot rock.

## CHEMICAL TERMS IN HYDROLOGY

Several terms that are widely used to describe the chemistry of natural waters are defined here for convenience.

*Total dissolved solids* (TDS) represents the total amount of solids (milligrams per liter, mg/l) remaining when a water sample is evaporated to dryness. In principle, it is the sum of all dissolved constituents, with bicarbonate converted to equivalent carbonate. *Salinity* has essentially the same meaning as TDS, although a slightly more complex definition is used in oceanography.

*Fresh* waters are sufficiently dilute to be potable, that is, less than about 1,000 mg/l TDS. *Brackish* waters are too saline to be potable, but are significantly less saline than seawater; the range is approximately 1,000 to 20,000 mg/l. *Saline* waters have salinities similar to or greater than that of seawater (35,000 mg/l TDS), and *brines* are waters significantly more saline than seawater.

A convenient approximate way to measure salinity is to measure the electrical conductivity (or specific conductance) of a water sample. Conductivity (measured in siemens) is the reciprocal of electrical resistivity. The more ions a solution contains, the higher its conductivity. Conductivity cannot be converted precisely to salinity unless information is available on the proportions of the different ions contributing to the conductivity.

The *hardness* of a water is the concentration of ions in the water that will react with a sodium soap to precipitate an insoluble residue. It is usually reported as milligrams per liter of equivalent  $\text{CaCO}_3$ . From the atomic weights involved:

$$\text{equivalent CaCO}_3 = 2.5(\text{mg Ca/l}) + 4.1(\text{mg Mg/l})$$

Hydrogeologists commonly display water compositions on what are called *trilinear diagrams* or *Piper diagrams*. These are explained in Appendix I.

## SUGGESTED READING

- BARNES, I., and J. D. HEM. (1973). Chemistry of subsurface waters. *Annual Review of Earth Planetary Science*, 1, 157–301.
- BERNER, E. K., and R. A. BERNER. (1996). *Global Environment: Water, Air, and Geochemical Cycles*. Upper Saddle River, NJ: Prentice-Hall.
- DOMENICO, P. A., and F. W. SCHWARTZ. (1990). *Physical and Chemical Hydrogeology*. New York: Wiley.
- FREEZE, R. A., and J. A. CHERRY. (1979). *Groundwater*. Englewood Cliffs, NJ: Prentice-Hall.
- GARRELS, R. M., F. T. MACKENZIE, and C. HUNT. (1975). *Chemical Cycles and the Global Environment: Assessing Human Influences*. Los Altos, CA: William Kaufmann. Easy-to-understand introduction to box models and examples of the use of box models in assessing importance of particular human activities in changing natural cycles.
- HEM, J. D. (1985). Study and interpretation of the chemical characteristics of natural water (3rd ed.). U. S. Geological Survey Water-Supply Paper 2254. An authoritative treatment of many aspects of natural water chemistry.

# 2

## Chemical Background

To understand the geochemistry of natural waters, it is necessary to have some understanding of physical chemistry. In this chapter we review briefly a few important general ideas, but for a more complete treatment, consult the books listed at the end of the chapter.

### UNITS AND TERMINOLOGY

Several different sets of units are currently used by chemists and hydrologists. To promote uniformity among different disciplines and different countries, the SI system (System International d'Unites) has been introduced, and its use is being encouraged (in some instances demanded) by many professional organizations. The SI system uses the meter as the basic unit of length, the kilogram as the basic unit of mass, and the second as the unit of time; derived from them is the joule as the unit of energy. Some conversion factors among units are provided in the front endpaper of this book.

This book generally follows the SI system. We have "violated" the SI system by continued use of the liter ( $= 10^{-3} \text{ m}^3$ ) as a unit of volume and the atmosphere ( $1 \text{ atmosphere} = 1.01325 \times 10^5 \text{ Pa}$ ) as a unit of pressure, and we have retained some examples of calorie-based units. The conversion between joules and calories is

$$1 \text{ calorie} = 4.184 \text{ joules}$$

In physical chemistry, concentrations of solutes in aqueous solutions are usually expressed in molal units (m), that is, moles of solute per kilogram of solvent. A mole of a substance is its formula weight expressed in grams. Molar units (M) measure concentration in moles of solute per liter of solution. For most natural waters, molal and molar units are essentially the same; it is only in concentrated brines or at high temperatures that the difference becomes significant.

Concentrations in solid solutions (and sometimes other solutions) are generally expressed as mole fractions. The mole fraction of A is simply the number of moles of A in some unit of solution divided by the total number of moles in that unit.

**Example 1**

A  $\text{CaCO}_3$ – $\text{MgCO}_3$  solid solution contains 5 weight percent Mg. What is the mole fraction of  $\text{MgCO}_3$  in the solid solution?

The formula weights of Mg, Ca and  $\text{CO}_3$  are 24, 40 and 60, respectively; hence

$$\text{Wt\% MgCO}_3 = \frac{5 \times (24 + 60)}{24} = 17.5$$

$$\text{Wt\% CaCO}_3 = 100 - 17.5 = 82.5$$

$$\text{Relative number of moles MgCO}_3 = \frac{17.5}{84} = 0.21$$

$$\text{Relative number of moles CaCO}_3 = \frac{82.5}{100} = 0.825$$

$$\begin{aligned} \text{Mole fraction} &= \frac{\text{moles MgCO}_3}{\text{moles MgCO}_3 + \text{moles CaCO}_3} \\ &= \frac{0.21}{0.21 + 0.825} \\ &= 0.20 \end{aligned}$$

The mole fraction of  $\text{MgCO}_3$  is thus 0.20.

Concentrations in geochemistry are often expressed as millimoles per kilogram (mmol/kg) or micromoles/kg ( $\mu\text{mol/kg}$ ), which, except in concentrated brines, are essentially the same as molal units  $\times 10^{-3}$  (or  $\times 10^{-6}$ ). Weight units such as parts per million (ppm) or parts per billion (ppb) are also widely used.

$$1 \text{ ppm} = \frac{1 \text{ g}}{10^6 \text{ g}} = 1 \text{ mg/kg} = 1 \text{ g/metric ton}$$

$$1 \text{ ppb} = \frac{1 \text{ g}}{10^9 \text{ g}} = 1 \mu\text{g/kg} = 1 \text{ mg/metric ton}$$

A useful conversion to remember is

$$\text{Conc. in ppm} = \text{conc. in mmol/kg} \times \text{formula weight}$$

As units, mmol/kg or  $\mu\text{mol/kg}$  are generally preferable to weight units because most calculations are performed in molal units, and because there is sometimes ambiguity with weight units. For example, nitrate concentrations are sometimes reported as ppm nitrate (formula weight 62) and sometimes as ppm nitrogen (formula weight 14) and it is not always clear which formula weight has been assumed. Concentrations are also reported as milliequivalents per kg (meq/kg) or microequivalents per kg ( $\mu\text{eq/kg}$ ). Equivalents are simply moles multiplied by ionic charge:

$$\text{Conc. in meq/kg} = \text{conc. in mmol/kg} \times \text{ionic charge}$$

a solution containing 1 mmol/kg of  $\text{Ca}^{2+}$  thus contains 2 meq/kg of  $\text{Ca}^{2+}$ .

Three terms that are widely used in chemistry and geochemistry are *system*, *species*, and *component*. A *system* represents a group of chemicals we wish to consider. Thus if we are interested in calcite dissolving in pure water, we would talk about the system  $\text{CaCO}_3\text{-H}_2\text{O}$ . If  $\text{CO}_2$  gas were also involved, we would talk about the system  $\text{CaCO}_3\text{-H}_2\text{O-CO}_2$ . A “system” is something of an abstraction, since a real solution would have a container that is not  $\text{CaCO}_3$ ,  $\text{H}_2\text{O}$ , or  $\text{CO}_2$ . A *species* is a chemical entity: ion, molecule, solid phase, and so on. Thus in the system  $\text{CaCO}_3\text{-H}_2\text{O-CO}_2$ , some of the possible species would be (Chapter 3)  $\text{Ca}^{2+}$ ,  $\text{CO}_2(\text{g})$ ,  $\text{CO}_2(\text{aq})$ ,  $\text{H}_2\text{CO}_3$ ,  $\text{HCO}_3^-$ ,  $\text{CO}_3^{2-}$ ,  $\text{H}^+$ ,  $\text{OH}^-$ ,  $\text{H}_2\text{O}(\text{l})$ ,  $\text{H}_2\text{O}(\text{g})$ ,  $\text{CaCO}_3(\text{s})$ , plus various complexes. A set of *components* is defined as a group of entities such that every species in the system can be written as the product of a reaction involving only the components, and no component can be written as the product of a reaction involving only the other components. The components thus represent the minimum number of chemical entities necessary to define the compositions of all species in the system. When the expression “the system A-B-C” is used, A, B, and C are always a set of components. Any system can usually be described by several different sets of components. In the system  $\text{CaCO}_3\text{-H}_2\text{O-CO}_2$ , for example, another set of components would be  $\text{CaO-H}_2\text{O-CO}_2$ . Various sets involving ions could also be written, but because of the requirement of electrical neutrality in real systems, it is generally preferable to use uncharged entities as components.

## EQUILIBRIUM THERMODYNAMICS

Most of the discussions in this book are based on equilibrium thermodynamics. That is, we calculate what a particular system would look like if complete chemical equilibrium were attained. In natural systems, complete chemical equilibrium is rarely attained, particularly where biological processes are involved. Nevertheless, the equilibrium approach is useful in that (1) it often provides a good approximation to the real world, (2) it indicates the *direction* in which changes can take place. In the absence of some energy input, systems, including biological systems, can move only toward equilibrium, and (3) it is the basis for calculation of rates of natural processes since, in general, the farther a system is from equilibrium, the more rapidly it will react toward equilibrium, although it is rarely possible to predict reaction rates quantitatively from thermodynamic data.

A system at equilibrium is characterized by being in a state of minimum energy. A system not at equilibrium can move toward equilibrium by releasing energy. For systems at constant temperature ( $T$ ) and pressure ( $P$ ), which we shall be dealing with in this book, the appropriate measure of energy is the Gibbs free energy ( $G$ ), which is related to enthalpy (heat content) ( $H$ ) and entropy ( $S$ ) by the equation:

$$G = H - TS$$

The units of  $G$  and  $H$  are commonly kJ/mol (or kcal/mol); the unit of  $S$  is kJ/mol.K (kcal/mol.K).  $T$  is the temperature on the kelvin scale. For changes at constant  $P$  and  $T$ ,

$$\Delta G = \Delta H - T\Delta S \quad (2-1)$$

When a system moves toward equilibrium, it may release heat, its entropy may increase, or some combination of heat and entropy change may take place that causes a net decrease in  $G$ . Thus  $\Delta G$  is negative for spontaneous processes, and  $\Delta G = 0$  for processes occurring at

equilibrium. The idea of heat being given off in a spontaneous process is a familiar one; the concept of an increase in entropy is perhaps less familiar. Entropy is related to disorder. Consider two vessels filled with nitrogen and argon at the same temperature and pressure separated by a valve. Initially each vessel contains a pure gas. If the valve is opened, the gases will spontaneously mix (by diffusion). At equilibrium, each vessel will contain a 50:50 mixture of the two gases. Conversely, if we start with a 50:50 mixture in each vessel, the gases will never spontaneously separate into pure argon in one and pure nitrogen in the other. Mixing of the gases did not cause any evolution of heat, and no mechanical work was performed by the gases. The reason that mixing occurred is that the mixture is more disordered, more statistically probable, than the separate pure gases. In this example, the entropy term reflects the difference in order.

A quantity closely related to  $G$  is the *chemical potential* ( $\mu$ ), which is defined by the equation:

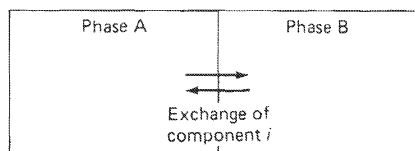
$$\mu_i = \left( \frac{\partial G}{\partial n_i} \right)_{T,P}$$

where the subscript  $i$  refers to a particular component in the system and  $n$  is the number of moles of that component being added to the system. The chemical potential is thus the partial molar Gibbs free energy or the amount (per mole) by which the Gibbs free energy of the system changes with the addition of an infinitesimal amount of a particular component. For a one-component system, the chemical potential is simply the Gibbs free energy per mole. Gibbs free energy is an extensive quantity, whereas chemical potential is an intensive quantity. Thus, if we have two systems that are identical except that one has twice the mass and volume of the other, the large system will have twice the Gibbs free energy of the small one, but the chemical potentials of all components in the large system will be identical to those in the small system. Temperature is another example of an intensive quantity.

When two or more phases coexist at equilibrium, the chemical potential of all the components in the system must be identical in each phase. Consider the system in Fig. 2-1. If  $(\mu_i)_A$  is greater than  $(\mu_i)_B$ , the transfer of some component  $i$  from A to B will result in a release of energy ( $\Delta G$  negative), and thus the system cannot be at equilibrium. If  $(\mu_i)_A = (\mu_i)_B$ , transfer of component  $i$  from A to B will result in zero change in  $G$ , which is a criterion of chemical equilibrium. The phases A and B could be gas-liquid, gas-solid, liquid-liquid, liquid-solid, or solid-solid. For stoichiometric solids (ones that have a unique, invariable chemical composition), there may be practical problems in defining  $\mu$  for particular components, but the principle is still valid: in a system at equilibrium, the chemical potential of each component is the same in all phases.

The final quantities directly related to  $G$  that we introduce at this stage are activity  $a$  and fugacity  $f$ . *Fugacity*, which can be thought of as an effective pressure, is commonly used in

FIGURE 2-1 Exchange of a component between two phases.



connection with gases, and *activity*, which can be thought of as an effective concentration, is commonly used in connection with liquid and solid phases. They are defined by the equations:

$$\mu_i = \mu_i^0 + RT \ln \alpha_i \quad (2-2)$$

$$\mu_i = \mu_i^0 + RT \ln f_i$$

where  $\mu_i^0$  is a constant which is the chemical potential of component  $i$  in its *standard state*,  $R$  is the gas constant (8.3143 J/mol.K; 1.98717 cal/mol.K), and  $T$  is the temperature on the kelvin scale. In an ideal system (discussed below),  $\alpha_i$  and  $f_i$  are numerically equal to the concentration or pressure in the units used to define the standard state. They are formally dimensionless, although they are often reported in the units corresponding to the standard state. Activity and fugacity are both defined by chemical potential and hence by Gibbs free energy.

Several different conventions are used to define standard states, and the choice of a particular convention is determined by convenience for solving a particular problem rather than by any theoretical considerations. The overall concept is that  $\mu_i$  is a defined, in principle measurable, quantity. It is convenient for calculation purposes to divide it into two parts: one part representing the intrinsic properties of  $i$  (the chemical potential of  $i$  in some well-defined reference state) and one part representing the concentration of  $i$  in solution. For solid solutions, solutions of two miscible liquids, and for the *solvent* in aqueous solutions, the standard state is commonly taken to be the pure substance at the same temperature and pressure as the solution of interest. Thus, for aqueous solutions,  $\mu_{\text{H}_2\text{O}} = \mu_{\text{H}_2\text{O}}^0$  and  $\alpha_{\text{H}_2\text{O}} = 1$  when the solution is infinitely dilute. For *solutes* in aqueous solutions, the pure solute is not a convenient standard state, and the most commonly used approach is the *infinite dilution convention*. By this convention, the activity of a solute approaches its concentration, in molal units, as the concentration of dissolved species approaches zero.

$$\alpha_i \rightarrow m_i \text{ as } \sum m_i \rightarrow 0$$

We can also define an *activity coefficient*  $\gamma$  by the equation:

$$\gamma_i = \frac{\alpha_i}{m_i}$$

and hence,

$$\gamma_i \rightarrow 1 \text{ as } \sum m_i \rightarrow 0$$

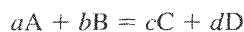
Under this convention, the standard state is a hypothetical ideal 1 m solution (an ideal solution in this context is one in which activities equal concentrations). Other conventions, such as the constant ionic medium convention:

$$\alpha_i \rightarrow m_i \text{ as } m_i \rightarrow 0, \sum m_j = \text{constant}$$

are in use, but will not be discussed here. For gases, the fugacity approaches the partial pressure as the total gas pressure approaches zero.

## Equilibrium Constant

The familiar expression for the equilibrium constant can easily be derived from the expressions for chemical potential and Gibbs free energy. Consider the reaction:



The Gibbs free energy per mole of reaction,  $\Delta G_R$ , is the difference between the Gibbs free energy of the products and that of the reactants:

$$\Delta G_R = G_{\text{products}} - G_{\text{reactants}}$$

which can be written, in terms of chemical potential:

$$\Delta G_R = c\mu_C + d\mu_D - a\mu_A - b\mu_B$$

Substituting Eq. (2-2), we obtain

$$\Delta G_R = c\mu_C^0 + cRT \ln \alpha_C + d\mu_D^0 + dRT \ln \alpha_D - a\mu_A^0 - aRT \ln \alpha_A - b\mu_B^0 - bRT \ln \alpha_B$$

Collecting terms and rearranging yields

$$\Delta G_R = c\mu_C^0 + d\mu_D^0 - a\mu_A^0 - b\mu_B^0 + RT \ln \left( \frac{\alpha_C^c \alpha_D^d}{\alpha_A^a \alpha_B^b} \right)$$

which is equivalent to

$$\Delta G_R = \Delta G_R^0 + RT \ln \left( \frac{\alpha_C^c \alpha_D^d}{\alpha_A^a \alpha_B^b} \right) \quad (2-3)$$

$\Delta G_R^0$  is the *standard free energy* of the reaction, that is, the change in free energy when  $a$  moles of A and  $b$  moles of B are converted to  $c$  moles of C and  $d$  moles of D, all in their standard states. At equilibrium,  $\Delta G_R = 0$  and hence:

$$RT \ln \left( \frac{\alpha_C^c \alpha_D^d}{\alpha_A^a \alpha_B^b} \right) = -\Delta G_R^0$$

or

$$\begin{aligned} \left( \frac{\alpha_C^c \alpha_D^d}{\alpha_A^a \alpha_B^b} \right) &= \exp \left( \frac{-\Delta G_R^0}{RT} \right) \\ &= K_{\text{eq}} \end{aligned}$$

where  $K_{\text{eq}}$  is the *equilibrium constant*. The equilibrium constant is thus related to the standard free energy of reaction by the equation:

$$\ln K_{\text{eq}} = \frac{-\Delta G_R^0}{RT}$$

or

$$\log K_{\text{eq}} = \frac{-\Delta G_R^0}{2.303 RT}$$

which gives

$$\log K_{\text{eq}} = -\frac{\Delta G_R^0}{5.708} \text{ at } 25^\circ\text{C, where } \Delta G_R^0 \text{ is in kJ/mol}$$

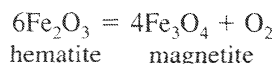


$$\log K_{\text{eq}} = -\frac{\Delta G_R^0}{1.364} \text{ at } 25^\circ\text{C, where } \Delta G_R^0 \text{ is in kcal/mol}$$

The equilibrium constant can thus be calculated directly if the free energy of reaction is known.

Appendix II lists the *standard free energies of formation* ( $\Delta G_f^0$ ) of various species—solid phases, liquids, gases, and solutes. These represent the free energy change when 1 mole of the species in its standard state is formed from the elements of which it is composed, the elements all being in their standard states. Thus the standard free energy of formation of calcite ( $\text{CaCO}_3$ ) ( $-1129.07$  kJ/mole) represents the energy change when 1 mole of calcite at  $25^\circ\text{C}$  and 1 atm. is formed from 1 mole of metallic calcium, 1 mole of graphite, and 1.5 moles of  $\text{O}_2$ , all of them at  $25^\circ\text{C}$  and 1 atm. The standard free energy of formation of calcite is negative, indicating that energy is released when calcite is formed from its elements. By convention, the standard free energies of formation of elements in their standard states are zero. The definition of the standard free energy of formation of ions in solution is based on the convention (Chapter 7) that the standard free energy of formation of a hydrogen ion in solution is zero. *Standard enthalpies of formation* ( $\Delta H_f^0$ ) are defined in an analogous way: they represent the enthalpy (heat) change when 1 mole of a species is formed from its constituent elements, everything being in its standard state. The standard entropy ( $S^0$ ) is defined on a slightly different convention. Instead of the entropy of elements in their standard states being zero, the entropy of perfectly crystalline solids at  $0^\circ\text{K}$  is taken to be zero (the third law of thermodynamics).

*Standard free energies of reaction, standard enthalpies of reaction, and standard entropies of reaction* are all calculated in the same way. Let us use the reaction between hematite and magnetite plus oxygen as an example. First, a balanced chemical reaction is written



The standard free energy (enthalpy, entropy) of reaction is the standard free energy (enthalpy, entropy) of the products (species appearing on the right of the equation) minus that of the reactants (species appearing on the left of the equation). The free energy (enthalpy, entropy) associated with each species is its standard free energy (enthalpy, entropy) of formation multiplied by its coefficient in the chemical equation. For the reaction, we are considering

	$\Delta G_f^0$ (kJ/mol)	$\Delta H_f^0$ (kJ/mol)	$S^0$ (kJ/mol.K)
hematite	-742.8	-824.7	$87.7 \times 10^{-3}$
magnetite	-1012.9	-1116.1	$146.1 \times 10^{-3}$
oxygen	0	0	$205.0 \times 10^{-3}$

$$\Delta G_R^0 = 4 \times (-1012.9) + 0 - 6 \times (-742.8) = +405.2 \text{ kJ/mole}$$

$$\Delta H_R^0 = 4 \times (-1116.1) + 0 - 6 \times (-824.7) = +483.8 \text{ kJ/mole}$$

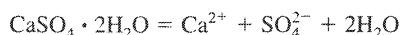
$$\Delta S_R^0 = 4 \times (146.1 \times 10^{-3}) + 205.0 \times 10^{-3} - 6 \times (87.7 \times 10^{-3}) = 263.2 \times 10^{-3} \text{ kJ/mole.K}$$

Note that  $\Delta G_R^0 = \Delta H_R^0 - T\Delta S_R^0$ , where  $T = 298.15 \text{ K}$  ( $25^\circ\text{C}$ ).

The standard free energy of reaction is used to calculate equilibrium constants at 25°C. The standard enthalpy and entropy of reaction can be used to calculate the equilibrium constant at different temperatures, as discussed later in this chapter.

### Example 2

Calculate the solubility product of gypsum at 25°C from the data in Appendix II (a *solubility product* is an equilibrium constant for a simple solubility reaction).



$$K_{\text{eq}} = \frac{\alpha_{\text{Ca}^{2+}} \alpha_{\text{SO}_4^{2-}} \alpha_{\text{H}_2\text{O}}^2}{\alpha_{\text{CaSO}_4 \cdot 2\text{H}_2\text{O}}}$$

If the solution is reasonably dilute,  $\alpha_{\text{H}_2\text{O}}$  will equal 1;  $\text{CaSO}_4 \cdot 2\text{H}_2\text{O}$  is in its standard state (pure solid), so its activity is unity. Therefore,

$$K_{\text{eq}} = \alpha_{\text{Ca}^{2+}} \alpha_{\text{SO}_4^{2-}} = K_{\text{sp}}$$

$K_{\text{eq}}$  is the solubility product ( $K_{\text{sp}}$ ) of gypsum.

Standard free energies of formation in kJ/mol are (Appendix II)

CaSO <sub>4</sub> · 2H <sub>2</sub> O	-1797.36	Ca <sup>2+</sup>	-552.8
H <sub>2</sub> O	-237.14	SO <sub>4</sub> <sup>2-</sup>	-744.0

$$\Delta G_R^0 = -552.8 - 744.0 - 2 \times 237.14 - (-1797.36)$$

$$= +26.28 \text{ kJ/mol}$$

$$\log K_{\text{eq}} = \frac{-\Delta G_R^0}{5.708} = -4.60$$

The solubility product ( $K_{\text{sp}}$ ) of gypsum at 25°C is therefore  $10^{-4.60}$ .

For temperatures not far from 25°C, the variation of  $K_{\text{eq}}$  with temperature can be calculated from the equations:

$$\begin{aligned} \Delta G_R^0 &= \Delta H_R^0 - T\Delta S_R^0 \\ &= -RT \ln K_{\text{eq}} \end{aligned}$$

which rearranges to

$$\ln K_{\text{eq}} = \frac{-\Delta H_R^0}{RT} + \frac{\Delta S_R^0}{R} \quad (2-4)$$

Values of  $\Delta H_R^0$  and  $\Delta S_R^0$  can be obtained from the standard-state enthalpies and entropies of formation of the reactants and products (see Appendix II). This method of calculation is based on the assumption that  $\Delta H_R^0$  and  $\Delta S_R^0$  are independent of temperature. The assumption is reasonable for temperatures within 20°C or so of the standard state. For extrapolation to much different temperatures, the effect of temperature on  $\Delta H_R^0$  and  $\Delta S_R^0$  can be calculated from the heat capacities of the reactants and products (e.g., Nordstrom and Munoz, 1994).

An alternative method based on the same assumptions comes from differentiating Eq. (2-4)

$$\frac{d \ln K_{\text{eq}}}{dT} = \frac{\Delta H_R^0}{RT^2} \quad (2-5)$$

and integrating this from  $T_1$  (the reference temperature) to  $T_2$  (the temperature of interest):

$$\ln K_{T_2} - \ln K_{T_1} = \frac{\Delta H_R^0}{R} \left( \frac{1}{T_1} - \frac{1}{T_2} \right)$$

or

$$\log K_{T_2} - \log K_{T_1} = \frac{\Delta H_R^0}{2.303 R} \left( \frac{1}{T_1} - \frac{1}{T_2} \right) \quad (2-6)$$

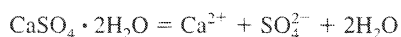
Thus, if the equilibrium constant at one temperature and the standard enthalpy of reaction are known, the equilibrium constant at another temperature can readily be calculated. Again, if  $T_2$  is far from  $T_1$ , the variation of  $\Delta H_R^0$  with  $T$  must be calculated from heat capacity data. Eq. (2-6) is sometimes referred to as the *Van't Hoff equation*.

### Example 3

By how much does the solubility of gypsum at 40°C differ from the value at 25°C?

This problem can be solved in several different ways, depending on the tabulated data that are available. We can use a tabulated equilibrium constant and  $\Delta H_R^0$  from Appendix III in Eq. (2-6), or we can use the standard free energies, enthalpies, and entropies of formation in Appendix II and either Eq. (2-4) or (2-6).

From Appendix III, the equilibrium constant for the reaction



is

$$\log K_{\text{eq}} = -4.58$$

and

$$\Delta H_R^0 = -0.46 \text{ kJ/mol}$$

rewriting Eq. (2-6):

$$\log K_{T_2} = \log K_{T_1} + \frac{\Delta H_R^0}{2.303R} \left( \frac{1}{T_1} - \frac{1}{T_2} \right) \quad (2-7)$$

where 2.303 represents the conversion from base  $e$  to base 10 logarithms. We can see right away from Eq. (2-7) that whether the solubility increases or decreases with increasing temperature will depend on the sign of  $\Delta H_R^0$ . If  $\Delta H_R^0$  is positive, solubility will increase with increasing temperature. If  $\Delta H_R^0$  is negative (as in this example), solubility will decrease with increasing temperature. Substituting the numbers gives

$$\log K_{T_2} = -4.58 - 0.00386 = -4.584$$

The solubility product at 40°C is thus  $10^{-4.584}$ . The percent difference between the 40°C value and the 25°C value is given by

$$100 \times (10^{-4.58} - 10^{-4.584}) / 10^{-4.58} = -0.9\%$$

The solubility of gypsum is thus about 1 percent less at 40°C than at 25°C. The small difference reflects the small numerical value of  $\Delta H_R^0$ .

We can perform exactly the same calculation using the data in Appendix II. From the previous example:

$$\log K_{T_1}(25^\circ\text{C}) = -4.60$$

The  $\Delta H_R^0$  of reaction is given by

$$\Delta H_R^0 = \Delta H_f^0(\text{Ca}^{2+}) + \Delta H_f^0(\text{SO}_4^{2-}) + 2\Delta H_f^0(\text{H}_2\text{O}) - \Delta H_f^0(\text{CaSO}_4 \cdot 2\text{H}_2\text{O})$$

Substituting the numbers from Appendix II:

$$\Delta H_R^0 = -1.08 \text{ kJ/mol}$$

Substituting in Eq. (2-7) gives

$$\log K_{T_2} = -4.60 - 0.009 = -4.61$$

The solubility product at 40°C would thus be  $10^{-4.62}$ , which is about 2 percent smaller than the 25°C value; the slightly greater effect of temperature compared to the previous calculation reflects the slightly greater (absolute) value of  $\Delta H_R^0$ .

Alternatively, we can use the data in Appendix II with Eq. (2-4). The numbers in Appendix II yield  $\Delta H_R^0 = -1.08 \text{ kJ/mol}$ ,  $\Delta S_R^0 = -91.7 \text{ J/mol}\cdot\text{K}$  (note that entropies are commonly reported in J rather than kJ units; this is simply a matter of convenience, as the numerical values for entropies are generally much smaller than those for enthalpies and Gibbs free energies).

At 40°C,

$$\begin{aligned} \Delta G_R^0 &= \Delta H_R^0 - T\Delta S_R^0 \\ &= -1.08 - (313.15 \times -91.7 \times 10^{-3}) \text{ kJ/mol} \\ &= +27.64 \text{ kJ/mol} \end{aligned}$$

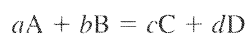
The equilibrium constant is calculated from

$$\begin{aligned} -2.303 RT \log K_{40} &= \Delta G_R^0 \\ \log K_{40} &= \frac{-27.64}{2.303 \times 8.314 \times 10^{-3} \times 313.15} \\ &= -4.61 \end{aligned}$$

Thus the solubility product at 40°C is  $10^{-4.61}$ , which is essentially the same as the value obtained by using the data from Appendix II and Eq. (2-7). The different approaches and data sets give similar temperature dependence, and similar solubility products at 40°C. The slight discrepancies are an example of inconsistencies among different thermodynamic data sets that commonly arise in geochemistry. (The problem of inconsistency is further discussed in Chapter 10.) As a general rule, tabulated equilibrium constants are likely to be more accurate than equilibrium constants calculated from tabulated free energies.

### Measurements of Disequilibrium

Consider again the reaction:



If the system is at equilibrium,

$$\frac{a_C^c a_D^d}{a_A^a a_B^b} = K_{\text{eq}} \quad (2-8)$$

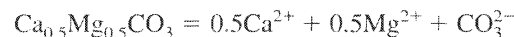
If the system is not at equilibrium, the expression on the left side of Eq. (2-8) is called the *activity product (AP)* or the *ion activity product (IAP)* if the species involved are ions. Unless the system is exactly in equilibrium, the activity product will not be equal to  $K_{\text{eq}}$ . If  $AP/K_{\text{eq}} > 1$ , the reaction will tend to go to the left; if  $AP/K_{\text{eq}} < 1$ , the reaction will tend to go to the right. Expressions used by various authors to indicate how far a system is from equilibrium include  $AP/K_{\text{eq}}$  (which will be 1 at equilibrium),  $\log (AP/K_{\text{eq}})$  (which will be zero at equilibrium), and  $RT \ln (AP/K_{\text{eq}})$ . This last expression has the significance [compare Eq. (2-3)] that it represents the free-energy change in converting 1 mole of reactants to products under the conditions at which the AP was measured. The most common use of these expressions is in describing the extent to which a particular solution is supersaturated or undersaturated with respect to a particular solid phase. The term *saturation index* is often used for  $\log (IAP/K_{\text{eq}})$  for a dissolution reaction. The saturation index (*SI*) for gypsum, for example, would be

$$SI = \log \frac{(a_{\text{Ca}^{2+}} a_{\text{SO}_4^{2-}})_{\text{solution}}}{K_{\text{sp}(\text{gypsum})}}$$

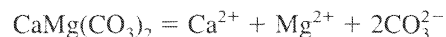
A useful modification to all these expressions for state of saturation is to normalize for the number of ions ( $\nu$ ) in the expression for the ion activity product. This gives the *saturation ratio (SR)* (Zhang and Nancollas, 1990):

$$SR = \left( \frac{IAP}{K_{\text{sp}}} \right)^{1/\nu}$$

The expressions for the saturation index and saturation state in free energy units ( $RT \ln IAP/K_{\text{eq}}$ ) can be normalized in the same way. The advantage of normalization is that it makes the state of saturation independent of the way the formula of the solid phase is written. For example, the dissolution of dolomite could be written as



or as



If the equation is written in the second way, the  $IAP/K_{\text{sp}}$  ratio will be the square of what it would be if the equation were written in the first way, and the SI and free energy expressions will be double. Logically, the state of saturation should not depend on the way we choose to write the reaction; use of the normalized saturation ratio avoids this problem.

#### Example 4

A water has a calcium activity of  $10^{-3.5}$  and a sulfate activity of  $10^{-1.5}$ . By how much is it undersaturated (or supersaturated) with respect to gypsum? By how much would it have to be concentrated (or diluted) for it to be in equilibrium with gypsum?

The ion activity product (*IAP*) is  $10^{-3.5} \times 10^{-1.5} = 10^{-5.0}$ . The solubility product ( $K_{\text{sp}}$ ) from Example 2 is  $10^{-4.60}$ . Since *IAP* is less than  $K_{\text{sp}}$ , the solution is undersaturated. The ratio

$$\frac{IAP}{K_{sp}} = \frac{10^{-5.0}}{10^{-4.60}} = 10^{-0.40} = 0.40$$

Since two ions are involved in the IAP, the saturation ratio is given by

$$\left(\frac{IAP}{K_{sp}}\right)^{1/2} = 10^{-0.20} = 0.63$$

The amount by which it would have to be concentrated to reach saturation is simply the reciprocal of the saturation ratio (another advantage of using the normalized ratio!); i.e.,  $1/0.63 = 1.58$ .

For the other measures of saturation state, the saturation index is  $-0.40$  ( $-0.20$  normalized), and  $RT \ln (IAP/K_{sp}) = -2.28$  kJ/mol ( $-1.14$  kJ normalized).

This last number indicates that, if gypsum were to dissolve in the water in question, 2.28 kJ of energy would be released per mole of gypsum dissolved. This, of course, is the instantaneous rate at which energy would be released at the given solution conditions. As gypsum dissolved, the activities of  $\text{Ca}^{2+}$  and  $\text{SO}_4^{2-}$  would increase, and the energy released per mole of dissolving gypsum would decrease until it became zero when the solution became saturated with respect to gypsum.

## ACTIVITY-CONCENTRATION RELATIONSHIPS

If a solution of two species A and B has the properties that the energy of interaction between two A molecules is identical to the energy of interaction between an A molecule and a B molecule, or between two B molecules, the solution will be ideal. It can be shown by statistical arguments that the activities of both species in an ideal solution will equal their concentrations (provided that appropriate standard states and concentration units are used). In real solutions, particularly solutions of ionic species in water, these conditions are not met. There are electrostatic interactions between charged ions, and the ions are generally surrounded by regions in which the water molecules are ordered in a structure different from that of pure water (a hydration shell). The ionic interactions and the ordering of the water both cause the free energy of the real solution to be different from that of the ideal solution and, hence, for the activities of both solute and solvent to differ from their concentrations. In practice, for aqueous solutions less concentrated than seawater, the activity of water is very close to unity (in seawater it is 0.98). Uncharged solutes (such as dissolved  $\text{CO}_2$  or  $\text{H}_4\text{SiO}_4$ ) approximate ideal solution behavior much more closely than do charged species because there is not the same electrostatic interaction. The ratio of the activity of a species to its concentration is called the *activity coefficient* ( $\gamma$ ). In general, activity coefficients of uncharged species are near unity in dilute solutions and rise above unity in concentrated solutions, largely because much of the water in concentrated solutions is involved in the hydration shells of ions and less water is available to solvate uncharged species. The activity coefficients of uncharged species can be represented approximately by the equation (Plummer and Mackenzie, 1974)

$$\gamma = 10^{0.1I}$$

where  $I$  is the ionic strength of the solution (defined below). As a point of reference, the activity coefficient of dissolved carbon dioxide in seawater is about 1.12.

### Activities of Ionic Species

From a purely thermodynamic point of view, there is no way in which the activity coefficient of a single ion can be measured without introducing non-thermodynamic (and non-verifiable) assumptions. In principle, to measure the activity coefficient of, for example,  $\text{Na}^+$  in solution, we would have to measure how much the free energy of a solution varied as the concentration of  $\text{Na}^+$  varied. The problem is that it is impossible to vary the concentration of  $\text{Na}^+$  without also varying the concentration of some anion or some other cation. It is therefore impossible, in principle, to say how much of the free-energy change should be attributed to  $\text{Na}^+$  and how much to the other ion. The thermodynamically correct way to treat activity coefficients of ionic species is not in terms of ionic components ( $\text{Na}^+$ ,  $\text{K}^+$ ,  $\text{Cl}^-$ ,  $\text{SO}_4^{2-}$ , etc.), but in terms of uncharged components ( $\text{NaCl}$ ,  $\text{K}_2\text{SO}_4$ , etc.). For dilute solutions, however, it is convenient to use single-ion activity coefficients even though they are not rigorously defined thermodynamically. For concentrated brines, it may be advantageous to consider uncharged species rather than ions. The conceptual approach that is used to relate activities to concentrations is called a *solution model*. We shall generally use the *single-ion activity coefficient/ion pair model* in this text. The model is explained in the following sections.

**Debye-Hückel Theory.** The Debye-Hückel theory is a model that allows activity coefficients for single ions to be calculated on the basis of the effect ionic interactions should have on free energy. In an ionic solution, positive ions will tend to have a cloud of negative ions around them, and negative ions a cloud of positive ions. This will result in a system with a lower free energy than would be the case if the distribution of ions were completely random, and hence an activity for the solutes lower than it would be for the random (ideal) case. Activity coefficients for ions in solution should thus be less than 1. If it is assumed that the ions are point charges, the interactions are entirely electrostatic, and the ions around any particular ion follow a Boltzmann distribution, it is possible to derive the equation

$$\log \gamma_i = -Az_i^2\sqrt{I} \quad (2-9)$$

where  $A$  is a constant depending only on  $P$  and  $T$ ,  $z_i$  is the charge on the particular ion, and  $I$  is the *ionic strength* of the solution. Ionic strength is given by

$$I = \frac{1}{2} \sum m_i z_i^2$$

Ionic strength ( $m_i$  is the concentration of the  $i$ th ion; the summation sign means that the contributions from all ions in solution must be summed) is a quantity that occurs frequently in solution chemistry. It differs from total concentration in that it takes account of the greater electrostatic effectiveness of polyvalent ions. Thus the ionic strength of a 1 m solution of  $\text{NaCl}$  is 1, of a 1 m solution of  $\text{Na}_2\text{SO}_4$  is 3, and of a 1 m solution of  $\text{MgSO}_4$  is 4. Eq. (2-9), the original form of the Debye-Hückel equation, holds reasonably well up to ionic strengths of about  $10^{-3}$ .

At higher ionic strengths the simple model fails because it requires an impossibly high concentration of anions around each cation, and vice versa. The equation can be modified to take account of the finite size of the ions, giving the extended Debye-Hückel equation:

$$\log \gamma_i = \frac{-Az_i^2\sqrt{I}}{1 + Ba_0\sqrt{I}} \quad (2-10)$$

$B$  is a constant depending only on  $P$  and  $T$ , and  $a_0$  is, in theory, the hydrated radius of the particular ion. In practice, the value of  $a_0$  is chosen to give the best fit to experimental data. Some values for the parameters in the Debye-Hückel equation [Eq. (2-10)] are given in Table 2-1. Equation (2-10) is reasonably accurate up to ionic strengths of about  $10^{-1}$ .

Note in Table 2-1 that the product  $Ba_0$  has a numerical value of about 1. A commonly used alternative form of Eq. (2-10) is

$$\log \gamma_i = \frac{-Az_i^2\sqrt{I}}{1 + \sqrt{I}} \quad (2-11)$$

Eq. (2-11) is commonly called the *Güntelberg equation*.

For higher ionic strengths, Eq. (2-10) and (2-11) can be modified by adding a further term:

$$\log \gamma_i = \frac{-Az_i^2\sqrt{I}}{1 + Ba_0\sqrt{I}} + bI \quad (2-12)$$

and

$$\log \gamma_i = \frac{-Az_i^2\sqrt{I}}{1 + \sqrt{I}} + bI \quad (2-13)$$

where  $b$  may be a general constant (Davies, 1962), or may be a constant specific to the individual ion  $i$  (Parkhurst, 1990). Eq. (2-13) with  $b$  set equal to 0.3 is called the *Davies equation*. The additional term can be justified on theoretical grounds, or it can be justified as an empirical fit to experimental data. An important consequence of the additional term is that it predicts that activity coefficients should increase with increasing ionic strength at high ionic strengths, in accord with experimental observations (Fig. 2-2).

There are many ions for which  $a_0$  values have not been measured experimentally. The Güntelberg or Davies equation rather than the Debye-Hückel equation must be used for such ions.

**TABLE 2-1** Parameters for the Debye-Hückel Equation at 1 Atmosphere Pressure (Adapted from Truesdell and Jones, 1974; Ball and Nordstrom, 1991)

$T(^{\circ}\text{C})$	$A$	$B(\times 10^8)$	Ion	$a_i(\times 10^{-8})$	$b$
0	0.4883	0.3241	$\text{Ca}^{2+}$	5.0	0.165
5	0.4921	0.3249	$\text{Mg}^{2+}$	5.5	0.20
10	0.4960	0.3258	$\text{Na}^{+}$	4.0	0.075
15	0.5000	0.3262	$\text{K}^{+}, \text{Cl}^{-}$	3.5	0.015
20	0.5042	0.3273	$\text{SO}_4^{2-}$	5.0	-0.04
25	0.5085	0.3281	$\text{HCO}_3^{-}, \text{CO}_3^{2-}$	5.4	0.0
30	0.5130	0.3290	$\text{NH}_4^{+}$	2.5	
40	0.5221	0.3305	$\text{Sr}^{2+}, \text{Ba}^{2+}$	5.0	
50	0.5319	0.3321	$\text{Fe}^{2+}, \text{Mn}^{2+}, \text{Li}^{+}$	6.0	
60	0.5425	0.3338	$\text{H}^{+}, \text{Al}^{3+}, \text{Fe}^{3+}$	9.0	



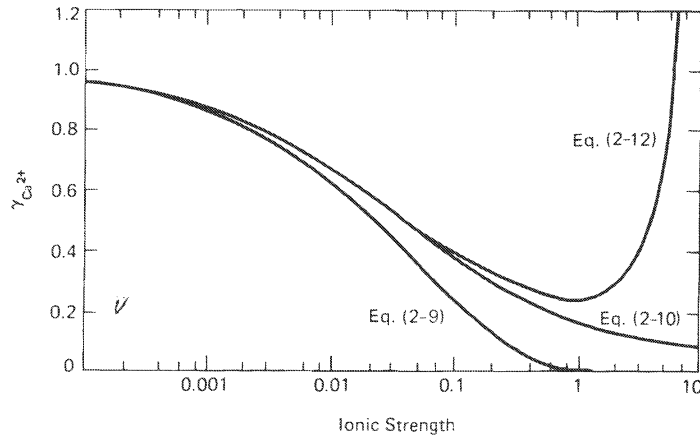


FIGURE 2-2 Variation of the activity coefficient for  $\text{Ca}^{2+}$  according to the three forms of the Debye-Hückel equation.

### Example 5

The Rio Grande at Laredo has the following approximate composition:

	mg/l	mmol/l
$\text{Ca}^{+2}$	109	2.72
$\text{Mg}^{+2}$	24	0.99
$\text{Na}^{+}$	117	5.09
$\text{K}^{+}$	7	0.18
$\text{HCO}_3^{-}$	183	3.00
$\text{SO}_4^{2-}$	238	2.48
$\text{Cl}^{-}$	171	4.82
$\text{H}_4\text{SiO}_4$	48	0.50
Temp.	25°C	

- What is the ionic strength of the solution?
  - What are the activity coefficients for  $\text{Ca}^{2+}$  and  $\text{SO}_4^{2-}$ , based on the extended Debye-Hückel equation?
  - By how much is the water undersaturated with respect to gypsum?
- The ionic strength is given by

$$\begin{aligned}
 I &= \frac{1}{2} \sum m_i z_i^2 \\
 &= 0.5[(2.72 + 0.99 + 2.48) \times 4 + 5.09 + 0.18 + 3.00 + 4.82] \times 10^{-3} \\
 &= 18.9 \times 10^{-3}
 \end{aligned}$$

(The factor  $10^{-3}$  is to convert millimolar units to molar units.  $\text{H}_4\text{SiO}_4$  does not appear in the ionic strength calculation because it is uncharged.)

2. The activity coefficients are given by

$$\log \gamma_i = \frac{-A z_i^2 \sqrt{I}}{1 + B a_0 \sqrt{I}}$$

At 25°C,  $A = 0.5085$ ,  $B = 0.3281 \times 10^8$ , and  $a_0 = 5 \times 10^{-8}$  for both  $\text{Ca}^{2+}$  and  $\text{SO}_4^{2-}$ . Substituting these values and the value for  $I$  calculated above gives

$$\log \gamma = -0.228$$

$$\gamma = 0.591 \text{ for both } \text{Ca}^{2+} \text{ and } \text{SO}_4^{2-}$$

3. The ion activity product is given by

$$\begin{aligned} \text{IAP} &= \alpha_{\text{Ca}^{2+}} \alpha_{\text{SO}_4^{2-}} = m_{\text{Ca}^{2+}} \gamma_{\text{Ca}^{2+}} \cdot m_{\text{SO}_4^{2-}} \gamma_{\text{SO}_4^{2-}} \\ &= (2.72 \times 10^{-3}) \times 0.591 \times (2.48 \times 10^{-3}) \times 0.591 \\ &= 2.36 \times 10^{-6} = 10^{-5.63} \end{aligned}$$

The solubility product of gypsum (from Example 2) is  $10^{-4.60}$ . The ratio  $\text{IAP}/K_{\text{sp}}$  is thus  $10^{-5.63}/10^{-4.60}$ , or  $10^{-1.03}$ . This number is less than 1, indicating undersaturation. The saturation ratio is  $(10^{-1.03})^{1/2} = 10^{-0.52}$  ( $= 0.31$ ), and the saturation index ( $= \log \text{IAP}/K_{\text{sp}}$ ) is  $-1.03$ .

### Example 6

On the basis of Eq. (2-10), what are the activity coefficients of  $\text{Ca}^{2+}$  and  $\text{SO}_4^{2-}$  in a solution in equilibrium with gypsum at 25°C in the system  $\text{CaSO}_4\text{-H}_2\text{O}$ ? What is the solubility of gypsum in water assuming these activity coefficients? How does it differ from the value calculated on the assumption that activities equal concentrations?

This calculation requires an iteration procedure. The solubility product of gypsum (previous examples) is  $10^{-4.60}$ . As a first approximation, let us assume that  $m_{\text{Ca}^{2+}} = m_{\text{SO}_4^{2-}} = (10^{-4.60})^{1/2} = 5.01 \times 10^{-3}$  (dissolution of gypsum in pure water must result in equal molar concentrations of calcium and sulfate).

$$\begin{aligned} I &= \frac{1}{2} ([5.01 \times 10^{-3} \times 4] + [5.01 \times 10^{-3} \times 4]) \\ &= 2.01 \times 10^{-2} \end{aligned}$$

From Table 2-1,  $A = 0.5085$ ,  $B = 0.3281 \times 10^8$ , and  $a_0 = 5 \times 10^{-8}$  for both  $\text{Ca}^{2+}$  and  $\text{SO}_4^{2-}$ .

Substituting these numbers in Eq. (2-10) gives

$$\log \gamma_{\text{Ca}^{2+}} = \log \gamma_{\text{SO}_4^{2-}} = -0.234$$

$$\gamma_{\text{Ca}^{2+}} = \gamma_{\text{SO}_4^{2-}} = 0.584$$

With these provisional values, we can compute more accurate calcium and sulfate concentrations, and hence a more accurate ionic strength.

$$(m_{\text{Ca}^{2+}} \times 0.584)(m_{\text{SO}_4^{2-}} \times 0.584) = 10^{-4.60}$$

Since  $m_{\text{Ca}^{2+}}$  must equal  $m_{\text{SO}_4^{2-}}$  when gypsum dissolves,

$$m_{\text{Ca}^{2+}} = m_{\text{SO}_4^{2-}} = \left( \frac{10^{-4.60}}{0.584 \times 0.584} \right)^{1/2} = 8.58 \times 10^{-3}$$

On the basis of this number, the ionic strength is

$$I = 3.43 \times 10^{-2}$$

and

$$\gamma_{\text{Ca}^{2+}} = \gamma_{\text{SO}_4^{2-}} = 0.514$$

These values will be more accurate than the provisional estimate, and they can be used to calculate a more accurate ionic strength, and hence more accurate activity coefficients. The iteration procedure can be repeated any number of times to give values of any desired mathematical accuracy. Doing this, we obtain the final answer:

$$I = 4.08 \times 10^{-2}$$

$$\gamma_{\text{Ca}^{2+}} = \gamma_{\text{SO}_4^{2-}} = 0.491$$

The solubility of gypsum in water will then be

$$\begin{aligned} \left( \frac{10^{-4.60}}{0.491 \times 0.491} \right)^{1/2} &= 10.2 \times 10^{-3} \text{ mol/kg} \\ &= 1.39 \text{ g/l CaSO}_4 \\ &= 1.75 \text{ g/l CaSO}_4 \cdot 2\text{H}_2\text{O} \end{aligned}$$

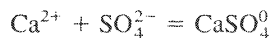
If we had assumed activities were equal to concentrations, the solubility of gypsum would have been

$$(10^{-4.60})^{1/2} = 5.01 \times 10^{-3} \text{ mol/kg}$$

This value is about half the value calculated with activity corrections, so, in this example, neglecting activity coefficients would have resulted in an error of a factor of about 2.

### Activity-Concentration Relationships in More Concentrated Solutions.

Several different approaches have been used to calculate activity coefficients in more concentrated electrolytes. One is to retain the use of single-ion activity coefficients and postulate that departures from the behavior predicted by the Debye-Hückel equation are due to the formation of *ion pairs*. Thus, for example, in a solution containing calcium and sulfate ions, the ion pair  $\text{CaSO}_4^0$  will be present. (The ion pair is a dissolved species: it has nothing to do with solid calcium sulfate.) Its formation can be described by the equation:



for which the equilibrium constant is

$$K_{\text{stab}} = \frac{a_{\text{CaSO}_4^0}}{a_{\text{Ca}^{2+}} \cdot a_{\text{SO}_4^{2-}}}$$

$K_{\text{stab}}$  is the *stability constant* for the ion pair. Sometimes in the literature *instability constants* (or *dissociation constants*) are tabulated rather than stability constants. The instability constant is the reciprocal of the stability constant. Ion-pair formation has two effects on the relationship between activity and concentration: the concentrations of free  $\text{Ca}^{2+}$  and  $\text{SO}_4^{2-}$  are decreased because some of the calcium and sulfate present in the solution are tied up in ion pairs, and the ionic strength of the solution is decreased because ions are “converted” into uncharged species. The first effect is by far the most important. The net effect of ion-pair formation is that the activities of  $\text{Ca}^{2+}$  and  $\text{SO}_4^{2-}$  are lower than would be predicted from their concentrations by the Debye-Hückel equation.

The single-ion activity coefficient/ion-pair solution model is widely used for waters less concentrated than seawater because it is convenient, the necessary data are generally available, and it is sufficiently accurate. It is not able, however, to predict accurately activity-concentration relations in brines.

### Example 7

The ion pair  $\text{CaSO}_4^0$  (an uncharged dissolved species) has a stability constant of  $10^{2.30}$ . What will be the concentration of this species in the water of Example 5? How does the existence of this complex affect the state of saturation with respect to gypsum?

The activity of the complex is given by

$$a_{\text{CaSO}_4^0} = 10^{2.30} a_{\text{Ca}^{2+}} a_{\text{SO}_4^{2-}}$$

If we assume the activity of  $\text{CaSO}_4^0$  is equal to its concentration (it is an uncharged species) and, as an initial approximation, use the total concentrations of  $\text{Ca}^{2+}$  and  $\text{SO}_4^{2-}$  and the activity coefficients from Example 5, then

$$\begin{aligned} m_{\text{CaSO}_4^0} &= 10^{2.30} [(2.72 \times 10^{-3}) \times 0.591 \times (2.48 \times 10^{-3}) \times 0.591] \\ &= 4.70 \times 10^{-4} \end{aligned}$$

This is not the final answer, because the formation of  $\text{CaSO}_4^0$  will decrease the concentrations of free  $\text{Ca}^{2+}$  and  $\text{SO}_4^{2-}$  in solution, and will also decrease the ionic strength and change the activity coefficients.

$$\begin{aligned} m_{\text{Ca}^{2+} \text{ free}} &= m_{\text{Ca}^{2+} \text{ total}} - m_{\text{CaSO}_4^0} \\ &= 2.72 \times 10^{-3} - 4.70 \times 10^{-4} \\ &= 2.25 \times 10^{-3} \end{aligned}$$

$$\begin{aligned} m_{\text{SO}_4^{2-} \text{ free}} &= m_{\text{SO}_4^{2-} \text{ total}} - m_{\text{CaSO}_4^0} \\ &= 2.48 \times 10^{-3} - 4.70 \times 10^{-4} \\ &= 2.01 \times 10^{-3} \end{aligned}$$

The new ionic strength, calculated using these revised  $\text{Ca}^{2+}$  and  $\text{SO}_4^{2-}$  numbers instead of the original (total) values gives

$$I = 8.51 \times 10^{-3}$$

$$\gamma = 0.604 \text{ for both } \text{Ca}^{2+} \text{ and } \text{SO}_4^{2-}$$

With the new values for free  $\text{Ca}^{2+}$  and  $\text{SO}_4^{2-}$  concentrations, and the new activity coefficients,

$$\begin{aligned} m_{\text{CaSO}_4^0} &= 10^{2.30} [(2.25 \times 10^{-3}) \times 0.604 \times (2.01 \times 10^{-3}) \times 0.604] \\ &= 3.29 \times 10^{-4} \end{aligned}$$

$$m_{\text{Ca}^{2+} \text{ free}} = 2.72 \times 10^{-3} - 3.29 \times 10^{-4} = 2.39 \times 10^{-3}$$

$$m_{\text{SO}_4^{2-} \text{ free}} = 2.48 \times 10^{-3} - 3.29 \times 10^{-4} = 2.15 \times 10^{-3}$$

In principle we should use these new values to calculate a new ionic strength and new activity coefficients, but the differences from the values calculated on the first iteration are trivial. We can see that 12 percent of the calcium and 13 percent of the sulfate is present in the form of the  $\text{CaSO}_4^0$  complex.

The new ion activity product for gypsum is given by

$$\begin{aligned} \text{IAP} &= (2.39 \times 10^{-3}) \times 0.604 \times (2.15 \times 10^{-3}) \times 0.604 \\ &= 1.87 \times 10^{-6} = 10^{-5.73} \end{aligned}$$

The ratio  $\text{IAP}/K_{\text{sp}}$  is thus  $10^{-5.73}/10^{-4.60}$ , or  $10^{-1.13}$ . The saturation ratio is  $(10^{-1.13})^{1/2} = 10^{-0.56}$  ( $=0.27$ ), and the saturation index ( $=\log \text{IAP}/K_{\text{sp}}$ ) is  $-1.13$ . Inclusion of the complex  $\text{CaSO}_4^0$  in the calculation has increased slightly the computed degree of undersaturation. If we had used a more concentrated water as our example, the effect of the complex would have been greater.

**Activity-Concentration Relationships in Brines.** Several different models have been used to calculate activity-concentration relationships in more concentrated solutions. Most are based on the use of mean ionic activity coefficients. The mean ionic activity coefficient ( $\gamma_{\pm}$ ) for a 1:1 electrolyte (e.g., NaCl) is defined by the equation:

$$\gamma_{\pm} = (\gamma_+ \gamma_-)^{1/2}$$

where  $\gamma_+$  is the activity coefficient of the cation and  $\gamma_-$  that of the anion. The general definition for an electrolyte in which the cation has a charge  $n^+$  and the anion a charge  $m^-$  is

$$\gamma_{\pm} = (\gamma_+^m \gamma_-^n)^{1/(m+n)}$$

Mean ion-activity coefficients are rigorously defined thermodynamically and can be measured experimentally. It turns out that the behavior of mean ion-activity coefficients in concentrated solutions is easier to predict than that of single ion-activity coefficients.

The most successful solution model for concentrated brines is that of Pitzer (1973, 1979, 1980, 1987). In very simplified form, this model postulates that departures from ideality in ionic solutions are due to interactions between the various ions in solution. Thus,

$$\frac{G_{\text{ex}}}{RT} = (D - H) + \sum_i \sum_j \lambda_{ij}(I) m_i m_j + \sum_i \sum_j \sum_k \mu_{ijk} m_i m_j m_k$$

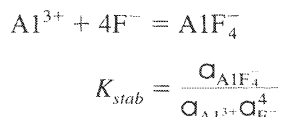
$G_{\text{ex}}$  is the excess Gibbs free energy per kilogram of water (the difference between the actual free energy and the free energy the system would have if activities equaled concentrations),  $(D-H)$  represents a Debye-Hückel term similar to Eq. (2-11),  $\lambda_{ij}(I)$  represents binary interactions (interactions between pairs of ions), and  $\mu_{ijk}$  represents ternary interactions, which are significant only at very high ionic strengths. The activity coefficient can be readily calculated from the relationship:

$$RT \ln \gamma_{\pm i} = \frac{\partial G_{\text{ex}}}{\partial n_i}$$

Pitzer's model provides a functional relationship between the values of  $\lambda$  and  $I$  and a means of calculating the interaction coefficients from measurements on solutions of simple salts. It does not include ion pairs as species in solution. The interactions represented by ion pair formation in the ion-pair model are described by the interaction coefficients in the Pitzer model. The model has been used successfully to predict the solubilities of highly soluble evaporite minerals in solutions as concentrated as 20 m (Eugster et al., 1980; Harvie and Weare, 1980; Harvie et al., 1982; Monnin and Schott, 1984; Weare, 1987).

### Complex Formation

For the purposes of this book, I define a complex as a dissolved species formed from two or more simpler species, each of which can exist in aqueous solution. For example,  $\text{Al}^{3+}$  forms complexes with fluoride ions ( $\text{AlF}^{2+}$ ,  $\text{AlF}_2^+$ ,  $\text{AlF}_4^-$ ), and numerous organic species. The strength of a complex is usually represented by its stability constant, for example:

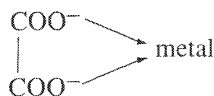


The larger the stability constant, the more stable the complex is. It is convenient to divide complexes into ion pairs, discussed earlier in this chapter, and *coordination compounds*, in which the complex has a well-defined structure and generally a large stability constant. The terms *outer-sphere complex* and *inner-sphere complex* are also used for ion pairs and coordination compounds respectively. The idea of an outer-sphere complex is that the ions involved remain fully hydrated, so they remain separated by their hydration shells. In an inner-sphere complex, the ions are not separated by water molecules and interact directly with each other.

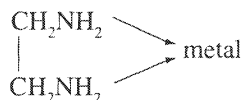
One effect of complex formation is to modify relationships between activity and concentration as illustrated in Example 7. For example, the Debye-Hückel theory gives a relationship between  $\alpha_{\text{Al}^{3+}}$  and  $m_{\text{Al}^{3+}}$ . If complexes of aluminum are present, however,  $m_{\text{Al}^{3+}}$  is less than the total concentration of dissolved aluminum, which represents the sum of free  $\text{Al}^{3+}$  and all Al complexes present in solution.

In the coordination compound type of complex, a *central atom* (usually a metal ion) is surrounded by several (most commonly six) *ligands*. The ligands are usually anions or neutral species and have a definite geometrical arrangement around the central atom. In a solution without other ligands present, most transition metals are in the form of aquo complexes [e.g.,  $\text{Fe}(\text{H}_2\text{O})_6^{3+}$  where  $\text{Fe}^{3+}$  is the central atom and the six water molecules are ligands], and complex formation can be regarded as displacement of some or all of the coordinated water molecules by other ligands. As pH rises, water molecules coordinating metal ions deprotonate, giving rise to species such as  $\text{Fe}(\text{H}_2\text{O})_5(\text{OH})^{2+}$ ,  $\text{Fe}(\text{H}_2\text{O})_4(\text{OH})_2^+$ , etc. This process is referred to as *hydrolysis*. Hydrolyzed cations are generally written and treated algebraically as simple hydroxide complexes, e.g.,  $\text{Fe}(\text{OH})^{2+}$ ,  $\text{Fe}(\text{OH})_2^+$ .

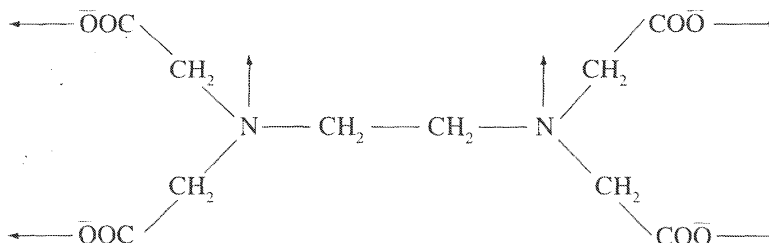
If a ligand has only one site by which it can bond to a metal (e.g.,  $\text{NH}_3$ ,  $\text{Cl}^-$ ,  $\text{F}^-$ ,  $\text{H}_2\text{O}$ ,  $\text{OH}^-$ ), it is called a *unidentate* (one-toothed) ligand. Some molecules have more than one site by which they can bond to a metal ion and are called *multidentate* ligands. For example, the oxalate ion,



can coordinate to a metal ion through two of its oxygen atoms and be a bidentate ligand. Ethylenediamine,

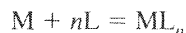


can coordinate through two nitrogen atoms, and the anion of ethylenediaminetetraacetic acid (EDTA),



can coordinate to a single metal ion through four oxygen and two nitrogen atoms, making it a hexadentate ligand. Much of the dissolved organic matter in natural waters, the humic and fulvic acids (Chapter 6), functions as multidentate ligands for transition metals. Complexes involving multidentate ligands are called *chelates*. In general, chelates are much more stable than are complexes involving unidentate ligands, and the more complexing groups there are on a multidentate ligand, the more stable the complex.

Chelates are very important in the chemistry of transition metals and some polyvalent cations (e.g.,  $\text{Al}^{3+}$ ) in natural waters. Consider the formation of a complex between a metal ion  $M$  and a ligand  $L$ :



$$K_{stab} = \frac{\alpha_{ML_n}}{\alpha_M \alpha_L^n}$$

Because of the exponent  $n$ , when the concentration of the ligand is low, only complexes containing one or two ligand groups are likely to be present in significant concentrations. Chelating ligands contain several complexing groups in one molecule, so  $n$  is automatically small. The combination of a high value of  $K_{stab}$  with a low value of  $n$  makes chelate-type complexes important even when the concentrations of both metal and chelating agent are very low.

The ionic form of a chelating agent

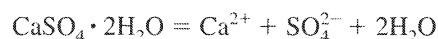


may have a major influence on the stability constant of a chelate complex. For this reason, the stabilities of many such complexes are strongly pH dependent.

All outer-sphere complexes are kinetically labile; that is, they form and decompose rapidly in response to changes in solution composition. Some inner-sphere complexes are labile and some are inert.

### Apparent Equilibrium Constants

A different approach to the problem of determining activity-concentration relationships is through the use of apparent equilibrium constants. Consider a solution in equilibrium with gypsum:



$$\begin{aligned}
 K_{sp} &= a_{\text{Ca}^{2+}} a_{\text{SO}_4^{2-}} \\
 &= m_{\text{Ca}T} m_{\text{SO}_4T} \gamma_{\text{Ca}^{2+}}^* \gamma_{\text{SO}_4^{2-}}^*
 \end{aligned}$$

The subscript  $T$  indicates total analytical concentration, including complexed forms.  $\gamma_{\text{Ca}^{2+}}^*$  and  $\gamma_{\text{SO}_4^{2-}}^*$  are *stoichiometric activity coefficients*, which relate the activities of single ions to the total analytical concentrations of the ions. Stoichiometric activity coefficients differ from the ionic activity coefficients discussed previously in that stoichiometric activity coefficients include the effect of complexing, whereas ionic activity coefficients do not.

The apparent equilibrium constant (or apparent solubility product)  $K'_{sp}$ , is given by

$$K'_{sp} = m_{\text{Ca}T} m_{\text{SO}_4T} = \frac{K_{sp}}{\gamma_{\text{Ca}^{2+}}^* \gamma_{\text{SO}_4^{2-}}^*}$$

The apparent equilibrium constant is thus analogous to the thermodynamic equilibrium constant, but total analytical concentrations are used rather than activities. Activity-concentration corrections and the effects of complexing are included in the apparent constant. The apparent constant cannot be derived from standard thermodynamic data, but can often be measured experimentally (see, for example, the discussion of the alkalinity titration in Chapter 3). The approach is used most in marine chemistry because in seawater the concentrations of the major ions (which largely determine activity coefficients) are almost constant. Since activity coefficients are essentially constant, the apparent constants, once measured, can be used reliably throughout the oceanic system (see, e.g., Edmond and Gieskes, 1970). The compositions of most other natural waters are so variable that an apparent constant measured for one water is useful for calculations involving that particular water only, so the approach is not widely used.

## COMPUTER CODES

Most of the calculations discussed in this chapter can be performed by widely available computer codes. One of the first such codes was WATEQ (Truesdell and Jones, 1974), which is now available for use on a PC (both IBM-compatible and Macintosh) as the version WATEQ4F (Ball and Nordstrom, 1991). Another one that is widely used in environmental studies is MINTEQ, with the current PC version MINTEQA2. We shall use WATEQ4F as an example here. WATEQ4F takes as an input a chemical analysis of a water, including temperature and pH, and performs the following types of calculation:

1. It corrects all equilibrium constants to the temperature of the sample using either the Van't Hoff equation or an empirical polynomial.
2. It calculates *speciation*, the distribution of species for each element, by solving a matrix of equations consisting of a stability constant for each complex and a conservation of mass equation for each element. Thus, for example, the total calcium concentration is distributed among the species  $\text{Ca}^{2+}$ ,  $\text{CaSO}_4^0$ ,  $\text{CaHCO}_3^+$ , and so on.
3. It calculates activity coefficients by either the extended Debye-Hückel equation or the Davies equation. This calculation requires iteration with the speciation calculation because speciation affects ionic strength, which affects activity coefficients, as illustrated in Example 7.



4. It calculates the state of saturation of the solution with respect to all the solids in its database that contain the elements in the input analysis.
5. It performs a variety of calculations related to oxidation-reduction processes. We shall defer discussion of redox processes until Chapter 7.

**Example 8**

A water has the following chemical analysis:

Na <sup>+</sup>	120 ppm	SO <sub>4</sub> <sup>2-</sup>	1115 ppm
K <sup>+</sup>	15 ppm	Cl <sup>-</sup>	15 ppm
Ca <sup>2+</sup>	380 ppm	HCO <sub>3</sub> <sup>-</sup>	150 ppm
Mg <sup>2+</sup>	22 ppm	SiO <sub>2</sub>	21 ppm
pH	7.4	Temp.	15°C

Use WATEQ4F to calculate the state of saturation of this solution with respect to gypsum.

Selected parts of the output from the WATEQ4F run are shown in Table 2-2. The answer to the question is underlined

$$\log IAP/KT = -0.236$$

which means that the solution is undersaturated by 0.236 log units ( $KT$  represents the equilibrium constant corrected to the temperature of the sample). The corresponding saturation ratio is

$$SR = (10^{-0.236})^{1/2} = 0.762$$

The printout also shows that 70% of the calcium and 73% of the sulfate are in the form of free ions, the remainder forming ion pairs. The activity coefficient for Ca<sup>2+</sup> is 0.5198, and for SO<sub>4</sub><sup>2-</sup> is 0.5111. The solution is slightly supersaturated with respect to calcite, aragonite, and various polymorphs of silica, but undersaturated with respect to all other solid phases in the database. It would have been possible to calculate all this by hand, but when more than three or four elements are to be considered, a computer becomes almost essential.

Several other codes, for example MINTEQA2 (Allison et al., 1991) and PHREEQC (Parkhurst, 1995) perform the same calculations as WATEQ. However they also perform other calculations as well, which makes them somewhat more complex to use. We shall discuss both codes in subsequent chapters. These codes all use the single-ion activity coefficient/ion pair solution model, so they are not suitable for brines. A code PHRQPTZ (Plummer and Parkhurst, 1990) is available for calculations involving brines. It is limited to calculations involving the major ions (Na, K, Ca, Mg, Cl, SO<sub>4</sub>, carbonate species) at present because very few data are available for interaction coefficients involving other ions.

**REVIEW QUESTIONS**

Use data from Appendix II or tables in the text. Assume a temperature of 25°C, assume activities equal concentrations, and ignore complexing unless directed otherwise.

1. Which is more stable at 25°C, gypsum or anhydrite plus water?
2. What is the solubility product of gibbsite (Al(OH)<sub>3</sub>)?

TABLE 2-2 Selected Output from WATEQ4F for Example 8

1 Example 7

TEMP = 15.000000  
 PH = 7.400000  
 EH (0) = 9.900000  
 FLG = PPM  
 DENS = 1.000000  
 Index No Input Concentration

Ca : 0 : 380.00000000  
 Mg : 1 : 22.00000000  
 Na : 2 : 120.00000000  
 K : 3 : 15.00000000  
 Cl : 4 : 15.00000000  
 SO4 : 5 : 1115.00000000  
 HCO3 : 6 : 150.00000000  
 Fe total : 16 : .00000000  
 H2S aq : 13 : .00000000  
 CO3 : 17 : .00000000  
 SiO2 tot : 34 : 21.00000000  
 NH4 : 38 : .00000000  
 B tot : 86 : .00000000  
 PO4 : 44 : .00000000  
 Al : 50 : .00000000  
 F : 61 : .00000000  
 NO3 : 84 : .00000000

Anal EPMCAT = 26.4238 Anal EPMAN = 26.1439 Percent difference in input cation/anion balance = 1.0651  
 Calc EPMCAT = 20.2254 Calc EPMAN = 19.9456 Percent difference in calc cation/anion balance = 1.3933  
 Total Ionic Strength (T.I.S.) from input data = .04832  
 Effective Ionic Strength (E.I.S.) from speciation = .03591

T pH TDS ppm Effective  
 15.00 7.400 1838.0 .03592  
 Ionic Str pO2 Atm ppm O2 Atm pCO2 Atm ppm CO2 Atm log pCO2 CO2 Tot Ncrb Alk aH2O  
 .03592 0.00E-01 0.00E-01 4.58E-03 2.01E+02 2.65E-03 1.20E-06 .9995

Sato

TABLE 2-2 Continued

I	Species	Anal ppm	Calc ppm	Anal Molal	Calc Molal	% of Total	Activity	Act Coeff	-Log Act
0	Ca	2 380.000	267.325	9.498E-03	6.682E-03	70.35	3.473E-03	.5198	2.459
31	CaSO4 aq	0	369.720		2.721E-03	28.64	2.743E-03	1.0083	2.562
4	Cl	-1 15.000	15.000	4.239E-04	4.239E-04	100.00	3.546E-04	.8365	3.450
6	HCO3	-1 150.000	142.211	2.463E-03	2.335E-03	88.00	1.982E-03	.8488	2.703
85	H2CO3 aq	0	12.693		2.050E-04	7.73	2.069E-04	1.0093	3.684
63	H	1	.000046		4.581E-08	.00	3.981E-08	.8690	7.400
3	K	1 15.000	14.628	3.843E-04	3.748E-04	97.52	3.135E-04	.8365	3.504
45	KSO4	-1	1.284		9.520E-06	2.48	8.020E-06	.8425	5.096
1	Mg	2 22.000	15.427	9.066E-04	6.357E-04	70.12	3.366E-04	.5294	3.473
22	MgSO4 aq	0	31.402		2.614E-04	28.83	2.635E-04	1.0083	3.579
2	Na	1 120.000	117.475	5.229E-03	5.119E-03	97.90	4.323E-03	.8444	2.364
43	NaSO4	-1	12.479		1.050E-04	2.01	8.847E-05	.8425	4.053
26	OH	-1	.002282		1.344E-07	.00	1.133E-07	.8425	6.946
34	SiO2 tot	0 21.000	33.490	3.501E-04	3.491E-04	99.70	3.520E-04	1.0083	3.453
23	H4SiO4aq	0	818.055	1.163E-02	8.532E-03	73.37	4.360E-03	.5110	2.360
5	SO4	-2 1115.000							
1	Example 7								

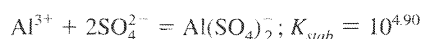
Phase	Log IAP/KT	Log IAP	Sigma (A)	Log KT	Sigma (T)
17 Anhydrite	-.484	-4.820		-4.335	
21 Aragonite	.089	-8.190		-8.279	.020
19 Brucite	-6.203	11.327		17.529	
12 Calcite	.240	-8.190		-8.430	.020
97 Chalcedony	.218	-3.453		-3.671	
20 Chrysotile	-6.407	27.074		33.481	
99 Cristobalite	.274	-3.453		-3.727	
11 Dolomite (d)	-1.137	-17.395		-16.258	
401 Dolomite (c)	-.545	-17.395		-16.850	
340 Epsomite	-3.623	-5.835		-2.212	
18 Gypsum	-.236	-4.820		-4.585	
64 Halite	-7.373	-5.814		1.559	
10 Magnesite	-1.332	-9.204		-7.872	
101 Quartz	.680	-3.453		-4.133	
153 Sepiolite (d)	-6.366	12.294		18.660	
36 Sepiolite (c)	-3.738	12.294		16.032	
395 SiO2 (a)	-.656	-3.453		-2.797	

- Calculate the concentration of dissolved  $\text{Al}^{3+}$  in equilibrium with gibbsite at pH 4 and  $5^\circ\text{C}$  using the data from (a) Appendix II and (b) Appendix III. Does the solubility of gibbsite increase or decrease with decreasing temperature? How do the results from the two data sets compare?
- $\text{Al}^{3+}$  forms a complex  $\text{AlSO}_4^+$  in the presence of sulfate.



How many ppm of Al (total) would be in equilibrium with gibbsite at pH 4 and  $25^\circ\text{C}$  in the presence of  $10^{-3}$  m  $\text{SO}_4^{2-}$ ? (Consider only this one complex and assume activities equal concentrations.)

- $\text{Al}^{3+}$  also forms a complex  $\text{Al}(\text{SO}_4)_2^-$



How much does the presence of this complex increase the dissolved Al concentration in equilibrium with gibbsite at pH 4 in the presence of  $10^{-3}$  m  $\text{SO}_4^{2-}$ ? How does the existence of each of the aluminum sulfate complexes affect the Al concentration in equilibrium with gibbsite at pH 4 and  $10^{-1}$  m  $\text{SO}_4^{2-}$ ?

- What is the solubility of  $\text{BaSO}_4$  in water? How does the result compare, depending on whether you use data from Appendix II or Appendix III? How much difference does it make whether it is assumed that activities equal concentrations or activities are calculated from the Debye-Hückel equation?
- A water has the following chemical analysis:

$\text{Na}^+$	120 ppm	$\text{SO}_4^{2-}$	1115 ppm
$\text{K}^+$	15 ppm	$\text{Cl}^-$	15 ppm
$\text{Ca}^{2+}$	380 ppm	$\text{HCO}_3^-$	150 ppm
$\text{Mg}^{2+}$	22 ppm	$\text{SiO}_2$	21 ppm
$\text{Sr}^{2+}$	0.8 ppm	pH	7.4
Temp.	$25^\circ\text{C}$		

- What are these concentrations in mmol/kg?
  - Do the charges balance (total positive charges = total negative charges)?
  - What are the activity coefficients for  $\text{Sr}^{2+}$  and  $\text{SO}_4^{2-}$  in the water?
  - By how much is the water supersaturated or undersaturated with respect to  $\text{SrSO}_4$ ?
- Perform the calculations in Problem 7 using WATEQ4F or MINTEQA2 and compare the computed results with your hand-calculated results. Is the state of saturation with respect to  $\text{SrSO}_4$  the same? Account for any discrepancies between the two results.

## SUGGESTED READING

- GARRELS, R. M., and C. L. CHRIST. (1965). *Solutions, Minerals, and Equilibria*. New York: Harper & Row. A classic in the field. Clear and understandable introduction to thermodynamics applied to low-temperature geochemistry.
- MELCHIOR, D. C., and R. L. BASSETT (Eds.) (1990). *Chemical Modeling of Aqueous Systems II*. American Chemical Society Symposium Series 416. Washington, DC: American Chemical Society. A series of papers covering various aspects of chemical modeling applied to natural systems.
- MOREL, F., and J. G. HERING. (1993). *Principles and Applications of Aquatic Chemistry*. New York: Wiley.
- NORDSTROM, D. K., and J. L. MUNOZ. (1994). *Geochemical Thermodynamics* (2nd ed.). Boston: Blackwell Scientific Publications.
- STUMM, W., and J. J. MORGAN. (1996). *Aquatic Chemistry* (3rd ed.). New York: Wiley-Interscience. This book gives extensive treatment of solution chemistry applied to natural water systems.

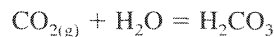
# 3

## The Carbonate System and pH Control

### CARBONIC ACID SYSTEM

The pH of most natural waters is controlled by reactions involving the carbonate system. The carbonate system is also used here as an example of acid-base systems in general; the relationships developed for carbonate equilibria can be used with little modification for equilibria involving such species as phosphate, sulfide, and silicic acid.

When  $\text{CO}_2$  gas is brought into contact with water, the  $\text{CO}_2$  will dissolve until equilibrium is reached. At equilibrium, the concentration (or, more strictly, activity) of dissolved carbon dioxide will be proportional to the pressure (or, more strictly, fugacity) of  $\text{CO}_2$  in the gas phase. At earth-surface conditions, the difference between partial pressure and fugacity can be ignored. The usual convention is to refer to all dissolved carbon dioxide as  $\text{H}_2\text{CO}_3$  (carbonic acid), and thus the dissolution of carbon dioxide in water can be represented by the equation:



for which an equilibrium constant can be written

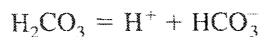
$$K_{\text{CO}_2} = \frac{\alpha_{\text{H}_2\text{CO}_3}}{P_{\text{CO}_2} \alpha_{\text{H}_2\text{O}}} \quad (3-1)$$

For dilute solutions,  $\alpha_{\text{H}_2\text{O}}$ , the activity of water, is very close to 1 (in seawater, it is 0.98, for example); deviations from 1 will be ignored here. In fact, most of the dissolved carbon dioxide is in the form of solvated  $\text{CO}_2$  rather than  $\text{H}_2\text{CO}_3$ , but, provided that equilibrium is established, the exact chemical form of dissolved carbon dioxide does not affect the equilibrium relationships presented here. It is convenient to adopt the convention that dissolved carbon dioxide is all  $\text{H}_2\text{CO}_3$  and to use equilibrium constants consistent with this convention. Eq. (3-1) thus simplifies to:

$$\alpha_{\text{H}_2\text{CO}_3} = K_{\text{CO}_2} P_{\text{CO}_2} \quad (3-2)$$

For every  $P_{\text{CO}_2}$ , there is a corresponding  $\alpha_{\text{H}_2\text{CO}_3}$ , and for every  $\alpha_{\text{H}_2\text{CO}_3}$ , there is a corresponding  $P_{\text{CO}_2}$ . In the literature, it is quite common to report  $\alpha_{\text{H}_2\text{CO}_3}$  as the corresponding  $P_{\text{CO}_2}$ , even when no gas phase is present.  $K_{\text{CO}_2}$  is often referred to as a *Henry's law constant*; Henry's law states that the concentration of a dissolved gas is proportional to its pressure in the gas phase.

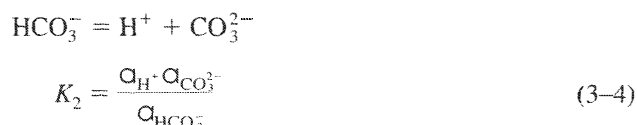
$\text{H}_2\text{CO}_3$  is an acid, so it will tend to dissociate into hydrogen and bicarbonate ions:



An equilibrium constant can be written for this reaction:

$$K_1 = \frac{\alpha_{\text{H}^+} \alpha_{\text{HCO}_3^-}}{\alpha_{\text{H}_2\text{CO}_3}} \quad (3-3)$$

Bicarbonate ion itself dissociates also:



Numerical values for  $K_{\text{CO}_2}$ ,  $K_1$ , and  $K_2$  are listed in Table 3-1.

From Eqs. (3-3) and (3-4), the ratios  $\alpha_{\text{H}_2\text{CO}_3}/\alpha_{\text{HCO}_3^-}$  and  $\alpha_{\text{HCO}_3^-}/\alpha_{\text{CO}_3^{2-}}$  depend on the pH of the solution. When we talk about pH as an independent variable, we are no longer talking about the system  $\text{CO}_2$ - $\text{H}_2\text{O}$ . To obtain a pH above 7, for example, it is necessary to introduce some cation other than  $\text{H}^+$ . If we consider a solution containing a total activity of dissolved carbonate species of  $10^{-2}$  (which implies that the solution cannot exchange  $\text{CO}_2$  with a gas phase), we can calculate the activity of each individual species as a function of pH:

$$10^{-2} = \alpha_{\text{H}_2\text{CO}_3} + \alpha_{\text{HCO}_3^-} + \alpha_{\text{CO}_3^{2-}}$$

From Eq. (3-3) and Table 3-1:

$$\frac{\alpha_{\text{H}_2\text{CO}_3}}{\alpha_{\text{HCO}_3^-}} = \frac{\alpha_{\text{H}^+}}{K_1} = 10^{+6.35} \alpha_{\text{H}^+} \text{ at } 25^\circ\text{C}$$

Ignoring  $\text{CO}_3^{2-}$  for the moment and rounding the value of  $K_1$  to  $10^{-6.4}$ , at a pH of 6.4 the activity of  $\text{H}_2\text{CO}_3$  will equal that of  $\text{HCO}_3^-$ .

**TABLE 3-1** Equilibrium Constants<sup>a</sup> for the Carbonate System  
( $pK = -\log_{10} K$ ) [after Plummer and Busenberg, 1982]

$T(^{\circ}\text{C})$	$pK_{\text{CO}_2}$	$pK_1$	$pK_2$	$pK_{\text{cal}}$	$pK_{\text{arag}}$	$pK_{\text{CaHCO}_3^{\ominus}}$ <sup>b</sup>	$pK_{\text{CaCO}_3^{\ominus}}$	$pK_w$
0	1.11	6.58	10.63	8.38	8.22	-0.82	-31.3	14.94
5	1.19	6.52	10.55	8.39	8.24	-0.90	-3.13	14.73
10	1.27	6.46	10.49	8.41	8.26	-0.97	-3.13	14.53
15	1.34	6.42	10.43	8.43	8.28	-1.02	-3.15	14.35
20	1.41	6.38	10.38	8.45	8.31	-1.07	-3.18	14.17
25	1.47	6.35	10.33	8.48	8.34	-1.11	-3.22	14.00
30	1.52	6.33	10.29	8.51	8.37	-1.14	-3.27	13.83
45	1.67	6.29	10.20	8.62	8.49	-1.19	-3.45	13.40
60	1.78	6.29	10.14	8.76	8.64	-1.23	-3.65	13.02

<sup>a</sup>based on the infinite dilution standard state

<sup>b</sup> $K_{\text{CaHCO}_3^{\ominus}} = \alpha_{\text{CaHCO}_3^{\ominus}} / (\alpha_{\text{Ca}^{2+}} \alpha_{\text{HCO}_3^-})$

<sup>c</sup> $K_{\text{CaCO}_3^{\ominus}} = \alpha_{\text{CaCO}_3^{\ominus}} / (\alpha_{\text{Ca}^{2+}} \alpha_{\text{CO}_3^{2-}})$

$$\frac{a_{\text{H}_2\text{CO}_3}}{a_{\text{HCO}_3^-}} = 10^{+6.4} \cdot 10^{-6.4} = 1$$

$$a_{\text{H}_2\text{CO}_3} + a_{\text{HCO}_3^-} = 10^{-2}$$

$$a_{\text{H}_2\text{CO}_3} = a_{\text{HCO}_3^-} = 0.5 \times 10^{-2} = 10^{-2.3}$$

Similarly, at pH 5.4,

$$\frac{a_{\text{H}_2\text{CO}_3}}{a_{\text{HCO}_3^-}} = 10^{+6.4} \cdot 10^{-5.4} = 10^{+1}$$

$$a_{\text{H}_2\text{CO}_3} + a_{\text{HCO}_3^-} = 10^{-2}$$

Solving these two equations,

$$a_{\text{H}_2\text{CO}_3} = 0.91 \times 10^{-2} = 10^{-2.04}$$

$$a_{\text{HCO}_3^-} = 0.09 \times 10^{-2} = 10^{-3.04}$$

The same procedure at pH 4.4 gives

$$a_{\text{H}_2\text{CO}_3} = 0.99 \times 10^{-2} = 10^{-2}$$

$$a_{\text{HCO}_3^-} = 0.01 \times 10^{-2} = 10^{-4}$$

At pH values above  $\text{p}K_1$  (the notation  $\text{p}K$  is used to denote  $-\log_{10} K$ , exactly analogous to the notation for pH), the ratios are reversed. At pH 7.4,

$$a_{\text{H}_2\text{CO}_3} = 0.09 \times 10^{-2} = 10^{-3.04}$$

$$a_{\text{HCO}_3^-} = 0.91 \times 10^{-2} = 10^{-2.04}$$

and at pH 8.4,

$$a_{\text{H}_2\text{CO}_3} = 0.01 \times 10^{-2} = 10^{-4}$$

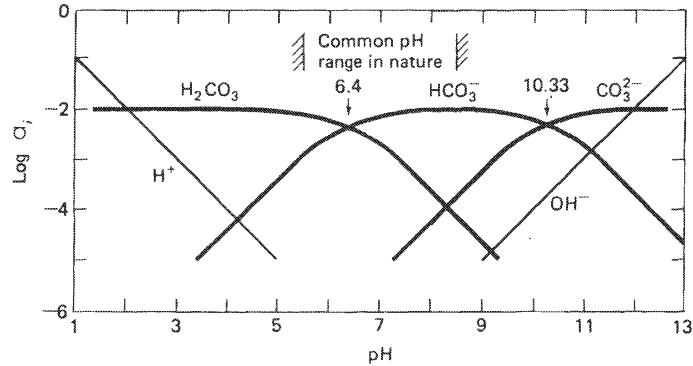
$$a_{\text{HCO}_3^-} = 0.99 \times 10^{-2} = 10^{-2}$$

Thus it is only at pH values close to 6.4 (the pH corresponding to  $\text{p}K_1$ ) that both species are present at comparable activities and hence comparable concentrations. Below pH 6, essentially all of the dissolved carbonate species are present in the form of  $\text{H}_2\text{CO}_3$ , and above pH 7 essentially all are in the form of  $\text{HCO}_3^-$ .

For the  $\text{HCO}_3^-/\text{CO}_3^{2-}$  pair, Eq. (3-4) gives:

$$\frac{a_{\text{HCO}_3^-}}{a_{\text{CO}_3^{2-}}} = \frac{a_{\text{H}^+}}{10^{-10.33}}$$

This equation is exactly analogous to the one for the  $\text{H}_2\text{CO}_3/\text{HCO}_3^-$  pair except that the crossover point is at the  $\text{p}K_2$  value for carbonic acid (pH 10.33) instead of the  $\text{p}K_1$  value. Above pH 10.33, the activity of  $\text{HCO}_3^-$  rapidly becomes small, and below pH 10.33 the activity of  $\text{CO}_3^{2-}$  becomes small. These relationships are displayed in Fig. 3-1. This type of plot is sometimes called a *Bjerrum plot*. Since the crossover points are far apart, we were quite justified in ignoring  $\text{CO}_3^{2-}$  when discussing the  $\text{H}_2\text{CO}_3/\text{HCO}_3^-$  pair and in ignoring  $\text{H}_2\text{CO}_3$  when discussing the  $\text{HCO}_3^-/\text{CO}_3^{2-}$  pair.



**FIGURE 3-1** Activities of different species in the carbonate system as a function of pH, assuming  $\Sigma\text{CO}_2 = 10^{-2}$ , temperature = 25°C. Activities of  $\text{H}^+$  and  $\text{OH}^-$  are defined by pH. This diagram is an example of a Bjerrum plot.

An important conclusion from Fig. 3-1 is that in most natural waters the  $\text{CO}_3^{2-}$  concentration is small compared to the  $\text{HCO}_3^-$  concentration. It is only in unusual, generally saline, waters that pH values above 9 are encountered.

#### Example 1

What is the pH of pure water in equilibrium with the atmosphere ( $P_{\text{CO}_2} = 10^{-3.5}$  atm) at 25°C? Assume activities equal concentrations.

The relevant equations are:

$$a_{\text{H}_2\text{CO}_3} = K_{\text{CO}_2} P_{\text{CO}_2} \quad (\text{Eq. 3-2})$$

$$= 10^{-1.47} \cdot 10^{-3.5} = 10^{-4.97}$$

$$K_1 = \frac{a_{\text{H}^+} a_{\text{HCO}_3^-}}{a_{\text{H}_2\text{CO}_3}} \quad (\text{Eq. 3-3})$$

$$a_{\text{H}^+} a_{\text{HCO}_3^-} = K_1 a_{\text{H}_2\text{CO}_3} \quad (3-5)$$

$$= 10^{-6.35} \cdot 10^{-4.97} = 10^{-11.32}$$

The final constraint is *charge balance*: solutions must be electrically neutral, which means that the total concentration of cations must equal the total concentration of anions. In the system  $\text{CO}_2$ - $\text{H}_2\text{O}$ , the only ions present are  $\text{H}^+$ ,  $\text{OH}^-$ ,  $\text{HCO}_3^-$ , and  $\text{CO}_3^{2-}$ . The charge balance equation is thus:

$$m_{\text{H}^+} = m_{\text{HCO}_3^-} + 2m_{\text{CO}_3^{2-}} + m_{\text{OH}^-}$$

The coefficient 2 before  $m_{\text{CO}_3^{2-}}$  results from the fact that each carbonate ion contributes 2 negative charges.

We know the solution will have to have a pH less than 7 (mathematically, if  $m_{\text{HCO}_3^-}$  or  $m_{\text{CO}_3^{2-}}$  is finite,  $m_{\text{H}^+}$  must be greater than  $m_{\text{OH}^-}$ ). Thus, from Fig. 3-1, the charge balance equation simplifies to:

$$m_{\text{H}^+} = m_{\text{HCO}_3^-}$$



Assuming  $\alpha = m$ , Eq. (3-5) above becomes:

$$\begin{aligned}\alpha_{\text{H}^+} \alpha_{\text{HCO}_3^-} &= \alpha_{\text{H}^+}^2 = 10^{-11.32} \\ \alpha_{\text{H}^+} &= 10^{-5.66}\end{aligned}$$

The pH would thus be 5.66. At this pH,  $m_{\text{CO}_3^{2-}} = 10^{-10.33}$  and  $m_{\text{OH}^-} = 10^{-8.34}$ , which are negligible compared to  $10^{-5.66}$ , confirming that it was reasonable to ignore them in the charge balance equation. We would thus expect the pH of rain to be around 5.66. In reality the pH of rain is quite variable, influenced by other solutes (particularly acids) derived from the atmosphere (see Chapter 1).

## ALKALINITY AND TITRATION CURVES

We mentioned in the preceding section that solutions with pH values greater than 7 must contain cations other than  $\text{H}^+$ . This can be seen from considerations of charge balance. It is a fundamental principle of solution chemistry that solutions are electrically neutral, that is, that the total number of positive charges carried by cations must equal the total number of negative charges carried by anions. The formula is:

$$\sum m_i z_i = 0$$

where  $m$  is the concentration and  $z$  the charge of the  $i$ th ion.

For the system  $\text{H}_2\text{O}-\text{CO}_2$ , the charge balance equation is

$$m_{\text{H}^+} = m_{\text{HCO}_3^-} + 2m_{\text{CO}_3^{2-}} + m_{\text{OH}^-}$$

At pH 7,  $m_{\text{H}^+} = m_{\text{OH}^-}$  (the dissociation constant of water,  $K_w$ , is  $10^{-14}$  at  $25^\circ\text{C}$ ). As mentioned in Example 1 above, if  $m_{\text{HCO}_3^-}$  or  $m_{\text{CO}_3^{2-}}$  has any finite value,  $m_{\text{H}^+}$  must be correspondingly greater than  $m_{\text{OH}^-}$ , and the solution will have a pH lower than 7. If we introduce  $\text{NaOH}$  or  $\text{NaHCO}_3$  into the system, the charge balance equation becomes

$$m_{\text{H}^+} + m_{\text{Na}^+} = m_{\text{HCO}_3^-} + 2m_{\text{CO}_3^{2-}} + m_{\text{OH}^-}$$

There are no immediate constraints on the value of  $m_{\text{H}^+}$  and hence pH. For solutions that are approximately neutral,  $m_{\text{H}^+}$ ,  $m_{\text{OH}^-}$ , and  $m_{\text{CO}_3^{2-}}$  are generally negligible compared to  $m_{\text{Na}^+}$  and  $m_{\text{HCO}_3^-}$ . In this case the charge balance equation simplifies to

$$m_{\text{Na}^+} = m_{\text{HCO}_3^-}$$

Eq. (3-2) and (3-3) can be combined to give

$$\alpha_{\text{H}^+} \alpha_{\text{HCO}_3^-} = K_1 K_{\text{CO}_2} P_{\text{CO}_2}$$

Thus, at constant  $P_{\text{CO}_2}$  hydrogen ion activity is inversely related to bicarbonate concentration. In waters in which bicarbonate is the dominant anion (which are common in nature), the total cation concentration (weighted according to charge) will approximately equal the bicarbonate concentration, and hence pH and salinity in bicarbonate-rich waters are inversely related.

The charge balance equation can be extended to cover all dissolved species:

$$\begin{aligned}m_{\text{H}^+} + m_{\text{Na}^+} + m_{\text{K}^+} + 2m_{\text{Ca}^{2+}} + 2m_{\text{Mg}^{2+}} \dots \\ = m_{\text{Cl}^-} + 2m_{\text{SO}_4^{2-}} + m_{\text{HCO}_3^-} + 2m_{\text{CO}_3^{2-}} + m_{\text{OH}^-} \\ + m_{\text{B}(\text{OH})_4^-} + m_{\text{H}_2\text{SiO}_4} + m_{\text{HS}^-} + m_{\text{organic anions}} + \dots\end{aligned}\quad (3-6a)$$

Ions such as  $\text{Na}^+$ ,  $\text{K}^+$ ,  $\text{Ca}^{2+}$ ,  $\text{Mg}^{2+}$ ,  $\text{Cl}^-$ ,  $\text{SO}_4^{2-}$ , and  $\text{NO}_3^-$  can be regarded as *conservative* in the sense that their concentrations are unaffected by changes in pH, pressure, or temperature (within the ranges normally encountered near the earth's surface and assuming no precipitation or dissolution of solid phases or biological transformations). Ion pair formation (Chapter 2) will not affect the charge balance equation provided that total analytical concentrations of each species are used. When solutions are mixed, the concentration of a conservative species in the mixture is simply the weighted average of its concentrations in the original solutions.

Eq. (3-6a) can be written:

$$\begin{aligned} & \sum \text{conservative cation (in equivalents)} - \sum \text{conservative anions (in equivalents)} \\ & = m_{\text{HCO}_3^-} + 2m_{\text{CO}_3^{2-}} + m_{\text{B(OH)}_4^-} + m_{\text{H}_4\text{SiO}_4} + m_{\text{HS}^-} + m_{\text{organic anions}} + m_{\text{OH}^-} - m_{\text{H}^+} \quad (3-6b) \end{aligned}$$

The expression on the right side of Eq. (3-6b) is the *total alkalinity*, which is formally defined as the equivalent sum of the bases that are titratable with strong acid (Stumm and Morgan, 1996). If the pH of the solution is progressively lowered by addition of a strong acid (HCl, for example), all the anions on the right will be converted to uncharged species [ $\text{H}_2\text{CO}_3$ ,  $\text{B(OH)}_3$ ,  $\text{H}_4\text{SiO}_4$ ,  $\text{H}_2\text{S}$ , organic acids,  $\text{H}_2\text{O}$ ]. The amount of acid required to complete the conversion can easily be measured (see below), so that total alkalinity can easily be measured. Also, since the terms on the left side of Eq. (3-6b) are not affected by changes in  $P$  or  $T$ , total alkalinity must also be unaffected by changes in  $P$  and  $T$ . Total alkalinity is thus a conservative quantity. Note that the individual terms on the right side of Eq. (3-6b) are not conservative. A change in  $T$ , for example, will cause a change in  $K_2$ , which will cause a change in the ratio  $m_{\text{HCO}_3^-}/m_{\text{CO}_3^{2-}}$ .

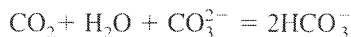
In most natural waters, borate, ionized silicic acid, bisulfide, organic anions, hydrogen ion, and hydroxyl ion are present in concentrations that are very small compared to bicarbonate and carbonate. Under these circumstances,

$$\text{Alkalinity} = m_{\text{HCO}_3^-} + 2m_{\text{CO}_3^{2-}}$$

The expression  $(m_{\text{HCO}_3^-} + 2m_{\text{CO}_3^{2-}})$  is the *carbonate alkalinity*. In most natural waters,

$$\text{Carbonate alkalinity} \approx \text{Total alkalinity}$$

and hence carbonate alkalinity is generally conservative. Alkalinity is independent of  $P_{\text{CO}_2}$ , because neither the  $P_{\text{CO}_2}$  nor the uncharged species  $\text{H}_2\text{CO}_3$  is involved directly in the charge balance equation. Although an increase in  $P_{\text{CO}_2}$  will cause an increase in  $m_{\text{HCO}_3^-}$ , the reaction is either



or



In the first case, the alkalinity gained by increasing  $m_{\text{HCO}_3^-}$  is exactly balanced by the alkalinity lost by decreasing  $m_{\text{CO}_3^{2-}}$ . In the second case, the increased  $\text{HCO}_3^-$  is exactly balanced by increased  $\text{H}^+$ , so the net effect on alkalinity is zero.

Total dissolved carbonate species,  $\Sigma\text{CO}_2$ , is also a conservative quantity, provided the solution cannot exchange with a gas phase.

$$\Sigma\text{CO}_2 = m_{\text{H}_2\text{CO}_3} + m_{\text{HCO}_3^-} + m_{\text{CO}_3^{2-}}$$

$\Sigma\text{CO}_2$  simply represents the sum of all dissolved oxidized carbon species. It can change only

if oxidized carbon is added to or removed from the solution. It could also change by oxidation-reduction processes involving carbon (including biological processes), but such processes are in a different class from those considered in defining conservative quantities.

### Alkalinity Titration

The alkalinity titration is an important analytical procedure in natural-water chemistry. The titration curve also provides insights into pH stability and buffering, so we shall consider it in some detail. The treatment is more complicated than that found in most elementary chemistry textbooks because I am deriving equations that are valid for the entire pH range from 14 to 0. As discussed above, different species are important over different parts of the pH range.

**Problem:** Suppose that we have 1 ℓ of a  $5 \times 10^{-3}$  m solution of  $\text{Na}_2\text{CO}_3$  in a closed container with no gas phase present, and add  $v$  ml of 1m HCl. How does the pH vary with  $v$ , assuming that activity coefficients are all unity, no gas phase forms, and the total volume remains effectively 1 ℓ?

Starting conditions (before addition of any acid):

$$m_{\text{Na}^+} = 10^{-2}, \quad \Sigma\text{CO}_2 = 5 \times 10^{-3} \text{ m}$$

The charge balance equation is:

$$m_{\text{Na}^+} = m_{\text{HCO}_3^-} + 2m_{\text{CO}_3^{2-}} + m_{\text{OH}^-} - m_{\text{H}^+}$$

Until HCl is added,  $m_{\text{H}^+}$  will be negligible compared to the other terms; therefore,

$$m_{\text{Na}^+} = m_{\text{HCO}_3^-} + 2m_{\text{CO}_3^{2-}} + m_{\text{OH}^-} \quad (3-7)$$

$$\Sigma\text{CO}_2 = m_{\text{H}_2\text{CO}_3} + m_{\text{HCO}_3^-} + m_{\text{CO}_3^{2-}} \quad (3-8)$$

Since a solution of  $\text{Na}_2\text{CO}_3$  will be alkaline, we can provisionally assume that  $m_{\text{H}_2\text{CO}_3}$  will be small compared to  $m_{\text{HCO}_3^-}$  and  $m_{\text{CO}_3^{2-}}$ . Eq. (3-8) then becomes

$$\Sigma\text{CO}_2 = m_{\text{HCO}_3^-} + m_{\text{CO}_3^{2-}} \quad (3-9)$$

Multiplying Eq. (3-9) by 2 and subtracting from Eq. (3-7) gives

$$m_{\text{Na}^+} - 2 \Sigma\text{CO}_2 = -m_{\text{HCO}_3^-} + m_{\text{OH}^-}$$

Since  $m_{\text{Na}^+} = 2 \Sigma\text{CO}_2$  (there are two Na atoms per  $\text{CO}_3$  in  $\text{Na}_2\text{CO}_3$ ),

$$m_{\text{HCO}_3^-} = m_{\text{OH}^-} = \frac{K_w}{m_{\text{H}^+}} \quad (3-10)$$

The result of Eq. (3-10) can also be deduced intuitively; if any  $\text{CO}_3^{2-}$  is converted to  $\text{HCO}_3^-$ , there will be a net loss of one negative charge per molecule converted. Since the solution must remain electrically neutral, an additional unit of charge must come from somewhere. The only possibility is formation of  $\text{OH}^-$ , so one  $\text{OH}^-$  ion must be formed for each  $\text{HCO}_3^-$  that is formed from  $\text{CO}_3^{2-}$ .

Eq. (3-4) is (assuming that activities equal concentrations)

$$K_2 = \frac{m_{\text{H}^+} m_{\text{CO}_3^{2-}}}{m_{\text{HCO}_3^-}}$$

Substituting Eq. (3-10) gives

$$K_2 = \frac{m_{\text{H}^+}^2 m_{\text{CO}_3^{2-}}}{K_w} \quad (3-11)$$

Substituting Eq. (3-11) and (3-10) into (3-7) gives

$$m_{\text{Na}^+} = \frac{K_w}{m_{\text{H}^+}} + \frac{2K_2 K_w}{m_{\text{H}^+}^2} + \frac{K_w}{m_{\text{H}^+}}$$

Substituting numerical values for  $m_{\text{Na}^+}$  and the equilibrium constants and solving the resulting quadratic gives

$$m_{\text{H}^+} = 10^{-10.96}$$

The pH of the solution before adding any acid would be 10.96. At this pH the assumption that  $m_{\text{H}_2\text{CO}_3}$  could be ignored in the expression of  $\Sigma\text{CO}_2$  is obviously justified.

When we start to add acid, the  $\text{H}^+$  in the acid will be involved in reaction, and the  $\text{Cl}^-$  will simply accumulate. After  $v$  ml of acid has been added, the charge balance equation will be

$$\begin{aligned} m_{\text{Na}^+} - m_{\text{Cl}^-} &= m_{\text{HCO}_3^-} + 2m_{\text{CO}_3^{2-}} + m_{\text{OH}^-} - m_{\text{H}^+} \\ 10^{-2} - 10^{-3}v &= m_{\text{HCO}_3^-} + 2m_{\text{CO}_3^{2-}} + m_{\text{OH}^-} - m_{\text{H}^+} \end{aligned} \quad (3-12)$$

Equations (3-3) and (3-4) can be rewritten as:

$$m_{\text{HCO}_3^-} = \frac{K_1 m_{\text{H}_2\text{CO}_3}}{m_{\text{H}^+}} \quad (3-13)$$

$$m_{\text{CO}_3^{2-}} = \frac{K_2 m_{\text{HCO}_3^-}}{m_{\text{H}^+}} \quad (3-14)$$

Substituting Eq. (3-13) in (3-14) gives

$$m_{\text{CO}_3^{2-}} = \frac{K_1 K_2 m_{\text{H}_2\text{CO}_3}}{m_{\text{H}^+}^2} \quad (3-15)$$

Substituting (3-13) and (3-15) and the expression for  $K_w$  in (3-12) gives

$$10^{-2} - 10^{-3}v = \frac{K_1 m_{\text{H}_2\text{CO}_3}}{m_{\text{H}^+}} + \frac{2K_1 K_2 m_{\text{H}_2\text{CO}_3}}{m_{\text{H}^+}^2} + \frac{10^{-14}}{m_{\text{H}^+}} - m_{\text{H}^+} \quad (3-16)$$

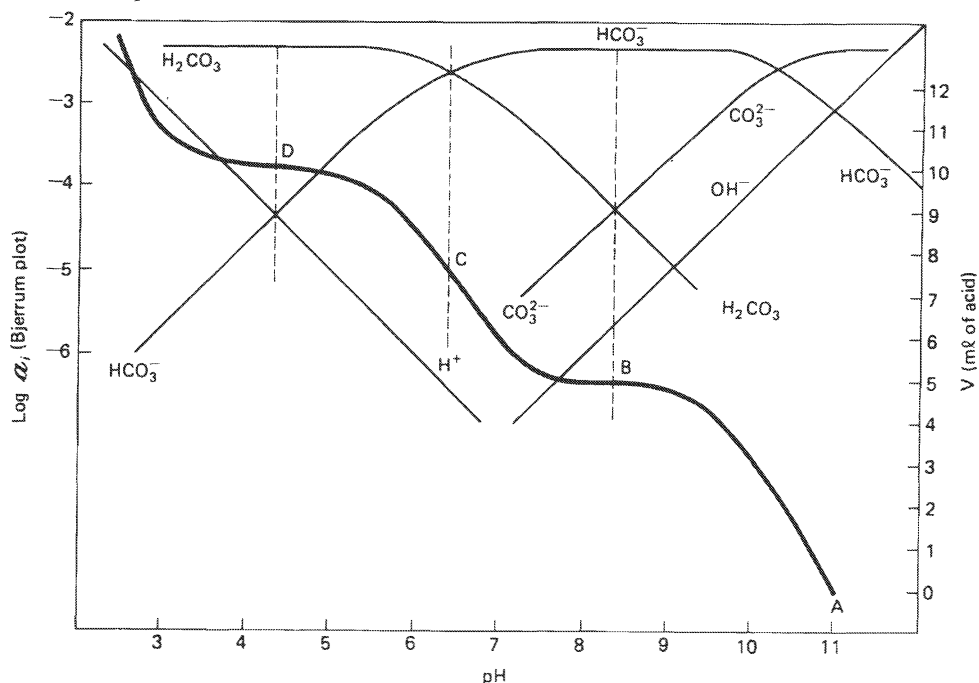
and substituting (3-13) and (3-15) in (3-8) gives

$$5 \times 10^{-3} = m_{\text{H}_2\text{CO}_3} + \frac{K_1 m_{\text{H}_2\text{CO}_3}}{m_{\text{H}^+}} + \frac{K_1 K_2 m_{\text{H}_2\text{CO}_3}}{m_{\text{H}^+}^2} \quad (3-17)$$

Elimination of  $m_{\text{H}_2\text{CO}_3}$  between (3-16) and (3-17) gives

$$10^{-3}v = 10^{-2} - \frac{5 \times 10^{-3} K_1 (1 + 2K_2/m_{\text{H}^+})}{m_{\text{H}^+} + K_1 - K_1 K_2/m_{\text{H}^+}} - \frac{10^{-14}}{m_{\text{H}^+}} + m_{\text{H}^+} \quad (3-18)$$

Values for  $m_{\text{H}^+}$  can be substituted directly into (3-18) to give the graph shown in Fig. 3-2. Fig. 3-2 also includes the Bjerrum plot discussed earlier.



**FIGURE 3-2** Titration curve (heavy line ABCD) for  $5 \times 10^{-3}$  m  $\text{Na}_2\text{CO}_3$  with acid, and Bjerrum plot for  $\Sigma\text{CO}_3 = 5 \times 10^{-3}$  m. B is the carbonate end point. C is a region of strong buffering, and D is the bicarbonate end point.

The titration curve contains two inflections, or *end points*, at pH values of 8.35 and 4.32. The corresponding volumes of acid are 5 and 10 ml. At the first end point, we have added just enough acid to convert all of the  $\text{CO}_3^{2-}$  to  $\text{HCO}_3^-$ , and at the second end point, we have converted all of the  $\text{HCO}_3^-$  (derived from  $\text{CO}_3^{2-}$ ) to  $\text{H}_2\text{CO}_3$ . The expression “converted all the  $\text{CO}_3^{2-}$  to  $\text{HCO}_3^-$ ” is confusing at first, as some  $\text{CO}_3^{2-}$  remains at all pH values. The actual equivalence condition is that

$$m_{\text{CO}_3^{2-}} = m_{\text{H}_2\text{CO}_3}$$

In terms of proton balance, 1 unit of  $\text{CO}_3^{2-}$  plus 1 unit of  $\text{H}_2\text{CO}_3$  is equivalent to 2 units of  $\text{HCO}_3^-$ , so that, at the equivalence point, all the dissolved carbonate species are effectively  $\text{HCO}_3^-$ . Note that in Fig. 3-2 the inflection point on the titration curve corresponds to the point on the Bjerrum plot where  $m_{\text{CO}_3^{2-}} = m_{\text{H}_2\text{CO}_3}$ . By similar reasoning, the second end point corresponds to the condition  $m_{\text{H}^+} = m_{\text{HCO}_3^-}$ , so all the dissolved carbonate species are effectively  $\text{H}_2\text{CO}_3$ .

For purposes of chemical analysis, the carbonate concentration and alkalinity can be determined by titration to the two end points. At the end points, the pH changes rapidly with small additions of acid so that determination of the exact equivalence pH is not critical unless a high degree of accuracy is required. Traditionally, the carbonate concentration has been measured by titration to the point where the indicator phenolphthalein changes color (pH approximately 9), and alkalinity by titration to the methyl orange end point (pH approximately 4). More accurate analyses use a pH electrode rather than indicators, and either the titration curve

is drawn out in full, or the titration is performed to a particular pH that is known to be close to the correct end point.

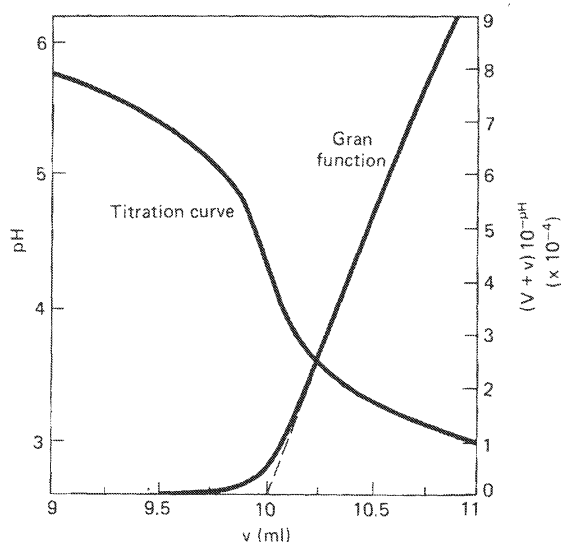
### Gran Plots

For the highest accuracy, a special graphical technique, the *Gran plot*, is used to determine the end points (Stumm and Morgan, 1996; Edmond, 1970). The principle of a Gran plot is illustrated by the following example: well below point *D* on the titration curve (Fig. 3-2), the shape of the curve is determined simply by the buildup of  $H^+$  in solution from the added acid. The curvature results from the logarithmic relationship between pH and hydrogen ion activity/concentration. If  $10^{-pH}$  is plotted against  $v$  for the region around the end point (Fig. 3-3), a straight line results in the pH region below the end point. Extrapolation of the straight line to  $m_{H^+} = 0$  locates the end point with great precision. Conceptually, an added hydrogen ion during the titration is used first to convert  $HCO_3^-$  to  $H_2CO_3$ , and when that is “complete,” it builds up in solution. The Gran plot identifies the point at which stoichiometrically all the alkalinity has been titrated and the buildup of free hydrogen ions begins.

The Gran plot can also be used to locate an end point when the titration curve is incomplete. It would be very difficult (Fig. 3-3) to identify visually the end point for a sample whose initial pH was below about 5. With the Gran plot this is no problem, and it can even be used to locate the “end point” of a sample with a slightly negative alkalinity. In Fig. 3-2 we ignored the change in volume of the system resulting from the added acid. To allow for this, we would plot  $(V + v) 10^{-pH}$  instead of  $10^{-pH}$  against  $v$  ( $V$  is the initial volume of sample,  $v$  the volume of acid added). Analogous Gran functions can be formulated for the first end point in the alkalinity titration.

In determining Eq. (3-18) and Fig. 3-2, a necessary input was the value of  $\Sigma CO_2$  (here  $5 \times 10^{-3}$  m). Thus the titration curve can be used to measure  $\Sigma CO_2$  as well as alkalinity. The procedure is explained in detail by Edmond (1970). When alkalinity and  $\Sigma CO_2$  are known, in situ values for  $P_{CO_2}$ , pH, bicarbonate, and carbonate concentrations can be calculated. The titration can be used to measure  $\Sigma CO_2$  only if  $CO_2$  does not exchange with a gas phase (the system

**FIGURE 3-3** Titration curve and Gran function for the alkalinity titration of Fig. 3-2. Note that the straight-line portion of the Gran function extrapolates to 10.00 ml, which corresponds to the inflection point on the titration curve.



is closed to  $\text{CO}_2$  exchange). In the particular example given,  $P_{\text{CO}_2}$  would increase from about  $10^{-14}$  atm in the pure  $\text{Na}_2\text{CO}_3$  solution to about 0.15 atm at the end point. If the titration was done in contact with the atmosphere ( $P_{\text{CO}_2} = 10^{-3.5}$ ),  $\text{CO}_2$  would have entered the solution from the atmosphere at the beginning of the titration and would have diffused out of the solution into the atmosphere at the end of the titration. Alkalinity can be measured whether the solution is open or closed to  $\text{CO}_2$  exchange, but  $\Sigma\text{CO}_2$  can be measured only if the system is closed.

At a pH of about 6.4 (Fig. 3-2), the pH of the solution changes very slowly as acid is added. In this region the solution is strongly buffered with respect to pH change. Buffering occurs when a protonated species (here  $\text{H}_2\text{CO}_3$ ) and an unprotonated species (here  $\text{HCO}_3^-$ ) are both present in significant concentrations. When acid is added, the protons combine with  $\text{HCO}_3^-$  to form  $\text{H}_2\text{CO}_3$ , and the net change in pH is small. Similar buffering by the  $\text{HCO}_3^-/\text{CO}_3^{2-}$  pair occurs around pH 10.3.

In deriving Eq. (3-18) and Fig. 3-2, we assumed that activities and concentrations were equal, which is obviously not true. Eq. (3-18) is correct in this regard, however, if the  $K$  values represent apparent equilibrium constants (Chapter 2) rather than thermodynamic constants. The titration curve can thus be used to determine apparent constants in natural waters, although the apparent constants may be slightly changed by the addition of HCl. The change is likely to be significant only if carbonate species are the major anions in solution. This information is important in determining the stabilities of various complexes and in determining the state of saturation of a water with respect to carbonate minerals. Eq. (3-18) can be modified to include the change in total volume as acid is added.

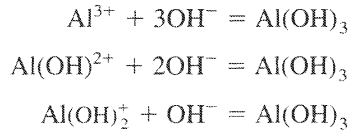
Organic anions present both conceptual and practical problems for the definition of alkalinity. If the corresponding organic acid had the same  $\text{p}K_a$  value as  $\text{H}_2\text{CO}_3$  (6.35), there would be no problem, and the measured alkalinity would be the sum of the carbonate alkalinity and the concentration of the organic anion. Most organic acids, however, have  $\text{p}K_a$  values around 4 or 5 (Table 6-1). At the pH of the bicarbonate end point (about 4.5), some fraction of the organic anions will be converted to undissociated acid, and some will remain as anions. If the concentration of organic anions is much less than that of bicarbonate, the titration curve will show an inflection at the bicarbonate end point, and the measured alkalinity (defined by the bicarbonate end point) will equal the sum of carbonate alkalinity and that fraction of the organic anions that has been titrated by the pH of the carbonate end point. As the concentration of organic anions increases relative to carbonate species, the inflection at the bicarbonate end point gradually disappears and cannot be used to define the pH corresponding to zero alkalinity. One approach is to define a certain pH (say 5.0) arbitrarily as the zero point of alkalinity; the alkalinity would then be the amount of acid required to bring the sample to that pH. This definition is convenient, but the alkalinity so defined is not conservative. Another approach is to include all organic anions in the definition of alkalinity. The problem with this approach is that some organic acids are quite strong (e.g., oxalic acid has a  $\text{p}K_a$  of 1.2, which makes it a stronger acid than  $\text{HSO}_4^-$ ). It is impossible to measure anions of such strong "weak" acids by acid-base titrations; thus, although alkalinity so defined is conservative, it is not directly measurable.

*Acidity* (equivalent to the terms *mineral acidity* or *strong acidity* of other authors) can be defined as the negative of alkalinity, that is, as the amount of base required to raise the pH of the sample to the bicarbonate end point. If acidity is positive,

$$m_{\text{H}^+} > m_{\text{HCO}_3^-} + 2m_{\text{CO}_3^{2-}} + m_{\text{OH}^-}$$

which means, from charge balance considerations, that an anion of an acid stronger than carbonic acid must be present. In nature, the anion is commonly sulfate.

Hydrolyzable cations such as aluminum also contribute to acidity, because they are titratable by base. If a solution containing  $\text{Al}^{3+}$  is titrated with strong base, the following reactions will occur:



The acidity (the negative alkalinity) thus becomes (ignoring  $\text{CO}_3^{2-}$  and  $\text{OH}^-$ )

$$\text{Acidity} = m_{\text{H}^+} - m_{\text{HCO}_3^-} + 3m_{\text{Al}^{3+}} + 2m_{\text{Al}(\text{OH})^{2+}} + m_{\text{Al}(\text{OH})_2^+} - m_{\text{Al}(\text{OH})_3}$$

The contribution of Al species to the titration acidity is called *aluminum acidity*. The solubility of  $\text{Al}(\text{OH})_3$  at around pH 5 is small, so the presence of dissolved Al species does not in practice complicate the definition of the pH corresponding to zero acidity/alkalinity. The behavior of  $\text{Fe}^{3+}$  is analogous to that of  $\text{Al}^{3+}$ .

## CALCIUM CARBONATE SOLUBILITY

The solubility of calcium carbonate can be understood by adding one more equation to the equations for the carbonate system discussed in the preceding section. The solubility products of calcite and aragonite are defined by the equations

$$\begin{aligned}K_{\text{cal}} &= a_{\text{Ca}^{2+}} a_{\text{CO}_3^{2-}} = 10^{-8.48} \text{ at } 25^\circ\text{C} \\ K_{\text{arag}} &= a_{\text{Ca}^{2+}} a_{\text{CO}_3^{2-}} = 10^{-8.34} \text{ at } 25^\circ\text{C}\end{aligned}$$

Values for the solubility product at other temperatures are listed in Table 3-1. Aragonite is the less stable polymorph of calcium carbonate at 1 atm pressure, and hence it is more soluble than calcite.

Garrels and Christ (1965) discuss at length calculations involving calcite solubility, and only a few examples will be given here. Most problems reduce to setting up a set of equations consisting of equilibrium conditions (the expressions for  $K_{\text{CO}_2}$ ,  $K_1$ ,  $K_2$ ,  $K_w$ , and  $K_{\text{cal}}$ ), a charge balance equation, and some other condition. The other condition is usually either a fixed value of  $P_{\text{CO}_2}$  if an open system is being considered, or a fixed value of  $\Sigma\text{CO}_2$  if a closed system is being considered. This set of equations usually describes the system completely, and all that remains is algebraic manipulation to get the desired answer.

### Example 2

What is the pH of pure water in equilibrium with the atmosphere ( $P_{\text{CO}_2} = 10^{-3.5}$  atm) and calcite at  $25^\circ\text{C}$ ? Assume activities equal concentrations.

This example is similar to Example 1, with the addition of calcite. From Example 1:

$$\begin{aligned}a_{\text{H}_2\text{CO}_3} &= K_{\text{CO}_2} P_{\text{CO}_2} \\ &= 10^{-1.47} \cdot 10^{-3.5} = 10^{-4.97} \\ K_1 &= \frac{a_{\text{H}^+} a_{\text{HCO}_3^-}}{a_{\text{H}_2\text{CO}_3}} \\ a_{\text{H}^+} a_{\text{HCO}_3^-} &= K_1 K_{\text{CO}_2} P_{\text{CO}_2}\end{aligned}\tag{3-19}$$



The charge balance equation, however, becomes

$$m_{\text{H}^+} + 2m_{\text{Ca}^{2+}} = m_{\text{HCO}_3^-} + 2m_{\text{CO}_3^{2-}} + m_{\text{OH}^-}$$

If the pH is near-neutral (which we can verify later), this simplifies to:

$$2m_{\text{Ca}^{2+}} = m_{\text{HCO}_3^-} \quad (3-20)$$

The solubility of calcite is defined by:

$$K_{\text{cal}} = \alpha_{\text{Ca}^{2+}} \alpha_{\text{CO}_3^{2-}} \quad (3-21)$$

and since we have introduced  $\alpha_{\text{CO}_3^{2-}}$  as a variable, we shall need the expression for  $K_2$ :

$$K_2 = \frac{\alpha_{\text{H}^+} \alpha_{\text{CO}_3^{2-}}}{\alpha_{\text{HCO}_3^-}} \quad [\text{Eq. (3-4)}] \quad (3-22)$$

We now have six unknowns ( $P_{\text{CO}_2}$ ,  $\alpha_{\text{H}_2\text{CO}_3}$ ,  $\alpha_{\text{HCO}_3^-}$ ,  $\alpha_{\text{CO}_3^{2-}}$ ,  $\alpha_{\text{Ca}^{2+}}$ ,  $\alpha_{\text{H}^+}$ ) and, assuming  $\alpha = m$ , six equations relating them (fixed  $P_{\text{CO}_2}$ , equations for  $K_{\text{CO}_2}$ ,  $K_1$ ,  $K_2$ ,  $K_{\text{cal}}$ , charge balance equation). It is now a matter of manipulating the equations to get the desired answer. There are several ways of eliminating the “unwanted” variables: the method shown here leads directly to an equation relating pH and  $P_{\text{CO}_2}$ .

Rewriting Eq. (3-22):

$$\alpha_{\text{CO}_3^{2-}} = K_2 \frac{\alpha_{\text{HCO}_3^-}}{\alpha_{\text{H}^+}}$$

Substituting this in Eq. (3-21):

$$\alpha_{\text{Ca}^{2+}} K_2 \frac{\alpha_{\text{HCO}_3^-}}{\alpha_{\text{H}^+}} = K_{\text{cal}}$$

Substituting for  $\alpha_{\text{Ca}^{2+}}$  from Eq. (3-20) (assuming  $\alpha = m$ ),

$$\left(\frac{1}{2} \alpha_{\text{HCO}_3^-}\right) K_2 \left(\frac{\alpha_{\text{HCO}_3^-}}{\alpha_{\text{H}^+}}\right) = K_{\text{cal}}$$

and for  $\alpha_{\text{HCO}_3^-}$  from Eq. (3-19),

$$\frac{1}{2} \left(\frac{K_1 K_{\text{CO}_2} P_{\text{CO}_2}}{\alpha_{\text{H}^+}}\right)^2 \frac{K_2}{\alpha_{\text{H}^+}} = K_{\text{cal}}$$

which rearranges to:

$$\alpha_{\text{H}^+}^3 = \frac{K_1^2 K_{\text{CO}_2}^2 P_{\text{CO}_2}^2 K_2}{2 K_{\text{cal}}}$$

Substituting the numerical values for the constants and  $P_{\text{CO}_2}$ ,

$$\alpha_{\text{H}^+} = 10^{-8.26}$$

The pH would thus be 8.26.

We can now check whether we were justified in neglecting  $m_{\text{CO}_3^{2-}}$  and  $m_{\text{H}^+}$  in the charge balance equation. Rearranging Eq. (3-22):

$$\frac{\alpha_{\text{CO}_3^{2-}}}{\alpha_{\text{HCO}_3^-}} = \frac{K_2}{\alpha_{\text{H}^+}} = \frac{10^{-10.33}}{10^{-8.26}} = 10^{-2.07}$$

The carbonate activity (concentration) is thus less than 1% of the bicarbonate activity (concentration), so it was reasonable to ignore it. The  $\text{Ca}^{2+}$  activity in the solution (see following examples) is  $10^{-3.35}$ , which is much larger than  $\alpha_{\text{H}^+}$  ( $10^{-8.26}$ ). It was thus reasonable to neglect  $\text{H}^+$  in the charge balance equation. As a general rule,  $m_{\text{Ca}^{2+}}$  will be orders-of-magnitude larger than  $m_{\text{H}^+}$  in solutions that are in equilibrium with calcite.

### Example 3

Express the solubility product of calcite in terms of bicarbonate activity and  $P_{\text{CO}_2}$  instead of carbonate activity. Recalling Eqs. (3-1 to 3-3):

$$K_{\text{CO}_2} = \frac{\alpha_{\text{H}_2\text{CO}_3}}{P_{\text{CO}_2}} \quad (3-23)$$

$$K_1 = \frac{\alpha_{\text{H}^+} \alpha_{\text{HCO}_3^-}}{\alpha_{\text{H}_2\text{CO}_3}} \quad (3-24)$$

$$K_2 = \frac{\alpha_{\text{H}^+} \alpha_{\text{CO}_3^{2-}}}{\alpha_{\text{HCO}_3^-}} \quad (3-25)$$

$$K_{\text{cal}} = \alpha_{\text{Ca}^{2+}} \alpha_{\text{CO}_3^{2-}} \quad (3-26)$$

Rearranging Eq. (3-24) gives

$$\alpha_{\text{H}^+} = \frac{K_1 \alpha_{\text{H}_2\text{CO}_3}}{\alpha_{\text{HCO}_3^-}} \quad (3-27)$$

Rearranging Eq. (3-25) gives

$$\alpha_{\text{CO}_3^{2-}} = \frac{K_2 \alpha_{\text{HCO}_3^-}}{\alpha_{\text{H}^+}} \quad (3-28)$$

Substituting Eq. (3-27) in Eq. (3-28) gives

$$\alpha_{\text{CO}_3^{2-}} = \frac{K_2 \alpha_{\text{HCO}_3^-}^2}{K_1 \alpha_{\text{H}_2\text{CO}_3}}$$

Substituting this in Eq. (3-26) gives

$$K_{\text{cal}} = \alpha_{\text{Ca}^{2+}} \frac{K_2 \alpha_{\text{HCO}_3^-}^2}{K_1 \alpha_{\text{H}_2\text{CO}_3}}$$

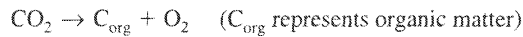
or

$$\frac{\alpha_{\text{Ca}^{2+}} \alpha_{\text{HCO}_3^-}^2}{\alpha_{\text{H}_2\text{CO}_3}} = \frac{K_{\text{cal}} K_1}{K_2} = 10^{-4.30} \text{ at } 25^\circ\text{C}$$

or, from Eq. (3-23):

$$\frac{\alpha_{\text{Ca}^{2+}} \alpha_{\text{HCO}_3^-}^2}{P_{\text{CO}_2}} = \frac{K_{\text{cal}} K_1 K_{\text{CO}_2}}{K_2} = 10^{-5.97} \text{ at } 25^\circ\text{C} \quad (3-29)$$

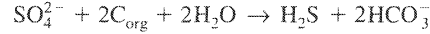
Eq. (3-29) is useful in understanding natural waters, because controlling variables in many natural systems are  $\text{CO}_2$  and  $m_{\text{HCO}_3^-}$ . For example, photosynthesis



will remove dissolved  $\text{CO}_2$ , which will increase the state of saturation (i.e., it would tend to cause calcite to precipitate). Aerobic respiration or decay



will decrease the state of saturation and tend to cause calcite to dissolve. Anaerobic decay with sulfate reduction (see Chapter 8) can be represented in a simplified way by the equation



Sulfate reduction causes an increase in alkalinity and thus tends to cause precipitation of calcite.

#### Example 4

How does the calcium concentration of pure water in equilibrium with calcite vary as a function of  $P_{\text{CO}_2}$ ?

In this example we shall not assume activities equal concentrations. We can start from Eq. (3-29) from the previous example:

$$\alpha_{\text{Ca}^{2+}} \alpha_{\text{HCO}_3^-}^2 = \frac{K_{\text{cal}} K_1 K_{\text{CO}_2} P_{\text{CO}_2}}{K_2} \quad (3-30)$$

The charge balance equation is

$$m_{\text{H}^+} + 2m_{\text{Ca}^{2+}} = m_{\text{HCO}_3^-} + 2m_{\text{CO}_3^{2-}} + m_{\text{OH}^-} \quad (3-31)$$

If we restrict our attention to the pH region below 9,  $m_{\text{H}^+}$ ,  $m_{\text{OH}^-}$ , and  $2m_{\text{CO}_3^{2-}}$  will be small compared to  $2m_{\text{Ca}^{2+}}$  and  $m_{\text{HCO}_3^-}$  in the charge balance equation (small quantities can be neglected when they are added to or subtracted from large quantities; they may not be neglected when they multiply or divide large quantities). Eq. (3-31) then simplifies to

$$2m_{\text{Ca}^{2+}} = m_{\text{HCO}_3^-} \quad (3-32)$$

or

$$\frac{2\alpha_{\text{Ca}^{2+}}}{\gamma_{\text{Ca}^{2+}}} = \frac{\alpha_{\text{HCO}_3^-}}{\gamma_{\text{HCO}_3^-}}$$

or

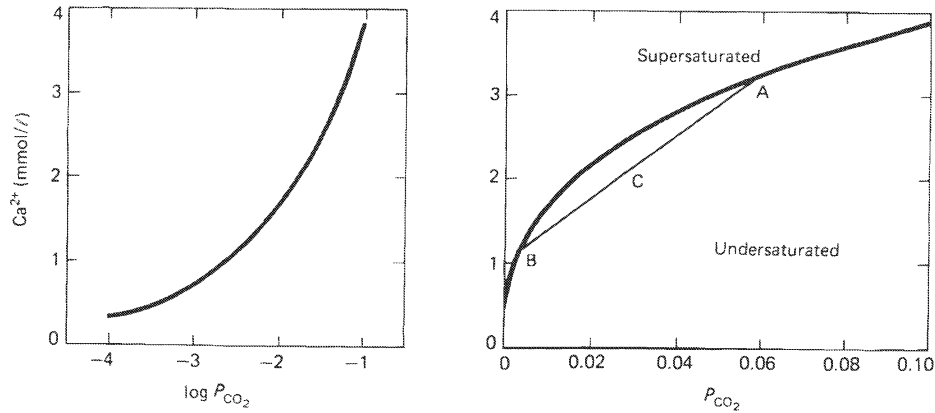
$$\alpha_{\text{HCO}_3^-} = 2\alpha_{\text{Ca}^{2+}} \frac{\gamma_{\text{HCO}_3^-}}{\gamma_{\text{Ca}^{2+}}}$$

Substituting this in Eq. (3-30) and rearranging gives

$$m_{\text{Ca}^{2+}}^3 = P_{\text{CO}_2} \frac{K_1 K_{\text{cal}} K_{\text{CO}_2}}{4K_2 \gamma_{\text{Ca}^{2+}} \gamma_{\text{HCO}_3^-}^2} \quad (3-33)$$

which is the desired relationship.

The relationship is shown graphically in Fig. 3-4, assuming 25°C and a total pressure of 1 atm. The calculation of the activity coefficients can be done by an iteration procedure similar to that used in Example 6 of Chapter 2. For each value of  $P_{\text{CO}_2}$ , a preliminary calculation is made, assuming that activity coefficients are unity; the concentrations of all species are calculated on this assumption, and these concentrations are used to calculate  $\gamma_{\text{Ca}^{2+}}$  and  $\gamma_{\text{HCO}_3^-}$  by the Debye-Hückel equation. These  $\gamma$  values are then used in Eq. (3-33) to give better values for  $m_{\text{Ca}^{2+}}$  and, hence, the concentrations of other dissolved species, and the cycle is repeated until consistent results are achieved.



**FIGURE 3-4** Concentration of calcium in equilibrium with calcite as a function of  $P_{\text{CO}_2}$  in the system  $\text{CaCO}_3\text{--CO}_2\text{--H}_2\text{O}$  at  $25^\circ\text{C}$  and 1 atm total pressure. For explanation of points A, B, and C, see text.

It is interesting to note on Fig. 3-4 that the relationship between  $m_{\text{Ca}^{2+}}$  and  $P_{\text{CO}_2}$  is not linear. For example, if a water in equilibrium with calcite at  $P_{\text{CO}_2} = 0.06$  atm (A in Fig. 3-4) is mixed with a water in equilibrium with calcite at  $P_{\text{CO}_2} = 0.006$  atm (B in Fig. 3-4), the resulting water (C in Fig. 3-4) is not in equilibrium with calcite. In fact, it is undersaturated and could cause dissolution of calcite. In general, mixing of two waters of different compositions, both of which are in equilibrium with calcite, can frequently result in a water that is not in equilibrium with calcite. It may be supersaturated or undersaturated, depending on the particular compositions or the waters involved (Runnells, 1969; Wigley and Plummer, 1976). Supersaturation would occur if, for example, a water with high calcium concentration and low alkalinity mixed with a water of high alkalinity and low calcium concentration.

#### Example 5

How does the presence of dissolved sodium bicarbonate affect the concentration of dissolved calcium in equilibrium with calcite at different  $\text{CO}_2$  pressures?

The equations for solving this problem are identical with those for Example 4 except that the charge balance equation becomes (for pH values below 9)

$$m_{\text{Na}^+} + 2m_{\text{Ca}^{2+}} = m_{\text{HCO}_3^-}$$

Substituting this equation for Eq. (3-32) in Example 4 and following the same derivation, Eq. (3-33) becomes

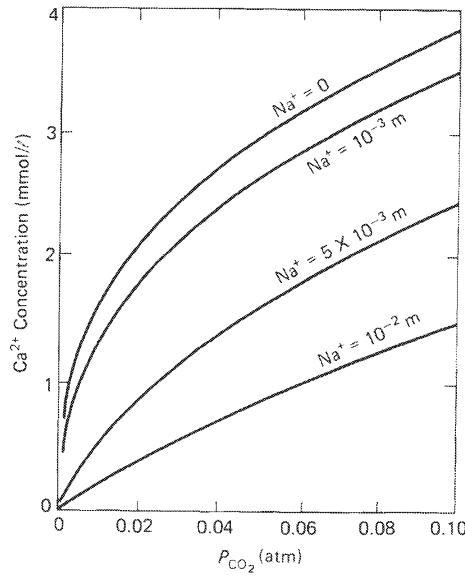
$$m_{\text{Ca}^{2+}}(m_{\text{Na}^+} + 2m_{\text{Ca}^{2+}})^2 = P_{\text{CO}_2} \frac{K_1 K_{\text{cal}} K_{\text{CO}_2}}{K_2 \gamma_{\text{Ca}^{2+}} \gamma_{\text{HCO}_3^-}^2} \quad (3-34)$$

This relationship is shown graphically in Fig. 3-5. The presence of excess  $\text{NaHCO}_3$  decreases the concentration of  $\text{Ca}^{2+}$  in equilibrium with calcite. This is the familiar common-ion effect in solution chemistry. In alkaline brines where the  $\text{Na}^+$  concentration is very high, the dissolved  $\text{Ca}^{2+}$  concentration is often vanishingly small (see Chapter 15).

#### Example 6

How does the presence of dissolved calcium chloride affect the concentration of dissolved calcium in equilibrium with calcite at different  $\text{CO}_2$  pressures?

**FIGURE 3-5** Concentration of calcium in equilibrium with calcite as a function of  $P_{\text{CO}_2}$  and  $\text{Na}^+$  concentration in the system  $\text{CaCO}_3\text{-Na}_2\text{CO}_3\text{-CO}_2\text{-H}_2\text{O}$  at 25°C and 1 atm total pressure.



Again, the basic equations are the same as in Example 4, except that the charge balance equation is now

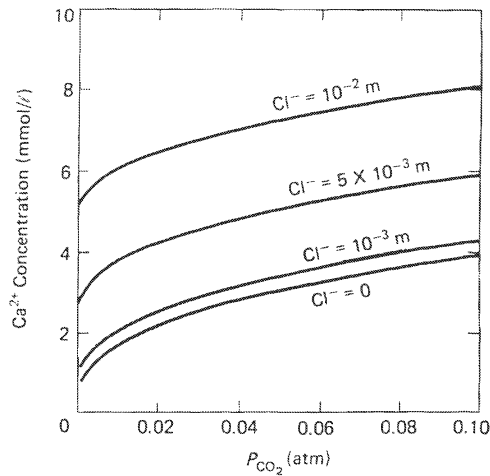
$$2m_{\text{Ca}^{2+}} = m_{\text{HCO}_3^-} + m_{\text{Cl}^-}$$

Using the same procedure as in Examples 4 and 5 gives the final equation:

$$m_{\text{Ca}^{2+}}(2m_{\text{Ca}^{2+}} - m_{\text{Cl}^-})^2 = P_{\text{CO}_2} \frac{K_1 K_{\text{cal}} K_{\text{CO}_2}}{K_2 \gamma_{\text{Ca}^{2+}} \gamma_{\text{HCO}_3^-}^2} \quad (3-35)$$

This relationship is shown in Fig. 3-6. The concentration of calcium equivalent to chloride is not affected by changes in  $P_{\text{CO}_2}$ . The additional  $\text{Ca}^{2+}$  balanced by carbonate species is related to  $P_{\text{CO}_2}$  in a way that is rather similar to that of the simple system without  $\text{Cl}^-$  or  $\text{Na}^+$ .

**FIGURE 3-6** Concentration of calcium in equilibrium with calcite as a function of  $P_{\text{CO}_2}$  and  $\text{Cl}^-$  concentration in the system  $\text{CaCO}_3\text{-CaCl}_2\text{-CO}_2\text{-H}_2\text{O}$  at 25°C and 1 atm total pressure.



These three examples cover all of the possibilities in common natural-water systems. The general charge balance equation is

$$m_{\text{Na}^+} + m_{\text{K}^+} + 2m_{\text{Ca}^{2+}} + 2m_{\text{Mg}^{2+}} = m_{\text{HCO}_3^-} + 2m_{\text{CO}_3^{2-}} + m_{\text{Cl}^-} + 2m_{\text{SO}_4^{2-}} + m_{\text{minor species}}$$

This can be rewritten as (ignoring minor species):

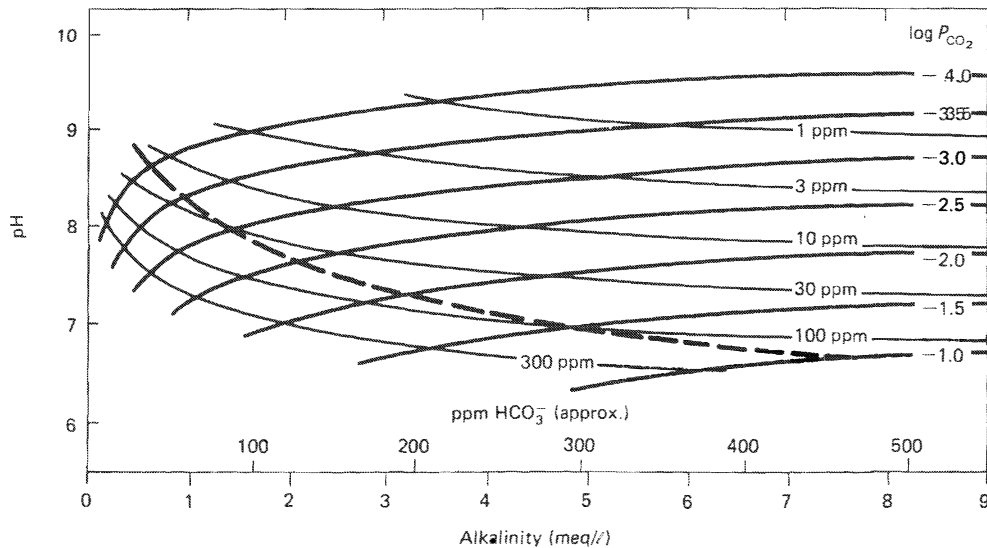
$$\underbrace{m_{\text{Na}^+} + m_{\text{K}^+} + 2m_{\text{Mg}^{2+}} - m_{\text{Cl}^-} - 2m_{\text{SO}_4^{2-}} + 2m_{\text{Ca}^{2+}}}_M = m_{\text{HCO}_3^-} + 2m_{\text{CO}_3^{2-}}$$

If the expression  $M$  is positive, then  $M$  is exactly analogous to  $\text{Na}^+$  in Example 5, and  $M$  can be substituted for  $m_{\text{Na}^+}$  in Eq. (3-34). If  $M$  is negative, then  $M$  will be analogous to  $\text{Cl}^-$  in Example 6, and  $M$  may be substituted for  $m_{\text{Cl}^-}$  in Eq. (3-35). Seawater is a good example of a water in which  $M$  is negative.

Some general relationships among species in the carbonate system are shown in Fig. 3-7. In constructing Fig. 3-7, it was assumed that, when  $2m_{\text{Ca}^{2+}}$  was less than alkalinity, the difference was made up by  $\text{Na}^+$ ; when  $2m_{\text{Ca}^{2+}}$  was greater than alkalinity, the difference was made up by  $\text{Cl}^-$ .

## DOLOMITE

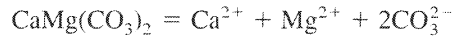
Dolomite has a chemical formula  $\text{CaMg}(\text{CO}_3)_2$  and a crystallographic structure similar to that of calcite, except that the Ca and Mg atoms are arranged in separate planes. The ordering of the Ca and Mg atoms distinguishes dolomite from a high-magnesium calcite of the same composition.



**FIGURE 3-7** Relation among pH, alkalinity,  $P_{\text{CO}_2}$ , and calcium concentration in waters saturated with respect to calcite at 25°C and 1 atm total pressure. Heavy lines are contours of equal  $P_{\text{CO}_2}$ , light lines are contours of equal calcium concentration, and the dashed line is the locus of compositions where the calcium concentration exactly balances the alkalinity. For assumptions, see text (after Drever, 1972).

Protodolomite is a partially disordered form of dolomite; it usually contains more Ca and less Mg than the ideal formula.

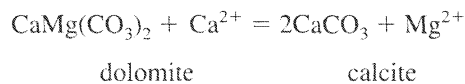
The solubility of dolomite can be represented by the equation:



$$K_{\text{dol}} = \alpha_{\text{Ca}^{2+}} \alpha_{\text{Mg}^{2+}} \alpha_{\text{CO}_3^{2-}}^2$$

There has been considerable disagreement in the literature as to the correct value of  $K_{\text{dol}}$ . The disagreement results from the fact that dolomite is very unreactive at low temperatures. At 25°C it is almost impossible to make dolomite grow in the laboratory, and dolomite dissolves only slowly in solutions that are strongly undersaturated with respect to it. The most accepted value for  $K_{\text{dol}}$  is about  $10^{-17.2}$ , which is deduced from the compositions of groundwaters that have spent a long time in dolomite aquifers (Hsü, 1967).

In nature, dolomite is generally formed by alteration of calcite (or aragonite). The equilibrium constant for the reaction can be written



$$K_{\text{cd}} = \frac{\alpha_{\text{Mg}^{2+}}}{\alpha_{\text{Ca}^{2+}}}$$

In solutions in which the ratio  $\alpha_{\text{Mg}^{2+}}/\alpha_{\text{Ca}^{2+}}$  is higher than  $K_{\text{cd}}$ , dolomite is more stable than calcite, and vice versa.  $K_{\text{cd}}$  is related to  $K_{\text{dol}}$  by the equation:

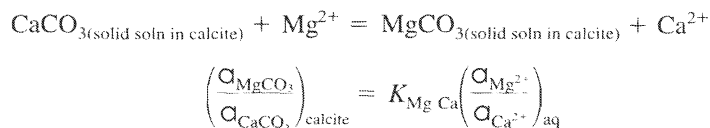
$$\begin{aligned} K_{\text{cd}} &= \frac{K_{\text{dol}}}{K_{\text{cal}}^2} \\ &= \frac{10^{-17.2}}{10^{-16.96}} = 10^{-0.2} \\ &= 0.6 \end{aligned}$$

There is a large uncertainty associated with this number, but calcite is probably unstable with respect to dolomite in surface waters in which the  $\alpha_{\text{Mg}^{2+}}/\alpha_{\text{Ca}^{2+}}$  ratio is greater than 1. However, because the reaction is kinetically slow, calcite is rarely converted to dolomite at low temperatures unless the  $\alpha_{\text{Mg}^{2+}}/\alpha_{\text{Ca}^{2+}}$  ratio is considerably higher than 1. The conversion is more rapid in the absence of sulfate (Baker and Kastner, 1981).

## HIGH-MAGNESIUM CALCITE

Magnesium can substitute for calcium in the calcite structure. The calcite formed in modern shallow-marine environments commonly contains 11 to 19 mole percent  $\text{MgCO}_3$  and is called high-magnesium calcite. Calcite containing 5 percent or less  $\text{MgCO}_3$  is referred to as low-magnesium calcite. In discussing the stability of high-magnesium calcites, it is important to define what is meant by stability. All high-magnesium calcites are unstable with respect to low-magnesium calcite plus dolomite. This is of little importance in surface-water chemistry because dolomite is so kinetically inert.

Equilibrium between high-magnesium calcite and a solution can be defined in terms of a cation-displacement reaction and in terms of a solubility reaction. For cation-displacement equilibrium between a high-magnesium calcite and solution,



In general, the Ca–Mg carbonate solid solution will be highly nonideal, so no simple linear relationship will exist between the concentration ratio in the solid and the concentration ratio in solution. However, for any particular ratio in solution, there is a corresponding unique ratio in the solid, and when the ratio in solution varies, so should the ratio in the solid.

Solubility equilibrium or, more strictly, *stoichiometric saturation* can be defined by the equations:

$$\text{Mg}_x\text{Ca}_{(1-x)}\text{CO}_3 = x\text{Mg}^{2+} + (1-x)\text{Ca}^{2+} + \text{CO}_3^{2-}$$

$$K_{\text{sp}} = a_{\text{Mg}^{2+}}^x a_{\text{Ca}^{2+}}^{(1-x)} a_{\text{CO}_3^{2-}} \quad (3-36)$$

$$= \left( \frac{a_{\text{Mg}^{2+}}}{a_{\text{Ca}^{2+}}} \right)^x a_{\text{Ca}^{2+}} a_{\text{CO}_3^{2-}}$$

Measurement of  $K_{\text{sp}}$  is complicated by the fact that, when high-magnesium calcites are placed in water, they initially dissolve congruently,\* but as the concentration of ions in solution increases, dissolution becomes incongruent. During incongruent dissolution, a low-magnesium calcite precipitates as the high-magnesium calcite dissolves. Plummer and Mackenzie (1974) and Bischoff et al. (1987) estimated the solubility of high-magnesium calcites by measuring the rate of dissolution when dissolution was congruent and extrapolating the results to infinite time. There is some disagreement about the validity of this approach, but there is a consensus that calcites containing *some* magnesium, probably up to at least 5 mole percent  $\text{MgCO}_3$ , are more stable than pure calcite in seawater.

For true equilibrium, the equations describing cation displacement and stoichiometric saturation must both be satisfied. Stoichiometric saturation is commonly attained much more rapidly than cation displacement equilibrium.

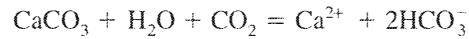
## GROUND- AND SURFACE WATERS IN CARBONATE TERRAINS

The equations derived in this chapter provide a good framework for understanding the chemistry of waters in limestone aquifers. Rainwater is in equilibrium with atmospheric carbon dioxide, which has a partial pressure of  $10^{-3.5}$  atm. The gases in soils commonly contain much more  $\text{CO}_2$  (typically  $10^{-2.5}$  to  $10^{-1.5}$  atm) than the atmosphere as a consequence of respiration and decay of organic matter. As rain percolates through soil, its  $\text{CO}_2$  content increases, typically to an equivalent  $P_{\text{CO}_2}$  of  $10^{-2}$  or so. The additional  $\text{CO}_2$  from the soil greatly increases the amount of  $\text{CaCO}_3$  the water can dissolve. The amount of  $\text{CaCO}_3$  dissolved per liter of percolating water (and hence

\*Congruent dissolution occurs when the entire solid dissolves; incongruent dissolution occurs when part of the solid dissolves, leaving behind a solid phase different in composition from the original.



the  $\text{Ca}^{2+}$  concentration in the water) depends on the initial  $\text{CO}_2$  concentration and on the extent to which the  $\text{CO}_2$  in the water can be replenished by exchanging with a gas phase. If  $\text{CO}_2$  is not replenished (the system is *closed* to exchange of  $\text{CO}_2$  gas), the amount of calcite that a water can dissolve is essentially limited by the amount of  $\text{CO}_2$  present initially, since dissolution follows the equation:



If the system is *open* to  $\text{CO}_2$ , the  $P_{\text{CO}_2}$  of the water will remain constant, and  $\text{CO}_2$  will be transferred from the gas phase to replace the  $\text{CO}_2$  consumed by dissolution of calcite. In this case, the dissolution of calcite is not limited by the availability of  $\text{CO}_2$ ; more calcite will dissolve under open-system conditions than under closed-system conditions.

### Example 7

Pure water at 25°C is in equilibrium with  $\text{CO}_2$  at a partial pressure of  $10^{-2}$  atm. How much calcite can the water dissolve, assuming (a) a closed system (no exchange of  $\text{CO}_2$  with a gas phase); (b) an open system ( $P_{\text{CO}_2}$  remains constant)? In case (a), what will be the final  $P_{\text{CO}_2}$  of the system? Assume that all activity coefficients are unity.

The equilibrium equations for the carbonate system are:

$$K_{\text{CO}_2} = \frac{a_{\text{H}_2\text{CO}_3}}{P_{\text{CO}_2}} \quad (3-37)$$

$$K_1 = \frac{a_{\text{H}^+} a_{\text{HCO}_3^-}}{a_{\text{H}_2\text{CO}_3}} \quad (3-38)$$

$$K_2 = \frac{a_{\text{H}^+} a_{\text{CO}_3^{2-}}}{a_{\text{HCO}_3^-}} \quad (3-39)$$

$$K_{\text{ca}} = a_{\text{Ca}^{2+}} a_{\text{CO}_3^{2-}} \quad (3-40)$$

The charge balance equation is

$$m_{\text{H}^+} + 2m_{\text{Ca}^{2+}} = m_{\text{HCO}_3^-} + 2m_{\text{CO}_3^{2-}} + m_{\text{OH}^-}$$

If the final pH is less than about 9,  $m_{\text{H}^+}$ ,  $m_{\text{OH}^-}$ , and  $m_{\text{CO}_3^{2-}}$  will all be small compared to  $2m_{\text{Ca}^{2+}}$  and  $m_{\text{HCO}_3^-}$ . Assuming that these terms can be neglected, and introducing the assumption  $a = m$ , the charge balance equation becomes

$$2a_{\text{Ca}^{2+}} = a_{\text{HCO}_3^-} \quad (3-41)$$

We now have five equations in six unknowns. The other equation necessary to solve the system in case (b) is simply

$$P_{\text{CO}_2} \text{ constant} = 10^{-2}$$

In case (a) the condition is conservation of carbonate species; that is

$$\begin{aligned} \Sigma \text{CO}_2 &= \Sigma \text{CO}_2 \text{ initial} + \Sigma \text{CO}_2 \text{ from dissolution of CaCO}_3 \\ &= (m_{\text{H}_2\text{CO}_3})_{\text{initial}} + m_{\text{Ca}^{2+}} \end{aligned} \quad (3-42)$$

where  $(\ )_{\text{initial}}$  means before any  $\text{CaCO}_3$  dissolves ( $10^{-2} \times 10^{-1.47}$  m), and  $m_{\text{Ca}^{2+}}$  comes from the fact that each mole of  $\text{CaCO}_3$  that dissolves adds 1 mol of  $\text{Ca}^{2+}$  and 1 mole of  $\Sigma \text{CO}_2$ . If  $m_{\text{CO}_3^{2-}}$  can be neglected in the expression of  $\Sigma \text{CO}_2$ , Eq. (3-42) becomes

$$m_{\text{H}_2\text{CO}_3} + m_{\text{HCO}_3^-} = (m_{\text{H}_2\text{CO}_3})_{\text{initial}} + m_{\text{Ca}^{2+}}$$

which rearranges to

$$(m_{\text{H}_2\text{CO}_3})_{\text{initial}} = m_{\text{H}_2\text{CO}_3} + m_{\text{HCO}_3^-} - m_{\text{Ca}^{2+}} \quad (3-43)$$

All that remains now is algebraic manipulation. Dividing Eq. (3-38) by (3-39) gives

$$\frac{K_1}{K_2} = \frac{\alpha_{\text{HCO}_3^-}^2}{\alpha_{\text{H}_2\text{CO}_3} \alpha_{\text{CO}_3^{2-}}}$$

Substituting (3-40), (3-43), and (3-41) in this gives

$$\frac{K_1}{K_2} = \frac{4\alpha_{\text{Ca}^{2+}}^3}{K_{\text{cal}}[(m_{\text{H}_2\text{CO}_3})_{\text{initial}} - m_{\text{Ca}^{2+}}]}$$

which, assuming that  $\alpha = m$ , rearranges to:

$$m_{\text{Ca}^{2+}}^3 + \frac{K_1 K_{\text{cal}}}{4K_2} m_{\text{Ca}^{2+}} - \frac{K_1 K_{\text{cal}} K_{\text{CO}_2}}{4K_2} (P_{\text{CO}_2})_{\text{initial}} = 0$$

This cubic equation is solved to give

$$\begin{aligned} m_{\text{Ca}^{2+}} &= 3.34 \times 10^{-4} \text{ m} \\ &= 33.4 \text{ mg CaCO}_3/\text{kg of water} \end{aligned}$$

The equations for case (b) were derived in Example 4. Substituting the appropriate numerical values in Eq. (3-33) gives

$$\begin{aligned} m_{\text{Ca}^{2+}} &= 1.39 \times 10^{-3} \\ &= 139 \text{ mg CaCO}_3/\text{kg of water} \end{aligned}$$

Thus the amount of  $\text{CaCO}_3$  dissolved under open-system conditions is approximately four times that dissolved under closed-system conditions. The factor of 4 applies only to the example of  $P_{\text{CO}_2} = 10^{-2}$ ; other factors apply at other  $P_{\text{CO}_2}$  values.

To calculate the final  $P_{\text{CO}_2}$  in the closed system, we can rearrange Eq. (3-33) to

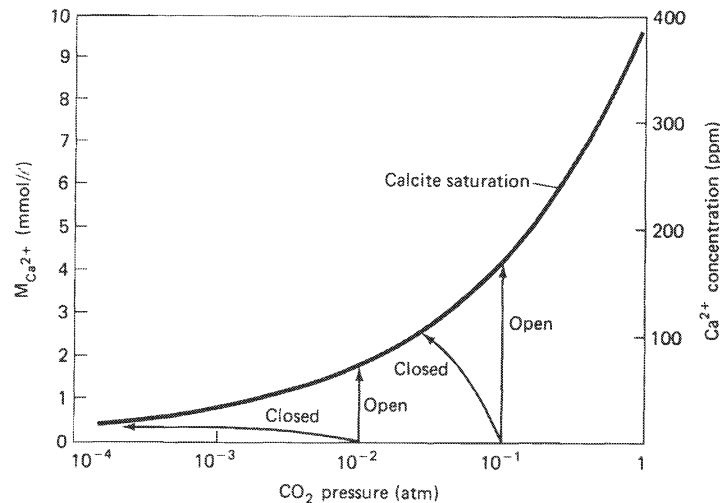
$$P_{\text{CO}_2} = \frac{m_{\text{Ca}^{2+}}^3 + 4K_2}{K_1 K_{\text{cal}} K_{\text{CO}_2}}$$

Substituting the value we calculated for  $m_{\text{Ca}^{2+}}$  gives

$$P_{\text{CO}_2} = 10^{-4.46}$$

Thus the dissolution of calcite in a closed system has reduced the  $P_{\text{CO}_2}$  from the relatively high value of  $10^{-2}$  to the below-atmospheric value of  $10^{-4.46}$ . Finally, we can calculate the pH from Eq. (3-38). The result is 8.50; at this pH our assumption that  $m_{\text{H}^+}$ ,  $m_{\text{OH}^-}$ , and  $m_{\text{CO}_3^{2-}}$  could all be neglected in the charge balance equation and the equation for  $\Sigma\text{CO}_2$  is justified.

The conclusion from Example 7 is that the amount of  $\text{CaCO}_3$  dissolved by a percolating water depends critically on whether the water is in communication with a gas phase while the mineral is dissolving (Fig. 3-8). Measured  $P_{\text{CO}_2}$  values in groundwaters in limestone aquifers are almost always above atmospheric (e.g., Back and Hanshaw, 1970; Holland et al., 1964;



**FIGURE 3-8** Changes in composition of carbonated water as it equilibrates with calcite when the system is either open or closed to exchange of CO<sub>2</sub> gas. Initial  $P_{\text{CO}_2}$  values of 10<sup>-2</sup> and 10<sup>-1</sup> atm. (After Holland et al., 1964. Reprinted from *Journal of Geology* by permission of The University of Chicago Press.)

Langmuir, 1971), suggesting that dissolution takes place largely under open-system conditions. Plummer (1977) showed that the main Floridan aquifer (a limestone aquifer underlying most of Florida) was receiving soil-derived CO<sub>2</sub> over a significant distance “downstream” from its recharge area.

In summary, waters in limestone aquifers generally have Ca<sup>2+</sup> and HCO<sub>3</sub><sup>-</sup> as the major dissolved species and are generally close to equilibrium with calcite. The Ca<sup>2+</sup> concentration (and TDS) depends on the  $P_{\text{CO}_2}$  of the water, which is generally controlled by the soil atmosphere in the recharge area. The main exceptions to these generalizations are waters in deeper aquifers which have received solutes by mixing with waters from other sources or which have received solutes by dissolution of gypsum or halite.

Two examples of groundwaters from limestone aquifers are shown in Table 3-2. The first, from central Florida, shows the typical dominance of calcium and bicarbonate. Some magnesium is also present, derived from either magnesian calcite or dolomite, but other species are generally minor. The silica was probably derived from siliceous microfossils in the rock. The water is close to equilibrium with calcite at a  $P_{\text{CO}_2}$  of about 10<sup>-2.9</sup> atm. The second analysis shows several differences. The calcium and bicarbonate concentrations are higher and the pH is lower because the water is in equilibrium with calcite at a higher  $P_{\text{CO}_2}$  value (10<sup>-2.0</sup> atm). The strikingly higher nitrate concentration is an indication of contamination by sewage, agricultural wastes, or fertilizers. Indeed, Langmuir (1971) concluded that the nitrate, sulfate, chloride, potassium, and sodium were all largely derived from human activities—sewage, fertilizer, and salting of roads in winter. Near-surface carbonate aquifers are particularly vulnerable to contamination because water commonly moves rapidly both vertically and horizontally in relatively large openings and because the aquifer material has little sorptive capacity.

The weathering of dolomite is closely analogous to that of calcite, except that rates are slower, and nearly half the HCO<sub>3</sub><sup>-</sup> in the water is balanced by Mg<sup>2+</sup> rather than Ca<sup>2+</sup>. Dolomite

**TABLE 3-2** Chemical Analyses (mg/l) of Groundwaters in Carbonate Aquifers from Central Florida (from Back and Hanshaw, 1970) and Central Pennsylvania (from Langmuir, 1971)

	Florida	Pennsylvania
Ca <sup>2+</sup>	34	83
Mg <sup>2+</sup>	5.6	17
Na <sup>+</sup>	3.2	8.5
K <sup>+</sup>	0.5	6.3
HCO <sub>3</sub> <sup>-</sup>	124	279
SO <sub>4</sub> <sup>2-</sup>	2.4	27
Cl <sup>-</sup>	4.5	17
NO <sub>3</sub> <sup>-</sup>	0.1	38
SiO <sub>2</sub>	12	—
pH	8.00	7.36
T	25°C	10°C

normally dissolves congruently. In a rock containing both calcite and dolomite, the water should ultimately come to equilibrium with calcite and dolomite, in which case:

$$\frac{a_{\text{Mg}^{2+}}}{a_{\text{Ca}^{2+}}} \approx 0.6$$

$$a_{\text{Ca}^{2+}} a_{\text{CO}_3^{2-}} = 10^{-8.48}$$

In practice, establishment of equilibrium with dolomite is slow. Such waters usually contain more calcium than magnesium near the recharge area because calcite dissolves more rapidly than dolomite. Over time periods of thousands of years, however, the magnesium/calcium ratio of the water rises to the “equilibrium” value (e.g., Plummer, 1977). Quotation marks are used because, as mentioned earlier, the equilibrium solubility of dolomite is calculated from analyses of groundwaters from dolomite aquifers, which are presumed to have had sufficient time to reach equilibrium.

#### Example 8

Use WATEQ4F to calculate the equilibrium  $P_{\text{CO}_2}$  and the state of saturation of the Pennsylvania water in Table 3-2 with respect to calcite and dolomite.

The data input is straightforward. When an item is requested for which you have no data, or which does not apply (e.g., redox calculations in this example), it is usually sufficient to hit a carriage return to move on to the next question. There are some complications associated with how alkalinity is entered into the data input file: (a) Only one set of input units is allowed. If the input units chosen are mmol/kg, alkalinity is simply entered as meq/kg. However, if the input units chosen are ppm or mg/l and alkalinity is reported in meq/kg, the alkalinity must be converted to the equivalent ppm HCO<sub>3</sub><sup>-</sup> (multiplied by 61); (b) You are given a choice of whether you want to correct the alkalinity for contributions from species such as B(OH)<sub>4</sub><sup>-</sup> and H<sub>3</sub>SiO<sub>4</sub><sup>-</sup> or whether alkalinity should be considered entirely carbonate alkalinity; (c) You are given the choice of entering a  $\Sigma\text{CO}_2$  value instead of an alkalinity value.

Selected parts of the output are shown in Table 3-3. For the Pennsylvania sample,  $P_{\text{CO}_2} = 9.67 \times 10^{-3}$  ( $10^{-2.015}$ ) atm and  $\log(IAP/K)$  is 0.027 for calcite, -0.513 for dolomite (c)

**TABLE 3-3 Selected Parts of the WATEQ4F Output for Example 8**

Pennsylvania Water from Table 3-2

```

0 0 000000      0 0 0 0 0 0 0 0 0
TEMP           = 10.000000
PH             = 7.360000
EH (0)        = 9.900000
DOC           = .000000
DOX          = .000000
CORALK       = 0
FLG          = MG/L
DENS        = 1.000000
    
```

Species Index No Input Concentration

```

-----
Ca : 0 : 83.00000000
Mg : 1 : 17.00000000
Na : 2 : 8.50000000
K : 3 : 6.30000000
Cl : 4 : 17.00000000
SO4 : 5 : 27.00000000
HCO3 : 6 : 279.00000000
H2S aq : 13 : .00000000
CO3 : 17 : .00000000
SiO2 tot : 34 : .00000000
NO3 : 84 : 38.00000000
    
```

```

Anal Cond = .0 Calc Cond = 597.0 Activity H2S calc from SO4 and pe = 0.00E+00
Anal EPMCAT = 6.0740 Anal EPMAN = 6.2300 Percent difference in input cation/anion balance = -2.5362
Calc EPMCAT = 5.8819 Calc EPMAN = 6.0378 Percent difference in calc cation/anion balance = -2.6168
Total Ionic Strength (T.I.S.) from input data = .00920
Effective Ionic Strength (E.I.S.) from speciation = .00883
    
```

Effective

```

T pH TDS ppm Ionic Str pO2 Atm ppm O2 Atm pCO2 Atm ppm CO2 Atm log pCO2 CO2 Tot Ncrb Alk aH2O
10.00 7.360 475.8 .00883 0.00E+00 0.00E+00 9.67E-03 4.25E+02 -2.015 5.08E-03 7.38E-08 .9998
    
```

TABLE 3-3 Continued

I	Species	Anal ppm	Calc ppm	Anal Molal	Calc Molal	% of Total	Activity	Act Coeff	-Log Act
0	Ca	83.000	79.002	2.072E-03	1.972E-03	95.19	1.362E-03	.6907	2.866
29	CaHCO3	1	5.735		5.676E-05	2.74	5.159E-05	.9090	4.287
31	CaSO4 aq	0	5.081		3.734E-05	1.80	3.742E-05	1.0020	4.427
4	Cl	17.000	16.999	4.797E-04	4.797E-04	100.00	4.354E-04	.9076	3.361
6	HCO3	-1	272.710	4.575E-03	4.472E-03	88.04	4.077E-03	.9118	2.390
85	H2CO3 aq	0	31.983		5.159E-04	10.16	5.171E-04	1.0023	3.286
63	H	1	.000048		4.750E-08	.00	4.365E-08	.9191	7.360
3	K	1	6.294	1.612E-04	1.611E-04	99.92	1.462E-04	.9076	3.835
1	Mg	2	16.131	6.996E-04	6.638E-04	94.89	4.611E-04	.6946	3.336
21	MgHCO3	1	1.979		2.320E-05	3.32	2.109E-05	.9090	4.676
22	MgSO4 aq	0	1.379		1.146E-05	1.64	1.148E-05	1.0020	4.940
2	Na	1	8.476	3.699E-04	3.689E-04	99.72	3.356E-04	.9099	3.474
84	NO3	-1	37.999	6.131E-04	6.131E-04	100.00	5.574E-04	.9090	3.254
26	OH	-1	.001254		7.377E-08	.00	6.706E-08	.9090	7.174
5	SO4	-2	22.275	2.812E-04	2.320E-04	82.50	1.596E-04	.6878	3.797
	Phase	Log IAP/KT	Log IAP	Sigma (A)	Log KT	Sigma (T)			
17	Anhydrite	-2.327	-6.663		-4.336				
21	Aragonite	-.128	-8.383		-8.255	.020			
19	Brucite	-6.509	11.384		17.892				
12	Calcite	.027	-8.383		-8.411	.020			
11	Dolomite (d)	-1.127	-17.237		-16.109				
401	Dolomite (c)	-.513	-17.237		-16.724				
340	Epsomite	-4.884	-7.134		-2.249				
18	Gypsum	-2.072	-6.663		-4.591				
64	Halite	-8.382	-6.835		1.546				
10	Magnesite	-1.064	-8.854		-7.789				

and  $-1.127$  for dolomite (d). The (c) and (d) refer to well-crystallized (ordered) and disordered dolomite respectively. Well-ordered crystals are always less soluble than disordered crystals (which commonly form at low temperatures in nature). The WATEQ4F database includes separate solubilities for crystalline and disordered forms for some solids and not others, depending on whether data are available. The water is thus very slightly supersaturated with respect to calcite and undersaturated with respect to both forms of dolomite.

## REVIEW QUESTIONS

In the following problems, assume activities equal concentrations and ignore complexing unless instructed otherwise. Use the constants in Table 3-1.

- What is the pH of pure water in equilibrium with 1 atmosphere of carbon dioxide at  $25^{\circ}\text{C}$ ?
- What is the pH and calcium concentration of pure water in equilibrium with calcite and one atmosphere of  $\text{CO}_2$  at  $25^{\circ}\text{C}$ ?
- What is the calcium concentration in a water in equilibrium with calcite at a  $P_{\text{CO}_2}$  of  $10^{-2.5}$  atm at  $5^{\circ}\text{C}$ ?
- The water in question 3 is warmed from  $5^{\circ}$  to  $25^{\circ}\text{C}$ . How much calcite should precipitate, assuming chemical equilibrium and (a) constant  $P_{\text{CO}_2}$ ; (b) no loss or gain of  $\text{CO}_2$  gas? In case (b), what will be the final pH and  $P_{\text{CO}_2}$ ?
- A 0.01-m  $\text{NaHCO}_3$  solution is allowed to equilibrate with calcite at a  $P_{\text{CO}_2}$  of  $10^{-1}$  atm at  $25^{\circ}\text{C}$ . How much  $\text{Ca}^{2+}$  (in ppm) will the solution contain, and what will be its pH?
- A 0.01-m  $\text{CaCl}_2$  solution is allowed to equilibrate with calcite at a  $P_{\text{CO}_2}$  of  $10^{-3.5}$  atm and  $25^{\circ}\text{C}$ . What will be the resulting pH and  $\text{HCO}_3^-$  concentration?
- What should be the pH of a puddle of rain on an outcrop of dolomite at  $25^{\circ}\text{C}$ ? (Assume chemical equilibrium.)
- An "ideal" rain consists of pure water in equilibrium with  $\text{CO}_2$  at a partial pressure of  $10^{-3.5}$  atm. By how many millimeters per century should limestone exposed to this rain be dissolved if equilibrium is attained? Assume a rainfall of 1 m/year,  $25^{\circ}\text{C}$ , a system open to  $\text{CO}_2$ , and a density for calcite of  $2.7 \text{ g/cm}^3$ .
- If the rain in question 8 were "acid," containing 0.1 meq/kg of free acidity, how many millimeters per century would be dissolved?
- A river water has the following chemical analysis:
 

$\text{Na}^+$	11.4 ppm	$\text{SO}_4^{2-}$	58 ppm
$\text{K}^+$	1.56 ppm	Alkalinity	1.30 meq/kg
$\text{Ca}^{2+}$	24.0 ppm	pH	8.10
$\text{Mg}^{2+}$	10.0 ppm	Temp.	$10^{\circ}\text{C}$
$\text{Cl}^-$	1.9 ppm		

With what  $P_{\text{CO}_2}$  would the water be in equilibrium? By how much is it supersaturated or undersaturated with respect to calcite? (Calculate activity coefficients by the Debye-Hückel equation, Chapter 2.)

- Perform the same calculations as in Problem 10 using the WATEQ4F code. How do the results compare to your "hand-calculated" values?

## SUGGESTED READING

- BUTLER, J. N. (1982). *Carbon Dioxide Equilibria and Their Applications*. Reading, MA: Addison-Wesley.
- HOLLAND, H. D., et al. (1964). On some aspects of the chemical evolution of cave waters. *Journal of Geology*, 72, 36–67. Example of the application of simple calculations to a natural system.
- MOREL, F., and J. G. HERING. (1993). *Principles and Applications of Aquatic Chemistry*. New York: Wiley.
- MORSE, J. W., and F. T. MACKENZIE. (1990). *Geochemistry of Sedimentary Carbonates*. Amsterdam, Netherlands: Elsevier.
- PLUMMER, L. N. (1977). Defining reactions and mass transfer in part of the Floridian Aquifer. *Water Resources Research*, 13, 801–812.
- REEDER, R. J., (Ed.). (1983). *Carbonates: Mineralogy and Chemistry*. Reviews in Mineralogy (vol. 11). Washington, DC: Mineralogical Society of America.
- STUMM, W., and J. J. MORGAN. (1996). *Aquatic Chemistry* (3rd ed.). New York: Wiley-Interscience. Chaps. 3 and 4. Detailed systematics of acid-base reactions, the carbonate system, and alkalinity titrations.



# 4

## Clay Minerals and Cation Exchange

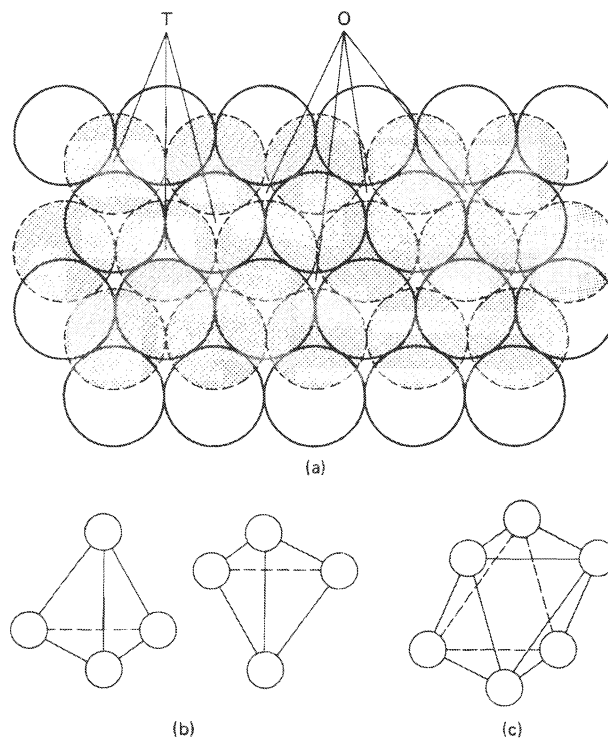
The clay minerals are defined as fine-grained, crystalline, hydrous silicates with structures of the layer lattice type. They are the most common products of water-rock interaction under earth-surface conditions. As a consequence of their structures, clay minerals are effective ion exchangers. Since clay minerals are so closely involved in processes regulating the chemistry of natural waters, some knowledge of their structure and chemistry is essential.

The term *clay* is also used in geology to denote a grain size (measured by settling velocity in water) of less than 2  $\mu\text{m}$  (or, less commonly, less than 4  $\mu\text{m}$ ). Although most clay-sized materials in nature are clay minerals, and most clay mineral particles are clay-sized, the correspondence between the terms is by no means exact. The clay fraction (grain size) of soils and sediments usually contains quartz, feldspars, iron oxides, and carbonates in addition to clay minerals, and clay minerals, particularly kaolinite and chlorite, often occur with grain sizes larger than 2  $\mu\text{m}$ .

### MINERALOGY AND COMPOSITION

#### **Brucite [Mg(OH)<sub>2</sub>] and Gibbsite [Al(OH)<sub>3</sub>]**

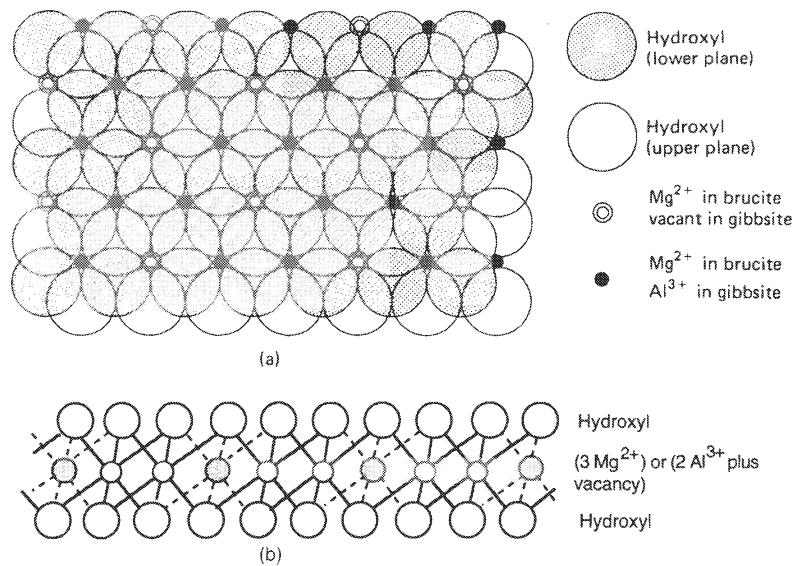
Although not strictly clay minerals, brucite and gibbsite form a good starting point for discussion of clay mineral structures. Both consist essentially of two close-packed sheets of hydroxyl ions (Fig. 4-1) with magnesium or aluminum ions in octahedral coordination between them. A close-packed layer is one in which the hydroxyl ions (which, for the purposes of the present discussion, can be regarded as rigid spheres) are arranged in the most compact way possible in a single plane. The second close-packed layer of hydroxyl ions is positioned so that the spheres in the upper plane sit in depressions between the spheres of the lower plane, just as a second layer of tennis balls would lie on an initial layer (in the absence of constraints, such as a box). Between the layers of hydroxyl ions are two types of hole: smaller *tetrahedral* holes, as they are called, in which the hole is surrounded by four hydroxyl ions in positions equivalent to the corners of a regular tetrahedron, and larger *octahedral* holes, in which there



**FIGURE 4-1** Two close-packed sheets of hydroxyl ions, superimposed as in the structures of brucite and gibbsite. (a) The two-layer sheet (lower sheet shaded) viewed from above; T and O are tetrahedral and octahedral sites, respectively. (b) Arrangement of hydroxyl ions around a tetrahedral site. (c) Arrangement of hydroxyl ions around an octahedral site. In (b) and (c), and in subsequent diagrams, hydroxyl (and oxygen) ions are shown for clarity as small circles separated from each other. In fact, the hydroxyls (oxygens) are "touching," and cations such as  $\text{Al}^{3+}$  and  $\text{Mg}^{2+}$  fit in the holes between them.

are six surrounding hydroxyls in positions corresponding to the corners of a regular octahedron (Fig. 4-1). In the brucite structure, each octahedral hole is occupied by a magnesium ion (Fig. 4-2). Thus each  $\text{Mg}^{2+}$  ion is coordinated by six  $\text{OH}^-$  ions, and each hydroxyl ion is coordinated by three  $\text{Mg}^{2+}$  ions, which corresponds to the formula  $\text{Mg}(\text{OH})_2$ . If trivalent  $\text{Al}^{3+}$  is substituted for  $\text{Mg}^{2+}$ , the brucite structure shown would not be possible, because there would be more positive than negative charges. This problem is overcome in the gibbsite structure by leaving every third octahedral hole empty (Fig. 4-2). The formula is then  $\text{Al}(\text{OH})_3$ , and the charges balance. Clay minerals related to gibbsite are called *dioctahedral*, because two out of every three octahedral sites are occupied. Clay minerals related to brucite are called *trioctahedral*. Natural gibbsites appear to be close to the ideal composition; some  $\text{Fe}^{3+}$  sometimes substitutes for  $\text{Al}^{3+}$ . Some  $\text{Fe}^{2+}$  may substitute for  $\text{Mg}^{2+}$  in the brucite structure.  $\text{Al}^{3+}$ ,  $\text{Fe}^{3+}$ ,  $\text{Fe}^{2+}$ ,  $\text{Mg}^{2+}$ , and  $\text{Li}^+$  all have ionic radii between 0.5 and 0.75 Å, which allows them to fit into the octahedral holes. The radii of  $\text{Ca}^{2+}$  (0.99 Å),  $\text{Na}^+$  (0.95 Å), and  $\text{K}^+$  (1.33 Å) are too large to allow these ions to fit into octahedral holes.

The individual sheets of brucite and gibbsite are held together by *van der Waals forces*. The van der Waals force is a weak attraction that exists between any two atoms (or planes of



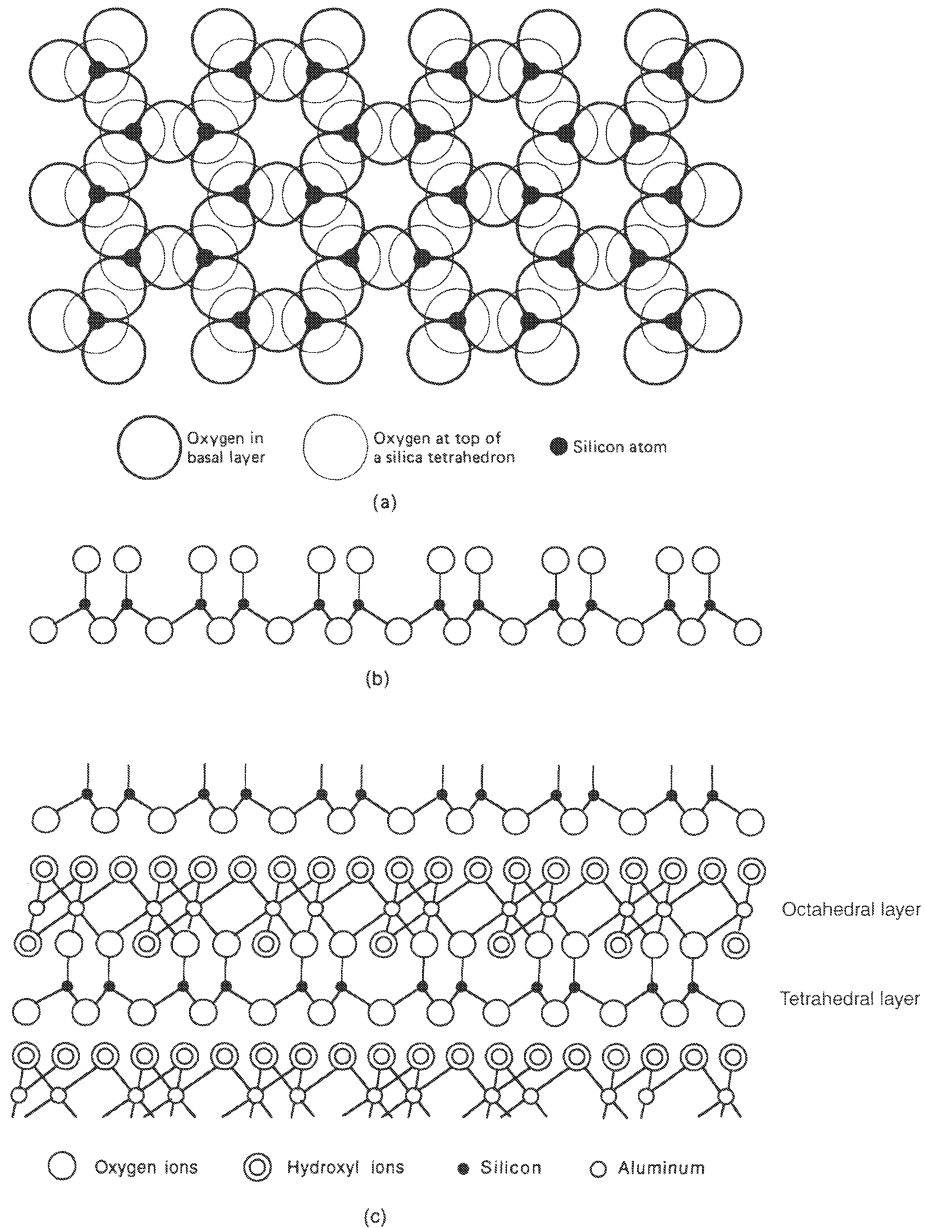
**FIGURE 4-2** The structures of brucite and gibbsite. (a) Vertical view of a sheet, showing location of cations and (in gibbsite) vacancies in octahedral sites. (b) Schematic cross section of sheet; hydroxyls shown are not in the same vertical plane as the cations.

atoms). Compared to electrostatic forces, such as those that bind the Mg<sup>2+</sup> and OH<sup>-</sup> ions within each brucite layer, the van der Waals force is much weaker and is effective over shorter distances. Brucite and gibbsite are very soft minerals because the cohesive forces between successive planes are so weak.

## Kaolinite and Related Minerals

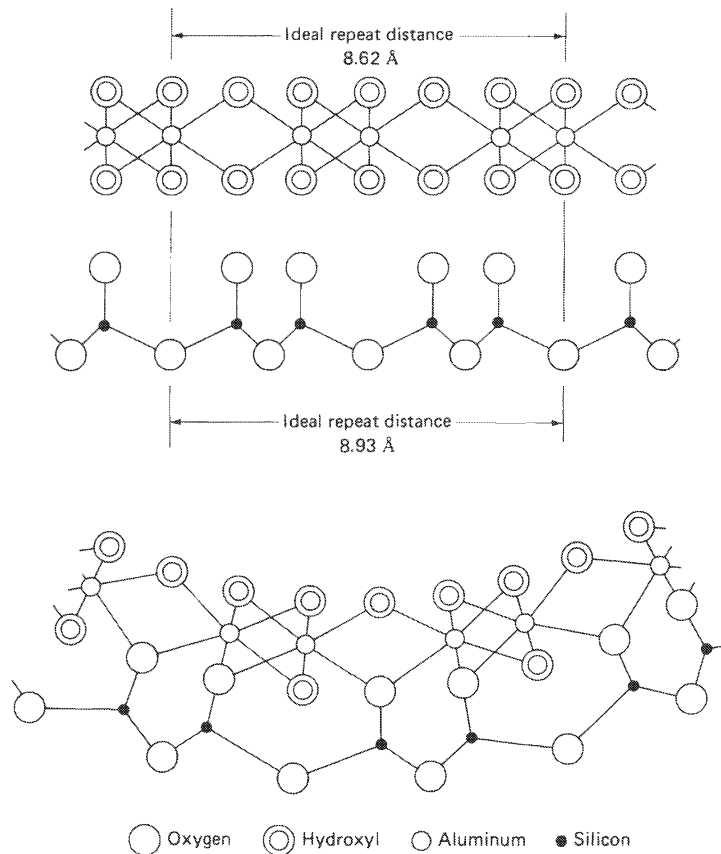
**Kaolin Group.** Kaolinite consists of an octahedrally coordinated layer of aluminum ions closely analogous to gibbsite and a layer of tetrahedrally coordinated silicon atoms (Fig. 4-3). The silicon ion (smaller than Al<sup>3+</sup>) is so small relative to oxygen and hydroxyl ions that it fits into tetrahedral sites similar to those illustrated in Fig. 4-1. Oxygen and hydroxyl ions are essentially the same size, so interchanging oxygen and hydroxyl ions makes no difference to the geometry of the brucite/gibbsite layer, provided that electrical charges are balanced in the structure as a whole.

The ideal formula of kaolinite (half the crystallographic unit cell) is Al<sub>2</sub>Si<sub>2</sub>O<sub>5</sub>(OH)<sub>4</sub>, and most minerals of the kaolin group appear to be close to ideal in composition (halloysite is discussed below). The unit layer is about 7 Å thick, which gives rise to a characteristic X-ray diffraction peak. Successive layers in the kaolin group are held together by van der Waals forces. The layers can stack in different ways, giving rise to the polymorphs kaolinite (*sensu stricto*), dickite, and nacrite. Successive layers in kaolins formed under earth-surface conditions are usually stacked in a random manner. The term *kaolinite* is often used loosely to cover all members of the kaolin group.



**FIGURE 4-3** The kaolinite structure. (a) The tetrahedral layer viewed from above. Note that the oxygen ions in the basal layer are in a close-packed arrangement, but with some vacancies. (b) Cross section of tetrahedral layer. (c) Cross section of kaolinite structure showing oxygens at the top of the tetrahedra replacing some hydroxyls in the gibbsite structure.

The ideal octahedral (gibbsite) layer in kaolinite would have a slightly smaller horizontal dimension than the ideal tetrahedral (silica) layer (Fig. 4-4). The “misfit” can be accommodated by distorting the tetrahedral layer (in kaolinite, dickite, and nacrite) or by having the



**FIGURE 4-4** Schematic illustration of how the mismatch between the octahedral and tetrahedral layers causes curvature of the lattice, which results in the tubular structure of halloysite.

layers curl and form tubes, with the octahedral layers toward the inside (Fig. 4-4). The tubular varieties of the kaolin group are generally called *halloysite*. Some varieties of halloysite have extra water molecules between the aluminosilicate layers.

**Serpentine Group.** The serpentine group minerals are the trioctahedral analogs of kaolinite, having an idealized formula  $\text{Mg}_3\text{Si}_2\text{O}_5(\text{OH})_4$ . The various members of the serpentine group (antigorite, chrysotile, lizardite) are polymorphs with curved, tubular, or very small crystallites, resulting from the fact that the ideal brucite layer is considerably larger than the ideal tetrahedral silica layer. Natural serpentines are close to the ideal chemical composition.

**7-Å Chlorite (Septechlorite) Group.** Minerals of the 7-Å chlorite (or septechlorite) group are also trioctahedral analogs of kaolinite, but differ from serpentines in having significant Fe (both  $\text{Fe}^{2+}$  and  $\text{Fe}^{3+}$ ) and Al substituting for Mg in the octahedral layer, and some Al substituting for Si in the tetrahedral layer. The substitution of an atom larger than Si in the tetrahedral layer and an atom smaller than Mg in the octahedral layer reduces the misfit between the two layers, and, as a result, crystallite morphology is usually simple. The only important member of the group forming under earth-surface conditions today is

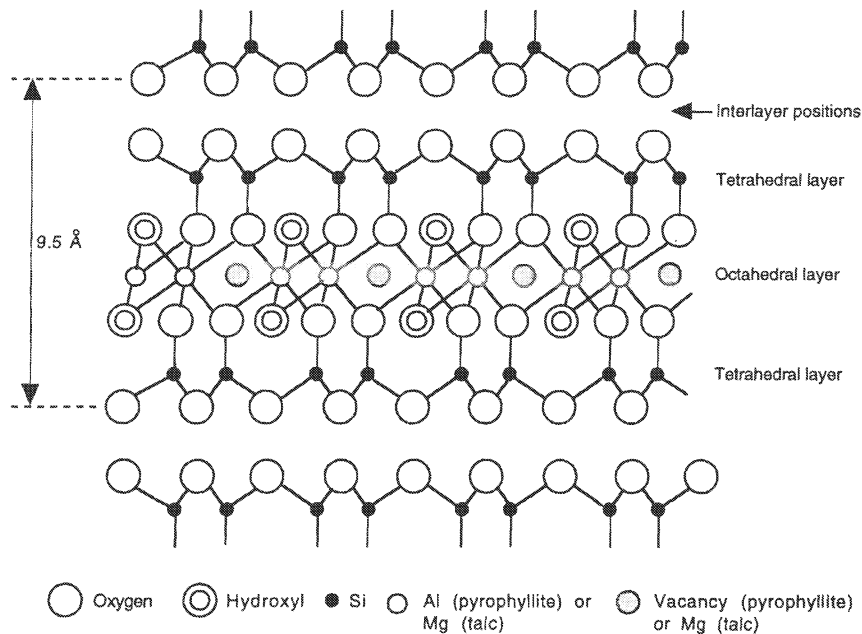
berthierine, which has an approximate formula  $(Mg_{0.3}Fe_{2.0}^{2+}Al_{0.7})(Si_{1.3}Al_{0.7})O_5(OH)_4$ , where the parentheses indicate octahedral and tetrahedral cations.

## 2:1 Clay Minerals

This large and complex group includes the micas, vermiculite, the smectite (montmorillonite) group, pyrophyllite, talc, and various mixed-layer species. They are all based on a structure consisting of two tetrahedral layers with one octahedral layer in between. Pyrophyllite  $[Al_2Si_4O_{10}(OH)_2]$  and talc  $[Mg_3Si_4O_{10}(OH)_2]$  are the simplest end members of the group (Fig. 4-5). The structures are the same except that pyrophyllite is dioctahedral and talc is trioctahedral. Other members of the 2:1 group are related to pyrophyllite or talc by one or more of the following (Fig. 4-6):

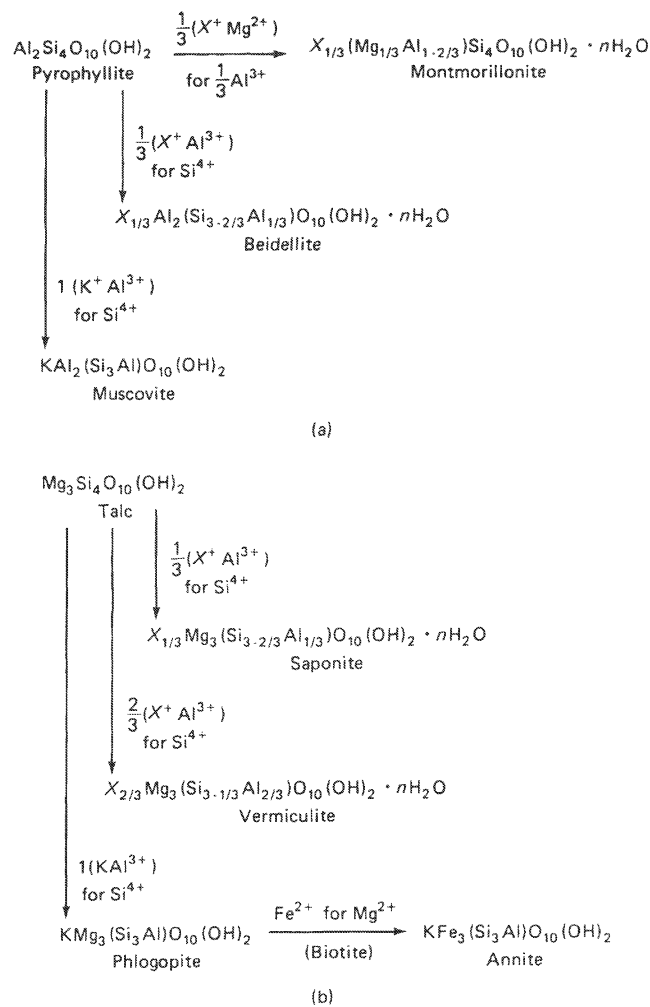
1. Substitution of  $Al^{3+}$  for  $Si^{4+}$  in the tetrahedral layers. This causes a net deficiency of charge on the 2:1 unit, which is balanced by additional cations located between the 2:1 sheets, in what are called the *interlayer positions*. When the number of interlayer cations is small, these cations are exchangeable (see below). When the number of cations is large,  $K^+$ , for geometrical reasons, is commonly the cation present, and it is not readily exchangeable.

2. Substitution of  $Mg^{2+}$  or  $Fe^{2+}$  for  $Al^{3+}$  in the octahedral layer, and the introduction of exchangeable cations into the interlayer positions to balance the resulting negative charge on the 2:1 sheets.



**FIGURE 4-5** The structure of pyrophyllite and talc. In pyrophyllite, the octahedral cation is Al, and the shaded positions are vacant. In talc, the octahedral cation is Mg, and all the octahedral positions are occupied. In pyrophyllite and talc, there is nothing in the interlayer positions and the layers are held together by van der Waals forces only. In other members of the 2:1 clay mineral group, cations and, in some minerals, water are present in the interlayer positions.

**FIGURE 4-6** Relationship of some common (a) dioctahedral and (b) trioctahedral sheet silicates to pyrophyllite and talc. Substitutions in the tetrahedral layer are shown by vertical arrows; substitutions in the octahedral layer by horizontal arrows,  $X^+$  represents exchangeable cations in the interlayer positions ( $\text{Na}^+$ ,  $\text{K}^+$ ,  $\frac{1}{2}\text{Ca}^{2+}$ ,  $\frac{1}{2}\text{Mg}^{2+}$ , etc.), and  $n\text{H}_2\text{O}$  represents interlayer water. Dioctahedral vermiculites would be similar to beidellite or montmorillonite, but with substitution of approximately  $\frac{2}{3}$  unit rather than  $\frac{1}{3}$ .



3. Substitution of  $\text{Fe}^{2+}$ ,  $\text{Fe}^{3+}$ ,  $\text{Mg}^{2+}$ , and similar cations for  $\text{Al}^{3+}$  or substitution of  $\text{Fe}^{2+}$ ,  $\text{Fe}^{3+}$ ,  $\text{Al}^{3+}$ , and similar cations for  $\text{Mg}^{2+}$  in the octahedral layer. Charge balance can be maintained either by changes in the interlayer cations or by introducing vacancies (sites not occupied by a cation) in the octahedral layer. It appears that natural minerals are generally either dioctahedral or trioctahedral in terms of the number of cations in the octahedral layer and are usually not intermediate between the two, although clays of the smectite group are so fine grained and hard to study that the existence of intermediates cannot be easily proved or disproved.

**Smectite Group.** The term *smectite* is used to describe any clay whose basal spacing (the thickness of the 2:1 sheet plus the interlayer space) expands to 17 Å on treatment with ethylene glycol. Such minerals have been traditionally called *montmorillonite*; this has caused confusion because the term *montmorillonite* was also used for a specific member of the smectite group. Expansion by ethylene glycol is indicative of a structure in which the number

of cations in the interlayer positions corresponds to a positive charge of about 0.2 to 0.5 unit per formula unit [ $O_{10}(OH)_2$ ]. In montmorillonite (*sensu stricto*), the balancing negative charge is derived by substitution of  $Mg^{2+}$  for  $Al^{3+}$  in the octahedral layer of pyrophyllite. In beidellite, another smectite, the charge is derived by substitution of  $Al^{3+}$  for  $Si^{4+}$  in the tetrahedral layer of pyrophyllite. Substitution of  $Al^{3+}$  for  $Si^{4+}$  in the tetrahedral layer of talc results in the mineral saponite. The compositional variations in the smectite group are enormous, resulting from substitution of different amounts of  $Mg^{2+}$ ,  $Al^{3+}$ ,  $Fe^{2+}$ ,  $Fe^{3+}$ ,  $Li^+$ , and other cations in the octahedral layer and substitution of  $Al^{3+}$  and probably  $Fe^{3+}$  for  $Si^{4+}$  in the tetrahedral layer. Smectites normally occur as extremely small crystals (less than 1  $\mu m$ ), so identification is usually based on X-ray powder diffraction. Since it is usually impossible to separate pure smectite from fine-grained mixtures\*, there are relatively few reliable data available on the compositions of smectites in soils and sediments.

The interlayer cations in smectites are exchangeable: if the clay is placed in a solution of NaCl, the interlayer cations will be largely  $Na^+$ , in a solution of  $CaCl_2$  they will be largely  $Ca^{2+}$  and similarly for other cations. Various organic molecules (such as ethylene glycol mentioned above) can also enter the interlayer space, causing characteristic interlayer spacings in X-ray diffraction.

Water is also normally present in the interlayer space of smectites. The amount of water is determined by the nature of the interlayer cation, the net charge on the 2:1 layer, and the humidity of the environment to which the clay is exposed. When the interlayer cation is divalent ( $Mg^{2+}$  or  $Ca^{2+}$ ), two layers of water molecules are normally present unless the humidity is very low. This gives a basal spacing of about 14 Å. When the interlayer cation is  $Na^+$ , the amount of interlayer water may increase almost indefinitely as the relative humidity approaches 100 percent, causing the grains to expand or swell. The swelling behavior of sodium-saturated smectites has important practical consequences. If a smectite-containing soil becomes sodium saturated, its permeability decreases and its structure breaks down, making it unsuitable for agriculture. If the clays in an aquifer become sodium saturated, permeability is likely to decrease. The shrinking-swelling behavior of smectites may make slopes unstable and may cause severe problems for the foundations of buildings. Potassium-saturated smectites do not swell as sodium-saturated ones do, but their basal spacings are more variable than those of smectites saturated with  $Mg^{2+}$  or  $Ca^{2+}$ . As humidity decreases, water may be completely excluded from the interlayers.

**Vermiculite.** When the charge on the 2:1 sheet is greater than about 0.5 unit per  $O_{10}(OH)_2$ , the electrostatic forces holding the 2:1 layers together are sufficiently strong that the interlayer space is no longer easily expandable by organic molecules, and the interlayer cations are less readily exchangeable. Vermiculites have a higher charge on the 2:1 sheets than smectites\*\* [about 0.5 to 0.7 per  $O_{10}(OH)_2$ ], and as a consequence, vermiculite does not expand to 17 Å when treated with ethylene glycol. When the interlayer cation in vermiculite

\*The  $<0.1 \mu m$  size-fraction of soils and sediments is often almost pure smectite, but there is always a question of whether this very fine material is representative of the bulk of the smectite in the sample.

\*\*The practical definition of vermiculite is based on swelling properties in organic liquids. Swelling behavior does not necessarily correspond exactly to interlayer charge, so there is some overlap in the interlayer-charge values for vermiculites and smectites.



is  $\text{Mg}^{2+}$ , two layers of water are normally present in the interlayer space, giving a basal spacing of about 14 Å. When the interlayer cation is  $\text{K}^+$ , water may be excluded from the interlayer space, giving a basal spacing of about 10 Å. Macroscopic vermiculite crystals are all trioctahedral; dioctahedral vermiculite occurs as very small crystals in some soils and sediments. In general, the structure and properties of vermiculites are similar to those of smectites. The differences are a result of the higher electrostatic charge on the silicate framework, balanced by more interlayer cations.

**Mica Group.** The structure of the common micas is related to those of pyrophyllite and talc by substitution of one  $\text{Al}^{3+}$  ion for one of the four  $\text{Si}^{4+}$  ions in the tetrahedral layer and introduction of one  $\text{K}^+$  ion into the interlayer position. The layers in the micas are held together by relatively strong electrostatic forces between the negatively charged silicate layers and the  $\text{K}^+$  ions between them. Thus the micas are much harder than talc, no water is present in the interlayer space, and the  $\text{K}^+$  ions are not exchangeable under normal conditions. The basal spacing of the micas is about 10 Å.

The common dioctahedral mica is *muscovite*  $[\text{KAl}_2(\text{Si}_3\text{Al})\text{O}_{10}(\text{OH})_2]$ ; the common trioctahedral micas are *phlogopite*  $[\text{KMg}_3(\text{Si}_3\text{Al})\text{O}_{10}(\text{OH})_2]$  and *biotite*. Biotite is similar to phlogopite but has some  $\text{Fe}^{2+}$  in place of  $\text{Mg}^{2+}$ .

The term *illite* was originally introduced to cover all clay-sized (less than 2 μm) minerals belonging to the mica group, that is, clay minerals that show a 10-Å basal spacing in X-ray diffraction (Grim et al., 1937). Illites are the most common clay minerals in nature, making up the bulk of ancient shales. The illites in ancient shales are not ideal muscovite. Compared to muscovite, they contain less K and Al and more Si. They also contain some Mg and Fe. Most natural illites have a mixed-layer structure; about 80 percent of the layers are similar to muscovite, and 20 percent are similar to smectite (Srodon et al., 1986; Hower and Mowatt, 1966). The term *illite* is sometimes used in the more restricted sense of an 80:20 mica:smectite mixed-layer clay mineral rather than the original definition given above; the precise meaning varies from author to author.

*Glaucosite* is an iron-rich variety of illite, which forms (or whose precursor mixed-layer mineral forms) in sedimentary environments, commonly on the sea floor.

## Chlorite

The chlorite structure can be thought of as the talc structure with an additional brucite layer between the 2:1 layers, making it a 2:2 clay mineral (Fig. 4-7). The resultant basal spacing is about 14 Å. Natural chlorites have variable amounts of  $\text{Al}^{3+}$ ,  $\text{Fe}^{2+}$ , and  $\text{Fe}^{3+}$  substituting for  $\text{Mg}^{2+}$  and  $\text{Al}^{3+}$  substituting for  $\text{Si}^{4+}$ . Names have been assigned to the various compositional varieties (see, e.g., Bailey, 1988), but they will not be listed here. The ideal formula is  $(\text{Mg,Fe,Al})_3(\text{Si,Al})_4\text{O}_{10}(\text{OH})_2 \cdot (\text{Mg,Al,Fe})_3(\text{OH})_6$  or  $(\text{Mg,Fe,Al})_6(\text{Si,Al})_4\text{O}_{10}(\text{OH})_8$ , where the atoms within each set of parentheses can be in any relative proportion provided charges balance for the structure as a whole. The true (or 14 Å) chlorites have the same chemical formula as the 7-Å chlorites. It appears that for most compositions the 14-Å structure is more stable than the 7-Å structure, which would explain why 7-Å chlorites are rare. Chlorites form most

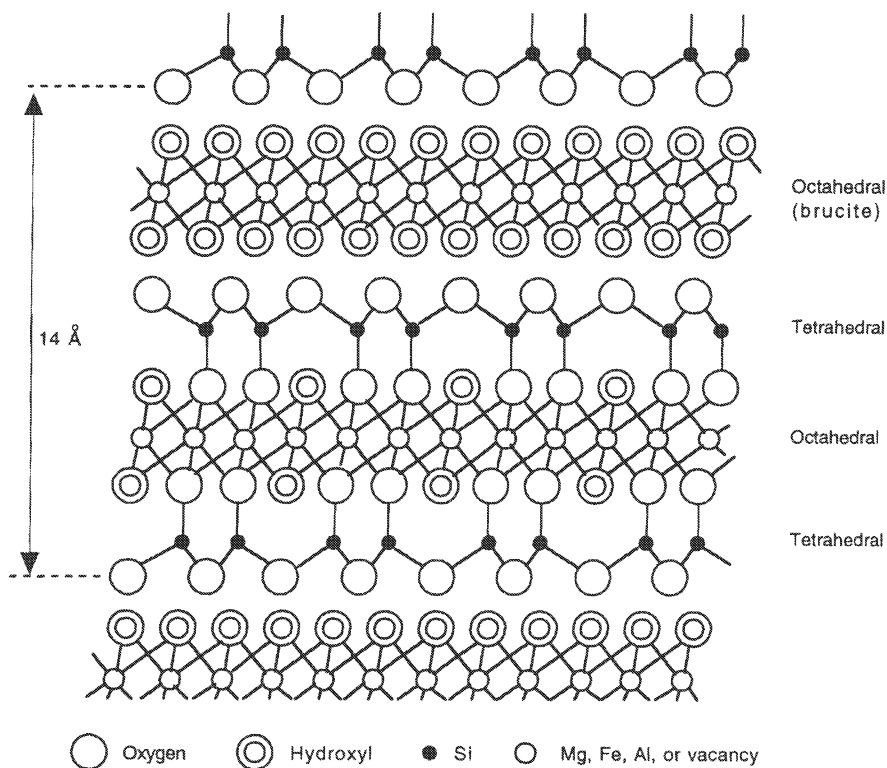
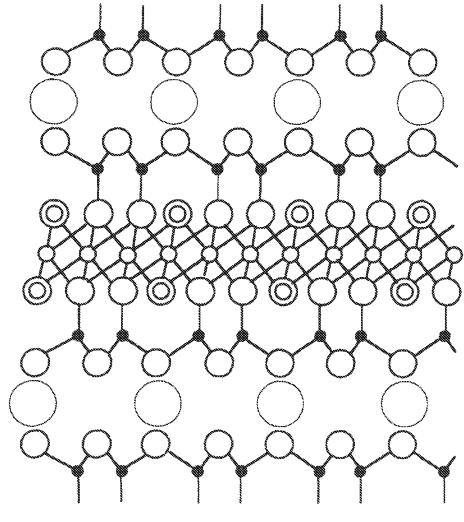


FIGURE 4-7 The structure of chlorite.

commonly during diagenesis and low-grade metamorphism; they are formed in minor amounts in soils and on the sea floor.

### Mixed-Layer Clays

The structures of all the 2:1 clays and chlorite are closely related (Fig. 4-8). It is not surprising, therefore, that minerals occur that contain more than one type of interlayer behavior. As mentioned above, some layers in a crystal may be of the smectite type and some of the mica type, giving a mixed-layer illite-smectite. Also, regions of gibbsite or brucite may occur between the layers of a smectite or vermiculite, giving what is called either a mixed-layer chlorite-smectite (-vermiculite) or a hydroxy-interlayer smectite (vermiculite). The different layers may be distributed randomly or may exhibit several types of ordering, making precise identification of mixed-layer structures difficult. The most successful approach has been to simulate the X-ray diffraction patterns of the various possible mixed-layer structures on the computer and compare the simulations with the X-ray diffraction pattern of the natural material (Reynolds, 1980, 1985, 1988; Reynolds and Hower, 1970). There is some uncertainty whether the mixed-layer structures identified by X-ray diffraction are really present in the natural material or whether they result in part from stacking of very thin crystallites on the X-ray mount (Wilson and Nadeau, 1985).



	Mica (common)	Smectite	Chlorite
Interlayer positions	$K_1$	(Exchange cations) $_{1/3}$ + $H_2O$	$Mg(OH)_2$ $Al(OH)_1$ sheets
Tetrahedral positions	$Si_3Al$	$Si_4$ (some Al and $Fe^{3+}$ in some varieties)	$Si_4$ to $Si_2Al_2$
Octahedral positions	$Al_2$ (muscovite) ( $Mg, Fe$ ) $_3$ (biotite)	Al, $Fe^{2+}$ , $Fe^{3+}$ , Mg	Mg, Al, Fe
Thickness of unit layer	10 Å	Varies with $H_2O$ content. Commonly 14 Å; expands to 17 Å with glycol	14 Å
Simplest formula	$KAl_3Si_3O_{10}(OH)_2$ (muscovite)	$Na, Al, Mg, Si_4O_{10}(OH)_2$ $\frac{1}{3}, \frac{2}{3}, \frac{1}{3}$ (montmorillonite)	$Mg_6Si_4O_{10}(OH)_8$

FIGURE 4-8 Summary of the 2:1 and 2:2 clay mineral structures. Vermiculite is similar to smectite, but with (exchange cations) $_{2/3}$ .

### Sepiolite and Palygorskite

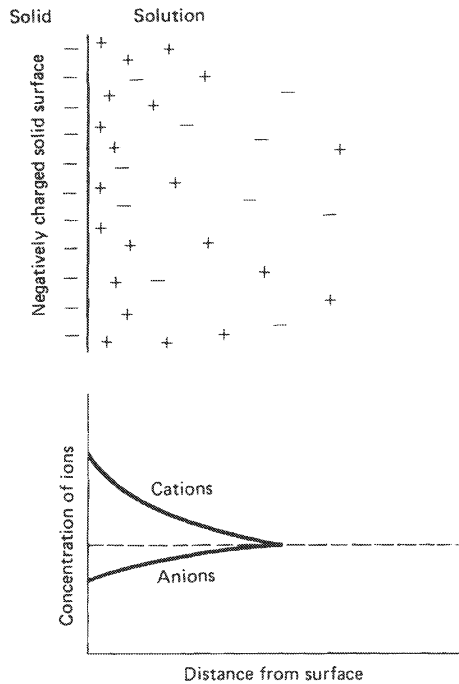
In *sepiolite* and *palygorskite* (synonymous with *attapulgit*), the 2:1 layers do not form continuous sheets, but form fibers six (sepiolite) or four (palygorskite) silicon tetrahedra wide. Simplified formulas are  $Mg_4Si_6O_{15}(OH)_2 \cdot 6H_2O$  and  $(Mg, Al, Fe)_4Si_8O_{20} \cdot nH_2O$ , respectively. Sepiolite may occur as the pure Mg end member, but most sepiolites and all natural palygorskites contain some aluminum and usually some exchangeable cations.

## COLLOID PROPERTIES

When a clay particle such as a smectite is suspended in water, some of the interlayer cations pass into solution, resulting in a negatively charged silicate framework surrounded by a diffuse cloud of cations (Fig. 4-9). The charged surface and diffuse cloud of oppositely charged ions (called counterions) are called a *double layer*. A double layer may also consist of a positively charged surface surrounded by a cloud of anions. The stability of colloidal suspensions (see below) and the ion-exchange properties of solids are closely related to the behavior of the double layer.

In smectites, the surface charge results from substitutions in the silicate framework, so the charge is more or less independent of pH. In most other natural colloids (e.g., oxides of Si, Al, Fe, Mn, or colloidal organic matter), the surface charge results from ionization of, or adsorption on, the surface of the solid, which will be discussed in Chapter 5.

**FIGURE 4-9** Simple picture of the electrical double layer, in which excess negative charge on a solid surface is balanced by an excess concentration of cations in solution near the solid–solution interface.

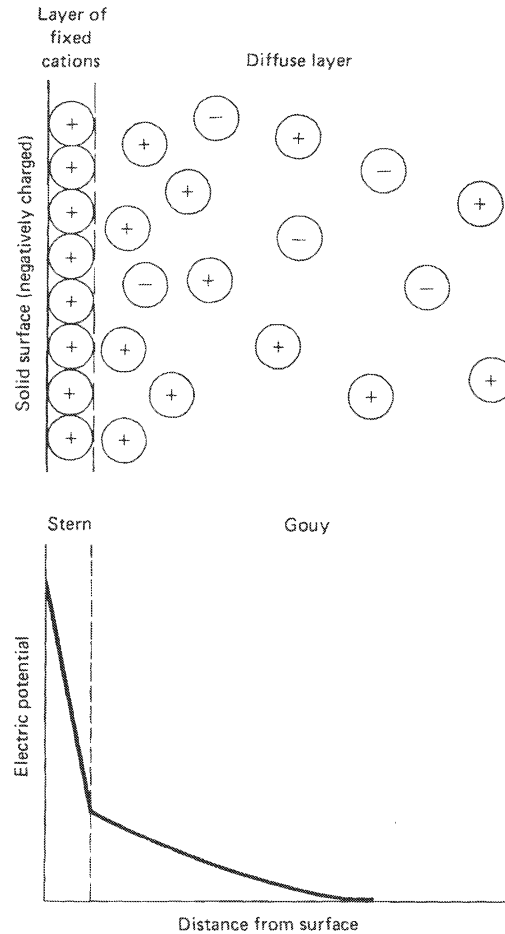


### The Double Layer

The structure of the double layer has been the subject of a great deal of study, and several mathematical models are available to describe the distribution of ions within it (Westall and Hohl, 1980). In general terms, the double layer consists of ions more or less attached to the solid surface (the *fixed* or *Stern* layer) and outside that a *diffuse* (or *Gouy*) layer in which the ions are free to move (Fig. 4-10). In smectites (and most other clays under most conditions), the silicate framework is negatively charged and exchangeable cations form the fixed and diffuse layers. In the Gouy layer the concentration of cations not balanced by anions decreases exponentially away from the boundary with the fixed layer. The ions in the fixed layer may be held by purely electrostatic forces or by formation of complexes with groups on the surface of the solid (see Chapter 5).

The stability of a colloidal suspension depends on the thickness of the Gouy layer, which depends on the electrical potential at the outside of the fixed layer and, approximately, on the ionic strength of the solution. When two particles approach each other, the Gouy layer on one particle is repelled electrostatically by the Gouy layer on the other. This keeps the particles apart, and a stable suspension results. As ionic strength increases, the Gouy layer becomes compressed close to the particle. When this happens, the electrostatic repulsion that tends to keep the particles apart is not sufficient to counteract the van der Waals force, which attracts the particles toward each other, and the suspension is no longer stable. This is why clay minerals commonly form stable suspensions in fresh water but flocculate in more saline solutions such as seawater. Although the stability of colloidal suspensions is approximately related to ionic

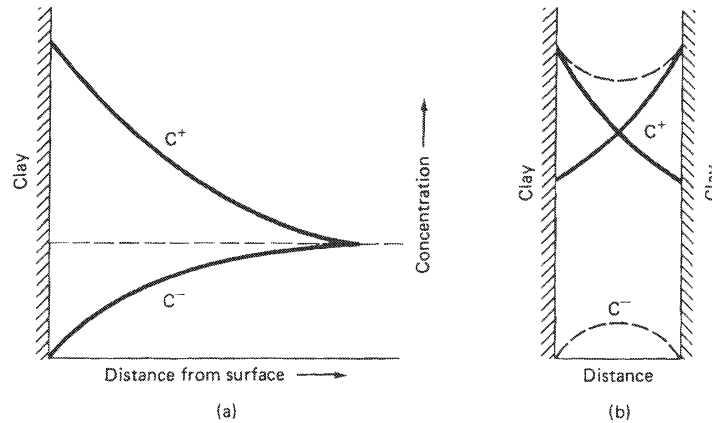
**FIGURE 4-10** Schematic picture of the fixed (Stern) and diffuse (Gouy) layers.



strength, polyvalent cations have a disproportionately greater effect in causing flocculation than monovalent cations. For this reason polyvalent cations are often used in water treatment to cause flocculation.

### Membrane Filtration

When the solid particles in a clay-water system are compacted, the Gouy layers on adjacent particles overlap. The solution in pores between adjacent grains will be made up of the Gouy layers only, and consequently anions will be almost excluded from the pores (Fig. 4-11), an effect called *anion exclusion*. When a pressure gradient is imposed on the solution in a clay-water system, water molecules can move through the pores but, as a consequence of anion exclusion, ions cannot (the theory is discussed by Hanshaw and Coplen, 1973). The clay thus behaves as a semipermeable membrane, allowing the passage of water but not ions. Clays do not act as perfect semipermeable membranes; they retain different ions with different degrees



**FIGURE 4-11** Concentrations of cations ( $C^+$ ) and anions ( $C^-$ ) (a) in the diffuse double layer of a single particle, and (b) in a pore between two closely approaching clay particles. Note how anions are excluded from the narrow pore.

of effectiveness, causing a chemical fractionation as water passes through (Kharaka and Berry, 1973). Membrane filtration has been suggested to be a major process affecting the composition of water trapped in deeply buried sedimentary rocks (e.g., Graf, 1982). It would be effective only when the original sediments have undergone compaction, so it is not an important process in near-surface (depth less than 1 km or so) environments. It could be effective at shallower depths where the solution is very dilute (lake sediments) and hence the Gouy layers extend far from the particle, but this has not been documented in nature. There is considerable disagreement in the literature as to the overall importance of membrane filtration in influencing the chemistry of underground waters.

### Ion Exchange

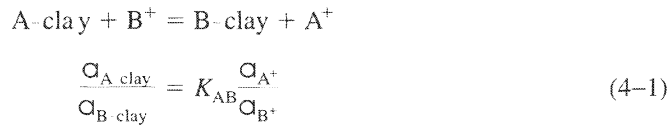
Clay minerals all exhibit ion exchange behavior to some degree, as do zeolites, colloidal oxyhydroxides, and natural organic compounds. In soil science and geology, cation exchange capacity (CEC) is often measured by (and hence defined by) uptake and release of ammonium ions from 1M ammonium acetate solution at pH 7.0, although other cations are sometimes used in place of  $NH_4^+$ . Some reported cation-exchange capacities are shown in Table 4-1. Cation-exchange capacity in clay minerals is not a very precise or fundamental quantity. It varies as a function of pH and it varies as a function of the nature of the ions

**TABLE 4-1** Cation-Exchange Capacities (meq/100g) of Clay Materials

Smectites	80–150
Vermiculites	120–200
Illites	10–40
Kaolinite	1–10
Chlorite	<10

occupying the exchange sites. For example, a river clay from the Rio Ameca in Mexico had a CEC of 76 meq/100 g. When the same clay was placed in seawater for 2 weeks and the CEC remeasured, the value was only 66 meq/100 g (Russell, 1970). The difference did not reflect any fundamental change in the clay; it appears to be a consequence of the fact that the  $K^+$  picked up in seawater in exchange for  $Ca^{2+}$  was not rapidly displaced by  $NH_4^+$ . In general, we would expect cations located in the Gouy layer to exchange rapidly, whereas cations in the Stern layer might exchange rapidly or slowly, depending on their bonding to the particle surface. Oxides and organic matter, which commonly form coatings on clay minerals (Jenne, 1977), often have high exchange capacities; specific values must be interpreted with caution because the surface charge (and hence CEC) of such material is strongly dependent on pH (Chapter 5).

Exchange equilibrium between two monovalent (or two divalent) cations can be represented by the mass action equation



where  $\alpha_{A\text{-clay}}$  and  $\alpha_{B\text{-clay}}$  represent the activities of A and B on the exchange sites,  $\alpha_{A^+}$  and  $\alpha_{B^+}$  are the activities in solution, and  $K_{AB}$  is the exchange constant. If Eq. (4-1) is written with equivalent fractions (the fractions of the CEC represented by the particular ion) instead of activities in the solid phase and concentrations instead of activities in solution, then

$$\frac{X_{A\text{-clay}}}{X_{B\text{-clay}}} = K'_{AB} \frac{m_{A^+}}{m_{B^+}} \quad (4-2)$$

$K'_{AB}$  is called the *selectivity coefficient*. The selectivity coefficient is not a constant because the activity-equivalent fraction correction will vary as a function of the ratio of A to B on the solid. Several authors (see Sayles and Mangelsdorf, 1979) have suggested that exchange between  $Ca^{2+}$  and  $Mg^{2+}$  on clays can be described by the equation

$$\frac{X_{Ca\text{-clay}}}{X_{Mg\text{-clay}}} = K \left( \frac{\alpha_{Ca^{2+}}}{\alpha_{Mg^{2+}}} \right)^p$$

where the exponent  $p$  (related to the nonideal solid solution behavior of the exchanger) has a value of about 0.7 to 0.9. An alternative approach to selectivity coefficients based on electrostatic processes in the double layer is given by Neal and Cooper (1983).

If A and B are the only cations in the system, Eq. (4-2) can be rewritten as

$$\frac{m_{A\text{-clay}}}{CEC m_{A\text{-clay}}} = K'_{AB} \frac{m_{A^+}}{M m_{A^+}} \quad (4-3)$$

where  $m_{A\text{-clay}}$  is the concentration of A adsorbed on the clay (in units of meq/kg of solid),  $CEC$  is the cation exchange capacity of the clay (meq/kg), and  $M$  is the total concentration of cations in solution (meq/kg of solution). If the concentrations of A in solution and on the clay are small compared to  $M$  and  $CEC$ , respectively, Eq. (4-3) reduces to

$$m_{A\text{-clay}} = K'_{AB} \frac{CEC}{M} m_{A^+}$$

or

$$m_{A \text{ clay}} = K_d m_{A^+} \quad (4-4)$$

$K_d$  is the *distribution coefficient* for A between solid and solution. Thus the amount of an ion that is present in trace amounts that is adsorbed on an ion exchanger is directly proportional to the concentration in solution. For calculation of the migration of minor species in an aquifer, the distribution coefficient is the quantity that must be known. Note that  $K_d$  is a function of the other ions in solution ( $M$ ), so a distribution coefficient measured for a particular ion on a particular sediment in a particular solution cannot be used for calculations involving other solutions or other sediments.

**Monovalent-Divalent Exchange.** For exchange between a monovalent and a divalent cation, Eq. (4-1) becomes

$$2 A \text{-clay} + C^{2+} = C \text{-clay} + 2A^+ \quad (4-5)$$

$$\frac{\alpha_{C \text{-clay}}}{\alpha_{A \text{-clay}}^2} = K_{AC} \frac{\alpha_{C^{2+}}}{\alpha_{A^+}^2}$$

where  $\alpha_{C \text{-clay}}$  is the activity of C on the solid phase and  $K_{AC}$  is the equilibrium constant. If equivalent fractions are substituted for activities in the solid phase and concentrations are substituted for activities in solution, Eq. (4-2) becomes

$$\frac{X_{C \text{ clay}}}{X_{A \text{ clay}}^2} = K'_{AC} \frac{m_{C^{2+}}}{m_{A^+}^2} \quad (4-6)$$

$K'_{AC}$  will not be a true constant because activity coefficients in the solid are dependent on composition.

There are some important consequences of the squared terms in Eq. (4-6). Consider a system in which  $K'_{AC} = 1$ ,  $m_{C^{2+}} = 1$ , and  $m_{A^+} = 1$  (these are arbitrary numbers for illustration purposes). Solving Eq. (4-6) subject to the condition that  $X_A + X_C = 1$  gives  $X_A = 0.62$ ,  $X_C = 0.38$ ; the ratio of the concentration of C on the exchanger to that of A (in equivalents) is 0.61. Suppose that we now dilute the solution by a factor of  $10^3$ , keeping the ratio of C to A in solution constant; what will be the ratio of C to A on the clay?

If we assume a constant cation-exchange capacity,

$$X_C = 1 - X_A$$

Substituting this and the numerical values in Eq. (4-6) gives

$$\frac{1 - X_A}{X_A^2} = 1 \times \frac{10^{-3}}{10^{-6}} = 10^{+3}$$

$$10^3 X_A^2 + X_A - 1 = 0$$

$$X_A = 0.03 \text{ and } X_C = 0.97$$

Now instead of  $X_C/X_A = 0.61$ , we have  $X_C/X_A = 31$ . The divalent cation has almost completely displaced the monovalent cation on the exchange sites. The monovalent-divalent effect is important in nature. In fresh (dilute) waters, the dominant exchangeable cation is calcium (divalent), whereas in the ocean (concentrated), the dominant exchangeable cation is sodium (monovalent) (Table 4-2). The effect has also led to problems in measuring the exchangeable cations on clay minerals in marine sediments. If the sediment is washed with distilled water to



**TABLE 4-2** Equivalent Fractions of Exchangeable Cations (Excluding H<sup>+</sup>) on Amazon River Sediment and on Amazon River Sediment Equilibrated with Seawater<sup>a</sup> (from Sayles and Mangelsdorf, 1979)

	$X_{\text{Na}^+}$	$X_{\text{Ca}^{2+}}$	$X_{\text{Mg}^{2+}}$	$X_{\text{K}^+}$
Amazon River sediment	0.004	0.80	0.17	0.014
Equilibrated with seawater	0.38	0.16	0.38	0.08

<sup>a</sup>Since oxides and the edges of clay particles gain and lose protons as pH changes, there is a problem in the definition of exchangeable H<sup>+</sup>. If exchangeable H<sup>+</sup> is defined to be zero in clays equilibrated with seawater, the river clay would contain an equivalent fraction of 0.17 exchangeable H<sup>+</sup>.

remove enclosed seawater, the resulting dilution causes divalent cations in solution to displace monovalent cations from the clay (Sayles and Mangelsdorf, 1977).

Eq. (4-6) can be generalized for cations of any valence. Consider exchange between cations A<sup>p+</sup> and B<sup>q+</sup>

$$qA\text{-clay} + pB^{q+} = pB\text{-clay} + qA^{p+}$$

$$\left(\frac{X_B^p}{X_A^q}\right)_{\text{clay}} = K'_{AB} \frac{m_{B^{q+}}^p}{m_{A^{p+}}^q} \quad (4-7)$$

Eq. (4-7) is referred to in the soils literature as the *Gaines-Thomas equation*. Another equation that is sometimes used to describe exchange among ions of different valence is the *Gapon Equation*

$$\left(\frac{X_B}{X_A}\right)_{\text{clay}} = K_{\text{gapon}} \frac{m_{B^{q+}}^{1/q}}{m_{A^{p+}}^{1/p}}$$

The difference between the Gaines-Thomas equation and the Gapon equation is essentially that no exponents are applied to the adsorbed concentrations in the Gapon equation. One would think that one of these equations would have to be “right” and the other “wrong.” However, both can be derived theoretically (from slightly different assumptions) and because adsorbed ions do not form an ideal solid solution, experimental data can often be fitted equally well to either.

Ion-exchange reactions will exert an important control on water chemistry whenever water is in contact with sediments. For example, in an aquifer with a cation-exchange capacity of 5 meq/100 g and a porosity of 20 percent (typical values), the exchange capacity of the solids is equivalent to about 500 meq/l of groundwater. This number is much larger than the concentration of dissolved cations in dilute groundwater, so exchangeable ions exert a strong buffering action on the composition of groundwaters. (The effect of ion exchange on the migration of pollutant cations is discussed in Chapter 16.)

## REVIEW QUESTIONS

1. The mineral nontronite has an ideal formula  $\text{Na}_{0.33}\text{Fe}^{3+}\text{Al}_{0.33}\text{Si}_{3.67}\text{O}_{10}(\text{OH})_2 \cdot n\text{H}_2\text{O}$ . To which of the 2:1 mineral groups does it belong? Is it dioctahedral or trioctahedral?
2. Sketch the structure of chlorite. What bonds have to be rearranged, and what atoms shifted, to go from the regular chlorite structure to the 7-Å chlorite structure?

3. If an illite consists of 80 percent ideal muscovite layers and 20 percent ideal montmorillonite layers, what should its chemical composition and cation-exchange capacity be?
4. What should be the range in cation-exchange capacity of a sediment consisting of 60 percent montmorillonite, 20 percent kaolinite, and 20 percent illite? (Use Table 4-1.)
5. Ten grams of a sodium-saturated smectite (CEC = 100 meq/100 g) are mixed with 1 l of water containing 10 ppm Na<sup>+</sup> and 10 ppm K<sup>+</sup> as the only cations. If

$$\left( \frac{X_{K^+}}{X_{Na^+}} \right)_{clay} = 2 \frac{m_{K^+}}{m_{Na^+}}$$

what will be the resulting concentrations of Na<sup>+</sup> and K<sup>+</sup> in solution?

### SUGGESTED READINGS

- |   |   |
|---|---|
| <p>BAILEY, S. W., (Ed.). (1988). <i>Hydrous Phyllosilicates</i>. Reviews in Mineralogy 19, Mineralogical Society of America.</p> <p>DIXON, J. B., and S. B. WEED, (Eds.). (1977). <i>Minerals in Soil Environments</i>. Madison, WI: Soil Science Society of America.</p> | <p>VAN OLPHEN, H. (1963). <i>An Introduction to Clay Colloid Chemistry</i>. New York: Wiley-Interscience.</p> <p>WEAVER, C. E. (1989). <i>Clays, Muds, and Shales</i>. Development in Sedimentology 44. Amsterdam, Netherlands: Elsevier.</p> |
|---|---|

# 5

## Adsorption

In the context of this book, adsorption is attachment of a solute to the surface of a solid or, more generally, the accumulation of solutes in the vicinity of a solid-solution interface. We can subdivide adsorption mechanisms into *physical adsorption*, where the attraction to the surface is due to relatively weak van der Waals forces; *electrostatic adsorption*, where ions in solution are attracted by a surface of the opposite electrical charge; and *chemical adsorption*, where there is chemical bonding between the solute molecule and one or more atoms on the surface of the solid. Cation exchange, discussed in the previous chapter, is an example of electrostatic adsorption. Adsorption is probably the most important chemical process affecting the movement of contaminants in groundwater (Chapter 16) and is an important influence on mineral dissolution rates (Chapter 11). Typically, the concentrations of heavy metals in natural waters are far below the values that would be predicted for saturation with respect to a solid phase. The most common reason for the low concentrations is adsorption onto a solid phase such as an iron or manganese oxide or hydroxide (collectively referred to as oxyhydroxides). If we are to predict the movement of heavy metals in soils and groundwater, we need to be able to model adsorption processes quantitatively. The mathematical approach that is used to describe adsorption ranges from relatively simple empirical equations to sophisticated mechanistic models of interactions at the solid-solution interface. The discussion here is presented in terms of adsorption of inorganic ions. However, many of the same principles and equations apply to the adsorption of organic solutes (Chapter 6).

### EMPIRICAL EQUATIONS

There are many situations where a relatively simple equation is adequate to describe adsorption. For example, in the previous chapter we saw that, for an ion present in trace concentrations in a solution of constant composition, the equations describing cation exchange could be reduced to a simple distribution coefficient (Eq. 4-4). Use of a simple equation is advantageous when adsorption is added to an already complex hydrologic

model, and in many instances the amount of data available is insufficient to justify a more sophisticated approach. The equation (or its graphical representation) relating the concentration of a species adsorbed on a solid to its concentration in solution is often referred to as an *isotherm*, stemming originally from the fact that the measurements were made at constant temperature.

### Linear Distribution Coefficient

The simplest adsorption isotherm is the linear distribution coefficient or linear  $K_d$  (Fig. 5-1)

$$m_{i(\text{ads})} = K_d m_{i(\text{soln})}$$

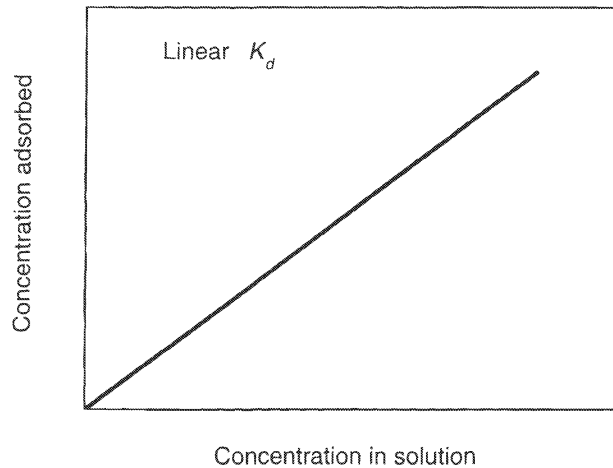
where  $m_{i(\text{ads})}$  is the concentration of the species of interest adsorbed on the solid phase (commonly moles/kg of solid) and  $m_{i(\text{soln})}$  is the concentration of the species in solution (commonly moles/l). The distribution coefficient thus has the units l/kg. Various other systems of units are also used. A closely related quantity is the “activity  $K_d$ ,” which is defined by

$$m_{i(\text{ads})} = K_d \alpha_{i(\text{soln})}$$

where  $\alpha_{i(\text{soln})}$  represents the activity rather than the concentration of the species in solution. The activity  $K_d$  is commonly used in conjunction with computer codes such as MINTEQA2, in which speciation and activity coefficients have already been calculated.

The linear  $K_d$  is widely used in hydrologic models that incorporate some chemical transport (see Chapter 16). The fact that it is linear and involves no variables other than the concentration of the species of interest make it computationally simple. Many more complex adsorption models may reduce to a linear  $K_d$  under certain restrictive assumptions, as is the case with cation exchange discussed above. The numerical value of a distribution coefficient is a function of the properties of the solid substrate and the composition of the solution. It must generally be measured experimentally for each system of interest and cannot be easily transferred from one system to another.

**FIGURE 5-1** Linear distribution coefficient.



### Freundlich Isotherm

The Freundlich isotherm takes the form

$$m_{i(\text{ads})} = K_f m_{i(\text{soln})}^n$$

where  $n$  is a constant, usually less than 1. The exponent causes the isotherm to curve, becoming less steep at higher concentrations (Fig. 5-2). It can be regarded as strictly empirical or it can be justified theoretically in several ways. It would result from the adsorbed species forming a non-ideal solid solution on the solid surface, or it could result from heterogeneity in the sites to which the solute binds on the surface. If the surface contained sites with different binding energies for the solute, the first solute molecules to be adsorbed would be adsorbed at the sites with the strongest binding energy, which corresponds to the steep portion of isotherm. As the sites became filled, adsorption would take place at sites with lower binding energies, decreasing the slope of the isotherm.

### Langmuir Isotherm

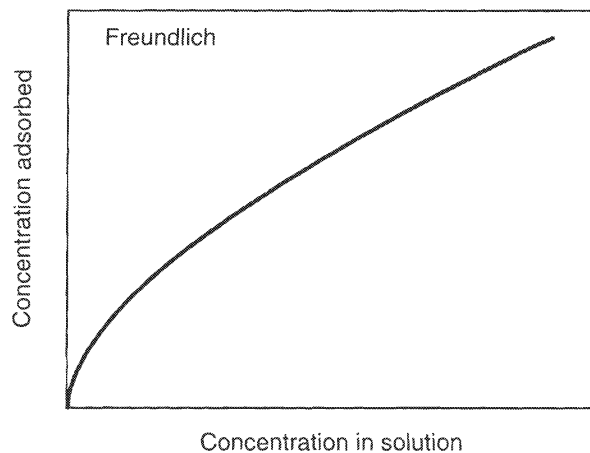
The Langmuir isotherm was originally derived to describe the adsorption of a gas monolayer on a solid surface. An analogous form can be derived for aqueous systems (Stumm, 1992). Consider a surface in which the total concentration of sites for adsorption is  $m_{i(\text{ads, max})}$ , the concentration of sites to which solute  $i$  is adsorbed is  $m_{i(\text{ads})}$  and the concentration of sites not occupied by  $i$  is  $m_{\text{vacant sites}}$ . These concentrations can all be expressed in moles per liter of solution. The adsorption reaction can be written



The corresponding equilibrium constant for this reaction can be written

$$K_{\text{Lang}} = \frac{m_{i(\text{ads})}}{m_{i(\text{soln})} m_{\text{vacant sites}}}$$

**FIGURE 5-2** Example of a Freundlich isotherm (exponent = 0.6).



Substituting  $m_{i(\text{ads}, \text{max})} = m_{i(\text{ads})} + m_{\text{vacant sites}}$  and rearranging gives

$$m_{i(\text{ads})} = m_{i(\text{ads}, \text{max})} \frac{K_{\text{Lang}} m_{i(\text{soln})}}{1 + K_{\text{Lang}} m_{i(\text{soln})}}$$

The form of this equation is shown in Fig. 5-3. At high concentrations the Langmuir isotherm flattens, owing to saturation of the available surface sites. However high  $m_{i(\text{soln})}$  becomes,  $m_{i(\text{ads})}$  can never exceed  $m_{i(\text{ads}, \text{max})}$ . The Langmuir isotherm can also be transformed to a linear form:

$$\frac{1}{m_{i(\text{ads})}} = \frac{1}{m_{i(\text{ads}, \text{max})}} + \frac{1}{K_{\text{Lang}} m_{i(\text{ads}, \text{max})}} \frac{1}{m_{i(\text{soln})}}$$

A plot of  $1/m_{i(\text{ads})}$  against  $1/m_{i(\text{soln})}$  will give a straight line of slope  $1/K_{\text{Lang}} m_{i(\text{ads}, \text{max})}$  and an intercept of  $1/m_{i(\text{ads}, \text{max})}$ .

At low concentrations, the term  $K_{\text{Lang}} m_{i(\text{soln})}$  becomes small compared to 1 and the Langmuir isotherm reduces to the linear  $K_d$ , where

$$K_d = m_{i(\text{ads}, \text{max})} K_{\text{Lang}}$$

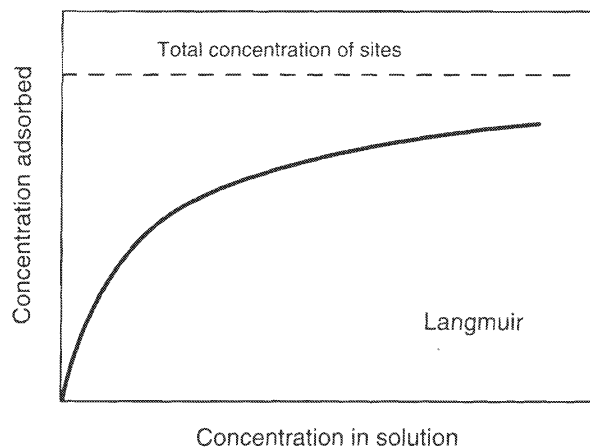
This is an example of how a more complex isotherm can be represented by a linear  $K_d$  under certain restricted circumstances.

Cation exchange reactions involving clay minerals are analogous to the Langmuir isotherm because the concentration of cations adsorbed can never be greater than the cation exchange capacity of the solid.

## SURFACE COMPLEXATION

Mechanistic models for adsorption of inorganic species are generally based on the idea of *surface complexation*. The detailed models are conceptually and mathematically quite complex, and only an overview is provided here. For more detailed information, see Stumm (1992),

**FIGURE 5-3** Example of a Langmuir isotherm. The dashed line represents the maximum concentration that can be adsorbed.



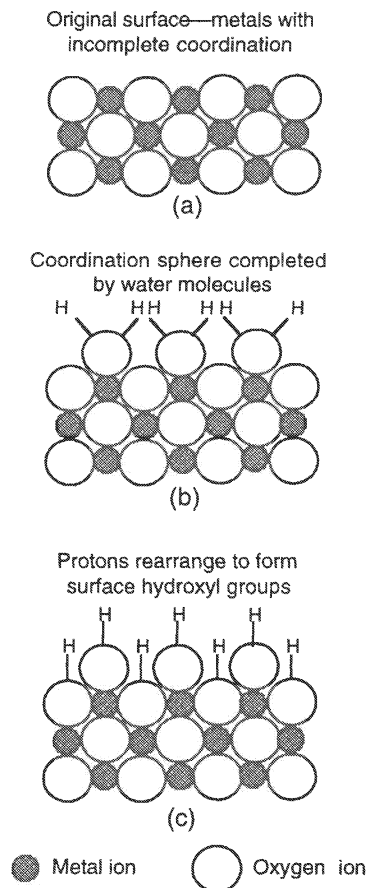
Davis and Kent (1990), or Dzombak and Morel (1990). Surface complexation is incorporated into the computer code MINTEQA2 and is currently regarded as the most accurate way of modeling adsorption of inorganic species at mineral surfaces. The objective of such modeling is usually to predict the concentration of an environmentally important cation or anion in groundwater or surface water following some perturbation such as waste disposal, mining activities, or a chemical spill.

Conceptually, the surface of an oxide or a silicate can be regarded as a plane of hydroxyl groups. A hypothetical oxide mineral is shown in Fig. 5-4a. Cations in the interior of the structure are coordinated on all sides by oxygen ions. Cations at the surface, however, are not fully coordinated. They adsorb a water molecule from solution to complete their coordination shell (Fig. 5-4b). The protons attached to the adsorbed water molecules then tend to redistribute themselves, as shown in Fig. 5-4c (Stumm, 1992). In the discussion that follows, OH groups at the surface of an oxide are shown as  $\equiv\text{S}-\text{OH}$ .

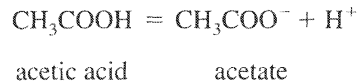
The hydroxyl groups at the surface of an oxide behave in a similar way to  $-\text{OH}$  groups attached to dissolved species. They can dissociate



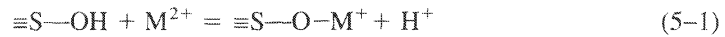
**FIGURE 5-4** Schematic representation of the cross section of a metal oxide: (a) Metal ions at the surface have vacancies in their coordination sphere; (b) Vacant positions occupied by  $\text{H}_2\text{O}$  molecules; (c) Protons rearrange to form surface hydroxyl groups (after Schindler, 1981; Stumm, 1992).



which is completely analogous to the dissociation of an organic acid



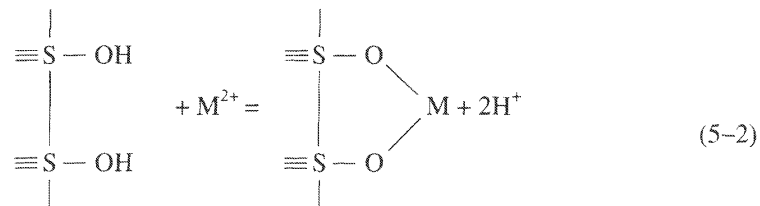
They can also form complexes with a metal (represented here as a divalent cation  $\text{M}^{2+}$ ), which is again analogous to complex formation in solution. The surface may act as a monodentate ligand



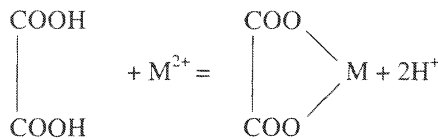
as in the analogous reaction



or as a bidentate ligand



analogous to complexation by oxalate in solution



Adsorption of anions at the surface of an oxide can also take place by a process analogous to ligand exchange



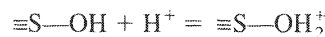
where  $\text{L}^-$  represents a simple anionic ligand such as  $\text{F}^-$ . Some possible schematic configurations of surface complexes are shown in Fig. 5-5.

### Acid-Base Equilibria

As mentioned above, surface hydroxyl groups can dissociate

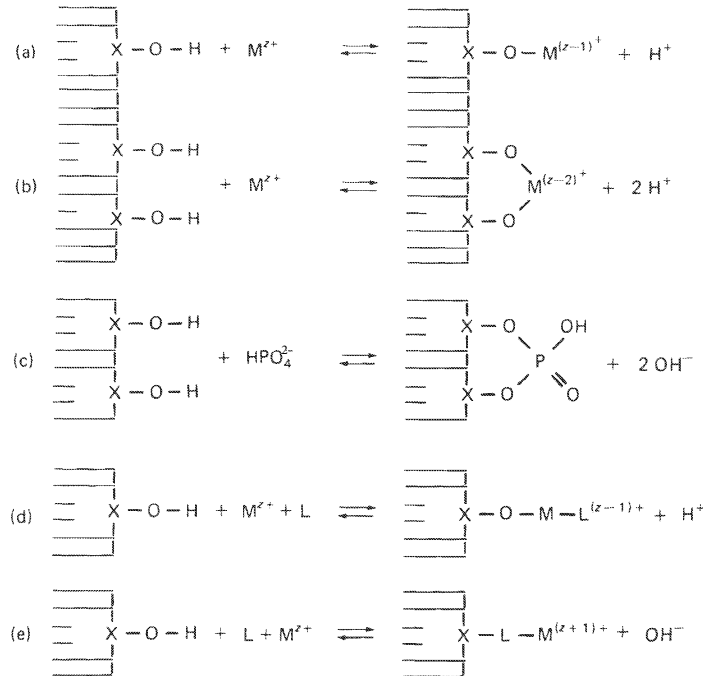


and they can also be protonated



Dissociation tends to give the surface a negative electrical charge, whereas protonation tends to give it a positive charge. This process gives oxides a variable surface charge, unlike the fixed charge that results from substitution of  $\text{Al}^{3+}$  for  $\text{Si}^{4+}$  and  $\text{Mg}^{2+}$  for  $\text{Al}^{3+}$  in clay minerals. From the law of mass action, low pH will favor protonation; high pH will favor deprotonation. For each oxide there exists a pH at which the positive charge on the surface due to protonated

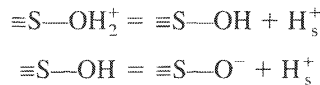




**FIGURE 5-5** Some possible surface coordination reactions. X represents a metal cation forming the oxide surface (after Schindler, 1981).

groups equals the negative charge on the surface due to deprotonated groups. At that pH the net charge on the surface will be zero. That pH is called the *zero point of charge (ZPC)*. If the only process affecting surface charge is loss or gain of protons (as distinct from adsorption–desorption of other ions such as metals) the ZPC is also referred to as the *zero point of net proton charge (ZPNPC)* or *isoelectric point (IEP)*. Some isoelectric points are shown in Table 5-1.

For convenience, protonation–deprotonation equilibria can be written as the dissociation of acids:



The subscript s indicates the hydrogen ions are in the immediate vicinity of the surface. The corresponding equilibrium constants are

$$K_{a1}^{\text{intr}} = \frac{[\equiv\text{S}-\text{OH}][\text{H}^+]_s}{[\equiv\text{S}-\text{OH}_2^+]} \quad (5-3)$$

$$K_{a2}^{\text{intr}} = \frac{[\equiv\text{S}-\text{O}^-][\text{H}^+]_s}{[\equiv\text{S}-\text{OH}]} \quad (5-4)$$

where [ ] formally represent activities, with the [ ]<sub>s</sub> indicating an activity in solution close to the surface. The differences between activities and concentrations of surface species are often

**TABLE 5-1** Isoelectric Points (pH) of Some Naturally Occurring Substances (from James and MacNaughton, 1977; Leckie and James, 1974; Parks, 1965)

SiO <sub>2</sub> (quartz)	2.0
SiO <sub>2</sub> (gel)	1.0–2.5
Al <sub>2</sub> O <sub>3</sub> (corundum)	9.1
Al(OH) <sub>3</sub> (gibbsite)	~9
TiO <sub>2</sub> (anatase)	7.2
Fe <sub>3</sub> O <sub>4</sub> (magnetite)	6.5
Fe <sub>2</sub> O <sub>3</sub> (hematite)	5–9 (commonly 6–7)
FeO(OH) (goethite)	6–7
Fe <sub>2</sub> O <sub>3</sub> • nH <sub>2</sub> O	6–9
δ-MnO <sub>2</sub>	2
Kaolinite	~3.5
Montmorillonite	<2.5

ignored in surface complexation modeling (Stumm, 1992). The units of the surface species (moles per kg of solid, moles per liter of solution, moles per square meter of surface) do not really have to be specified at this point because any conversion factor among units will cancel in Eqs. (5-3) and (5-4). The most generally useful units are moles per kg of solution. This is related to more fundamental quantities by

$$[\text{total surface sites}]_{\text{moles/l soln}} = \frac{N_s S_A C_s}{N_A} \quad (5-5)$$

where  $N_s$  is the number of sites per m<sup>2</sup>,  $S_A$  is the specific surface area of the solid (m<sup>2</sup>/g),  $C_s$  is the concentration of the solid (g solid/l of solution), and  $N_A$  is Avogadro's number ( $6.02 \times 10^{23}$ ).  $N_s$  can be measured (or estimated) in several ways, for example by deuterium exchange or from the known structure of the solid, but is most commonly derived from surface titration experiments (see below).  $S_A$  is commonly measured by the BET method (Brunauer, Emmett, and Teller, 1938), in which the amount of a gas (most commonly nitrogen) required to form a monolayer on the surface of the solid is measured.

The activity  $[H^+]_s$  in Eqs. (5-3) and (5-4) represent the activity of hydrogen ions in solution *at the surface of the solid*. This will generally not be the same as the activity of hydrogen ions in bulk solution because, if the surface is charged, the concentration of ions close to the surface will be affected by the charge on the surface (see Fig. 4-9). If the surface is positively charged, the activity of H<sup>+</sup> near it will be less than in bulk solution, and if the surface charge is negative, the activity of H<sup>+</sup> near it will be greater than in bulk solution. The electrostatic or *coulombic* effect can be quantified by

$$[H^+]_{\text{location } x} = [H^+]_{\text{bulk soln}} \exp\left(\frac{-zF\Psi_{(x)}}{RT}\right) \quad (5-6)$$

where  $z$  is the charge on the ion (1 in the case of H<sup>+</sup>),  $F$  is Faraday's constant (96,485 Coulombs per mole of electrons),  $\Psi_{(x)}$  is the electrical potential at location  $x$ ,  $R$  is the gas constant and  $T$  the temperature on the Kelvin scale (Stumm, 1992). The expression  $\exp\left(\frac{-zF\Psi_{(x)}}{RT}\right)$  is referred to as the *electrostatic* or *coulombic* term in the equation.

Eqs. (5-3) and (5-4) can thus be rewritten as

$$K_{a1}^{\text{intr}} = \frac{[\equiv\text{S}-\text{OH}][\text{H}^+]_{\text{bulk}}}{[\equiv\text{S}-\text{OH}_2^+]} \exp\left(\frac{-zF\Psi_{(\text{surface})}}{RT}\right) \quad (5-7)$$

and

$$K_{a2}^{\text{intr}} = \frac{[\equiv\text{S}-\text{O}^-][\text{H}^+]_{\text{bulk}}}{[\equiv\text{S}-\text{OH}]} \exp\left(\frac{-zF\Psi_{(\text{surface})}}{RT}\right) \quad (5-8)$$

where  $[\text{H}^+]_{\text{bulk}}$  represents the hydrogen ion activity in the bulk solution.  $K_{a1}^{\text{intr}}$  and  $K_{a2}^{\text{intr}}$  are *intrinsic constants*. The intrinsic constant is the value of the equilibrium constant written in terms of concentrations at the surface rather than in bulk solution. It is a function of the nature of the solid surface and adsorbing ion only and is not a function of the charge on the surface.  $K_{a2}^{\text{intr}}$  reflects only the chemical energy involved in an adsorption reaction, whereas  $K_{a1}$ , written in terms of activities in bulk solution,

$$K_{a1} = \frac{[\equiv\text{S}-\text{OH}][\text{H}^+]_{\text{bulk}}}{[\equiv\text{S}-\text{OH}_2^+]}$$

includes both chemical and electrostatic effects.

Substitution of  $[\equiv\text{S}-\text{OH}_2^+] = [\equiv\text{S}-\text{O}^-]$  and  $\Psi = 0$  (the definition of the ZPNPC; when the charge is zero the potential is zero) into Eqs. (5-7) and (5-8) gives

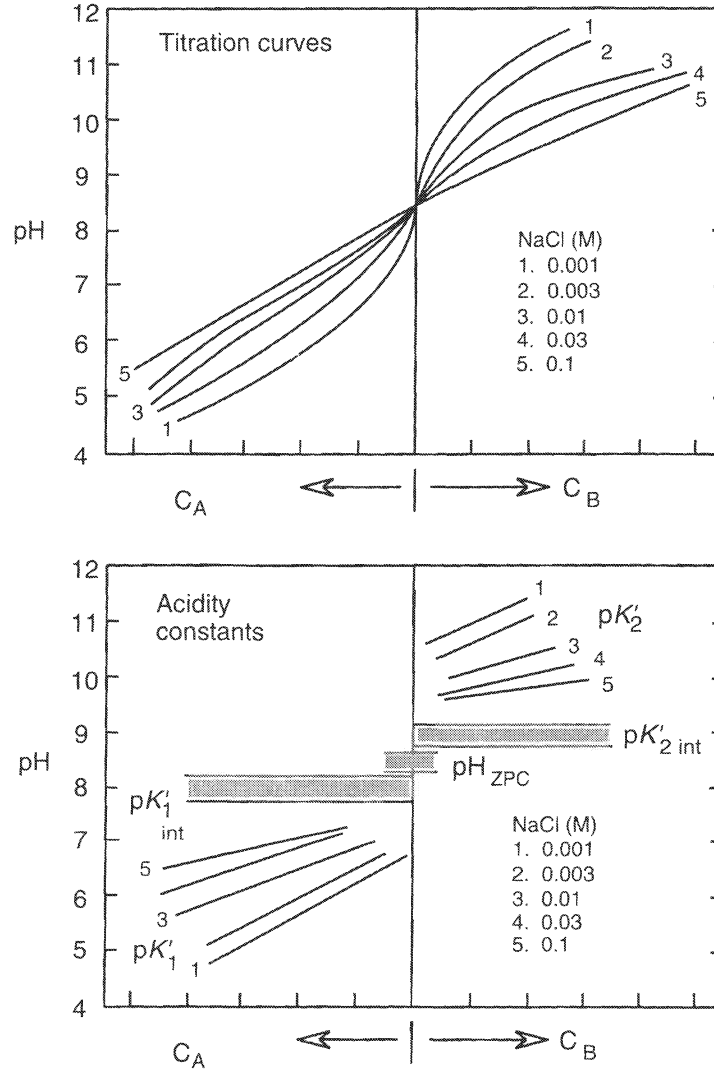
$$\text{pH}_{\text{ZPNPC}} = 0.5(\text{p}K_{a1}^{\text{intr}} + \text{p}K_{a2}^{\text{intr}})$$

**Surface Titrations.** The quantities  $[\equiv\text{S}-\text{OH}_2^+]$  and  $[\equiv\text{S}-\text{O}^-]$  and hence the intrinsic acidity constants, can be measured by what are called *surface titrations*. In a surface titration, a stirred suspension of the solid in a solution containing (usually) a supporting electrolyte (a solution of a salt whose ions do not interact strongly with the surface, commonly  $\text{NaNO}_3$  or  $\text{NaClO}_4$ ) is titrated by addition of a strong acid (commonly  $\text{HNO}_3$  or  $\text{HCl}$ ) or strong base (commonly  $\text{NaOH}$ ). Of the added  $\text{H}^+$  or  $\text{OH}^-$  ions, some are adsorbed by the surface and some accumulate in solution. If the amount of acid added is  $C_A$  and the amount of base  $C_B$  (in units of moles per liter of the solution being titrated), then

$$C_A - C_B + m_{\text{OH}^-} - m_{\text{H}^+} = [\equiv\text{S}-\text{OH}_2^+] - [\equiv\text{S}-\text{O}^-]$$

where  $m_{\text{OH}^-}$  and  $m_{\text{H}^+}$  are concentrations present in solution, and  $[\equiv\text{S}-\text{OH}_2^+]$  and  $[\equiv\text{S}-\text{O}^-]$  are also in units of moles per liter of solution. Titration curves for  $\gamma\text{-Al}_2\text{O}_3$  are shown in Fig. 5-6. The curves show the pH of the solution as a function of the amount of acid or base added. The curves corresponding to different supporting electrolyte concentrations intersect at a single pH and diverge away from that pH in either direction. The reason for the divergence is the electrostatic term in Eqs. (5-7) and (5-8). The distribution of charge and hence  $\Psi$  close to the surface is a function of the ionic strength of the solution. At the ZPC of the surface, however, the charge is zero,  $\Psi$  is zero, and the titration curves intersect. This represents one way of identifying the ZPC of the surface. If it is assumed that at a pH less than the ZPC the concentration of  $[\equiv\text{S}-\text{O}^-]$  is small compared to that of  $[\equiv\text{S}-\text{OH}_2^+]$ , then titration of the surface with acid yields

$$C_A - m_{\text{H}^+} = [\equiv\text{S}-\text{OH}_2^+] \quad (\text{below ZPC})$$



**FIGURE 5-6** Titration curves in different concentrations of NaCl background electrolyte and corresponding acidity constants for hydrous  $\gamma\text{-Al}_2\text{O}_3$  (1.56 g/l). The uncorrected acidity constants ( $pK'_1$  and  $pK'_2$ ) are calculated from the corresponding individual points on the titration curves. They vary as a function of surface charge whereas the corresponding intrinsic constants ( $pK_{1\text{int}}$  and  $pK_{2\text{int}}$ ) do not; they all plot in the shaded areas on the figure. The titration curves all intersect at the ZPC (after Huang and Stumm, 1973). Reprinted with permission of Academic Press, Inc.

and titration with base above the ZPC yields

$$C_B - m_{\text{OH}^-} = [\equiv\text{S}-\text{O}^-] \text{ (above ZPC)}$$

$[\equiv\text{S}-\text{OH}_2^+]$  and  $[\equiv\text{S}-\text{O}^-]$  can thus be measured as a function of pH from the titration curves. If the total concentration of sites is known (by deuterium exchange or titration to

extreme pH, for example) then the values of  $K_{a1}$  and  $K_{a2}$  can be calculated. Plotting these values and extrapolating to the ZPC (Fig. 5-6) gives the intrinsic constants  $K_{a1}^{\text{intr}}$  and  $K_{a2}^{\text{intr}}$ .

### Adsorption of Metal Cations

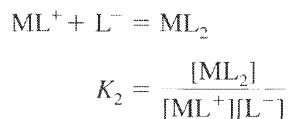
Analogous intrinsic constants can be written for formation of complexes between a metal and the surface. For example, constants for Eq. (5-1) and (5-2) can be written

$$K_M^{\text{intr}} = \frac{[\equiv\text{S}-\text{OM}^+][\text{H}^+]}{[\equiv\text{S}-\text{OH}][\text{M}^{2+}]} \exp\left(\frac{-\Delta z F \Psi_{(\text{surface})}}{RT}\right)$$

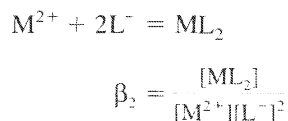
and

$$\beta_{2(\text{M})}^{\text{intr}} = \frac{[(\equiv\text{S}-\text{O})_2\text{M}][\text{H}^+]^2}{[(\equiv\text{S}-\text{OH})_2][\text{M}^{2+}]} \exp\left(\frac{-\Delta z F \Psi_{(\text{surface})}}{RT}\right)$$

The convention for writing equilibrium constants follows that of Sillén and Martell (1971): when a metal forms a constant with more than one ligand,  $K_n$  refers to individual steps and  $\beta_n$  refers to a cumulative reaction. For formation of a complex  $\text{ML}_2$ ,  $K_2$  would refer to the reaction



whereas  $\beta_2$  would refer to the reaction



The coulombic term is written with  $\Delta z$  rather than  $z$ .  $\Delta z$  represents the net change in the charge on the surface corresponding to the adsorption reaction as written (Dzombak and Morel, 1990). For reaction (5-1),  $\Delta z$  would be +1 (one  $\text{M}^{2+}$  gained, one  $\text{H}^+$  lost). For reaction (5-2),  $\Delta z$  would be zero (one  $\text{M}^{2+}$  gained, two  $\text{H}^+$  lost). Intrinsic constants for surface complexation reactions can be measured by methods analogous to surface titrations for adsorbed  $\text{H}^+$  (Davis and Kent, 1990; Dzombak and Morel, 1990). Dzombak and Morel give an extensive compilation of constants for hydrous ferric oxide, the most important substrate for adsorption of heavy metals in natural systems.

It is useful to distinguish between *inner sphere* and *outer sphere* surface complexes (Fig. 5-7), analogous to inner- and outer-sphere complexes in solution (Chapter 2). In an outer-sphere complex, the ion remains surrounded by a hydration shell so it does not bind directly to the surface. Adsorption is essentially electrostatic, caused by attraction between a positively charged ion in solution and a negatively charged surface (or between an anion in solution and a positively charged surface). In an inner sphere complex, the ion bonds directly to the surface groups. The bond is generally stronger and does not depend on electrostatic attraction: a cation can adsorb to a positively charged surface.

Adsorption of cations can be regarded as a competition between cations and  $\text{H}^+$  for surface sites. At low pH, adsorption of cations is minimal. As the pH rises, there is a relatively

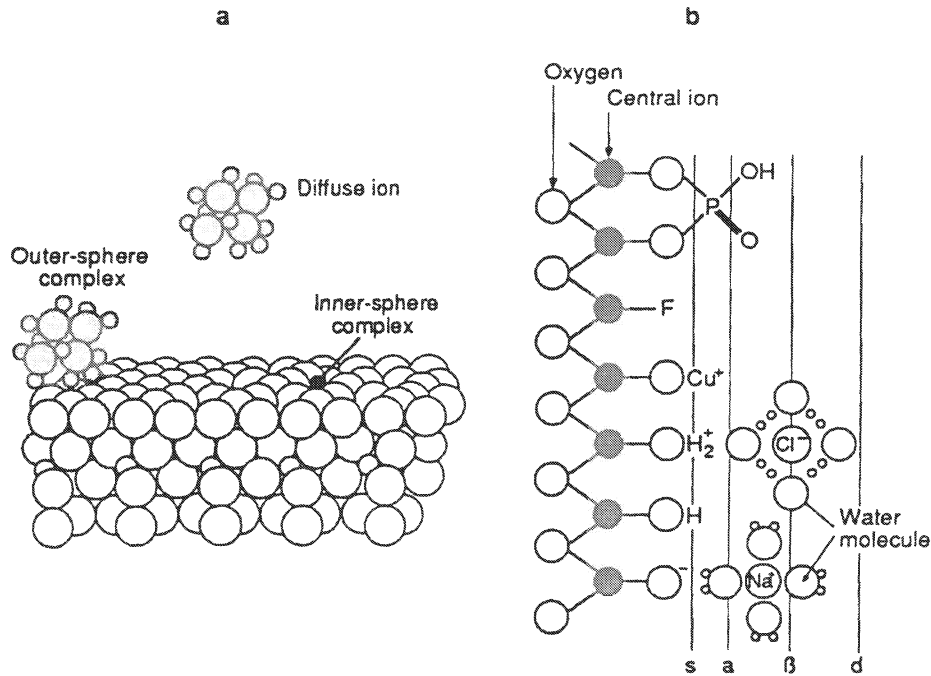


FIGURE 5-7 Schematic representation of inner-sphere (phosphate, fluoride, copper) and outer-sphere (sodium, chloride) complexes. The labels on the layers correspond to the triple-layer model (discussed in text) (after Stumm, 1992).

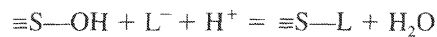
narrow interval (about 2 pH units) over which adsorption changes from essentially zero to essentially complete (Fig. 5-8) (assuming the amount of cation present is small compared to the number of available surface sites). This pH interval is different for different metal cations and for different solid substrates.

### Adsorption of Anions

Equations for the adsorption of anions are very similar to those for adsorption of cations. For example

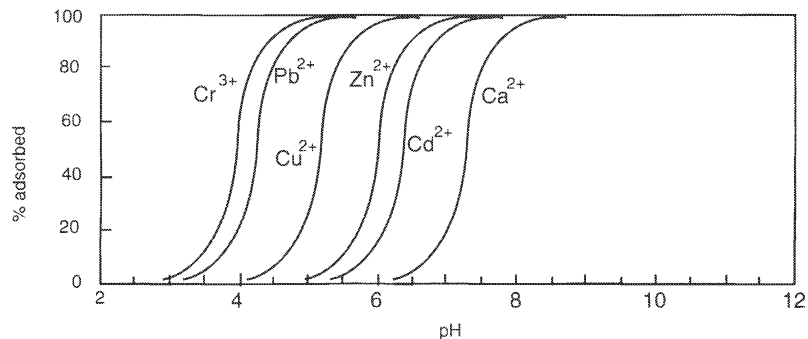


or, written in terms of  $\text{H}^+$  rather than  $\text{OH}^-$ :



$$K_{\text{L}^-}^{\text{intr}} = \frac{[\equiv\text{S}-\text{L}]}{[\equiv\text{S}-\text{OH}][\text{L}^-][\text{H}^+]} \exp\left(\frac{-\Delta z F \Psi_{(\text{surface})}}{RT}\right)$$

In this particular instance  $\Delta z$  would be zero (no net change in surface charge). Other possible anion adsorption reactions would result in non-zero values for  $\Delta z$ . As with cations, anions may adsorb as inner-sphere or outer-sphere complexes.

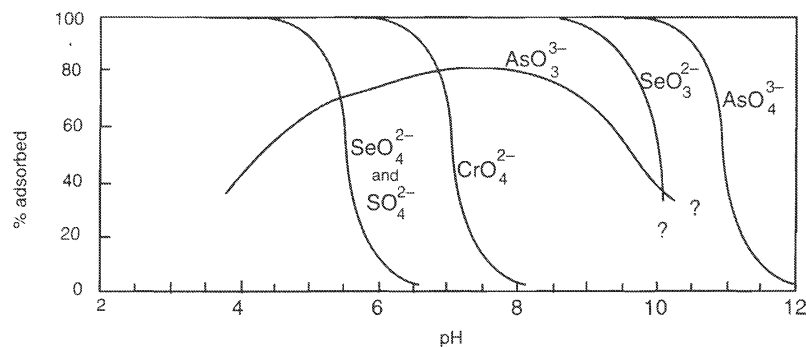


**FIGURE 5-8** Adsorption of metal cations on hydrous ferric oxide as a function of pH (data from Dzombak and Morel, 1990).

Anions are essentially competing with  $\text{OH}^-$  for adsorption sites, so their behavior is the mirror image of cation adsorption (Fig. 5-9). Adsorption increases from essentially zero at high pH to essentially complete at low pH. The transition occurs over a relatively narrow pH range which is specific to the anion and the oxide surface. The adsorption of anions is often complicated by a change in speciation of the solute as a function of pH. For example, at low pH the dominant form of dissolved arsenic in oxidizing environments is  $\text{H}_3\text{AsO}_4$ . As the pH rises, this acid dissociates into, progressively,  $\text{H}_2\text{AsO}_4^-$ ,  $\text{HAsO}_4^{2-}$ , and  $\text{AsO}_4^{3-}$ . Each species has different adsorption properties, so the overall adsorption behavior is quite complex.

### The Electric Double Layer

The treatment so far has been quite general. We have developed a series of equations that describe the adsorption of ions at the surface of an oxide in terms of measurable equilibrium constants and an electrostatic term involving the electrical potential,  $\Psi$ , at the surface of the solid. Before we can apply this modeling approach to a real system, we need to be able to calculate  $\Psi$ .  $\Psi$  itself is a function of surface charge, so it is a function of the extent



**FIGURE 5-9** Adsorption of selected anions on hydrous ferric oxide as a function of pH (data from Dzombak and Morel, 1990).

of protonation–deprotonation reactions and the extent of the adsorption of ions from solution. It is thus a function of solution composition. The electrostatic potential at the surface of the solid and the surface charge are mathematically related

$$\sigma = f(\Psi) \quad (5-9)$$

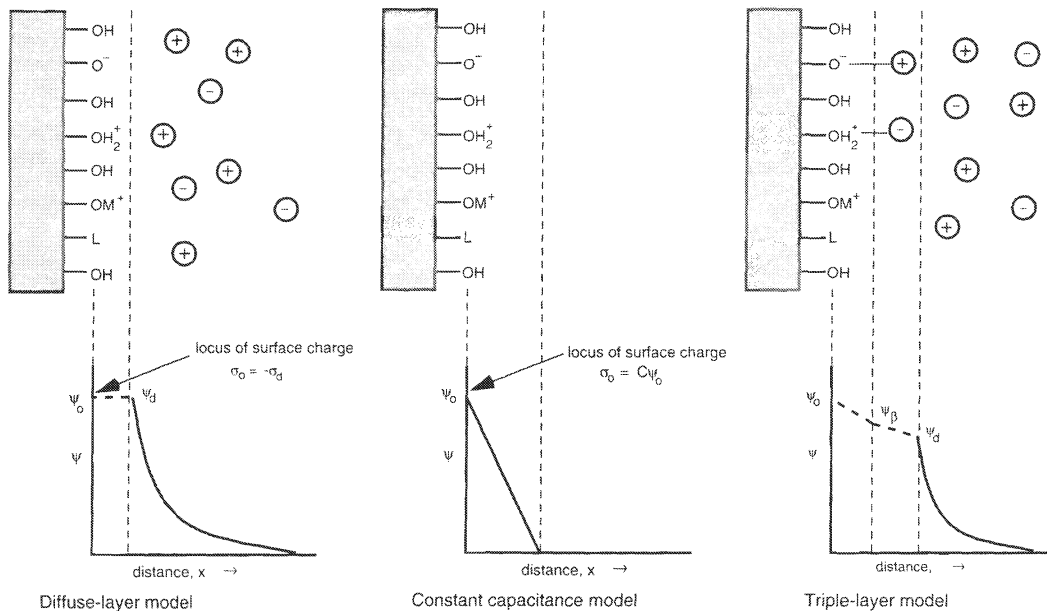
where  $\sigma$  is the charge on the surface in units of coulombs/m<sup>2</sup>. It is the form of the functional relationship,  $f$ , that distinguishes the various surface complexation models discussed below. It is more convenient to express  $\sigma$  in molar units; the conversion is

$$T_\sigma = \frac{S_A C_s}{F} \sigma$$

where  $T_\sigma$  is the surface charge in moles per liter of solution,  $S_A$  is the specific surface area of the solid (m<sup>2</sup>/g),  $C_s$  is the concentration of the solid (g solid/l of solution), and  $F$  is Faraday's constant.  $T_\sigma$  is zero at the ZPC and represents the net charge (adsorbed cations—adsorbed anions) away from the ZPC.

**The Constant Capacitance Model (CCM).** In this model it is assumed that the double layer can be represented by a parallel plate capacitor (Fig. 5-10).

1. Only one plane in the interfacial region is considered. All adsorbed protons, negative sites from deprotonation, and specifically adsorbed ions occur in a single plane, defined as the surface of the solid. Ions that do not form inner-sphere complexes (e.g., Na<sup>+</sup>, K<sup>+</sup>, Cl<sup>-</sup>, and NO<sub>3</sub><sup>-</sup>) are assumed to be excluded from this inner plane.



**FIGURE 5-10** Idealized distribution of electrical potential ( $\psi$ ) in the vicinity of a hydrated oxide surface according to (a) the diffuse-layer model; (b) the constant capacitance model; (c) the triple-layer model (after Hayes et al., 1991).



2. The relationship between charge and potential at the surface plane is given by

$$\sigma_{(0)} = C\Psi_{(0)}$$

where  $C$  is the capacitance of the double layer (Farads/m<sup>2</sup>) and is assumed to be a constant.  $C$  is essentially a fitting parameter rather than being derived theoretically.

The model is appropriate for solutions of high ionic strength, where the double layer is compressed close to the mineral surface. It has also been widely applied in dilute solution.

**The Diffuse Double-Layer Model (DDLDM).** The DDLDM is based on the Gouy-Chapman model of the diffuse double layer (for detailed discussions, see Bolt, 1982, and Sposito, 1984). The Gouy-Chapman model was coupled with surface complexation modeling by Stumm et al. (1970) and Huang and Stumm (1973). The approach was extended and modified by Dzombak and Morel (1990). The main difference from the CCM is that the counterions are assumed to form a diffuse layer extending from the surface out into solution, which can be described by Gouy-Chapman theory. In the DDLDM, the relationship between charge and potential is given by

$$\sigma_d = -0.1174\sqrt{I} \sinh \frac{zF\Psi}{2RT} \quad (5-10)$$

where the subscript  $d$  refers to the diffuse layer and  $I$  is the ionic strength (Chapter 2). The electrical potential at the innermost edge of the diffuse layer is assumed to be equal to the surface potential (Fig. 5-10). In this model the capacitance of the double layer is inherently defined by Eq. (5-10); it is a function of solution composition rather than being a fitting parameter. In principle, this model should be appropriate for solutions of low ionic strength and low concentrations of adsorbing ions.

**The Triple-Layer Model (TLM).** The CCM and the DDLDM both make the assumption that all adsorbed ions are present at a single plane at the surface of the solid. In the TLM (Davis et al., 1978; Hayes et al., 1991) it is assumed that different species are adsorbed at different distances from the surface. Somewhat different versions of the triple-layer model are in use; the description here follows Hayes et al. (1991). In the triple-layer model (Fig. 5-10c), proton and deprotonation reactions occur in a layer directly adjacent to the surface, the  $\alpha$ -plane. Inner-sphere complexes are also assigned to the  $\alpha$ -plane. Outer-sphere complexes are assigned to a plane (the  $\beta$ -plane) slightly farther from the surface, and all ions that interact only through electrostatic forces are assigned to a diffuse layer outside the  $\beta$ -layer. In the original version of the TLM (Davis et al., 1978), which is the version implemented in MINTEQA2, only proton-deprotonation reactions occurred at the  $\alpha$ -plane; inner-sphere complexes were assigned to the  $\beta$ -plane, and outer-sphere complexes were assigned to the diffuse layer. The approach (in both forms) is conceptually reasonable: protons should be attached directly to the surface, physically larger adsorbed species should be centered at a greater distance, and ions that do not bond directly to the surface would form a diffuse layer. The two regions closest to the surface are modeled as a constant capacity layer and the region outside the  $\beta$ -layer as a diffuse (Gouy-Chapman) layer. The advantage of this model is that it is (presumably) a better representation

of reality or, alternatively, it has more fitting parameters, which should result in a better fit to experimental data. The disadvantage is that it is mathematically more complex and requires more parameters to describe the system. It should be stressed, following Westall (1987), that although these models may describe macroscopic data well, they should not be regarded as a literal description of processes occurring at the molecular scale.

**Comparison of the Models.** The ability of each of the three models (and two others) to describe experimental data from acid-base titrations of hydrous oxides was evaluated rigorously by Westall and Hohl (1980). They showed that each model had sufficient adjustable parameters and that each could describe the experimental titration data equally well. Subsequent comparisons are reviewed by Davis and Kent (1990). They conclude that all surface complexation models can simulate ion adsorption data adequately in simple mineral-water systems, so there is no obvious reason to choose one over the other. Computational complexity is not really an issue because computer codes handle the calculations for all of them. A major limitation is the availability of data to implement any model. The most extensive compilation at present is that of Dzombak and Morel (1990) for hydrous ferric oxide. Dzombak and Morel used a modified DDLM; it is convenient and advisable to maintain consistency by using their model with their data.

Realistically, when it comes to predicting adsorption in field situations, the choice of a specific surface complexation model is likely to be a very minor source of uncertainty. A far greater source of uncertainty is specifying the amount and properties (specific surface area, site density, complexation constants) of the adsorption substrates present in the natural environment.

### Modeling Adsorption with MINTEQA2

Conceptually, modeling adsorption is simply an extension of the speciation calculation discussed in Chapter 2. If we were to add a new dissolved component to WATEQ4F or MINTEQA2, we would need to add:

1. An equation for the conservation of the total mass of the component

$$\text{Total concentration} = \text{Sum of concentrations of all species (complexes) containing the component}$$

2. An equilibrium constant for the formation of each species containing the component.

We would thus add  $n$  unknowns (the concentration of each complex and the concentration of the free component), and  $n$  equations (a total concentration for the component), and  $(n - 1)$  equilibrium constant expressions.

Mathematically, if the electrostatic term is omitted, adsorption at a surface site is identical to complex formation in solution. To model adsorption at a single surface site, we need to specify:

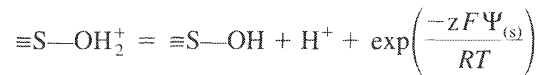
1. The total concentration of "sites" ( $[=S-OH]$  in the terminology above) in units of moles/l of solution (MINTEQA2 prompts for the variables shown on the right hand side of Eq. (5-5) above).

2. An equilibrium constant for formation of each complex between the surface site and components in solution. For surface complexation models, these would correspond to the intrinsic constants.

The electrostatic term is modeled mathematically by treating it as an additional component. This “works” because Eq. (5-7),

$$K_{al}^{intr} = \frac{[\equiv S-OH][H^+]}{[\equiv S-OH_2^+]} \exp\left(\frac{-zF\Psi_{(s)}}{RT}\right)$$

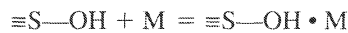
corresponds to the equilibrium constant for the reaction



The electrostatic term is thus analogous to an activity in solution. It is calculated by MINTEQA2 to be consistent with the particular adsorption model chosen. The other equations needed to define the system are an equation for conservation of charge at the surface (at each layer in the triple-layer model), and expressions corresponding to equilibrium constants, which determine the appropriate value for the electrostatic term for each reaction being modeled. These calculations are performed by MINTEQA2 to correspond to the adsorption model chosen. Thus addition of adsorption reactions, including electrostatic effects, is mathematically equivalent to adding additional components in solution and does not require anything fundamentally different from the program.

The adsorption equations available in MINTEQA2 are

1. *The Activity  $K_d$  Model.* The model implemented by MINTEQA2 differs slightly from the common usage in that the concentration in solution is expressed as the activity of the free ion rather than as the total concentration of the ion in solution. The relevant equations are:



and

$$K_d^{act} = \frac{[\equiv S-OH \cdot M]}{a_M}$$

where  $[\equiv S-OH \cdot M]$  represents the adsorbed concentration of M (which may have any charge, including zero).  $[\equiv S-OH]$  does not appear in the equation because in the  $K_d$  model it is assumed that the number of available sites is infinite and does not change. This is analogous to the assumption that the activity of a solid phase is 1. The only input data needed to implement the model is a numerical value for the  $K_d$  for each species of interest. There is no interaction among solutes: adsorption of solute A has no effect on adsorption of solute B.

2. *The Activity Langmuir Model.* As with the activity  $K_d$  above, the activity of the relevant species in solution is used rather than the concentration, and the charge of the solute (M) is unimportant. The relevant equations are



and

$$K_{Lang}^{act} = \frac{[\equiv S-OH \cdot M]}{a_M[\equiv S-OH]} \quad (5-11)$$

If the total concentration of sites is  $[\equiv\text{SOH}]_T (= [\equiv\text{S—OH}] + [\equiv\text{S—OH} \cdot \text{M}])$ , then Eq. (5-11) can be rewritten in the more familiar Langmuir form:

$$[\equiv\text{S—OH} \cdot \text{M}] = \frac{K_{\text{Lang}}^{\text{act}} [\equiv\text{S—OH}]_T \alpha_M}{1 + K_{\text{Lang}}^{\text{act}} \alpha_M}$$

The input data required to implement the activity Langmuir model are numerical values for  $K_{\text{Lang}}^{\text{act}}$  for each species of interest and a numerical value for  $[\equiv\text{SOH}]_T$ . Because the number of sites is fixed, there is competition among solutes. Adsorption of solute A will tend to decrease the adsorption of solute B.

**3. The Activity Freundlich Model.** This model is similar to the activity  $K_d$  model, with the addition of an exponent  $n$ . The concentration/activity of unreacted sites is assumed constant and equal to 1.

$$[\equiv\text{S—OH} \cdot \text{M}] = K_{\text{Freun}}^{\text{act}} \alpha_M^n$$

The required inputs are  $K_{\text{Freun}}^{\text{act}}$  and  $n$  (somewhat confusingly, MINTEQA2 asks for  $1/n$  rather than  $n$ ). As with the  $K_d$  model, there is no interaction among solutes.

**4. Ion Exchange Model.** This model uses selectivity coefficients, as discussed in Chapter 4. For ions of the same charge,

$$[\equiv\text{S—OH} \cdot \text{M}_1] + \text{M}_2 = [\equiv\text{S—OH} \cdot \text{M}_2] + \text{M}_1$$

$$K_{\text{ex}} (= K_{\text{M}_1\text{M}_2} \text{ in the terminology of Chapter 4}) = \frac{m_{\text{M}_1} [\equiv\text{S—OH} \cdot \text{M}_2]}{m_{\text{M}_2} [\equiv\text{S—OH} \cdot \text{M}_1]}$$

The calculation uses concentrations of free ions (calculated from activity divided by activity coefficient) rather than activities for solutes. The required inputs are a cation exchange capacity and a selectivity coefficient for each pair of ions to be modeled. For ions of different charge, the model implements the Gaines-Thomas equation (Eq. 4-7) discussed in Chapter 4.

**5. Constant Capacitance Model, Diffuse-Layer Model, and Triple-Layer Model.** The implementation of these models follows the theory outlined above. The necessary inputs are surface area(s) of the solid(s), surface site densities, and intrinsic constants for all species of interest, and a capacitance or capacitances for the double (triple) layers. Five different surfaces (which would correspond to different mineral phases) and can be modeled simultaneously by MINTEQA2, and each surface may have up to two different sites. It is not often that people model more than one surface at a time. There is interaction among solutes both because of competition for a fixed number of sites and because adsorption of any ion affects the electric charge of the surface. MINTEQA2 normally comes with the Dzombak and Morel (1990) data base for calculating adsorption on hydrous ferric oxides with the diffuse double layer model.

## REVIEW QUESTIONS

The adsorption properties of ammonium in an aquifer were evaluated by mixing 1 g of an ammonium-saturated sediment with different volumes of ammonium-free groundwater from the aquifer, and the concentration of ammonium in the groundwater was measured. The cation exchange capacity of the sediment was 20 meq/kg.

ml soln/g sediment	0.5	1	2	5	10	20	50	100	200	500	1000
Conc in solution (mM)	6.8	5.0	3.5	2.0	1.3	0.75	0.35	0.186	0.0963	0.03938	0.01984

1. How well do the data fit a Langmuir isotherm? Estimate the values of  $K_{\text{Lang}}$  and  $m_{(\text{ads}, \text{max})}$  that best fit the data.
2. What value of  $K_d$  would fit the data at low concentration? Up to what concentration is the linear  $K_d$  a reasonable fit (say  $\pm 10$  percent) to the data?
3. How well do the data fit a Freundlich isotherm? Up to what concentration is the Freundlich isotherm a reasonable fit (say  $\pm 10$  percent) to the data? What value of  $n$  gives the best fit at low concentration?
4. The data in the table above fit a cation-exchange equation (Eq. 4-3):

$$\frac{m_{\text{A-clay}}}{\text{CEC} - m_{\text{A-clay}}} = K'_{\text{AB}} \frac{m_{\text{A}^+}}{M - m_{\text{A}^+}}$$

with  $K'_{\text{AB}} = 6$  and  $M = 15 \text{ meq/l}$ . How does this equation differ from the Langmuir isotherm? Can you relate the constants in this equation (CEC,  $K'_{\text{AB}}$ ,  $M$ ) to the constants in the Langmuir isotherm and its linearized equivalent ( $K_{\text{Lang}}$ ,  $m_{(\text{ads}, \text{max})}$ )?

### SUGGESTED READING

- DAVIS, J. A., and D. B. KENT. (1990). Surface complexation modeling in aqueous geochemistry. In M. F. HOCELLA and A. F. WHITE, (Eds.), *Mineral-Water Interface Geochemistry*, (pp. 177–260). Reviews in Mineralogy, Vol. 23, Washington, DC: Mineralogical Society of America.
- DZOMBAK, D. A., and F. M. M. MOREL. (1990). *Surface Complexation Modeling: Hydrous Ferric Oxide*. New York: Wiley-Interscience.
- SPOSITO, G. (1984). *The Surface Chemistry of Soils*. Oxford, England: Oxford University Press.
- STUMM, W. (1992). *Chemistry of the Solid-Water Interface*. New York: Wiley-Interscience.
- WESTALL, J. C. (1987). Adsorption mechanisms in aquatic surface chemistry. In W. STUMM, (Ed.), *Aquatic Surface Chemistry*, (pp. 3–32). New York: Wiley-Interscience.



# 6

## Organic Compounds in Natural Waters

### NATURAL ORGANIC MATTER

All natural waters contain dissolved organic compounds. In the past, geochemists have tended to ignore organic solutes because of the complexity of the mixture and the analytical difficulties. Recently, however, there have been numerous studies of dissolved organic compounds, both natural and anthropogenic, and the role they play in geochemical processes. It is now recognized that organic solutes play a major role in weathering processes, in diagenesis, in light attenuation and photochemical reactions, and in the transport of trace metals.

The simplest measure of the total concentration of organic solutes is the concentration of *dissolved organic carbon* (DOC), which is measured by converting all the organic material in solution to  $\text{CO}_2$  and then measuring the  $\text{CO}_2$  produced. Organic matter is considered dissolved if it passes through a 0.45- $\mu\text{m}$  filter, and it is particulate if it is retained by the filter. This definition, although easy to apply, is arbitrary, as organic materials occur in a range of molecular sizes, and 0.45  $\mu\text{m}$  does not represent a fundamental break, except that a 0.45  $\mu\text{m}$  filter excludes almost all bacteria. The term *TOC* (*total organic carbon*) is the organic carbon content of an unfiltered sample.

Rainwater has DOC concentrations of about 0.5 to 1.5 mg/l (Hoffman et al., 1980), much of it in the form of formate, acetate, and oxalate, derived largely from photochemical reactions involving larger organic molecules (Keene and Galloway, 1984; Sedlak and Hoigné, 1993). These compounds tend to biodegrade rapidly, so the rain must be analyzed or preserved quickly if these simple organic solutes are to be observed. DOC concentrations in groundwaters and the ocean are typically about 0.5 mg/l, in rivers and lakes they are typically 2 to 10 mg/l with values up to 60 mg/l in rivers draining swamps and wetlands (Thurman, 1985); values in soil water can be as high as 260 mg/l (Antweiler and Drever, 1983). Some typical values for DOC in natural waters are shown in Fig. 6-1.

River waters with DOC concentrations above about 10 mg/l are distinctly colored. High-DOC waters, most common in tropical lowlands, are called *black waters*.

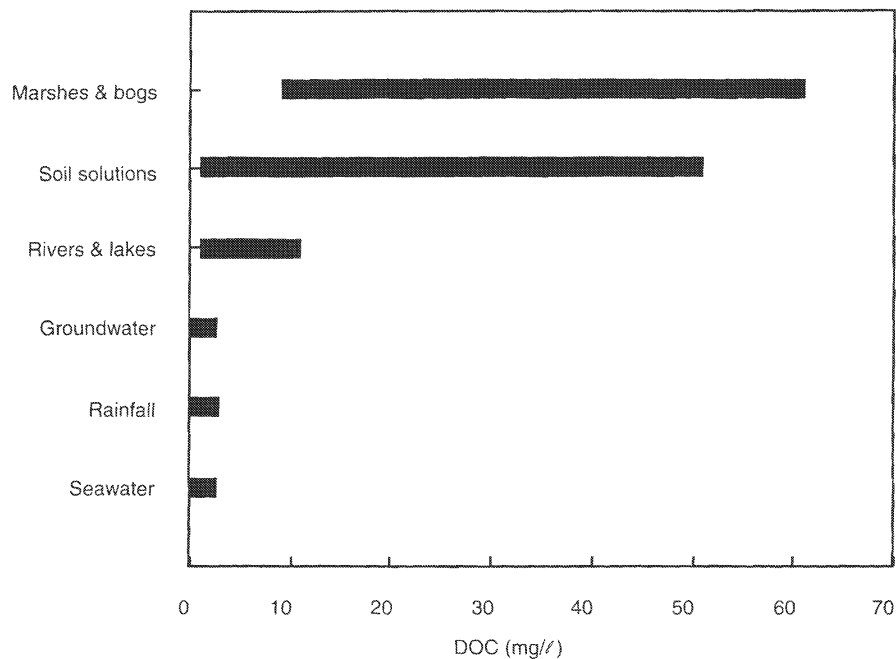
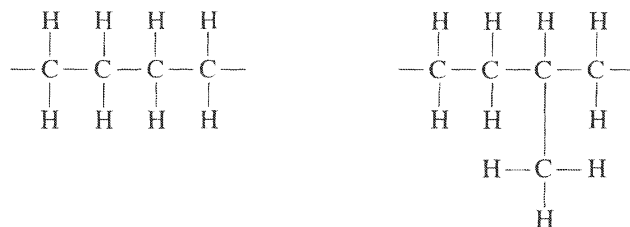


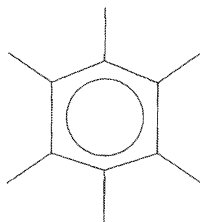
FIGURE 6-1 Typical values for natural DOC in natural waters (data from Thurman, 1985, and other sources).

### Structure of Natural Organic Solutes

In the simplest view, organic compounds can be regarded as a carbon skeleton to which various functional groups are attached. The main components of the carbon skeleton are straight-chained or branched carbon units (aliphatic units):



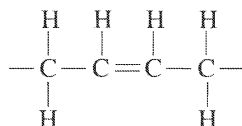
and aromatic units based primarily on the benzene ring:



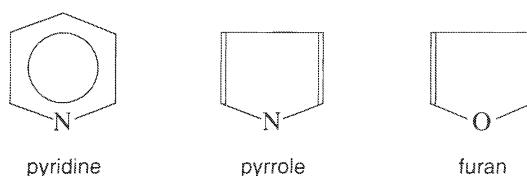


The color in black waters is due to conjugated aromatic units.

The carbon skeleton may also contain olefinic (double-bonded) groups:



and heterocyclic units (rings containing one or more atom that is not carbon):



## Functional Groups

Functional groups are small groups of atoms attached to the carbon skeleton. They normally contain atoms other than carbon (typically oxygen, nitrogen, or sulfur) and have specific chemical properties that affect the properties of the molecule as a whole. Functional groups containing oxygen and nitrogen are typically *polar*, that is to say they either have an electrical charge (ionized groups such as  $-\text{COO}^-$  or  $\equiv\text{NH}^+$ ) or an electric dipole—a separation of charge in the group such that one “end” has a partial negative charge and the other a partial positive charge. Polarity is important because water is a highly polar solvent: polar functional groups tend to increase solubility in water, whereas organic molecules without polar functional groups tend to be relatively insoluble.

**Carboxylic Acids.** The most important group in natural DOC is the carboxylic acid group:



The carboxylic group is important because it is the most abundant functional group in natural DOC. In fact, it is largely the presence of this functional group that makes natural organic matter soluble in water (see discussion below). It is the dominant contributor to the acid-base behavior of natural DOC and a major contributor to complexation of metals. Carboxylic acids are produced by microbial oxidation of other (particularly plant-derived) organic matter. The diversity of carboxylic acids in nature reflects the diversity of precursor plant material and the diversity of microbial oxidation pathways.

As the name implies, this group behaves as an acid. If R is used to represent the remainder of the molecule, dissociation of the acid is described by

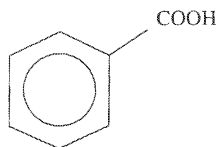


$$K_a = \frac{\alpha_{\text{H}^+} \alpha_{\text{RCOO}^-}}{\alpha_{\text{RCOOH}}} \quad (6-1)$$

The “strength” of an acid is measured by its dissociation constant,  $K_a$ , which is commonly reported (by analogy with pH) as  $pK_a$ , where  $pK_a = -\log_{10} K_a$ . As can be seen from Eq. (6-1), the  $pK_a$  is numerically equal to the pH at which half of the acid is dissociated and half is undissociated. The smaller the  $pK_a$ , the lower the pH at which dissociation occurs and hence the stronger the acid. The  $pK_a$  value of a particular carboxylic acid group depends on the nature and position (see, e.g., Schwarzenbach et al., 1993) of other functional groups close to it in the same molecule (Table 6-1). Note that oxygen-containing functional groups adjacent to the carboxylic acid group generally cause an increase in acid strength (compare, for example benzoic and salicylic acids in Table 6-1). Most carboxylic acid groups have  $pK_a$  values around 3.5 to 5 (Fig. 6-2); thus most are completely dissociated in most natural waters. In high-DOC waters with low concentrations of inorganic ions, organic acids typically buffer the pH at about 4.5 (McKnight et al., 1985).

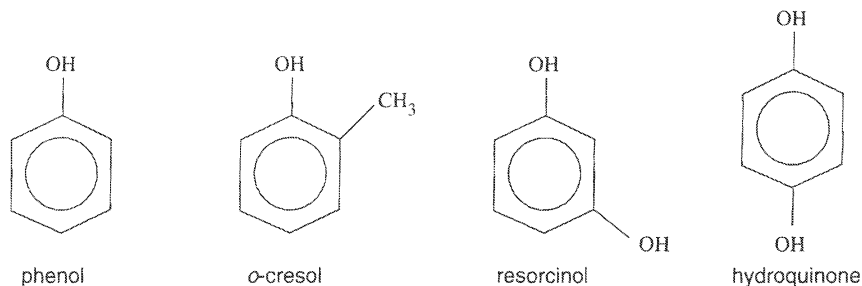
A second important property of carboxylic acids (or, more importantly, the corresponding anions) is the ability to complex metals, especially transition metals and aluminum. Complexation is particularly strong when two adjacent functional groups on a single molecule can coordinate with a cation and form a chelate (see Chapter 2).

A third important property of the carboxylic acid group is its effect on solubility and related properties. An ionized carboxylic acid greatly increases the solubility in water of the compound to which it is attached. Thus, for example, undissociated benzoic acid

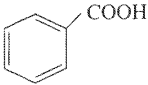
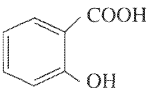
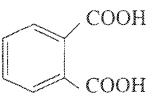


is relatively insoluble in water (3 g/l), but sodium benzoate is highly soluble (660 g/l). Even undissociated carboxylic acid groups contribute to solubility; benzoic acid is more soluble in water than is benzene. Somewhat related to solubility is the *hydrophobic* (water-hating) or *hydrophilic* (water-loving) property of an organic compound. Hydrophobic compounds are more soluble in organic solvents (e.g., octanol or dichloromethane) than in water, and hydrophilic compounds are more soluble in water than in organic solvents. This is important in fractionation schemes for dividing natural organic compounds into classes and in determining the adsorption properties of the compound. Compounds with a high ratio of polar functional groups (such as carboxylic acid groups) to framework carbon atoms tend to be hydrophilic, whereas those with a lower ratio tend to be hydrophobic.

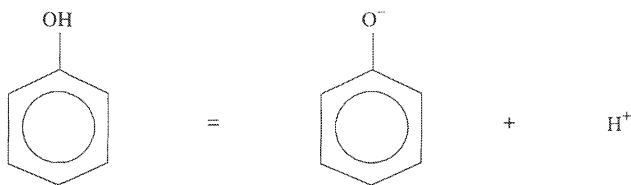
**Phenols.** A phenolic group is an —OH group attached to an aromatic ring, for example:



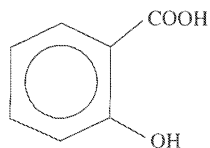
**TABLE 6-1** Dissociation Constants for Some Organic Acids

		$pK_a$
Acetic	$\text{CH}_3\text{COOH}$	4.9
Lactic	$\begin{array}{c} \text{CH}_3-\text{CH}-\text{COOH} \\   \\ \text{OH} \end{array}$	3.1
Oxalic	$\begin{array}{c} \text{COOH} \\   \\ \text{COOH} \end{array}$	1.2, 4.2
Benzoic		4.2
Salicylic		2.9
<i>o</i> -Phthalic		2.9, 5.5

The properties of phenols resemble those of carboxylic acids in several ways. They can dissociate into  $\text{H}^+$  and the corresponding anion:

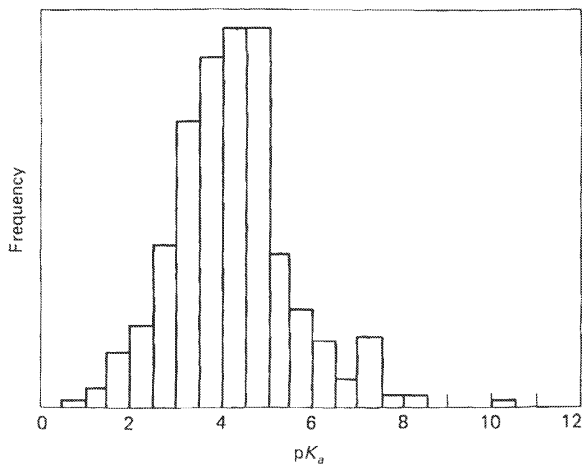


Although they are generally much weaker acids than carboxylic acids (Fig. 6-3), the  $pK_a$  value likewise depends on the nature of other functional groups nearby in the molecule. Phenolic groups form strong complexes with metal cations, and a phenolic group adjacent to a carboxylic acid group as in salicylic acid,



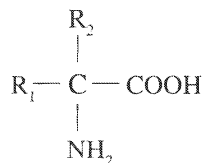
is a very effective chelator. Phenolic groups also contribute to the hydrophilic properties of a compound.

**FIGURE 6-2** Distribution of  $pK_a$  values for simple carboxylic acids (after Perdue, 1985).



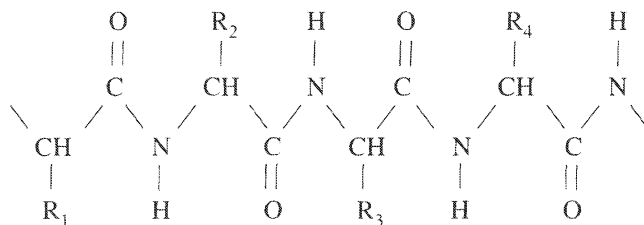
**Amines and Amino Acids.** The amino group ( $-\text{NH}_2$ ) behaves like ammonia in that it can accept a proton and become  $-\text{NH}_3^+$ . The nitrogen atom can coordinate with metal cations and contributes to the hydrophilic character of the molecule.

Natural amino acids contain an amino group adjacent to a carboxylic acid group:



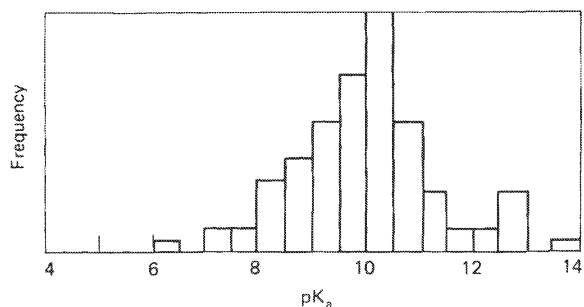
The remainder of the molecule (represented by  $\text{R}_1$  and  $\text{R}_2$ ) may be quite complex and commonly contains other functional groups. The group can behave as both an acid (from the  $-\text{COOH}$ ) group and as a base (from the  $-\text{NH}_2$  group).

Amino acids are the building blocks of proteins and are essential components of all living organisms. They may be present in natural waters as free amino acids, as peptides (chains of amino acids linked through their amino and carboxylic acid groups),

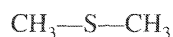


or as components of humic substances (see below). As a group, amino acids make up about 1 percent to 3 percent of the DOC in natural waters (Thurman, 1985).

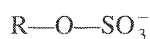
**FIGURE 6-3** Distribution of  $pK_a$  values for phenolic groups (after Perdue, 1985).



**Sulfur-Containing Functional Groups.** Relatively little is known about sulfur-containing functional groups in natural DOC. Microbial processes produce dimethyl sulfide:



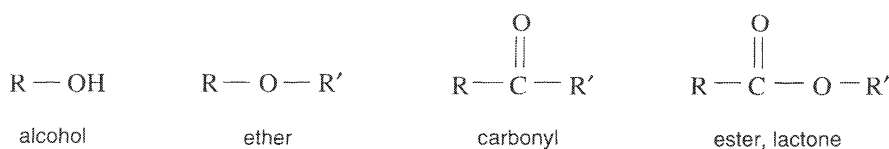
and various other reduced sulfur compounds. Leenheer et al. (1994) speculate that sulfur in fulvic acids (see below) is present as an ester sulfate:



Synthetic detergents commonly contain sulfonate groups:



**Neutral Functional Groups.** Natural organic matter contains several oxygen-containing functional groups,



that do not contribute directly to the acid-base properties of the molecule, but, because they are polar, they increase (to varying degrees) the solubility in water and the hydrophilic properties of molecules in which they are present.

## Humic Substances

Humic substances have been defined as “A general category of naturally occurring, biogenic, heterogeneous organic substances that can generally be characterized as being yellow to black in color, of high molecular weight, and refractory” (Aiken et al., 1985). In general terms, they are the products of the decomposition of primarily plant material by microbes. They are refractory in the sense that they are not easily decomposed further by microbes. Humic substances are subdivided into: *humins*, the fraction of humic substances that is insoluble in water at all pH values; *humic acid*, the fraction that is insoluble in water at pH 2 but becomes soluble at higher

pH; and *fulvic acid*, the fraction that is soluble under all pH conditions. Most of the dissolved organic carbon in natural waters is in the form of humic and fulvic acid, with fulvic acid predominating in surface waters and humic acid tending to predominate in soil solutions. Humic and fulvic acids are general terms that cover a wide range of individual compounds. The exact structures of the individual compounds have not been elucidated. Since *humic* and *fulvic acid* are general terms for mixtures of compounds, the detailed properties of humic or fulvic acid from one location may be different from those of humic or fulvic acid from another location. The differences are presumably related to different original source material and different degradation pathways.

Attempts to characterize soluble humic substances by identifying the individual compounds present have generally been unsuccessful (Hayes et al., 1989), and the common approach has been to measure the properties of either the bulk mixture or of fractions separated from the mixture. The simplest fractionation is the division into humic and fulvic acid on the basis of solubility at low pH. Fractionation can also be based on molecular size, electrical charge characteristics, and adsorption. The main purpose of fractionation is to provide more uniform material for characterization by other techniques.

Some of the more important characterization methods are:

**Elemental Analysis.** The composition of the humic material (C, H, O, N, S, and sometimes other elements) is measured by standard chemical techniques (Huffman and Stuber, 1985). Bulk analysis constrains the amount of individual functional groups that can be present and constrains the relative amounts of aliphatic versus aromatic carbon. The chemical compositions of fulvic and humic acids are shown in Table 6-2.

**Molecular Size and Weight Determinations.** *Colligative properties:* A colligative property is a property of a solution that depends only on the number of solute molecules present and not on their properties. Thus, if the number of molecules associated with a given concentration of fulvic acid is determined, a number-averaged molecular weight can be calculated. Colligative properties include vapor-pressure lowering, changes in freezing point and boiling point, and changes in osmotic pressure (Aiken and Gillam, 1989). Because solutions of humic substances are generally dilute in terms of the number of molecules present in solution, measuring these properties with sufficient precision is technically difficult. The most commonly used technique is vapor-pressure osmometry (e.g., Aiken et al., 1994). They report number-averaged molecular weights for aquatic fulvic acid of about 600 to 900 daltons. (The dalton is the standard unit of molecular weight; the weight of the isotope  $^{12}\text{C}$  is defined as

**TABLE 6-2** Average Values for Elemental Composition of Soil Humic Substances (from Steelink, 1985)

	<i>Humic Acids</i>	<i>Fulvic Acids</i>
Carbon	53.8–58.7%	40.7–50.6%
Hydrogen	3.2–6.2	3.8–7.0
Oxygen	32.8–38.3	39.7–49.8
Nitrogen	0.8–4.3	0.9–3.3
Sulfur	0.1–1.5	0.1–3.6

12,000 daltons.) One disadvantage of colligative-property measurements is that they provide only a mean molecular weight and provide no information on the spread or distribution of molecular weights.

*Gel permeation chromatography:* The most commonly used method for molecular size determination is gel permeation chromatography. A solution of the humic substance is passed through a column of Sephadex gel, and the extent to which fractions are retarded is a measure of their molecular size. Conceptually, the gel can be regarded as a framework with holes of a certain size in it. Molecules that are too large to fit the holes pass straight through the column and are not retarded. Smaller molecules diffuse through the holes into the gel, and hence take longer to pass through the column. If gels with different-sized "holes" (characterized by retention of known compounds) are used, the molecular size distribution of the humic substance can be measured. Molecular "size" is usually reported as molecular weight, although the conversion is only approximate.

Other methods for molecular size determination include ultrafiltration, and scattering of light or X-rays (Wershaw and Aiken, 1985). The general molecular-weight range of fulvic acids is 500 to 2,000 daltons and that of humic acids is 2,000 to  $10^6$  or more daltons.

**Acid-base Titration.** Acidic functional groups can be determined by titration with a strong base, such as barium hydroxide (see the discussion of alkalinity titrations in Chapter 3). In the past, such titration curves were "fitted" by assuming the existence of two types of functional groups: carboxylic acid with a  $pK_a$  of about 4 and phenol with a  $pK_a$  of about 10 (cf. Figs. 6-2 and 6-3). With this assumption, the number of carboxylic and phenolic groups per gram of humic substance could be readily measured. Unfortunately, the functional groups of "real" humic substances show a large spread in  $pK_a$  values, and there are several theoretical complications to the titration of a polyelectrolyte such as humic or fulvic acid (Ephraim et al., 1986; Marinsky and Ephraim, 1986; Perdue, 1985.)

**Nuclear Magnetic Resonance (NMR) Spectroscopy.** NMR spectroscopy measures transitions involving the nuclear spin of a suitable nucleus ( $^{13}\text{C}$  or  $^1\text{H}$ ) in an externally imposed magnetic field. The resonant frequency of the nucleus depends on the strength of the magnetic field to which it is exposed. The electrons surrounding the nucleus shield it partially from the external magnetic field, and so the resonant frequency varies as a function of the distribution of electrons around the nucleus. Thus NMR gives information on the electron configuration surrounding the  $^1\text{H}$  or  $^{13}\text{C}$  atom; the electron configuration is itself determined by the functional group in which the nucleus occurs. Proton NMR is capable of distinguishing between and estimating the relative amounts of protons on aromatic rings, aliphatic chains (several subclasses), carboxylic acids, hydroxyl groups, methoxyl groups, and lactone groups (Wershaw, 1985).  $^{13}\text{C}$  NMR can distinguish between aromatic carbon, aliphatic (alkyl) carbon, carboxyl carbon, carbon in aldehydes and ketones, and carbon in alcohols, esters, ethers, and so on. NMR (especially  $^{13}\text{C}$  NMR) is thus capable of estimating the amounts of various functional groups present and also the amounts of different types of carbon atom in the carbon skeleton.

**Suwannee River Humic Substances.** The Suwannee River drains the Okefenokee Swamp in the southeast portion of the state of Georgia. It is a "black" river, with low concentrations of inorganic ions, and a DOC concentration of 35-50 mgC/l. Interestingly, the DOC appears to be derived from decomposition of contemporary vegetation and not from the peat that

underlies the swamp (Malcolm et al., 1994) Large quantities of fulvic acid have been extracted from the Suwannee by workers at the U.S. Geological Survey. This fulvic acid has been extensively analyzed and characterized (Averett et al., 1994). It is thought to be typical of fulvic acid in rivers. Some properties of Suwannee River fulvic acid are listed in Table 6-3. Three proposed structural models consistent with the information are shown in Fig. 6-4. Note that the structures contain only two aromatic rings and have a large number of oxygen-containing functional groups. It must be emphasized, however, that fulvic acid is not a single compound; these models would thus be typical of the types of molecule that might make up a major fraction of the mixture.

Humic acids would be expected to be similar in structure to fulvic acids with the exception that the average molecular weight is higher and the proportion of oxygen-containing functional groups lower.

**TABLE 6-3** Average Properties of Suwannee River Fulvic Acid (from Leenheer et al., 1994)

Number-average molecular weight	800 daltons
Elemental composition (corrected for ash & moisture)	
Carbon	53.8%
Hydrogen	4.3%
Oxygen	40.9%
Nitrogen	0.7%
Sulfur	0.6%
Phosphorus	<0.1%
Average molecular formula	$C_{33}H_{32}O_{19}$
Carbon distribution by type of carbon by $^{13}C$ NMR (normalized to 33 total carbon atoms)	
Aliphatic	7
H-C-O (alcohol, ether, acetal, ketal)	5
O-C-O (acetal, ketal, inc. aromatic)	2
Aromatic	8
Phenols, phenolic esters, aromatic ethers	3
Carboxyl plus ester	6
Ketone	2
Hydrogen distribution (normalized to 32 total)	
Carboxyl	4
Phenol	2
Alcohol	1
Bound to carbon	25
Oxygen distribution (normalized to 19 total)	
Carboxyl	8
Ester	4
Ketone	2
Phenol	2
Alcohol	1
Acetal and ketal	1
Ether	1



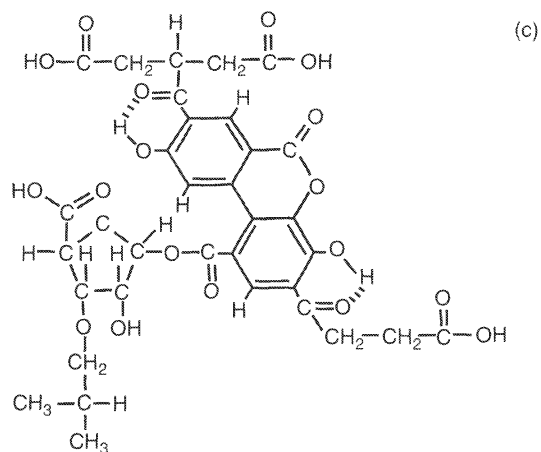
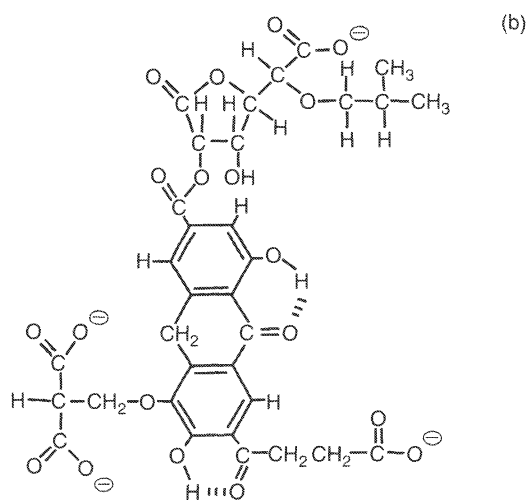
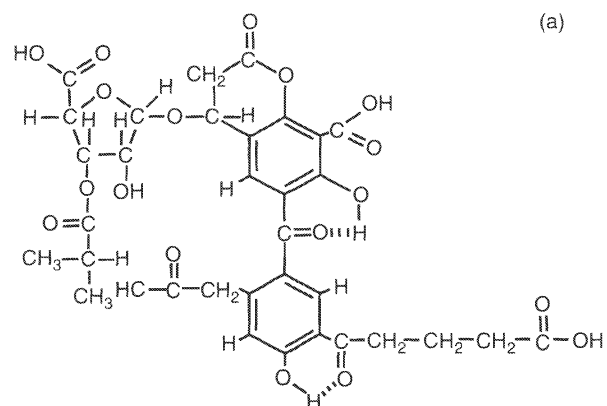


FIGURE 6-4 Three proposed average structural models of Suwannee River fulvic acid (from Leenheer et al., 1994).

## Dissolved Organic Carbon (DOC) in Natural Environments

**Soil Solutions.** The organic layer in soils is a major source of soluble organic compounds. Cronan and Aiken (1985) report concentrations of 21 to 32 mg C/l in solutions from the O/A horizon of soils from the Adirondack Mountains of New York State; concentrations there decreased to 5 to 7 mg C/l in the B horizon (50 cm depth). Yavitt and Fahey (1985) showed a similar decrease in DOC with depth in soils from the Rocky Mountains of Wyoming. Yavitt and Fahey also observed a strong seasonal effect: solutions from the organic layer at the time of first snowmelt contained high (greater than 70 mg C/l) concentrations of DOC, and the concentrations decreased to less than 20 mg C/l as the season advanced. The early-season solutions contained relatively high concentrations of low-molecular-weight, readily metabolizable compounds such as amino acids and short-chain aliphatic acids, whereas the late-season solutions were dominated by refractory humic substances. The seasonal changes are a result of seasonal changes in microbial activity. The decrease in DOC with depth is caused by some combination of microbial decomposition, adsorption, and precipitation as a solid (Stevenson, 1994).

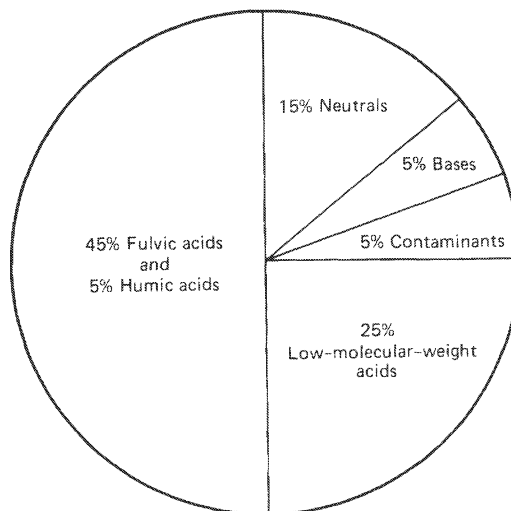
The presence of organic acids has a strong influence on weathering and soil formation (e.g., Antweiler and Drever, 1983; Fahey et al., 1985; Graustein et al., 1977). They control the pH of soil solutions and hence, in part at least, the rate of mineral weathering. Aluminum and iron are complexed by organic solutes, which results in leaching of these elements from upper horizons and deposition in deeper horizons (as the DOC is removed from solution), forming the characteristic profiles of podsols or spodosols (although there is some debate about the relative importance of transport of Al in solution and transport by physical movement of particles in soil profile development).

**Groundwater.** Most groundwaters that are not affected by pollution have DOC concentrations below 2 mg C/l, with a median value of about 0.7 mg C/l (Leenheer et al., 1974). As mentioned previously, water percolating through soil loses its DOC by several processes. By the time the water reaches the water table, most of the DOC has been removed. Locally, groundwaters associated with swamps or with coal or oil shale may have much higher DOC concentrations. Oilfield brines may contain very high (more than 1,000 mg C/l) concentrations of short-chain aliphatic acids produced by thermal degradation of kerogen (Lundegard and Kharaka, 1994).

**Rivers and Lakes.** DOC concentrations in rivers vary with the size of the river, climate, and the nature of vegetation in the river basin (Thurman, 1985). Excluding waters draining swamps and wetlands, the normal range is about 2 to 15 mg C/l with a mean of about 4 to 6 mg C/l (Degens, 1982). About half of the DOC is fulvic/humic acids (Fig. 6-5). Waters draining swamps and wetlands range from about 5 to 60 mg C/l with a mean of 25 mg C/l (Thurman, 1985). Again, the major component is fulvic acids. Organic species are often the dominant anions in such waters, and aluminum and iron, complexed by dissolved organic matter, may be major cations (Beck et al., 1974). DOC concentrations in rivers commonly vary with discharge. At low flow, when most of the water is derived from groundwater, DOC concentrations tend to be low. At high flow, when water is entering the river directly from the soil, DOC concentrations tend to be higher.

The DOC concentration in lakes varies with the biological productivity of the lake. Lakes with low productivity typically have 1 to 3 mg C/l, whereas eutrophic (see Chapter 8) lakes

**FIGURE 6-5** Distribution of different classes of organic compounds in surface water DOC in rivers of the United States (after Malcolm, 1985).



typically have 2 to 5 mg C/l (Thurman, 1985). Lakes associated with swamps or peat bogs may have much higher values. The DOC in lakes is a mixture of substances from river input (with a higher proportion of humic substances) and substances produced by the biota, primarily algae, in the lake (a wide range of compounds with a smaller portion of humic substances) (Wetzel, 1983). The relative importance of the two sources depends on the size of the lake; very roughly, the larger the lake, the smaller the relative contribution from river input.

DOC in surface waters is strongly involved in photochemical reactions (e.g., Sulzberger and Hug, 1994). Humic substances absorb ultraviolet and visible light, which both breaks down the humic molecules and provides free radicals that may influence the redox chemistry of iron, manganese, and other metals. Such photochemical reactions may be important in providing iron in a bioavailable form to phytoplankton, and in converting humic substances to smaller molecules that can be metabolized by microorganisms.

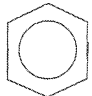
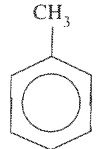
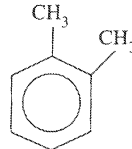
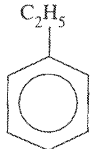
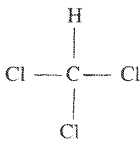
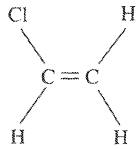
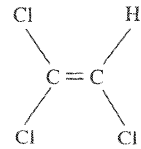
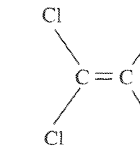
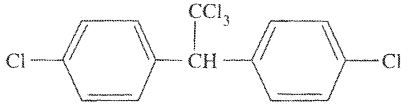
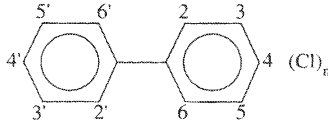

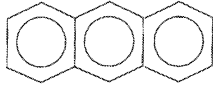
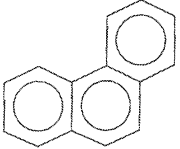
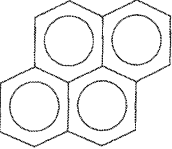
**The Oceans.** The mean DOC concentration in the surface layers (0 to 300 m) of the oceans is 1 mg C/l, with a range of 0.3 to 2.0 mg C/l (Williams, 1971). The mean DOC concentration of deeper water is 0.5 mg C/l. The DOC is derived both from marine biota and from continental runoff. Marine DOC contains a wide range of compounds, of which fulvic/humic acids are a relatively small proportion. Marine humic substances are quite different in chemical character from terrestrial humic substances, reflecting derivation, in part at least, from planktonic organisms rather than terrestrial plant material (Harvey and Boran, 1985).

## ORGANIC POLLUTANTS

Human activities have introduced a vast number of synthetic organic compounds into the environment, and many are causing significant pollution of ground and surface waters. Although many different compounds cause problems locally, the most important overall are aromatic

hydrocarbons (mostly from gasoline, diesel, and other fuels), chlorinated hydrocarbons (used in various industrial processes, mostly as solvents), and pesticides (Table 6-4). Aromatic hydrocarbons and chlorinated hydrocarbons have a number of properties in common: they are relatively nonpolar, they are somewhat soluble in water, they are volatile, and some members of each group are relatively resistant to biodegradation. Although aliphatic hydrocarbons are also a major component of fuels, they are generally less of a problem as pollutants in groundwater

**TABLE 6-4** Examples of Some Common Organic Pollutants

<i>Aromatic Hydrocarbons</i>			
			
benzene	toluene (methylbenzene)	<i>o</i> -xylene (1, 2-dimethylbenzene)	ethylbenzene
<i>Chlorinated Hydrocarbons</i>			
			
chloroform (trichloromethane)	vinyl chloride (chloroethene)	trichloroethylene, TCE (trichloroethene)	perchloroethylene, PCE (tetrachloroethene)
			
DDT		polychlorinated biphenyls (PCB) (Chlorine atoms attached at various points around both benzene rings)	
<i>Polynuclear Aromatic Hydrocarbons</i>			
			
naphthalene	anthracene	phenanthrene	pyrene

because they are much less soluble in water and are generally biodegradable. Another class of compound associated with petroleum is *polynuclear aromatic hydrocarbons* (PAH) (Table 6-4). These are relatively insoluble in water but are of environmental concern because many members of the group are carcinogens. The properties of pesticides are highly variable, so one cannot assign general properties to the group. Some (e.g., DDT) are chlorinated hydrocarbons (non-polar, insoluble), whereas others are highly polar and soluble in water.

### Solubility and Related Properties

Much of the behavior of organic pollutants is determined by their hydrophobicity, that is the extent to which they tend to partition into an organic phase such as octanol rather than into water. The most general measure of hydrophobicity is the *octanol-water partition coefficient*. If a compound is allowed to distribute itself between octanol and water in contact with each other, the octanol-water partition coefficient ( $K_{OW}$ ) is simply the ratio of its concentration in the octanol phase to its concentration in the aqueous phase. There is nothing “special” about octanol; other organic solvents would give a similar pattern. The octanol–water partition coefficient is a good predictor of adsorption behavior and of bioaccumulation. Compounds with very high  $K_{OW}$  values (for example the pesticide DDT) tend to accumulate in fat and not be excreted, and as a result their concentration increases up the food chain. The solubilities of nonpolar organic compounds also correlate fairly well with their octanol-water partition coefficients (Table 6-5). Note that the solubilities of many aromatic hydrocarbons and chlorinated hydrocarbons are quite high, as high as several hundred mg/l. Note also that low solubility in water corresponds to a high octanol-water partition coefficient, reflecting the “incompatibility” of that compound with water.

Because of their limited solubilities in water, nonpolar organic liquids commonly form a separate phase in the subsurface; such liquids are referred to as NAPLs (Non-Aqueous Phase Liquids). NAPLs are subdivided into LNAPLs (Light NAPLs), whose density is less than that of water, and DNAPLs (Dense NAPLs), whose density is greater than that of water. The most common LNAPLs are gasoline and other fuels; the most common DNAPLs are chlorinated hydrocarbons (particularly chlorinated ethylenes) used as solvents. If an LNAPL is spilled on the ground (Fig. 6-6), it tends to flow down through the unsaturated zone and form a pool at the water table. A DNAPL, by contrast (Fig. 6-7), will flow downward through the ground-water until it encounters an impermeable layer. It then tends to spread laterally, following the topography of the surface of the impermeable layer.

The theory of multiphase flow in a porous medium is complex, and will not be discussed here (for an introduction, see Fetter, 1993). As a liquid percolates downward through the unsaturated zone, it does not drain completely; some of the liquid remains in the pores, held by capillary forces. The amount of liquid remaining is referred to as the *residual saturation*. Similarly, if an NAPL is displaced by moving groundwater, the NAPL is not completely displaced by the water; a fraction, the *irreducible saturation*, remains behind. These phenomena contribute greatly to the difficulty of cleaning up aquifers contaminated by NAPLs. Even if all the “free” NAPL is pumped from the ground, a significant fraction remains behind in the pores of the vadose zone and the aquifer. The common pollutants are sufficiently soluble (Table 6-5) that the residual amounts can severely contaminate any groundwater moving through an affected volume, yet they are sufficiently insoluble that cleanup by pumping water through the affected volume to dissolve the residual amounts (“pump and treat”) is rarely an effective treatment by

**TABLE 6-5 Solubilities and Octanol-Water Partition Coefficients for Some Common Organic Pollutants** (from Mackay et al., 1992; Sangster, 1991; and other sources)\*

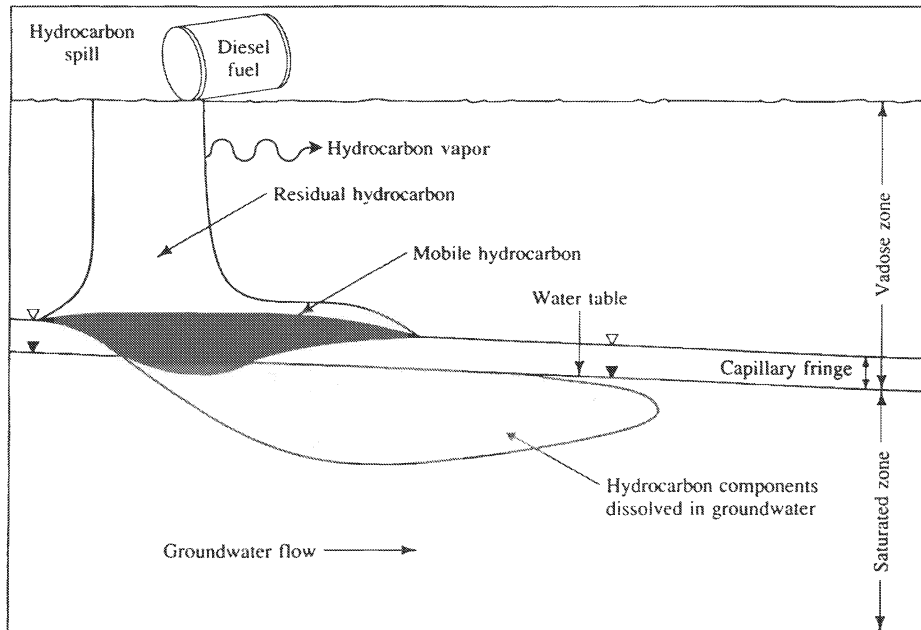
<i>Compound</i>	<i>Specific gravity</i>	<i>Solubility in water at 25°C (mg/l)</i>	<i>log K<sub>OW</sub></i>
<i>Aliphatic hydrocarbons</i>			
<i>n</i> -heptane	0.68	3	4.50
<i>n</i> -octane	0.70	0.7	5.15
<i>Aromatic hydrocarbons</i>			
Benzene	0.88	1800	2.13
Toluene	0.87	500	2.73
<i>o</i> -Xylene (1,2-dimethylbenzene)	0.88	180	3.12
Ethylbenzene	0.87	170	3.15
<i>Chlorinated hydrocarbons</i>			
Chloroform (trichloromethane)	1.48	8000	1.97
Carbon tetrachloride (tetrachloromethane)	1.59	800	2.83
1, 2 Dichloroethane	1.25	8500	1.48
1,1,2 Trichloroethane	1.44	4500	2.1
1,1,2,2 Tetrachloroethane	1.59	3000	2.4
Vinyl chloride	gas		1
Trichloroethylene (trichloroethene)	1.46	1200	2.4
Perchloroethylene (tetrachloroethene)	1.62	200	3
Chlorobenzene	1.11	450	2.84
1,3 Dichlorobenzene	1.29	120	3.5
<i>p,p'</i> -DDT		0.003	6.19
2,4,2',4'-Tetrachlorobiphenyl (PCB-47)	1.20	0.1	6.0
<i>Polynuclear aromatic hydrocarbons (PAH)</i>			
Naphthalene	1.15	32	3.35
Anthracene	1.3	0.07	4.50
Phenanthrene	1.2	1.2	4.52
Pyrene	1.3	0.13	5.00

\*There is considerable uncertainty associated with some of the solubility and log  $K_{OW}$  numbers.

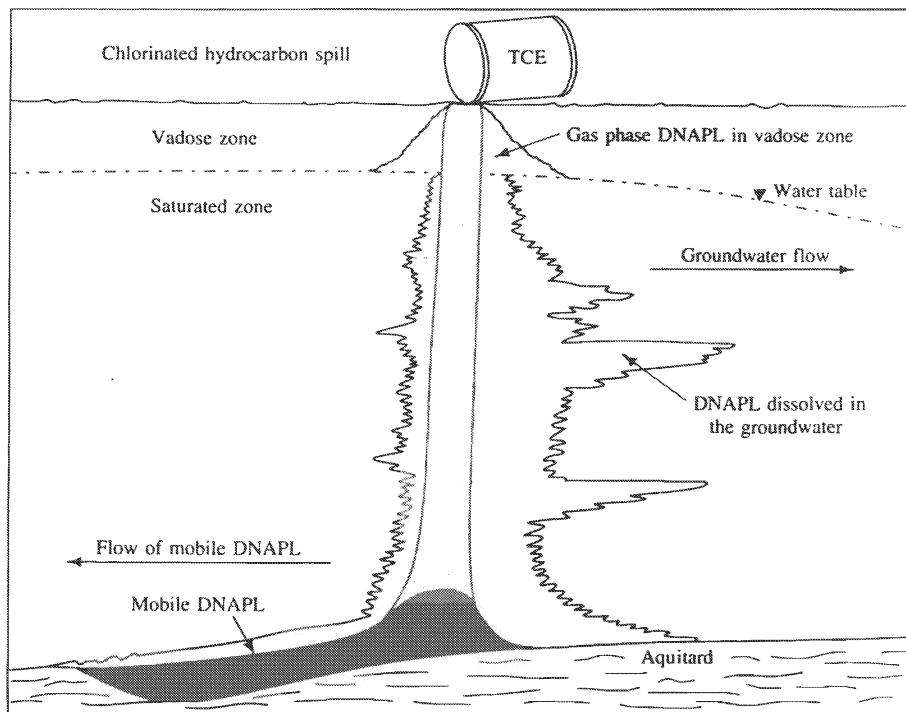
itself. "Pump and treat" may, however, be an effective way of containing the contaminant and preventing its spread. It is also used in combination with other strategies such as bioremediation (see below). For volatile NAPLs, circulating air through the vadose zone (vapor extraction) can be an effective cleanup strategy. These topics are well reviewed in the National Research Council (1994) publication "Alternatives for Ground Water Cleanup."

## Adsorption

**Nonpolar Compounds.** Dissolved organic compounds are often strongly adsorbed by solid phases in the subsurface, which greatly affects their mobility in groundwater. For nonpolar compounds such as hydrocarbons and chlorinated hydrocarbons, the important substrate is solid organic matter in the aquifer. "Solid organic matter" does not generally consist of large particles such as coal or wood fragments, but organic coatings on minerals. Natural minerals are very commonly coated by organic matter and, as a result, a



**FIGURE 6-6** General distribution of an LNAPL in the subsurface following a spill. CONTAMINANT HYDROGEOLOGY by Fetter, C. W., ©1993. Reprinted by permission of Prentice-Hall, Inc., Upper Saddle River, NJ.



**FIGURE 6-7** General distribution of a DNAPL in the subsurface following a spill. CONTAMINANT HYDROGEOLOGY by Fetter, C. W., ©1993. Reprinted by permission of Prentice-Hall, Inc., Upper Saddle River, NJ.

relatively small weight percent organic matter can correspond to a relatively large surface area available for adsorption. The principal adsorption mechanism is *hydrophobic partitioning*. Hydrophobic compounds are, by definition, incompatible with water and so tend to partition out of water onto any available organic substrate. Since the main driving energy is the incompatibility with water, the extent of adsorption is relatively insensitive to the exact nature of the solid organic matter. On the other hand, adsorption of nonpolar organic compounds by silicate minerals is generally unimportant. In aquifers containing more than about 0.1 to 1 percent organic carbon, adsorption of nonpolar compounds follows a simple distribution law:

$$C_{\text{ads}} = K_d C_{\text{soln}}$$

where  $C_{\text{ads}}$  is the concentration of the adsorbed solute (commonly moles or g per kg solid),  $C_{\text{soln}}$  is the concentration of the solute in aqueous solution (commonly moles or g per  $\ell$ ) and  $K_d$  is a distribution coefficient (Chapter 5) which commonly has units  $\ell/\text{kg}$ . Because adsorption is determined by the amount of organic matter present, the distribution coefficient,  $K_d$ , is proportional to the fraction of the aquifer solids that is organic matter

$$K_d = K_{\text{OM}} f_{\text{OM}} \quad (6-2)$$

where  $f_{\text{OM}}$  is the fraction of the aquifer solids that is organic matter and  $K_{\text{OM}}$  is the extrapolated value that  $K_d$  would have if the aquifer solids were 100 percent organic matter.

$K_{\text{OM}}$  reflects basically the hydrophobicity of the organic solute, and it can thus be predicted from the octanol-water partition coefficient,  $K_{\text{OW}}$ . For adsorption onto natural organic matter, many nonpolar organic compounds follow the equation (Schwarzenbach et al., 1993)

$$\log K_{\text{OM}} = 0.82 \log K_{\text{OW}} + 0.14$$

Combining these equations gives

$$\log K_d = 0.82 \log K_{\text{OW}} + \log f_{\text{OM}} + 0.14 \quad (6-3)$$

Slightly different coefficients for this equation have been reported by different authors (for reviews, see Karickhoff, 1984, and Schwarzenbach et al., 1993).

Organic matter is usually measured and reported as organic carbon, in which case Eq. (6-2) becomes

$$K_d = K_{\text{OC}} f_{\text{OC}}$$

where  $f_{\text{OC}}$  is the fraction of the aquifer that is organic carbon (the weight percentage organic carbon divided by 100), and  $K_{\text{OC}}$  is the (extrapolated) value that  $K_d$  would have if the aquifer were 100 percent organic carbon. Natural organic matter is approximately 50 percent C (Schwarzenbach et al., 1993), so  $f_{\text{OM}} = 2f_{\text{OC}}$  and, written in terms of organic carbon, Eq. (6-3) becomes

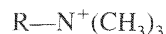
$$\log K_d = 0.82 \log K_{\text{OW}} + \log f_{\text{OC}} + 0.44$$

**Polar Compounds.** Adsorption of polar organic compounds, including many pesticides, is a complex subject (for reviews, see Schwarzenbach et al., 1993, and Stevenson, 1994). If the compound contains a cationic functional group (typically an amino group or pyridine), it will be adsorbed electrostatically by negatively charged surfaces such as clay min-

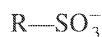


erals. Oxygen-containing functional groups may be adsorbed by ligand exchange with surface OH groups, by hydrogen bonding, or by dipole–dipole interaction. Many polar organic compounds are strongly adsorbed by clay minerals and oxides. The mechanisms are not well understood.

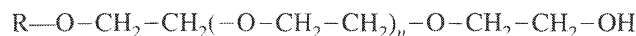
**Surfactants (Detergents).** Surfactants are molecules containing a hydrophilic “head” and a hydrophobic “tail.” The hydrophilic part may be a cationic group such as a quaternary ammonium group:



It may be an anionic group such as a carboxylate or a sulfonate:



or it may be a neutral group such as a polyether:



where  $n$  is typically about 8. The hydrophobic part of the molecule (R— in the examples above) is generally a straight-chain aliphatic hydrocarbon with 10–20 carbon atoms; it may also contain a benzene ring.

Cationic surfactants adsorb strongly on negatively charged surfaces such as clay minerals, including the interlayer spaces in smectites. Neutral surfactants generally adsorb less strongly onto minerals; anionic surfactants are much less adsorbed. Once a layer of surfactant has been adsorbed, the hydrophobic “tails,” which project into the solution away from the surface, form a hydrophobic organic layer that can adsorb nonpolar organic solutes. In general, the behavior of nonpolar solutes can be manipulated through addition of surfactants. The surfactants affect surface tension and “wetting,” miscibility/solubility, and adsorption/desorption. They are used extensively in enhanced oil recovery; their use in cleanup of NAPLs is the subject of considerable research. One problem is that surfactants themselves are not necessarily environmentally benign, so any surfactant that is injected into an aquifer must itself be cleaned up.

### Biodegradation and Bioremediation

The concept of bioremediation is relatively simple: microbes are capable of breaking down many organic compounds, ultimately to environmentally benign compounds such as  $\text{CO}_2$ , water, and inorganic forms of Cl, N, and S. They do this basically to obtain energy from the carbon in the contaminant molecule. Although the concept is simple, the implementation is complex and there are many limitations to the applicability of the method. The enzyme systems of microorganisms have evolved to deal with the compounds commonly encountered by the microorganisms in their natural environments. Such enzyme systems are not adapted to dealing with many synthetic organic compounds (or *xenobiotics*, as they are sometimes called), which limits the ability of such organisms to degrade organic pollutants. However, microorganisms have a remarkable ability to adapt, by a variety of mechanisms, and to develop enzymatic pathways that result in a breakdown of xenobiotic compounds (Schwarzenbach et al., 1993). It may require some considerable time for a natural community of organisms to acquire the ability to degrade an introduced contaminant and, of course, some organic compounds are not biodegraded to any significant extent.

Bioremediation (or, more strictly, *in-situ bioremediation*) may simply involve allowing naturally occurring microbes to act on the contaminant without further intervention, it may involve addition of oxygen and/or nutrients\*, it may involve extracting indigenous microbes, adapting them to the specific contaminant and reinjecting, or it may involve injecting specific organisms cultured in the laboratory. Although the concept of injecting a specific organism has received a great deal of publicity, the approach has not been particularly successful in practice. This is in part, at least, because biodegradation is usually not the result of a single organism, but of a *consortium* of microorganisms that interact with each other in complex ways. A further complication of bioremediation is that microorganisms may not degrade the target compound all the way to CO<sub>2</sub> and water, but to some intermediate compound that may itself be hazardous. As an example, vinyl chloride is commonly produced as an intermediate in the biodegradation of various chlorinated hydrocarbon solvents. Vinyl chloride is a carcinogen and considerably more hazardous than the original solvents.

Microorganisms use various metabolic pathways to oxidize organic carbon to CO<sub>2</sub> (see Chapter 8). The different pathways are characterized by the *terminal electron acceptor*, that is to say the "oxidizing agent." For aerobic microorganisms, the terminal electron acceptor is molecular oxygen. For anaerobic organisms, it may be nitrate, ferric iron, sulfate, or bicarbonate (and some other less important species). Although biodegradation of contaminants does occur under anaerobic conditions, particularly when nitrate is available as an electron acceptor, many more compounds are degraded under aerobic conditions, and the rate of degradation is generally much faster; however, some chlorinated hydrocarbons degrade more rapidly (by reductive dehalogenation) under anaerobic conditions (Mohn and Tiedje, 1992). Thus, in general, one requirement for successful bioremediation is the availability of oxygen. The solubility of oxygen in water is quite small. Water in equilibrium with the atmosphere contains about 10 mg/l (0.3 mM) of dissolved oxygen (the exact amount depends on temperature; see Table 8-1). This is a rather small amount. If much organic matter is present to be metabolized, oxygen in the groundwater will be rapidly depleted, and the bioremediation process is likely to be limited by the rate at which oxygen is transported to the site of reaction, either by advection (flow) of groundwater or by diffusion. Because of this limitation, bioremediation is currently most useful as a "polishing" step once the bulk of a contaminant has been removed. A great deal of research is currently being conducted on bioremediation under both aerobic and anaerobic conditions. The subject is reviewed in National Research Council (1993).

## REVIEW QUESTIONS

1. Suppose a river water contains 10 mg/l DOC, and that the DOC represents ionized fulvic acid with the composition described in Table 6-3:
  - a. Now many milliequivalents per liter of organic anions would be present?

\*Nutrients may be inorganic species such as nitrogen and phosphorus compounds, or may include a readily metabolized substrate such as acetate to stimulate microbial growth and degradation of the target compound by a process called *cometabolism*.

- b. If the organic anions were balanced by  $\text{Ca}^{2+}$ , how many ppm calcium would this represent?
- c. If it requires two functional groups (either two carboxyl acid groups or a phenol group plus a carboxylic acid group) to complex an aluminum ion, how many ppm aluminum could be present in the water as complexes with fulvic acid?
2. What should be the distribution coefficient for toluene in an aquifer containing 0.5 percent organic carbon? What would be a reasonable estimate for the retardation coefficient (Chapter 16) of toluene in the aquifer?
3. A groundwater contains a dissolved oxygen concentration of 5 mg/l. How many liters of groundwater would it take to oxidize 1 g of toluene to  $\text{CO}_2$ ?

### SUGGESTED READING

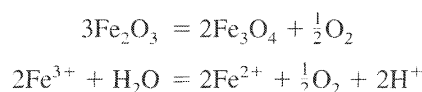
- AIKEN, G. R., et al., (Eds.). (1985). *Humic Substances in Soil, Sediment, and Water*. New York: Wiley-Interscience.
- AVERETT, R. C., J. A. LEENHEER, D. M. MCKNIGHT, and K. A. THORN. (1994). *Humic Substances in the Suwannee River, Georgia: Interactions, Properties, and Proposed Structures*. U.S. Geological Survey Water-Supply Paper 2373. An up-to-date presentation of techniques for studying aquatic humic substances and a synthesis of the results.
- CHAPPELLE, F. H. (1993). *Ground-Water Microbiology and Geochemistry*. New York: Wiley.
- FETTER, C. W. (1993). *Contaminant Hydrogeology*. New York: Macmillan.
- HAYES, M. B. H., et al., (Eds.). (1989). *Humic Substances II: In Search of Structure*. New York: Wiley-Interscience.
- NATIONAL RESEARCH COUNCIL. (1993). *In Situ Bioremediation: When Does It Work?*. Washington, DC: National Academy of Sciences.
- NATIONAL RESEARCH COUNCIL. (1994). *Alternatives for Ground Water Cleanup*. Washington, DC: National Academy Press.
- PITTMAN, E. D., and M. D. LEWAN. (1994). *Organic Acids in Geological Processes*. New York: Springer-Verlag.
- SCHWARZENBACH, R. P., P. M. GSCHWEND, and D. M. IMBODEN. (1993). *Environmental Organic Chemistry*. New York: Wiley-Interscience.
- STEVENSON, F. J. (1994). *Humus Chemistry: Genesis, Composition, Reactions*. New York: Wiley.
- THURMAN, E. M. (1985). *Organic Geochemistry of Natural Waters*. Dordrecht, Netherlands: Martinus Nijhoff/Dr. W. Junk.



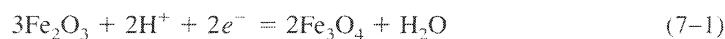
# 7

## Redox Equilibria

Most of the chemical reactions we have discussed so far, such as the solubility of carbonates, have been acid-base processes; that is, they have involved transfer of protons. We now consider the other great class of reactions, those which involve transfer of electrons. Oxidation-reduction (or redox) reactions can be thought of as reactions involving transfer of oxygen. For example:



Or they can be thought of as transfers of electrons:

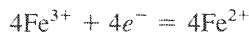


where  $e^-$  represents an electron. In solution chemistry it is generally more convenient to consider redox reactions as electron transfers. Many redox reactions do not involve molecular oxygen directly, and even where molecular oxygen is involved, there are usually kinetic problems that complicate the use of activity of oxygen as a thermodynamic variable. At elevated temperatures and pressures, on the other hand, thermodynamic functions involving electrons may not be well defined, and oxygen fugacity is the more convenient variable to use.

Eqs. (7-1) and (7-2) do not represent complete chemical reactions. There is no such thing as a free electron in aqueous solution, so some complementary reaction must take place to provide or consume electrons. Consider, for example, the reduction of  $\text{Fe}^{3+}$  by organic matter [represented by (C)]:



Eq. (7-3) is a balanced redox reaction in which neither electrons nor molecular oxygen are shown explicitly. This equation can be broken into two half-reactions, one involving only iron and the other only carbon:



A thermodynamic convention has been established based on the standard hydrogen electrode, which allows each half-reaction to be considered in isolation.

### THE STANDARD HYDROGEN ELECTRODE AND THERMODYNAMIC CONVENTIONS

The standard hydrogen electrode (SHE) consists of a piece of finely divided platinum in contact with a solution containing hydrogen ions at unit activity and hydrogen gas at a pressure of 1 atm, with the whole system at 25°C (Fig. 7-1). The purpose of the platinum is simply to provide electrical contact and to catalyze equilibrium among the other species. The thermodynamic conventions related to the SHE are:

1. The difference in electrical potential between the metal electrode and solution is zero.
2. The standard free energy of formation of a proton in solution is zero.
3. The standard free energy of formation of an electron in solution is zero.

These conventions assign arbitrary values to quantities that cannot, in principle, be measured. Once these assignments have been made, however, a scale has been defined on which the free energies of other dissolved ions can be measured. The logic is analogous to the arbitrary assumption that the standard free energies of formation of elements in their standard states is zero.

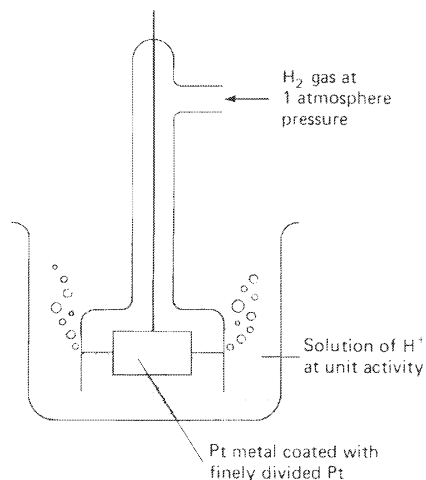
Consider the electrochemical cell shown in Fig. 7-2, which consists of two half-cells, A and B, that are connected by a salt bridge. A salt bridge is a solution of a salt, such as KCl, which establishes electrical contact between the two half-cells. We shall assume for the moment that the salt bridge behaves ideally; that is, it acts simply as a conductor of electricity.

In half-cell A, the platinum wire acts as an inert means of transferring electrons to or from solution. The chemical reaction taking place at the electrode can be represented by the equation



If this reaction is to go to the left, the platinum wire must remove electrons from half-cell A. If it is to go to the right, the wire must provide electrons to the solution. If the wire is not connected to a source or sink for electrons, there can be no net reaction, but the wire will acquire an electrical potential that reflects the tendency for electrons to leave the solution. We can, by convention, represent this tendency by an "activity of electrons,"  $\alpha_{e^{-}}$ , in solution. The activity of electrons does not correspond to a concentration, as is the case with most solutes, but to the tendency (which can be thought of as being analogous to pressure) of the system to provide electrons to any electron acceptor (electrode or chemical system).  $\alpha_{e^{-}}$  and  $pe$  ( $pe = -\log_{10} \alpha_{e^{-}}$  by analogy with  $pH = -\log_{10} \alpha_{\text{H}^{+}}$ ) are not strictly analogous to the activities of "normal" solutes (Hostettler, 1984; Hostettler, 1985; Stumm and Morgan, 1996). They do, however, provide a convenient formalism for discussion of redox reactions.

FIGURE 7-1 The standard hydrogen electrode.



An equilibrium constant can be written for Eq. (7-4):

$$K_{eq} = \frac{a_{Fe^{2+}}}{a_{Fe^{3+}} a_{e^-}}$$

or, alternatively,

$$a_{e^-} = \frac{1}{K_{eq}} \frac{a_{Fe^{2+}}}{a_{Fe^{3+}}}$$

The activity of electrons is thus proportional to the ratio of the activity of the reduced species to that of the oxidized species.

Consider now half-cell B in Fig. 7-2. The reaction is

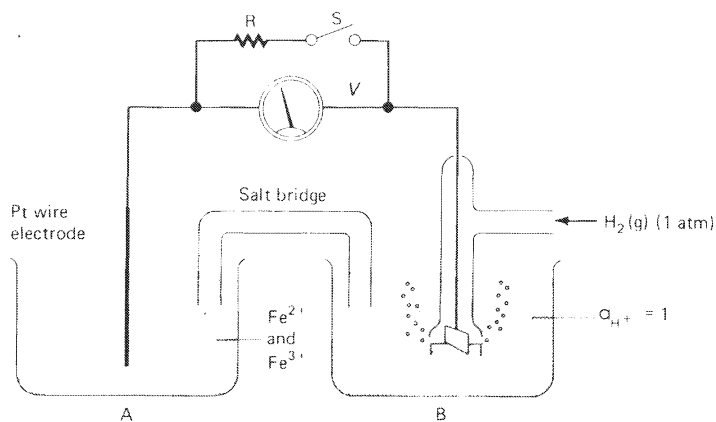
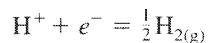


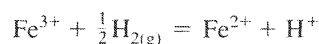
FIGURE 7-2 Redox cell discussed in text.

As in half-cell A, the direction in which the reaction goes depends on whether the platinum is acting as a source or sink for electrons. If the wire is electrically isolated, it can do neither, but it will acquire an electrical potential controlled by the relative activities of oxidized and reduced species. We can again represent this by an activity of electrons and write an equilibrium constant:

$$K_{\text{SHE}} = \frac{P_{\text{H}_2}^{1/2}}{\alpha_{\text{H}^+} \alpha_{e^-}}$$

By convention,  $\alpha_{e^-} = 1$  in the SHE. This is consistent with the definition of the SHE and the conventions that the standard free energies of formation of  $\text{H}^+$  and  $e^-$  are zero.

Consider now the whole system in Fig. 7-2. If the switch S is closed, electrons will move from the solution with the higher activity of electrons to the solution with the lower activity of electrons. Energy will be released, largely in the form of heat in the resistance  $R$ . The overall reaction will be

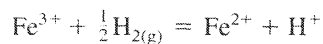


The direction of the reaction will depend on which half-cell has the higher activity of electrons.

If switch S is opened, there will no longer be any transfer of electrons from one half-cell to the other. The voltage meter V will register the difference in potential  $E$  between the two electrodes. Since, by convention, the potential of the SHE is zero,  $E$  represents the potential of the electrode in half-cell A. This potential is called the Eh of the solution, the h derived from the fact that it is measured (or expressed) relative to the standard hydrogen electrode. The Eh may be positive or negative, depending on whether the activity of electrons in solution A is less or greater than the activity of electrons in the SHE. By convention, the Eh is positive if the activity of electrons in half-cell A is less than that in the SHE. The half-cell convention is based on the idea that the complementary half-cell is the standard hydrogen electrode. For thermodynamic purposes, the reaction



is equivalent to



where  $\text{H}_2$  and  $\text{H}^+$  are in their standard states (unit activity).

The activity of electrons in a solution (and hence its redox level) can thus be expressed in units of volts (Eh) or in units of electron activity ( $\alpha_{e^-}$ , or  $pe$ ). Eh and  $pe$  are related by the equation

$$pe = \frac{F}{2.303RT} \text{Eh}$$

where  $F$  is Faraday's constant (96,484 kJ per volt gram equivalent, the unit consistent with the others used here),  $R$  is the gas constant ( $8.314 \times 10^{-3}$  kJ/K.mol),\*  $T$  is temperature in kelvins, and 2.303 is the conversion from natural to base 10 logarithms. At 25°C,  $pe = 16.9 \text{ Eh}$ , and  $\text{Eh} = 0.059pe$ .

\* In calorie units  $F$  is 23.06 kcal per volt gram equivalent, and  $R$  is  $1.987 \times 10^{-3}$  kcal/K.mol.



**Use of Eh as a Variable**

Consider again the reaction



From Eq. (2-3),

$$\Delta G_R = \Delta G_R^0 + RT \ln \left( \frac{a_{\text{Fe}^{2+}} a_{\text{H}^+}}{a_{\text{Fe}^{3+}} P_{\text{H}_2}^{1/2}} \right)$$

Since  $a_{\text{H}^+} = P_{\text{H}_2} = 1$ ,

$$\Delta G_R = \Delta G_R^0 + RT \ln \left( \frac{a_{\text{Fe}^{2+}}}{a_{\text{Fe}^{3+}}} \right) \quad (7-5)$$

It is a basic result from electrochemistry that Eh and Gibbs free energy are related by the equation

$$\Delta G_R = -nFEh \quad (7-6)$$

where  $n$  is the number of electrons involved in the reaction and  $F$  is Faraday's constant. The sign of Eh has been established by convention; Eq. (7-6) is correct only if the half-reaction is written with electrons appearing on the left side of the equation. Dividing Eq. (7-5) by  $-nF$  gives

$$\frac{-\Delta G_R}{nF} = \frac{-\Delta G_R^0}{nF} + \frac{RT}{nF} \ln \left( \frac{a_{\text{Fe}^{2+}}}{a_{\text{Fe}^{3+}}} \right)$$

Substituting Eq. (7-6) yields

$$Eh = E^0 - \frac{RT}{nF} \ln \left( \frac{a_{\text{Fe}^{2+}}}{a_{\text{Fe}^{3+}}} \right) \quad (7-7)$$

$E^0$  is the *standard electrode potential*, which is the Eh the cell would have if all the chemical species involved (here  $\text{Fe}^{2+}$  and  $\text{Fe}^{3+}$ ) were in their standard states (unit activity). Standard electrode potentials are tabulated in the literature and can readily be calculated from standard free energies of formation. Eq. (7-7) can be rewritten (remembering that  $\log 1/x = -\log x$ ) as

$$Eh = E^0 + \frac{2.303RT}{nF} \log \left( \frac{a_{\text{Fe}^{3+}}}{a_{\text{Fe}^{2+}}} \right)$$

or, at 25°C

$$Eh = E^0 + \frac{0.059}{n} \log \left( \frac{a_{\text{Fe}^{3+}}}{a_{\text{Fe}^{2+}}} \right)$$

This can be generalized for any redox reaction at 25°C:

$$Eh = E^0 + \frac{0.059}{n} \log \left( \frac{\text{activity product of oxidized species}}{\text{activity product of reduced species}} \right)$$

which is the form most commonly used in calculations.

Consider, for example, the redox pair sulfate– $\text{H}_2\text{S}$ . The half-reaction, with electrons appearing on the left, is



The expression for Eh for this reaction is (at 25°C)

$$Eh = E^0 + \frac{0.059}{8} \log \left( \frac{a_{\text{SO}_4^{2-}} a_{\text{H}^+}^{10}}{a_{\text{H}_2\text{S}} a_{\text{H}_2\text{O}^+}^4} \right) \quad (7-8)$$

$E^0$  can be calculated from Eq. (7-6) and the free energy values in Appendix II:

$$\begin{aligned} E^0 &= \frac{-1}{nF} (\Delta G_{\text{H}_2\text{S}}^0 + 4\Delta G_{\text{H}_2\text{O}}^0 - \Delta G_{\text{SO}_4^{2-}}^0) \\ &= \frac{-1}{8 \times 96.48} (-232.3) \\ &= +0.30 \text{ V} \end{aligned}$$

### Use of pe as a Variable

The formalism for pe is similar to that for Eh but simpler because pe is an “activity” unit and we do not have the conversion between volts and activities. Consider the ferrous–ferric system



(When pe is used as a variable, it does not matter on which side electrons appear in the reaction.)

$$\begin{aligned} K_{\text{eq}} &= \frac{a_{\text{Fe}^{2+}}}{a_{\text{Fe}^{3+}} a_{e^-}} \\ \frac{1}{a_{e^-}} &= K_{\text{eq}} \frac{a_{\text{Fe}^{3+}}}{a_{\text{Fe}^{2+}}} \\ pe &= \log K_{\text{eq}} + \log \frac{a_{\text{Fe}^{3+}}}{a_{\text{Fe}^{2+}}} \quad (7-10) \end{aligned}$$

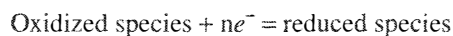
$K_{\text{eq}}$  is the equilibrium constant for Eq. (7-9). It can be calculated from the standard free energies in Appendix II:

$$\begin{aligned} -RT \ln K_{\text{eq}} &= \Delta G_{\text{Fe}^{2+}}^0 - \Delta G_{\text{Fe}^{3+}}^0 \quad (\Delta G_{e^-}^0 \text{ is zero}) \\ &= -74.3 \text{ kJ/mol} \\ \log K_{\text{eq}} &= 13.0 \end{aligned}$$

and hence,

$$pe = 13.0 + \log \left( \frac{a_{\text{Fe}^{3+}}}{a_{\text{Fe}^{2+}}} \right)$$

In general, for the reaction



$$pe = \frac{1}{n} \log K_{\text{eq}} + \frac{1}{n} \log \left( \frac{\text{activity product of oxidized species}}{\text{activity product of reduced species}} \right)$$

For the sulfate reduction reaction,

$$\text{SO}_4^{2-} + 8e^- + 10\text{H}^+ = \text{H}_2\text{S} + 4\text{H}_2\text{O}$$

$$pe = \frac{1}{8} \log K_{\text{eq}} + \frac{1}{8} \log \left( \frac{a_{\text{SO}_4^{2-}} a_{\text{H}^+}^{10}}{a_{\text{H}_2\text{S}} a_{\text{H}_2\text{O}}^4} \right) \quad (7-11)$$

where

$$-RT \ln K_{\text{eq}} = \Delta G_{\text{H}_2\text{S}}^0 + 4\Delta G_{\text{H}_2\text{O}}^0 - \Delta G_{\text{SO}_4^{2-}}^0$$

from the example above

$$= -232.3 \text{ kJ/mol}$$

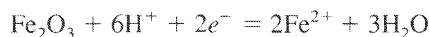
and at 25°C

$$\log K_{\text{eq}} = \frac{-\Delta G_{\text{R}}^0}{5.708} = 40.7$$

This equilibrium constant is also listed directly in Appendix III.

### Definition of *pe* and *Eh* by Redox Pairs

The discussion so far has been based on the electrochemical cell shown in Fig. 7-2, which included a platinum wire and a standard hydrogen electrode. These items are necessary for understanding the derivation of *pe* and *Eh*, but the activity of electrons in solution A will be exactly the same whether the platinum electrode and the SHE are present or not. A *pe* or *Eh* is defined whenever both members of a redox pair are present either in solution together or in contact with solution. In any solution containing ferrous and ferric ions, *pe* and *Eh* are defined by Eqs. (7-10) and (7-7) respectively. In any solution containing sulfate and hydrogen sulfide, *pe* and *Eh* are defined by Eqs. (7-11) and (7-8). Redox reactions that define a *pe* and an *Eh* may involve solid phases; for example,



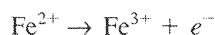
$$Eh = E^0 + \frac{RT}{2F} \ln \frac{a_{\text{H}^+}^6}{a_{\text{Fe}^{2+}}^2}$$

$$pe = \frac{1}{2} \log K_{\text{eq}} + \frac{1}{2} \log \left( \frac{a_{\text{H}^+}^6}{a_{\text{Fe}^{2+}}^2} \right)$$

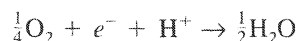
What happens if a solution contains more than one redox pair, for example,  $\text{Fe}^{3+}$ ,  $\text{Fe}^{2+}$ ,  $\text{SO}_4^{2-}$ , and  $\text{H}_2\text{S}$ ? Each pair will define a *pe* (or *Eh*), but the two values may not be the same. If the system is at chemical equilibrium, the two values will be identical, but if all species are not in equilibrium with each other (a common situation in nature), the values will be different. Unless all redox couples are in equilibrium, one cannot speak of “the *pe* (*Eh*) of a solution.” One *can* speak of the *pe* (*Eh*) defined by a particular couple in the solution, but it is misleading to attribute that *pe* (*Eh*) to the solution as a whole without careful justification of what is implied.

## MEASUREMENT OF Eh

The preceding discussion might have given the impression that Eh could always be measured by inserting a platinum wire into the solution of interest and comparing the potential to that of a SHE.\* This is true only if the redox reaction occurs rapidly and reversibly at the surface of the platinum, and if the electrode is responding to a single redox pair and not to some process involving two or more redox pairs that are not in mutual equilibrium. (These questions are discussed in detail by Stumm and Morgan, 1996). In general, the platinum electrode responds satisfactorily to very few of the redox pairs important in natural waters. Examples of systems to which the electrode does *not* respond are O<sub>2</sub>-H<sub>2</sub>O, SO<sub>4</sub><sup>2-</sup>-H<sub>2</sub>S, CO<sub>2</sub>-CH<sub>4</sub>, NO<sub>3</sub><sup>-</sup>-N<sub>2</sub>, N<sub>2</sub>-NH<sub>4</sub><sup>+</sup>, and almost all reactions involving solid phases. Mixed potentials, which are potentials that result from a combination of parts of two different redox systems, are common in natural waters. For example, in a solution containing Fe<sup>2+</sup> and dissolved oxygen, the reactions



and



might be taking place (the latter via several steps). These two reactions would fix the potential measured by the platinum electrode at some value, but the value would have no meaning for any individual redox pair.

In relatively oxidizing waters, Eh values measured with a platinum electrode can rarely be related to a specific redox pair and are rarely of much value in quantitative interpretations of natural water chemistry. In waters from strongly reducing environments, minor species are often present to which the electrode does respond, so Eh measurement may be of value. In strongly reducing waters, great care must be taken to avoid any contact of the solution with air, either before or during the measurement.

In using the term Eh, it is important to distinguish between the quantity that is measured with a platinum electrode and the quantity that is calculated from the activities of a redox pair. In this book, Eh is used in the latter sense; it is thus regarded as a thermodynamic variable, which cannot generally be measured directly. The most important way of “measuring” Eh is in fact to measure both members of a redox couple such as iron species, sulfur species, or forms of a trace element such as arsenic (Cherry et al., 1979b).

## REDOX CALCULATIONS USING WATEQ4F

WATEQ4F calculates the speciation of redox-sensitive elements in accordance with a *pe* or Eh specified by the user. *pe* (Eh) can be defined in several different ways in the input:

1. As a numerical value for *pe* or Eh.
2. By the concentrations of both members of a redox pair (e.g., Fe<sup>2+</sup> and Fe<sup>3+</sup>). The code includes thirteen possible pairs. It also includes the option of using different redox pairs

\*The SHE is almost never used in practice. A reference electrode (calomel or silver-silver chloride) whose potential is known relative to the SHE is used instead.

to define the speciation of different elements. This allows considerable flexibility in modeling natural systems where redox disequilibrium is present.

Problems can arise when  $pe$  is defined in more than one way. For example, if the input specifies a numerical value for  $pe$  and concentrations of both  $Fe^{2+}$  and  $Fe^{3+}$ ,  $pe$  will be defined in two different ways, which will generally be inconsistent. WATEQ4F will give a warning message in such situations. If a numerical value for  $pe$  or Eh is to be used, total concentrations for each element (e.g.,  $Fe_{total}$ ) should be entered rather than individual species (e.g.,  $Fe^{2+}$  and  $Fe^{3+}$ ).

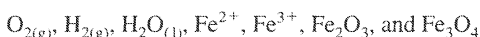
## pe-pH AND Eh-pH DIAGRAMS

These diagrams are a convenient way of displaying stability relationships where redox reactions are involved. They show strictly equilibrium relationships, but it must always be remembered that departures from equilibrium, particularly redox equilibrium, are common in natural waters. Equilibrium calculations tell us what reactions *should* take place, but they cannot tell us the rate at which these reactions will occur.

### System Fe-O-H<sub>2</sub>O

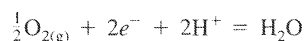
#### Example 1

Construct a  $pe$ -pH diagram for the system Fe-O-H<sub>2</sub>O at 25°C and 1 atm total pressure, considering initially the species:



The first consideration is the stability of liquid water. At very high  $pe$ , the pressure of  $O_2$  in equilibrium with liquid water will exceed 1 atm, and at very low  $pe$ , the pressure of hydrogen in equilibrium with water will exceed 1 atm. Since we are interested only in environments where water is stable at a total pressure of 1 atm, the stability of water defines the  $pe$ -pH region of interest.

The upper stability limit of water is defined by the reaction:



$$K_{eq} = \frac{a_{H_2O}}{P_{O_2}^{1/2} a_e^2 a_{H^+}^2}$$

Since  $a_{H_2O} = 1$  (pure water in its standard state),

$$\log K_{eq} = -\frac{1}{2} \log P_{O_2} + 2pe + 2pH$$

$$pe = \frac{1}{2} \log K_{eq} + \frac{1}{4} \log P_{O_2} - pH \quad (7-12)$$

$$\Delta G_R^0 = \Delta G_{H_2O}^0 = -237.14 \text{ kJ (the other standard free energies of formation are zero)}$$

$$\log K_{eq} = \frac{-\Delta G_R^0}{2.303RT} = \frac{237.14}{5.708} = +41.55 \text{ at } 25^\circ\text{C}$$

For  $P_{O_2} = 1$  (the upper stability limit for water),  $\log P_{O_2} = 0$ , so:

$$pe = 20.77 - pH$$

This plots as a straight line of slope  $-1$  on the  $pe$ - $pH$  diagram (Fig. 7-3). From Eq. (7-12), lines of equal  $P_{O_2}$  plot parallel to the line for  $P_{O_2} = 1$  atm. Note the rapid change in  $P_{O_2}$  (Fig. 7-3) on moving away from the line  $P_{O_2} = 1$ . The  $P_{O_2} = 0.2$  atm line is indistinguishable from the  $P_{O_2} = 1$  atm line.

The lower stability limit of water is defined by the reaction:

$$H^+ + e^- = \frac{1}{2}H_{2(g)}$$

$$K_{eq} = \frac{P_{H_2}^{1/2}}{\alpha_{H^+}\alpha_{e^-}}$$

$$\log K_{eq} = \frac{1}{2} \log P_{H_2} + pe + pH$$

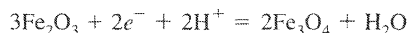
The standard free energies of formation of all species in the reaction are zero, so  $\Delta G_R^0 = 0$  and  $\log K_{eq} = 0$ ,

$$pe = -\frac{1}{2} \log P_{H_2} - pH$$

Again, this represents a straight line with a slope of  $-1$ . Lines of constant  $P_{H_2}$  will be parallel to this line; some examples are shown on Fig. 7-3. At the lower stability limit for water,  $P_{H_2} = 1$ ,  $\log P_{H_2} = 0$ , so

$$pe = -pH$$

Next, consider the boundary  $Fe_2O_3$ - $Fe_3O_4$ :



The solids and water are all in their standard states, so

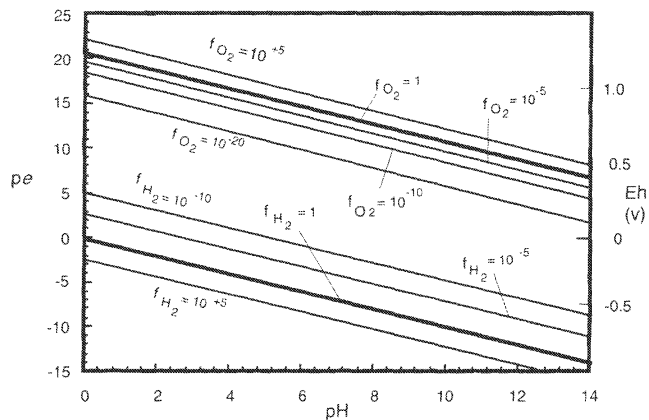
$$K_{eq} = \frac{1}{\alpha_e^2 \alpha_{H^+}^2}$$

$$\log K_{eq} = 2pe + 2pH$$

$$pe = \frac{1}{2} \log K_{eq} - pH$$

This boundary will also be a straight line of slope  $-1$ . Its intercept will be given by the value of  $K_{eq}$ :

**FIGURE 7-3** Contours of equal oxygen fugacity and hydrogen fugacity as a function of  $pe$  and  $pH$  at 25°C.



$$\begin{aligned}\Delta G_R^0 &= 2\Delta G_{\text{Fe}_2\text{O}_3}^0 + \Delta G_{\text{H}_2\text{O}}^0 - 3\Delta G_{\text{Fe}^{3+}}^0 \\ &= -34.5 \text{ kJ}\end{aligned}$$

$$\log K_{\text{eq}} = 6.05$$

The equation for the boundary is thus:

$$pe = 3.03 - pH$$

which is plotted on Fig. 7-4.

Next, consider the boundary  $\text{Fe}^{3+}$ - $\text{Fe}_2\text{O}_3$ :



$$K_{\text{eq}} = \frac{\alpha_{\text{Fe}^{3+}}^2}{\alpha_{\text{H}^+}^6}$$

$$\log K_{\text{eq}} = 2 \log \alpha_{\text{Fe}^{3+}} + 6pH \quad (7-13)$$

pe is not involved in this equation (both  $\text{Fe}^{3+}$  and  $\text{Fe}_2\text{O}_3$  are in the same oxidation state), so the boundary will plot as a vertical line on a pe-pH diagram. Before the line can be plotted, we must arbitrarily choose a value of  $\alpha_{\text{Fe}^{3+}}$  to represent the boundary between "solubility" and "insolubility." The limit of "solubility" is generally taken to be an activity of the dissolved species of  $10^{-6}$ , corresponding to a concentration of  $10^{-6}$  m (Garrels and Christ, 1965). The choice of  $10^{-6}$  is arbitrary but reasonable: for most purposes anything much less soluble than  $10^{-6}$  m would generally be considered insoluble, and anything much more soluble than  $10^{-6}$  m would be considered soluble. To illustrate the effect of different choices, boundaries for  $\alpha_{\text{Fe}^{3+}} = 10^{-3}$  and  $10^{-9}$  are also shown on Fig. 7-4. With the value of  $10^{-6}$ , Eq. (7-13) becomes

$$pH = \frac{1}{6} \log K_{\text{eq}} + 2$$

$\log K_{\text{eq}} = -2.50$  (from free energy values), so the boundary for  $\alpha_{\text{Fe}^{3+}} = 10^{-6}$  plots at pH 1.58. The boundaries for  $\alpha_{\text{Fe}^{3+}} = 10^{-3}$  and  $10^{-9}$  plot at pH 0.58 and 2.58 respectively. The oxides become more soluble as the solution becomes more acid, so the  $\text{Fe}^{3+}$  field is to the left of the boundary, and the  $\text{Fe}_2\text{O}_3$  field to the right.

The boundary  $\text{Fe}^{3+}$ - $\text{Fe}^{2+}$  is given by



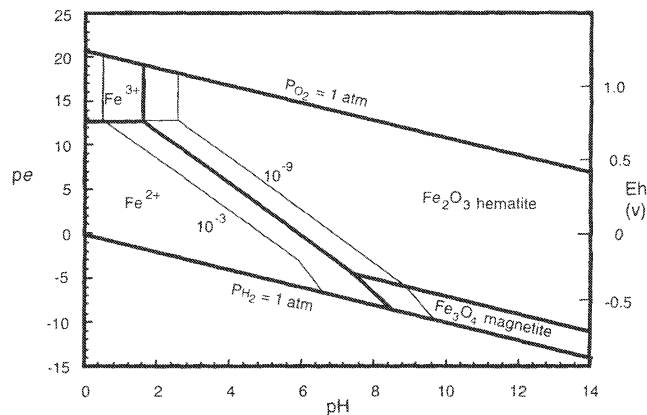
$$K_{\text{eq}} = \frac{\alpha_{\text{Fe}^{2+}}}{\alpha_{\text{Fe}^{3+}} \alpha_{e^-}}$$

$$\begin{aligned}pe &= \log K_{\text{eq}} - \log \left( \frac{\alpha_{\text{Fe}^{2+}}}{\alpha_{\text{Fe}^{3+}}} \right) \\ &= 13.02 - \log \left( \frac{\alpha_{\text{Fe}^{2+}}}{\alpha_{\text{Fe}^{3+}}} \right)\end{aligned}$$

Since this boundary is independent of pH, it must plot as a horizontal line. To draw the boundary, we must assign a value to the ratio  $\alpha_{\text{Fe}^{2+}}/\alpha_{\text{Fe}^{3+}}$ . The normal choice is 1, but it must be remembered that the boundary represents this ratio; nonzero concentrations of  $\text{Fe}^{2+}$  will be present above it, and nonzero concentrations of  $\text{Fe}^{3+}$  will be present below it.

The  $\text{Fe}^{2+}$ - $\text{Fe}^{3+}$  and the  $\text{Fe}^{3+}$ - $\text{Fe}_2\text{O}_3$  boundaries intersect at a point on Fig. 7-4, and both boundaries have been terminated at that point. They terminate because we are interested only in

**FIGURE 7-4**  $pe$ - $pH$  diagram for the system  $Fe-O-H_2O$  at  $25^\circ C$  with hematite as the stable ferric oxide phase. The heavy lines are boundaries for  $\alpha_{Fe^{3+}} = 10^{-6}$ . The light lines are boundaries for  $\alpha_{Fe^{3+}} = 10^{-3}$  and  $10^{-9}$ .



stable boundaries. To the right of the  $Fe^{3+}$ - $Fe_2O_3$  boundary,  $Fe^{3+}$  is not the stable form of  $Fe$ , so any boundary involving  $Fe^{3+}$  must be metastable. Similarly,  $Fe^{3+}$  is not the stable form below the  $Fe^{2+}$ - $Fe^{3+}$  boundary, so any boundary involving  $Fe^{3+}$  must be metastable. It is clear from the topology of Fig. 7-4 that we need a boundary between  $Fe_2O_3$  and  $Fe^{2+}$ .

The boundary  $Fe_2O_3$ - $Fe^{2+}$  is calculated from the equation

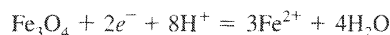


$$K_{eq} = \frac{\alpha_{Fe^{2+}}^2}{\alpha_e^2 \alpha_{H^+}^6}$$

$$\begin{aligned} pe &= \frac{1}{2} \log K_{eq} - \log \alpha_{Fe^{2+}} - 3pH \\ &= 11.77 + 6 - 3pH \end{aligned} \quad (7-15)$$

Here again we must choose a value of  $\alpha_{Fe^{3+}}$  to represent the boundary between solubility and insolubility. If we choose the same values as we did for  $Fe^{3+}$ , we do not actually have to calculate  $K_{eq}$ . The  $Fe_2O_3$ - $Fe^{2+}$  boundary is a straight line of slope  $-3$  [Eq. (7-15)] that passes through the intersection of the  $Fe_2O_3$ - $Fe^{3+}$  and the  $Fe^{3+}$ - $Fe^{2+}$  boundaries. It is usually a good idea, however, to calculate  $K_{eq}$  and verify that the new boundary does pass through the intersection of the other two. If the three boundaries do not meet in a single point, it indicates arithmetic error. Inaccurate free-energy values would cause the position of the point to be in error, but they would result in a single point.

The  $Fe_3O_4$ - $Fe^{2+}$  boundary is calculated from the reaction



$$K_{eq} = \frac{\alpha_{Fe^{2+}}^3}{\alpha_e^2 \alpha_{H^+}^8}$$

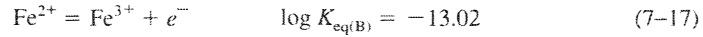
$$pe = \frac{1}{2} \log K_{eq} - \frac{3}{2} \log \alpha_{Fe^{2+}} - 4pH$$

Here, again, it is not strictly necessary to calculate  $K_{eq}$  since the boundary must be a straight line of slope  $-4$  passing through the intersection of the  $Fe_2O_3$ - $Fe^{2+}$  and  $Fe_2O_3$ - $Fe_3O_4$  boundaries.

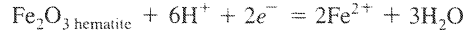
The boundaries can also be calculated from the equilibrium constants in Appendix III instead of the free energy values in Appendix II. As an example, let us calculate the  $Fe^{2+}$ - $Fe_2O_3$  boundary. The relevant reactions listed in Appendix III are:







Multiplying Eq. (7-17) by 2 and subtracting from Eq. (7-16) gives



which is identical to Eq. (7-14) above. The equilibrium constant for this reaction is given by

$$\log K_{\text{eq}} = \log K_{\text{eq(A)}} - 2 \log K_{\text{eq(B)}} = 22.03$$

When reactions are added or subtracted, the logarithms of the equilibrium constants can be added or subtracted in the same way. This can readily be derived algebraically or from the fact that  $\log K_{\text{eq}}$  is proportional to  $\Delta G_R^0$ .

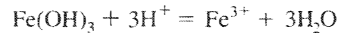
From Fig. 7-4 we would conclude that  $\text{Fe}^{3+}$  is likely to be a major species only under unusually acidic oxidizing conditions, such as acid mine drainage. At alkaline pH values, iron should be insoluble at all pe values; at nearly neutral and mildly acidic pH values, iron should be insoluble under oxidizing conditions and soluble (as  $\text{Fe}^{2+}$ ) under reducing conditions.

### Example 2

If ferrihydrite ( $\text{Fe}(\text{OH})_3$ ) rather than  $\text{Fe}_2\text{O}_3$  is considered as the ferric oxide mineral and  $\text{Fe}(\text{OH})_2$  is considered instead of  $\text{Fe}_3\text{O}_4$ , how will the diagram be changed? (Ferrihydrite is a poorly crystalline hydrous ferric oxide; it is roughly equivalent to amorphous  $\text{Fe}(\text{OH})_3$  in older literature.)

The equations for the various boundaries involving  $\text{Fe}(\text{OH})_3$  will be essentially the same as those involving  $\text{Fe}_2\text{O}_3$ , but the  $K_{\text{eq}}$  values will be different, reflecting the lesser stability of  $\text{Fe}(\text{OH})_3$ . These boundaries will have the same slopes as in Fig. 7-4, but different intercepts.

Consider the boundary  $\text{Fe}(\text{OH})_3\text{-Fe}^{3+}$ :



$$K_{\text{eq}} = \frac{\alpha_{\text{Fe}^{3+}}}{\alpha_{\text{H}^{+}}^3}$$

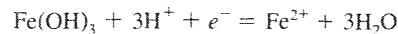
$$\text{pH} = \frac{1}{3}(\log K_{\text{eq}} - \log \alpha_{\text{Fe}^{3+}})$$

From the free-energy values in Appendix II, and substituting  $\alpha_{\text{Fe}^{3+}} = 10^{-6}$ :

$$\text{pH} = 3.63$$

This boundary (Fig. 7-5) is about 2 pH units higher than the corresponding boundary for hematite, reflecting the lesser stability and hence greater solubility of ferrihydrite. Fig. 7-5 and subsequent diagrams are shown for the pH range 2 to 12 rather than 0 to 14. Few natural waters are more acid than pH 2 or more alkaline than pH 12.

The boundary  $\text{Fe}(\text{OH})_3\text{-Fe}^{2+}$  is given by



$$\log K_{\text{eq}} = \log \alpha_{\text{Fe}^{2+}} + \text{pe} + 3\text{pH}$$

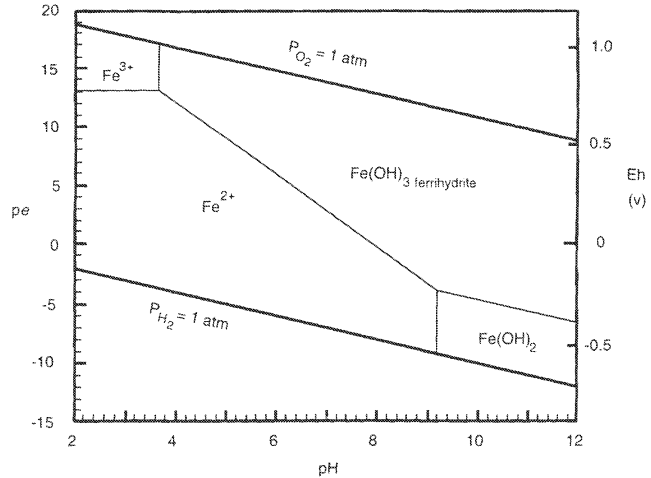
$$\text{pe} = \log K_{\text{eq}} - 3\text{pH} - \log \alpha_{\text{Fe}^{2+}}$$

Substituting  $\log K_{\text{eq}} = 17.9$  (from data in Appendix II) and  $\log \alpha_{\text{Fe}^{2+}} = -6$ ,

$$\text{pe} = 23.9 - 3\text{pH}$$

Note that this line passes through the intersection of the  $\text{Fe}(\text{OH})_3\text{-Fe}^{3+}$  line calculated above and the  $\text{Fe}^{3+}\text{-Fe}^{2+}$  boundary, which is unchanged from Fig. 7-4.

**FIGURE 7-5**  $pe$ - $pH$  diagram for the system  $Fe-O-H_2O$  at  $25^\circ C$  with ferrihydrite ( $Fe(OH)_3$ ) as the ferric oxide instead of hematite and  $Fe(OH)_2$  instead of magnetite. Solid-solution boundaries are drawn for an activity of dissolved Fe species of  $10^{-6}$ .



The boundaries involving  $Fe(OH)_2$  are



$$pH = \frac{1}{2}(\log K_{eq} - \log a_{Fe^{2+}})$$

$$= 9.2$$

(from Appendix II and  $\log a_{Fe^{2+}} = -6$ )

and:



$$pe = \log K_{eq} - pH$$

$$= 5.53 - pH$$

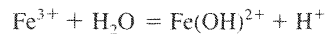
The final diagram, Fig. 7-5, shows that the effect of substituting the less stable phases [ferrihydrite for hematite and  $Fe(OH)_2$  for magnetite] is to expand the area of solubility (the  $Fe^{2+}$  and  $Fe^{3+}$  fields), but the general topology of the diagram is unchanged.

In calculations on natural water systems, we would probably use the  $Fe_2O_3$  (hematite) value in considering the dissolution of well-crystallized hematite and the  $Fe(OH)_3$  (ferrihydrite) value in considering the precipitation of a ferric oxide from a supersaturated solution, because the initial precipitate would probably be amorphous. Likewise, well-crystallized magnetite is unlikely to precipitate at low temperatures, so it is appropriate to include some less stable phase than magnetite. As we shall see later, the exact choice of a reduced oxide is not important because its stability field will be replaced by that of a carbonate or sulfide in most natural environments.

### Example 3

So far, we have ignored the hydrolyzed species (or hydroxy complexes)  $Fe(OH)^{2+}$ ,  $Fe(OH)_2^+$ ,  $Fe(OH)_3^0$ , and  $Fe(OH)_4^-$ . If we include them, how will Figs. 7-4 and 7-5 change?

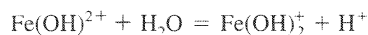
The first hydrolysis constant of  $Fe^{3+}$  is given by



From Appendix III (or the free energy values in Appendix II), we find

$$\log K_{\text{eq}} = -2.19$$

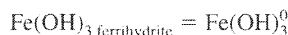
Thus at pH 2.19 the activities of  $\text{Fe}^{3+}$  and  $\text{Fe}(\text{OH})^{2+}$  are equal; above pH 2.19  $\text{Fe}(\text{OH})^{2+}$  becomes the dominant species and below pH 2.19  $\text{Fe}^{3+}$  becomes the dominant species. The relationship is exactly analogous to that between  $\text{H}_2\text{CO}_3$  and  $\text{HCO}_3^-$  discussed in the context of the Bjerrum plot in Chapter 3. In Fig. 7-4, the boundary between  $\text{Fe}^{3+}$  and  $\text{Fe}_2\text{O}_3$  is at pH 1.58, which is below pH 2.19. Thus, the pH at the boundary is sufficiently low that  $\text{Fe}(\text{OH})^{2+}$  is not an important species in the region of solubility and so its existence does not affect the diagram. On Fig. 7-5, by contrast, the  $\text{Fe}^{3+}$ - $\text{Fe}(\text{OH})_3$  boundary is at pH 3.63, which means that there should be a stability field for  $\text{Fe}(\text{OH})^{2+}$ . Next, consider the reaction



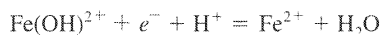
The  $\log K_{\text{eq}}$  for this reaction is  $-3.48$ . The stability field for  $\text{Fe}(\text{OH})_2^+$  will thus be above pH 3.48. pH 3.48 is still below our original solubility boundary (pH 3.63), so there will be a stability field for  $\text{Fe}(\text{OH})_2^+$ . The upper limit of this field will be given by



for which  $\log K_{\text{eq}} = -0.78$ , so for  $\log a_{\text{Fe}(\text{OH})_2^+} = -6$ , pH = 5.22. This boundary now represents the solubility limit of  $\text{Fe}(\text{OH})_3$ . We can test whether  $\text{Fe}(\text{OH})_3^0$  should appear on the diagram by writing the reaction



The  $\log K_{\text{eq}}$  for this reaction is  $-7.67$ . This means that the activity of  $\text{Fe}(\text{OH})_3^0$  in equilibrium with ferrihydrite is always  $10^{-7.67}$ , which is smaller than  $10^{-6}$ , our criterion for solubility. This means that  $\text{Fe}(\text{OH})_3^0$  has no stability field on Fig. 7-5 (or on Fig. 7-4). To complete the low-pH part of the diagram, we need the boundaries

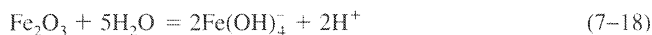


and



These boundaries are plotted on Fig. 7-6.

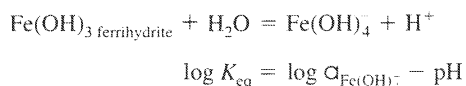
The activity of  $\text{Fe}(\text{OH})_4^-$  in equilibrium with hematite (the relevant phase in Fig. 7-4) is given by the reaction



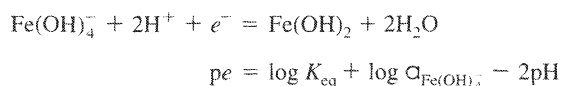
Note that with the anionic species,  $\text{Fe}(\text{OH})_4^-$ , the dissolved iron species, and  $\text{H}^+$  appear on the same side of the equation (they are on opposite sides for cationic species). This means that the activity of  $\text{Fe}(\text{OH})_4^-$  in equilibrium with  $\text{Fe}_2\text{O}_3$  increases with increasing pH. The equilibrium constant for Eq. (7-18) is given by

$$\log K_{\text{eq}} = 2 \log a_{\text{Fe}(\text{OH})_4^-} - 2\text{pH}$$

substituting  $\log K_{\text{eq}} = -47.2$  and  $\log a_{\text{Fe}(\text{OH})_4^-} = -6$  gives pH = 17.6, which is far beyond the boundaries of Fig. 7-4. The species  $\text{Fe}(\text{OH})_4^-$  would thus not appear on Fig. 7-4. On Fig. 7-5, the relevant reaction is



substituting  $\log K_{\text{eq}} = -16.7$  and  $\log \alpha_{\text{Fe}(\text{OH})_4^-} = -6$  gives  $\text{pH} = 10.7$ .  $\text{Fe}(\text{OH})_4^-$  would thus have a stability field above  $\text{pH} 10.7$  on Fig. 7-5. The final boundary to complete the diagram is one between  $\text{Fe}(\text{OH})_4^-$  and  $\text{Fe}(\text{OH})_2$ . This is given by the equation



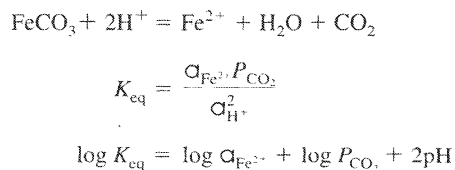
The revised version of Fig. 7-5, including the hydrolysis products, is shown as Fig. 7-6. The conclusion from this calculation is that the existence of the hydrolysis products has essentially no effect on the  $pe$ - $\text{pH}$  diagram when hematite is chosen as the ferric oxide phase, but a quite significant effect when ferrihydrite is the phase chosen. In particular, the existence of these complexes significantly increases the solubility of ferrihydrite at low  $\text{pH}$ . The graphical presentation used here (the  $pe$ - $\text{pH}$  diagram) is not really the best way of displaying the effects of the complexes; their existence does increase the solubility of hematite but not enough to bring it above  $10^{-6}$  m, the threshold to appear on the diagram. (The topic is discussed in more detail in the context of Al species in Chapter 10.)

### System Fe-O-H<sub>2</sub>O-CO<sub>2</sub>

#### Example 4

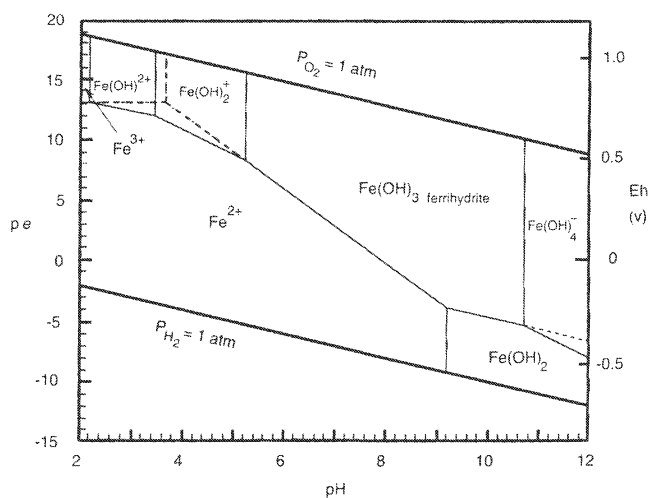
What is the effect in Figs. 7-4 and 7-6 of introducing carbonate species on the assumption (a) an open system with  $P_{\text{CO}_2} = 1$  atm and  $P_{\text{CO}_2} = 10^{-3}$  atm; and (b) a closed system with  $\Sigma\text{CO}_2 = 10^{-2}$  m?

When  $\text{CO}_2$  is added to the system, the phase siderite ( $\text{FeCO}_3$ ) must be considered. The  $\text{Fe}^{2+}$ - $\text{FeCO}_3$  boundary is given by

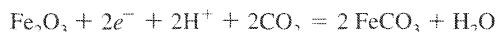


Substituting  $\alpha_{\text{Fe}^{2+}} = 10^{-6}$  and  $\log K_{\text{eq}} = 7.24$  (from free-energy values) gives  $\text{pH} = 6.62$  for  $P_{\text{CO}_2} = 1$  and  $\text{pH} = 8.12$  for  $P_{\text{CO}_2} = 10^{-3}$ . These boundaries will plot as vertical lines in the  $\text{Fe}^{2+}$  field on

**FIGURE 7-6**  $pe$ - $\text{pH}$  diagram for the system Fe-O-H<sub>2</sub>O with ferrihydrite as the ferric oxide, including the hydrolyzed forms of  $\text{Fe}^{3+}$ . Dashed lines are copied from Figure 7-5. Solid-solution boundaries are drawn for an activity of dissolved Fe species of  $10^{-6}$ .



Figs. 7-4 and 7-6 (Figs. 7-7 and 7-8). On Fig. 7-4, we can see by inspection that the  $P_{\text{CO}_2} = 1$  atm line will intersect the  $\text{Fe}^{2+}$ - $\text{Fe}_2\text{O}_3$  boundary, and the  $P_{\text{CO}_2} = 10^{-3}$  line will intersect the  $\text{Fe}^{2+}$ - $\text{Fe}_3\text{O}_4$  boundary. For  $P_{\text{CO}_2} = 1$  we need a  $\text{FeCO}_3$ - $\text{Fe}_2\text{O}_3$  boundary:

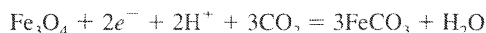


$$K_{\text{eq}} = \frac{1}{a_e^2 a_{\text{H}^+}^2 P_{\text{CO}_2}}$$

$$pe = \frac{1}{2} \log K_{\text{eq}} + \log P_{\text{CO}_2} - pH$$

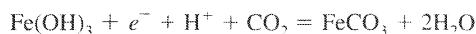
For a given  $P_{\text{CO}_2}$ , this will plot as a straight line of slope  $-1$  on the pe-pH diagram, and will pass through the intersection of the  $\text{Fe}^{2+}$ - $\text{FeCO}_3$  and  $\text{Fe}_2\text{O}_3$ - $\text{FeCO}_3$  lines. The field of siderite completely replaces the field for magnetite and part of the field for hematite. [Note that all reactions not involving ions plot as straight lines of slope  $-1$  on pe-pH diagrams, parallel to lines of equal oxygen pressure (Fig. 7-3). This stems from the requirement that the number of  $\text{H}^+$  ions must equal the number of electrons for the charges to balance in the chemical reaction.]

For  $P_{\text{CO}_2} = 10^{-3}$  atm we need a  $\text{FeCO}_3$ - $\text{Fe}_3\text{O}_4$  boundary:



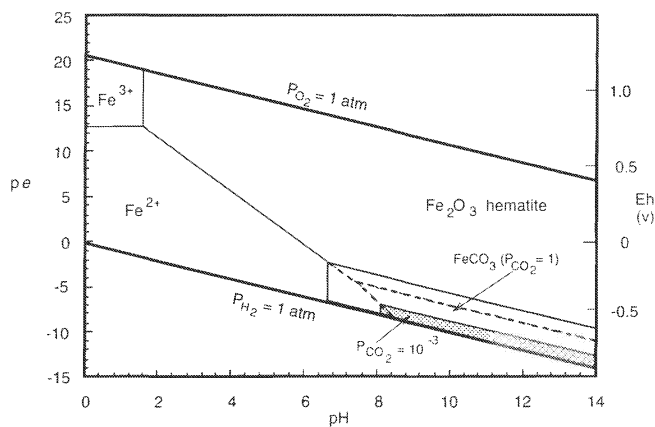
It can be seen by inspection that this will also plot as a straight line of slope  $-1$  on the pe-pH diagram. Again, there is no real need to calculate an equilibrium constant, since the boundary must pass through the intersection of the  $\text{Fe}_3\text{O}_4$ - $\text{Fe}^{2+}$  and  $\text{Fe}^{2+}$ - $\text{FeCO}_3$  ( $P_{\text{CO}_2} = 10^{-3}$  atm) boundary. The final diagram is shown on Fig. 7-7. Several features of the diagram are reasonably intuitive:  $\text{FeCO}_3$  contains only iron in the reduced state ( $\text{Fe}^{2+}$ ) so it occurs under more reducing conditions (lower pe) than hematite ( $\text{Fe}^{3+}$ ). Also, it is stable at high pH and dissolves at low pH, as we would expect for any carbonate mineral (compare  $\text{CaCO}_3$ , Chapter 3).

When  $\text{Fe}(\text{OH})_3$  is chosen as the oxide phase (Fig. 7-8), the  $\text{Fe}^{2+}$ - $\text{FeCO}_3$  boundaries are unchanged. They intersect the  $\text{Fe}^{2+}$ - $\text{Fe}(\text{OH})_3$  boundary for both  $P_{\text{CO}_2}$  values, so we need boundaries between  $\text{Fe}(\text{OH})_3$  and  $\text{FeCO}_3$ :

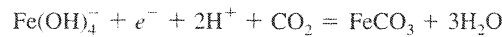
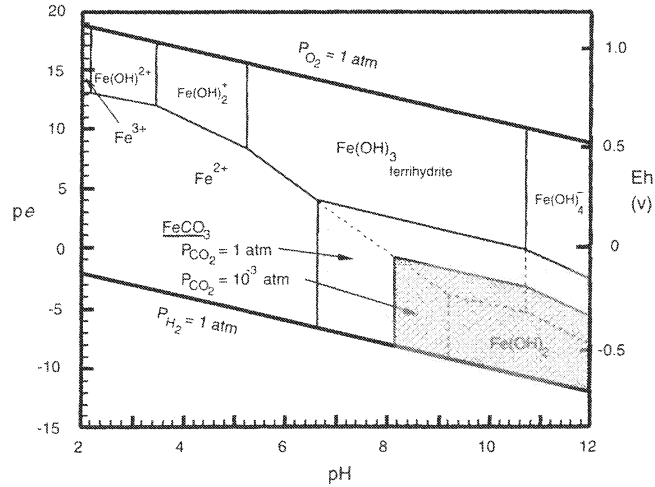


Again, for each value of  $P_{\text{CO}_2}$ , this will plot as a straight line of slope  $-1$  through the intersections of the  $\text{Fe}^{2+}$ - $\text{FeCO}_3$  and the  $\text{Fe}^{2+}$ - $\text{Fe}(\text{OH})_3$  boundaries. To complete the diagram, we need  $\text{FeCO}_3$ - $\text{Fe}(\text{OH})_4^-$  boundaries:

**FIGURE 7-7** pe-pH diagram for the system  $\text{Fe-O-H}_2\text{O-CO}_2$  at  $25^\circ\text{C}$ , assuming hematite as the ferric oxide and  $P_{\text{CO}_2} = 1$  atm (light shading) and  $10^{-3}$  atm (darker shading). Dashed lines are the boundaries for magnetite first shown in Fig. 7-4. Solid-solution boundaries are drawn for an activity of dissolved Fe species of  $10^{-6}$ .



**FIGURE 7-8**  $pe$ - $pH$  diagram for the system  $Fe-O-H_2O-CO_2$  at  $25^\circ C$ , assuming ferrihydrite is the ferric oxide and  $P_{CO_2} = 1$  atm (light shading) and  $10^{-3}$  atm (darker shading). Dashed lines are stability field for  $Fe(OH)_2$  first shown in Fig. 7-5. Solid-solution boundaries are drawn for an activity of dissolved Fe species of  $10^{-6}$ .



$$pe = \log K_{eq} + \log P_{CO_2} + \log \alpha_{Fe(OH)_4^-} - 2 pH$$

This will plot as a straight line of slope  $-2$  through the intersection(s) of the  $Fe(OH)_3$ - $Fe(OH)_4^-$  and  $Fe(OH)_3$ - $FeCO_3$  boundaries.

The final diagram is shown in Fig 7-8. Note that the stability field of  $Fe(OH)_2$  is completely eliminated by the field of  $FeCO_3$  at both  $P_{CO_2}$  values.  $Fe(OH)_2$  would be stable only at very low  $P_{CO_2}$  values. Note also that, as one would expect, the size of the stability field of the carbonate mineral increases as  $P_{CO_2}$  increases.

The constant  $\Sigma CO_2$  case is a little more complicated. We can write the  $Fe^{2+}$ - $FeCO_3$  boundary in the form:



$$K_{eq} = \frac{\alpha_{H^+}}{\alpha_{Fe^{2+}} \alpha_{HCO_3^-}}$$

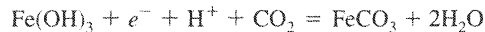
$$pH = -\log K_{eq} - \log \alpha_{Fe^{2+}} - \log \alpha_{HCO_3^-}$$

If we assume that  $\alpha_{HCO_3^-} = \Sigma CO_2 = 10^{-2}$  and  $\alpha_{Fe^{2+}} = 10^{-6}$ , then:

$$pH = 7.41$$

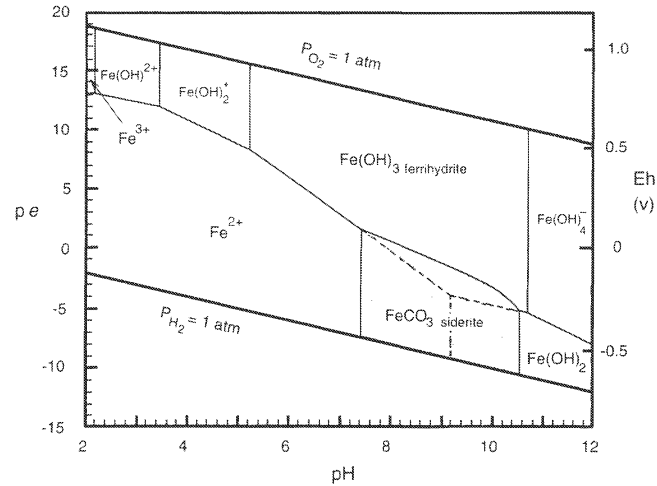
At this pH, the assumption that essentially all carbonate species are  $HCO_3^-$  is clearly justified (see Chapter 3). We have introduced the assumption that  $\alpha_{HCO_3^-} = m_{HCO_3^-}$ ; the error in the calculated pH resulting from this assumption should be trivial on the type of  $pe$ - $pH$  diagram we are considering.

In Figs. 7-4 and 7-7, the  $Fe^{2+}$ - $FeCO_3$  ( $\Sigma CO_2 = 10^{-2}$ ) boundary intersects the  $Fe^{2+}$ - $Fe_3O_4$  boundary very close to the  $P_{H_2} = 1$  boundary. The stability field of  $FeCO_3$  is thus very small and will not be plotted. In Figs. 7-5 and 7-8, the  $Fe^{2+}$ - $FeCO_3$  boundary intersects the  $Fe^{2+}$ - $Fe(OH)_3$  boundary (Fig. 7-9), so we need a  $FeCO_3$ - $Fe(OH)_3$  boundary:



$$pe = \log K_{eq} + \log P_{CO_2} - pH \quad (7-19)$$

**FIGURE 7-9** pe-pH diagram for the system Fe-O-H<sub>2</sub>O-CO<sub>2</sub> at 25°C, considering the phases ferrihydrite, siderite, and Fe(OH)<sub>2</sub>.  $\Sigma\text{CO}_2 = 10^{-2}$  m. Solid-solution boundaries are drawn for an activity of dissolved Fe species of  $10^{-6}$ .



If we neglect activity coefficients, we can express  $P_{\text{CO}_2}$  in terms of  $\Sigma\text{CO}_2$  from the relationship (Chapter 3):

$$\begin{aligned}\Sigma\text{CO}_2 &= m_{\text{H}_2\text{CO}_3} + m_{\text{HCO}_3^-} + m_{\text{CO}_3^{2-}} \\ &= K_{\text{CO}_2} P_{\text{CO}_2} \left( 1 + \frac{K_1}{\alpha_{\text{H}^+}} + \frac{K_1 K_2}{\alpha_{\text{H}^+}^2} \right)\end{aligned}$$

or

$$P_{\text{CO}_2} = \frac{\Sigma\text{CO}_2}{K_{\text{CO}_2} (1 + K_1/\alpha_{\text{H}^+} + K_1 K_2/\alpha_{\text{H}^+}^2)}$$

Substituting this in Eq. (7-19) gives

$$pe = \log K_{\text{eq}} - \text{pH} + \log \Sigma\text{CO}_2 - \log K_{\text{CO}_2} \left( 1 + \frac{K_1}{\alpha_{\text{H}^+}} + \frac{K_1 K_2}{\alpha_{\text{H}^+}^2} \right)$$

This is clearly not a linear relationship between  $pe$  and  $\text{pH}$ . It is actually linear with a slope of  $-2$  so long as  $\text{HCO}_3^-$  is the dominant carbonate species, but it curves downwards as the  $\text{p}K_2$  of carbonic acid is approached ( $\text{pH}$  10.33). The boundary is plotted in Fig. 7-9. This boundary intersects the  $\text{Fe(OH)}_3$ - $\text{Fe(OH)}_2$  boundary at a  $\text{pH}$  of 10.54. We therefore need a  $\text{FeCO}_3$ - $\text{Fe(OH)}_2$  boundary below the intersection. Since  $\text{FeCO}_3$  and  $\text{Fe(OH)}_2$  are both in the same oxidation state ( $\text{Fe}^{\text{II}}$ ), the boundary will be a vertical line. We can calculate the position of the line from the equations:



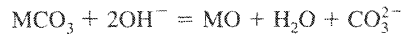
$$K_{\text{eq}} = P_{\text{CO}_2} = 10^{-5.14}$$

and

$$P_{\text{CO}_2} = \frac{\Sigma\text{CO}_2}{K_{\text{CO}_2} (1 + K_1/\alpha_{\text{H}^+} + K_1 K_2/\alpha_{\text{H}^+}^2)}$$

Substitution of the numerical values of  $P_{\text{CO}_2}$  and  $\Sigma\text{CO}_2$  and solving the resulting quadratic gives  $\alpha_{\text{H}^+} = 10^{-10.54}$ , or a  $\text{pH}$  of 10.54.

When  $\Sigma\text{CO}_2$  is fixed rather than  $P_{\text{CO}_2}$ , oxides or hydroxides become stable relative to carbonates at high pH. In general, the relative stability of carbonates versus oxides and hydroxides (of the same oxidation state) can be considered in terms of an equation of the following type:



or



Here  $M$  is any divalent cation. The same logic applies to cations of other valence. For either equation,

$$K_{\text{eq}} = \frac{\alpha_{\text{CO}_3^{2-}}}{\alpha_{\text{OH}^-}^2}$$

Combining the equations for  $K_{\text{CO}_3}$ ,  $K_1$  and  $K_2$  in Chapter 3.

$$\alpha_{\text{CO}_3^{2-}} = \frac{K_1 K_2 K_{\text{CO}_2} P_{\text{CO}_2}}{\alpha_{\text{H}^+}^2}$$

Substituting  $K_w = \alpha_{\text{H}^+} \alpha_{\text{OH}^-}$  and rearranging gives

$$\frac{\alpha_{\text{CO}_3^{2-}}}{\alpha_{\text{OH}^-}^2} = \frac{K_1 K_2 K_{\text{CO}_2} P_{\text{CO}_2}}{K_w^2}$$

Thus, as long as  $P_{\text{CO}_2}$  is constant, the ratio  $\alpha_{\text{CO}_3^{2-}}/\alpha_{\text{OH}^-}^2$  will be constant and independent of pH. However, if  $\Sigma\text{CO}_2$  is constant rather than  $P_{\text{CO}_2}$ ,  $\alpha_{\text{CO}_3^{2-}}$  cannot increase indefinitely as pH increases, so  $\alpha_{\text{OH}^-}^2$  increases more than  $\alpha_{\text{CO}_3^{2-}}$  with increasing pH, and oxides and hydroxides become stable relative to carbonates. By the same argument, ferrous silicates will become stable relative to ferrous carbonates at high pH if  $\Sigma\text{CO}_2$  is constant, but the relative stability will be independent of pH if  $P_{\text{CO}_2}$  is constant. At an arbitrary  $P_{\text{CO}_2}$  and  $\alpha_{\text{H}_4\text{SiO}_4}$ , either a ferrous carbonate will be more stable than the silicate, or the silicate will be more stable than the carbonate. Both phases can be stable together only at a unique  $P_{\text{CO}_2}$  for each  $\alpha_{\text{H}_4\text{SiO}_4}$  value.

In the discussions so far, we have not considered redox reactions involving  $\text{CO}_2$  itself. At low  $pe$  values,  $\text{CO}_2$  may be reduced to graphite, carbon monoxide, or methane. As an example, let us consider the pressure of methane in equilibrium with 1 atm  $\text{CO}_2$  pressure as a function of  $pe$  and pH.



$$\log K_{\text{eq}} = \log P_{\text{CH}_4} - \log P_{\text{CO}_2} + 8pe + 8\text{pH}$$

Calculating  $K_{\text{eq}}$  and introducing  $P_{\text{CO}_2} = 1$  gives

$$pe = 2.86 - \frac{1}{8} \log P_{\text{CH}_4} - \text{pH}$$

The relationship is shown in Fig. 7-10. As the  $pe$  approaches the lower stability limit of water, the  $\text{CH}_4$  pressure in equilibrium with  $\text{CO}_2$  becomes very high. It must be remembered, however, that formation of methane at  $25^\circ\text{C}$  occurs only with the help of organisms, and disequilibrium is common.

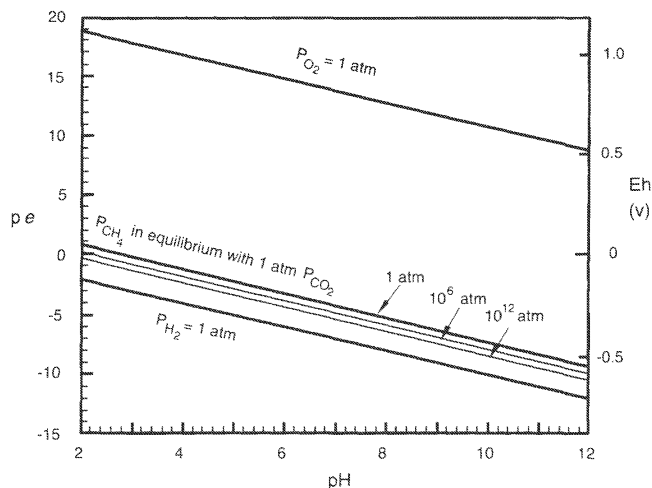
## System Fe-O-H<sub>2</sub>O-S

### Example 5

How can the stabilities of sulfur compounds and iron sulfides be added to the  $pe$ -pH diagram? The first problem is to choose a variable to describe the total activity or concentration of sulfur

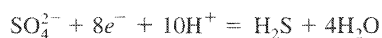


**FIGURE 7-10** Pressure of methane in equilibrium with CO<sub>2</sub> (1 atm) at 25°C as a function of pe and pH.



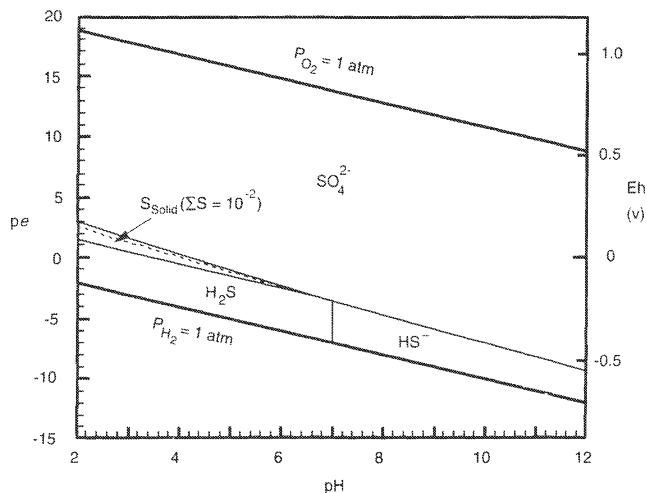
species. At high pe values, all sulfur will be in the form of sulfate, and at low pe values all sulfur will be in the form of sulfide species. Elemental sulfur may also be a significant species at intermediate pe values (Fig. 7-11). Keeping the activity of any single species constant over the whole pe-pH range is thus not a satisfactory approach; the best approach, in general, is to fix  $\Sigma S$  ( $= \alpha_{SO_4^{2-}} + \alpha_{HSO_4^-} + \alpha_{H_2S} + \alpha_{HS^-} + \alpha_{S^{2-}}$ ) at some value. If  $\Sigma S$  is defined, the values of pe and pH define uniquely the equilibrium activity of each individual sulfur species. Although many other oxyacids and anions of sulfur exist (such as sulfite, thiosulfate, dithionite, etc.), it is doubtful whether any of them is a stable species at 25°C and 1 atm.

The boundaries in Fig. 7-11 are calculated from the following equations:



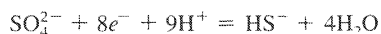
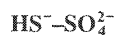
$$\log K_{eq} = \log \left( \frac{\alpha_{H_2S}}{\alpha_{SO_4^{2-}}} \right) + 8pe + 10pH$$

**FIGURE 7-11** Stability fields for dissolved sulfur species and solid sulfur ( $\Sigma S = 10^{-2}m$ ) as a function of pe and pH. Only boundaries involving solid sulfur change position as the value of  $\Sigma S$  changes. HSO<sub>4</sub><sup>-</sup> and S<sup>2-</sup> are not predominant species in the pH range shown. Dashed line is the SO<sub>4</sub><sup>2-</sup>-H<sub>2</sub>S boundary.



Setting the ratio equal to 1 and calculating  $\log K_{eq}$  from the data in Appendix II, we obtain

$$pe = 5.09 - \frac{5}{4} \text{pH}$$



$$\log K_{eq} = \log \left( \frac{\alpha_{\text{HS}^-}}{\alpha_{\text{SO}_4^{2-}}} \right) + 8pe + 9\text{pH}$$

Setting the ratio equal to 1 and calculating  $\log K_{eq}$ , we obtain

$$pe = 4.21 - \frac{9}{8} \text{pH}$$



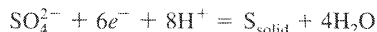
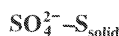
$$\log K_{eq} = \log \left( \frac{\alpha_{\text{HS}^-}}{\alpha_{\text{H}_2\text{S}}} \right) - \text{pH}$$

Again setting the ratio equal to 1 and calculating  $\log K_{eq}$ , we obtain

$$\text{pH} = 6.99 \text{ (the first dissociation constant of H}_2\text{S)}$$

The stability fields of  $\text{HSO}_4^-$  and  $\text{S}^{2-}$  are not in the pH range shown in Fig. 7-11.

Before we can calculate boundaries involving solid elemental sulfur (or any solid sulfide), we must assign a value to  $\Sigma\text{S}$ . Here we shall use  $10^{-2}\text{m}$  as an example. (The sulfate concentration in seawater is  $10^{-1.5}\text{m}$ ; "typical" fresh waters would be  $10^{-3}$  to  $10^{-5}\text{m}$ .) Above the  $\text{SO}_4^{2-}$ - $\text{H}_2\text{S}$  (or  $\text{HS}^-$ ) boundary, essentially all dissolved sulfur will be in the form of sulfate, so  $\alpha_{\text{SO}_4^{2-}} \approx 10^{-2}$ . Below the boundary and below pH 7,  $\alpha_{\text{H}_2\text{S}} = 10^{-2}$ ; below the boundary and above pH 7,  $\alpha_{\text{HS}^-} = 10^{-2}$ . It is only very close to the boundaries that these simplifying assumptions cannot be used.

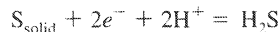
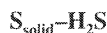


$$\log K_{eq} = 6pe + 8\text{pH} - \log \alpha_{\text{SO}_4^{2-}}$$

Setting  $\alpha_{\text{SO}_4^{2-}} = 10^{-2}$  and calculating  $\log K_{eq}$ , we obtain

$$pe = 5.64 - \frac{4}{3} \text{pH}$$

At this boundary, the activity of dissolved sulfur species in equilibrium with solid sulfur is  $10^{-2}$ . Below the boundary, the equilibrium activity of sulfur species is less than  $10^{-2}$ . Thus, as the value chosen for  $\Sigma\text{S}$  decreases, the size of the stability field of solid sulfur becomes smaller.



$$\log K_{eq} = 2pe + 2\text{pH} + \log \alpha_{\text{H}_2\text{S}}$$

Setting  $\alpha_{\text{H}_2\text{S}} = 10^{-2}$  and calculating  $\log K_{eq}$ , we obtain:

$$pe = 3.43 - \text{pH}$$

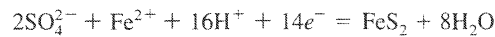
Where these two boundaries converge on the  $\text{SO}_4^{2-}$ - $\text{H}_2\text{S}$  boundary (Fig. 7-11), precise calculation requires consideration of the fact that both  $\text{H}_2\text{S}$  and  $\text{SO}_4^{2-}$  contribute significantly to  $\Sigma\text{S}$ . At

the scale of Fig. 7-11, however, the results of the more precise calculation are almost indistinguishable from those based on the assumption that  $\Sigma S$  is either all  $SO_4^{2-}$  or all  $H_2S$ .

The sulfate-sulfide boundary is probably the most important redox boundary in natural water chemistry. For many transition metals it represents (approximately) the dividing line between where oxides, carbonates, or dissolved ions are stable and where insoluble sulfides are stable (assuming some sulfur is present). The onset of sulfate reduction also has a major impact on biological systems.

The upper stability limit of pyrite is given by the boundaries between  $FeS_2$  and either  $Fe^{2+}$  or  $Fe_2O_3$ . Iron sulfides are precipitated by extremely small concentrations of dissolved sulfide species, so we would anticipate that the upper stability limit of pyrite would be above the sulfate-sulfide boundary in Fig. 7-11. If this is correct,  $\alpha_{SO_4^{2-}} \approx \Sigma S$  at the upper stability limit of pyrite.

#### $Fe^{2+}$ - $FeS_2$ ( $SO_4^{2-}$ field)

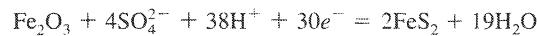


$$\log K_{eq} = -2 \log \alpha_{SO_4^{2-}} - \log \alpha_{Fe^{2+}} + 16pH + 14pe$$

Setting  $\alpha_{SO_4^{2-}} = 10^{-2}$ ,  $\alpha_{Fe^{2+}} = 10^{-6}$ , and calculating  $\log K_{eq}$ , we obtain

$$pe = 5.46 - \frac{16}{14}pH$$

#### $Fe_2O_3$ - $FeS_2$ ( $SO_4^{2-}$ field)



$$\log K_{eq} = -4 \log \alpha_{SO_4^{2-}} + 38pH + 30pe$$

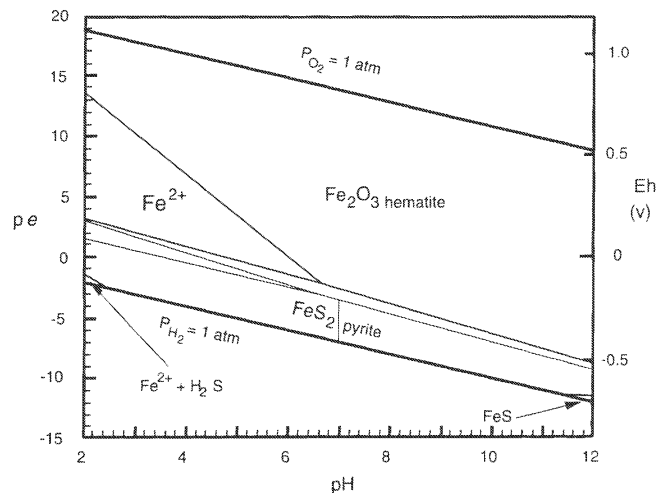
Setting  $\alpha_{SO_4^{2-}} = 10^{-2}$  and calculating  $\log K_{eq}$ , we obtain

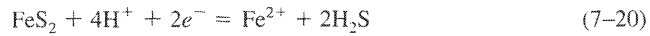
$$pe = 6.28 - \frac{38}{30}pH$$

These boundaries are plotted in Fig. 7-12.

The sulfur in pyrite is in a higher formal oxidation state than is the sulfur in  $H_2S$  or the equivalent ferrous sulfide,  $FeS$ . Thus, at low  $pe$ , pyrite becomes unstable with respect to  $Fe^{2+}$  at low pH:

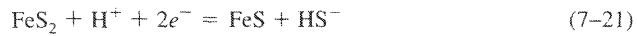
**FIGURE 7-12**  $pe$ - $pH$  diagram for the system  $Fe$ - $O$ - $H_2O$ - $S$  at  $25^\circ C$  assuming hematite as the ferric oxide and  $\Sigma S = 10^{-2}m$ . Solid-solution boundaries are drawn for an activity of dissolved  $Fe$  species of  $10^{-6}$ . Light lines are the distribution of sulfur species first seen in Fig. 7-11.





$$pe = 2.49 - 2p\text{H}$$

and unstable with respect to FeS at high pH:



$$pe = -2.54 - \frac{1}{2}p\text{H}$$

The boundaries representing Eqs. (7-20) and (7-21) plot close to the  $P_{\text{H}_2} = 1$  line close to pH 2 and pH 11, respectively, in Fig. 7-12. At the  $\Sigma\text{S}$  value ( $10^{-2}$ ) used to construct the diagram, the lower stability limits of pyrite appear unimportant, but as  $\Sigma\text{S}$  decreases, the stability field of pyrite shrinks, and these boundaries occur in the  $pe$ -pH region more typical of natural waters. Likewise, magnetite does not have a stability field below pH 12 when  $\Sigma\text{S} = 10^{-2}$ , but as  $\Sigma\text{S}$  decreases, a field for magnetite appears at high pH.

When an iron sulfide mineral forms in natural waters, the first phase to precipitate is usually an unstable monosulfide (Berner, 1970). These monosulfides are generally transformed rapidly to pyrite, and pyrite is the common iron sulfide in both modern sediments and ancient sedimentary rocks. Marcasite is a mineral with the same chemical composition as pyrite but with a different crystal structure. It is not known why marcasite is sometimes formed instead of pyrite.

We can add other compounds such as  $\text{CO}_2$  to the Fe-O-S system and generate diagrams such as Fig. 7-13, but such diagrams tend to confuse rather than simplify the interpretation of natural water chemistry. If hematite is the iron oxide phase, for both iron sulfides and iron carbonates to appear as significant stable phases on a  $pe$ -pH diagram,  $\Sigma\text{S}$  must be fixed at a very low value and  $P_{\text{CO}_2}$  (or  $\Sigma\text{CO}_2$ ) at a high value. For natural systems, it is generally simpler and more realistic to consider two cases: (1) sulfur is present, in which case a diagram as Fig. 7-12 is appropriate, or (2) sulfur is absent, in which case a diagram such as Fig. 7-7 or 7-8 is appropriate.

When ferrihydrite is chosen as the iron oxide, both siderite and pyrite can be stable at reasonable values of  $P_{\text{CO}_2}$  and  $\Sigma\text{S}$  (Fig. 7-14). The reason is that ferrihydrite is reduced to  $\text{Fe}^{2+}$  at a higher  $pe$  than sulfate is reduced to sulfide. At high pH, the  $\text{Fe}^{2+}$  forms siderite. It seems confusing at first that the siderite, which contains fully reduced iron, occurs under more oxidizing conditions than pyrite. The reason is that the stability field of pyrite is determined by reduction of sulfate, not reduction of iron.

### Eh-pH Diagrams

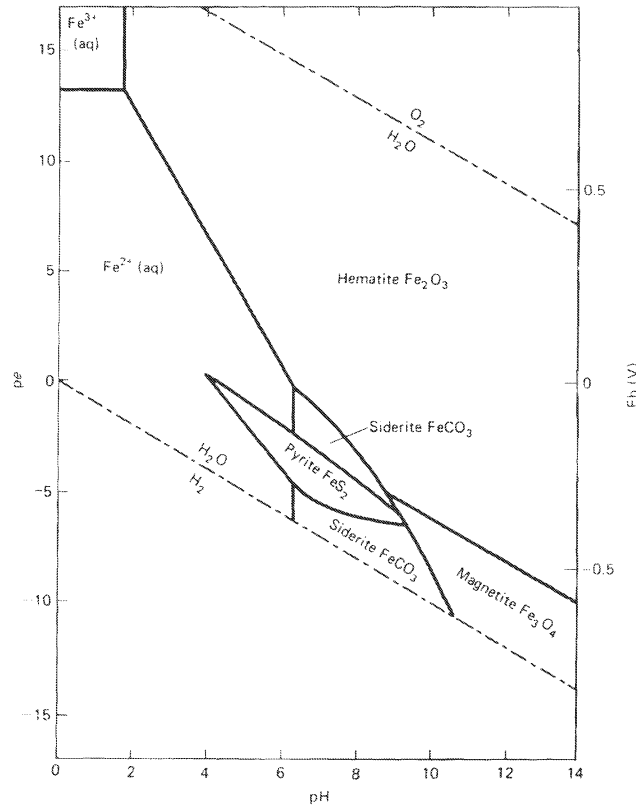
The formalism and equations for an Eh-pH diagram are very similar to those for a  $pe$ -pH diagram. The diagrams are identical except for the scale on the vertical axis, which is changed according to the equation:

$$\text{Eh} = \frac{2.303RT}{F} pe$$

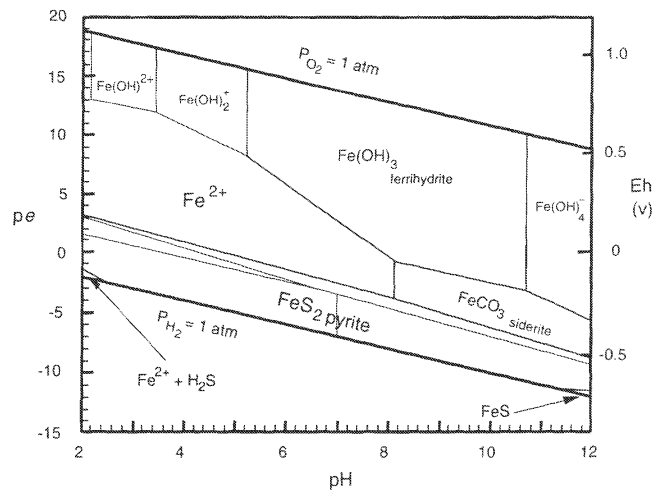
as discussed earlier in this chapter. At 25°C:

$$\text{Eh} = 0.059 pe$$

**FIGURE 7-13** Stability relations in the system Fe–O–H<sub>2</sub>O–S–CO<sub>2</sub> at 25°C, assuming  $\Sigma S = 10^{-6}$ ,  $\Sigma \text{CO}_2 = 10^0$  (after Garrels and Christ, 1965). Solid–solution boundaries are drawn for an activity of dissolved Fe species of  $10^{-6}$ .

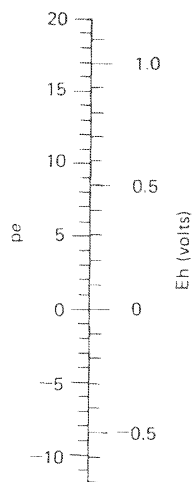


**FIGURE 7-14** Stability relations in the system Fe–O–H<sub>2</sub>O–S–CO<sub>2</sub> at 25°C, assuming ferrihydrite as the ferric oxide phase,  $\Sigma S = 10^{-7}$  m and  $P_{\text{CO}_2} = 10^{-3}$  atm. Solid–solution boundaries are drawn for an activity of dissolved Fe species of  $10^{-6}$ . Light lines are boundaries for sulfur species from Fig. 7-11.



Eh is shown on the right side of each of the pe–pH diagrams in this chapter. The two scales are compared graphically in Fig. 7-15. One disadvantage of using Eh as a variable is that the slopes of the various stability boundaries change as a function of  $T$ , which is not the case when the variable is pe.

FIGURE 7-15 Comparison of  $pe$  and Eh scales at 25°C.



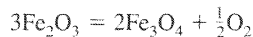
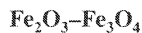
## PARTIAL PRESSURE OR FUGACITY-FUGACITY DIAGRAMS

As mentioned at the beginning of the chapter, the activity of oxygen can be used instead of  $pe$  as an indicator of redox conditions. Oxygen activity is most conveniently expressed as the fugacity of oxygen in a gas phase with which the solution would be in equilibrium. Fugacity (see Chapter 2) is essentially the same numerically as partial pressure, although it is questionable whether a partial pressure of  $10^{-80}$  atm has much physical reality.

### Example 6

Draw stability diagrams for the system Fe–O–CO<sub>2</sub>–H<sub>2</sub>O, using  $\log f_{O_2}$  as the indicator of redox conditions.

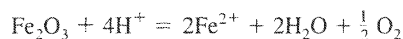
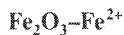
There are several possible choices of a second axis; we shall illustrate the use of pH and  $\log f_{CO_2}$ . This is equivalent to drawing sections through a three-dimensional diagram with  $\log f_{O_2}$ ,  $\log f_{CO_2}$ , and pH as axes. The upper and lower limits of the diagram are defined by  $\log f_{O_2} = 0$  and  $\log f_{H_2} = 0$ .



$$K_{\text{eq}} = f_{O_2}^{1/2}$$

$$\log f_{O_2} = 2 \log K_{\text{eq}} = -70$$

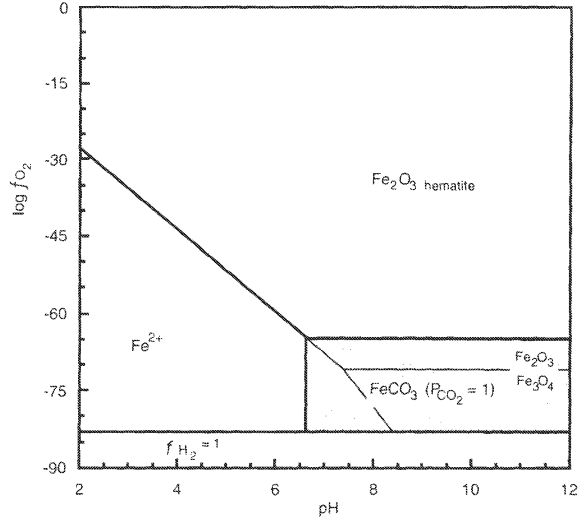
This plots as a horizontal line in both Fig. 7-16 and Fig. 7-17.



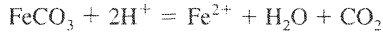
$$\log K_{\text{eq}} = 2 \log \alpha_{\text{Fe}^{2+}} + \frac{1}{2} \log f_{O_2} + 4\text{pH}$$

If we assign a value of  $\alpha_{\text{Fe}^{2+}}$ , this plots as a line of slope  $-8$  on a  $\log f_{O_2}$ –pH diagram (Fig. 7-16) and as a horizontal line on a  $\log f_{O_2}$ – $\log f_{CO_2}$  diagram (Fig. 7-17).

**FIGURE 7-16** Stability relations in the system Fe–O–H<sub>2</sub>O–CO<sub>2</sub> at 25°C drawn as a function of log *f*<sub>O<sub>2</sub></sub> and pH. Shaded area is stability field of siderite at *P*<sub>CO<sub>2</sub></sub> = 1 atm. Solid-solution boundaries are drawn for an activity of dissolved Fe species of 10<sup>-6</sup>.



**FeCO<sub>3</sub>–Fe<sup>2+</sup>**



$$\log K_{\text{eq}} = \log a_{\text{Fe}^{2+}} + \log f_{\text{CO}_2} + 2\text{pH}$$

This plots as a vertical line in Figs. 7-16 and 7-17.

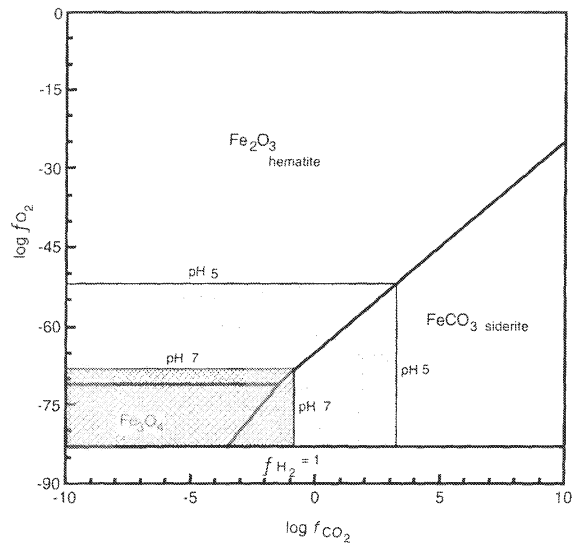
**Fe<sub>2</sub>O<sub>3</sub>–FeCO<sub>3</sub>**



$$\log K_{\text{eq}} = \frac{1}{2} \log f_{\text{O}_2} - 2 \log f_{\text{CO}_2}$$

$$\log f_{\text{O}_2} = 2 \log K_{\text{eq}} + 4 \log f_{\text{CO}_2}$$

**FIGURE 7-17** Stability relations in the system Fe–O–H<sub>2</sub>O–CO<sub>2</sub> at 25°C, drawn as a function of log *f*<sub>O<sub>2</sub></sub> and log *f*<sub>CO<sub>2</sub></sub>. Shaded areas indicate stability field of Fe<sup>2+</sup> (greater than 10<sup>-6</sup>) at pH 5 and pH 7.



This plots as a line with a slope of +4 in Fig. 7-17, and, if  $f_{\text{CO}_2}$  is held constant, as a horizontal line in Fig. 7-16.

Other boundaries can be calculated in the same way to give the completed figures. An analogous diagram to Fig. 7-16 could be calculated on the assumption of constant  $\Sigma\text{CO}_2$  rather than constant  $f_{\text{CO}_2}$  by the approach illustrated in Example 4.

Fig. 7-16 is very similar in essence to Fig. 7-7. The angles of some of the boundaries are different, but the basic topology is the same. This should not be surprising, as both types of diagram are simply convenient graphic ways of displaying free-energy data. The stability relationships are the same regardless of which variable is used on the redox axis, and for systems at equilibrium, interpretations made within the framework of one type of diagram can be made equally well within the framework of the other.

In this chapter we have illustrated the construction of the most common types of stability diagrams for redox reactions in natural waters. The application of these diagrams will be discussed in other chapters. There are many possible choices of axes for stability diagrams, and the two most useful ones for a particular problem may not be  $pe$  (or  $Eh$ ) and  $pH$ . In many environments—for example, groundwater in a particular aquifer or interstitial water in marine sediments— $pH$  is almost constant, so it makes sense to construct diagrams in which  $pH$  is fixed, and some other variable (e.g.,  $\log f_{\text{CO}_2}$ ,  $\Sigma S$ , or  $\log \alpha_{\text{HS}^-}$ ) is used as an axis. Such diagrams can readily be constructed by the same general approach as was used for the  $pe$ - $pH$  diagram.

Finally, we must stress that the diagrams we have discussed show only equilibrium relationships. Complete equilibrium among redox systems in natural waters is the exception rather than the rule. Stability diagrams are of great value, particularly in semiquantitative interpretations, but their limitations must be recognized.

## REVIEW QUESTIONS

Use free-energy values from Appendix II and assume a temperature of 25°C to answer the following questions.

1. Surface seawater has a  $pH$  of 8.2 and the following redox couples present:
  - a.  $\text{O}_2$  at a pressure of 0.21 atm and water
  - b.  $\text{N}_2$  at a pressure of 0.76 atm and  $\text{NO}_3^-$  at a concentration of  $4 \times 10^{-5}$  M
  - c.  $\text{CO}_2$  at a pressure of  $3 \times 10^{-4}$  atm and  $\text{CH}_4$  at a pressure of  $1.5 \times 10^{-6}$  atm
 What  $pe$  does each couple define? Are they the same as each other? What do you think are the reasons for the discrepancies?
2. Plot the stability field of fayalite ( $\text{Fe}_2\text{SiO}_4$ ) on Fig. 7-4, assuming:
  - a. Equilibrium with amorphous silica
  - b. Equilibrium with quartz
3. When sulfate reduction occurs in modern sediments, the first sulfide minerals to form are often mackinawite ( $\text{FeS}$ ) and greigite ( $\text{Fe}_3\text{S}_4$ ). Redraw Fig. 7-12 considering each of these phases instead of pyrite. In general, how much difference does it make which iron sulfide phase is chosen?



4. Construct a  $pe$ - $pH$  diagram for the system  $Mn-O-H_2O-CO_2$ , considering  $Mn^{2+}$  and the phases of  $MnO_2$  (birnessite),  $Mn_2O_3$ ,  $Mn_3O_4$ ,  $Mn(OH)_2$  (pyrochroite), and  $MnCO_3$ , and assuming that:
  - a. No  $CO_2$  is present
  - b.  $P_{CO_2} = 1$  atm
  - c.  $P_{CO_2} = 10^{-3}$  atm
5. Plot the field of  $MnS$  (alabandite) on the graph(s) of question 4, using appropriate values for  $\Sigma S$ . Should  $MnS$  be a significant phase in modern sediments (marine and non-marine)? Justify your reasoning.
6. Construct a  $f_{O_2}$ - $pH$  diagram using the same phases and the same set of assumptions as in question 4.
7. Construct a  $f_{O_2}$ - $f_{CO_2}$  diagram for the system in question 4 and:
  - a.  $pH$  5
  - b.  $pH$  7
  - c.  $pH$  8
8. Compare the  $pe$ - $pH$  diagrams for the Fe systems in the text of the chapter with the Mn systems in questions 4 and 5. Which element would you expect to be mobilized first as an environment becomes reducing? If seawater is trapped with organic matter in a sediment, how would you expect the concentration of dissolved (a) iron and (b) manganese to change as the  $pe$  is progressively lowered?

### SUGGESTED READING

- BROOKINS, D. G. (1988). *Eh-pH Diagrams for Geochemistry*. New York: Springer-Verlag. A compilation of Eh-pH diagrams for many elements of interest in water studies.
- GARRELS, R. M., and C. L. CHRIST. (1965). *Solutions, Minerals, and Equilibria*. New York: Harper & Row. Chaps. 5, 6, and 7. This is the classic work on Eh-pH diagrams.
- NORDSTROM, D. K., and J. L. MUNOZ. (1994). *Geochemical Thermodynamics*. (2nd ed.). Oxford: Blackwell Scientific Publications. Chap. 10.
- STUMM, W., and J. J. MORGAN. (1996). *Aquatic Chemistry*. (3rd ed.). New York: Wiley-Interscience. Chap. 8.



# 8

## Redox Conditions in Natural Waters

Redox conditions in rivers, lakes, and the ocean are largely controlled by the processes of photosynthesis and bacterial decomposition of organic matter.

### PHOTOSYNTHESIS

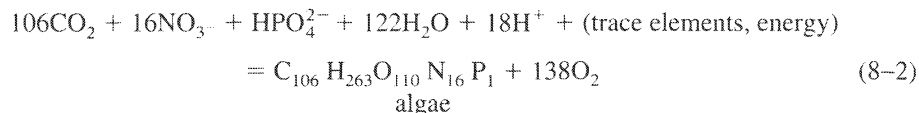
Photosynthesis is the process by which carbon dioxide (which may be derived from  $\text{HCO}_3^-$ ) is converted to organic matter and oxygen:



Photosynthesis uses energy from the sun to form unstable compounds (organic matter and oxygen) from the stable compound  $\text{CO}_2$ . In the absence of photosynthesis, the oxygen in the atmosphere would be steadily consumed by the oxidation of organic matter until no free oxygen remained (Garrels and Perry, 1974; Holland, 1978).

Carbon and oxygen are not the only elements involved in photosynthesis. Plants also require nitrogen compounds, phosphorus compounds, and a wide range of trace elements. Plants (in aquatic systems, primarily microscopic algae) will grow and multiply until all available phosphate or nitrate is used up, at which point photosynthesis ceases. In unpolluted fresh waters phosphate is normally the *limiting nutrient*; nitrate is sometimes limiting in polluted waters. The availability of particular trace elements is occasionally limiting for short periods of time, but this is rare. Photosynthesis is the ultimate source of food for all organisms in surface waters.

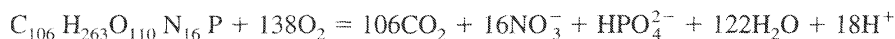
The average composition of the organic matter in plankton is approximately  $\text{C}_{106} \text{H}_{263} \text{O}_{110} \text{N}_{16} \text{P}_1$  (Redfield et al., 1963), so photosynthesis can be represented by the more complex equation:



rather than the simple form of Eq. (8-1). Eq. (8-2) illustrates the enormous importance of phosphate in the carbon-oxygen balance of waters, particularly lakes. Each atom of phosphorus (as phosphate) added to a surface water results in fixation of about 106 atoms of carbon in organic matter, and when the organic matter produced from one atom of phosphorus decays, it has the potential to consume 138 molecules of oxygen.

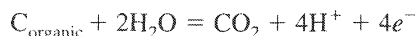
## RESPIRATION AND DECAY

As long as free oxygen is available, the net results of respiration and decay are essentially the reverse of photosynthesis:

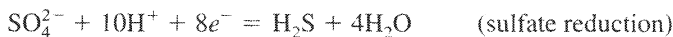
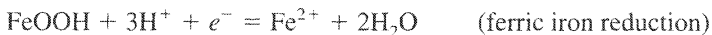
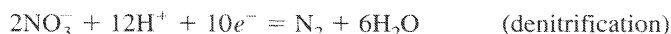


Carbon is released as  $CO_2$ , organically combined nitrogen as  $NO_3^-$ , and organically combined phosphorus as  $HPO_4^{2-}$ . The release of  $CO_2$  causes an increase in  $P_{CO_2}$  and hence a decrease in pH.

When molecular oxygen is not available, or when it has been used up, decay of organic matter continues by a series of reactions that represent successively lower  $pe$  levels (Fig. 8-1). The essential difference between the reactions is the *terminal electron acceptor*. Oxidation of carbon to  $CO_2$  can be viewed (Chapter 7) as a reaction that generate electrons:



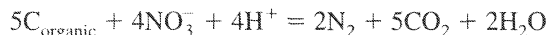
Since free electrons cannot accumulate, there must be some corresponding chemical system to accept the electrons, such as



Electron acceptors are essentially "oxidizing agents," compounds capable of being reduced. From a biochemical viewpoint, it is much more realistic to think in terms of electron transfers than transfers of oxygen.

Some of the most important reactions are:

1. *Nitrate reduction.* In nitrate reduction, in a complex series of reactions bacteria use nitrate ion as the terminal electron acceptor to oxidize organic carbon to  $CO_2$ . If molecular nitrogen is the final product, the process is called *denitrification* or *dissimilatory nitrate reduction*.

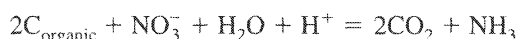
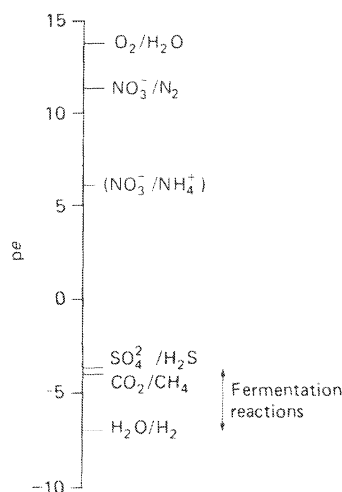


The importance of this reaction is that it converts nitrate, an essential nutrient, into biologically inert molecular nitrogen; it is important in the nutrient balance of lakes and rivers. Many bacteria reduce nitrate only as far as nitrite:



whereas other bacteria reduce nitrate all the way to ammonia:

**FIGURE 8-1** Approximate *pe* values at which various redox reactions occur in water at pH 7 and 25°C.

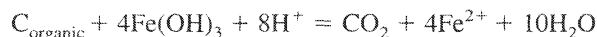


Ammonia may also be released from the decomposition of the amino acids in proteins. Ammonia that is released by microbial processes reacts with water



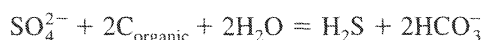
to form ammonium ion,  $\text{NH}_4^+$ , causing a net rise in pH. The rise in pH may cause precipitation of calcium as a carbonate or as a soap (the calcium salt of a fatty acid) (Berner, 1969, 1971), which may be important in the formation of concretions.

**2. Ferric iron reduction.** Reduction of ferric oxyhydroxides (and sometimes manganese oxyhydroxides) is an important process in groundwater systems where the oxyhydroxides are present. It is relatively less important in surface waters because the mass of oxyhydroxide available is usually quite small. Stoichiometrically, the reaction is



The  $\text{Fe}^{2+}$  produced may remain in solution, it may precipitate as  $\text{FeCO}_3$  (siderite) or, if iron reduction is followed by sulfate reduction, it may precipitate as a sulfide such as pyrite ( $\text{FeS}_2$ ). Iron reduction is commonly microbially mediated.

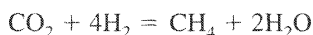
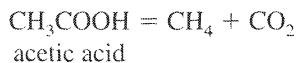
**3. Sulfate reduction.** In sulfate reduction, bacteria use  $\text{SO}_4^{2-}$  as a terminal electron acceptor in the oxidation of organic matter to  $\text{CO}_2$ . Sulfide species are the final reduction product, although various sulfur species such as thiosulfate may be produced as intermediates. The overall stoichiometry of the reaction is



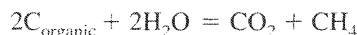
If the pH is above 7,  $\text{HS}^-$  will form rather than  $\text{H}_2\text{S}$ . If the pH is below 6,  $\text{CO}_2$  will form rather than  $\text{HCO}_3^-$ . If any reactive iron compounds are present, the sulfide species will react with them to form solid sulfides. Sulfate-reducing bacteria are capable of utilizing only relatively simple organic molecules such as formate, acetate, lactate and a range of other compounds containing up to about 20 carbon atoms (and also hydrogen) (Chapelle, 1993; Hansen, 1993). They are thus typically dependent on fermentative bacteria (see below) to produce these simple molecules.

There are many consequences of ferric iron and sulfate reduction.  $\text{H}_2\text{S}$  and  $\text{HS}^-$  are highly toxic to most organisms, so the biota in the environment are strongly affected. Conversion of iron oxides to sulfides generally causes a color change from red or brown to black or gray. Species (e.g., heavy metals and phosphate ion) that were adsorbed onto ferric oxyhydroxides (see Chapter 9) will be released to solution, and many heavy metals (e.g., Cu, Zn, Mo, Pb, and Hg) that are relatively soluble in oxidizing waters (provided that the pH is not too high) are highly insoluble (as sulfides) in the presence of dissolved sulfide species.

4. *Fermentation reactions and methanogenesis.* When no external electron acceptors are available, organisms use a wide variety of organic transformations as a source of energy in fermentation reactions. The reactions are fundamentally transformation of complex molecules such as carbohydrates into simple compounds such as  $\text{CO}_2$ , formate, acetate, and hydrogen. Measurable hydrogen concentrations are commonly present in fermentative systems. Associated with these fermentative organisms are another group of microorganisms that use the products of fermentation to derive energy by reactions involving methane formation such as



The overall result of fermentation and methanogenesis is thus to convert organic matter into methane and  $\text{CO}_2$ . It can be represented in a very simplified way as



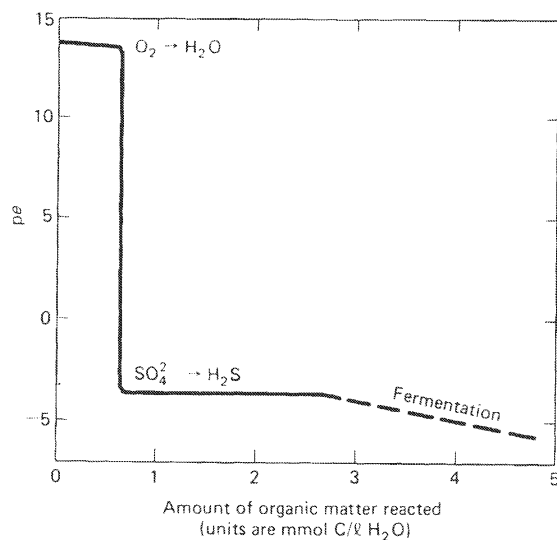
whose equilibrium  $p_e$  is shown in Fig. 8-1. Fermentation reactions typically generate hydrogen as a biochemical intermediate and can drive the  $p_e$  down to the  $\text{H}_2$ - $\text{H}_2\text{O}$  boundary.

Fundamentally, the various anaerobic decay reactions represent mechanisms by which microorganisms use decomposition of the products of photosynthesis as a source of energy. Since the bacteria derive energy from the reactions, their function is essentially to catalyze the conversion of thermodynamically unstable systems to more stable systems. In general, each reaction is mediated by a specific type of bacterium, and the reactions occur more or less in succession, with the reactions that yield most energy to the bacteria occurring earliest. Sulfate reduction does not occur until all molecular oxygen has been used up, and methane generation generally does not occur significantly until all sulfate has been used up. The succession is not strict, and there is commonly some overlap between the ranges of activities of the different microorganisms. Molecular oxygen is toxic to many anaerobic bacteria, so nitrate and sulfate reduction do not generally occur until all oxygen has been removed from the system.

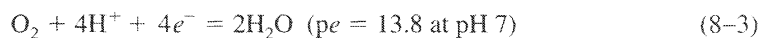
## REDOX BUFFERING

In addition to  $p_e$  (redox level or redox intensity), *redox buffering* (or redox capacity) is an important concept. A system is buffered or poised with respect to redox processes if oxidizable or reducible compounds are present that prevent a significant change in  $p_e$  in response to additions of small amounts of strong oxidizing or reducing agents. Fig. 8-2 shows schematically how  $p_e$  might change as organic matter decomposes in a typical surface water. It is assumed that the water was initially in equilibrium with atmospheric oxygen, but no additional oxygen is added as the organic matter decomposes.

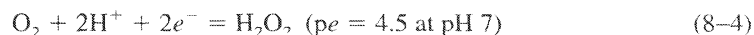
**FIGURE 8-2** Change in  $pe$  of a fresh water (dissolved  $O_2 = 10$  mg/l, dissolved  $SO_4^{2-} = 96$  mg/l) as a function of the amount of organic matter decomposed. Reactions involving nitrogen compounds may provide a small amount of buffering between the  $O_2/H_2O$  and the  $SO_4^{2-}/H_2S$  levels. pH is assumed constant at 7.0.



As long as free oxygen is present,  $pe$  remains high. There has been some disagreement in the literature as to the “correct”  $pe$  of oxygenated water. The overall reduction of oxygen



generally does not occur as a single step, but as a series of separate reactions, two of the most important of which are



and



Breck (1974) argued that reaction (8-5) was much slower than reaction (8-4), and hence  $pe$  was essentially controlled by reaction (8-4). The effective  $pe$  for oxygenated waters would then be 4.5 (at pH 7), rather than the value of 13.8 predicted by reaction (8-3). Stumm (1978) disagreed, pointing out that some natural redox systems seemed to respond as if reaction (8-3) determined  $pe$ , and some as if reaction (8-4) controlled  $pe$ . Stumm concluded that the use of a single  $pe$  to characterize oxygenated waters is meaningless because the various redox couples in natural waters are not in equilibrium with each other. Since a single  $pe$  for all redox systems cannot be defined, it is probably best to think of  $pe$  as being “high” without specifying an exact number. For general discussion purposes, it is as logical to use the value defined by the  $O_2$ - $H_2O$  couple as any other.

As soon as all free oxygen is consumed,  $pe$  drops abruptly to the value where sulfate reduction takes place (the amount of nitrate in an unpolluted water is usually too small for denitrification to be a significant buffer).  $pe$  remains essentially constant until all sulfate is reduced and then decreases gradually as various fermentation reactions take place. We would expect the  $pe$  values in natural waters to be generally in one of the buffered ranges because values in the unbuffered range are unstable; any trace of oxygen or reactive organic matter should shift the  $pe$  from an unbuffered range into a buffered range. The only place where we

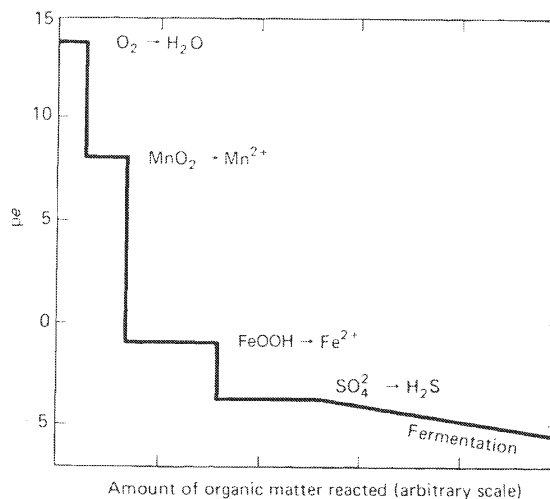
would expect an “unbuffered”  $pe$  to persist in a region where  $pe$  is controlled by diffusion between an anaerobic water (e.g., interstitial water in sediments) and an aerobic water (e.g., oxygenated lake or ocean water).

In this discussion we have considered only redox reactions involving organic matter and the solutes in water. In groundwaters and waters in effective contact with sediments, redox reactions involving solid phases may also buffer  $pe$ . Fig. 8-3 shows how Fig. 8-2 might be modified to include such reactions. The lengths of the various horizontal segments in Fig. 8-3 are arbitrary, as it is hard to generalize on the distribution and reactivity of specific minerals in sediments.

Some of the effects of bacterial decomposition of organic matter in marine sediments are shown in Figs. 8-4 and 8-5. Fig. 8-4 shows profiles of dissolved nitrate, manganese, and iron in a core from the eastern equatorial Atlantic (Froelich et al., 1979). First nitrate is reduced (denitrification), then manganese oxides are reduced to  $Mn^{2+}$ , and then iron oxides are reduced to  $Fe^{2+}$ . There was no reduction of sulfate in the core studied (sulfate reduction probably occurred at greater depth in the sediment), reflecting the relatively low organic matter content of the sediment. Fig. 8-5 shows the interstitial water chemistry in a core containing abundant organic matter from a near-shore environment off North Carolina (Martens and Goldhaber, 1978). Sulfate is completely reduced to sulfide in the top 40 cm, and methane is generated in the deeper part of the core. The high concentrations of ammonia and phosphate illustrate the release of inorganic nutrients accompanying the decomposition of organic matter. The profiles indicate that the nutrient elements are diffusing upward into the overlying water. These processes have been synthesized into a general model by Van Cappellen and Wang (1996).

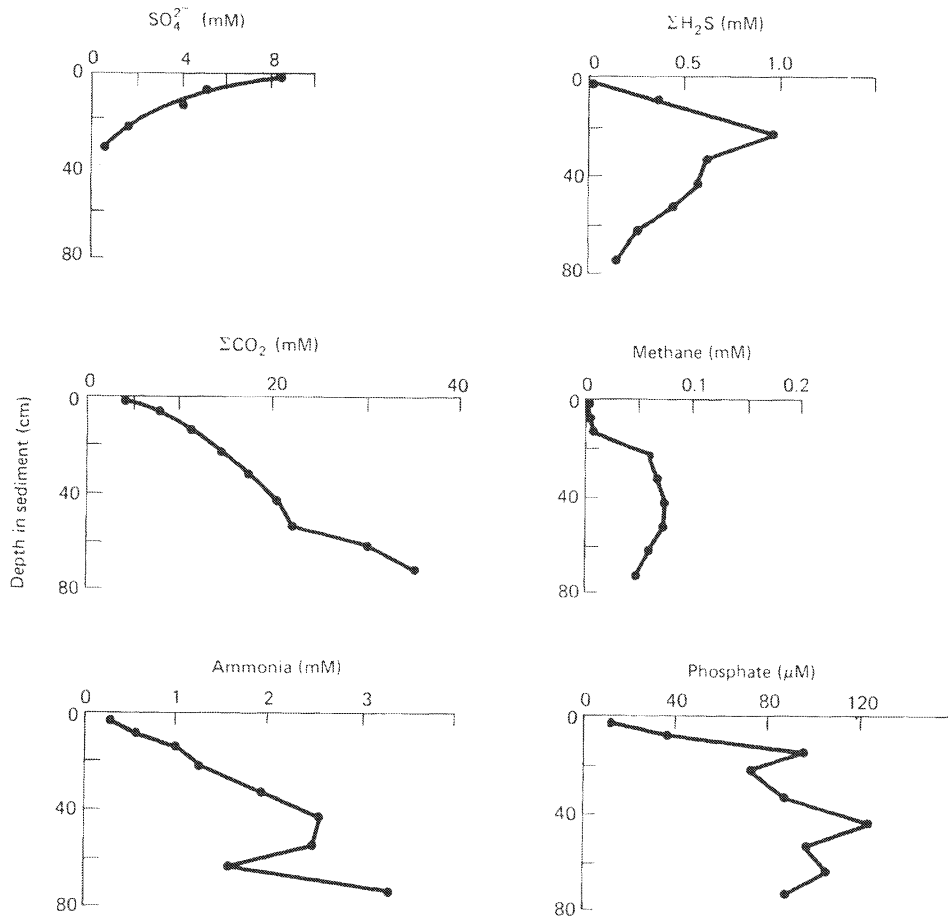
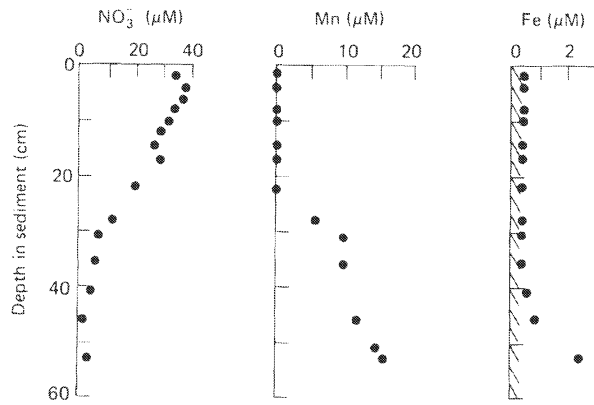
Although organic matter is the common reducing agent in natural waters, lowering of  $pe$  can also be brought about by oxidation of minerals containing ferrous iron or reduced sulfur species. Solutions emerging from basalt at oceanic spreading centers contain high concentrations of dissolved iron and manganese, or sometimes high concentrations of sulfide. Presumably, these solutions represent seawater, the  $pe$  of which has been lowered by reaction with ferrous minerals in the basalt. Some springs emerging from ultramafic rocks (rocks composed largely of Mg-Fe silicates) on land actually produce bubbles of hydrogen gas from the reduction of water by ferrous minerals (Barnes et al., 1972).

**FIGURE 8-3** Change in  $pe$  of a fresh water in contact with sediment as a function of the amount of organic matter decomposed. The lengths of the various horizontal segments are arbitrary, depending on the amounts of specific solid phases available for reaction. pH is assumed constant at 7.0.





**FIGURE 8-4** Profiles of nitrate, dissolved manganese, and dissolved iron in interstitial water from a sediment core from the eastern equatorial Atlantic (Froelich et al., 1979).



**FIGURE 8-5** Profiles of dissolved species in interstitial water from a sediment core from an estuary in North Carolina (Martens and Goldhaber, 1978).

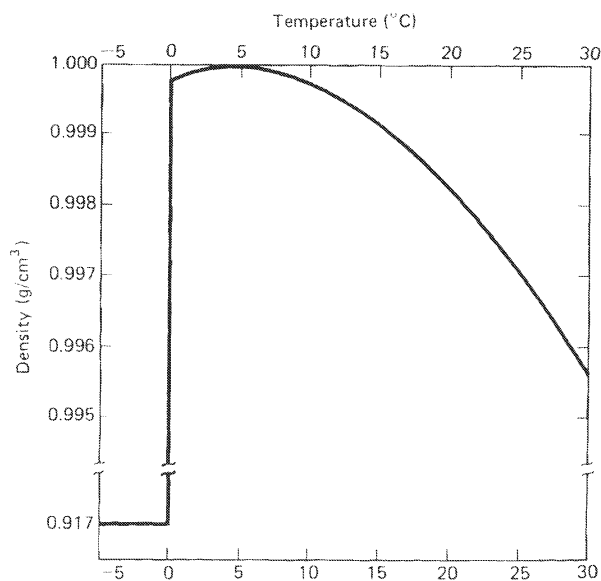
## LAKES

Redox conditions in lakes are determined by the balance between the decomposition of organic matter, normally from photosynthesis in the lake, and the supply of oxygen by circulation or vertical mixing of the water. The circulation in lakes is largely controlled by density differences, which are generally a consequence of temperature differences. The density of pure water as a function of temperature is shown in Fig. 8-6. Note that the maximum density occurs at 4°C, not at 0°C.

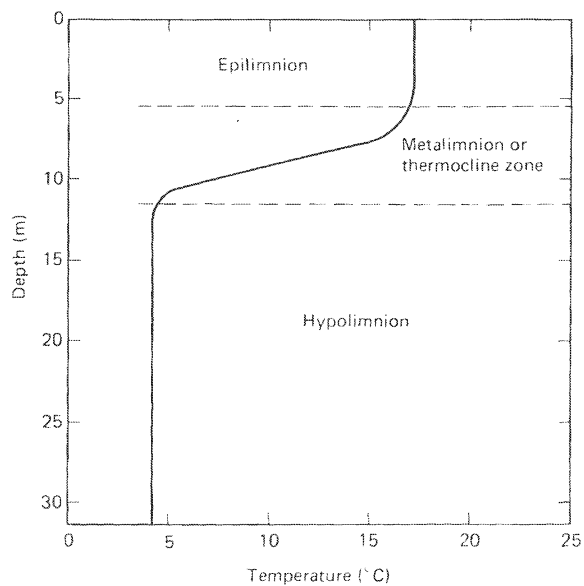
A typical vertical temperature profile for a lake in a temperate climate in summer is shown in Fig. 8-7 (tropical lakes are discussed below). The upper layer or *epilimnion* is warm as a result of solar radiation. The temperature within the epilimnion is fairly uniform because the surface zone is stirred by wave action. Immediately below the epilimnion is the *metalimnion* or *thermocline* zone, a region in which temperature decreases rapidly with depth. Below the metalimnion is a mass of uniformly cold water, the *hypolimnion*. In real lakes, the situation may be complicated by the presence of more than one metalimnion, and, of course, very shallow lakes and ponds will consist of an epilimnion only. The situation shown in Fig. 8-7 represents stable stratification. Warm, low-density water floats above cold, high-density water, and the density contrast results in little mixing or exchange of solutes between epilimnion and hypolimnion.

At the end of summer, the temperature of the epilimnion starts to decrease. When it reaches a value close to that of the hypolimnion (about 4°C in deep lakes in cold-winter climates), the density contrast between epilimnion and hypolimnion disappears. Storms, or even normal winds, cause complete mixing between the epilimnion and hypolimnion, an event called the *fall turnover*. If surface temperatures become even colder, stable stratification may again develop, with water (and ice) at about 0°C overlying more dense water at 4°C. This stratification breaks down at the *spring turnover*, when the surface layers again warm to 4°C. Lakes that turn over twice a year are called *dimictic*; those that turn over once a year are called *monomictic*.

**FIGURE 8-6** Density of pure water at 1 atm as a function of temperature.



**FIGURE 8-7** Typical summer temperature distribution for a lake in a temperate climate.



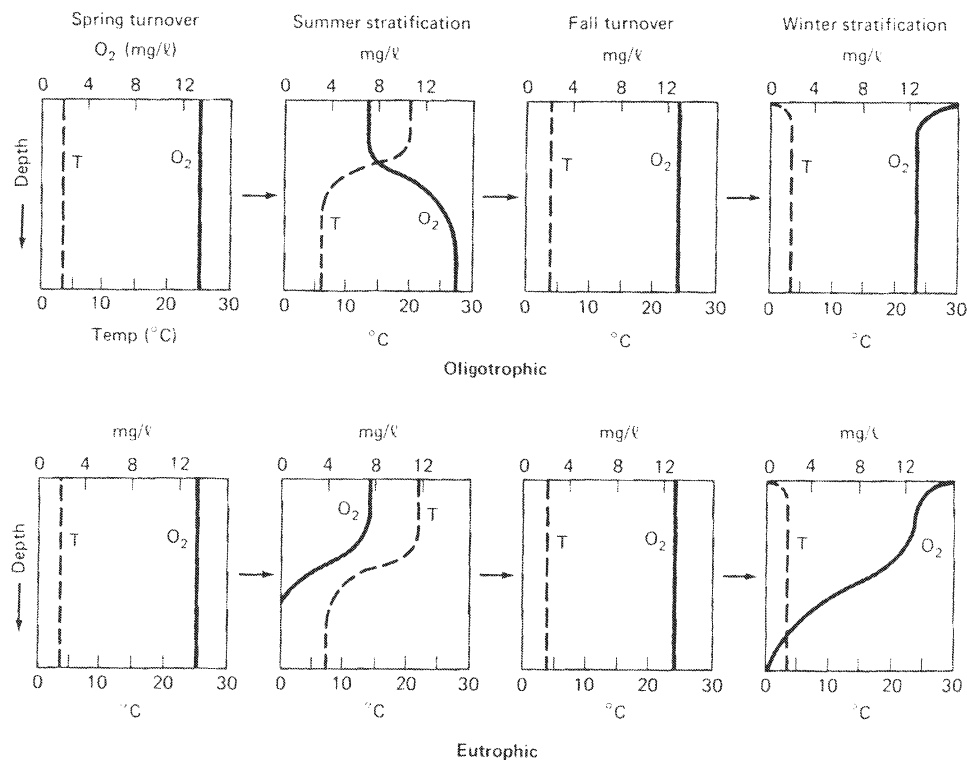
At times of turnover, the dissolved oxygen content of the entire lake is essentially determined by equilibrium with oxygen in the atmosphere (Table 8-1). When the lake becomes stratified, the oxygen content of the hypolimnion steadily decreases as a consequence of aerobic decomposition of organic matter falling from the epilimnion. Whether or not the hypolimnion

**TABLE 8-1** Concentration of Dissolved Oxygen in Water in Equilibrium with Air at a Total Pressure of 1 atm [from data of Truesdale et al., 1955]

Temperature (°C)	Oxygen (mg/l)	Oxygen (mM)	Temperature (°C)	Oxygen (mg/l)	Oxygen (mM)
0	14.16	0.443	18	9.18	0.287
1	13.77	0.430	19	9.01	0.282
2	13.40	0.419	20	8.84	0.276
3	13.05	0.408	21	8.68	0.271
4	12.70	0.397	22	8.53	0.267
5	12.37	0.387	23	8.38	0.262
6	12.06	0.377	24	8.25	0.258
7	11.76	0.368	25	8.11	0.253
8	11.47	0.358	26	7.99	0.250
9	11.19	0.350	27	7.86	0.246
10	10.92	0.341	28	7.75	0.242
11	10.67	0.333	29	7.64	0.239
12	10.43	0.326	30	7.53	0.235
13	10.20	0.319	31	7.42	0.232
14	9.98	0.312	32	7.32	0.229
15	9.76	0.305	33	7.22	0.226
16	9.56	0.299	34	7.13	0.223
17	9.37	0.293	35	7.04	0.220

becomes anaerobic depends on the total amount of organic matter falling into it during a period of stratification. The amount of organic matter produced in the epilimnion is largely controlled by the availability of inorganic nutrients, particularly phosphate. An *oligotrophic* lake is one in which the supply of nutrients is low, so there is little photosynthetic production and the water is oxygenated at all depths. A *eutrophic* lake is one in which the supply of nutrients is high, photosynthetic production is high, and the hypolimnion is anaerobic (Fig. 8-8). In an oligotrophic lake, the  $p_e$  of the hypolimnion remains high at all depths; in a eutrophic lake it will decrease with depth and with time since the onset of stratification. When turnover occurs in a eutrophic lake, hydrogen sulfide and other toxic compounds may be mixed into the epilimnion, which may cause widespread mortality among fish that were living in the epilimnion.

Pollution may affect the oxygen balance in lakes by introducing reactive organic matter, by introducing nutrients (phosphate and/or nitrate), or by introducing chemicals (e.g., heavy metals or persistent organic compounds) that interfere with biological systems in the lake. The common ways in which organic matter in wastewater is measured are as biochemical oxygen demand (BOD) and chemical oxygen demand (COD). BOD is measured by diluting the sample with oxygenated water, incubating it in the dark at 20°C for five days, and measuring the amount of oxygen that has been consumed. BOD is a predictor of how much direct oxygen



**FIGURE 8-8** Idealized distributions of temperature and dissolved oxygen in oligotrophic and eutrophic lakes. The increase in dissolved  $O_2$  with depth in the oligotrophic case in summer is due to the greater solubility of  $O_2$  at lower temperatures (after Wetzel, 1983).

consumption will be caused by a particular pollution source. COD is measured by the amount of a strong chemical oxidizer (potassium dichromate) consumed in oxidizing the organic matter in the water. It is (approximately) a measure of the total concentration of organic matter, both reactive and nonbiodegradable, in the water. COD can be measured more reproducibly and more conveniently than BOD, but BOD is probably a better predictor of oxygen consumption in the environment.

Normal sewage treatment processes reduce BOD and COD to low levels but are relatively ineffective in removing phosphate and nitrogen. Agricultural fertilizers also contribute these nutrients to surface waters. The most important way in which pollution affects lakes is thus by increasing the supply of nutrients, particularly phosphate, to the epilimnion. The phosphate content of sewage was significantly decreased when the phosphate content of commercial detergents was reduced in the late 1960s. Advanced waste treatment methods to remove phosphate from sewage are now becoming more common.

When an oligotrophic lake becomes eutrophic as a result of pollution, it is difficult to reverse the process. One might think that in a eutrophic lake undecomposed organic matter would be deposited in sediments, and this would remove phosphorus from lake waters. Although this does occur, the effect is usually overwhelmed by the consequences of reduction of ferric compounds. Ferric oxides adsorb phosphate strongly, and when the oxides are reduced (to  $\text{Fe}^{2+}$ ,  $\text{FeS}_2$ , or  $\text{FeCO}_3$ ), a large amount of phosphate is released to solution (Williams et al., 1976). Bacteria in the surface sediments of anaerobic lakes may also store significant quantities of phosphate, which is released to the water column when the water becomes aerobic (Gächter and Meyer, 1993). Thus, when a lake first becomes eutrophic, phosphate is transferred from the sediment to the hypolimnion, and when turnover occurs, this additional phosphate will be mixed into the epilimnion. The extra supply of phosphate will further aggravate the problem of eutrophication.

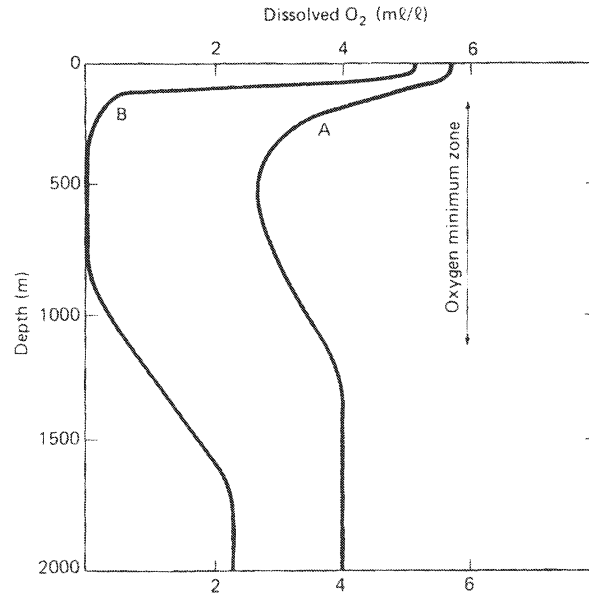
The circulation in tropical lakes is less straightforward than that of lakes in which circulation is controlled by seasonal temperature changes. In many tropical lakes, temperature differences between night and day are sufficient to cause frequent mixing, and hence prevent stratification. Thermal stratification may occur when a mass of cold water is formed during an unusually cold period, and a permanent epilimnion forms above it. Chemical stratification is also common. This occurs where water of higher salinity, formed in an arid period or by dissolution of salts in the lake bed, underlies more dilute surface water. Such chemical stratification may persist for many years. Lakes that do not turn over annually, usually because the deep water is more saline than the surface water, are called *meromictic*.

## THE OCEAN

The ocean differs from lakes in many respects other than scale. "Turnover" in the oceans is continuous, as cold surface water sinks at the poles, circulates at depth, and returns to the surface. The distribution of nutrients (and hence photosynthesis) in the oceans is controlled almost entirely by regeneration of nutrients in the water column and redistribution by circulation, whereas in lakes the distribution of nutrients is controlled more by the concentration of nutrients in the inflow waters than by processes in the lake itself (although there are exceptions to this generalization).

Typical profiles of dissolved oxygen in the ocean are shown in Fig. 8-9. The surface zone is well oxygenated as a result of both photosynthesis and exchange with the atmosphere.

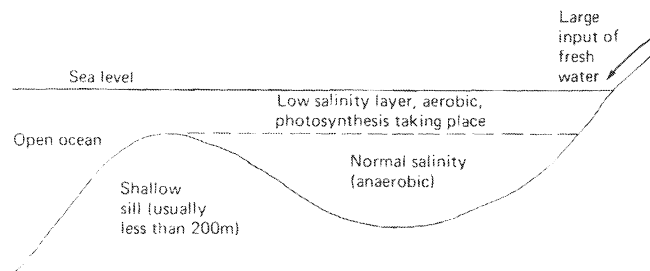
**FIGURE 8-9** Schematic illustration of the distribution of  $O_2$  with depth in the ocean. Curve A is a region of average surface productivity. Curve B is a region of very high surface productivity.



Below the surface zone is the oxygen minimum zone. This is the depth interval where most of the organic matter falling from the surface zone undergoes decomposition. Over most of the ocean, decomposition of organic matter is not sufficient to use up all the oxygen in the oxygen minimum zone, so the entire water column is aerobic. Under areas of exceptionally high surface productivity, areas of upwelling where nutrients are returned to the surface, water in the oxygen minimum zone may be anaerobic. The deep water below the oxygen minimum is generally well aerated. Most readily decomposable organic matter from the surface has already been decomposed before it reaches the deep zone, and oxygen in the deep zone is constantly replenished by the sinking of oxygenated water at the poles.

Anaerobic basins occur in the oceans where the circulation of deep water is obstructed and surface productivity is high (e.g., the Cariaco Basin off Venezuela). Such basins always have a sill depth near the oxygen minimum zone (Fig. 8-10). At greater depths, the supply of readily decomposable organic matter is so slow that even closed basins with little apparent circulation remain aerobic. Anaerobic conditions also occur in coastal basins such as the Black Sea and the fjords of northern Europe and North America, where a layer of relatively fresh

**FIGURE 8-10** Schematic illustration of anaerobic conditions in a fjord.



(low salinity) water traps a body of normal salinity water out of contact with the atmosphere or the open ocean.

The sediments of anaerobic basins are commonly black and rich in organic matter and iron sulfide. They also commonly show annual layering, caused by seasonal variations in the supply of sediment from land or in the production of calcite skeletons by planktonic organisms. The fine layering of the sediments is preserved because burrowing organisms which normally disrupt sea-floor sediments cannot live where the overlying water is anaerobic.

Although anaerobic conditions are rare in open ocean water, they are common in the interstitial waters of near-shore marine sediments. After a sediment is deposited, organic matter in it decays, consuming oxygen and then sulfate from the interstitial water. The detailed mechanisms controlling redox conditions in interstitial waters are complex (e.g., Berner, 1974, 1980), depending primarily on the amount of organic matter supplied to the sediment and the overall sedimentation rate. Sedimentation rate is particularly important because it controls the amount of time during which organic matter can undergo decomposition in oxygenated water at or near the sediment-water interface. In general, the interstitial waters of sediments around the margins of the continents are anaerobic, because sedimentation rates are high, and because, in shallower water, organic matter has not had as much time to decompose as it falls through the water column. Continental-margin sediments below wave base are generally black, green, or gray in color, and contain pyrite. At greater distances from the continents (deeper water and slower sedimentation rates), the sediments near the sediment-water interface are oxidizing, but the sediments at greater depths below the interface are reducing. Toward the centers of the ocean basins, far from the continents, the interstitial water of the entire sediment column is likely to be oxidizing.

## GROUNDWATER

Redox levels in groundwater are determined essentially by the relative rates of introduction of oxygen by circulation and the consumption of oxygen by bacterially mediated decomposition of organic matter (or occasionally sulfides or ferrous silicates or carbonates). The most important variables in natural systems appear to be:

1. *Oxygen content of recharge water.* Recharge water may enter an aquifer through fractures in bare rock, or it may percolate through a soil rich in organic matter. In the first case the recharge water will be oxidizing and will have significant redox buffer capacity at high  $p_e$  values. In the second case it may be anaerobic when it enters the aquifer, and it is unlikely to have much redox buffer capacity at high  $p_e$  values.

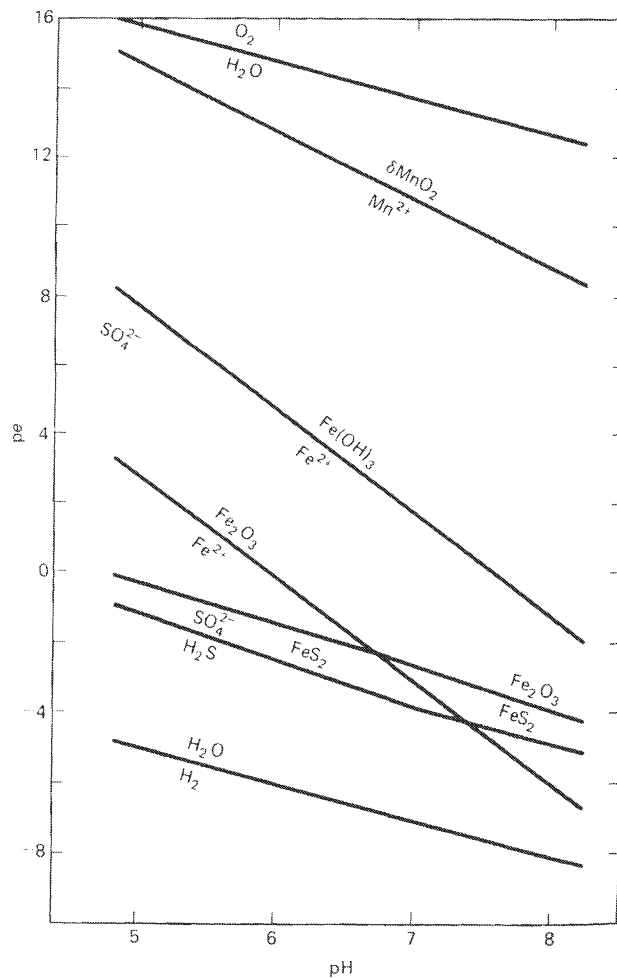
2. *Distribution and reactivity of organic matter and other potential reductants in the aquifer.* Aquifers vary greatly in the amount of organic matter present and, more important, in the reactivity of that organic matter. The organic matter of sedimentary rocks is generally refractory; that is, it is not easily utilized by bacteria. It is refractory both because the more easily metabolized components have already been utilized, and because the effects of elevated temperature and pressure are to convert the original organic compounds into compounds that are less readily utilized by bacteria. Most sedimentary rocks (and hence most aquifers) have been buried under a thickness of younger rocks at some time in their history, and hence have been exposed, to some degree or another, to elevated temperatures and pressures. As an example, coal (organic matter) should reduce any sulfate in groundwater

in a coal seam. However, groundwaters in coal seams often have high sulfate contents, and sometimes show no evidence of dissolved sulfide. Sulfate-reducing bacteria are incapable of utilizing directly the organic compounds that are common in coal, so sulfate reduction in groundwaters in coal is generally a slow process. The sulfides present in many coals were formed in the environment of deposition (an anaerobic sediment) rather than from later groundwater.

3. *Distribution of potential redox buffers in the aquifer.* In a groundwater system, the mass of potential redox buffers (for example,  $\text{MnO}_2$ ,  $\text{Fe}(\text{OH})_3$ , and  $\text{Fe}_2\text{O}_3$ ) per unit volume of groundwater is often large, and the reactions tending to lower  $pe$  are generally slow. The redox levels in groundwaters thus often correspond to buffering by the  $\text{Mn}^{2+}$ - $\text{MnO}_2$ , the  $\text{Fe}^{2+}$ - $\text{Fe}(\text{OH})_3$ , or the  $\text{Fe}^{2+}$ - $\text{Fe}_2\text{O}_3$  pair (Fig. 8-11).

4. *Circulation rate of the groundwater.* Since bacterial reactions that tend to lower  $pe$  are usually slow, the  $pe$  of a particular water depends very much on the residence time of water in the aquifer. The residence time depends on both the velocity of the water and the "length"

**FIGURE 8-11** Some possible redox buffers in a groundwater system. Solid-solution boundaries are drawn for activity of solute =  $10^{-6}$ .

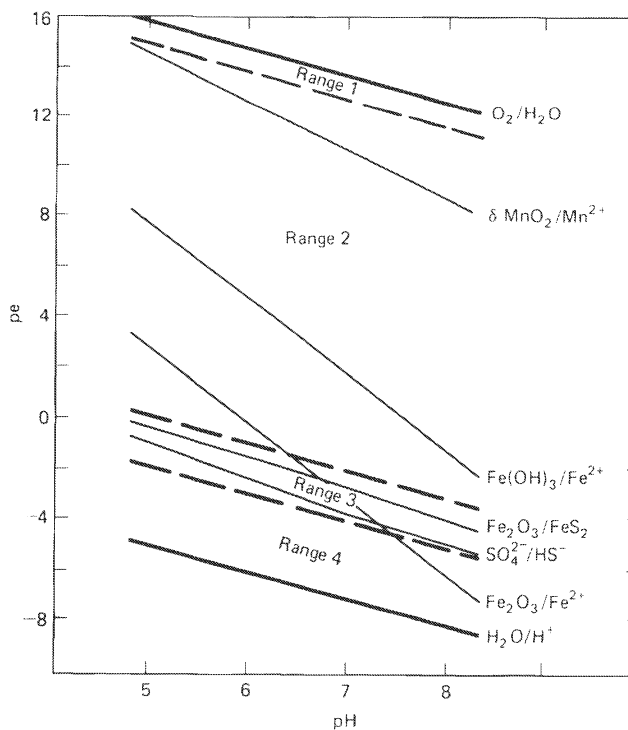




of the aquifer system from recharge to discharge. In general, the longer the residence time, the lower the resulting  $pe$ .

It is difficult to generalize about redox conditions in groundwater, as all four factors vary from place to place. If a groundwater contains free oxygen (range 1 on Fig. 8-12), either its residence time underground is short, or the aquifer contains essentially no metabolizable organic matter. The absence of organic matter may be inherited from the time the aquifer rock was deposited, or it may be that organic matter originally present has been removed by prolonged passage of oxygenated groundwater. Aerobic bacteria can utilize a greater variety of organic compounds than can sulfate-reducing bacteria. Most shallow groundwaters probably plot in Range 1. Many groundwaters also plot in range 2 of Fig. 8-12. The water contains no free oxygen, but no significant sulfate reduction has taken place. This redox level does not cause the water to be unsuitable for domestic supply purposes, although high (1 ppm or greater) concentrations of dissolved iron or manganese are sometimes a problem. Groundwaters in range 3 (buffered by sulfate reduction) are common where residence times are long or where much reactive organic matter is present. A high concentration of sulfide makes a water unsuitable for domestic supply purposes. Although waters in range 4 (well below the sulfate-sulfide boundary) are common in modern muds, they are relatively uncommon in aquifers, which are normally ancient rocks. The organic matter (with notable exceptions such as petroleum) in most ancient rocks is utilized so slowly by bacteria that many thousands of years are required for all the sulfate to be reduced and for the  $pe$  to reach the very low values.

**FIGURE 8-12** Positions of redox ranges discussed in text.



## SUMMARY

1. Redox conditions in natural waters are usually determined by the balance between the supply of oxygen from the atmosphere and the consumption of oxygen by microbial decomposition of organic matter.

2. After all free oxygen has been consumed,  $pe$  decreases progressively as a sequence of biological reactions occurs. The most important of these reactions are ferric iron reduction, sulfate reduction, and fermentation.

3. In lakes and the ocean, production of organic matter (and hence subsequent consumption of oxygen) is largely controlled by the availability of the inorganic nutrients phosphate and nitrate.

4. Changes in  $pe$  have a large effect on the solubility and hence mobility of many metals.

## REVIEW QUESTIONS

A lake in a cold-winter climate has a mean depth of 20 m, a surface area of 10 km<sup>2</sup>, an epilimnion thickness of 3 m, and an inflow and outflow of  $5 \times 10^8$  m<sup>3</sup>/y.

1. What is the residence time (Chapter 1) of water in the lake?
2. If organic water can be approximated by the formula CH<sub>2</sub>O, how many moles of organic matter per m<sup>2</sup> of lake surface would it take to consume all of the oxygen introduced to the metalimnion and hypolimnion during spring turnover? (Assume 4°C and the solubility of oxygen in Table 8-1.)
3. If summer stratification lasted six months, and all the phosphate in the inflow were used to produce organic matter [Eq. (8-2)] which fell into the metalimnion and hypolimnion, what concentration of phosphate in the inflow would result in depletion of all the oxygen in the metalimnion and hypolimnion?

## SUGGESTED READING

- BERNER, R. A. (1971). *Principles of Chemical Sedimentology*. New York: McGraw-Hill. Chap. 7.
- BRECK, W. G. (1974). Redox levels in the sea. In E. D. Goldberg (Ed.), *The Sea*, (Vol. 5). (p. 153-179). New York: Wiley-Interscience.
- CHAPELLE, F. H. (1993). *Ground-Water Microbiology and Geochemistry*. New York: John Wiley & Sons.
- STUMM, W., and P. BACCINI. (1978). Man-made chemical perturbation of lakes. In A. Lerman, (Ed.), *Lakes-Chemistry, Geology, Physics*. (p. 91-126), New York: Springer-Verlag.
- STUMM W., and J. J. MORGAN. (1996). *Aquatic Chemistry: Chemical Equilibria and Rates in Natural Waters* (3rd ed.). New York: Wiley-Interscience. Chap. 8, 10, and 11.
- WETZEL, R. G. (1983). *Limnology* (2nd. ed.). Philadelphia: Saunders.

# 9

## Heavy Metals and Metalloids

The term *heavy metals* is used generally to mean metallic elements with atomic numbers greater than about 20, the atomic number of calcium. Metalloids are elements such as arsenic and selenium that have both metallic and non-metallic properties. The term *heavy metals* will be used loosely to include metalloids. By and large, the concentrations of heavy metals in unpolluted natural waters are quite low. The main question we are trying to answer is: Why does a particular element have the concentration we observe in a particular water? Once we understand the answer to that question, we shall be in a position to predict the consequences of specific human interventions such as waste disposal and mining. Many elements—for example, selenium and molybdenum—are essential in trace amounts for biological systems. Understanding the circumstances that make such elements unavailable is sometimes as important as understanding the causes of toxic concentrations. Some economic ore deposits, such as those of uranium, are formed when elements present in trace concentrations in solution are extracted from solution at a particular location. To understand (and hence locate) such deposits, we need to understand the factors controlling the dissolution, transport, and precipitation of specific elements.

### SOURCES OF HEAVY METALS

Heavy metals may be derived from the weathering of rocks or, increasingly, they may be introduced into the atmosphere and hydrosphere by human activities. Average concentrations of some trace elements in rocks and in waters are shown in Table 9-1. For some elements, there are few reliable measurements, so the numbers should be taken as qualitative indicators only.

Whether a particular metal goes into solution during weathering depends on the mineral in which the element occurs and on the intensity of chemical weathering. Many of the metals do not substitute readily in feldspars or the common ferromagnesian minerals. They may be present in chemically resistant accessory minerals such as zircon, apatite, or monazite, or as sulfides, which generally weather rapidly in oxygenated water. The resistant minerals generally remain unaltered unless weathering is very intense (gibbsite formation, see Chapter 12).

**TABLE 9-1 Typical Concentrations of Selected Elements in Rocks [mg/kg (ppm)] and in Streams and the Ocean [ $\mu\text{g}/\text{kg}$  (ppb)]**  
 [from Turekian, 1971; Martin and Meybeck, 1979; and other sources]

	Granite	Basalt	Shale	Sandstone	Limestone	Streams	Ocean
Lithium	30	17	66	15	5	10	170
Beryllium	3	1	3				0.006
Boron	10	5	100	35	20	20	4,450
Fluorine	800	400	740	270	330	100	1,300
Aluminum	Major	Major	Major	Major	4,200	50	1
Scandium	10	30	13	1	1	0.004	0.0004
Titanium	Major	Major	Major	Major	400	10	1
Vanadium	50	250	130	20	20	1	2
Chromium	10	170	90	35	11	1	0.2
Manganese	450	1,500	850	50	1,100	8	0.2
Iron	Major	Major	Major	Major	Major	40	2
Cobalt	4	48	19	0.3	0.1	0.2	0.05
Nickel	10	130	68	2	20	2	0.5
Copper	20	87	45	2	4	7	0.5
Zinc	50	105	95	16	20	30	2
Gallium	17	17	19	12	4	0.1	0.03
Germanium	1	1	2	1	0.2		0.06
Arsenic	2	2	13	1	1	2	3
Selenium	0.05	0.05	0.6	0.05	0.9	0.2	0.1
Bromine	4	4	4		6	20	67,300
Rubidium	150	130	140	60	3	1	120
Strontium	250	465	300	20	600	60	8,100
Yttrium	40	25	35	10	4	0.07	0.001
Zirconium	150	140	160	220	20		0.03
Molybdenum	1	1.5	2.6	0.2	0.4	0.5	10
Silver	0.04	0.1	0.07			0.3	0.04
Cadmium	0.13	0.2	0.3		0.03		0.05
Antimony	0.2	0.1	1	0.4	0.3	1	0.3
Iodine	0.5	0.5	2	1	1	7	64
Cesium	3	1	6	6	6	0.03	0.3
Barium	600	330	580		10	50	10
Rare earths	0.5-70	1-80	1-80	0.05-15	0.05-8	0.001-0.1	0.001
Tungsten	1.7	0.7	1.8	1.6	0.6	0.03	<0.001
Gold	0.002	0.002	0.005	0.006	0.006	0.002	0.004
Mercury	0.03	0.01	0.4	0.03	0.04	0.07	0.03
Thallium	1.5	0.2	1.4	0.8			<0.01
Lead	17	6	20	7	9	1	0.03
Thorium	14	2.7	12	5.5	2	0.1	<0.0005
Uranium	3	1	4	2	2	0.1	3.3

and so their alteration never causes high trace-metal concentrations in waters (where weathering is intense, dilution prevents high concentrations). Many metals (e.g., copper, zinc, molybdenum, silver, mercury, and lead), occur in high concentrations in sulfide deposits and these sulfides often contain selenium, arsenic, and cadmium. Since sulfides weather rapidly, such ore deposits can give rise to locally high concentrations of dissolved trace elements (e.g., Alpers and Blowes, 1994). One aspect of *geochemical prospecting* is to use the concentrations of trace elements in water as a means of locating ore deposits.

Human activities introduce heavy metals to the hydrosphere in many ways. Burning of fossil fuels and smelting of ores put metals into the atmosphere, where they are washed out by rain and dry deposition into surface waters. Municipal sewage and industrial effluent introduce metals directly. Mining activities can result in release of metals, both because previously impermeable rocks are broken up and exposed to water, and because sulfide-containing rocks are exposed to oxygen, resulting in rapid alteration and dissolution. Landfills and underground toxic waste disposal, including radioactive wastes, have the potential to release a variety of substances to groundwater, and hence to surface waters. In many rivers and lakes, the human input of trace elements is many times greater than the natural input (Nriagu et al., 1979; Stumm and Baccini, 1978), and even in the oceans the human input is significant (Galloway, 1979).

High concentrations of heavy metals, regardless of their source, generally do not persist as the metals are transported through aquatic systems. The purpose of this chapter is to discuss some of the processes regulating trace element concentrations in natural waters.

## SPECIATION

For any calculations involving chemical equilibria, adsorption, or, indeed, toxicity, it is necessary to know the chemical form in which the element is present. For example, in Chapter 7 we discuss the solubility of  $\text{Fe}(\text{OH})_3$  in terms of the species  $\text{Fe}^{3+}$ ,  $\text{Fe}^{2+}$ ,  $\text{Fe}(\text{OH})^{2+}$ ,  $\text{Fe}(\text{OH})_2^+$ , and  $\text{Fe}(\text{OH})_4^-$ . If we had simply assumed that all dissolved iron was  $\text{Fe}^{3+}$ , we would have very little understanding of the processes regulating dissolved iron concentrations.

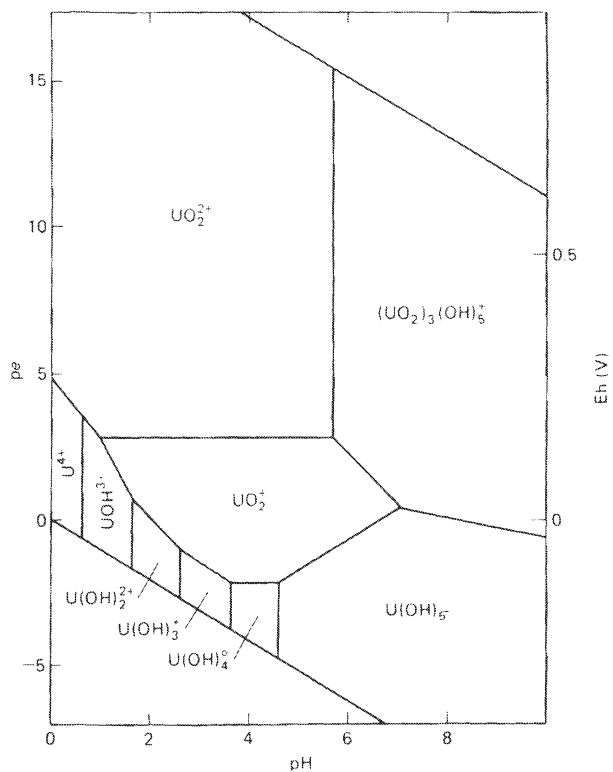
Dissolved uranium provides a more complicated example (Hostetler and Garrels, 1962; Langmuir, 1978). If we simply consider the system  $\text{U}-\text{O}-\text{H}_2\text{O}$ , the predominant dissolved species at different  $pe$  and  $pH$  values are as shown in Fig. 9-1. If we add  $\text{CO}_2$  to the system, various carbonate complexes become stable (Fig. 9-2). In typical ground- or surface water, phosphate, fluoride, and sulfate complexes may all be important (Fig. 9-3). The presence of carbonate and phosphate complexes makes the total dissolved uranium concentration in equilibrium with any uranium mineral much higher than it would be in carbonate- and phosphate-free water.

In order to calculate the concentration of a dissolved metal in equilibrium with a solid phase, it is necessary to know the concentrations of all potential complexing agents, and the stability constants (Chapter 2) of the various possible complexes. The databases of geochemical codes such as WATEQ4F and MINTEQA2 (Chapter 2) include a large number of elements and complexes.

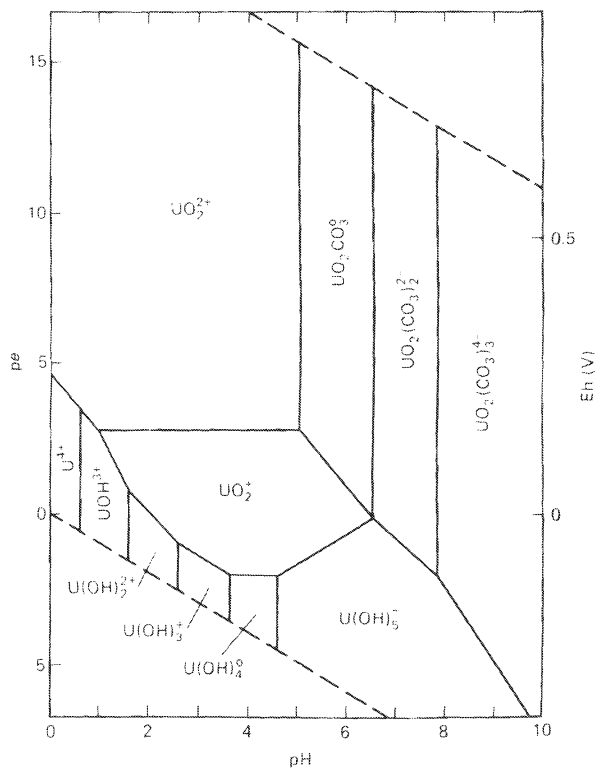
### Organic Matter and Complex Formation

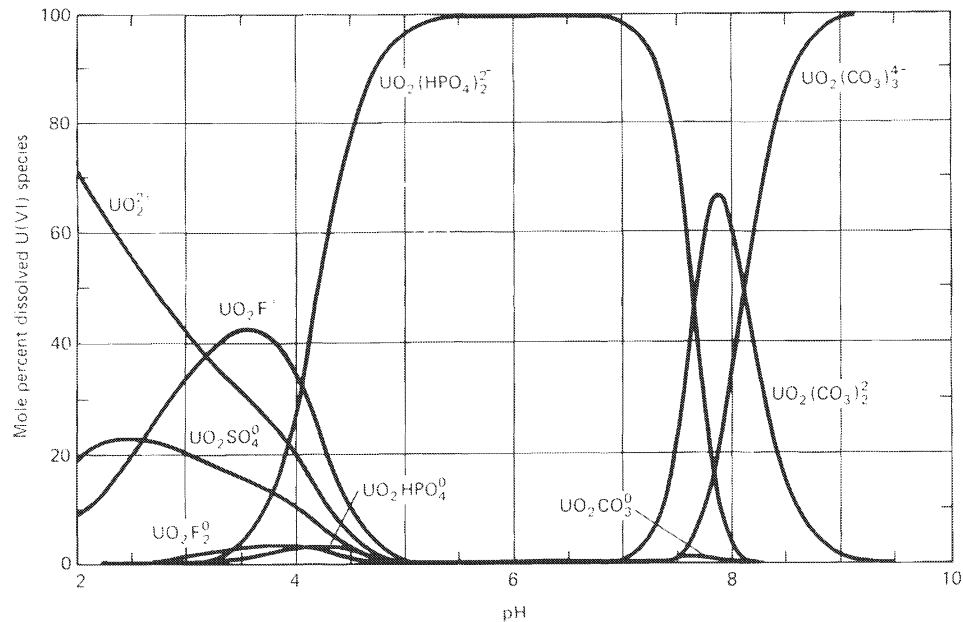
It is straightforward, in principle (Chapter 2), to calculate the effects of complexing by simple inorganic ligands such as  $\text{OH}^-$ ,  $\text{Cl}^-$ ,  $\text{SO}_4^{2-}$ , carbonate species, and phosphate species (although

**FIGURE 9-1** Distribution of dissolved uranium species in the system U–O–H<sub>2</sub>O at 25°C (after Langmuir, 1978).



**FIGURE 9-2** Distribution of dissolved uranium species in the system U–O–H<sub>2</sub>O–CO<sub>2</sub> at 25°C, assuming a  $P_{\text{CO}_2}$  of 10<sup>-2</sup> atm (after Langmuir, 1978).





**FIGURE 9-3** Distribution of uranyl complexes (uranyl,  $\text{UO}_2^{2+}$ , is the oxidized form of dissolved uranium) as a function of pH for some typical ligand concentrations in groundwater.  $P_{\text{CO}_2} = 10^{-2.5}$ , total F = 0.3 ppm, Cl = 10 ppm,  $\text{SO}_4^{2-} = 100$  ppm,  $\text{PO}_4^{3-} = 0.1$  ppm,  $\text{SiO}_2 = 30$  ppm (Tripathi, 1979).

the stabilities of some complexes are not well known). Complexing by organic ligands is much more difficult to evaluate. The dissolved organic matter in natural waters includes a wide range of compounds (Chapter 6), many of which have not been well characterized, and hence it is difficult to assign stability constants that have any general applicability. Complexing by organic matter may have a major effect on toxicity. Several metals, notably Al and Cu, are much less toxic to aquatic organisms when strongly complexed by organic matter than when present as free ions or hydroxy complexes.

The presence of organic ligands in solution also modifies the adsorption of trace metals by oxide and silicate surfaces (see below). If the metal ion in solution is strongly complexed, adsorption may be decreased, but in some systems adsorption is actually increased through formation of a ternary metal-ligand surface complex (Ali and Dzombak, 1996; Davis, 1984; Tessier et al., 1996).

## EQUILIBRIUM SOLUBILITY CONTROL

The simplest process that might regulate the concentration of a trace element in solution is equilibrium with respect to a solid phase containing the element as a major component. For example, Jones et al. (1974) showed that the dissolved aluminum concentration in a river in California corresponded well to equilibrium with kaolinite, and dissolved iron in the same samples corresponded to equilibrium with amorphous  $\text{Fe}(\text{OH})_3$ . Li et al. (1969) showed that the dissolved manganese concentration in interstitial water in a marine sediment first increased with depth as  $\text{MnO}_2$  was reduced, and then leveled off at a value corresponding to

the solubility of rhodochrosite ( $\text{MnCO}_3$ ). Emerson (1976) and Emerson and Widmer (1978) showed that the ion activity product

$$K_{\text{eq}} = \alpha_{\text{Fe}^{2+}}^3 \alpha_{\text{PO}_4^{3-}}^2$$

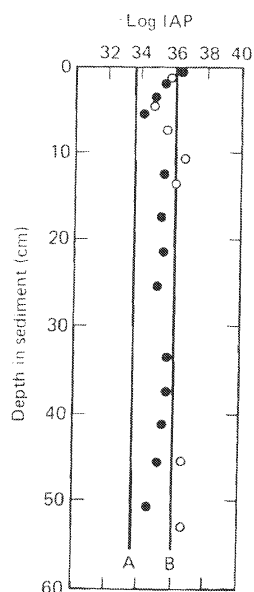
in interstitial waters in anaerobic sediments from a lake in Switzerland was very close to the solubility product of the mineral vivianite,  $\text{Fe}_3(\text{PO}_4)_2 \cdot 8\text{H}_2\text{O}$  (Fig. 9-4), and that the solubility of vivianite was a major control on the concentrations of iron and phosphorus in the water. On the other hand, these waters were quite strongly supersaturated with respect to pyrite ( $\text{FeS}_2$ ) and siderite ( $\text{FeCO}_3$ ); the solubility of these minerals did not appear to be a significant influence on the chemistry of the interstitial water.

The fact that a suite of waters appears to be close to saturation with respect to a solid phase is often taken as evidence that saturation with respect to the phase is in fact controlling solute concentrations. This logical leap is not necessarily justified, as other processes may give rise to similar concentrations. Controls on dissolved aluminum concentrations in acid soils provide a good example in this regard (Neal, 1988a, b). At first sight (Fig. 9-5 is an example) it appears that Al concentrations track closely the solubility of an  $\text{Al}(\text{OH})_3$  phase, and the assumption of equilibrium with  $\text{Al}(\text{OH})_3$  became an essential part of models for predicting the interaction of acid deposition with surface waters (Chapter 13). However, Neal showed that the apparent closeness to equilibrium was in part an artifact of the way the data had been plotted, and that concentrations of Al in many acidic waters were controlled more by mixing than by equilibration with an  $\text{Al}(\text{OH})_3$  phase.

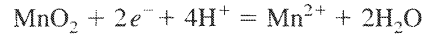
### Solubility in Redox Reactions

When an element occurs in a different oxidation state in the solid from that in solution (e.g.,  $\text{Fe}^{2+}$ – $\text{Fe}_2\text{O}_3$ ,  $\text{Mn}^{2+}$ – $\text{MnO}_2$ ,  $\text{Cu}^{2+}$ – $\text{Cu}_2\text{O}$ ), the “solubility product” must involve  $pe$  or some other redox couple. For example,

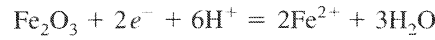
**FIGURE 9-4** Ion activity product  $\alpha_{\text{Fe}^{2+}}^3 \alpha_{\text{PO}_4^{3-}}^2$  in interstitial waters in two cores (open and closed circles) from the Greifensee (Switzerland), compared to the solubility product of vivianite (ferrous phosphate) as reported by (a) Tessenow (1974) and (b) Nriagu (1972) (after Emerson, 1976).







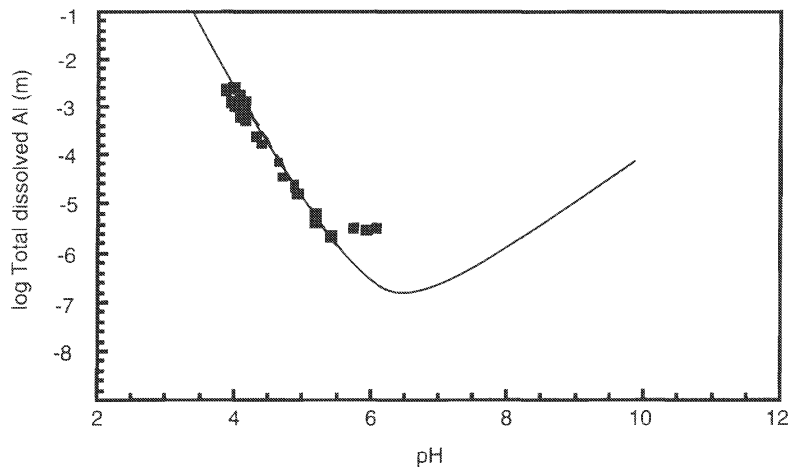
$$K_{\text{eq}} = \frac{\alpha_{\text{Mn}^{2+}}}{\alpha_e^2 \alpha_{\text{H}^+}^4}$$



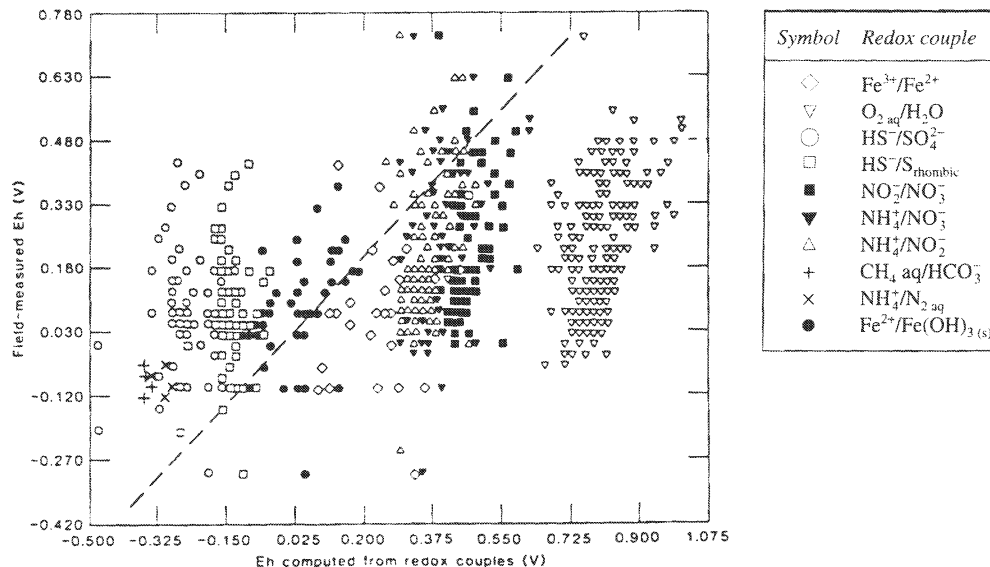
$$K_{\text{eq}} = \frac{\alpha_{\text{Fe}^{2+}}^2}{\alpha_e^2 \alpha_{\text{H}^+}^6}$$

To determine whether a solution is in equilibrium with  $\text{Fe}_2\text{O}_3$  or not, we need to know  $pe$ . Since  $pe$  can rarely be determined accurately (Chapter 7), it is rarely possible to test directly whether such a system is at equilibrium. One approach to testing for equilibrium is to calculate the  $pe$  corresponding to several different redox couples in solution. If the  $pe$  values are not the same, the system is not at equilibrium. Lindberg and Runnells (1984) compiled "high-quality analyses of groundwaters from diverse geographic areas" and computed  $pe$  values from ten different redox couples, which they compared to values calculated from Eh measured with a platinum electrode. The agreement was spectacularly poor (Fig. 9-6). Agreement was equally poor when speciation of Se (Runnells and Lindberg, 1990) and As (Runnells and Skoda, 1990) was compared to measured Eh. These results suggest that it is difficult, if not impossible, to assign a unique value to  $pe$  (or Eh) to use in quantitative calculations of redox-sensitive solubilities. They also suggest that modeling of the transport of redox-sensitive species by assuming thermodynamic equilibrium is likely to have limited success. This is borne out in field studies (for example, Kent et al., 1994). (Reasons for the lack of agreement are discussed in Chapter 8.)

In general, solubility equilibria provide upper limits to the concentrations of dissolved trace metals. It is unusual for a water to be supersaturated with respect to a simple solid phase by more than three orders of magnitude (observed concentration more than 1,000 times equilibrium concentration). Although a factor of 1,000 may seem a large range, precipitates often differ in



**FIGURE 9-5** Dissolved Al concentrations in soil solutions from a forest soil undergoing irrigation with acidified water compared to a solubility line for a poorly crystallized gibbsite (compare Fig. 10-3). The correspondence between the points and the line suggests (but does not prove) that Al concentrations are controlled by the solubility of a poorly crystallized Al-hydroxide phase (data from Swoboda-Colberg and Drever, unpublished).



**FIGURE 9-6** Comparison of field-measured Eh (platinum electrode) with Eh computed from 10 different redox couples. The dashed line corresponds to agreement between the electrode measurement and the redox couple. After Lindberg and Runnells, 1984, Groundwater redox reactions: an analysis of equilibrium state applied to Eh measurements and geochemical modeling. *Science*, 225, p. 925–927. Reprinted with permission. Copyright 1984 American Association for the Advancement of Science.

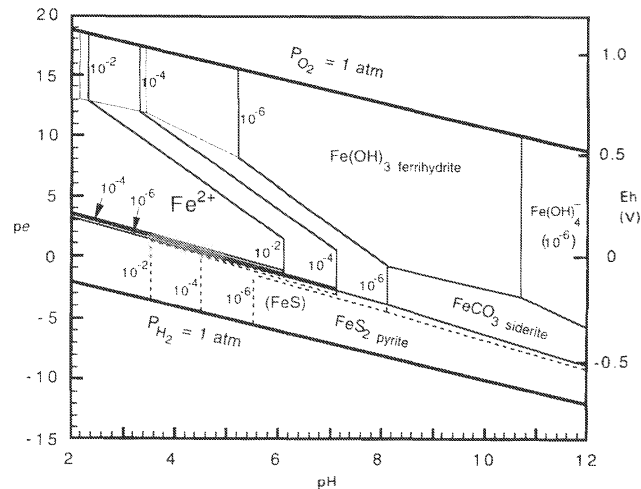
their solubilities by this much, depending on their state of crystallinity/disorder, and  $pe$  is often so poorly defined that an uncertainty of a factor of 1,000 makes little difference for purposes of interpretation (note the spacing of the contours of dissolved iron on Fig. 9-7). When large apparent supersaturations are observed, for example, several ppm iron in a neutral groundwater that contains oxygen or sulfide, it usually means that the speciation of the element (here iron) has not been evaluated correctly. The iron may be present as a complex (perhaps organic) or as a colloid that was not removed by filtration, so although the concentration of iron is high, the activity of Fe<sup>2+</sup> and/or Fe<sup>3+</sup> may be low, and the water may not be particularly supersaturated. Photo-reduction by sunlight (discussed later in this chapter) may also cause temporary high concentrations of Fe<sup>2+</sup> in oxygen-containing surface waters.

Solubility equilibria provide upper limits to the activities of dissolved species, but they do not generally provide lower limits. For example, we said that the solubility of MnCO<sub>3</sub> provided an upper limit to the concentration of manganese in a particular water, but MnCO<sub>3</sub> can be effective as a lower limit only if MnCO<sub>3</sub> is present in contact with water, and if it dissolves reasonably rapidly. MnCO<sub>3</sub> is not a common mineral, so that, by and large, it will not be available to be dissolved and will have no significance as a lower limit to dissolved manganese concentrations.

### pe–pH and Eh–pH Diagrams

pe–pH and related diagrams are graphical ways of displaying equilibrium solubility information. When they are used to interpret natural waters, the assumption is being made implicitly

**FIGURE 9-7** Contours of dissolved iron as a function of  $pe$  and  $pH$ , assuming  $P_{CO_2} = 10^{-2}$  atm, total activity of sulfur species =  $10^{-2}$ . The solid lines in lower part of diagram are drawn for pyrite ( $FeS_2$ ) as the iron sulfide mineral. Dashed lines are drawn for mackinawite ( $FeS$ ) as the iron sulfide mineral. In experiments (and presumably in nature), mackinawite or an amorphous equivalent is normally the first iron sulfide formed at approximately neutral  $pH$  values; at  $pH$  values below 6.5, pyrite, usually mixed with mackinawite, is the first sulfide to form (Berner, 1964; Roberts et al., 1969).



that equilibrium solubilities are important controls. Following are two examples of the use of such diagrams. Eh– $pH$  diagrams for many elements of geochemical interest are presented and discussed by Garrels and Christ (1965) and Brookins (1988).

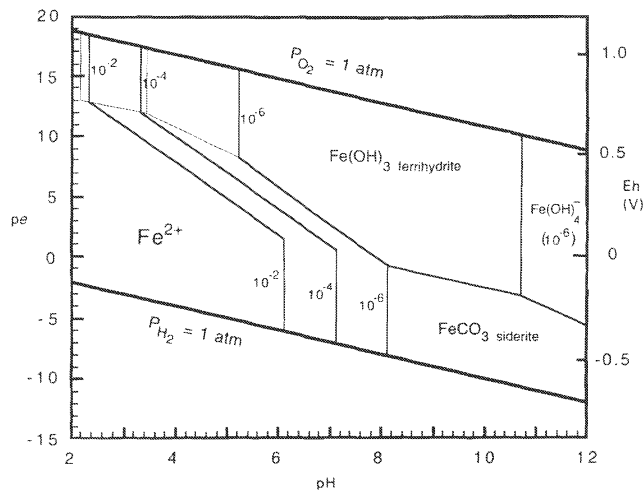
The solubilities of some iron minerals are shown as a function of  $pe$  and  $pH$  in Figs. 9-7 and 9-8. In oxygenated waters, we would expect dissolved iron concentrations to be low under neutral and alkaline conditions (in the absence of photochemical reduction), but high under strongly acid conditions. Over the common  $pH$  range of natural waters (5 to 9), as redox conditions become reducing we would expect iron concentrations to increase until the redox level is reached where sulfate reduction occurs. Under strongly reducing conditions, if dissolved sulfur species are present, we would expect low dissolved iron concentrations at all normal  $pH$  values; if sulfur is absent, we would expect iron concentrations to be controlled by the solubility of  $FeCO_3$ . At high  $pH$  values, concentrations should be low; at low  $pH$  values, they should be high (Fig. 9-8).

The following sequence would thus be expected in a dilute water reacting progressively with a sediment containing organic matter: initial iron concentrations should be low; the iron concentration should increase progressively until the onset of sulfate reduction; it should then drop to a low value; if all sulfate is consumed making iron sulfides, the iron concentration should again increase to the value corresponding to equilibrium with  $FeCO_3$ . This sequence could occur through time at a single location, as, for example, trapped interstitial water reacts with its enclosing sediment, or it could occur as a function of location as initially oxygenated water moves through an aquifer containing organic matter.

Qualitatively, iron behaves very much according to these predictions, even though we are not sure which ferric oxide/hydroxide to use in calculations, and the sulfide formed initially is rarely pyrite alone. The most common exceptions occur when iron is complexed by organic molecules, or when colloidal iron oxide is erroneously assumed to be dissolved.

The geochemistry of iron is exceptionally well suited to interpretation in terms of  $pe$ – $pH$  diagrams. The important phases containing iron do not generally contain large amounts of any other metal to complicate solubility calculations, and iron oxides or sulfides are almost ubiquitous in sediments and rocks.

**FIGURE 9-8** Contours of dissolved iron activity as a function of  $pe$  and  $pH$ .  $P_{CO_2} = 10^{-2}$ , no dissolved sulfur species present.



Uranium is another element whose behavior in nature has been successfully interpreted in terms of Eh–pH (or  $pe$ –pH) diagrams (Hostetler and Garrels, 1962; Langmuir, 1978). As mentioned earlier, uranium forms stable complexes with several commonly occurring ligands, so that the details of the  $pe$ –pH diagram depend critically on the assumptions made about potential complexing agents. In Fig. 9-9, a  $P_{CO_2}$  of  $10^{-2}$  atm and zero concentrations of phosphate, fluoride, and sulfate have been assumed. On the basis of Fig. 9-9, we would predict that uranium would be soluble at all pH values under oxidizing conditions and would be insoluble at all nonextreme pH values under reducing conditions. This appears to be the way uranium behaves in nature. A technique for mining uranium, which was introduced in the late 1970s, involves *in situ* extraction. A solution of hydrogen peroxide (oxidizer) and ammonium carbonate/bicarbonate (complexing agent), for example, is pumped into an aquifer containing uranium minerals. The uranium-containing minerals dissolve, and the solution is pumped out for processing above ground.

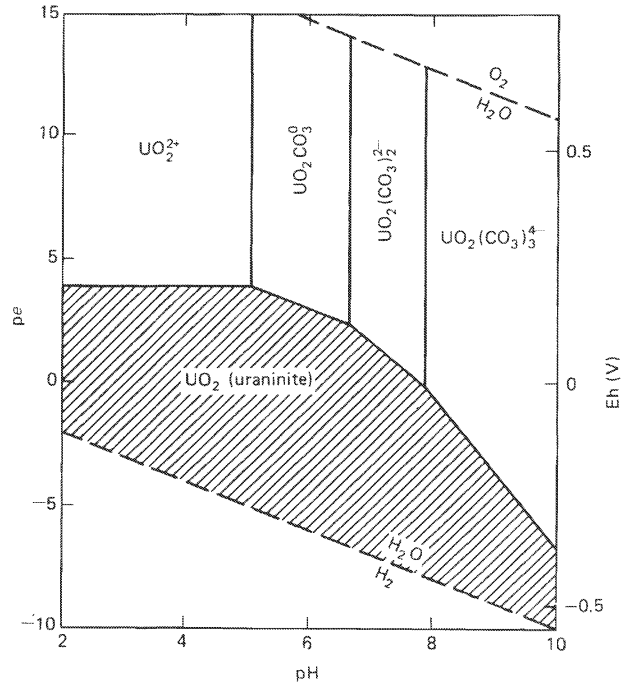
The solubility of uranium is extremely sensitive to traces of vanadium. If even 0.1 mg/l of dissolved vanadium is present, uranium becomes insoluble under all redox conditions over the pH range of approximately 4 to 8 (Fig. 9-10). If any dissolved vanadium is present in a water, the concentration of vanadium is at least as important a variable as  $pe$  or pH, so the simple  $pe$ –pH diagram may no longer be an adequate framework for discussing the solubility of uranium.

Uranium provides an excellent illustration of the value of  $pe$ –pH diagrams in qualitative discussions. Although the precise positions of the solubility boundaries are sensitive to the assumed concentrations of complexing agents, the general features of the diagram—soluble under oxidizing conditions unless vanadium is present, insoluble under reducing conditions—are sufficient for a general understanding of the behavior of uranium in natural waters.

### Roll-front Uranium Deposits

Some ore deposits, notably roll-front uranium deposits, are a consequence of redox reactions in groundwater. If oxygenated water starts to flow through an aquifer in which conditions were initially reducing, a redox front may develop between oxidizing and reducing

**FIGURE 9-9** Simplified  $pe$ - $pH$  diagram for the system  $U-O-H_2O-CO_2$  at  $25^\circ C$  and  $P_{CO_2} = 10^{-3}$  atm, showing the stability fields of ideal solid uraninite and dissolved species. Solubility boundaries are drawn at  $10^{-6}$  m dissolved uranium species (modified from Langmuir, 1978).



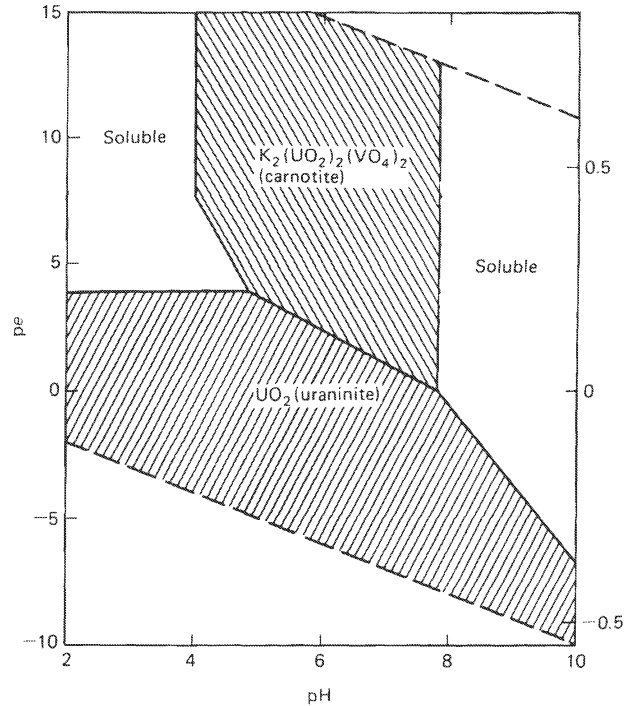
environments (Fig. 9-11). The front will move in the direction of groundwater flow but at a much slower rate than the water. The rate of movement of the front is determined by the capacity of the aquifer (particularly the organic matter in it) to consume oxygen. As an order of magnitude calculation, if a typical sedimentary aquifer contained 1.0 weight percent reactive organic carbon, and the groundwater contained 10 mg/l dissolved  $O_2$ , the front would migrate 13,000 times slower than the water velocity. Uranium and some other elements, notably selenium, arsenic, and molybdenum, are insoluble under reducing conditions and soluble under oxidizing conditions. As the oxidation front advances, any of these elements present in the aquifer are dissolved. The moving groundwater carries them through the front into a reducing environment, where they immediately reprecipitate. Thus the uranium that was distributed all through the aquifer before the front passed (or was transported from elsewhere in the groundwater system) is concentrated in the immediate vicinity of the front, and economic recovery may be possible.

## ADSORPTION AND COPRECIPITATION CONTROLS

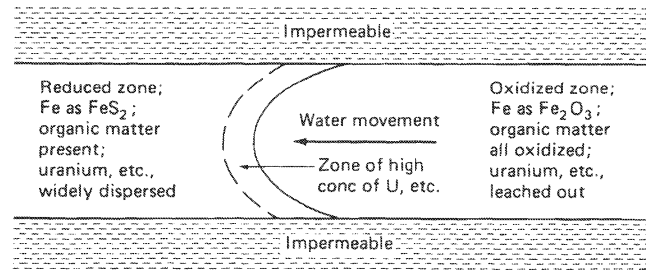
The concentrations of trace elements in natural waters are often much lower than would be expected on the basis of either equilibrium solubility calculations or of supply to the water from various sources. The most common reason for the low concentrations is adsorption of the element onto a solid phase.

Adsorption occurs when a dissolved ion or molecule becomes attached to the surface of a preexisting solid substrate. Coprecipitation occurs when a dissolved species is incorporated as a

**FIGURE 9-10** Simplified  $pe$ - $pH$  diagram for the system  $U-O-H_2O-CO_2$  at  $25^\circ C$  and  $P_{CO_2} = 10^{-2}$  atm,  $K^+ = 10^{-3}$  m,  $V = 10^{-6}$ . Solubility boundaries are drawn at  $10^{-6}$  m dissolved uranium species (modified from Langmuir, 1978).



**FIGURE 9-11** Idealized section through a roll-front uranium deposit in a sandstone aquifer.



minor component in a solid phase as that phase itself is precipitated. For example, if sulfate is added to a solution containing barium and traces of radium, barium sulfate will precipitate incorporating the radium, and the radium will be effectively removed from the solution. This is coprecipitation. On the other hand, if solid barium sulfate is added to a solution containing radium, some radium will be removed from the solution by adsorption onto the surface of the barium sulfate. In natural systems involving hydrous manganese and iron oxides, it is often impossible to distinguish between adsorption and coprecipitation, and the terms *adsorption* and *sorption* are sometimes used loosely to include both processes.

### Adsorption by Hydrous Iron and Manganese Oxides

Hydrous iron and manganese oxides (the term *oxyhydroxide* is often used to refer to hydroxides and hydrous oxides in general) are almost ubiquitous in soils and sediments where conditions

are not strongly reducing. They occur as coatings around silicate grains and as discrete grains of oxide mineral. The hydrous iron oxide is often amorphous although, of course, well-crystallized iron oxide minerals occur in ancient sedimentary rocks. Manganese generally occurs as poorly crystallized birnessite (also referred to as  $\delta$ -MnO<sub>2</sub>). In composition, this phase contains less oxygen than does ideal MnO<sub>2</sub> (typically between MnO<sub>1.6</sub> and MnO<sub>1.95</sub>) and may contain cations other than Mn as part of the structure. Both the manganese and the iron oxyhydroxides are exceedingly fine grained, with surface areas often on the order of 200 m<sup>2</sup>/g. Hydrous manganese oxides have extremely high adsorption capacities and high adsorption affinities for heavy metals. Jenne (1977) reviewed the literature on the distribution of trace elements in soils and sediments and concluded that the most important controls were adsorption by solid iron and manganese oxides and adsorption by solid organic matter. Suarez and Langmuir (1976) documented that Co, Ni, Cu, Zn, Pb, Ag, and Cd in a Pennsylvania soil were present largely in manganese and iron oxide phases. Means et al. (1978) showed that <sup>60</sup>Co and the actinides <sup>238</sup>Pu, <sup>241</sup>Am, and <sup>244</sup>Cm in sediments around a nuclear waste disposal site were present as adsorbed species on manganese oxides.

Synthetic  $\delta$ -MnO<sub>2</sub> (similar to natural birnessite) has a zero point of charge (see Chapter 5) of pH 2.8 in the absence of adsorbed ions other than H<sup>+</sup> and OH<sup>-</sup>. At higher pH values,  $\delta$ -MnO<sub>2</sub> is negatively charged and has a cation exchange capacity that increases with increasing pH, as would be expected from an oxide whose surface charge is controlled by loss or gain of protons. Murray (1975) summarized the adsorption properties of  $\delta$ -MnO<sub>2</sub> and demonstrated that there was significant adsorption of heavy metals at the point of zero charge, indicating that specific chemical forces are involved in the adsorption process in addition to electrostatic forces. He documented that the adsorption process is highly irreversible and suggested that the principal adsorption mechanism is



Hem (1978) argued that treating uptake by manganese oxides as a simple adsorption process is unrealistic. The uptake probably also involves phase transformations among the manganese oxides and catalysis of redox reactions by the Mn<sup>2+</sup>-Mn oxide system.

Where trace element concentrations are controlled by adsorption on manganese and iron oxides, we would expect dissolved concentrations to be sensitive to *pe* and pH. If the oxides are dissolved by reduction, any adsorbed metals will be released. They may appear in solution or they may be precipitated as some other phase such as a sulfide. The negative surface charge of manganese and iron oxides increases with increasing pH. At high pH values, metals are strongly adsorbed. This explains why alkaline soils often show deficiencies in the availability of trace elements required by plants. Photoreduction in surface waters may also cause dissolution of iron and manganese oxyhydroxide (McKnight and Bencala, 1990; Sulzberger, 1990; Sunda et al., 1983). This may result in release of adsorbed trace elements and may also be important in making iron and other metals bioavailable in surface waters.

Iron and manganese oxides are used as scavengers in wastewater treatment, and may be very important in retarding the migration of pollutants (including some radionuclides) in the subsurface (see Chapter 16). In planning underground disposal, consideration should be given to maintaining the high *pe* and pH conditions necessary for optimum adsorption.

Adsorption by iron and manganese oxyhydroxides can be modeled quantitatively with the geochemical code MINTQA2 (Chapter 5). The main limitation to such modeling is a lack of knowledge concerning the amounts and properties of oxyhydroxides in the natural environment, and also a lack of knowledge of specific flow paths of water in the subsurface.

### Adsorption by Silicates and Carbonates

Cation-exchange reactions involving clay minerals and zeolites (Chapter 4) can also maintain the concentrations of trace metals at low levels. Intuitively, one would not expect this to be an important process because the major cations ( $\text{Ca}^{2+}$ ,  $\text{Mg}^{2+}$ ,  $\text{K}^+$ , and  $\text{Na}^+$ ) should compete with trace metals for adsorption sites and should displace the trace metals into solution. This is probably true for species that adsorb as outer-sphere complexes (Chapter 5), but not necessarily for species that adsorb as inner-sphere complexes. The selectivity of an exchanger for a particular ion may be so great that the ion is removed from solution even when it is present in very low concentration. Some zeolites show high selectivities for specific cations (e.g., barium and ammonium). This is probably not very important for natural systems, because zeolites are not particularly widespread in nature. The use of zeolites to immobilize specific elements has, however, an important potential in the management of wastes.

Coston et al. (1995) investigated the adsorption of  $\text{Pb}^{2+}$  and  $\text{Zn}^{2+}$  on a natural aquifer sand. They concluded that most of the adsorption was due to coatings around quartz grains in the aquifer material. They were unable to characterize the coatings completely, but concluded that  $\text{—AlOH}$  groups played an important role; adsorption was not due simply to Fe or Mn oxyhydroxide coatings.

Calcite surfaces may also adsorb cations, notably  $\text{Cd}^{2+}$  (Davis et al., 1987), and anionic selenium species (see below). This does not appear to be a major process for most heavy metals, probably because the surface area of calcite in most aquifers is relatively small.

### Adsorption by Solid Organic Matter

The organic matter with which natural waters come in contact ranges from relatively small, soluble molecules to insoluble polymeric material such as coal and wood. Organic matter generally interacts strongly with trace metals, probably through formation of chelate-type complexes. Thus complexation by dissolved organic matter can lead to unexpectedly high concentrations of metals in solution, and adsorption onto solid organic matter can remove metals from solution. Rivers draining swamps in Georgia (abundant dissolved organic matter) contain as much dissolved iron as potassium or magnesium (Beck et al., 1974), whereas groundwaters from a coal seam in Wyoming (abundant solid organic matter) contain exceedingly low concentrations of trace metals (Drever et al., 1977).

So little is known about the details of adsorption of trace metals by solid organic matter that precise quantitative predictions cannot be made at this time. As discussed in Chapter 6, adsorption by solid organic matter is a major control on the migration of non-polar organic contaminants.

## UPTAKE BY LIVING ORGANISMS

Many trace elements are essential in minute quantities for plant and animal growth. Organisms are capable of extracting these elements from water in which the metals are present in very low concentrations. The main control on the distribution of trace elements in the ocean is uptake by living organisms and subsequent release as the organisms decay.

It is hard to generalize about the overall significance of biological uptake in controlling trace element concentrations in natural waters. For elements used in relatively large amounts



by organisms (nitrogen, phosphorus, sometimes carbon, potassium, and silica), biological processes are often the dominant control in surface waters. For elements utilized in only trace amounts (e.g., Mn, Cu, Ni, Mo, and Se), uptake by organisms in open waters such as lakes probably affects dissolved concentrations significantly only in environments where concentrations are low in general. In environments where concentrations are high as, for example, in polluted waters, the amounts taken up by organisms are likely to be small compared to the amounts in solution or to the amounts removed by adsorption processes.

In terrestrial systems uptake by plants can have a major influence on both heavy metals and organic compounds. One method of water treatment is to route a contaminated water through an artificially constructed wetland—a swamp with abundant plants (e.g., Wieder, 1993). Contaminants are removed by direct plant uptake, by adsorption on solid organic matter, and by precipitation as sulfides where the environment is anaerobic. One problem with artificial wetlands is that their lifetime is generally finite (a decade or so), and then the material that makes up the wetland must be disposed of.

## BEHAVIOR OF SPECIFIC ELEMENTS

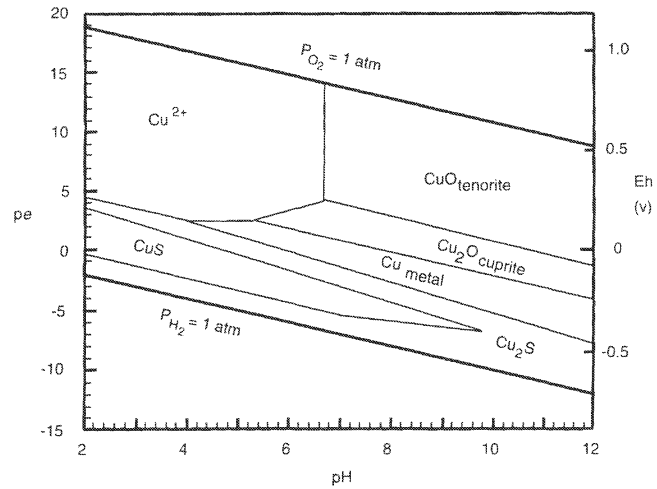
Several specific elements are discussed here to provide an overview of their behavior and to illustrate patterns of behavior that are common to many other elements.

### Copper, Zinc, Cadmium, and Lead

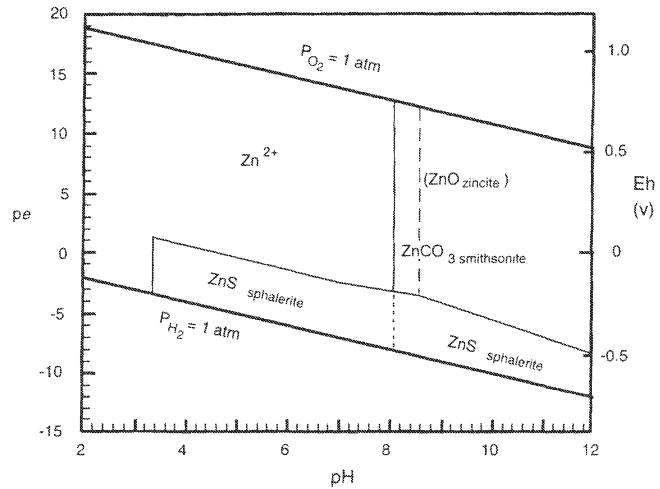
These elements have several features in common. The dominant species in solution is a divalent cation (free or complexed). Under oxidizing conditions, they are soluble under acid conditions and their solubilities at higher pH are limited by the solubility of a carbonate or oxide/hydroxide (Figs. 9-12 to 9-16; these and subsequent figures have been simplified by omission of some possible complexes in solution involving sulfate, sulfide species, carbonate species, and  $\text{OH}^-$ . These omissions do not significantly change the diagrams for the conditions commonly encountered in fresh waters). Under reducing conditions, in the presence of sulfur all form relatively insoluble sulfides. In the absence of sulfur, copper is insoluble as the native metal (Fig. 9-16). The others behave as they do in oxidizing environments: they are relatively soluble at low pH and insoluble as carbonates/oxides/hydroxides at high pH. Copper, zinc, and cadmium form anionic species at high pH. It is rare, however, for pH values in nature to be sufficiently high for such species to be important. The response of these elements to a change in redox conditions is determined less by redox reactions involving the elements themselves than by changes occurring in sulfur species, and in Fe and Mn oxyhydroxides, which are important substrates for adsorption.

All members of the group are complexed by natural organic matter. Some binding constants for complexing of the  $\text{M}^{2+}$  ion with humic substances are shown in Table 9-2. These constants give a general indication of the strength of interaction between the metal and dissolved organic matter. The constant for calcium is included for comparison. In general, copper is the most strongly complexed member of the group and is very commonly influenced by organic complexation. Lead is next, followed by zinc and cadmium. Complexing of zinc and cadmium by organic solutes is, generally speaking, important only where concentrations of dissolved organic carbon are relatively high.

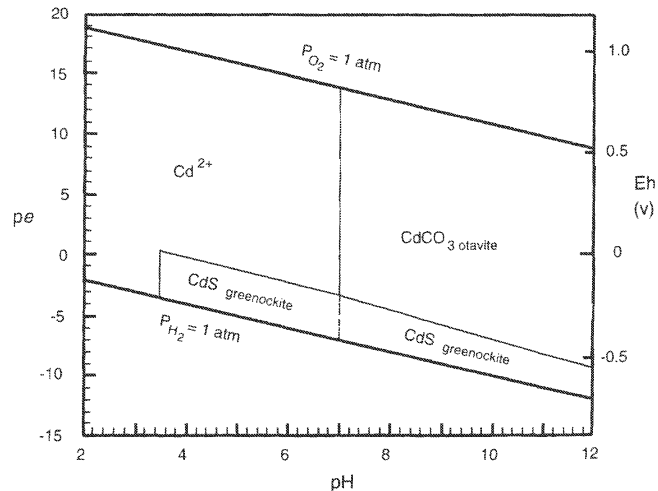
**FIGURE 9-12** Simplified  $pe$ - $pH$  diagram for the system Cu-S-O-H<sub>2</sub>O at 25°C and 1 atm. Solubility is defined as a dissolved Cu activity of  $10^{-6}$ . Total activity of sulfur species =  $10^{-2}$ . Malachite (Cu<sub>2</sub>(OH)<sub>2</sub>CO<sub>3</sub>) becomes stable at a  $P_{CO_2}$  of about 0.6 atm; its stability field replaces that of CuO (Fig. 9-16). Data are consistent with Appendix III.



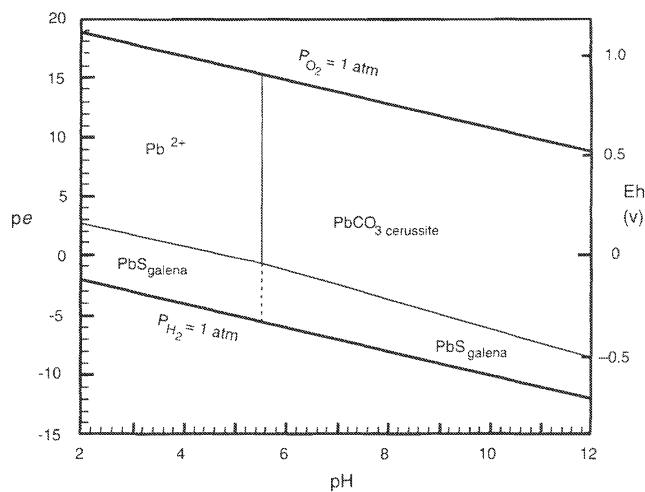
**FIGURE 9-13** Simplified  $pe$ - $pH$  diagram for the system Zn-CO<sub>2</sub>-S-O-H<sub>2</sub>O at 25°C and 1 atm. Solubility is defined as a dissolved Zn activity of  $10^{-6}$ . Total activity of sulfur species =  $10^{-2}$ ,  $P_{CO_2} = 10^{-2}$  atm. Dashed lines are the solubility of ZnO (zincite) in the absence of CO<sub>2</sub>, and short dashes are the solubility of the carbonate in the absence of S species. Data are consistent with Appendix III.



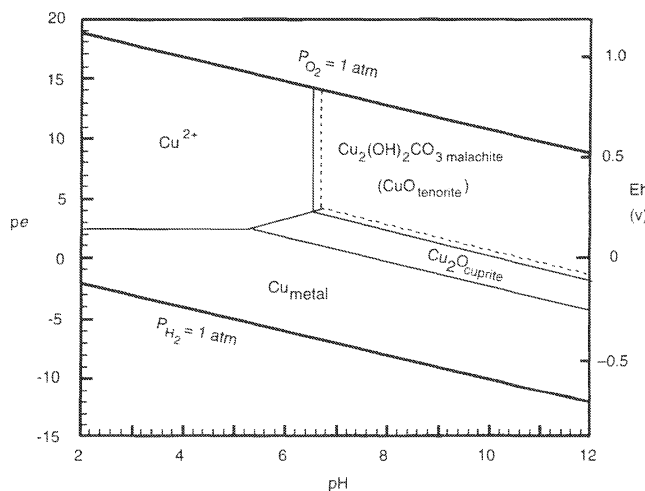
**FIGURE 9-14** Simplified  $pe$ - $pH$  diagram for the system Cd-CO<sub>2</sub>-S-O-H<sub>2</sub>O at 25°C and 1 atm. The  $P_{CO_2}$  has to be very low for the oxide, CdO (monteponite) to be stable relative to the carbonate. Solubility is defined as a dissolved Cd activity of  $10^{-6}$ . Total activity of sulfur species =  $10^{-2}$ ,  $P_{CO_2} = 10^{-2}$  atm. Solid lines are solubility in the presence of S species, and dashed line is solubility of the carbonate in the absence of S species. Data are consistent with Appendix III.



**FIGURE 9-15** Simplified  $pe$ - $pH$  diagram for the system  $Pb$ - $CO_2$ - $S$ - $O$ - $H_2O$  at  $25^\circ C$  and 1 atm. Solubility is defined as a dissolved  $Pb$  activity of  $10^{-6}$ . Total activity of sulfur species =  $10^{-2}$ ,  $P_{CO_2} = 10^{-2}$  atm. The  $P_{CO_2}$  has to be very low for the oxide,  $PbO$  (litharge) to be stable relative to the carbonate. Solid lines are solubility in the presence of  $S$  species, and the dashed line is solubility of the carbonate in the absence of  $S$  species. Data are consistent with Appendix III.



**FIGURE 9-16** Simplified  $pe$ - $pH$  diagram for the system  $Cu$ - $CO_2$ - $O$ - $H_2O$  at  $25^\circ C$  and 1 atm. Solubility is defined as a dissolved  $Cu$  activity of  $10^{-6}$ . No sulfur species present. The stability of malachite ( $Cu_2(OH)_2CO_3$ ) is shown for a  $P_{CO_2}$  of 1 atm. At  $P_{CO_2}$  values below about 0.6 atm, malachite becomes unstable, and tenorite ( $CuO$ ) becomes the stable phase. Dashed lines are the stability field of  $CuO$  in the absence of  $CO_2$ . Data are consistent with Appendix III.



**TABLE 9-2** Logarithms of Intrinsic Binding Constants<sup>a</sup> for Complexes Between Metals and Dissolved Humic Substances [from Tipping and Hurley, 1992]

	<i>log binding constant</i>
$Cu^{2+}$	-0.72
$Pb^{2+}$	-0.81
$Zn^{2+}$	-1.04
$Cd^{2+}$	-1.63
$Ca^{2+}$	-2.67

<sup>a</sup>The exact definition of intrinsic binding constant is rather complex; readers should consult the original reference before attempting to use the numbers. The numbers are a good indication of the relative extent of complexing to be expected between the individual metals and natural dissolved organic matter. A smaller number (larger negative logarithm) means weaker binding.

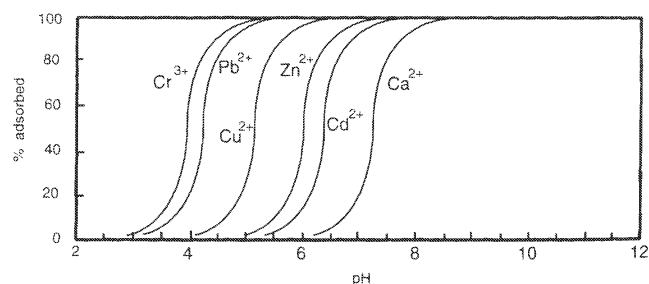
All members of the group are potentially affected by adsorption on iron and manganese oxyhydroxides (Fig. 9-17), and Cd is potentially affected by adsorption on calcite. As discussed in Chapter 5, adsorption is pH dependent. Lead adsorbs at the lowest pH, followed by Cu, Zn, and Cd. The curves shown in Fig. 9-17 illustrate the results of experiments conducted under a specific set of conditions and should not be overgeneralized.

The expected behavior of these metals in the environment can be summarized as follows: under oxidizing conditions at low pH, they are all soluble and mobile. As the pH rises, their concentrations tend to decrease, first because of adsorption (particularly for Pb and Cu), and then because of the limited solubility of carbonates and oxides/hydroxides. Under reducing conditions, if sulfur is present, all should be immobilized as sulfides. If sulfur is absent, for Zn, Cd, and Pb the solubility control will be the same as under oxidizing conditions; Cu should be insoluble at all pH values. Adsorption is generally less important under reducing conditions because the most important substrates for adsorption, Fe and Mn oxyhydroxides, tend themselves to dissolve.

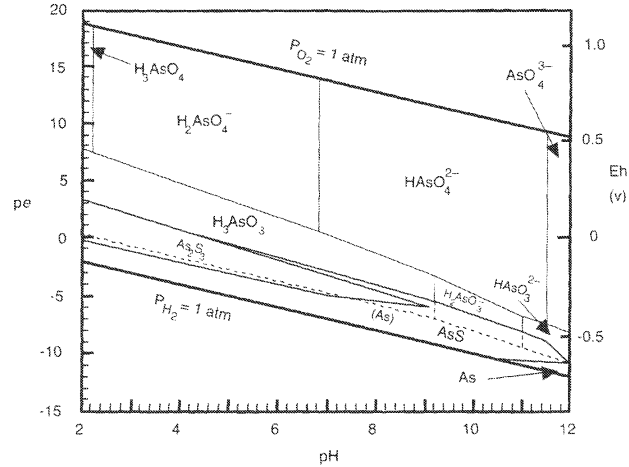
### Arsenic and Selenium

Arsenic and selenium differ strongly from the previous examples in that both elements undergo important changes in oxidation state themselves, and both occur in solution as anions or as neutral species rather than as cations.  $pE$ -pH diagrams are shown in Figs. 9-18 and 9-19. Under oxidizing conditions, the dominant form of arsenic is the +V oxidation state, which is present as arsenic acid and its anions (arsenate), corresponding closely to phosphoric acid and phosphate species. For selenium, the dominant form under oxidizing conditions is selenate, which is closely analogous to sulfate. As conditions become reducing, As(V) is reduced to As(III)—arsenious acid and arsenite anions. When sulfate reduction occurs, As precipitates as a sulfide; if sulfur is absent, it remains in solution as arsenious acid or an arsenite. Elemental arsenic should be a stable species under highly reducing conditions, but it does not occur commonly in nature. For selenium, selenite species (analogous to sulfite) occur at intermediate redox levels, followed by elemental selenium and hydrogen selenide (analogous to hydrogen sulfide) species under strongly reducing conditions. Both

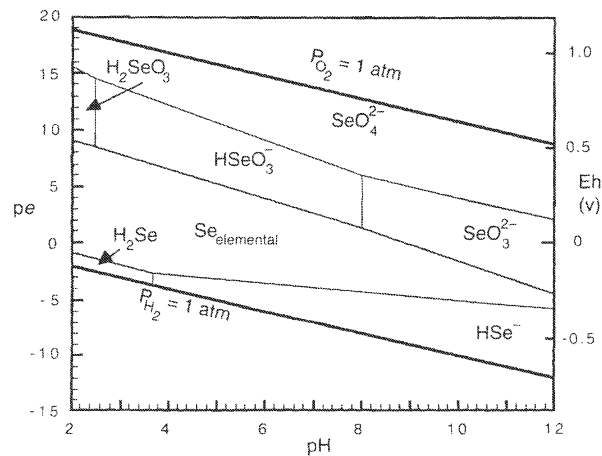
**FIGURE 9-17** Adsorption of  $\text{Cu}^{2+}$ ,  $\text{Cd}^{2+}$ ,  $\text{Zn}^{2+}$ ,  $\text{Pb}^{2+}$ ,  $\text{Cr}^{3+}$ , and  $\text{Ca}^{2+}$  (for comparison) on hydrous ferric oxide as a function of pH. Each metal shows an adsorption "edge": at pH values below the edge, the ion is not adsorbed or very weakly adsorbed. At pH values above the edge, the ion is strongly adsorbed. Conditions correspond to a high ratio of hydrous ferric oxide to adsorbing cation and an ionic strength of 0.1 M. The edges move towards higher pH as the ratio adsorbing cation:hydrous ferric oxide increases. From data in Dzombak and Morel (1990).



**FIGURE 9-18** Simplified  $pe$ - $pH$  diagram for the system As-O-H<sub>2</sub>O at 25°C and one atm. Total activity of sulfur species =  $10^{-2}$ . Light lines are boundaries involving dissolved species only. Dashed line is field of solid elemental arsenic in the absence of sulfur. Solubility is defined as a dissolved As species activity of  $10^{-6}$ .



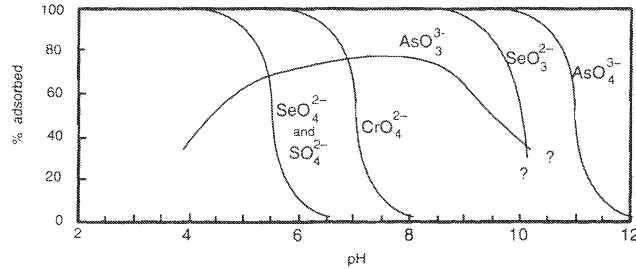
**FIGURE 9-19** Simplified  $pe$ - $pH$  diagram for the system Se-O-H<sub>2</sub>O at 25°C and one atmosphere. Solubility is defined as a dissolved Se activity of  $10^{-6}$ . Data are from Cowan (1988).



arsenic and selenium may be incorporated into iron sulfides under reducing conditions. The kinetics of redox transformations involving arsenic and selenium are slow, so disequilibrium is common (Kent et al., 1994; Runnells and Lindberg, 1990).

Arsenate species form inner-sphere complexes at the iron oxyhydroxide surface and are strongly adsorbed at near-neutral pH (Fig. 9-20). At high pH the strong negative charge on the oxide surface decreases adsorption of anions. As(III) apparently does not form inner-sphere complexes at the oxide surface. It is not strongly adsorbed at any pH value. For selenium, the adsorption picture is reversed. The oxidized form is only weakly adsorbed (similar to sulfate), whereas Se(IV) is strongly adsorbed under near-neutral conditions.

Organoarsenic compounds occur in nature but do not appear to be particularly important in the overall cycle of arsenic. Organic forms of selenium are more important, particularly in plants that accumulate selenium. Certain plants, notably vetches of the genus *Astragalus*, can accumulate high concentrations of selenium and may cause toxicity problems for livestock.

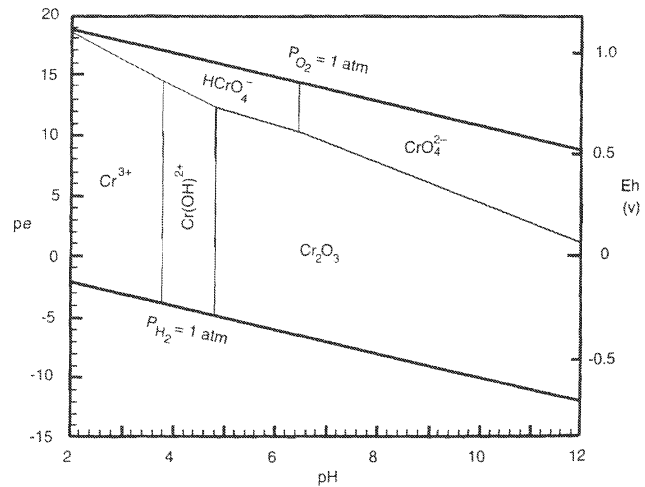


**FIGURE 9-20** Adsorption of arsenate, arsenite, selenate, selenite, chromate, and sulfate (for comparison) on hydrous ferric oxide as a function of pH. Most of the anions show an adsorption "edge": at pH values above the edge (for anions), the ion is not adsorbed or very weakly adsorbed. At pH values below the edge, the ion is strongly adsorbed. The anomalous behavior of arsenite is related to the fact that  $\text{AsO}_3^{3-}$  is fully protonated to  $\text{H}_3\text{AsO}_3$  below pH 9 (Fig. 9-18); the symbol  $\text{AsO}_3^{3-}$  is used for all As in the +III oxidation state. Conditions correspond to a high ratio of hydrous ferric oxide to adsorbing cation and an ionic strength of 0.1 m. The edges move towards lower pH as the ratio adsorbing anion:hydrous ferric oxide increases. From data in Dzombak and Morel (1990).

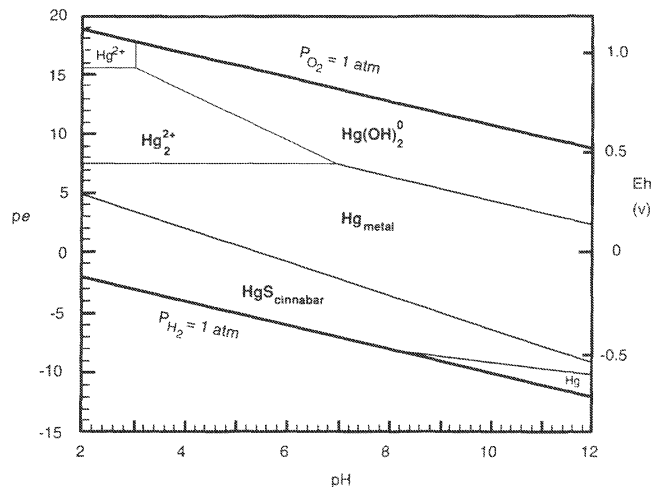
## Chromium

Chromium (Fig. 9-21) shows some similarities to both of the groups of elements discussed above. Under highly oxidizing conditions, the hexavalent form (chromate) is stable as an anion. It is not strongly adsorbed (adsorption edge at about pH 7, Fig. 9-20) and is therefore mobile in the environment. Under intermediate and reducing conditions, Cr(III) is the stable oxidation state. It is insoluble in the neutral and alkaline pH ranges. It is soluble (largely as  $\text{Cr}(\text{OH})^{2+}$ ) under acid conditions. In general, Cr(III) species are strongly adsorbed (Fig. 9-17). Where dissolved chromium pollution occurs, the problem form is generally Cr(VI).

**FIGURE 9-21**  $pe$ - $pH$  diagram for the system  $\text{Cr-O-H}_2\text{O}$  at  $25^\circ\text{C}$  and one atm. Solubility is defined as a dissolved Cr activity of  $10^{-6}$ . Data from Brookins (1988).



**FIGURE 9-22**  $pe$ - $pH$  diagram for the system  $Hg-S-O-H_2O$  at  $25^\circ C$  and one atm. Solubility is defined as a dissolved  $Hg$  activity of  $10^{-6}$ . Total activity of sulfur species =  $10^{-2}$ . The diagram is the same in the absence of  $S$  species, with the  $HgS$  (cinnabar) field replaced by  $Hg$  (metal). In the presence of chloride, the  $Hg_2^{2+}$  may be replaced by the insoluble mercurous chloride (calomel). Data are consistent with Allison et al. (1991).



## Mercury

The chemistry of mercury in the environment is highly complex. The thermodynamically stable forms are shown in Fig. 9-22. The common soluble form is the oxidized (mercuric)  $Hg^{2+}$  ion and its hydrolysis product  $Hg(OH)_2^0$ , with the reduced (mercurous)  $Hg_2^{2+}$  ion being less important. Elemental mercury has a large stability field. The elemental form is volatile and slightly soluble in water. The global cycle of mercury is dominated by vapor-phase transport of  $Hg^0$  through the atmosphere (Mason et al., 1994). Mercury is transformed by microorganisms into organic forms, notably monomethyl mercury ( $CH_3Hg$ ) and dimethyl mercury [ $(CH_3)_2Hg$ ]. These organic forms, in addition to being highly toxic, are volatile and tend to accumulate in the food chain. High concentrations of  $Hg$  in fish, which are common in polluted waters, generally result from accumulation of organomercury species. Pollutant  $Hg$  in sediments is partly transformed to organomercury species and partly to the sulfide.

Most of the metals discussed above— $Cu$ ,  $Zn$ ,  $Cd$ ,  $Pb$ ,  $As$ ,  $Hg$ , and, to a lesser extent,  $Se$ —are transformed to sulfides in anaerobic sediments. So long as conditions remain anaerobic and sulfur is available, they are relatively immobile. However, any disturbance, such as dredging, that brings the sediment into contact with oxygen will cause oxidation of the sulfides and release of the metals into solution. Cleaning up or moving contaminated sediments is a difficult problem because it may lead to oxidation and mobilization of these metals.

## SUMMARY

1. To understand the behavior of any trace element in natural waters, it is essential to know the chemical form of the element in the water of interest. Anomalously high concentrations are often related to the presence of stable complexes in solution.
2. The solubility of phases containing the element as a major constituent (commonly an oxide/hydroxide, carbonate, or sulfide) provides a general upper limit to the concentration of a specific element.

3. Adsorption, by iron and manganese oxyhydroxides in particular, is probably the most important process in maintaining the concentrations of trace elements at levels far below those predicted by equilibrium solubility calculations. In general, elements present in solution as cationic species are more likely to be adsorbed than those present as anionic species, although, depending on the pH, anionic species that form inner-sphere complexes may also be strongly adsorbed.

### REVIEW QUESTIONS

1. Figures 8-4 and 8-5 show the behavior of several solutes in the interstitial water of marine sediments. Predict qualitatively how the concentrations of Cu, Zn, As, and Hg would vary with depth in the same sediments.
2. A reservoir is accumulating fine-grained sediment being transported downstream from a mining area. The sediment contains abundant heavy metals (in the form of sulfides and adsorbed on iron oxyhydroxides) and abundant organic carbon. Water is infiltrating through the sediments and recharging an underlying oxygenated alluvial aquifer. Predict qualitatively or semiquantitatively how the concentrations of Cu, Zn, Pb, Cd, As, Se, Cr, and Hg would vary with depth in the porewaters of the reservoir sediment. Which of the elements are likely to pose a contamination problem in the underlying aquifer? (There is not one unique answer; several scenarios might be considered.)

### SUGGESTED READING

- ALPERS, C. N., and D. W. BLOWES, (Eds.). (1994). *Environmental Geochemistry of Sulfide Oxidation*. American Chemical Society Symposium Series 550. Washington, DC: American Chemical Society. Collection of papers covering various aspects of heavy-metal behavior in acidic systems.
- BROOKINS, D. G. (1988). *Eh-pH Diagrams for Geochemistry*. New York: Springer-Verlag.
- HEM, J. D. (1985). Study and interpretation of the chemical characteristics of natural water (3rd ed.). *U.S. Geological Survey Water-Supply Pap.* 2254.
- JENNE, E. A. (1977). Trace element sorption by sediments and soils—sites and processes. In W. Chappel and K. Peterson, (Eds.), *Symposium on Molybdenum in the Environment* (Vol. 2). (p. 425–553). New York: Marcel Dekker.
- LECKIE, J. O., and R. O. JAMES. (1974). Control mechanisms for trace metals in natural waters. In A. J. Rubin, (Ed.), *Aqueous-Environmental Chemistry of Metals*, (p. 1–76) Ann Arbor, MI: Ann Arbor Science Publishers.
- STUMM, W., and J. J. MORGAN. (1996). *Aquatic Chemistry* (3rd ed.). New York: Wiley-Interscience.



# 10

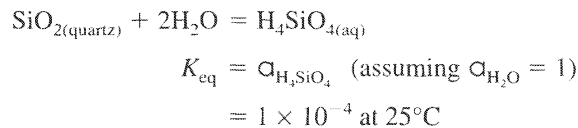
## Stability Relationships and Silicate Equilibria

Stability relationships among minerals can be thought of in several different ways; the most convenient approaches for understanding natural water systems are summarized by the following questions:

1. Is solution A supersaturated, undersaturated, or in equilibrium with mineral B?
2. Which is more stable, mineral B or mineral C, in contact with solution A?
3. Is solution A in equilibrium with mineral B if certain assumptions are made concerning a component that has not been measured?

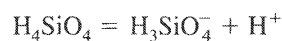
### SOLUBILITY EQUILIBRIA (CONGRUENT SOLUTION)

The simplest example of mineral-solution equilibrium would be dissolution of a mineral such as quartz. At pH values below about 9, this can be represented by the equation:



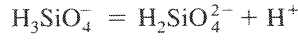
Any solution (at 25°C) in which  $\alpha_{\text{H}_4\text{SiO}_4} = 1 \times 10^{-4}$  would be in equilibrium with quartz. Solutions with higher  $\alpha_{\text{H}_4\text{SiO}_4}$  values would be supersaturated, and those with lower values would be undersaturated. Similar relationships hold for amorphous silica, which has a solubility constant of  $2 \times 10^{-3}$  at 25°C.

At high pH values, the solubility equilibrium is slightly more complicated.  $\text{H}_4\text{SiO}_4$  is an acid just as  $\text{H}_2\text{CO}_3$  is (Chapter 3), and at high pH values it dissociates into  $\text{H}_3\text{SiO}_4^-$  and  $\text{H}_2\text{SiO}_4^{2-}$ . The equilibrium constants are



$$K_1 = \frac{\alpha_{\text{H}_3\text{SiO}_4^-} \alpha_{\text{H}^+}}{\alpha_{\text{H}_4\text{SiO}_4}} \quad (10-1)$$

$$= 10^{-9.9} \text{ at } 25^\circ\text{C}$$



$$K_2 = \frac{\alpha_{\text{H}_2\text{SiO}_4^{2-}} \alpha_{\text{H}^+}}{\alpha_{\text{H}_3\text{SiO}_4^-}} \quad (10-2)$$

$$= 10^{-11.7} \text{ at } 25^\circ\text{C}$$

The total dissolved silica concentration,  $m_{(\text{SiO}_2)_T}$ , will be the sum of the ionized and un-ionized species:

$$(m_{\text{SiO}_2})_T = m_{\text{H}_4\text{SiO}_4} + m_{\text{H}_3\text{SiO}_4^-} + m_{\text{H}_2\text{SiO}_4^{2-}} \quad (10-3)$$

From Eqs. (10-1) and (10-2):

$$\alpha_{\text{H}_3\text{SiO}_4^-} = K_1 \frac{\alpha_{\text{H}_4\text{SiO}_4}}{\alpha_{\text{H}^+}} \text{ and } \alpha_{\text{H}_2\text{SiO}_4^{2-}} = K_1 K_2 \frac{\alpha_{\text{H}_4\text{SiO}_4}}{\alpha_{\text{H}^+}^2}$$

If activity coefficients are neglected, substitution of these in Eq. (10-3) gives

$$(m_{\text{SiO}_2})_T = m_{\text{H}_4\text{SiO}_4} \left( 1 + \frac{K_1}{\alpha_{\text{H}^+}} + \frac{K_1 K_2}{\alpha_{\text{H}^+}^2} \right) \quad (10-4)$$

The total dissolved silica concentration in equilibrium with quartz or amorphous silica will thus increase dramatically at high pH values (Fig. 10-1). Note the similarity between Eq. (10-4) and the corresponding equation for the carbonate system (Chapter 3):

$$\Sigma \text{CO}_2 = m_{\text{H}_2\text{CO}_3} \left( 1 + \frac{K_1}{\alpha_{\text{H}^+}} + \frac{K_1 K_2}{\alpha_{\text{H}^+}^2} \right)$$

where the  $K$  values refer to the carbonate system.

It must be emphasized that although total dissolved silica concentrations may be high in alkaline waters, this does not imply that the activity of  $\text{H}_4\text{SiO}_4$  is high in those waters, just as a high bicarbonate or carbonate concentration in a water does not imply a high  $P_{\text{CO}_2}$ . At high pH values, polymeric silicate ions (ions containing more than one silicon atom) may also be present in solution, but the presence of these species does not change significantly the solubility relationships.

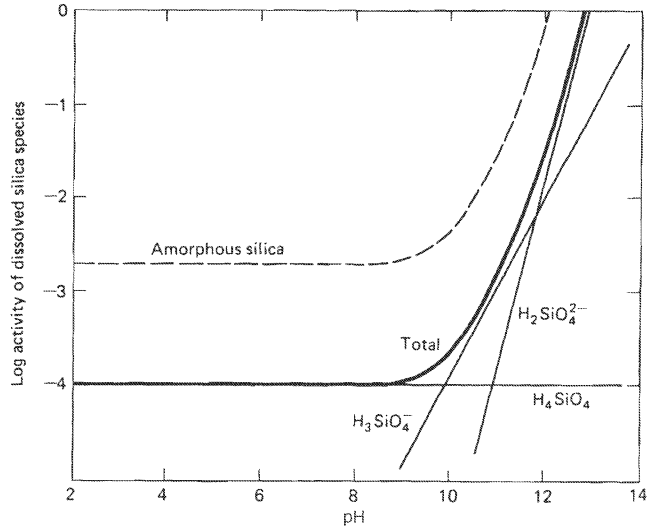
The next type of solubility equilibrium occurs when the solid contains more than one ion, such as brucite [ $\text{Mg}(\text{OH})_2$ ]. Equilibrium between brucite and solution can be represented by a solubility product,  $K_{\text{sp}}$ :



Since pH is a more convenient variable than  $\alpha_{\text{OH}^-}$ , we can write Eq. (10-5) in terms of  $\alpha_{\text{H}^+}$ :

$$\alpha_{\text{OH}^-} = \frac{K_w}{\alpha_{\text{H}^+}}$$

**FIGURE 10-1** Activities of dissolved silica species in equilibrium with quartz at 25°C. The heavy line represents the sum of the activities of individual species. The dashed line is the corresponding sum for equilibrium with amorphous silica.



where  $K_w$  is the dissociation constant of water;  $K_w = 10^{-14.0}$  at 25°C. Substituting in Eq. (10-5) gives

$$K_{sp} = \alpha_{Mg^{2+}} \frac{K_w^2}{\alpha_{H^+}^2}$$

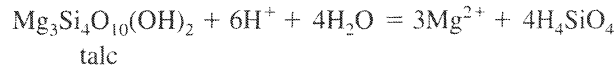
which can be rewritten as

$$K_{bru} = \frac{\alpha_{Mg^{2+}}}{\alpha_{H^+}^2} \quad (10-6)$$

where  $K_{bru} = K_{sp}/K_w^2$ . The purpose of this transformation is to allow equilibrium relationships to be written directly in terms of pH rather than  $\alpha_{OH^-}$ .

### Solubility of Magnesium Silicates

The solubilities of various magnesium silicates can be presented as more complicated solubility expressions. For talc,

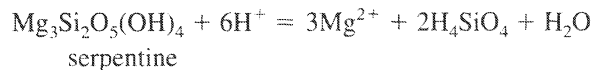


$$K_{\text{talc}} = \frac{\alpha_{Mg^{2+}}^3 \alpha_{H_4SiO_4}^4}{\alpha_{H^+}^6}$$

or

$$\log K_{\text{talc}} = 3 \log \left( \frac{\alpha_{Mg^{2+}}}{\alpha_{H^+}^2} \right) + 4 \log \alpha_{H_4SiO_4} \quad (10-7)$$

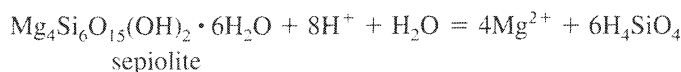
Similarly, for serpentine,



$$K_{\text{serp}} = \frac{\alpha_{\text{Mg}^{2+}}^3 \alpha_{\text{H}_4\text{SiO}_4}^2}{\alpha_{\text{H}^+}^6}$$

$$\log K_{\text{serp}} = 3 \log \left( \frac{\alpha_{\text{Mg}^{2+}}}{\alpha_{\text{H}^+}^2} \right) + 2 \log \alpha_{\text{H}_4\text{SiO}_4} \quad (10-8)$$

and for sepiolite,



$$K_{\text{sepiolite}} = \frac{\alpha_{\text{Mg}^{2+}}^4 \alpha_{\text{H}_4\text{SiO}_4}^6}{\alpha_{\text{H}^+}^8}$$

$$\log K_{\text{sepiolite}} = 4 \log \left( \frac{\alpha_{\text{Mg}^{2+}}}{\alpha_{\text{H}^+}^2} \right) + 6 \log \alpha_{\text{H}_4\text{SiO}_4} \quad (10-9)$$

We can generalize Eqs. (10-6) to (10-9) into the form

$$\text{Mg}_a\text{Si}_b\text{O}_{(a+2b)} \cdot n\text{H}_2\text{O} + 2a\text{H}^+ = a\text{Mg}^{2+} + b\text{H}_4\text{SiO}_4 + (n + a - 2b)\text{H}_2\text{O}$$

$$\log K = a \log \left( \frac{\alpha_{\text{Mg}^{2+}}}{\alpha_{\text{H}^+}^2} \right) + b \log \alpha_{\text{H}_4\text{SiO}_4}$$

which means the equations plot as straight lines on a graph with  $\log (\alpha_{\text{Mg}^{2+}}/\alpha_{\text{H}^+}^2)$  and  $\log \alpha_{\text{H}_4\text{SiO}_4}$  as axes (Fig. 10-2). The slopes of the lines,  $-b/a$ , are determined by the Si/Mg ratios in the magnesium silicates, and the intercepts by the specific values of the  $\log K$ 's, which are determined from the free energies of formation of the minerals (Chapter 2).

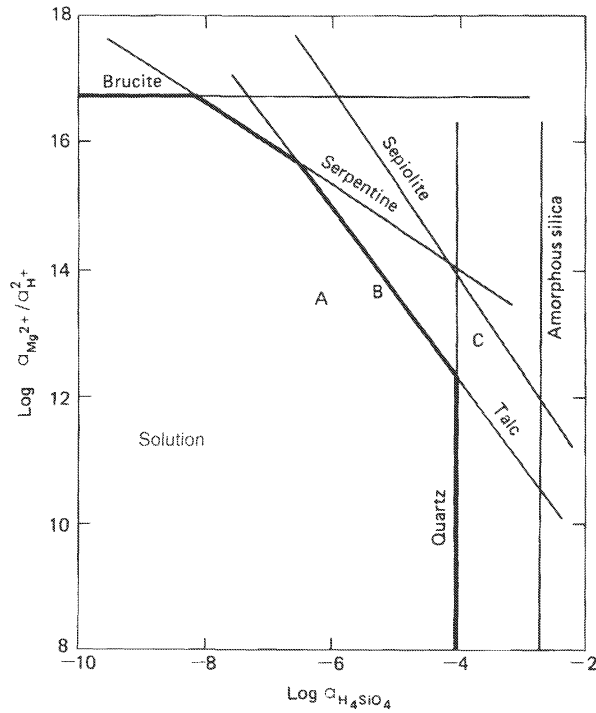
Only water compositions that plot on a specific line are in equilibrium with a particular phase. Thus a water whose composition plots at point A (Fig. 10-2) is undersaturated with respect to all the minerals under consideration. At point B, the water is in equilibrium with talc, but undersaturated with respect to serpentine, sepiolite, quartz, and amorphous silica. At point C, the water is supersaturated with respect to talc and quartz, but undersaturated with respect to sepiolite, amorphous silica, and serpentine. Note that any water composition plotting above or to the right of the heavy line surrounding the solution field cannot represent chemical equilibrium, since the water is supersaturated with respect to one or more solid phases. Note also that sepiolite must always be metastable in contact with water at 25°C, because solutions in equilibrium with sepiolite are always supersaturated with respect to one or more of the other solid phases.

### Solubility of Gibbsite

The solubility of gibbsite  $[\text{Al}(\text{OH})_3]$  is complicated by the fact that dissolved aluminum can exist in several forms in solution. In the absence of other ligands, the most important are  $\text{Al}^{3+}$  and its hydrolyzed forms  $\text{Al}(\text{OH})^{2+}$ ,  $\text{Al}(\text{OH})_2^+$ ,  $\text{Al}(\text{OH})_3^0$ , and  $\text{Al}(\text{OH})_4^-$ . The activity of  $\text{Al}^{3+}$  in equilibrium with gibbsite is given by

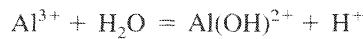


**FIGURE 10-2** Solubility relationships in the system MgO–SiO<sub>2</sub>–H<sub>2</sub>O at 25°C. Free energies of talc and serpentine from Bricker et al. (1973); free energy of sepiolite from Christ et al. (1973). For explanation of A, B, and C, see text.

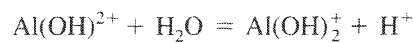


$$K_{\text{gib}} = \frac{a_{\text{Al}^{3+}}}{a_{\text{H}^+}^3} \quad (10-10)$$

At low pH,  $\text{Al}^{3+}$  is the dominant species in solution, and the solubility of gibbsite decreases rapidly as pH increases. As pH increases, however, the relative importance of the hydroxy complexes (or hydrolysis products) increases, and their behavior controls the solubility of gibbsite. Formation of the complexes can be described by the equations:

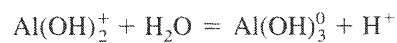


$$K_1 = \frac{a_{\text{Al}(\text{OH})^{2+}} a_{\text{H}^+}}{a_{\text{Al}^{3+}}} = \beta_1 \quad (10-11)$$



$$K_2 = \frac{a_{\text{Al}(\text{OH})_2^+} a_{\text{H}^+}}{a_{\text{Al}(\text{OH})^{2+}}}$$

$$\beta_2 = \frac{a_{\text{Al}(\text{OH})_2^+} a_{\text{H}^+}^2}{a_{\text{Al}^{3+}}} \quad (10-12)$$



$$K_3 = \frac{a_{\text{Al}(\text{OH})_3^0} a_{\text{H}^+}}{a_{\text{Al}(\text{OH})_2^+}}$$

$$\beta_3 = \frac{\alpha_{\text{Al(OH)}_3^0} \alpha_{\text{H}^+}^3}{\alpha_{\text{Al}^{3+}}} \quad (10-13)$$



$$K_4 = \frac{\alpha_{\text{Al(OH)}_4^-} \alpha_{\text{H}^+}}{\alpha_{\text{Al(OH)}_3^0}}$$

$$\beta_4 = \frac{\alpha_{\text{Al(OH)}_4^-} \alpha_{\text{H}^+}^4}{\alpha_{\text{Al}^{3+}}} \quad (10-14)$$

The convention is to use the symbol  $K_n$  for formation of a complex from the species with one fewer ligand, whereas the symbol  $\beta_n$  is used for formation of the complex from the free ions.

The total dissolved aluminum concentration is the sum of the concentrations of the individual species:

$$m_{\text{Al(total)}} = m_{\text{Al}^{3+}} + m_{\text{Al(OH)}_2^{2+}} + m_{\text{Al(OH)}_3^0} + m_{\text{Al(OH)}_4^-}$$

Substituting Eqs. (10-11) through (10-14) and neglecting activity coefficients gives

$$m_{\text{Al(total)}} = m_{\text{Al}^{3+}} \left[ 1 + \frac{K_1}{\alpha_{\text{H}^+}} + \frac{\beta_2}{\alpha_{\text{H}^+}^2} + \frac{\beta_3}{\alpha_{\text{H}^+}^3} + \frac{\beta_4}{\alpha_{\text{H}^+}^4} \right] \quad (10-15)$$

Combining Eqs. (10-15) and (10-10) gives the total concentration of dissolved aluminum in equilibrium with gibbsite:

$$m_{\text{Al(total)}} = K_{\text{gib}} \left[ \alpha_{\text{H}^+}^3 + K_1 \alpha_{\text{H}^+}^2 + \beta_2 \alpha_{\text{H}^+} + \beta_3 + \frac{\beta_4}{\alpha_{\text{H}^+}} \right] \quad (10-16)$$

Numerical values for the constants are shown in Table 10-1 and the activities of each of the species for a solution in equilibrium with gibbsite are shown in Fig. 10-3. Note the following:

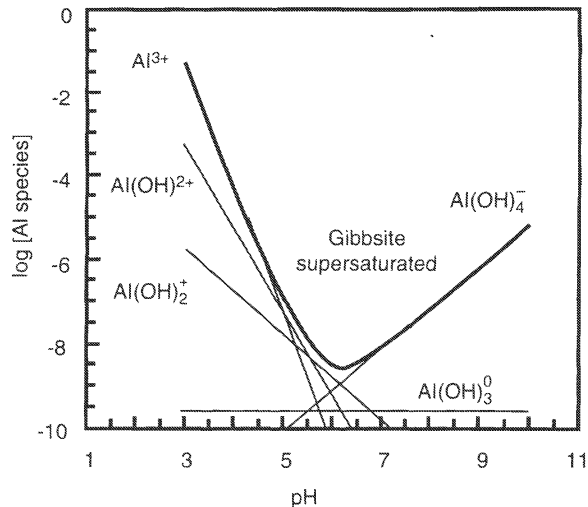
1. The solubility of gibbsite is very low except at either very low or very high pH.
2. As the pH increases, the complexes containing progressively more hydroxide groups become progressively more important.
3. When cationic species dominate, the solubility of gibbsite decreases with increasing pH.

**TABLE 10-1** Stability Constants<sup>a</sup> for the Formation of Aluminum-Hydroxy Species at 25°C (after Wesolowski and Palmer, 1994)

Species	log $K_n$	Log $\beta_n$
$\text{Al(OH)}_2^{2+}$	-4.95	-4.95
$\text{Al(OH)}_3^0$	-5.6	-10.6
$\text{Al(OH)}_4^-$	-6.7	-17.2
$\text{Al(OH)}_4^-$	-5.6	-22.8
Gibbsite solubility $\text{Al(OH)}_3 + 3\text{H}^+ = \text{Al}^{3+} + 3\text{H}_2\text{O}$	7.74	

<sup>a</sup>For explanation of  $K_n$  and  $\beta_n$ , see text.

**FIGURE 10-3** Activities of dissolved aluminum species in equilibrium with gibbsite  $[\text{Al}(\text{OH})_3]$  at 25°C. Heavy line is sum of individual activities. Data from Wesolowski and Palmer (1994).



When anionic species dominate, the solubility increases with increasing pH. This observation can be generalized to the solubilities of all oxides and hydroxides and of many other solids.

### Solubility of Aluminosilicates

The behavior of aluminum makes it impossible to present the solubility of aluminum silicates in as simple a way as was done for magnesium silicates. In principle, a three-dimensional diagram is needed with aluminum concentration, silica activity, and pH as axes. Three-dimensional diagrams can be represented by contours on a two-dimensional diagram. The solubilities of gibbsite, kaolinite  $[\text{Al}_2\text{Si}_2\text{O}_5(\text{OH})_4]$ , and pyrophyllite  $[\text{Al}_2\text{Si}_4\text{O}_{10}(\text{OH})_2]$  at four different silica activities are shown in Fig. 10-4. The aluminum concentration in equilibrium with gibbsite is independent of silica activity, as would be expected since gibbsite contains no silicon, but the aluminum activity in equilibrium with kaolinite and pyrophyllite decreases as silica activity increases. This can also be shown by plotting the aluminum concentration at the solubility minimum (pH 6.2) for each mineral (Fig. 10-5). There is some controversy over exact free-energy values and solubilities of these phases (see discussion on uncertainty below). The topology of Figs. 10-4 and 10-5 is not sensitive to the values chosen, but the numerical values of solubilities and “crossover points” do depend on the particular data set used.

An additional problem for most aluminosilicates is that the total dissolved aluminum concentrations at equilibrium are often extremely low. For typical fresh waters in equilibrium with kaolinite, the dissolved aluminum concentrations are 0.1 to 1  $\mu\text{g}/\text{L}$ . It is difficult to measure aluminum concentrations reliably at this level and almost impossible to determine accurately the aluminum species present (organic or fluoride complexes are often important). Uncertainties in the aluminum analyses commonly introduce large uncertainties into the solubility calculation.

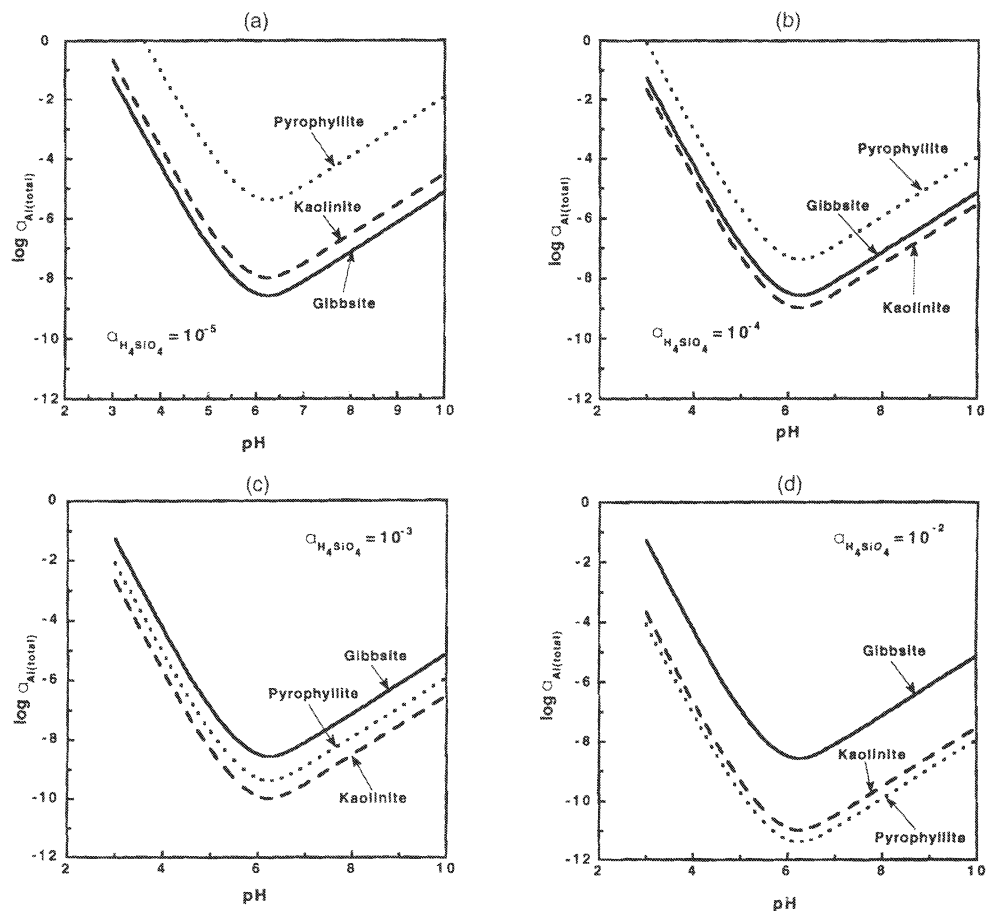
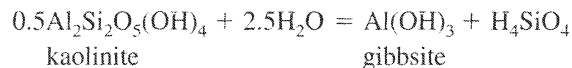


FIGURE 10-4 Sum of activities of dissolved aluminum species in equilibrium with gibbsite, kaolinite, and pyrophyllite at different activities of  $H_4SiO_4$ .

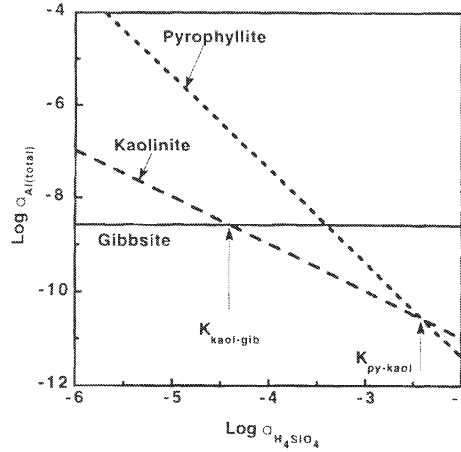
## INCONGRUENT SOLUTION AND STABILITY DIAGRAMS

Because the concentration of dissolved aluminum is usually very small, an alternative approach is to assume that aluminum is retained entirely in solid phases and to write reactions between minerals on this basis. This is equivalent to treating  $Al_2O_3$  as an inert component in the sense of Thompson (1955) or to saying that the chemical potential of  $Al_2O_3$  is controlled by reactions in the mineral-water system. An advantage of this approach is that it reduces the number of variables and allows stability relationships in some four-component systems to be displayed on two-dimensional diagrams. When this approach is used, we can no longer consider the precipitation-dissolution of a single mineral, but must consider reactions between two minerals. For example,





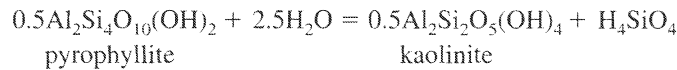
**FIGURE 10-5** Sum of activities of dissolved aluminum species in equilibrium with gibbsite, kaolinite, and pyrophyllite at pH 6.2 as a function of activity of  $H_4SiO_4$  in solution.



$$K_{kaol-gib} = a_{H_4SiO_4}$$

At  $H_4SiO_4$  activities above a particular value (about  $10^{-4.4}$  at  $25^\circ C$ ), kaolinite is more stable than gibbsite, and at  $H_4SiO_4$  activities below that value, gibbsite is more stable than kaolinite. It is impossible to say whether or not a particular solution is in equilibrium with kaolinite or gibbsite without knowing the dissolved aluminum concentration.

A similar equation can be written for the kaolinite–pyrophyllite reaction:



$$K_{py-kaol} = a_{H_4SiO_4} = 10^{-2.4} \text{ at } 25^\circ C$$

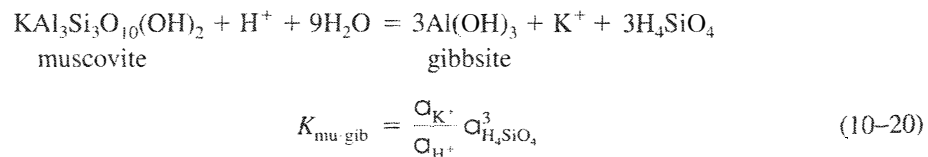
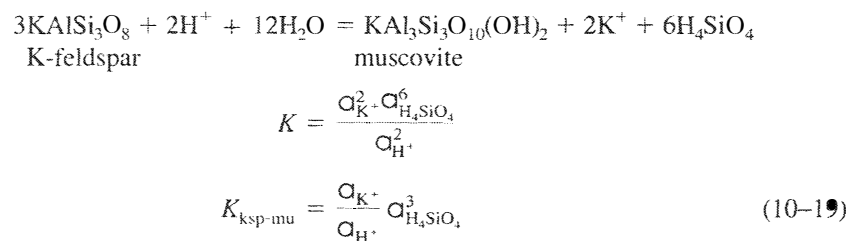
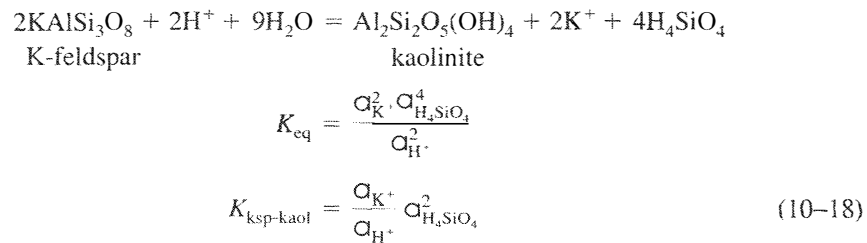
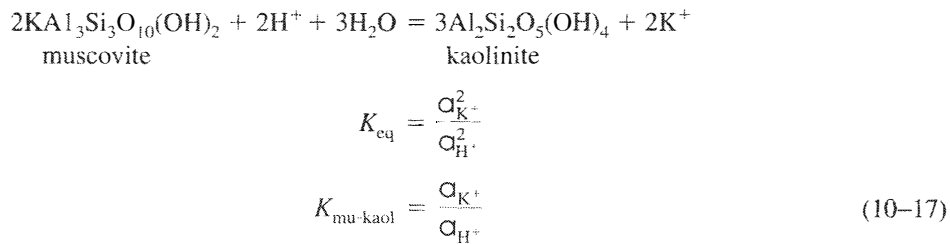
In this case the equilibrium silica activity ( $10^{-2.4}$ ) is greater than the solubility of amorphous silica ( $10^{-2.7}$ ), which implies that pyrophyllite is unstable in contact with water at  $25^\circ C$  and 1 atm.

It is instructive to compare the results of this approach with Figs. 10-4 and 10-5. Below the silica activity corresponding to  $K_{kaol-gib}$ , the concentration of Al in equilibrium with gibbsite is less than that in equilibrium with kaolinite. At silica activities above  $K_{kaol-gib}$ , the reverse is true. When the silica activity equals  $K_{kaol-gib}$ , the concentration of aluminum in equilibrium with both phases is identical. A similar set of relationships holds for the pair pyrophyllite-kaolinite at the silica activity corresponding to  $K_{py-kaol}$ .

In general, at any particular silica activity, the most stable aluminum hydroxide or silicate will be the one with the lowest equilibrium dissolved aluminum concentration. This can be seen by considering the kaolinite–gibbsite pair in Fig. 10-4(a). Any solution in equilibrium with kaolinite will contain aluminum species at a higher activity than corresponds to equilibrium with gibbsite. That is equivalent to saying that the solution is supersaturated with respect to gibbsite, and there will be a release of free energy if gibbsite precipitates. Conversely, any solution in equilibrium with gibbsite at the  $H_4SiO_4$  activity of Fig. 10-4(a) will be undersaturated with respect to kaolinite, and kaolinite cannot precipitate spontaneously. The same logic

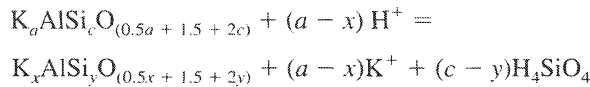
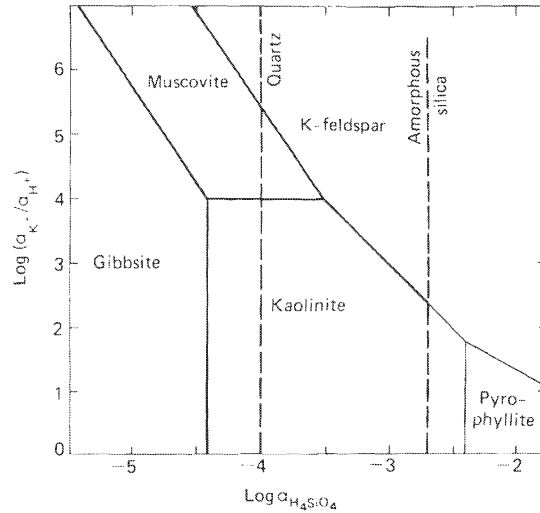
applies to all the curves in Fig. 10-4: whenever a solid phase that is more soluble (meaning here has a higher equilibrium dissolved Al activity) converts at constant  $H_4SiO_4$  to one that is less soluble, there is a net release of free energy. Equilibrium is the state of minimum free energy, and hence the least soluble phase is the most stable. Another conclusion from Figs. 10-4 and 10-5 is that a solution with any particular silica activity can be in equilibrium with any of the aluminum hydroxides or silicates, provided that the dissolved aluminum activity is appropriate. The equilibrium will be metastable if the solid phase is not the most stable one at that silica activity.

A similar approach can be used for minerals containing cations in addition to aluminum and silicon. Consider, for example, reactions between pairs of minerals in the system  $K_2O-Al_2O_3-SiO_2-H_2O$ :



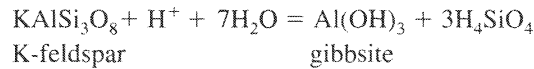
As with the solubility lines for Mg-silicates discussed earlier in this chapter, all these equilibrium constant expressions [Eqs. (10-17) through (10-20)] can be displayed as straight lines on a graph with  $\log(\alpha_{K^+}/\alpha_{H^+})$  and  $\log \alpha_{H_4SiO_4}$  as axes (Fig. 10-6). The slopes of the lines are determined by the stoichiometry of the reactions. Ignoring water and normalizing to 1 Al in both reactant and product, we can write the general reaction ( $a$ ,  $b$ ,  $c$ ,  $x$ , and  $y$  need not be integers):

**FIGURE 10-6** Stability relationships among some minerals in the system  $K_2O-Al_2O_3-SiO_2-H_2O$  at  $25^\circ C$ .



The slope will be given by  $-(c - y)/(a - x)$ , and the positions of the lines by the numerical values of the equilibrium constants, which are determined from the free energies of formation of the various species. (The free energies used to construct the diagrams in this chapter are shown in Table 10-2. Uncertainties associated with these numbers are discussed at the end of the chapter.)

The equations listed above and the lines of Fig. 10-6 are only a few of the possible reactions that could have been written among the same set of minerals. For example, we did not include the reaction:



$$K_{ksp-gib} = \frac{a_{K^+}}{a_{H^+}} a_{H_4SiO_4}^3$$

This boundary is shown as a dashed line in Fig. 10-7. It can be seen by inspection that it must be a metastable boundary; immediately to the right of the dashed line, K-feldspar is unstable with respect to muscovite or kaolinite. If K-feldspar is unstable in that region, any boundary involving K-feldspar cannot be a stable boundary. Similarly, gibbsite is not stable immediately to the left of the dashed line, so any boundary involving gibbsite must be metastable. The same logic can be applied to other possible boundaries in the system and to the various possible extensions of the boundaries shown in Fig. 10-7.

The significance of the lines and areas in Fig. 10-6 is different from those on Fig. 10-2. In Fig. 10-6 the area "kaolinite" represents solution compositions in which kaolinite is the most stable of the minerals considered in constructing the diagram. It is conceivable that a mineral exists (perhaps a K-beidellite) that would be more stable than kaolinite over part of the kaolinite field. It is also quite possible that gibbsite is not the most stable aluminum oxyhydroxide in contact with water at  $25^\circ C$ : diaspore  $[AlO(OH)]$  may in fact be more stable (Anovitz et al., 1991).

**TABLE 10-2** Free-Energy Values (kJ/mole) Used in Constructing Stability Diagrams

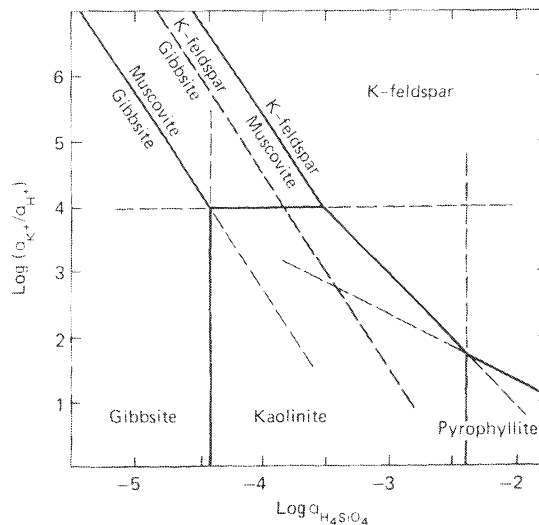
Gibbsite	$\text{Al}(\text{OH})_3$	-1151
Kaolinite	$\text{Al}_2\text{Si}_2\text{O}_5(\text{OH})_4$	-3800
Pyrophyllite	$\text{Al}_2\text{Si}_4\text{O}_{10}(\text{OH})_2$	-5275
Muscovite	$\text{KAl}_3\text{Si}_3\text{O}_{10}(\text{OH})_2$	-5606
K-feldspar	$\text{KAlSi}_3\text{O}_8$	-3767
Albite	$\text{NaAlSi}_3\text{O}_8$	-3715
Analcite	$\text{NaAlSi}_2\text{O}_6 \cdot \text{H}_2\text{O}$	-3090
Na-beidellite <sup>a</sup>	$\text{Na}_{0.33}\text{Al}_{2.33}\text{Si}_{3.67}\text{O}_{10}(\text{OH})_2$	-5382
Ca-beidellite <sup>a</sup>	$\text{Ca}_{0.16}\text{Al}_{2.33}\text{Si}_{3.67}\text{O}_{10}(\text{OH})_2$	-5388
Laumontite (zeolite)	$\text{CaAl}_2\text{Si}_4\text{O}_{12} \cdot 4\text{H}_2\text{O}$	-6711
$\text{K}^+$		-283.27
$\text{Na}^+$		-261.91
$\text{Ca}^{2+}$		-553.58
$\text{H}_4\text{SiO}_4$		-1316.6
$\text{H}_2\text{O}$		-237.13

<sup>a</sup>Formulas represent multiples of one-third rather than of 0.330.

Gibbsite is used here because it is the most common form in natural environments. Also, Fig. 10-6 shows only minerals in the system  $\text{K}_2\text{O}-\text{Al}_2\text{O}_3-\text{SiO}_2-\text{H}_2\text{O}$ . If a solution that plots in the kaolinite field on Fig. 10-6 contains sodium, for example, kaolinite might be unstable with respect to some sodium-containing mineral. It is possible to add another component to the system ( $\text{Na}_2\text{O}$ , for example) and plot a three-dimensional diagram or two-dimensional sections corresponding to a particular activity of one of the components. With this many components, however, the graphical approach tends to become unworkable.

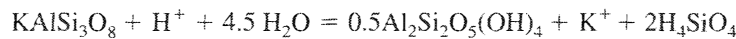
The lines labeled quartz and amorphous silica in Fig. 10-6 do not have the same significance as the other lines on the diagram. They are solubility lines similar to those on Fig. 10-2.

**FIGURE 10-7** Stability relationships among some minerals in the system  $\text{K}_2\text{O}-\text{Al}_2\text{O}_3-\text{SiO}_2-\text{H}_2\text{O}$  at 25°C, showing the metastable K-feldspar-gibbsite boundary and the metastable extensions of the stable boundaries.



Only solutions whose compositions plot on the quartz line are in equilibrium with quartz. Solutions that plot to the right of the quartz line are supersaturated with respect to quartz, and compositions that plot to the left are undersaturated. In theory, all solution compositions that plot to the right of the quartz line are metastable, but in practice, quartz is kinetically unreactive at low temperatures and rarely precipitates or dissolves at a significant rate. Amorphous silica, on the other hand, precipitates and dissolves relatively rapidly, so the solubility of amorphous silica is generally the upper limit for  $H_4SiO_4$  activities in natural waters.

As an alternative to the graphical approach, one can construct *disequilibrium indices* based on Eqs. (10–16) through (10–19) (Pačes, 1972; see also Chapter 12). Consider, for example, the reaction between K-feldspar and kaolinite:



The activity product  $Q$  for the reaction is (Chapter 2)

$$Q = \frac{a_{K^+}}{a_{H^+}} a_{H_4SiO_4}^2$$

and the disequilibrium index is defined as  $\log(Q/K)$ , where  $K$  is the equilibrium constant for the reaction. If kaolinite and K-feldspar are equally stable in the solution (i.e., the solution composition would plot on the K-feldspar-kaolinite boundary or its metastable extension in Fig. 10-6), the disequilibrium index will be zero. If the solution would plot to the left of that boundary in Fig. 10-6, the index would be negative (kaolinite more stable than K-feldspar), and if it would plot to the right of the K-feldspar-kaolinite boundary, the disequilibrium index would be positive (K-feldspar more stable than kaolinite). The disequilibrium index approach has two advantages: it gives a quantitative measure of how far a given solution composition is from the equilibrium boundary, and it can be used in a system of any number of components, since the result does not have to be displayed graphically.

Analogous stability diagrams can be constructed for the systems  $Na_2O-Al_2O_3-SiO_2-H_2O$  (Fig. 10-8) and  $CaO-Al_2O_3-SiO_2-H_2O$  (Fig. 10-9). These diagrams are less well established than those for the potassium system. Smectite (montmorillonite) is an important phase in nature, but natural smectites generally contain Mg and Fe, and the free energies of the pure Ca and Na-beidellite end members are somewhat conjectural. Also, a variety of sodium and calcium zeolites appear to be stable at 25°C. The compositions of the zeolites are variable, and their free energies are not well known, so it is difficult to plot their stability fields quantitatively. Qualitatively, the stability fields of zeolites would replace those of albite and laumontite in the upper part of the diagrams.

The solubility of calcite is an upper limit to the permitted  $a_{Ca^{2+}}/a_{H^+}^2$  ratio in natural waters. From Chapter 3,

$$a_{Ca^{2+}} a_{CO_3^{2-}} = K_{cal}$$

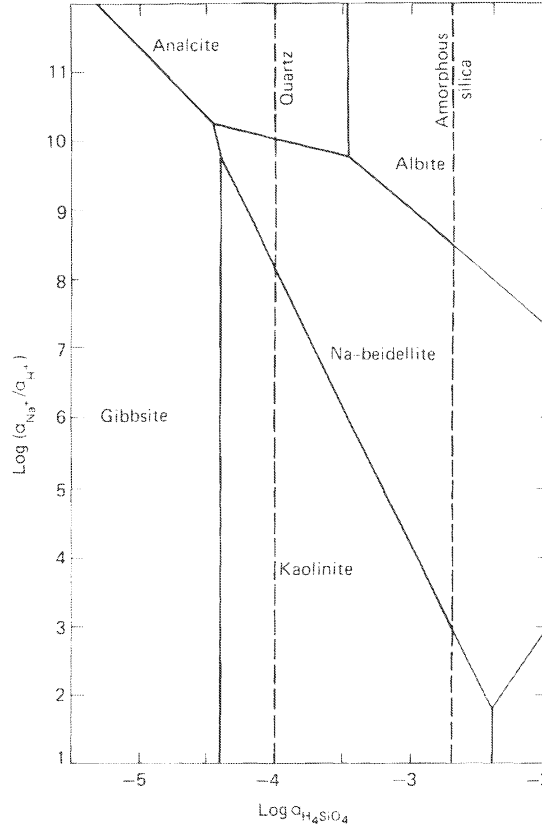
Substituting for  $a_{CO_3^{2-}}$  using Eqs. (3–2), (3–3), and (3–4) (Chapter 3) gives

$$a_{CO_3^{2-}} = \frac{K_{CO_2} K_1 K_2 P_{CO_2}}{a_{H^+}^2}$$

Combining these gives

$$a_{CO_3^{2-}} = \frac{K_{CO_2} K_1 K_2 P_{CO_2}}{a_{H^+}^2} = K_{cal}/a_{Ca^{2+}}$$

**FIGURE 10-8** Stability relationships among some minerals in the system  $\text{Na}_2\text{O}-\text{Al}_2\text{O}_3-\text{SiO}_2-\text{H}_2\text{O}$  at  $25^\circ\text{C}$ . The positions of boundaries involving Na-beidellite are uncertain; zeolites are probably more stable than albite in the upper part of the diagram, but free-energy data are not available.



which rearranges to

$$\frac{a_{\text{Ca}^{2+}}}{a_{\text{H}^+}^2} = \frac{K_{\text{cal}}}{K_{\text{CO}_2} K_1 K_2 P_{\text{CO}_2}}$$

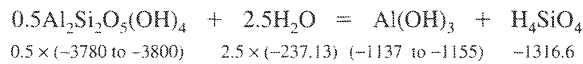
Values of  $a_{\text{Ca}^{2+}}/a_{\text{H}^+}^2$  for some particular values of  $P_{\text{CO}_2}$  are shown in Fig. 10-9.

**UNCERTAINTY IN MINERAL STABILITY DIAGRAMS**

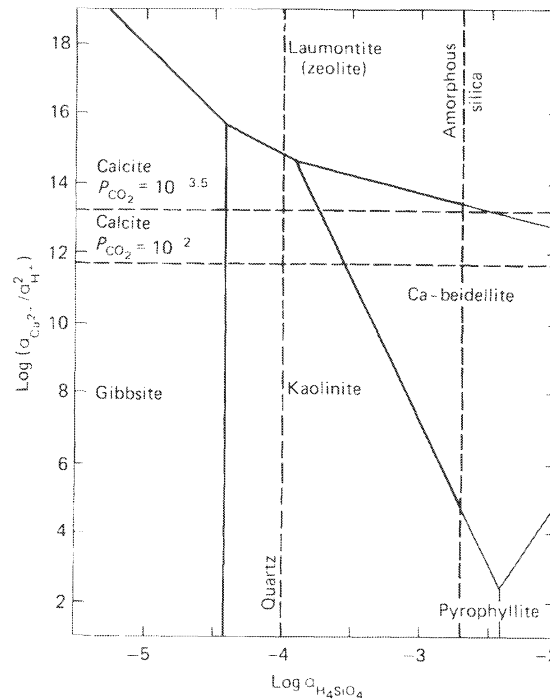
The positions of boundaries on stability diagrams are extremely sensitive to the exact values of the standard free energies of formation used in the calculations, and hence they are also sensitive to any errors or uncertainties in these values.

**Example 1**

Reported free-energy values in the literature range from about  $-1137$  to  $-1155$  kJ/mol ( $-272$  to  $-276$  kcal/mol) for gibbsite and from about  $-3780$  to  $-3800$  kJ/mol ( $-903$  to  $-908$  kcal/mole) for kaolinite. Accepting these numbers at face value, what is the corresponding uncertainty in the position of the gibbsite-kaolinite boundary?



**FIGURE 10-9** Stability relationships among some minerals in the system  $\text{CaO}-\text{Al}_2\text{O}_3-\text{SiO}_2-\text{H}_2\text{O}$  at  $25^\circ\text{C}$ . Other zeolites are probably more stable than laumontite, but free-energy data are not available. Horizontal dashed lines are solubility of calcite at  $P_{\text{CO}_2}$  values indicated.

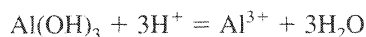


This gives a  $\Delta G_{\text{reaction}}^0$  of 11.23 to 39.23 kJ/mol, which corresponds to  $\log K_{\text{eq}}$  ( $= \log a_{\text{H}_4\text{SiO}_4}$ ) values of  $-1.97$  to  $-6.87$ . This represents an uncertainty of 4.9 orders of magnitude (a factor of almost 80,000) in the activity of silica at the equilibrium boundary. The real uncertainty is less than this because there are valid reasons for selecting among published free-energy values, but it indicates the potential magnitude of the problem.

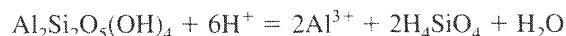
There are several sources of uncertainty in tabulated free-energy values. We shall discuss some of them here in the context of the gibbsite–kaolinite boundary.

- 1. Uncertainty in experimental measurements.** Free-energy values are derived from several types of measurement, for example, calorimetry (measurement of heats of dissolution and heat capacities), solubility measurements, and phase equilibria (measurement of conditions under which two or more phases coexist stably). Typically, the standard free energies of a few key compounds are measured by calorimetry, and those of other compounds are calculated from phase equilibria involving the key compounds or solubility studies calibrated against the solubilities of the key compounds. As a general rule, experimental uncertainties in individual measurements are not the main cause of uncertainties in tabulated standard free-energy values. The largest source of experimental uncertainty is often uncertainty as to whether a solid/solution system has reached true chemical equilibrium. A common complication is that, unless precautions are taken, the material used in solubility experiments may include fine particles and highly strained grains from crushing procedures. Such material is more soluble than bulk, unstrained material (see below). The solubility measurement may reflect this disordered material rather than the bulk solid.

2. *Inconsistencies in deriving standard free-energy values from experimental data.* The following is a simple hypothetical example of how this might arise. Suppose the standard free energy of formation of gibbsite was measured by calorimetry. The solubility of gibbsite,



could then be used to calculate a standard free energy of formation of  $\text{Al}^{3+}$  (assuming the  $\Delta G_f^0$  of water is known). If the solubility of kaolinite is then measured (and the  $\Delta G_f^0$  of  $\text{H}_4\text{SiO}_4$  is known),



then a standard free energy of formation of kaolinite can be calculated, which will be consistent with the value for gibbsite. Suppose, however, that a new and more accurate value for the  $\Delta G_f^0$  of gibbsite is measured by calorimetry and substituted for the old one in published tabulations. Although this value is intrinsically more accurate, it is no longer consistent with the calculated values for  $\text{Al}^{3+}$  and kaolinite, and a gibbsite–kaolinite stability boundary calculated using the “new” gibbsite value and the “old” kaolinite value would be in error and would be inconsistent with the solubility data. The answer is obviously to correct the  $\text{Al}^{3+}$  and kaolinite values to bring them into consistency, but this is often not done, and it is a major problem in using free-energy data from different sources. For many reactions, such as the solubility of gibbsite, equilibrium constants (or solubility products) are published as well as standard free energies of formation (Appendix III). When an equilibrium constant is available from the literature, it should generally be used in preference to an equilibrium constant calculated from tabulated standard free energies of formation because of the possibility of inconsistency (and other) errors. The equilibrium constant is usually more closely tied to experimental data than the standard free energy of formation.

In the discussion of calculating free-energy values from solubility measurements, it was assumed that the activity of  $\text{Al}^{3+}$  could be calculated from the measured concentration of aluminum in solution. The calculation depends on the solution model (Chapter 2) used to convert concentration to activity, and the stability constants of any complexes [e.g.,  $\text{Al(OH)}_n^{(3-n)}$ ] used in the calculation. Use of different solution models can also cause inconsistency among tabulated standard free energies of formation. Gibbsite in fact provides a very real example. Wesolowski (1992) pointed out that many previous measurements of gibbsite solubility had been conducted in acetate buffers without including any correction for complexation of  $\text{Al}^{3+}$  by acetate. Inclusion of this correction changed the solubility by a factor of up to 5.

3. *Real differences in the properties of individual phases.* In the discussion so far, we have assumed implicitly that “gibbsite” was a single substance that could be characterized by a unique free energy of formation. In fact, gibbsite exhibits a range of crystalline order/disorder and a range of grain sizes. Fine-grained material is less stable than coarse-grained because of the extra energy associated with surfaces, and disordered material is less stable than ordered. Thus gibbsite (and kaolinite and all other minerals) possesses a range of standard free energies of formation. Tabulations commonly give values for large, well-ordered crystals, but this may not correspond to the material of interest in nature. Thus, for example, kaolinite and gibbsite formed in soils tend to be fine grained and disordered, and the properties of well-crystallized minerals may not provide an adequate framework for understanding the behavior of the real system (e.g., Sposito, 1985). Many minerals are also variable in chemical composition, which is a further source of uncertainty.



Diagrams such as Figs. 10-6, 10-8, and 10-9 are widely used in low-temperature geochemistry, but one should be aware of their limitations. They show topological relationships among the stability fields for various minerals, but the exact positions of the lines are subject to a great deal of uncertainty. (The values in Table 10-1 reflect this author's prejudices rather than a single literature source). Boundaries involving smectites (beidellites) are particularly uncertain, as they are based (see Chapter 12) on the assumption that certain natural waters are in equilibrium with both smectite and kaolinite, and that the simple end-member compositions used in the diagrams are an adequate representation of the complex smectites occurring in nature.

### REVIEW QUESTIONS

Assume 25°C, 1 atm pressure, and activity coefficients of unity. Use free-energy values from Appendix II.

1. Calculate the total concentration of dissolved silica (as ppm  $\text{SiO}_2$ ) in equilibrium with quartz at (a) pH 9.0, (b) pH 10.0, and (c) pH 11.0.
2. A solution has a measured concentration of silica of 200 ppm  $\text{SiO}_2$  at pH 10.0. Estimate the activity of  $\text{H}_4\text{SiO}_4$  in the solution. Is it supersaturated with respect to (a) quartz, or (b) amorphous silica?
3. Calculate the  $\text{H}_4\text{SiO}_4$  activity at which talc, serpentine, and an aqueous solution are all in equilibrium.
4. The activity of  $\text{Mg}^{2+}$  in seawater is  $10^{-1.87}$ . At what pH would seawater, amorphous silica, and sepiolite all be in equilibrium?
5. Seawater has an activity of  $\text{Mg}^{2+}$  of  $10^{-1.87}$  and a pH of 8.2. At what dissolved silica concentration (as ppm  $\text{SiO}_2$ ) would seawater be saturated with respect to sepiolite?
6. Estimate the total dissolved aluminum concentration in equilibrium with kaolinite in a water containing 20 ppm  $\text{SiO}_2$  at pH 7.5.
7. Estimate the total dissolved aluminum concentration in equilibrium with albite in a water at a pH of 7.5 containing 20 ppm  $\text{SiO}_2$  and 20 ppm  $\text{Na}^+$ . Which is more stable in that water, albite or kaolinite?

### SUGGESTED READING

- |  |   |
|--|---|
| BOWERS, T. S., et al. (1984). <i>Equilibrium Activity Diagrams</i> . New York: Springer Verlag.              | Discussion of sources and tabulations of thermodynamic data.  |
| GARRELS, R. M., and F. T. MACKENZIE. (1971). <i>Evolution of Sedimentary Rocks</i> . New York: W. W. Norton. | STUMM, W., and J. J. MORGAN. (1996). <i>Aquatic Chemistry</i> , (3rd ed.). New York: Wiley-Interscience. Chapter 7. |
| NORDSTROM, D. K., and J. MUNOZ. (1994). <i>Geochemical Thermodynamics</i> , (2nd ed.). Boston: Blackwell.    |   |



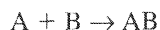
# 11

## Kinetics

In preceding chapters we have been concerned with chemical equilibrium. We have not been concerned with the path by which a system approached equilibrium, or with the rate of approach. There are two fundamental types of rate control: transport and reaction. *Transport*, which refers to the physical movement of chemical species to and from the site of reaction, will be discussed further in Chapter 16. *Reaction*—the rates of formation or destruction of chemical bonds—will be discussed here.

A *homogeneous* reaction is one in which only one phase is involved (gas, liquid, or solid); a *heterogeneous* reaction involves two or more phases, such as a solid and solution. Most reactions of geochemical interest are heterogeneous. Much more is known about the kinetics of homogeneous reactions than about those of heterogeneous reactions. The kinetics of heterogeneous reactions are extremely sensitive to the nature of the surface of the solid involved. The type and density of crystal defects and small traces of impurities can enormously increase or decrease reaction rates, which makes simple models difficult to apply. Almost all reactions, whether homogeneous or heterogeneous, consist of several steps. In the dissolution of calcite, for example, some of the steps might be detachment of  $\text{Ca}^{2+}$  and  $\text{CO}_3^{2-}$  from the crystal surface, diffusion of  $\text{Ca}^{2+}$  and  $\text{CO}_3^{2-}$  ions away from the crystal surface, conversion of  $\text{CO}_3^{2-}$  to  $\text{HCO}_3^-$  ions, conversion of  $\text{H}_2\text{CO}_3$  to  $\text{HCO}_3^-$ , conversion of  $\text{CO}_{2(\text{aq})}$  to  $\text{H}_2\text{CO}_3$ , and possibly dissolution and hydration of  $\text{CO}_2$  gas (the distinction between  $\text{H}_2\text{CO}_3$  and  $\text{CO}_{2(\text{aq})}$  is important for the kinetics of the system). Usually, one step in the reaction is much slower than all the others, and the rate of this one step, the *rate-determining* step, determines the rate of the overall reaction. Thus, when the kinetics of an overall reaction are described, what is usually being described is the kinetics of the slowest step.

The *order* of a reaction is an expression of the dependence of the reaction rate on the concentrations of the species involved. Consider, for example, the reaction



If the rate is proportional to the concentration of A, the reaction is first order with respect to A. If it is independent of the concentration of A, the reaction is zero order with respect to A. If it is proportional to  $m_A^2$ , the reaction is second order with respect to A, and so on. If the reaction rate

is proportional to the concentrations of both A and B, expressed by the product  $m_A m_B$ , the reaction is second order overall, but first order with respect to A and first order with respect to B.

Radioactive decay is an example of a first-order reaction; the amount of a radioactive element decaying in unit time is proportional to the amount present:

$$-\frac{dM}{dt} = kM \quad (11-1)$$

where  $M$  represents the amount (or concentration) of the radioactive element,  $t$  represents time, and  $k$  is a rate constant (the decay constant). Eq. (11-1) rearranges to

$$\frac{dM}{M} = -kdt$$

which integrates to

$$M = M_0 e^{-kt} \quad (11-2)$$

where  $M_0$  is the amount (concentration) present at  $t = 0$ . Eq. (11-2) represents an exponential decay, as shown in Fig. 11-1. Eq. (11-2) is also the basis of the concept of a half-life. When half of the original amount of the element has decayed,  $M = \frac{1}{2}M_0$ . Substituting this in Eq. (11-2) gives

$$\begin{aligned} \frac{1}{2} &= e^{-kt_{1/2}} \\ 2 &= e^{kt_{1/2}} \\ t_{1/2} &= \frac{\ln 2}{k} \end{aligned}$$

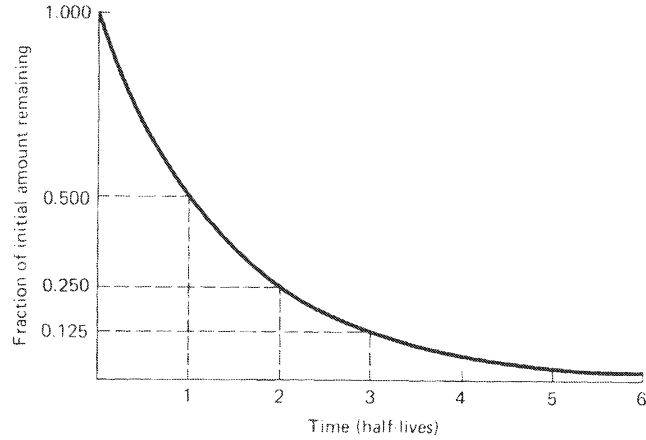
where  $t_{1/2}$  is the *half-life* of the radioactive element. The half-life is thus a constant independent of  $M_0$ . In each half-life, half of the element remaining undergoes decay. After one half-life, 1/2 of the original amount will remain; after two half-lives, 1/4 of the original amount will remain; after three half-lives, 1/8 will remain, and so on (Fig. 11-1). For any reaction whose order is not 1, the time required to remove half of the original amount will depend on the magnitude of the original amount, so the half-life is not a useful quantity.

Most rate processes conform approximately to the *Arrhenius equation*:

$$\text{Rate} = A \exp\left(\frac{-\Delta E}{RT}\right) \quad (11-3)$$

where  $R$  is the gas constant and  $T$  the absolute temperature.  $A$  (the *pre-exponential factor*) can be predicted by statistical mechanics for simple systems, but for complex systems, it is best regarded as an empirical constant.  $\Delta E$  is an activation energy. As the reactants go to products, they must usually pass through some intermediate stage of higher energy than the reactants.  $\Delta E$  can be regarded as the energy difference between the initial state and the maximum energy of the intermediate state. Consider, for example, the rearrangement of high-magnesium calcite to dolomite. To rearrange the calcium and magnesium ions into the dolomite configuration, the ions must be moved out of their crystallographic sites and through the crystal structure. This process will have a high energy of activation, and hence will be slow at low temperatures. The magnitude of  $\Delta E$  can sometimes be used to infer the nature of the rate-controlling process. For fixed  $\Delta E$  and  $A$ , Eq. (11-3) expresses the effect of temperature on reaction rate: reaction rates increase exponentially with increasing temperature.

**FIGURE 11-1** The exponential decay curve representing first-order kinetics.



## NUCLEATION

Nucleation is the formation of a new phase; the type of nucleation we consider here is formation of a solid phase from solution. If the nucleus forms in the bulk of the solution, nucleation is homogeneous; if it forms in contact with some surface (commonly another solid), nucleation is heterogeneous.

Nuclei must start out as small particles. Small particles have a very large surface area in comparison to their volume, and the free energy of the surface makes a significant contribution to the free energy of the particle as a whole. Since surface free energy is always positive in aqueous systems, small particles are always less stable and hence more soluble than large particles. The effect of surface energy on nucleation rate can be visualized in a simple way: Consider a spherical nucleus of radius  $r$ . If the solution is supersaturated with respect to the nucleating phase by  $\Delta G$  per cubic centimeter of the solid phase (Chapter 2), and the interfacial energy between the phase and solution is  $\gamma$  per square centimeter, then the energy  $W$  associated with the nucleus is

$$W = 4\pi r^2\gamma - \frac{4}{3}\pi r^3\Delta G \quad (11-4)$$

The first term represents the interfacial free energy (positive) and the second the free energy liberated by formation of the bulk solid. A schematic plot of  $W$  against  $r$  is shown in Fig. 11-2.

In most cases of nucleation, the maximum energy barrier  $W_1$  must be surmounted. Differentiation of Eq. (11-4) with respect to  $r$ , setting  $dW/dr = 0$  to obtain the maximum, substituting in Eq. (11-4) and rearranging, gives

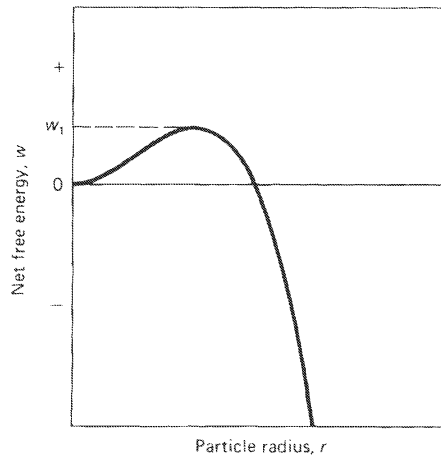
$$W_1 = \frac{16\pi\gamma^3}{3(\Delta G)^2}$$

From Eq. (11-3), the rate of nucleation should then be

$$\text{Rate} = A \exp\left(\frac{-W_1}{RT}\right) = A \exp\left(\frac{-16\pi\gamma^3}{3(\Delta G)^2 RT}\right)$$

where  $A$  is a constant,  $R$  is the gas constant, and  $T$  the absolute temperature. The rate of nucleation is thus enormously sensitive to interfacial energy. This has two implications for geochemical studies:

**FIGURE 11-2** Free energy (conceptual) of a small spherical particle as a function of particle radius.



1. Nucleation of a solid does not occur as soon as saturation is achieved. Some finite supersaturation is required to induce nucleation and the supersaturation required to induce nucleation is considerably greater than the supersaturation required to induce growth on a preexisting crystal.

2. At low degrees of supersaturation, nucleation can only take place if there is a way of minimizing interfacial energy. This is commonly accomplished by forming the nucleus in contact with some other solid phase, ideally where there is some similarity in the atomic structures of the two phases. In laboratory experiments nucleation commonly occurs on the walls of the reaction vessel or on dust particles in suspension, which tends to make results of experiments on nucleation highly nonreproducible.

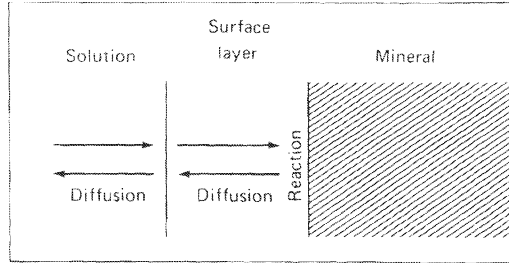
In general, for a particular degree of supersaturation it may be possible to predict whether the rate of nucleation will be rapid or essentially zero, but it is rarely possible to predict rates of nucleation more accurately than that.

## DISSOLUTION AND GROWTH

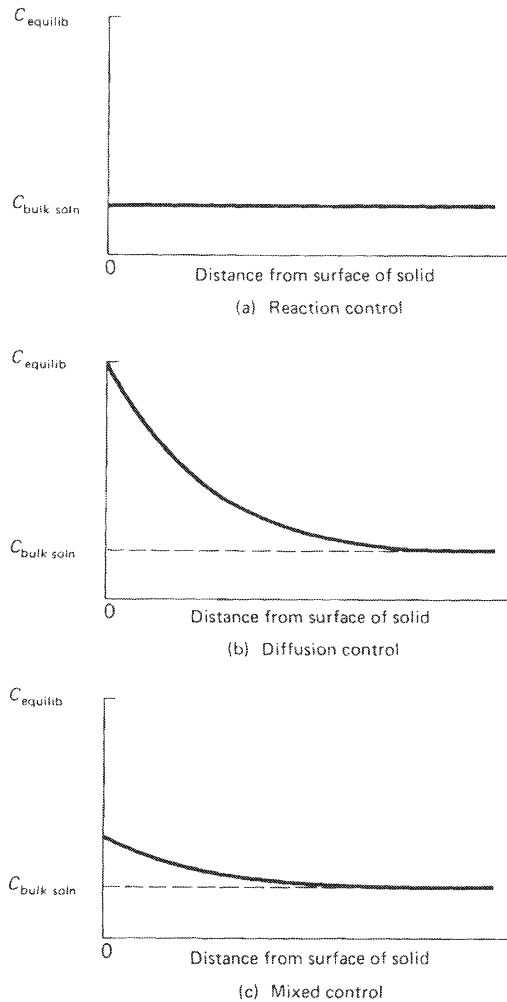
Three processes commonly control rates of dissolution or growth of a solid phase in inorganic geochemistry (Fig. 11-3):

1. Reaction at the surface of a mineral grain (reaction control), typically detachment or attachment of species at the mineral surface. When surface reaction is rate controlling, the concentration of solutes immediately adjacent to the grain will be very close to that in the bulk solution (Fig. 11-4a).
2. Transport (normally by diffusion) of ions or molecules in solution to or from the grain surface (diffusion or transport control). In this case, the solution immediately adjacent to the solid will be more or less in equilibrium with the solid, and concentration gradients will exist in solution (Fig. 11-4b).
3. Diffusion of ions or molecules through a layer of solid reaction products or a layer of partially altered primary mineral surrounding the solid. For many purposes this can be regarded as a type of surface reaction control; it will result in a uniform solution composition, as in Fig. 11-4a.

**FIGURE 11-3** Schematic drawing of a mineral reacting with solution. The rate-determining step may be reaction at the surface of the mineral, diffusion through a solid layer at the grain surface, or diffusion in solution.



**FIGURE 11-4** Distribution in solution of the concentration ( $C$ ) of a component released by dissolution of a solid phase. If the rate-controlling step is reaction at the surface, including diffusion through a solid layer, the concentration in solution will be uniform (a). If the rate-controlling step is aqueous diffusion, the concentration in solution close to the solid will be the value for equilibrium with the solid (b). If both reaction and diffusion are rate controlling, concentration gradients will be present in solution, but the concentration close to the solid will be lower than the equilibrium value (c) (after Berner, 1978).



Mixed kinetics (partly diffusion controlled, partly reaction controlled, Fig. 11-4c) may also occur, but generally either diffusion or reaction is the dominant control and the other can be neglected.

### Surface Reaction Mechanisms

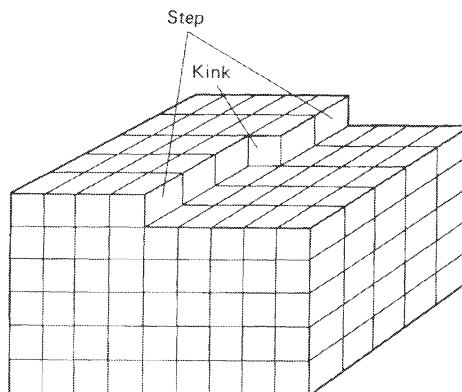
For low degrees of undersaturation and supersaturation, the rates of dissolution and crystal growth are often controlled by the detailed topography of the mineral surface. The surface normally includes “steps” and “kinks” (Fig. 11-5). The atoms that form a step have a higher energy than atoms in a plane surface, because they have two “sides” exposed to solution rather than one. Atoms at a kink have an even higher energy because they have three sides exposed to solution. During dissolution, the atoms with the highest energy detach most rapidly from the surface. Thus at low degrees of undersaturation atoms dissolve from the kinks, causing the kinks to migrate laterally along the steps. When the kink reaches the edge of the crystal, a new kink must be “nucleated,” and when the atoms above a step are all dissolved, a new step must be nucleated. The rate of dissolution may be controlled by the rate of “nucleation” of kinks and steps. During growth, the process is exactly reversed. New units of the crystal form at the points where they have the maximum surface area in common with the existing crystal. Kinks have three “sides” in common, steps two, and planar surfaces only one. Thus growth normally takes place at kinks, and the rate of growth may be limited by the rate of nucleation of new kinks and steps.

Crystals rarely have the ideal structure shown in Fig. 11-5. The structure normally shows various imperfections, particularly *dislocations*, in which one part of the crystal is offset relative to another. A particular type of dislocation, called a *screw dislocation* (Fig. 11-6), creates a step that can propagate continuously during either dissolution or growth, so the slow process of nucleating a new step is not required. The rate of dissolution or growth of a mineral is thus sensitive to the number and type of dislocations present. Because kinks are points of high surface energy, they are favored locations for adsorption of species from solution. The adsorbed species may “block” or immobilize the kink and so have a large effect on rates of dissolution or growth. Such species are called *inhibitors* or *surface poisons*. As an example, dissolved phosphate, even at very low concentrations (a few  $\mu\text{mol/kg}$ ), causes a large decrease in the rate of dissolution of calcite in seawater (Berner and Morse, 1974).

### Diffusion Control

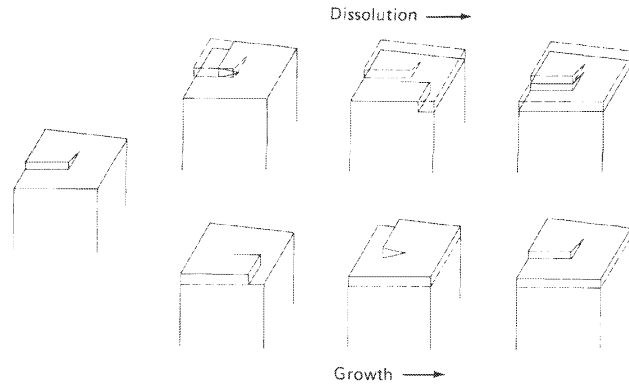
When diffusion in solution is rate controlling, this can usually be recognized because (Berner, 1978):

**FIGURE 11-5** Model of a crystal surface illustrating a step and a kink. Each cube corresponds to a molecule, atom, or pair of ions (from Berner and Morse, 1974).





**FIGURE 11-6** Illustration of how a spiral step (caused by a screw dislocation) can propagate endlessly during dissolution or growth.



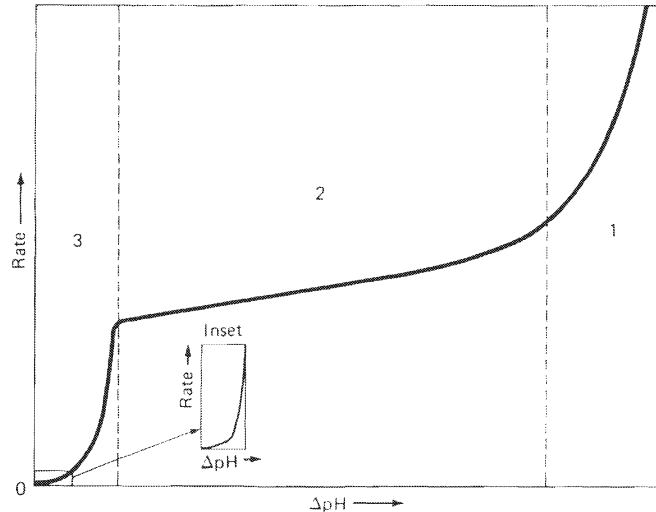
1. The rate to be expected on the basis of diffusion control can be calculated (approximately) and compared to the observed rate. If the observed rate is much slower, diffusion in solution is not the rate-controlling process.
2. If the rate is diffusion controlled, stirring should increase the rate of reaction. If surface reaction is rate controlling, the rate should be unaffected by stirring.
3. If the rate is measured at different temperatures,  $\Delta E$  can be calculated. Aqueous diffusion processes have characteristic low  $\Delta E$  values of about 20 kJ/mol (5 kcal/mol).
4. When the rate of dissolution of a grain is diffusion controlled, the grain becomes rounded, and dissolution is more or less uniform on all surfaces. When the dissolution rate is controlled by surface reaction, dissolution is selective; etch pits form around crystal defects, different crystallographic surfaces dissolve at different rates, and there is no general rounding of grains.

Biological processes also control the rates of many important geochemical processes, particularly redox processes (Chapter 8).

## DISSOLUTION OF CALCITE IN SEAWATER

In a series of papers, Morse and Berner (Morse and Berner, 1972; Berner and Morse, 1974; Morse, 1974a, 1974b) studied the kinetics of calcite dissolution in seawater, using an ingenious system for maintaining a constant degree of undersaturation. Their technique was to place powdered calcite in artificial seawater, the pH of which had been adjusted to give a particular degree of undersaturation. A burette containing acid was controlled by a pH electrode in the artificial seawater. As calcite dissolved, the pH tended to rise. When the pH started to rise, acid was automatically added to maintain the pH at its initial value. This maintained a constant degree of undersaturation, provided that the amount of  $\text{Ca}^{2+}$  added by calcite dissolution was small compared to the amount of  $\text{Ca}^{2+}$  already present in the seawater. The volume of acid added (recorded automatically) was exactly equivalent to the amount of calcite dissolved. The rate of dissolution as a function of degree of undersaturation is shown in Fig. 11-7.

Berner and Morse (1974) suggested that regions 1, 2, and 3 (Fig. 11-7) represented different mechanisms of dissolution, and hence different rate-controlling processes. In region 1 the



**FIGURE 11-7** Schematic plot of rate of dissolution of calcite as a function of  $\Delta\text{pH}$ , the difference between the pH of the solution and the pH at which the solution would be in equilibrium with calcite. The smaller  $\Delta\text{pH}$  is, the closer the solution is to equilibrium with calcite. The inset is a blown-up portion of the region near equilibrium, demonstrating the presence of a pronounced discontinuity, which is otherwise lost on the scale of the main diagram. The regions 1, 2, and 3 are discussed in the text (from Berner and Morse, 1974).

rate approached that calculated for control by diffusion in solution. This occurred only for extremely high degrees of undersaturation, corresponding to pH values below 4. Such degrees of undersaturation are rarely encountered in nature. At all less extreme degrees of undersaturation (region 2), the rate-controlling process was reaction at the surface of the crystal. In region 3, closest to saturation, the rate-controlling process appeared to be detachment of ions from kinks in monomolecular steps in the crystal surface. Kinks are points of high surface energy and are thus favored sites for adsorption of impurities from solution, particularly orthophosphate ion. When phosphate is adsorbed, the kink is immobilized, and dissolution at the kink stops. Thus the rate of dissolution of calcite in region 3 was very sensitive to traces of phosphate in solution. In region 2 the rate of dissolution was sensitive to  $P_{\text{CO}_2}$  and/or pH in addition to degree of undersaturation. Berner and Morse did not suggest a specific mechanism for dissolution in this region, although they suggested that adsorption of  $\text{H}^+$  on the crystal surface might be important.

Plummer and Wigley (1976) studied the kinetics of dissolution of calcite in  $\text{CO}_2$ -saturated water at  $25^\circ\text{C}$  and reached conclusions in general agreement with those of Berner and Morse. Dissolution rate was controlled by surface reaction and not diffusion; when the solution was far from equilibrium with calcite (region 2 of Berner and Morse), the dissolution rate was second order with respect to  $\text{Ca}^{2+}$ , and when the solution was close to equilibrium with calcite (region 3 of Berner and Morse), the reaction appeared to be fourth order with respect to  $\text{Ca}^{2+}$ . The somewhat complex apparent order of reaction was explained by Sjöberg and Rickard (1985) as being due to a mix of reaction-controlled and transport-controlled kinetics.

Two important general points should now be evident:

1. Even for a relatively simple system such as the dissolution of calcite in water, the relationship between degree of undersaturation and dissolution rate is not at all simple.

- The dissolution rate may depend on factors other than degree of undersaturation; here phosphate concentration and  $P_{\text{CO}_2}$  were also important.

It is important to stress these complexities, as mathematical models for natural water systems sometimes include the assumption that rates of both precipitation and dissolution are linearly related to degree of supersaturation or undersaturation. The relationship between dissolution rate and saturation state is discussed in the context of silicate dissolution later in this chapter.

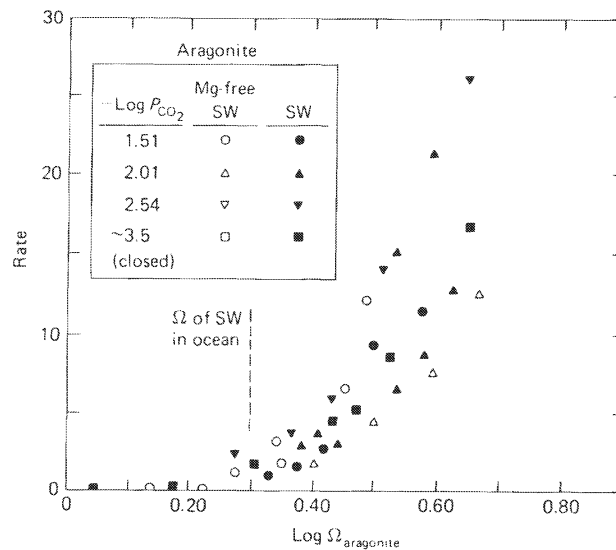
## GROWTH OF CALCITE AND ARAGONITE IN SEAWATER

Berner (1975) investigated the kinetics of the growth of calcite and aragonite in seawater. His main objective was to understand why aragonite and high-magnesium calcite, rather than low-magnesium calcite, formed in modern marine sediments. The technique was similar to that of Morse and Berner (preceding section), except that the solution was initially supersaturated rather than undersaturated, and base (NaOH or  $\text{Na}_2\text{CO}_3$ ) was added instead of acid to maintain supersaturation as  $\text{CaCO}_3$  precipitated. Solid  $\text{CaCO}_3$  (low-magnesium calcite or aragonite) was always present in the reaction vessel; the study concerned growth kinetics and not nucleation kinetics.

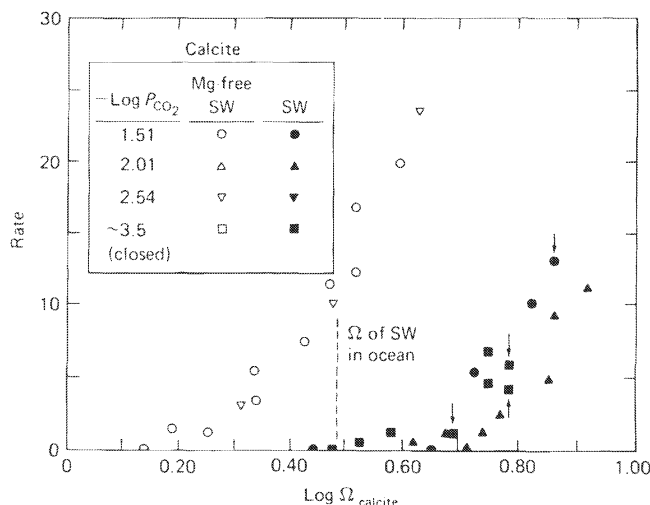
The rate of growth of aragonite crystals in seawater and in Mg-free artificial seawater is shown in Fig. 11-8. The rate increased rapidly as supersaturation increased, and the rate was independent of  $\text{Mg}^{2+}$  concentration and  $P_{\text{CO}_2}$  (at a constant degree of supersaturation).

The rate of growth of calcite, in contrast, was sensitive to the magnesium concentration in solution (Fig. 11-9). Whenever the concentration of magnesium in the artificial seawater exceeded about 3 mmol/kg (5 percent of its normal value in seawater), the growth rate of calcite was depressed. The 3-mmol/kg figure does not represent a "critical" level. Berner's experimental data showed no rate reduction compared to Mg-free seawater at 3 mmol/kg  $\text{Mg}^{2+}$ , a 20 percent rate reduction at 6 mmol/kg, and no growth at all at 48 mmol/kg at the degree of supersaturation of his experiments. The rate reduction is presumably a function of the  $\text{Mg}^{2+}/\text{Ca}^{2+}$  ratio in solution

**FIGURE 11-8** Rate of growth (arbitrary units) of aragonite versus degree of supersaturation with respect to aragonite ( $\Omega = IAP/K_{\text{arag}}$ ). SW = artificial seawater; Mg-free SW = artificial seawater of same ionic strength, but made up without magnesium (from Berner, 1975).



**FIGURE 11-9** Rate of growth (arbitrary units) of calcite versus degree of supersaturation with respect to calcite ( $\Omega = IAP/K_{\text{calcite}}$ ). Symbols as in Fig. 11-8 (Berner, 1975).



in addition to absolute  $\text{Mg}^{2+}$  concentration, although no data on this aspect were reported. At a given degree of supersaturation, the rate of growth of calcite in normal seawater was much less than the rate in Mg-free seawater. Or, put another way, a higher degree of supersaturation was needed to make calcite grow at a finite rate in the presence of  $\text{Mg}^{2+}$  than in the absence of  $\text{Mg}^{2+}$ .

These simple kinetic experiments explain why aragonite is so common in marine sediments. Before seawater becomes sufficiently supersaturated for calcite to precipitate at a finite rate, it has become supersaturated with respect to aragonite. Since the growth of aragonite is not inhibited by the presence of  $\text{Mg}^{2+}$ , aragonite can precipitate and grow. In fresh waters, the  $\text{Mg}^{2+}/\text{Ca}^{2+}$  ratio is usually well below 1. Calcite precipitation is not inhibited, so the common carbonate mineral to form is low-magnesium calcite and not aragonite.

According to Berner, the reason for the suppression of calcite growth was related to adsorption of  $\text{Mg}^{2+}$  on the surface of calcite, promoting formation of high-magnesium calcite. Ions on the surface of a crystal are in ion-exchange equilibrium with ions in solution (Chapter 4), and the equilibrium distribution of  $\text{Mg}^{2+}$  and  $\text{Ca}^{2+}$  between surface sites and solution may be quite different from the equilibrium distribution between ions in the bulk solid and solution. At  $\text{Mg}^{2+}/\text{Ca}^{2+}$  ratios in solution greater than about 1, virtually all the surface sites were occupied by  $\text{Mg}^{2+}$ . As the calcite grew, some of the adsorbed  $\text{Mg}^{2+}$  became trapped in the calcite structure to form a high-magnesium calcite. (The calcite precipitated from seawater in the experiments contained 7 to 10 mole percent Mg.) The high-magnesium calcite was thermodynamically less stable than low-magnesium calcite; hence it was more soluble, and a higher degree of supersaturation relative to pure  $\text{CaCO}_3$  was necessary to cause growth. This interpretation was confirmed (Mucci et al., 1985) by analysis of the surface layers formed when pure calcite was placed in artificial seawater supersaturated with respect to calcite ( $\Omega = 1.2$ ; see Fig. 11-9). The overgrowths contained about 8 mol percent  $\text{MgCO}_3$ , and appeared to be in exchange equilibrium with the solution.

Aragonite and high-magnesium calcite precipitation are two examples of a common phenomenon in geochemistry. When growth or nucleation of a thermodynamically stable phase is kinetically slow, a phase that is less thermodynamically stable but kinetically more labile is likely to form instead. Quartz (Chapter 10) is an example of a mineral whose formation is kinetically slow. We also mentioned in Chapter 10 that sepiolite is unstable with respect

to other magnesium silicates under earth–surface conditions. The reason that sepiolite occurs in nature (and it is not a very rare mineral) is that it precipitates rapidly from solutions that are only slightly supersaturated. Talc and serpentine, on the other hand, are slow to precipitate, so even though they may be more stable thermodynamically than sepiolite, they do not form so readily at low temperatures.

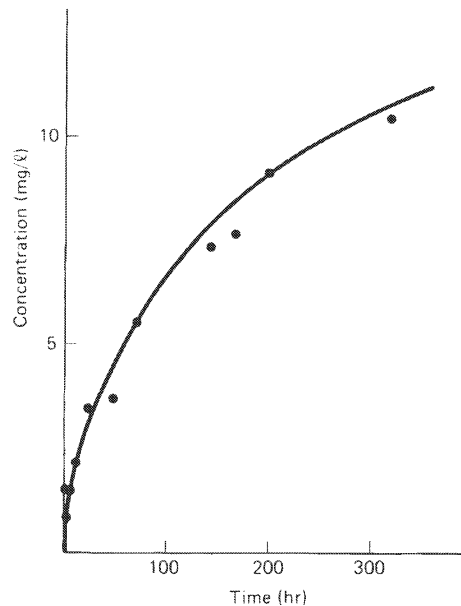
Amorphous phases are always thermodynamically unstable with respect to crystalline phases, but amorphous phases are usually kinetically labile. Amorphous phases [e.g.,  $\text{Fe}(\text{OH})_3$ ,  $\text{Al}(\text{OH})_3$ , and allophane (the amorphous equivalent of kaolinite)] often form by precipitation from solution. Over time, these unstable precipitates usually crystallize to more stable phases.

## DISSOLUTION OF SILICATES

A large amount of research has been conducted on silicate dissolution kinetics in the last two decades. The impetus has come from several directions, including prediction of the behavior of radioactive waste in the subsurface and prediction of the effect of acid deposition on soils and surface waters (Chapter 13). Early experiments were generally conducted in *batch reactors*. A batch reactor is simply a vessel containing a fixed volume of solution, commonly buffered at a particular pH, and a fixed mass of solid. Dissolution is followed by measuring the change in composition of the solution over time, usually by measuring a solute such as silica that is derived from the dissolving mineral. Such experiments typically show a concentration–time relationship such as that in Fig. 11-10. The slope of the curve, and hence the rate of dissolution of the mineral, decreases over time. The curve corresponds approximately to a parabola of the form

$$Q = kt^{1/2}$$

**FIGURE 11-10** Example of the parabolic rate law: release of silica from K-feldspar at pH 4 (after Wollast, 1967).



where  $Q$  is the amount in solution,  $k$  is a constant and  $t$  is time. This behavior is called the *parabolic rate law*. After a sufficiently long time, the increase in concentration may become linear, giving a *linear rate law* (Fig. 11-11):

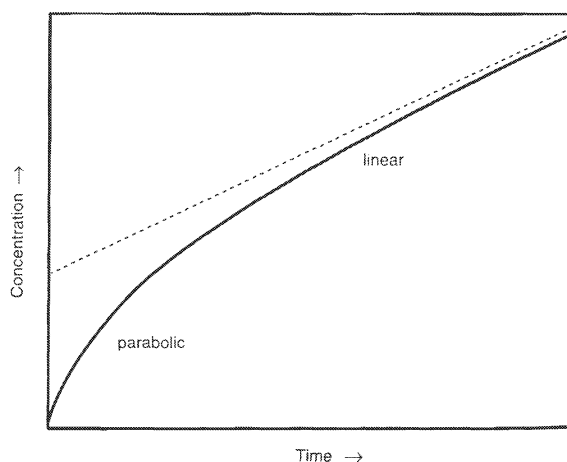
$$Q = kt + Q_0$$

The term  $Q_0$  simply represents the fact that the straight-line portion of the curve does not extrapolate to the origin of the graph.

The parabolic rate law was originally interpreted as indicating that the rate-controlling step was diffusion of solutes through a thickening, altered surface layer. The surface layer could be partially altered primary mineral or a layer of product material precipitated from solution. Either model will give rise to parabolic kinetics, the decrease in rate resulting from increasing layer thickness. The linear rate law observed after relatively long reaction times would correspond to a situation where the layer attained constant thickness, with dissolution at the outside of the layer proceeding at the same rate as alteration of the primary mineral.

The "leached layer" hypothesis (ignoring the distinction between leached primary mineral and secondary precipitate) was based solely on the rate of appearance of solutes as primary minerals dissolved. The surfaces of minerals undergoing dissolution had not been examined. Petrovic et al. (1976) and Berner and Holdren (1977, 1979) did examine the surfaces of experimentally and naturally leached feldspars by means of scanning electron microscopy and X-ray photoelectron spectroscopy (XPS). XPS is a technique for measuring the chemical composition of the surface layer of solids. These studies indicated that the postulated surface layers did not exist. There was no detectable chemical difference between the surface of the altered feldspar and its interior. If a surface layer of different composition did exist, it could not be more than a few tens of angstroms thick, and hence would be much too thin for diffusion through it to control the kinetics of ion and silica release. Scanning electron microscopy showed the absence of any coherent layers of secondary material. It appeared that the parabolic rate law was in fact an artifact of the grinding procedure used in the earlier experiments. Grinding of large feldspar crystals to produce material for the experiments produced a large number of very fine particles (less than 1  $\mu\text{m}$ ). These fine particles would dissolve more rapidly than larger grains because of the excess free energy associated with their surfaces. If the ultrafine particles were removed (by

**FIGURE 11-11** Illustration of a dissolution rate changing from parabolic at short times to linear at longer times.



sieving, washing, and etching with HF), the parabolic rate law was not observed; dissolution followed a linear rate law over the entire time range studied (Holdren and Berner, 1979). Similarly, Grandstaff (1986) showed that dissolution of unground olivine from Hawaiian beach sand followed a linear and not parabolic rate law.

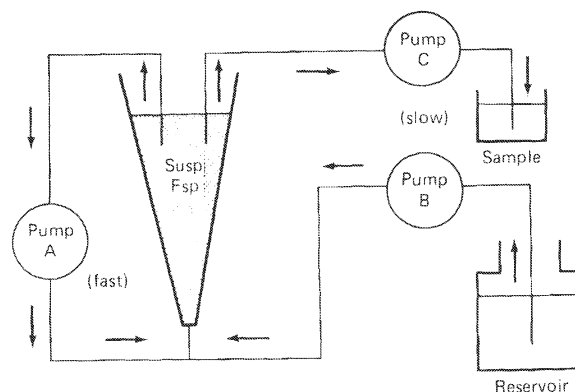
Regions of a crystal where the structure is disrupted, for example dislocations, are also regions of higher energy and hence greater solubility than the bulk crystal. Berner and Holdren (1977, 1979) showed that the dissolution of feldspars both in natural soils and in HF–H<sub>2</sub>SO<sub>4</sub> solutions in the laboratory produced well-defined etch pits, presumably related to dislocations in the original feldspars. Although dissolution rate increases with increasing dislocation density, the relationship is not simple. Experimentally, a large increase in dislocation density produces only a modest increase in dissolution rate (Blum et al., 1990).

Subsequent work, using more sophisticated analytical techniques (e.g., Casey et al., 1989; Casey and Bunker, 1990) has shown that cations may be depleted in the near-surface region of dissolving feldspars but the thickness of the depletion layer decreases with increasing pH. The existence of such layers is also implied by the fact that the initial dissolution of silicates is generally non-stoichiometric. The general consensus now is that non-stoichiometric zones exist in the vicinity of the surfaces of dissolving feldspars, but diffusion through such zones is not the major control on the dissolution rate. The primary control is detachment of atoms or ions from the outside of the solid. Diffusion through a partially leached surface layer may, however, control the rate of dissolution of volcanic glass (White, 1983).

Most experiments on dissolution rates are now conducted in *flow-through* reactors rather than batch reactors. The version shown in Fig. 11-12 was introduced by Chou and Wollast (1984). In this apparatus, rapid circulation of solution by pump A keeps the mineral in suspension, while solution is slowly introduced and removed by pumps B and C. The rates of introduction and removal are identical, maintaining a constant volume of solution in the system. The rate at which silica, sodium, and aluminum are removed in the output (= concentration × flow rate) is equal to the rate at which they are dissolved from the feldspar. The flow rate of B and C is maintained at a high enough rate that the solution does not become supersaturated with aluminum hydroxide or other secondary phases. A major advantage of this technique is that, once a steady state has been reached, the composition of the solution is constant throughout the experiment; in a batch reactor the solution composition changes as the mineral dissolves. The effect of different solution compositions can be easily investigated by changing the input solution. Alternative versions of the flow-through reactor have the mineral packed in a small column rather than being kept in suspension. This makes the system easier to use at higher temperatures, but the solution composition may not be the same throughout the column.

Rates are normally reported in moles per unit area of mineral undergoing dissolution; total dissolution rate is proportional to surface area rather than to mass of solid. Surface areas are commonly measured by the BET (Brunauer, Emmett and Teller, 1938) method. This method involves measuring the amount of a gas (commonly nitrogen, less commonly krypton) that adsorbs as a monolayer on the surface of the mineral at low temperature. The BET area is always larger than the geometrical area (calculated by assuming the minerals are simple geometrical forms such as spheres or cubes), and commonly changes significantly during a dissolution experiment (Anbeck, 1992a, 1992b). Dissolution rates are generally most easily interpreted when normalized to the BET area at the start of the experiment (Murphy, 1993).

FIGURE 11-12 Schematic illustration of a fluidized bed reactor.



### Effect of Solution Composition on Dissolution Rates

**pH.** Far from equilibrium, the dissolution rates of most silicate minerals have the form shown in Fig. 11-13. In the acid region, the rate increases exponentially with increasing hydrogen ion concentration, or

$$(\text{Rate})_{\text{H}} = k_{\text{H}} \alpha_{\text{H}^+}^n \quad (\text{acid region})$$

where  $k_{\text{H}}$  is a rate constant and  $n$  an exponent that is different for different minerals.  $n$  is typically about 0.5 (a slope of  $-0.5$  in Fig. 11-13); some values are shown in Table 11-1. An exponent of 0.5 means that for a change in pH of one unit, the rate should change by a factor of about 3 ( $=10^{0.5}$ ).

Above some transition pH, typically between about 4 and 5 (Table 11-1), dissolution rates are generally independent of pH.

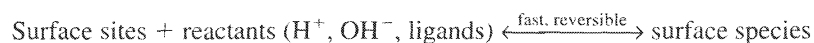
$$(\text{Rate})_{\text{neutral}} = k_{\text{N}} \quad (\text{neutral region})$$

and then at pH values above 8 or so, they increase with increasing pH.

$$(\text{Rate})_{\text{OH}} = k_{\text{OH}} \alpha_{\text{OH}^-}^m \quad (\text{basic region})$$

where  $m$  typically has a value of about 0.3 to 0.5 (Brady and Walther, 1989).

Rates of dissolution are commonly explained by *transition state theory*. This approach was originally developed to explain the kinetics of gas-phase reactions involving simple molecules. Its extension to silicate dissolution kinetics involves a certain amount of faith. The basic idea is that adsorption of a proton or a ligand to a cation at the surface of a solid weakens the bonds between the cation and the underlying solid and accelerates its release to solution. In brief, the dissolution reaction can be divided into two main steps (Stumm and Wieland, 1990). The first is formation of a complex at the surface of the mineral, which is assumed to be rapid:

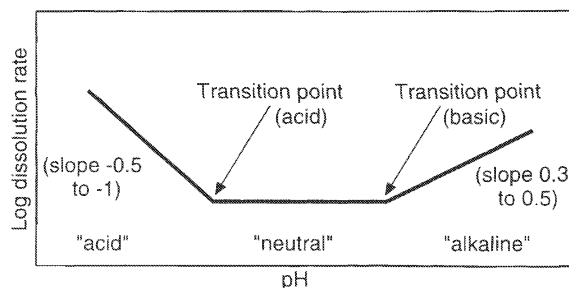


A simple example would be protonation of a surface OH site associated with a metal, M (Chapter 5):

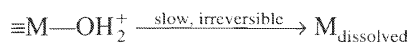




**FIGURE 11-13** Schematic representation of silicate dissolution rates far from equilibrium as a function of pH (after Drever, 1994).



The surface species would then decompose by a slow step, releasing M to solution:



This step would take place through a well-defined high-energy intermediate, the *activated complex*. The overall dissolution rate (the detachment rate of M from the solid) would be proportional to the concentration of the activated complex, which would in turn be proportional to the concentration of the precursor surface species (or *surface complex*). This model describes well the dissolution of simple oxides, where the rate of dissolution is directly related to the concentration of adsorbed protons (Stumm and Wieland, 1990).

In the discussion of pH dependence above, adsorption of protons results in a protonated surface complex, and the rate of dissolution is proportional to the concentration of this species. The exponent  $n$  reflects either a non-linear dependence of adsorbed protons on proton concentration in solution or the stoichiometry of the surface complex. A similar logic applies to formation of a surface complex involving  $\text{OH}^-$  (or deprotonation of a surface  $-\text{OH}$  group) under basic conditions.

Following Stumm and Wieland (1990), the total rate can be expressed as the sum of the individual rates

$$(\text{Rate})_{\text{total}} = k_{\text{H}}\alpha_{\text{H}^+}^n + k_{\text{N}} + k_{\text{OH}}\alpha_{\text{OH}^-}^m$$

**Organic Ligands.** Organic ligands may accelerate the dissolution rates of silicates by forming complexes with metals, particularly aluminum, on the mineral surface, thereby weakening the bonds between the metal and the solid. The effect can be described by the same equations as were used for proton adsorption:

$$(\text{Rate})_{\text{ligand}} = k_{\text{L}}\alpha_{\text{ligand}}^p$$

and the total rate can be represented as the sum of the individual rates

$$(\text{Rate})_{\text{total}} = k_{\text{H}}\alpha_{\text{H}^+}^n + k_{\text{N}} + k_{\text{OH}}\alpha_{\text{OH}^-}^m + k_{\text{L}}\alpha_{\text{ligand}}^p$$

The exponent  $p$  again reflects the stoichiometry of the complex and the relationship between adsorbed concentration and concentration in solution. The overall effect of organic ligands on dissolution rate will depend on how the magnitude of the term  $k_{\text{L}}\alpha_{\text{ligand}}^p$  compares to those of the other terms in the equation. There has been some controversy over the quantitative importance of organic ligands in nature (Drever, 1994). High concentrations of chelating ligands such as oxalate certainly accelerate the dissolution rates of silicates far from equilibrium, but the effect of organic ligands *at the concentrations commonly observed in soil solutions* on dissolution rate

**TABLE 11-1** pH of the Transition Points (See Fig. 11-13) and Slope of log (Rate) vs. pH Graph in the Acid Region for Silicate Minerals [after Drever, 1994]

Mineral	Transition pH (acid)	Slope in acid region	Transition pH (basic)	Source
Albite	4.5	-0.5	7.5	Sverdrup (1990) <sup>a</sup>
Oligoclase	4.5	-0.5		Oxburgh et al. (1994)
Andesine	4.5	-0.5		Oxburgh et al. (1994)
Bytownite	5	-0.75		Oxburgh et al. (1994)
Anorthite	4.5	-3		Amrhein & Suarez (1988)
K-feldspar	5	-0.5		Schweda (1990)
Forsterite	7 <sup>b</sup>	-0.9	7 <sup>b</sup>	Sverdrup(1990) <sup>a</sup>
Forsterite	4.5 (?)	-0.6	8(?)	Blum & Lasaga (1988)
Garnet	5.5	-0.9	8	Sverdrup (1990) <sup>a</sup>
Amphiboles	5.5	-0.8		Sverdrup (1990) <sup>a</sup>
Amphibole	<3			Mast & Drever (1987)
Diopside,				
Augite	ca. 6	-0.7 to -0.9	ca. 8	Sverdrup (1990) <sup>a</sup>
Phlogopite,				
Biotite		-0.4		Sverdrup (1990) <sup>a</sup>
Kaolinite	4	-0.4		Wieland & Stumm (1992)

<sup>a</sup>Sverdrup (1990) represents both original work and a compilation of data from the literature.

<sup>b</sup>No pH-independent region.

is probably minimal. The effects in microenvironments adjacent to roots and fungal hyphae, however, may be much greater.

The effect of organic ligands on state of saturation is a separate issue discussed below.

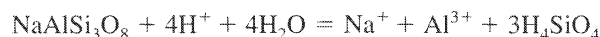
**Chemical Affinity and Other Ions in Solution.** Up to this point, we have been talking about dissolution rate “far from equilibrium” without really defining what was meant. At equilibrium, by definition, the rate of the forward reaction (dissolution of the solid phase) is exactly equal to the rate of the opposite (or backward) reaction, which is precipitation of the same solid phase, from solution. The net rate of reaction must be zero, but the forward and backward reactions individually proceed at a finite rate. As chemical reactions approach equilibrium, the rate of the back reaction becomes finite. Thus the net rate of reaction decreases as equilibrium is approached, ultimately becoming zero at equilibrium. The question is how close to equilibrium the reaction has to be before this effect becomes significant. This is a controversial question that has not been fully resolved in the literature. Transition state theory gives, for a *simple, elementary dissolution reaction* (Aagaard and Helgeson, 1982; Velbel, 1989),

$$\text{Rate} = k_a [1 - \exp(\Delta G_R / \sigma RT)]$$

where  $k_a$  is the apparent forward rate constant,  $\sigma$  is a “stoichiometric number,” conventionally set equal to 1,  $R$  is the gas constant and  $T$  temperature.  $\Delta G_R$  is the departure from equilibrium, or *chemical affinity*, in units of kJ or kcal per mole. It is related to the activity product for the reaction by

$$\Delta G_R = RT \ln (Q/K_{eq})$$

where  $Q$  is the activity product and  $K_{\text{eq}}$  the equilibrium constant. Thus for dissolution of albite in acid solution:



the activity product,  $Q$ , is given by

$$Q = \frac{a_{\text{Na}^+} a_{\text{Al}^{3+}} a_{\text{H}_4\text{SiO}_4}^3}{a_{\text{H}^+}^4}$$

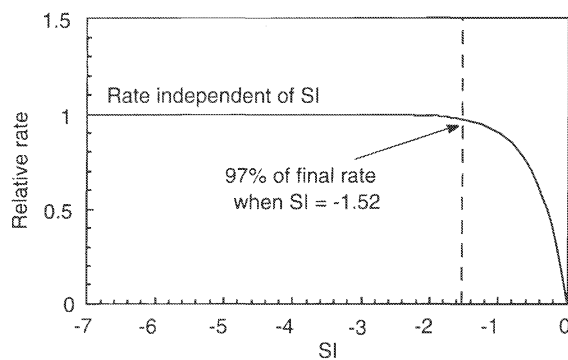
For undersaturated solutions, the value of  $Q$  is less than the equilibrium constant,  $K_{\text{eq}}$ .

The term  $\exp(\Delta G_R/\sigma RT)$  represents the “back reaction”—in this case reprecipitation of the primary mineral. It will be 3 percent of the forward reaction if  $\exp(\Delta G_R/\sigma RT) = 0.03$ , which corresponds to  $\Delta G_R = -8.7 \text{ kJ/mol}^{-1}$  at  $25^\circ\text{C}$  (assuming  $\sigma = 1$ ), or  $\log_{10}(Q/K_{\text{eq}}) = -1.52$ . If the departure from equilibrium is greater than this, the back reaction should be negligible and rate should be independent of affinity of reaction (Fig. 11-14). If this interpretation is correct, “far from equilibrium” would be defined by the criterion  $\log_{10}(Q/K_{\text{eq}}) \leq -1.52$ , and most experiments in the literature would meet the criterion of being “far from equilibrium.” The problem with this analysis is that it assumes that mineral dissolution behaves as a simple elementary reaction. In experiments conducted by Burch et al. (1993) at  $80^\circ\text{C}$ , the dissolution rate of albite seemed to be reduced by chemical affinity effects at much higher degrees of undersaturation than  $\log_{10}(Q/K_{\text{eq}}) = -1.52$  (Fig. 11-15).

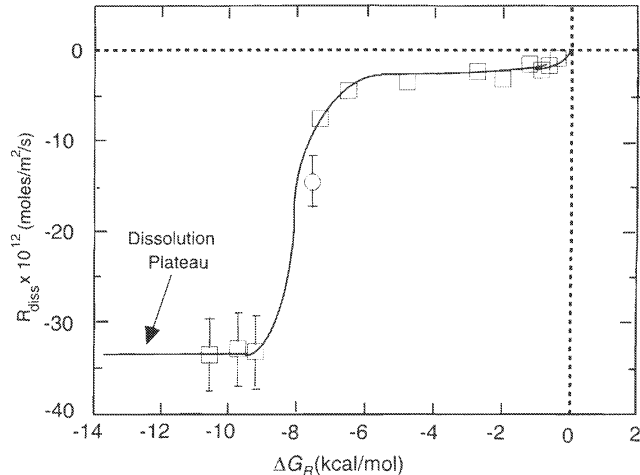
Oelkers et al. (1994), in experiments at  $150^\circ\text{C}$ , showed that the dissolution rates of albite at pH 9 and kaolinite at pH 2 were strongly affected by dissolved Al concentrations. It is hard to say how applicable these results from limited high-temperature experiments are to dissolution reactions at or below  $25^\circ\text{C}$ . Mast and Drever (1987) showed that oxalate ion at a concentration of  $10^{-3} \text{ M}$  had no effect on the dissolution rate of oligoclase feldspar. [Higher concentrations of oxalate do affect oligoclase dissolution rate, and  $10^{-3} \text{ M}$  oxalate has some effect on dissolution rates of more calcic feldspars (Stillings et al., 1996; Welch and Ullman, 1993).] Oxalate is a strong chelator of Al. The presence of  $10^{-3} \text{ M}$  oxalate has an enormous effect on the activity of free Al species and hence also on the affinity of reaction. The lack of a strong oxalate effect indicates a lack of sensitivity to dissolved Al activity or chemical affinity under the conditions of these experiments.

In summary, the effect of solution composition—particularly chemical affinity and Al concentration—on silicate dissolution rates is not well understood.

**FIGURE 11-14** Predicted effect of chemical affinity on reaction rate (after Drever and Clow, 1995).



**FIGURE 11-15** Experimentally measured dissolution rate of albite at 80°C and pH 8.8 as a function of chemical affinity. Reprinted from *Chemical Geology*, v. 5, Burch et al., 1993, "Free energy dependence of albite dissolution kinetics at 80°C and pH 8.8" (p. 137–162), with kind permission of Elsevier Science—NL, Sara Burgerhartstraat 25, 1055 KV Amsterdam, The Netherlands.



### Relative Dissolution Rates of Different Minerals

There has been a large amount of work done in the laboratory on the rates at which minerals dissolve (for reviews, see Sverdrup, 1990; Stumm, 1990). A simple way (Lasaga et al., 1994) of comparing rates is to calculate the time it would take for a 1 mm sphere of each mineral to dissolve completely in a dilute solution ("far from equilibrium") at pH 5 (Table 11-2). The rates vary enormously. Minerals such as quartz and kaolinite dissolve extremely slowly; feldspars and mafic minerals at intermediate rates, and carbonates very rapidly. The implications of these results for mineral weathering in the field will be discussed in the next chapter.

### Comparisons Between Laboratory and Field Dissolution Rates

One objective of measuring mineral dissolution rates in the laboratory is to predict rates in the field, particularly in the context of acid deposition (Chapter 13). The comparison is not an easy one to make because dissolution rate depends on mineral surface area exposed to solution, and it is not easy to measure or estimate mineral surface areas in the field. In order to apply laboratory-based dissolution rates to weathering in the field, we need to know the surface areas of all minerals exposed to weathering in the catchment (or soil profile) under study.

Pačes (1983) and Velbel (1985) compared the rates of weathering of silicate minerals based on cation export from field catchments to dissolution rates measured in the laboratory. Pačes estimated mineral surface areas on the basis of regolith thickness and a plausible fracture pattern in bedrock. Velbel calculated mineral surface area on the basis of a typical grain size for minerals in the regolith. Both Velbel and Pačes came up with rates for weathering in the field that were slower than would be predicted from the laboratory experiments. The magnitude of the discrepancy was about an order of magnitude, but it depends on the assumptions used in the calculations and is not well constrained. They attributed the discrepancy to, in part at least, "aging" of the mineral surfaces. The idea was that as minerals were exposed to weathering for a long time, sites of high energy such as dislocations would be dissolved out and

**TABLE 11-2** Approximate Time for a Hypothetical 1 mm Sphere of Various Minerals to Dissolve in Dilute Solution at pH 5 (modified from Lasaga et al., 1994, and other sources)

<i>Mineral</i>	<i>Lifetime (y)</i>
Quartz	34,000,000
Kaolinite	6,000,000
Muscovite	2,600,000
Epidote	923,000
Microcline	921,000
Biotite	900,000
Albite	575,000
Andesine	80,000
Bytownite	40,000
Enstatite	10,100
Diopside	6,800
Forsterite	2,300
Dolomite	1.6
Calcite	0.1

hence overall rates would decrease. Alternatively, secondary minerals might precipitate on the surface of the primary grains, isolating fresh mineral surfaces from the surrounding solution.

Swoboda-Colberg and Drever (1993) and Clow (Drever and Clow, 1995) measured weathering rates in smaller-scale (about 2m<sup>2</sup>) experiments where the mineral surface area could be well constrained. They also measured the dissolution rates of minerals from the same soils in laboratory experiments. The rates in the field were again slower than the rates in the laboratory but the difference could not be attributed to “aging” because the same minerals were used in both experiments. They attributed the difference to hydrologic effects: solutions in natural soils tended to pass rapidly through preferential channels in the soil without contacting all the mineral surfaces present. In laboratory experiments, by contrast, the minerals from the soil were maintained in suspension, so there was excellent contact between minerals and solution. The topic is discussed in more detail in Drever and Clow (1995).

## REVIEW QUESTIONS

1. Derive expressions for the time required for the initial amount of a substance,  $M_0$ , to be reduced to 50 percent of its initial value if the kinetics of removal are (a) zero order in the substance; (b) second order in the substance.
2. Prove mathematically that rate control by diffusion through a layer of constant thickness leads to a linear rate law. Discuss any assumptions that have been made.
3. List some instances, other than those mentioned in the chapter, where metastable rather than stable solids are formed in nature. Can you see any pattern to instances where metastable solids are formed?
4. The rates of dissolution of quartz, K-feldspar, albite, and anorthite at 25°C and pH 5 are  $10^{-13.39}$ ,

$10^{-12.50}$ ,  $10^{-12.26}$ ,  $10^{-8.55}$ , respectively (Lasaga et al., 1994). Assuming a density of 2.65, how long would it take a planar surface of each mineral to retreat 1 mm? How do these times relate to the preservation/loss of these minerals during weathering and transport?

5. The activation energy for the dissolution of enstatite ( $\text{MgSiO}_3$ ) is 49 kJ/mol (Schott et al., 1981). How much faster will enstatite dissolve at 25°C than at 10°C? Would you predict that mineral weathering rates in nature would be strongly affected by temperature?

### SUGGESTED READING

- BLUM, A. E. (1994). Feldspars in weathering. In I. Parsons, (Ed.), *Feldspars and their Reactions, NATO Advanced Study Institute* (pp. 595–629). Dordrecht, Netherlands: Kluwer Academic Publishers.
- LASAGA, A. C., J. M. SOLER; J. GANOR; T. E. BURCH; and K. L. NAGY. (1994). Chemical weathering rate laws and global geochemical cycles. *Geochimica et Cosmochimica. Acta*, 58, 2361–2386.
- STUMM W., and E. WIELAND. (1990). Dissolution of oxide and silicate minerals: Rates depend on surface speciation. In W. Stumm. (Ed.), *Aquatic Chemical Kinetics* (pp. 367–400). New York: Wiley-Interscience.
- WHITE, A. F., and S. L. BRANTLEY, (Eds.). (1995). *Chemical Weathering Rates of Silicate Minerals. Reviews in Mineralogy* (Vol. 31), Washington, DC: Mineralogical Society of America. This volume contains up-to-date reviews of the dissolution kinetics of the major silicate minerals.
- WOLLAST, R. (1990). Rate and mechanism of dissolution of carbonates in the system  $\text{CaCO}_3\text{--MgCO}_3$ . In W. Stumm, (Ed.), *Aquatic Chemical Kinetics* (pp. 431–446). New York: Wiley-Interscience.

# 12

## Weathering and Water Chemistry

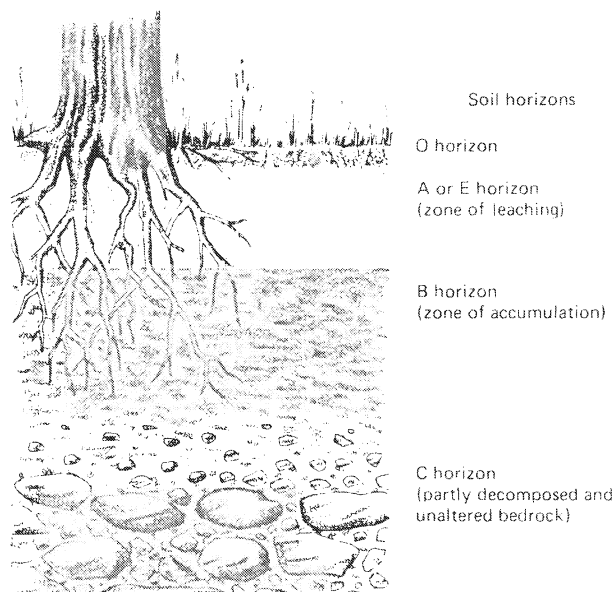
### SOIL FORMATION

The chemistry of most surface waters and groundwaters is the result of interaction between rain or snowmelt and rocks near the earth's surface. Much of the interaction takes place in the soil zone. Soil formation is an exceedingly complex process involving plants, animals, microorganisms, and inorganic processes; only the briefest summary will be presented here. Soil scientists have developed a complex and elaborate nomenclature system for classifying soils, which is beyond the scope of this book. Interested readers are referred to Soil Survey Staff (1992) and Buol et al. (1980).

In temperate, humid climates, soils commonly show a characteristic set of horizons (Fig. 12-1). Below a surface accumulation of organic matter (the O horizon), there is a coarse-grained layer from which iron and aluminum have been leached (the A or E horizon; the term A is used generally for the uppermost mineral horizon, the term E is used for a highly leached A horizon). Below the A (E) horizon is a layer in which iron and aluminum have accumulated as fine-grained, poorly crystallized hydroxides or clay minerals (the B horizon). The region below the B horizon containing partially altered bedrock is called the C horizon. A soil showing these horizons is called a *Spodosol* (roughly equivalent to the older term *Podsol*). A soil with an accumulation of clay in the B horizon but without a bleached A horizon is called an *Alfisol*. A highly leached soil from a more tropical environment, commonly with large accumulations of iron and aluminum oxyhydroxides, is called an *Ultisol*. The O, A, and B horizons are commonly subdivided into different recognizable horizons. The processes by which aluminum and iron are removed from the A horizon probably involve dissolution in the form of organic complexes and transport of colloidal particles. Precipitation in the B horizon is caused by several processes, including the loss of organic complexing agents by bacterial decomposition and adsorption.

In less humid environments, leaching is less important as a soil-forming process. Typically, not enough water flows through the soils to remove all the calcium released by weathering, and nodules of calcium carbonate (*calcrete* or *caliche*) form in the soil profile. The characteristic grassland soils with relatively high concentrations of organic matter are

FIGURE 12-1 Soil horizons formed in a temperate humid climate.



called *Mollisols* (roughly equivalent to the older term *Chernozem*), and the drier soils of desert environments are called *Aridisols*.

The type of soil formed under a particular climate is strongly influenced by the nature of the bedrock, topography, vegetation, and the time over which soil-forming processes have operated. These influences are discussed later in this chapter in the context of related effects on water chemistry.

Geochemical approaches to understanding the chemistry of surface waters have generally ignored the complexities of the soil zone. Many researchers have deduced the type of reactions that must take place between water and rock without being particularly concerned as to where the reactions were occurring. Until relatively recently, geochemists have tended to ignore or underestimate the effects of terrestrial biota on surface water composition, although the importance of the biota as a source of carbon dioxide (Chapter 3) and organic acids (Chapter 6) has been recognized for a long time.

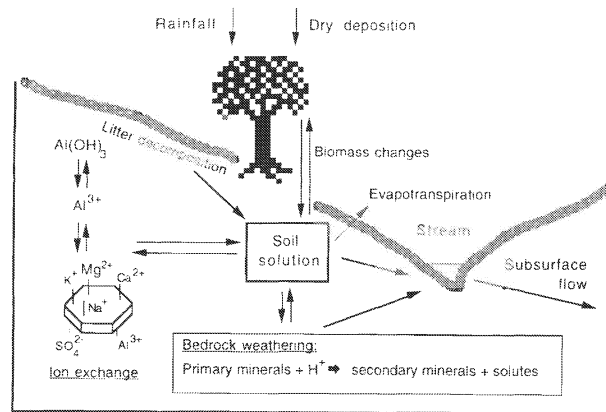
## THE MASS-BALANCE APPROACH TO CATCHMENT PROCESSES AND MINERAL WEATHERING REACTIONS

### Catchment Processes

A mass-balance calculation is simply a budget showing the sources from which the dissolved constituents in a water are derived. Such calculations can be performed on various scales. Here we shall first consider the catchment scale; that is to say, we will look at the composition of a stream and interpret its composition in terms of processes occurring over the whole catchment (drainage basin) upstream of the sampling point. Some of the processes affecting solute budgets are shown in Fig. 12-2.



**FIGURE 12-2** Some processes affecting solute budgets in a catchment.



If we ignore direct inputs of pollution, we can interpret the fluxes for a catchment in terms of a mass balance equation (Drever and Clow, 1995):

$$\text{solute in outflow} = \text{solute from atmosphere} + \text{solute from weathering of minerals} \\ \pm \text{solute from change in biomass} \pm \text{change in exchange pool} \quad (12-1)$$

In writing this equation we have already made the assumption that our time-scale is long enough that changes in water storage can be ignored. The question of time-scale is very important in catchment-scale studies: it is rarely possible to construct a meaningful catchment budget for a time-scale of less than a year. On the shorter time-scale, biomass effects tend to be large, whereas they tend to average out over an annual cycle. Let us discuss the individual terms in the above equation.

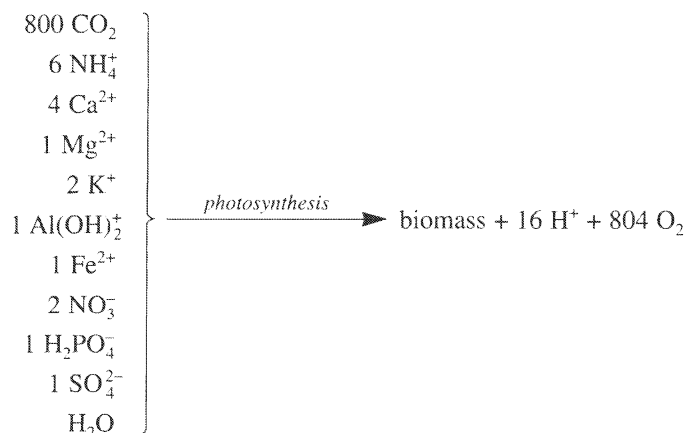
**Solutes in Outflow.** The information needed is the volume and chemical composition of water leaving the catchment. It is usually assumed that discharge via groundwater is negligible compared to surface runoff. The volume of surface runoff is commonly monitored continuously, ideally at a weir constructed for the purpose. Water chemistry is commonly measured at some fixed time interval, typically weekly. Interpolated values from these weekly samples are coupled with the continuous discharge record to calculate a continuous record of the flux of solutes leaving the catchment.

**Solutes from the Atmosphere.** Atmospheric deposition was discussed in Chapter 1. The atmospheric input comes in the form of *precipitation* (rain and snow) and *dry deposition* or *occult deposition*. Dry deposition consists of solid particles and gases such as SO<sub>2</sub> and NO<sub>x</sub> that are taken up directly by surfaces, particularly vegetation or moist foliage. The term *occult deposition* is sometimes used to cover dry deposition and deposition from mist or fog; the terms *dry deposition* and *occult deposition* are often used interchangeably to mean all inputs from the atmosphere other than those in precipitation. Occult deposition is difficult to quantify. One approach, which is useful in catchments with a reasonably uniform forest cover, is to measure *throughfall*, which is rain collected after it has passed through the forest canopy, and *stemflow*, which is water running down the outside of tree trunks. The solutes in throughfall and stemflow can be attributed to a combination of solutes in precipitation, solutes from occult deposition, and solutes translocated through the vegetation and

leached from the leaves. It is possible to distinguish *approximately* between occult deposition and translocation on the basis of tree physiology (Matzner, 1986), but ambiguities remain, particularly for trace elements. The amount of dry deposition is quite sensitive to the amount and type of vegetation present. Conifers are much more effective in trapping atmospheric solutes than deciduous trees, and trees are more effective than grassland. Significant dry deposition occurs even on rock outcrops (Clow and Mast, 1995; Peters, 1989). It is very difficult to measure dry deposition for a catchment containing different vegetation types.

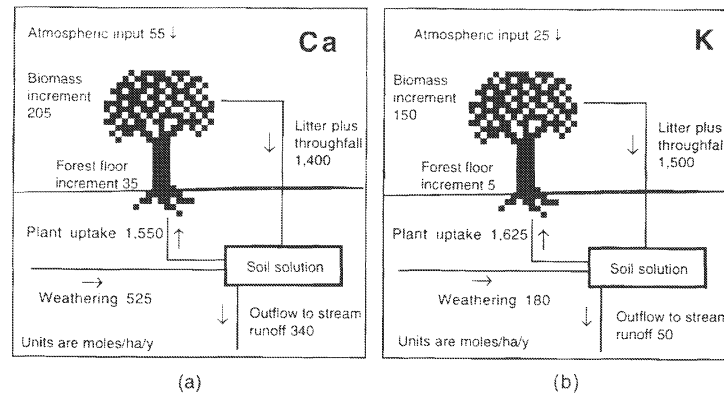
The solutes most affected by dry deposition are nitrogen species (nitrate, ammonium) and sulfate. The budgets of the major cations, which we shall be using later in the chapter to elucidate mineral weathering processes, are less influenced by dry deposition. Also, dry deposition is much lower in "pristine" areas than it is in areas where the atmosphere contains high concentrations of nitrogen and sulfur species from pollution.

**Solutes from Changes in the Biomass.** As plants grow, they extract inorganic nutrients from the soil solution and incorporate them into plant tissue. The stoichiometry is approximately (Schnoor and Stumm, 1985):



Plant growth may thus affect the budgets of most of the major solutes; the solutes least affected are Na and Cl. When plants die and decompose, the process is reversed and the elements are returned to the soil.

If a forest (or grassland) is in steady state, that is to say the growth of new vegetation is exactly balanced by the death and decay of old vegetation, the biomass will be neither a net source nor a sink in the mass-balance equation. However, in forested catchments, the biomass is rarely in a steady state. Even without human intervention such as tree cutting or planting, forests typically go through cycles of gradual biomass increase interrupted by catastrophic events, such as fire or disease, that result in rapid biomass loss (Vitousek and Reiners, 1975). It is only on a very long time scale—a scale of centuries—that the biomass of a forest can be considered in steady state. Hubbard Brook, New Hampshire, in the northeastern United States, is an example of a catchment where the biomass increment is large compared to the weathering term (Fig. 12-3). According to the data of Likens et al. (1977), the net uptake of Ca in the form of biomass increment and forest floor (organic) increment was 45 percent of the amount released by weathering. For potassium, the biomass increment was 86 percent of the amount



**FIGURE 12-3** (a) Calcium and (b) potassium fluxes at the Hubbard Brook Experimental Watershed (data from Likens et al., 1977).

released by weathering: the net outflow of K from the catchment (runoff–atmospheric deposition) was only 14 percent of the K calculated to be released by chemical weathering. More recent measurements have decreased the biomass uptake term relative to the weathering term, but it is still a major part of the budget.

The biomass term in Eq. (12–1) can be measured directly by measuring the rate of growth of trees and the chemical composition of different tissues. This requires long-term measurements over several years, implying a significant investment of time and resources (e.g., Likens et al., 1977). Even if the long-term average biomass uptake rate is known, the rate may vary from year to year depending on weather conditions, particularly the availability of moisture.

The term *biomass* as used here includes non-living organic matter on the ground surface and in the soil. This organic matter contains cations such as calcium (and, particularly, nitrogen species), so changes in its decomposition rate may also cause a net flux of inorganic solutes.

It is hard to generalize about the overall importance of biomass change in mass-balance budgets. It will be at a maximum where weathering rates are low and a large amount of aggrading biomass is present, as in New Hampshire. The effect will be much less where vegetation is sparse; in Loch Vale, Colorado, a high-elevation catchment on granitic bedrock, the biomass term is small compared to the weathering term (Baron, 1992). The relative effect of biomass will be less where the input of cations from weathering is greater, which corresponds to bedrock that is less resistant to chemical weathering. The elements most affected will, of course, be those that are used by plants as nutrients (phosphorus, nitrogen species, potassium, and calcium). The budgets of nitrogen species and phosphorus are normally dominated by biological processes.

**Solutes from Changes in the Exchange Pool.** Soils contain exchangeable cations and anions that are in equilibrium with the soil solution. As the composition of the soil solution changes, ions will be exchanged between the solid phase and solution. If the soil solution composition does not change with time, adsorbed ions will not change either, and ion exchange will make no net contribution to the solute budget. In the short term, changes in solution composition occur as a result of precipitation events, evaporation, and growth cycles

of plants. It is often assumed that these changes average out over an annual cycle, so that on a time scale longer than a year, they cause no net change to the exchange pool and hence no net contribution to solute flux.

If there is a permanent change in the chemistry of atmospheric input, this will cause a unidirectional change in the exchange pool. If, for example, the concentration of  $H^+$  in precipitation increases, the  $H^+$  [or  $Al^{3+}$  generated from dissolution of  $Al(OH)_3$  in response to the input of  $H^+$ ] will displace other cations (commonly mostly  $Ca^{2+}$ ) from exchange sites, and these cations will appear in the outflow from the catchment (e.g., Reuss and Johnson, 1986). If the composition of precipitation remained constant, the composition of the exchange pool would gradually adjust to the new input and a new steady state, in which there was no net change in the exchange pool over time, would be established. The time taken by the exchange pool to adjust to a change in atmospheric input is generally quite long—on a time-scale of decades—because the reservoir of exchangeable ions in the soil is generally large compared to the annual input from the atmosphere.

Sulfate may also be adsorbed by soil, particularly where the pH is low and abundant oxyhydroxides are present (Chapter 5). This is discussed in more detail in the following chapter.

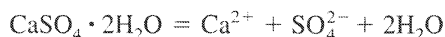
If a catchment does not receive a large input of anthropogenic acidity from the atmosphere, it is generally assumed that the exchange pool is in steady state, and is not a net contributor of (or removal process for) solutes.

**Solutes from Chemical Weathering of Minerals.** Mineral weathering is the dissolution or alteration of minerals present in the bedrock. In most unpolluted catchments it is the dominant source of solutes. Generally speaking, the solutes from chemical weathering are determined by difference: they are what is left after the solutes in the catchment outflow have been corrected for atmospheric input, biomass change, and ion exchange. In reality, the argument is often made that the biomass and ion exchange terms in Eq. (12-1) are negligible, and they are ignored.

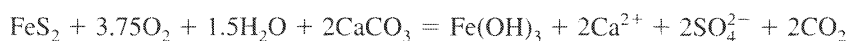
Catchment mass balances are usually normalized to unit area of land surface—fluxes are commonly reported in moles/ha/y. Calculations are also performed on the basis of l of runoff. This is no problem when only mineral weathering reactions are being considered; however, it may be difficult to convert biomass uptake rates from moles/ha/y to moles/l of runoff.

### Mineral Weathering Reactions

The main purpose of this section is to show how the chemistry of surface waters and groundwaters can be related to specific rock alteration reactions. Some examples are fairly obvious: a high concentration of sodium and chloride can usually be related to dissolution of halite (sodium chloride). A high concentration of calcium and sulfate is more ambiguous. It could come from dissolution of gypsum ( $CaSO_4 \cdot 2H_2O$ ) or anhydrite ( $CaSO_4$ ),



or it could come from oxidation of pyrite ( $FeS_2$ ) and reaction with calcite:



There is no way (except perhaps by a study of sulfur isotopes; Chapter 14) to distinguish between these alternatives without investigation of the rocks involved. Weathering of the minerals in silicate rocks is less straightforward and will be discussed in some detail.

**Sierra Nevada Springs, California and Nevada.** Garrels and Mackenzie (1967) discussed in detail the origin of the dissolved constituents of some springs in the Sierra Nevada (California and Nevada). This work was a “classic,” defining the logic that has been used in many subsequent studies. We shall review the original paper in some detail before going on to more recent studies. The rocks from which the springs issued were granitic, ranging from quartz diorite to quartz microcline gneiss (see the Glossary for explanations of mineral and rock names). Feldspars and quartz were the major minerals, with accessory hornblende and biotite. K-feldspar and plagioclase were about equally abundant; andesine was the dominant plagioclase. Kaolinite was identified as an important alteration product, and, although other secondary minerals were observed, the bulk of the residue apparently had a chemical composition near that of kaolinite.

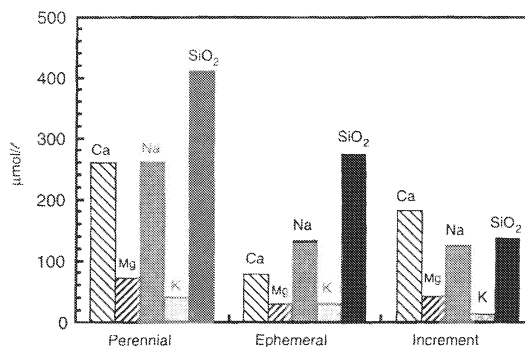
The *ephemeral* springs (flowing for only part of the year) and the *perennial* springs (flowing year round) of the area were considered separately (Table 12-1; Fig. 12-4). The ephemeral springs had a calculated  $P_{\text{CO}_2}$  of  $10^{-1.8}$  atm, illustrating the effect of soil biota in adding  $\text{CO}_2$  to the soil atmosphere. The perennial springs had approximately the same  $\Sigma\text{CO}_2$  as the ephemeral springs, but a lower  $P_{\text{CO}_2}$  because more of the original  $\text{H}_2\text{CO}_3$  had been converted to  $\text{HCO}_3^-$  by weathering reactions.

**Ephemeral Springs.** Garrels and Mackenzie (1967) performed a calculation to show that the dissolved constituents of the ephemeral springs could be explained by reaction of  $\text{CO}_2$ -charged rainwater with plagioclase feldspar and minor amounts of biotite and K-feldspar (Table 12-2). First, the cations and anions in snow were subtracted from the solutes in the spring water to determine the materials derived from the rock (possible biomass change and ion exchange were ignored). Next, a small correction was made to the  $\text{HCO}_3^-$  concentration to give exact charge balance (this step is of no real significance; it simply avoids possible artifacts that could arise from unbalanced charges). Then  $\text{Na}^+$ ,  $\text{Ca}^{2+}$ ,  $\text{HCO}_3^-$ , and dissolved  $\text{SiO}_2$  were subtracted in the proportions that would be derived from converting plagioclase into kaolinite, using up all the  $\text{Na}^+$  and  $\text{Ca}^{2+}$ . The calculated plagioclase composition was similar to that found

**TABLE 12-1** Mean Values for Compositions of Ephemeral and Perennial Springs of the Sierra Nevada [after Garrels and Mackenzie, 1967]

	<i>Ephemeral Springs</i>		<i>Perennial Springs</i>		<i>Difference</i> $\mu\text{mol/l}$
	ppm	$\mu\text{mol/l}$	ppm	$\mu\text{mol/l}$	
Ca	3.11	78	10.4	260	182
Mg	0.70	29	1.70	71	42
Na	3.03	134	5.95	259	125
K	1.09	28	1.57	40	12
$\text{HCO}_3^-$	20.0	328	54.6	895	567
$\text{SO}_4$	1.00	10	2.38	25	15
Cl	0.50	14	1.06	30	16
$\text{SiO}_2$	16.4	273	24.6	410	137
Al	0.03		0.02		
Fe	0.03		0.03		
F	0.07		0.09		
$\text{NO}_3^-$	0.02		0.28		
TDS	36.0		75.0		
pH (median value)	6.2		6.8		

**FIGURE 12-4** Major-element composition of Sierra Nevada springs (data from Garrels and Mackenzie, 1967). The “increment” represents the difference between the perennial and ephemeral springs.



in the rocks. Next, all the  $Mg^{2+}$  and proportionate amounts of  $K^+$ ,  $HCO_3^-$ , and  $SiO_2$  were assigned to conversion of biotite (end-member phlogopite for simplicity) into kaolinite. This left small amounts of  $K^+$ ,  $HCO_3^-$ , and  $SiO_2$ , which were assigned to the conversion of K-feldspar to kaolinite. Some dissolved  $SiO_2$ —about 4 percent of the original amount—remained unaccounted for. This amount is within the analytical uncertainties of the original analyses and was considered to be zero.

The balance worked so well that it was concluded that the weathering reactions chosen were a realistic representation of the natural system. Several general conclusions could be made:

1. The weathering reactions in Table 12-2 account for virtually all the dissolved  $SiO_2$ . Therefore, the dissolved silica came from the breakdown of silicates and not from dissolution of quartz.

2. About 80 percent of the rock-derived constituents came from the breakdown of plagioclase alone. Even though K-feldspar was abundant in the rocks, little breakdown occurred. It is a general observation that the more easily weathered minerals in a rock contribute disproportionately to the springs and streams, and is what would be expected on the basis of the different dissolution rates presented in Table 11-2. Minerals such as quartz and K-feldspar remain as a solid residue and would eventually be removed by physical erosion.

**Perennial Springs.** The perennial springs (Table 12-1) represent waters that have circulated deeper and have been in contact with the rocks for longer periods of time. The waters were less acidic because much of the original  $H_2CO_3$  had been converted to  $HCO_3^-$  by reaction with the rock, and they contained higher concentrations of ions and dissolved silica than the ephemeral springs. We might expect intuitively that different weathering reactions would occur in the different environment. The difference is obvious if the ephemeral spring composition is subtracted from the perennial spring composition (Table 12-1; Fig. 12-4). The ratio of  $SiO_2$  to  $Na^+$  in the increment was about 1:1, whereas it was about 2:1 in the ephemeral springs. Because weathering of plagioclase to kaolinite releases dissolved  $SiO_2$  and  $Na^+$  in a 2:1 ratio, and plagioclase was the only reasonable source of  $Na^+$ , a solid other than kaolinite must have been produced. A smectite (or montmorillonite type\*) clay mineral seems the most likely candidate. Garrels and Mackenzie’s reconstruction of the perennial springs is shown in

\*Smectite is preferred over montmorillonite as a general term for the expandable 2:1 clay mineral group. Many previous authors (including Garrels and Mackenzie) have used montmorillonite in the broad sense (see Chapter 4).

**TABLE 12-2** Reconstruction of Source Minerals for Ephemeral Springs of the Sierra Nevada (after Garrels and Mackenzie, 1967). Units are  $\mu\text{moles./l.}$ 

	<i>Na</i>	<i>Ca</i>	<i>Mg</i>	<i>K</i>	<i>HCO<sub>3</sub></i>	<i>SO<sub>4</sub></i>	<i>Cl</i>	<i>SiO<sub>2</sub></i>
Concentrations in spring	134	78	29	28	328	10	14	273
Corr. for atmos. input	110	68	22	20	310	0	0	270
Alteration of plagioclase to kaolinite: $177 \text{ Na}_{0.62}\text{Ca}_{0.38}\text{Al}_{1.38}\text{Si}_{2.62}\text{O}_8 + 246 \text{ CO}_2 + 367 \text{ H}_2\text{O} = 123 \text{ Al}_2\text{Si}_2\text{O}_5(\text{OH})_4 + 110 \text{ Na}^+ + 68 \text{ Ca}^{2+} + 246 \text{ HCO}_3^- + 220 \text{ SiO}_{2(\text{aq})}$								
Remainder	0	0	22	20	64	0	0	50
Alteration of biotite to kaolinite: $7.3 \text{ KMg}_3\text{AlSi}_3\text{O}_{10}(\text{OH})_2 + 51 \text{ CO}_2 + 26 \text{ H}_2\text{O} = 3.7 \text{ Al}_2\text{Si}_2\text{O}_5(\text{OH})_4 + 22 \text{ Mg}^{2+} + 7.3 \text{ K}^+ + 51 \text{ HCO}_3^- + 15 \text{ SiO}_2$								
Remainder	0	0	0	13	13	0	0	35
Alteration of K-feldspar to kaolinite: $13 \text{ KAlSi}_3\text{O}_8 + 13 \text{ CO}_2 + 19.5 \text{ H}_2\text{O} = 6.5 \text{ Al}_2\text{Si}_2\text{O}_5(\text{OH})_4 + 13 \text{ K}^+ + 26 \text{ SiO}_2 + 13 \text{ HCO}_3^-$								
Remainder	0	0	0	0	0	0	0	9
<b>Overall reaction:</b> $177 \text{ Plagioclase} + 7.3 \text{ Biotite} + 13 \text{ Kspar} (+ \text{H}_2\text{O} + \text{CO}_2) = 133 \text{ Kaolinite} + 110 \text{ Na}^+ + 68 \text{ Ca}^{2+} + 22 \text{ Mg}^{2+} + 20 \text{ K}^+ + 270 \text{ SiO}_2 + 310 \text{ HCO}_3^-$								

Table 12-3. The increased concentrations of  $\text{Cl}^-$  and  $\text{SO}_4^{2-}$  were assigned to  $\text{NaCl}$  and  $\text{CaSO}_4$ , respectively. The amounts were small, so the choice of phase did not matter much for subsequent calculations. Next, all of the  $\text{Mg}^{2+}$  and  $\text{K}^+$  were assigned to alteration of biotite to kaolinite (slight imbalance for  $\text{K}^+$  was ignored). This left  $\text{Na}^+$  equal to  $\text{SiO}_2$ , so the remaining  $\text{SiO}_2$  was apportioned between the alteration of plagioclase to kaolinite and to smectite. The ratio of smectite to kaolinite was chosen to give exact balance for dissolved  $\text{SiO}_2$ . The plagioclase composition used was the same as that deduced from the ephemeral spring compositions, and the smectite composition chosen was that of a calcium beidellite (Chapter 4). Aluminous smectites seemed to be prevalent under weathering conditions, and in such dilute waters the exchange positions should have been largely occupied by  $\text{Ca}^{2+}$ . After these steps, a considerable amount of  $\text{Ca}^{2+}$  and  $\text{HCO}_3^-$  remained, which was assigned to dissolution of minor amounts of carbonate minerals.

The mass balance on the perennial springs is less satisfying than the one on the ephemeral springs.  $\text{CaSO}_4$  is not a very plausible source for  $\text{SO}_4^{2-}$ , and the choice of a composition for the smectite is somewhat arbitrary. A major question is whether sufficient  $\text{CaCO}_3$  really existed in the rocks, or whether the requirement to invoke calcite dissolution showed a fundamental problem with the approach. The question will be discussed in the context of specific examples later in this chapter.

Despite the uncertainties, the mass balance calculation clearly indicates that some material with a higher Si/Al ratio than kaolinite is formed by prolonged contact between water and rock, and by far the most probable material is a member of the smectite group.

**Matrix Solutions to Mass-Balance Equations.** Mass-balance calculations of the type performed by Garrels and Mackenzie can be represented as a matrix of simultaneous equations (Velbel, 1986). They can be carried out by a relatively simple spreadsheet approach

**TABLE 12-3** Reconstruction of Weathering Reactions During Deeper Circulation, Sierra Nevada Sprints (after Garrels and Mackenzie, 1967). Units are  $\mu\text{moles/l}$ .

	<i>Na</i>	<i>Ca</i>	<i>Mg</i>	<i>K</i>	<i>HCO<sub>3</sub></i>	<i>SO<sub>4</sub></i>	<i>Cl</i>	<i>SiO<sub>2</sub></i>
Initial concentration (perennial – ephemeral)	125	182	42	12	539 <sup>a</sup>	15	16	137
Corr. for atmos. input	109	167	42	12	539	0	0	137
Alteration of biotite to kaolinite: $14 \text{ KMg}_3\text{AlSi}_3\text{O}_{10}(\text{OH})_2 + 98 \text{ CO}_2 + 49 \text{ H}_2\text{O} =$ $7 \text{ Al}_2\text{Si}_2\text{O}_5(\text{OH})_4 + 42 \text{ Mg}^{2+} + 14 \text{ K}^+ + 98 \text{ HCO}_3^- + 28 \text{ SiO}_2$								
Remainder	109	167	0	-2	441	0	0	109
Alteration of plagioclase to kaolinite: $38 \text{ Na}_{0.62}\text{Ca}_{0.38}\text{Al}_{1.38}\text{Si}_{2.62}\text{O}_8 + 52 \text{ CO}_2 + 78 \text{ H}_2\text{O} =$ $26 \text{ Al}_2\text{Si}_2\text{O}_5(\text{OH})_4 + 24 \text{ Na}^+ + 14 \text{ Ca}^{2+} + 52 \text{ HCO}_3^- + 47 \text{ SiO}_{2(\text{aq})}$								
Remainder	85	153	0	-2	389	0	0	62
Alteration of plagioclase to smectite: $137 \text{ Na}_{0.62}\text{Ca}_{0.38}\text{Al}_{1.38}\text{Si}_{2.62}\text{O}_8 + 162 \text{ CO}_2 + 162 \text{ H}_2\text{O} =$ $81 \text{ Ca}_{0.17}\text{Al}_{2.33}\text{Si}_{3.67}\text{O}_{10}(\text{OH})_2 + 85 \text{ Na}^+ + 38 \text{ Ca}^{2+} + 162 \text{ HCO}_3^- + 62 \text{ SiO}_{2(\text{aq})}$								
Remainder	0	115	0	-2	227	0	0	0
Dissolution of calcite: $115 \text{ CaCO}_3 + 115 \text{ H}_2\text{O} + 115 \text{ CO}_2 = 115 \text{ Ca}^{2+} + 230 \text{ HCO}_3^-$								
Remainder <sup>b</sup>	0	0	0	-2	-3	0	0	0
<b>Overall reaction:</b> $175 \text{ Plag} + 14 \text{ Biotite} + 115 \text{ Calcite} (+ \text{H}_2\text{O} + \text{CO}_2) =$ $81 \text{ Smectite} + 33 \text{ Kaol} + 109 \text{ Na}^+ + 167 \text{ Ca}^{2+} + 42 \text{ Mg}^{2+} + 12 \text{ K}^+ + 539 \text{ HCO}_3^- + 137 \text{ SiO}_2$								

<sup>a</sup>Bicarbonate number was adjusted slightly to make cations and anions balance.

<sup>b</sup>These numbers are effectively zero.

(Bowser and Jones, 1993; Finley and Drever, in press), or by more sophisticated computer programs such as BALANCE (Parkhurst et al., 1982), NETPATH (Plummer et al., 1991) and PHREEQC (Parkhurst, 1995). The matrix formulation for Garrels and Mackenzie's "increment" is shown in Fig. 12-5. The column for each mineral represents its stoichiometry; thus the column for plagioclase represents the formula  $\text{Ca}_{0.38}\text{Na}_{0.62}\text{Al}_{1.38}\text{Si}_{2.62}\text{O}_8$ ; the column for kaolinite represents  $\text{Al}_2\text{Si}_2\text{O}_5(\text{OH})_4$  [the relative proportions of O and (OH) do not matter]. The column vector on the right represents the water composition (or solute fluxes) being modeled (which can be in moles/l of solution or moles/ha of catchment). Al is shown with a concentration (flux) of zero to introduce the constraint that Al is conserved in the solid phases. The column vector "unknown coefficients" represents the coefficients to be determined. Each  $n$  represents the number of moles of that mineral that must react to satisfy the overall mass balance equation. The units of  $n$  are the same as the units of the water composition. A positive sign for  $n$  means that the mineral dissolves; a negative sign means that it precipitates. The values of  $n$  are obtained by a straightforward matrix inversion procedure. Mathematically, if the number of mineral phases in the calculation is equal to the number of chemical components in the system, a balanced reaction can generally be obtained. However, because the choice of minerals and the choice of compositions for these minerals is generally not unique; there are generally several sets of reactions that can "explain" the observed composition. The fact that a satisfactory balance is obtained does not prove that the reactions chosen are correct. A mass-balance calculation should incorporate as much information as possible on the compositions of minerals undergoing weathering, and being formed by weathering, in a particular catchment.



Element	Minerals used in calculation						Unknown	Solutes
	Plag	Bi	Ksp	Cc	Kaol	Smec	Coeff.	
Ca	0.38	0	0	1	0	0.17	$\begin{bmatrix} n_{\text{Plag}} \\ n_{\text{Bi}} \\ n_{\text{Ksp}} \\ n_{\text{Cc}} \\ n_{\text{Kaol}} \\ n_{\text{Smec}} \end{bmatrix} = \begin{bmatrix} 167 \\ 42 \\ 12 \\ 109 \\ 137 \\ 0 \end{bmatrix}$	
Mg	0	3	0	0	0	0		
K	0	1	1	0	0	0		
Na	0.62	0	0	0	0	0		
SiO <sub>2(aq)</sub>	2.62	3	3	0	2	3.67		
Al	1.38	1	1	0	2	2.33		

The solution to the matrix equation is:

Mineral	$n$ ( $\mu\text{moles per } \ell$ solution)
Plag	176
Biotite	14
Kspar	-2
Calcite	114
Kaol	-36
Smectite	-78

**FIGURE 12-5** Matrix formulation of the mass-balance equation for the "increment" (the difference between the mean compositions of perennial and ephemeral springs) of Garrels and Mackenzie (1967). Plag = plagioclase feldspar, Bi = biotite, Ksp = K-feldspar, Cc = calcite, Kaol = kaolinite, Smec = smectite.

### Mass-Balance Calculations in Groundwater Systems

The same general principles apply to using mass-balance calculations to understand the chemistry of groundwater. The simplest example would be to interpret the chemical evolution of water along a flow path, for which the program NETPATH (Plummer et al., 1991) was developed. NETPATH is incorporated into the newer code PHREEQC (Parkhurst, 1995). NETPATH performs the mineral dissolution-precipitation calculations discussed above. It also includes cation exchange as an option. Cation exchange (involving primarily Ca, Na, and Mg) turns out to be a major process affecting the chemistry of groundwater. Biomass change, in the sense discussed above, is not a major process affecting groundwater chemistry, but redox transformations involving organic matter, sulfur species, carbon species, and iron minerals may be very important. NETPATH has the capability of modeling such reactions, and also of keeping track of the isotopes of C, S, and O (Chapter 14), which serve as additional constraints to define the reactions that are taking place. NETPATH can also model mixing of waters in addition to reactions affecting a single water.

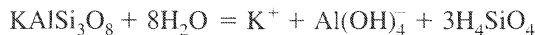
The results of mass-balance modeling based on NETPATH are, as with surface waters, generally not unique. Professional judgment is usually required to evaluate alternative scenarios. There may also be uncertainties associated with the assumptions behind the calculations. It is often assumed that two water samples (from two wells, for example) represent points along a flow path, and that the differences between them represent reactions along the flow path. It is also possible that (a) the waters are from different aquifers and are genetically unrelated, or (b) the composition of recharge water has changed with time, so that differences

are due to changes in the chemistry of the water reaching the first well rather than to reactions occurring between them. Provided these caveats are kept in mind, NETPATH provides a powerful tool for understanding the chemical evolution of groundwater.

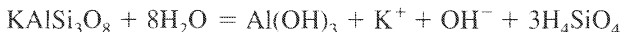
## THE THERMODYNAMIC APPROACH TO MINERAL WEATHERING REACTIONS

In this section we consider chemical equilibria among minerals and natural waters and try to evaluate the extent to which natural waters can be represented as equilibrium systems. We start by considering the reaction of K-feldspar with water. Helgeson et al. (1969) treated this problem as an example of irreversible mass transfer. The basic assumption of the calculations was that chemical equilibrium is maintained between the solution and all secondary minerals. It was also assumed that the alteration products are well-defined solids of fixed composition. A simpler way to view the calculation would be to consider what would happen if successive small amounts of K-feldspar were added to distilled water and the system were allowed to achieve chemical equilibrium between each addition. The chemical changes can best be shown on the stability diagram discussed in Chapter 11 (Fig. 12-6).

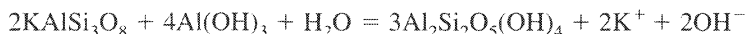
Initially, the feldspar would dissolve completely:



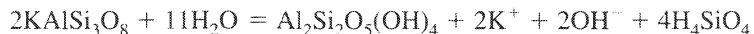
Pure water would have a pH of 7, so it is appropriate to write dissolved Al in the form of  $\text{Al}(\text{OH})_4^-$  (see Fig. 10-3). At some point (A on Fig. 12-6), the solution would become saturated with respect to gibbsite. K-feldspar would then alter to gibbsite:



The release of  $\text{K}^+$ ,  $\text{OH}^-$ , and  $\text{H}_4\text{SiO}_4$  would cause the solution composition to change along the path A–B (the composition moves to the right because  $\text{H}_4\text{SiO}_4$  is increasing, and upward because  $\text{K}^+$  is increasing and  $\text{H}^+$  decreasing). At B, the solution would be in equilibrium with kaolinite. The solution composition could not leave the gibbsite stability field as long as gibbsite remained in the system, so further additions of K-feldspar would cause the previously formed gibbsite to react to form kaolinite:

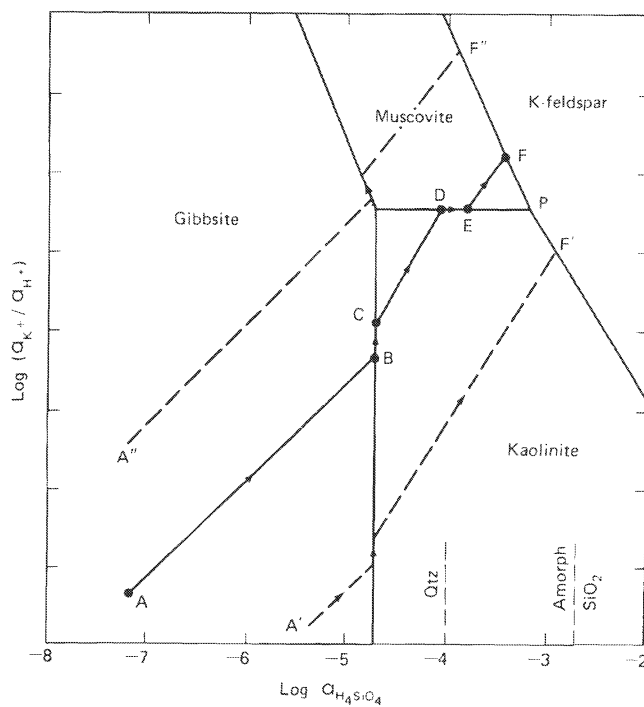


Another way to look at this reaction would be to say that K-feldspar would react with water, releasing ions and  $\text{H}_4\text{SiO}_4$ ; because the  $\text{H}_4\text{SiO}_4$  concentration in solution could not increase while gibbsite remained, the  $\text{H}_4\text{SiO}_4$  released would be consumed by conversion of gibbsite to kaolinite. The solution composition would move up the gibbsite-kaolinite stability boundary until all the gibbsite had been used up (point C). It might appear on Fig. 12-6 that the amount of gibbsite produced on the long segment A–B would not be consumed over the small segment B–C. On a log-log plot, however, the lengths of segments cannot be compared in this simple way. At point C, gibbsite would no longer be present in the system, the solution would no longer be constrained to the gibbsite stability field, and K-feldspar would alter to kaolinite:

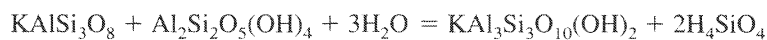


Because  $\text{K}^+$ ,  $\text{OH}^-$ , and  $\text{H}_4\text{SiO}_4$  would all be released, the solution composition would change diagonally across the kaolinite stability field. What happens next depends critically on the free-energy values used to calculate the positions of the stability boundaries on Fig. 12-6. With

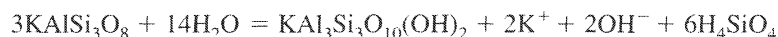
**FIGURE 12-6** Some possible theoretical paths of solution composition as K-feldspar reacts with water. The numerical scale on the vertical axis has been deliberately omitted because details of the diagram are highly sensitive to assumed free-energy values, and there is no overwhelming reason for choosing one particular set. Solid line A–F is the path discussed in the text, but paths A'–F' and A''–F'' would both be within the uncertainty of existing free-energy data.



the free-energy values used in drawing the solid line, the solution composition would intersect the kaolinite-muscovite stability boundary at D. The reaction would consist of dissolving feldspar reacting with previously-formed kaolinite to produce muscovite:



This reaction is analogous to the reaction at the kaolinite-gibbsite boundary, and the solution composition would move along the kaolinite-muscovite boundary until all the kaolinite was used up (point E). After that, K-feldspar would alter to muscovite:



The solution composition would then move to F. At F, the solution would be in equilibrium with K-feldspar, and no further reaction would take place. The only secondary mineral remaining would be muscovite.

With slightly different free-energy values for the phases involved (well within the uncertainties of existing values), the solution composition could reach the triple point P before all the kaolinite was used up, or it could intersect the kaolinite-K-feldspar boundary (point F') rather than the kaolinite-muscovite boundary.

In natural systems,  $\text{CO}_2$  is almost always present, so  $\text{HCO}_3^-$  is produced as an anion rather than  $\text{OH}^-$ :

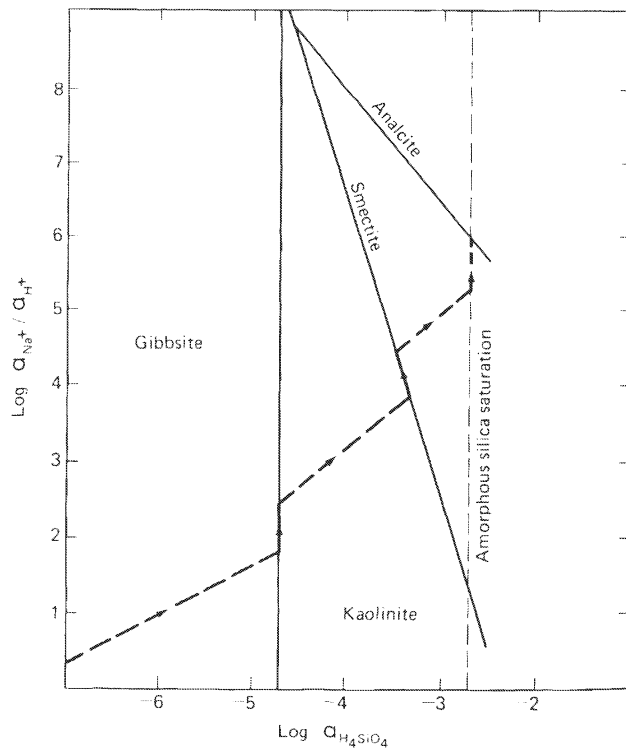


This decreases the pH rise associated with feldspar alteration, so the solution composition would probably follow approximately the dashed line A'–F' in Fig. 12-6.

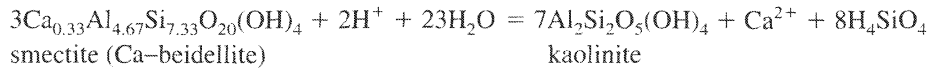
The alteration of albite on the same assumptions follows a similar path through the gibbsite and kaolinite stability fields (Fig. 12-7). The path would reach the kaolinite–smectite boundary (whose slope and position depend on the composition and free energy assumed for the smectite) and then enter the smectite stability field. Defining a composition and free energy for “smectite” to be used in calculations is a problem both because natural smectites are variable in composition and rarely approximate closely the idealized composition used in calculations, and because true chemical equilibrium is probably not attained. What we try to do is choose a hypothetical composition and free energy such that the computed behavior of our idealized phase corresponds as closely as possible to that of smectites in natural systems. This either implies that equilibrium between waters and smectites is commonly approached in natural waters, or that departures from equilibrium are systematic and can be represented adequately by equilibrium with a hypothetical phase. The path would probably reach the amorphous silica saturation line and then move up that line into the stability field of a zeolite or albite. It is not worth pursuing the calculation further, as the detailed stability relations among albite, smectite, and the various zeolites are not well known. The solubility of a sodium carbonate mineral would probably be the ultimate limit on how high up the amorphous silica saturation line a solution could go in nature.

If natural systems conform to the model, we would expect waters that have been in contact with igneous rock for a short time to plot toward the lower left in  $\log (a_{\text{M}^{n+}}/a_{\text{H}^+})$  versus  $\log a_{\text{H}_4\text{SiO}_4}$  diagrams and to produce gibbsite or kaolinite as a weathering product. As the time of contact between water and rock increases, the water composition should move diagonally across the diagram to the kaolinite–smectite boundary. Further alteration should produce smectite and not kaolinite.

**FIGURE 12-7** Predicted path of solution composition as albite reacts with water at 25°C (after Helgeson et al., 1969). Other zeolites are probably more stable than analcite at high silica activities, but free-energy data are lacking.



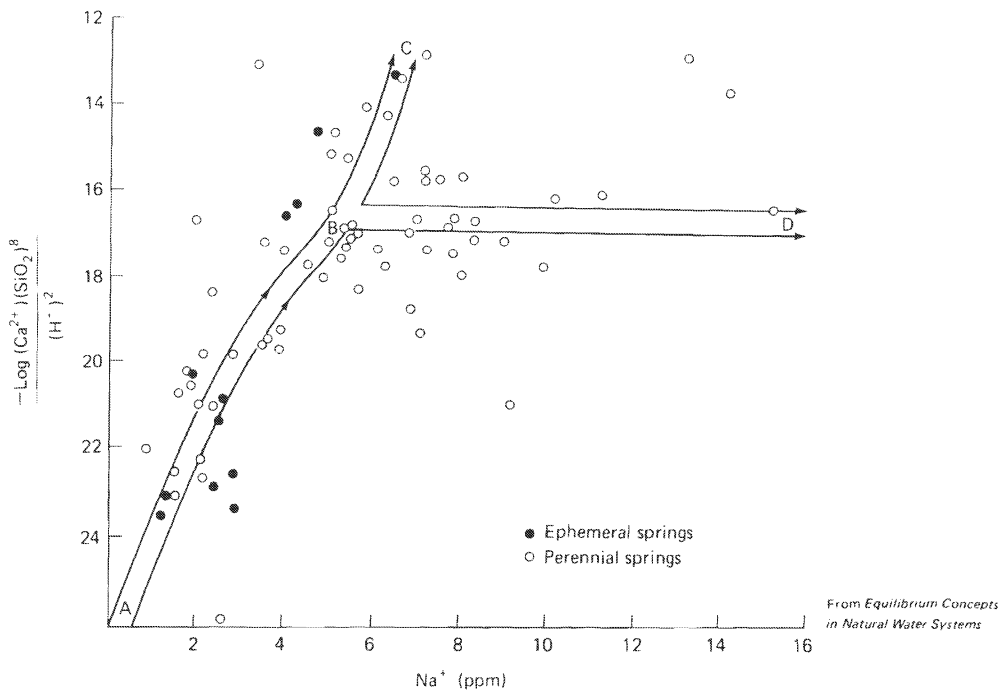
The Sierra Nevada springs studied by Feth et al. (1964) and by Garrels and Mackenzie (1967) seem to fit the prediction well. The mass-balance arguments discussed earlier indicated that brief interaction, represented by the ephemeral springs, produced only kaolinite, whereas prolonged interaction, represented by the perennial springs, produced both kaolinite and smectite. Garrels and Mackenzie tested the hypothesis of equilibrium control by considering the reaction:



for which the reaction quotient is

$$Q = \frac{a_{\text{Ca}^{2+}} \cdot a_{\text{H}_4\text{SiO}_4}^8}{a_{\text{H}^+}^2}$$

Waters in equilibrium with kaolinite and smectite should have a constant value for the quotient, equal to the equilibrium constant. Waters saturated with respect to kaolinite but undersaturated with respect to smectite should have a value for the quotient less than the equilibrium constant. The actual values of the quotient for the Sierra Nevada springs are shown in Fig. 12-8. If alteration to kaolinite in a closed system (constant  $\Sigma\text{CO}_2$ ) were the only process taking place, the



**FIGURE 12-8** Reaction quotient for the Ca-beidellite-kaolinite reaction plotted as a function of Na concentration in Sierra Nevada spring waters. Arrow ABC is the path of water evolution calculated for the reaction from plagioclase ( $\text{Na}_{0.62}\text{Ca}_{0.38}$ ) to kaolinite in a closed system with an initial dissolved  $\text{CO}_2$  concentration of 0.0006 mol/l. Arrow ABD is the expected path if evolution is also controlled by the two-phase equilibrium kaolinite-smectite.  $\text{SiO}_2$  on the figure is equivalent to  $\text{H}_4\text{SiO}_4$ . [Garrels, R. M., and Mackenzie, F. T., in *Equilibrium Concepts in Natural Water Systems*. Advances in Chemistry Series, No. 67, ed. W. Stumm (Washington, D.C.: American Chemical Society, 1967), p. 230.]

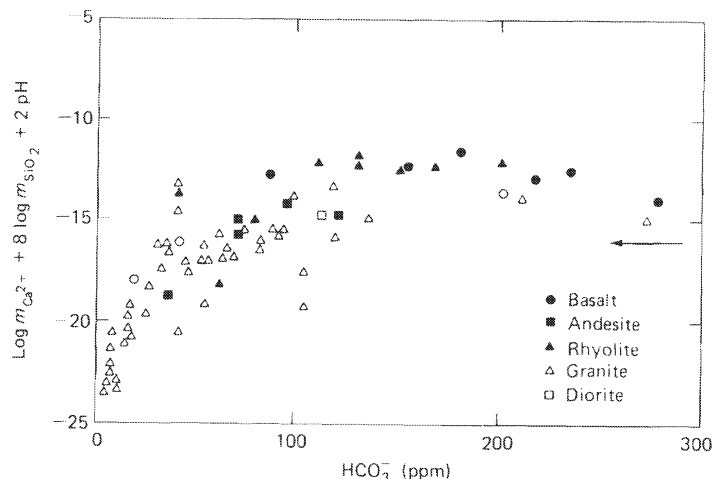
points should plot along the path ABC. If strict equilibrium were maintained with both kaolinite and smectite (when smectite is stable), the points should plot along ABD. The points show a great deal of scatter. Garrels and Mackenzie summarized by saying:

Despite the scatter, it is clear that the ephemeral springs alter feldspar chiefly to kaolinite and that many of the perennial springs, although their evolution is to kaolinite, have compositions that suggest a halt in that path of evolution and possible control by equilibration with both phases.

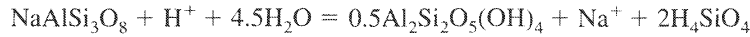
If this is true, and it must be regarded as a highly tentative conclusion, the upper limits of silica content of many natural waters, which are far less than saturation with amorphous silica (115 ppm), may well be controlled by equilibrium between the waters and various silicate phases. This does not mean that the controlling solids are well crystallized, clearly distinguishable substances, but there is definitely an interplay between the waters and solid aluminosilicates. Furthermore, the aluminosilicates apparently differ from each other in important compositional steps, and are not simply continuous gradations resulting from progressive adsorption and alteration as water compositions change. (p.232)

Garrels (1967) plotted a large number of published water analyses from different lithologies on a similar graph and obtained a more convincing cutoff (Fig. 12-9). The hypothesis is that the kaolinite–smectite boundary forms a limit on the compositions of most natural waters. It must be pointed out, however, that the position of the kaolinite–smectite boundary, and hence the free energy of formation of the smectite, is deduced from the distribution of points on graphs such as Figs. 12-8 and 12-9.

Pačes (1972, 1973) used a slightly different approach to study equilibrium and disequilibrium in groundwaters from granitic terrains. He presented his results in terms of a *disequilibrium index I*, which is the logarithm of the ratio of the reaction quotient  $Q$  to the equilibrium constant  $K_T$  for a particular reaction. Consider, for example, the reaction of albite to kaolinite:



**FIGURE 12-9** Plot of logarithm of kaolinite-smectite reaction quotient against  $\text{HCO}_3^-$  concentration (indicating extent of reaction) for waters from various igneous rocks. The roughly horizontal upper limit is attributed to control by equilibrium with kaolinite and smectite (from Garrels, 1967). Arrow shows the position of line B–D on Fig. 12-8.  $\text{SiO}_2$  on the figure is equivalent to  $\text{H}_4\text{SiO}_4$ .



$Q$  and  $K_T$  are given by expression:

$$\frac{a_{\text{Na}^+} \cdot a_{\text{H}_4\text{SiO}_4}^2}{a_{\text{H}^+}}$$

and the disequilibrium index for the albite–kaolinite reaction ( $I_{\text{ab-k}}$ ) is given by

$$\begin{aligned} I_{\text{ab-k}} &= \log \left[ \frac{(a_{\text{Na}^+} \cdot a_{\text{H}_4\text{SiO}_4}^2 / a_{\text{H}^+})_{\text{in situ}}}{K_T} \right] \\ &= \log a_{\text{Na}^+} + 2 \log a_{\text{H}_4\text{SiO}_4} + \text{pH} - \log K_T \end{aligned}$$

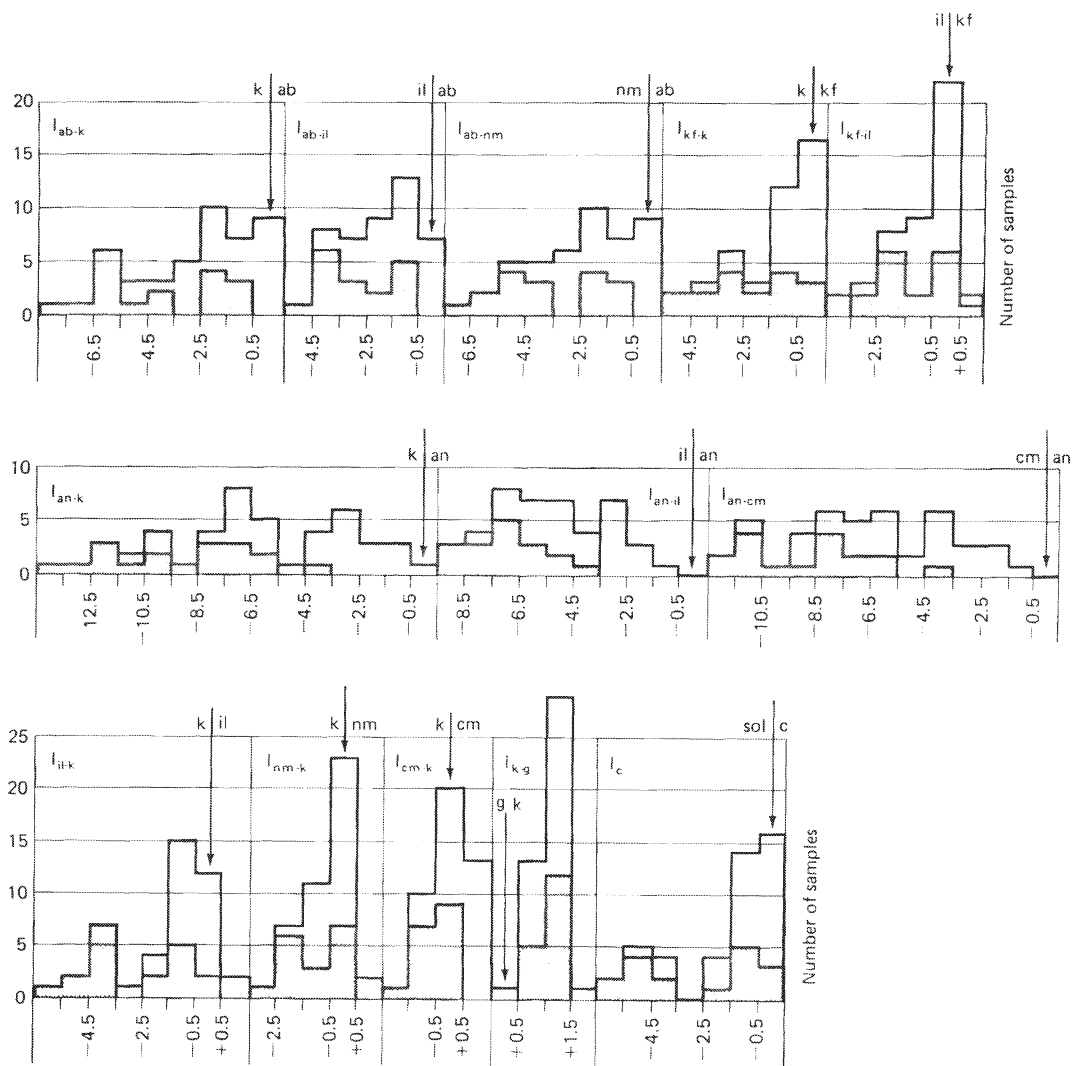
A similar disequilibrium index can be calculated for any mineral pair. The disequilibrium index can be regarded as a quantitative way of saying how far a water composition would be from a particular stability boundary on the type of stability diagram shown in Figs. 10-6, 10-8, and 10-9. It has the additional advantage that it can be used for multicomponent systems that cannot be projected conveniently on a two-dimensional diagram. A disadvantage of the approach is that it must rely on a specific set of assumed stoichiometries and thermodynamic data, and thus uncertainties in both stoichiometry and free energy tend to be ignored.

The distribution of disequilibrium indexes for waters from the Bohemian Massif of the Czech Republic (shaded) and other parts of the world is shown in Fig. 12-10. Pačes considered a disequilibrium index smaller than  $\pm 0.5$  to represent equilibrium and larger values to represent significant departures from equilibrium. The indexes for anorthite- and albite-clay mineral pairs are almost all negative, indicating that plagioclase feldspars are unstable with respect to clay minerals. K-feldspar–kaolinite and K-feldspar–illite are fairly close to equilibrium. Gibbsite and illite are generally unstable with respect to kaolinite. Some waters are in equilibrium with calcite, and some are undersaturated. Approximately half the waters appear to be in equilibrium with kaolinite plus Na- or Ca-smectite.

In summary, it appears that the compositions of many natural waters correspond approximately to what would be expected from equilibration with secondary clay minerals. Waters rarely achieve equilibrium with the primary minerals of igneous rocks, except quartz and sometimes K-feldspar. It would be unreasonable to expect complete equilibration between secondary clay minerals and solution. If a clay mineral is to form at a finite rate, some degree of supersaturation with respect to that mineral will be required. As the pH of a stream fluctuates daily owing to photosynthesis and decay, we would not expect smectite to grow from kaolinite in the daytime and revert to kaolinite at night. We should also be aware that there is a large uncertainty in the correct position of the kaolinite-smectite stability boundary, and the assumption that equilibrium exists in natural systems has been an influence in selecting the “correct” position of the boundary. Finally, as discussed in Chapter 10, we cannot really say whether a given aluminosilicate is in equilibrium with a particular water unless we know the dissolved aluminum content of the water. We shall address some of these questions again in the context of specific examples later in this chapter.

## THE STATISTICAL APPROACH

A third approach to understanding the chemistry of natural waters is to investigate statistical associations among dissolved constituents and environmental parameters, such as lithology,



**FIGURE 12-10** Distribution of disequilibrium indexes for partial systems consisting of groundwater, two aluminosilicates, gibbsite, or calcite. The arrows indicate the equilibrium value, and the stable phase on each side of the arrow is indicated. ab = albite; kf = K-feldspar; an = anorthite; k = kaolinite; il = illite; nm = Na-smectite; cm = Ca-smectite; g = gibbsite; c = calcite; sol = solution. Shaded columns represent waters from the Bohemian Massif (after Pačes, 1972).

climate, relief, and population. A statistical association does not establish any cause-and-effect relationship, but it frequently presents data in such a way that cause-and-effect relationships can be deduced. As a simple example, numerous analyses of streams in a particular region might show a strong association between  $\text{Ca}^{2+}$  and  $\text{SO}_4^{2-}$ . A possible deduction would be that they were both derived from the same source, gypsum. The deduction might be wrong, because pyrite associated with calcite would produce the same effect. If, however, the geographic occurrence of waters high in  $\text{Ca}^{2+}$  and  $\text{SO}_4^{2-}$  correlated strongly with the outcrop of a



geologic unit known to contain gypsum, the cause-and-effect relationship would be reasonably (although not unequivocally) established.

The sort of association described above can often be seen by inspection or can be demonstrated statistically by simple *correlation analysis*. In correlation analysis, correlation coefficients are calculated for all possible pairs of variables (here the variables would include geological variables such as percent gypsum in the drainage basin in addition to the chemical variables). The correlation coefficient expresses numerically the extent to which two variables are statistically associated. A value of +1 indicates the two variables are perfectly correlated, a value of 0 indicates that the variables have no correlation at all (i.e., they are completely independent), and a value of -1 indicates that they are perfectly negatively correlated (an increase in one corresponds to a decrease in the other). Whether or not a correlation coefficient of less than 1 (absolute value) is statistically significant depends on the nature of the data; there is no general arbitrary value (0.5, for example) above which correlations are significant and below which they are not significant. Other statistical tests can be used to determine significance.

Another way to examine the data would be by *multiple regression analysis*. The multiple regression model assumes that a *dependent variable*,  $Y$  (e.g.,  $\text{SO}_4^{2-}$  concentration in stream water), is a function of several *independent variables*,  $X_1, X_2, X_3, \dots$  (e.g., percent of gypsum-containing rocks in the drainage basin, rainfall, and population density). For the case of three independent variables,

$$Y = a + bX_1 + cX_2 + dX_3$$

where  $a, b, c,$  and  $d$  are coefficients to be determined from the data. The multiple regression program computes "best-fit" values for  $a, b, c,$  and  $d$  and normalizes these coefficients to give the percent of the variance of the dependent variable "explained" by each independent variable. If a nonlinear relationship is postulated between dependent and independent variables, the dependent variables can be transformed (into logarithms, for example) before the multiple regression calculation is performed.

The most widely used statistical technique in geochemistry is *R-mode factor analysis*, particularly where no relationship among the variables can be preassumed. Excellent descriptions of factor analysis applied to geochemical problems are provided by Klován (1975) and by Jöreskog et al. (1976). The basic purpose of *R-mode factor analysis* is to find a set of "factors," few in number, that will "explain" the variance of a large number of analytical data. Suppose that we had a data matrix consisting of  $N$  variables (e.g., the concentrations of dissolved or suspended species, discharge, etc.) measured on  $n$  samples, presumably from different locations. (The input data are sometimes transformed to logarithms for input into a factor analysis program; this is theoretically desirable if the original data have a log normal rather than a normal distribution, as is often the case with geochemical data and other natural phenomena.) The data matrix would have the form:

	Sample 1	Sample 2	Sample 3	...	Sample $n$
Variable 1	$d_{1,1}$	$d_{1,2}$	$d_{1,3}$		$d_{1,n}$
Variable 2	$d_{2,1}$	$d_{2,2}$	$d_{2,3}$		$d_{2,n}$
Variable 3	$d_{3,1}$	$d_{3,2}$	$d_{3,3}$		$d_{3,n}$
...					
Variable $N$	$d_{N,1}$	$d_{N,2}$	$d_{N,3}$		$d_{N,n}$

Thus  $d_{1,2}$  might represent the concentration of sodium (variable 1) in sample 2, and so on.

In general, the variables in such a set of data are intercorrelated, but the correlations are hard to see, and the data are hard to interpret as they stand. The purpose of *R*-mode factor analysis is to reduce the variables to a smaller set of “factors,” which are interpretable. The factors (“factor” here is used in a strictly mathematical sense; it does not imply a causative factor) group together correlated variables, and if they are interpretable, it means that they can be associated directly or indirectly with some specific source or process.

The mathematics of factor analysis are beyond the scope of this book. A very brief outline is given here, and the reader should consult the references mentioned above for more details. First the variables are standardized according to:

$$z_{i,j} = \frac{d_{i,j} - \bar{d}_i}{s_i}$$

where  $\bar{d}_i$  and  $s_i$  are the mean and standard deviation of all  $d_{i,j}$ ,  $j = 1, n$ . With this transformation, the mean of each transformed variable is zero and the standard deviation is 1. The *R*-mode factor analysis program (a computer is always required) then expresses the standardized variables in terms of  $k$  factors, the number  $k$  being (usually) selected by the person doing the study;  $k$  is normally much smaller than  $n$ .

$$\begin{aligned} z_1 &= L_{1,1}f_1 + L_{1,2}f_2 + \cdots + L_{1,k}f_k + e_1 \\ z_2 &= L_{2,1}f_1 + L_{2,2}f_2 + \cdots + L_{2,k}f_k + e_2 \\ &\cdot \\ &\cdot \\ z_N &= L_{N,1}f_1 + L_{N,2}f_2 + \cdots + L_{N,k}f_k + e_N \end{aligned}$$

$f_1, f_2$ , and so on, are the factors, which are common to all the variables, and  $e$  (sometimes called the *unique factor*) represents that part of the variance of each  $z$  that is not explained by the common factors. Mathematically, if  $k = n$ —that is, if we had as many factors as samples— $e$  would be zero; usually, we choose a value of  $k$  that is much smaller than  $n$ , and the magnitude of  $e$  is a measure of how well (or poorly) each variable is described by the set of factors chosen. The coefficient  $L_{i,j}$  is called the *loading* of variable  $i$  on factor  $j$ . The loadings are thus a measure of the extent to which each factor is associated with a particular variable. Loadings may have numerical values between +1 and -1. If two loadings on the same factor have the same sign, the variables are positively correlated, and if they have opposite signs, the variables are negatively correlated. The absolute sign (i.e., positive or negative) of a loading is unimportant.

Mathematically, the choice of a set of factors is not unique, and some criterion must be provided for the computer to calculate an “optimum” set. The method of adjustment of the factors according to a particular criterion is called a *rotation*. The most commonly used rotation, the varimax rotation, has the effect of producing a set of uncorrelated (*orthogonal*) factors, in which each variable has high loadings on some factors and near-zero loadings on the others. Other optimization criteria may result in different orthogonal sets of factors, and *oblique rotations*, in which the factors themselves are correlated, are also possible. The objective of trying different rotations is to find an “interpretable” set of factors; what constitutes an interpretable factor is a rather subjective question: basically it means that the person doing the analysis can associate them with some source or process.

The measure of how well the variance of a particular variable is described by a particular set of factors is called the *communality*. The communality for the  $i$ th variable is given by

$$\text{Communality} = \sum_{j=1}^k L_{i,j}^2$$

It is the fraction of the variance of the  $i$ th variable that is explained by the  $k$  factors chosen. Ideally, the communalities for all variables should be close to 1. If a factor analysis is successful,  $k$  will be small, communalities will be high, and the factors will be readily associated with particular sources or processes.

Let us consider a hypothetical example of how  $R$ -mode factor analysis might work in practice. Suppose that we had 100 water analyses from a particular region, each for fifteen elements. Suppose that the waters had three sources: weathering of granitic rocks, weathering of evaporites, and weathering of dolomite. Each of the 100 samples would then be the sum of different proportions of water from the three sources, and, in principle, all the variance in the 100 analyses could be explained by different proportions of water from the three sources. If an  $R$ -mode factor analysis were performed on the 100 analyses, the factor analysis should identify three factors that would account for all the variance in the original data. One of the factors would have high loadings of  $\text{Cl}^-$  and  $\text{SO}_4^{2-}$ , zero loadings for  $\text{SiO}_2$ ,  $\text{HCO}_3^-$ ,  $\text{K}^+$  and  $\text{Mg}^{2+}$ , and intermediate loadings for  $\text{Na}^+$  and  $\text{Ca}^{2+}$ . A second factor should have high loadings for  $\text{Mg}^{2+}$ , zero loadings for  $\text{K}^+$ ,  $\text{Na}^+$ ,  $\text{Cl}^-$ ,  $\text{SO}_4^{2-}$ , and  $\text{SiO}_2$ , and intermediate loadings for  $\text{Ca}^{2+}$  and  $\text{HCO}_3^-$ . A third factor would have high loadings for  $\text{SiO}_2$  and  $\text{K}^+$ , intermediate loadings for  $\text{Ca}^{2+}$ ,  $\text{Mg}^{2+}$ ,  $\text{Na}^+$ , and  $\text{HCO}_3^-$ , and zero loadings for  $\text{Cl}^-$  and  $\text{SO}_4^{2-}$ . These factors are easily interpretable in terms of the three sources mentioned. If we had started with just the analytical data, we would be able to identify the sources provisionally on the basis of the factor analysis, but we would probably check the distribution of water compositions against a geological map before drawing any firm conclusions.

In real situations, three factors will never explain all the variance in the data. What one hopes is that a few factors, much fewer than the number of variables, will explain 90 percent or so of the variance. The remaining variance can be ignored as "noise." It is usually possible to relate factors that explain a large percentage of the variance to specific sources or processes; factors that explain only a small percentage of the variance commonly have no obvious relationship to identifiable sources or processes.

$Q$ -mode factor analysis is similar mathematically to  $R$ -mode factor analysis, but it explores relationships among the samples rather than among the variables.  $Q$ -mode is often used in sedimentology but is used less commonly in studies of water chemistry.

## CASE STUDIES

### Mackenzie River System, Canada

A good example of the application of factor analysis is a study by Reeder et al. (1972) of the factors controlling the inorganic composition of surface waters in the Mackenzie River drainage basin, Canada. The Mackenzie drains a large part of western Canada, and has contrasting physiographic provinces with the Rocky Mountains in the west and the Canadian Shield in the east. Waters from 101 localities were analyzed for 22 major and minor inorganic components.

The approach used was strictly statistical. First, one highly saline sample and eight trace constituents that did not show normal or lognormal distributions were eliminated. The remaining 14 concentration variables were converted to logarithms, and *Q*-mode and *R*-mode factor analyses were performed. The *Q*-mode analysis indicated (among other things) that the data did not show any marked clustering and so were suitable for *R*-mode analysis.

In the *R*-mode analysis, seven factors accounted for 91 percent of the variance (Table 12-4). The factors are shown diagrammatically in Fig. 12-11. The rectangular boxes represent the factors and the center line represents zero loading for the variables. Points near the top of the boxes represent high positive loadings, and points near the bottom represent high negative loadings.

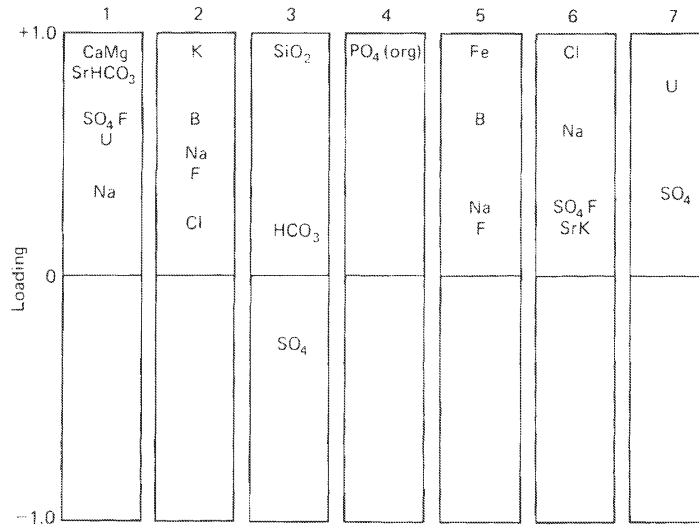
Factor 1 was interpreted as representing the weathering products of carbonate rocks and associated gypsum. Factor 2, which is essentially a potassium–boron factor with moderate loadings for Na and F, was interpreted as representing the weathering of illite in shales. Factor 3, which is essentially a silica factor, had no simple explanation. It did not represent siliceous rocks, but might have represented rocks containing easily dissolved silica or conceivably hot springs. Factor 4, whose only loading was organic PO<sub>4</sub>, was unrelated to a geological source. Factor 5, which was essentially an iron–boron factor with a small loading for Na, was interpreted as representing the weathering of glauconite. Factor 6 was an Na–Cl factor, and was interpreted as representing solution of evaporites at depth. Factor 7 had a high loading for U, but appeared unrelated geographically to areas of known uranium mineralization.

A second *R*-mode analysis was performed using the factors from the first *R*-mode analysis and some environmental parameters (Table 12-5, Fig. 12-12). Factor 1 simply showed that suspended matter, turbidity, and organic PO<sub>4</sub> were strongly correlated, which is not sur-

**TABLE 12-4** *R*-Mode Varimax Factor Matrix of Chemical Data for 100 Surface Waters from the Mackenzie River Drainage Basin, Canada<sup>a</sup> (from Reeder et al., 1972)

Variable	Factor							Communality
	1	2	3	4	5	6	7	
Na	0.335	<i>0.517</i>	0.057	-0.006	<i>0.300</i>	<i>0.613</i>	-0.054	0.852
K	0.082	<i>0.910</i>	-0.045	0.105	0.091	0.253	0.041	0.922
Mg	<i>0.921</i>	0.064	0.019	0.007	-0.068	0.111	0.176	0.901
Ca	<i>0.936</i>	0.143	0.055	0.056	0.069	0.012	0.163	0.933
Sr	<i>0.881</i>	-0.062	0.125	0.089	0.091	0.278	-0.013	0.889
B	0.180	<i>0.643</i>	-0.078	0.010	<i>0.647</i>	0.179	0.055	0.906
Fe	-0.142	0.125	0.190	0.179	<i>0.911</i>	0.023	0.018	0.934
U	<i>0.575</i>	0.030	0.055	0.080	0.024	-0.008	<i>0.784</i>	0.956
SiO <sub>2</sub>	0.198	-0.059	<i>0.937</i>	0.022	0.148	-0.099	0.030	0.954
F	<i>0.673</i>	<i>0.405</i>	-0.164	-0.079	<i>0.205</i>	0.331	-0.047	0.804
Cl	0.090	0.251	-0.126	0.005	-0.014	<i>0.935</i>	0.037	0.962
HCO <sub>3</sub>	<i>0.889</i>	0.117	0.230	0.016	-0.068	-0.142	0.118	0.896
SO <sub>4</sub>	<i>0.699</i>	0.147	-0.258	0.080	0.151	0.354	<i>0.378</i>	0.875
PO <sub>4</sub> (org.)	0.062	0.071	0.022	<i>0.978</i>	0.148	0.013	0.040	0.990
Percent of variance explained by factor								
	34.17	13.03	7.93	7.37	10.56	12.16	6.03	
Cumulative percent of variance								
	34.17	47.20	55.13	62.50	73.06	85.22	91.25	

<sup>a</sup>Significant loadings italicized.



**FIGURE 12-11** Diagrammatic representation of factors from *R*-mode varimax solution of chemical data for 100 surface waters from the Mackenzie River drainage basin, Canada (Reeder et al., 1972).

prising as organic PO<sub>4</sub> was measured on unfiltered samples. Factors 2 and 6 were interpreted as representing the products of weathering of Cretaceous shales. Factors 3, 4, and 9 were interpreted as showing that salinity was controlled largely by evaporites and carbonate minerals.

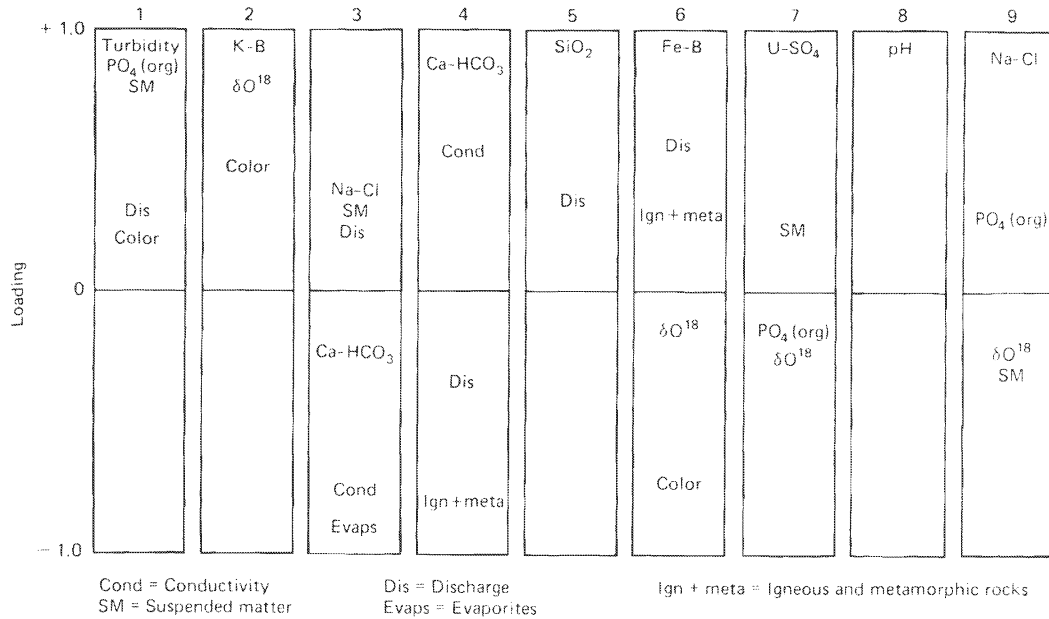
The paper by Reeder et al. illustrates many of the strengths and weaknesses of the statistical approach. The volume of data used in the study (101 samples, 22 chemical variables, several geological variables) would be unmanageable without some such approach. The factors revealed by the analysis are, by and large, too complex to be determined by inspection. On the other hand, the statistical study can find relationships only among the parameters used as input, which in this case were water analyses and lithology. Relief (compare with the Amazon later in the chapter), for example, was not included, so Reeder's conclusion that salinity was controlled by lithology and not relief is not really documented. Lithology and relief in the study area were highly correlated. Biological processes may strongly influence the concentrations of SiO<sub>2</sub>, K, and trace elements, and redox processes in the river may be much more important than source rock in determining Fe concentrations. This would not be revealed by the second factor analysis, because no appropriate environmental parameters were used as inputs. It is virtually impossible to include quantitative information on all possibly relevant environmental parameters in such a study. Finally, the study illustrates that, although the analysis identifies the factors more or less objectively, the interpretation of these factors in terms of actual controlling processes is highly subjective.

### Amazon and Orinoco River Systems

The geochemistry of the Amazon River system was studied by Gibbs in the mid-1960s (Gibbs, 1967, 1970, 1972), and subsequently in more detail by Stallard and Edmond (1981, 1983, 1987; Stallard, 1985). Related studies on the Orinoco were reported by Stallard (1985), Stallard and Edmond (1987), and Edmond et al. (1995). The Amazon is the world's largest

**TABLE 12-5 R-Mode Varimax Factor Matrix of Physical Properties and Factor Scores for 94 Surface Waters from the Mackenzie River Drainage Basin, Canada<sup>a</sup> [from Reeder et al., 1972]**

Variable	Factor							Community		
	1	2	3	4	5	6	7		8	9
Conductivity	-0.182	0.048	-0.779	0.492	-0.072	-0.073	0.017	0.033	-0.196	0.935
pH	0.087	-0.001	-0.025	0.057	0.129	0.066	-0.065	0.970	0.036	0.979
Color	0.247	0.475	-0.099	0.019	0.199	-0.720	-0.012	0.085	-0.162	0.889
Turbidity	0.924	-0.108	0.078	-0.025	0.003	-0.001	0.164	0.025	-0.150	0.922
Suspended matter	0.827	-0.038	0.269	0.006	0.022	-0.010	0.225	0.188	-0.215	0.891
Discharge	0.326	-0.161	0.258	-0.382	0.338	0.594	-0.035	-0.012	-0.181	0.845
$\delta^{18}\text{O}$ (SMOW)	-0.036	0.796	0.190	-0.086	-0.140	-0.230	-0.254	-0.042	-0.210	0.861
% evaporites	-0.086	-0.107	-0.916	0.064	0.011	-0.073	-0.031	0.032	-0.171	0.898
% igneous + metamorphic	-0.076	-0.155	-0.004	-0.835	-0.187	0.289	-0.107	-0.004	-0.156	0.881
Factor 1 (Ca-Mg-Sr-HCO <sub>3</sub> )	-0.073	-0.090	0.289	0.880	-0.024	0.139	-0.071	0.045	-0.071	0.904
Factor 2 (K-B)	-0.078	0.936	-0.068	0.113	0.084	-0.008	0.100	0.018	0.143	0.938
Factor 3 (SiO <sub>2</sub> )	0.007	-0.021	0.047	0.097	0.964	-0.034	0.010	0.129	-0.033	0.961
Factor 4 (organic PO <sub>4</sub> )	0.857	0.083	-0.105	-0.055	0.086	0.050	-0.201	-0.095	0.260	0.881
Factor 5 (Fe-B)	0.035	-0.009	-0.016	-0.016	0.003	0.956	0.032	0.114	0.009	0.931
Factor 6 (Na-Cl)	-0.124	-0.035	0.372	0.083	-0.055	0.057	0.014	0.069	0.856	0.906
Factor 7 (U-SO <sub>4</sub> )	0.113	-0.081	0.007	0.034	0.008	0.015	0.959	-0.060	-0.010	0.944
Percent of variance explained by factor	15.84	11.47	11.74	11.93	7.37	12.27	7.10	6.48	6.82	
Cumulative percent of variance	15.84	27.31	39.05	50.98	58.35	70.62	77.72	84.20	91.02	

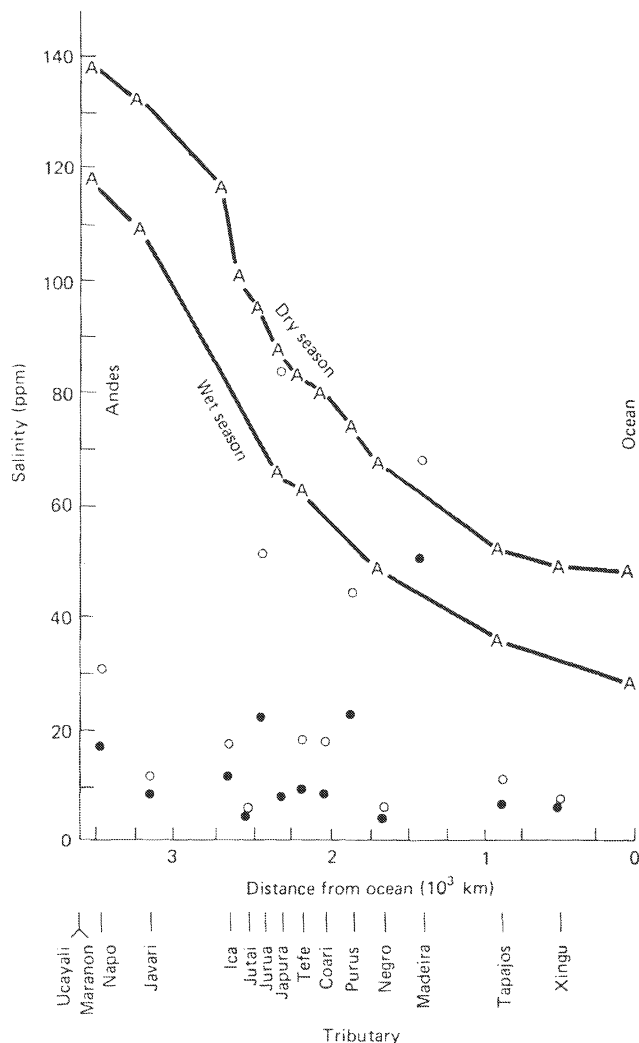


**FIGURE 12-12** Diagrammatic representation of factors from *R*-mode varimax factor matrix of physical properties and factors from previous *R*-mode analysis (Reeder et al., 1972).

river, contributing approximately 18 percent of the total runoff reaching the ocean. It is almost uninfluenced by human activities. Within the basin, climate varies from tropical rain forest to arctic mountains. Gibbs (1967) used a multiple regression and correlation analysis to relate the salinity and suspended sediments of 16 tributaries to nine environmental parameters—relief, temperature, precipitation, percent broadleaf evergreen vegetation—and five describing geology. From a statistical point of view, it would have been desirable to have more than 16 samples, but the results are nevertheless revealing. Relief accounted for 78 percent of the variance in salinity; the percent calcic (limestone, dolomite, and basic volcanics) rocks in the upper part of the tributary basin accounted for 4 percent of the variance, and the other seven parameters combined accounted for a total of 3 percent of the variance. The overwhelming importance of relief is obvious from the data (Fig. 12-13). The discharge-weighted mean salinity of eight tropical rivers was only 6 mg/l, so essentially all that is happening in the lowland region is dilution of solutes acquired in the Andes. Of the dissolved salts at the mouth of the Amazon (36 mg/l), approximately 86 percent are supplied by the 12 percent of the total area of the basin that is the mountainous region of the Andes. Of the suspended sediments at the mouth of the Amazon, 82 percent are derived from the same 12 percent of the basin area.

Gibbs's study illustrates a fundamental relationship between physical and chemical weathering: if fresh rock is not exposed by physical weathering, chemical weathering will become very slow. An important difference between the Andes and the lowland part of the basin is that in the Andes physical erosion continually removes the solid weathering residue, exposing fresh rock to chemical attack. In the lowlands, an enormous thickness of secondary material (mostly quartz, kaolinite, and gibbsite) effectively isolates the bedrock from incoming rainfall.

**FIGURE 12-13** Variation of salinity of the Amazon River and its tributaries with distance from the ocean. A indicates concentration of main stream of the Amazon; open circles indicate concentrations of tributaries in dry season; solid circles indicate concentrations of tributaries in wet season (Gibbs, 1967, courtesy the Geological Society of America).



Stallard and Edmond (1983, 1987) and Stallard (1985) greatly expanded on the relationships between water chemistry and both lithology and relief. They stressed the importance of denudation regimes, following geomorphological ideas presented by Carson and Kirkby (1972). Denudation regimes could be described as *weathering limited* and *transport limited*. In a *weathering-limited regime*, transport processes remove weathered material from a hillslope faster than weathering processes produce new material. As a result, soils are thin, and bedrock is not isolated from incoming rain. Weathering is highly selective: the more susceptible minerals are selectively weathered, and the less susceptible minerals are removed by physical erosion. Overall solute concentrations are relatively high because there is extensive interaction between fresh rock and incoming precipitation. The relative amounts of different elements in solution are quite different from the ratios in the rock; sodium and calcium are enriched in solution relative to potassium and magnesium. Under a *transport-limited regime*, by contrast, the



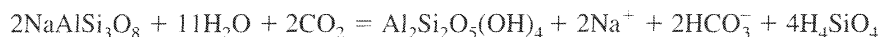
rate at which weathered material is removed by physical erosion is slower than the rate at which it is produced by chemical alteration of the bedrock. A thick mantle of weathered material builds up, isolating the rock from incoming precipitation. The rate of weathering gradually slows down until an approximate steady state is reached in which the rate at which fresh rock is altered equals the rate at which secondary minerals are removed, by either dissolution or erosion. The overall rate of weathering is controlled by the rate of removal of weathered products, not by the rate of weathering of fresh rock. Under such a regime, the ratios of various monovalent and divalent cations in solution are similar to those in the bedrock, because essentially all the cations in the original bedrock are dissolved out; none remain in the solid weathered products. The ratio of silica to cations in these waters is relatively high because the weathered products, typically gibbsite and kaolinite, have low Si/Al ratios; much of the silica present in the bedrock is transported away in solution, rather than remaining in solid phases.

Stallard and Edmond divided the waters of the Amazon basin into four groups:

1. Waters with a total cationic charge less than 200  $\mu\text{eq}/\ell$ . These are the waters draining silicate rocks under transport-limited regimes. Cationic ratios are similar to those in the rock, pH values are low, and the relative concentrations of dissolved  $\text{SiO}_2$ , Fe, and Al are high.
2. Waters with a total cationic charge between 200 and 450  $\mu\text{eq}/\ell$ . These are typically waters draining silicate rocks under weathering-limited regimes. Compared to ratios in the rock, Na is enriched over K, and Ca over Mg.
3. Waters with a total cationic charge between 450 and 3000  $\mu\text{eq}/\ell$ . These are typically waters draining marine sediments or red beds associated with carbonates and minor evaporites. Concentrations of Ca, Mg, and alkalinity are high as a result of carbonate dissolution, and sulfate concentrations are high in waters from pyrite-containing shales and from minor gypsum beds.
4. Waters with a total cationic charge greater than 3000  $\mu\text{eq}/\ell$ . These occur only in association with massive evaporites. They typically contain high concentrations of sodium and chloride in a 1:1 molar ratio.

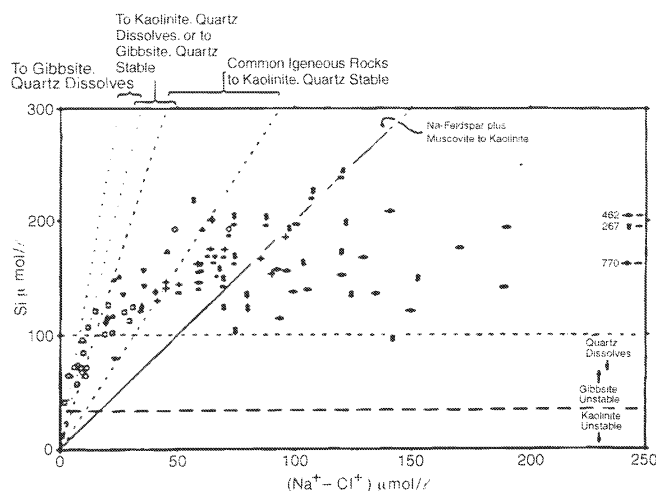
Water chemistry thus reflects both bedrock and erosional regime. The most concentrated waters are those draining evaporites, and waters draining limestone are more concentrated than those draining silicate rocks. The general relationship between solute concentration and lithology is not peculiar to the Amazon, although absolute concentrations are often higher in drier climates.

Some additional aspects of silicate weathering are illustrated in Fig. 12-14, in which rock-derived dissolved sodium (total sodium – sodium from precipitation – sodium balanced by chloride, assumed from halite) is plotted against dissolved silica. The idea is that the ratio of Si to Na is a reflection of weathering processes going on in the catchment. Assuming some sort of average composition for the bedrock, if all primary minerals weather to gibbsite and all quartz dissolves, the Si/Na ratio in the runoff will be very high (the steepest lines on Fig. 12-14). If quartz does not dissolve, the ratio will be somewhat lower; if kaolinite forms rather than gibbsite, more silica will be retained in the soil and hence the Si/Na ratio in solution will be even lower. An important boundary is represented by the weathering of albite to kaolinite



which generates a Si/Na ratio of 2. Any ratio lower than 2 cannot be derived by weathering of common rocks to kaolinite or gibbsite; a 2:1 silicate such as a smectite must be forming. The

**FIGURE 12-14** Silica versus silicate-derived sodium concentration for surface waters in the Amazon system. Open symbols represent lowland tributaries, crosses the Amazon mainstream, and other symbols Andean headwaters. The lines are explained in the text (after Stallard and Edmond, 1987).



waters from the Amazon and Orinoco basins show a systematic pattern of decreasing Si/Na ratio with increasing overall concentration. The most dilute samples, from the lowland and shield areas, have high Si/Na ratios reflecting formation of gibbsite. The most concentrated samples are all from the Andean headwaters. They have low Si/Na ratios, indicating formation of a 2:1 clay mineral. The gibbsite/kaolinite stability boundary (Chapter 10) and quartz solubility line are also shown on Fig. 12-14. The dilute samples appear to be in the kaolinite field but, as discussed in Chapter 10, there is considerable doubt about the position of the boundary and, even if the streams are in the kaolinite field, incoming precipitation and water in the soil would likely be in the gibbsite field. The extent to which quartz dissolves in different environments is not clear: it dissolves only very slowly, even in undersaturated solutions.

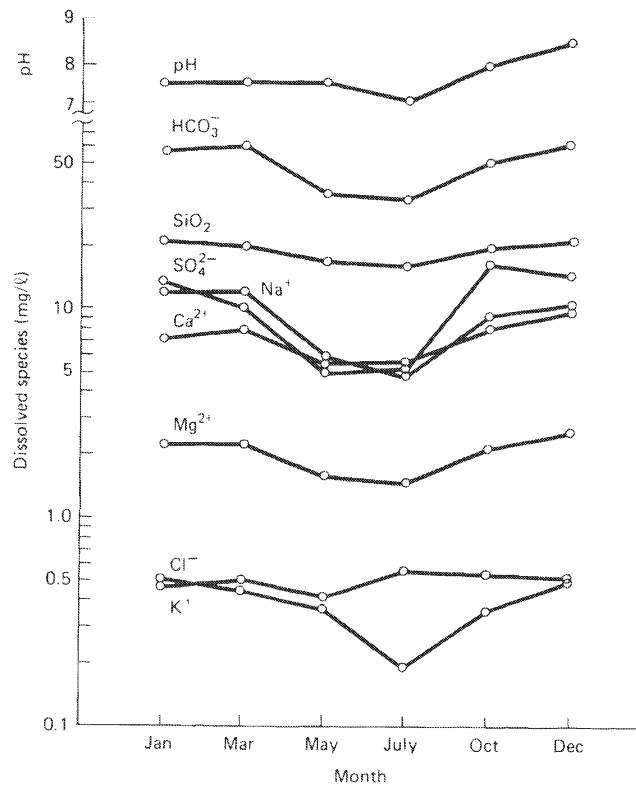
### Absaroka Mountains, Wyoming

Miller and Drever (1977a) studied chemical weathering in the drainage basin of the North Fork of the Shoshone River in northwest Wyoming. The bedrock was entirely andesitic volcanic rocks, the topography rugged (elevation 1760 to 3700 m), the mean annual temperature 7°C, and the mean annual precipitation 40 to 50 cm. The major clay mineral in all soils sampled was a smectite; traces of kaolinite were found in a few soils from areas of higher than average precipitation, and traces of illite and chlorite were found in a few samples from various parts of the basin.

In the stream waters, sodium and calcium were the major cations and bicarbonate was the major anion. The seasonal variation of the runoff composition is shown in Fig. 12-15. All ions except potassium decreased during the spring runoff. Potassium was apparently controlled by leaching from organic material, reflecting its importance as a plant nutrient and relatively low abundance in the bedrock.

The chemical compositions of waters from the North Fork and its tributaries are plotted on a  $\log (\alpha_{\text{Ca}^{2+}}/\alpha_{\text{H}^{+}}^2)$  versus  $\log \alpha_{\text{H}_2\text{SiO}_4}$  diagram in Fig. 12-16. Waters collected in December, when the discharge is lowest and water comes from the groundwater system, plot in the smectite field. Waters collected in May, when the runoff is a maximum, plot in the kaolinite field. Samples from other times of the year form a continuous band between the two extremes. The kaolinite–smectite stability boundary does not appear to control the distribution of points in

**FIGURE 12-15** Seasonal variation in the mean chemical composition of surface waters of the North Fork of the Shoshone River (Miller and Drever, 1977a).

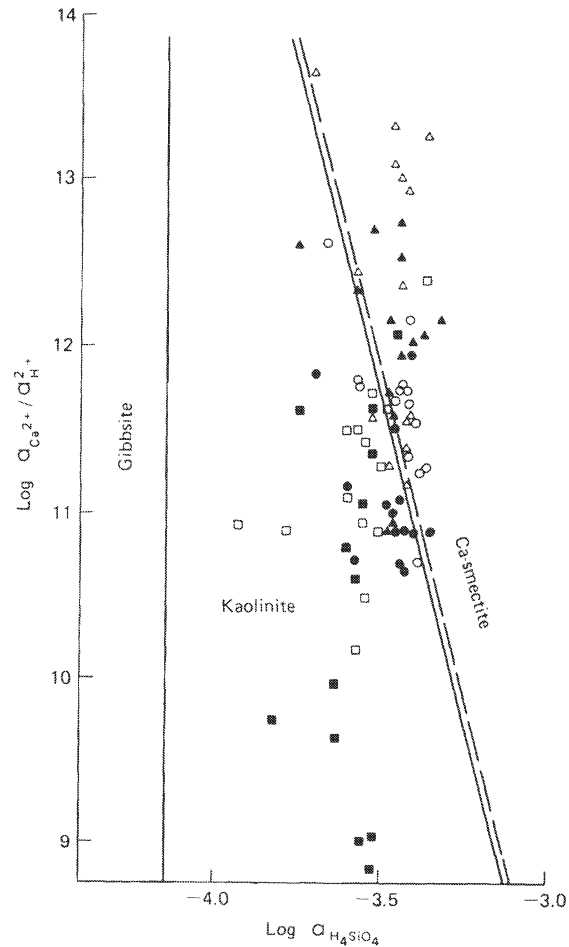


any convincing way. The relative constancy of the silica activity is remarkable, in agreement with the observations of Pačes (1972). Miller and Drever suggested that compositions within the kaolinite stability field were the result of dilution of relatively concentrated groundwaters by snowmelt. They summarized their views on equilibrium controls as follows:

In general, chemical equilibrium between solution and solid phases would not be expected in an open system through which water is fluxing rapidly. A more realistic approach would be to relate water chemistry to the kinetics of dissolution of primary phases and the kinetics of precipitation of secondary phases [cf. Pačes 1973, 1976]. At present we do not have sufficient data to apply this approach quantitatively to weathering in the North Fork basin. (p.1699)

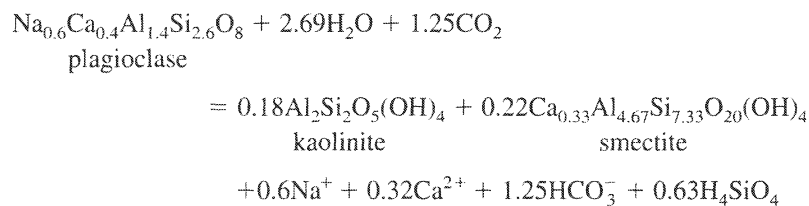
Attempts to calculate a mass balance for the weathering process presented an immediate problem. The MgO content of the clay fraction of the soils was much greater than the MgO content of the bedrock (Table 12-6). Thus, with any reasonable assumption such as conservation of Al<sub>2</sub>O<sub>3</sub>, an external source of Mg should be required to convert bedrock to soil. Miller and Drever suggested that the quantitatively important weathering process was slight alteration of large volumes of andesite during which no identifiable clay mineral was formed, rather than clay mineral formation in the soil zone. This was documented by the observation that all rock samples collected at lower elevations, including a drill core 3 m long from the base of a 20-m road cut, showed evidence of alteration of the ferromagnesian minerals. The bulk chemistry of the slightly altered rock was depleted in MgO, CaO, and total iron compared

**FIGURE 12-16** Compositions of water samples from the North Fork of the Shoshone River plotted on a stability diagram for the system  $\text{CaO}-\text{Al}_2\text{O}_3-\text{SiO}_2-\text{H}_2\text{O}$  at  $25^\circ\text{C}$  and at  $7^\circ\text{C}$  (dashed line). Solid circles = January; open circles = March; solid squares = May; open squares = July; solid triangles = October; open triangles = December (Miller and Drever, 1977a).



to fresh rock (Table 12-7). Rapid physical erosion presumably removed the feldspar-rich residue, re-exposing the bedrock and allowing the weathering process to continue.

This study was one of the few at that time in which the composition of the weathering products was actually measured rather than assumed. According to the mass-balance procedure of Garrels and Mackenzie (1967), the weathering process would be represented by the equation:



Thus, to achieve balance for  $\text{Na}^+$ ,  $\text{Ca}^{2+}$ , and  $\text{H}_4\text{SiO}_4$ , kaolinite and smectite should have been forming in approximately equal molar amounts. This illustrates that although a mass-balance

**TABLE 12-6** Chemical Analyses (wt %, Water-Free Basis) of Fresh Rock and Surface Soils from the Drainage Basin of the North Fork of the Shoshone River [from Miller and Drever, 1977a]

	(1) Sunlight group rocks <sup>a</sup> (19 samples)		(2) Bulk soils (10 samples)		(3) Clay fraction of soils (24 samples)		Differences	
	Mean	S. D.	Mean	S. D.	Mean	S. D.	(2)-(1)	(3)-(1)
SiO <sub>2</sub>	55.9	2.72	57.0	3.87	52.9	2.15	+1.5 (3%)	-2.6 (5%)
Al <sub>2</sub> O <sub>3</sub>	17.5	0.84	16.6	0.49	17.3	5.77	-0.9 (5%)	-0.2 (1%)
Fe <sub>2</sub> O <sub>3</sub> <sup>b</sup>	7.88	1.12	8.79	1.13	15.3	2.74	+0.9 (12%)	+7.4 (94%)
MgO	4.30	1.16	4.89	1.29	9.03	3.49	+0.6 (14%)	+4.73 (110%)
CaO	6.90	1.03	6.69	1.61	2.15	1.34	-0.21 (3%)	-4.75 (69%)
Na <sub>2</sub> O	3.38	0.45	2.95	0.51	0.48	0.25	-0.43 (13%)	-2.9 (86%)
K <sub>2</sub> O	3.00	0.79	2.06	0.33	1.77	0.65	-0.94 (31%)	-1.23 (41%)
TiO <sub>2</sub>	0.91	0.13	0.86	0.13	0.92	0.29	-0.04 (4%)	+0.02 (2%)

<sup>a</sup>From Nelson and Pierce (1968) and H. J. Prostka (unpublished data).

<sup>b</sup>Total iron reported as Fe<sub>2</sub>O<sub>3</sub>.

**TABLE 12-7** Chemical Analyses (wt %) of Fresh and Slightly Altered Andesites from the Drainage Basin of the North Fork of the Shoshone River [from Miller and Drever, 1977a]

	Analyses of Sunlight group rocks by the USGS <sup>a</sup> (19 samples)		Sunlight group rocks from surface out- crops, this study (11 samples)		Difference
	Mean	S. D.	Mean	S. D.	
SiO <sub>2</sub>	55.9	2.72	59.9	3.15	+4.0 (7%)
Al <sub>2</sub> O <sub>3</sub>	17.5	0.84	16.3	0.99	-1.2 (7%)
Fe <sub>2</sub> O <sub>3</sub> <sup>b</sup>	7.88	1.12	6.9	1.39	-0.98 (13%)
MgO	4.30	1.16	3.24	1.08	-1.06 (25%)
CaO	6.90	1.03	6.37	1.99	-0.53 (8%)
Na <sub>2</sub> O	3.38	0.45	3.92	0.68	+0.54 (16%)
K <sub>2</sub> O	3.00	0.79	2.59	1.16	-0.41 (14%)
TiO <sub>2</sub>	0.91	0.13	0.71	0.19	-0.20 (22%)

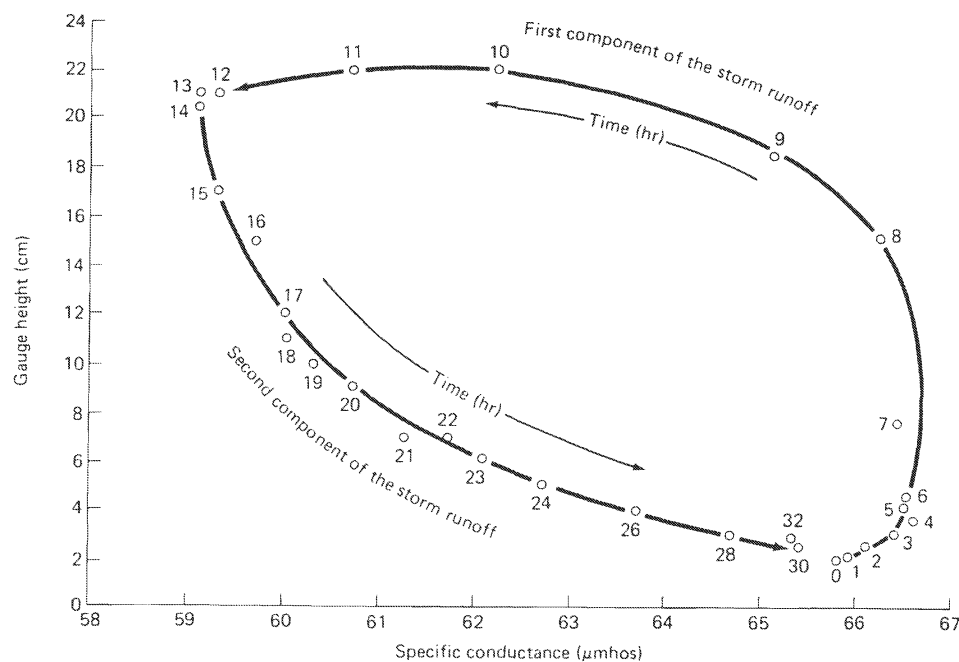
<sup>a</sup>From Nelson and Pierce (1968) and H. J. Prostka (unpublished data).

<sup>b</sup>Total iron reported as Fe<sub>2</sub>O<sub>3</sub>.

calculation using idealized mineral compositions may appear to give a reasonable result, the result may not correspond at all closely to what is actually happening in nature.

In a related study, Miller and Drever (1977b) studied the variation in the chemistry of the North Fork during and following a storm. The effect of rainfall is not simply to cause dilution of the base flow. During the first few hours of the storm, the salinity (represented by specific conductance) of the water actually rose (Fig. 12-17) and the path by which it returned to its initial value was not simple. The variation of the individual dissolved constituents is shown in Fig. 12-18.

As a means of interpreting the trends in Fig. 12-18, Miller and Drever used *R*-mode factor analysis. The data from the two components of the storm runoff (rising and falling water) were treated separately. The resulting factor matrices are shown in Tables 12-8 and 12-9.



**FIGURE 12-17** Variation of gauge height of flow (representing discharge) with specific conductance (representing salinity) for storm runoff, North Fork of the Shoshone River. Numbers near circles indicate sampling times in hours after beginning of storm (Miller and Drever, 1977b; courtesy the Geological Society of America).

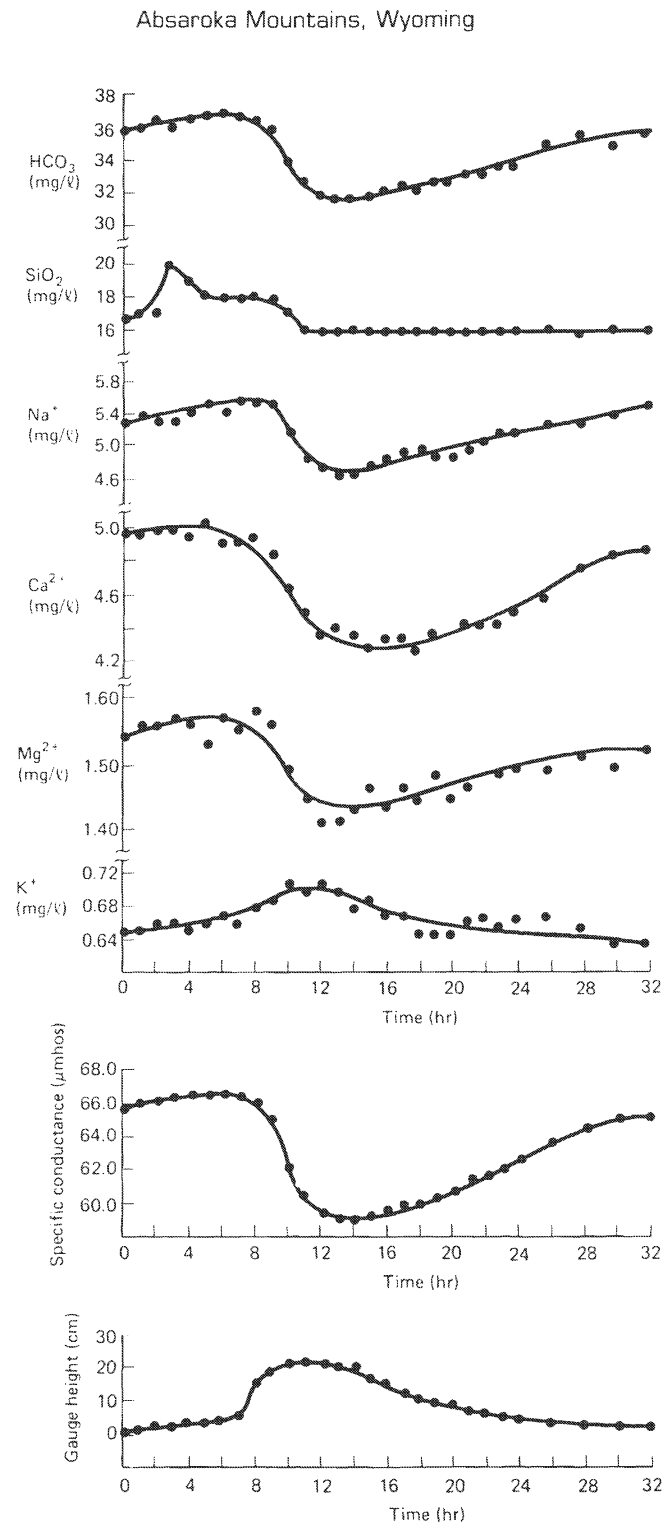
In the first component (0–13 hrs), factor 1 was represented by moderately high loadings for  $\text{Na}^+$ ,  $\text{HCO}_3^-$ ,  $\text{Mg}^{2+}$ , and  $\text{Ca}^{2+}$ . It was interpreted as representing highly soluble material that is first and easiest to be dissolved from the soil. Soils that are not continuously wet generally contain salts that form when water containing dissolved ions evaporates in the soil zone. When rainwater infiltrates the soil zone during the early part of a storm, these salts are dissolved and flushed out. Readily soluble salts may also be released by decaying vegetation. The loading for gauge height was essentially zero, indicating that factor 1 was unrelated to dilution by rainwater.

Factor 2 of the first component was represented by high negative loadings for gauge height and potassium and moderate loadings for  $\text{Ca}^{2+}$  and  $\text{HCO}_3^-$ . Potassium, unlike the other dissolved species, increased in concentration as streamflow increased. Potassium and, to a lesser degree, calcium and bicarbonate are probably leached from biological material. Likens et al. (1977) found that potassium was readily leached from biological material such as leaves, pollen, and insects in the Hubbard Brook watershed, and Cleaves et al. (1970) observed that leaf decay produced a short-term increase in the concentrations of calcium, potassium, and bicarbonate in a stream in Maryland.

Factor 3 of the first component was represented by moderate loadings for silica, magnesium, and bicarbonate. It was interpreted as representing the selective weathering of ferromagnesian minerals, which has already been discussed.

In the second component of the storm runoff (13 to 32 hrs), factor 1, which accounted for 59 percent of the total variance, was represented by high positive loadings for bicarbonate, calcium, and sodium, a high negative value for gauge height, and a moderate positive value for

**FIGURE 12-18** Variation in chemical composition and gauge height of flow of North Fork of Shoshone River following storm on July 20, 1973 (Miller and Drever, 1977b; courtesy the Geological Society of America).



**TABLE 12-8** R-Mode Factor Matrix for the First Component of Storm Runoff (rising gauge height), North Fork of the Shoshone River (from Miller and Drever, 1977b; courtesy of the Geological Society of America)

	<i>Factor<sup>a</sup></i>			<i>Communality</i>
	<i>1</i>	<i>2</i>	<i>3</i>	
Ca	0.703	0.582	—	0.981
Mg	0.715	—	0.571	0.982
Na	0.868	—	—	0.985
K	—	-0.849 <sup>b</sup>	—	0.945
SiO <sub>2</sub>	0.429	—	0.668	0.675
HCO <sub>3</sub>	0.774	0.465	0.409	0.984
Gauge height	—	-0.939	—	0.978
Percent of variance explained by factor	41	37	20	
Cumulative percent of variance	41	78	98	

<sup>a</sup>Factor loadings <0.4 are omitted.

<sup>b</sup>Variation of potassium accounted for by factor 2 is  $(-0.849)^2 = 0.72$ , or 72%.

**TABLE 12-9** R-Mode Factor Matrix for the Second Component of Storm Runoff, North Fork of the Shoshone River (from Miller and Drever, 1977b; courtesy of the Geological Society of America)

	<i>Factor<sup>a</sup></i>			<i>Communality</i>
	<i>1</i>	<i>2</i>	<i>3</i>	
Ca	0.914	—	—	0.964
Mg	0.567	0.761	—	0.911
Na	0.913	—	—	0.949
K	—	—	0.742	0.626
SiO <sub>2</sub>	—	0.797	—	0.743
HCO <sub>3</sub>	0.925	—	—	0.923
Gauge height	-0.931	—	0.245	0.977
Percent of variance explained by factor	59	22	13	
Cumulative percent of variance	59	81	94	

<sup>a</sup>Factor loadings <0.4 for chemical species are neglected.

magnesium. This factor was interpreted as representing simple dilution of the base flow by rainwater. Factor 2 was interpreted as being the same as factor 3 of the first component, and factor 3 was interpreted as being the same as factor 2 of the first component.

Thus rainfall does not simply cause dilution of the base flow, and the variations in water chemistry during a storm can be used to reveal information about processes occurring in the zone of weathering. The same concept is applied in a more comprehensive manner in the discussion of the Mattole River below.



### **Mattole River, California**

The chemistry of the Mattole River in northern California was studied by Kennedy (1971) and by Kennedy and Malcolm (1977); the emphasis in these studies was interpretation of variations in water composition with time and discharge. The basin studied had an area of 620 km<sup>2</sup>, an average relief of 460 m, a mean annual rainfall of 234 cm, and no significant population centers or industry. The bedrocks were mostly graywacke, sandstone, siltstone, and shale. The rocks were relatively impermeable, so no large groundwater reservoir was present to support river flow during the dry season.

The rainfall distribution in the area was markedly seasonal. The bulk occurred between November and March, and very little occurred from May to late October. Runoff closely paralleled rainfall, varying from about 1 m<sup>3</sup>/s in the early fall to 1000 m<sup>3</sup>/s or more in the middle of winter. The variation of the concentrations of the individual solutes, both seasonally and during individual storms, was used to elucidate the geochemical processes controlling the distribution of each solute.

During the summer, soluble salts from atmospheric deposition and decomposition of organic matter accumulate at the ground surface. These salts are carried down into the soil by early light rains in the fall, and each of the storms in early fall flushes some of them into the river. Later in the rainy season, these salts have all been washed out of the soil, and they no longer influence stream chemistry. Thus the proportion of chloride and sulfate in the dissolved salts is highest in the early part of the rainy season, and the proportion of bicarbonate and silica is highest toward the end of the rainy season. Potassium maintains a relatively uniform concentration, independent of discharge. Presumably, decaying organic matter served as an easily leached reservoir of potassium.

Toward the end of the rainy season, 60 to 80 percent of storm rainfall appeared as runoff within 24 h. However, the silica concentration in the runoff did not decrease by more than 40 percent, and the calcium concentration remained higher than would be expected on the basis of simple dilution of the base flow by rainwater. The relatively high silica and calcium concentrations mean that the rain must have interacted chemically with the soil before it reached the stream. The results of leaching experiments and simple calculations by Kennedy and Malcolm indicated that at least 50 percent of the incoming rain in a storm must have flowed through the soil before reaching a stream and that the soil must have been leached to a depth of several centimeters. Kennedy and Malcolm used the term *quick-return flow* for rainwater that infiltrates only a short distance into the soil and appears as runoff within 24 h. *Delayed-return flow* is rainwater that has penetrated deeper below the surface (but not to the permanent water table) and is discharged at the surface over a longer period of time. Kennedy and Malcolm suggested that during the early part of the rainy season, the runoff was largely quick-return flow and surface runoff. Around the end of the rainy season it was mostly delayed-return flow, and only during the dry season was inflow from the permanent groundwater significant (Fig. 12-19).

The paper by Kennedy and Malcolm illustrates the use of variations in chemical composition to evaluate the movement of water in the near subsurface. The use of oxygen isotopes to obtain similar information is discussed in Chapter 14.

### **Cascade Mountains, Washington; Loch Vale, Colorado**

These two studies focus on high-elevation catchments underlain by silicate rocks in the western United States.

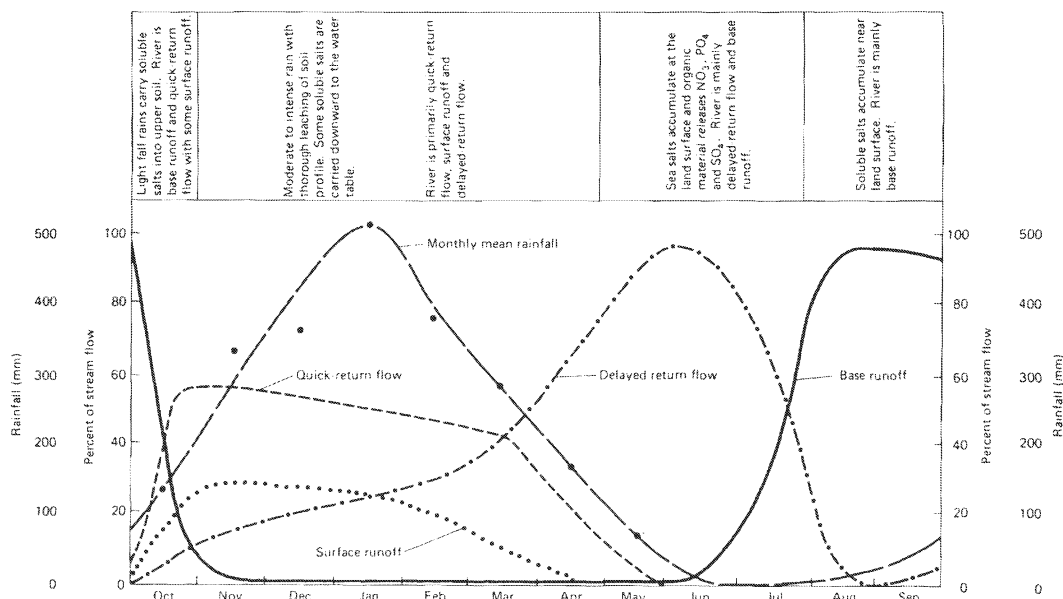


FIGURE 12-19 Conceptual model of sources of stream flow for the Mattole River, California (Kennedy and Malcolm, 1977).

**Cascade Mountains.** Chemical weathering in the temperate glacial environment in a small area of the northern Cascade Mountains in the state of Washington was studied by Reynolds and Johnson (Reynolds, 1971; Reynolds and Johnson, 1972), by Drever and Hurcomb (1986), and by Axtmann and Stallard (1995). The study area averaged 1970 m in elevation and was essentially free of megascopic biological activity. The mean annual rainfall was very high, approximately 384 cm. The bedrocks were migmatites, metadiorites, quartz diorite, and basaltic and lamprophyric dikes (rock names are explained in the glossary).

The waters in the area were dilute (Table 12-10), averaging about 15 mg/l total dissolved solids; calcium and magnesium were the dominant cations. Although the waters were dilute, the rainfall was so great that a large amount of material was being transported away in solution. In fact, the rate of chemical weathering in terms of mass removed in solution per unit area per year was approximately twice the average rate for the North American continent.

Three distinct clay mineral types were being formed, each restricted to a specific rock type. Vermiculite or a mixed-layer vermiculite–phlogopite was forming on phlogopite schists; saponite (see Chapter 4) was forming on the lamprophyres, and the clay forming on the quartz diorite was largely X-ray amorphous with minor vermiculite, gibbsite, and lepidocrocite ( $\text{FeOOH}$ ). Chemically, the clay forming on the quartz diorite was a ferruginous bauxite.

It is instructive to see how the data from this unusual environment agree with the principles discussed earlier in this chapter. On a log ( $\text{Ca}^{2+}/\text{Al}^{3+}$ ) versus log  $\text{Al}_2\text{SiO}_5$  diagram (Fig. 12-20), the points all plot in the gibbsite or the kaolinite stability field. This is in accord with the observation that the clay forming on the quartz diorite and metadiorite was a gibbsite-containing ferruginous bauxite. On the other hand, vermiculite and saponite, which were forming on other lithologies, are clearly not in equilibrium with the waters. Although there are no reliable

**TABLE 12-10** Mean Compositions ( $\mu\text{mol/kg}$ ) of Waters Draining Different Lithologies, South Cascade Lake Basin (after Drever and Hurcomb, 1988)

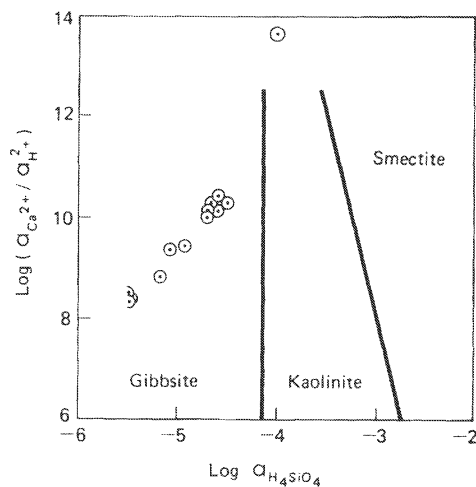
	$\text{HCO}_3^-$	$\text{SO}_4^{2-}$	$\text{Cl}^-$	$\text{Ca}^{2+}$	$\text{Mg}^{2+}$	$\text{Na}^+$	$\text{K}^+$	$\text{SiO}_2$
Migmatite (7 samples)	86	10.1	7.2	37	8.2	8.7	15.0	17.9
Quartz diorite (6 samples)	67	12.6	6.1	32	8.4	9.4	7.7	17.5
Quartz diorite and meta-quartz diorite (3 samples)	122	19.4	3.8	63	12	13	6.0	38
South Cascade Lake (6 samples)	171	19.1	13.2	73	15	18	21	25
Precipitation (from Dethier, 1979)		10.8		1.9	1.1	9.6	1.85	

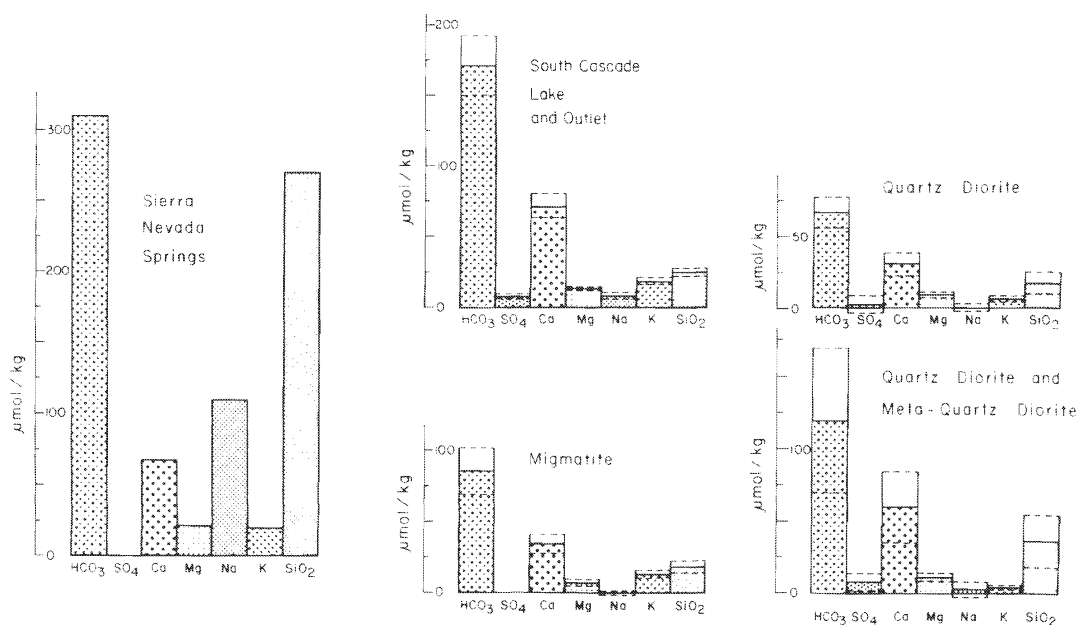
The mean nitrate content of all surface waters was  $1.28 \mu\text{mol/kg}$ . The pH values ranged from 6.19 to 7.14, with a mean of 6.62.

free-energy data for either mineral, a variety of evidence suggests that both would have stability relations similar to beidellite (smectite or montmorillonite), but requiring a high  $\alpha_{\text{Mg}^{2+}}/\alpha_{\text{H}^+}^2$  ratio in solution. The reason that vermiculite is formed is that it is a result of slight alteration of phlogopite. The two minerals are closely related (see Chapter 4), so vermiculite is not a "new" mineral in the sense that gibbsite is. It can be regarded as a partially leached phlogopite or biotite. Saponite probably represents a similar process. Reynolds did not detect kaolinite in any sample; Drever and Hurcomb observed very minor amounts. Kaolinite is thus not a major alteration product.

Drever and Hurcomb (1986) used mass-balance calculations to deduce the sources of solutes. The water compositions in the basin are quite different from those in the Sierra Nevada springs (Fig. 12-21). The high relative abundance of  $\text{Ca}^{2+}$  (and, to a lesser extent,  $\text{K}^+$ ) and the low relative abundance of  $\text{Na}^+$  and  $\text{SiO}_2$  are particularly striking. The low ratio of  $\text{Na}^+$  to  $\text{Ca}^{2+}$  implies that weathering of plagioclase feldspar cannot be an important

**FIGURE 12-20** Samples from the South Cascade Glacier region (Reynolds and Johnson, 1972) plotted on  $\log (\alpha_{\text{Ca}^{2+}}/\alpha_{\text{H}^+}^2)$  versus  $\log \alpha_{\text{H}_4\text{SiO}_4}$  stability diagram. Half-circles were below detection limit for silica ( $0.2 \text{ mg/l}$ ).



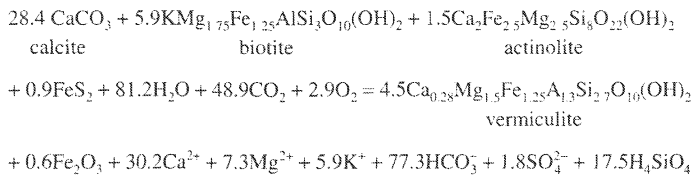


**FIGURE 12-21** Compositions of surface waters from South Cascade Lake Basin, and of Sierra Nevada ephemeral springs (Garrels and Mackenzie, 1967), all corrected for atmospheric input. Error bars represent one standard deviation of mean surface water composition; they do not include uncertainties in composition of precipitation (which would affect significantly only uncertainties for sulfate and sodium). From Drever and Hurcomb, 1986.

source of calcium in the waters. Weathering of plagioclase releases  $\text{Ca}^{2+}$  and  $\text{Na}^+$  to solution in approximately the same ratio as they occur in the solid. Plagioclase in the bedrock ranges in composition from about  $\text{An}_{28}$  to  $\text{An}_{55}$  (28 percent to 55 percent of the Ca end member, 62 percent to 45 percent of the Na end member), so weathering of it would release  $\text{Ca}^{2+}$  and  $\text{Na}^+$  in a ratio of no greater than about 1:1. Furthermore, the weathering of any ferromagnesian minerals (amphiboles or pyroxenes) would release at least as much  $\text{Mg}^{2+}$  and  $\text{SiO}_2$  as  $\text{Ca}^{2+}$ , and so they could not be the main source of  $\text{Ca}^{2+}$  either. In fact, the only plausible source for the bulk of the calcium is a phase such as calcite, which releases only  $\text{Ca}^{2+}$  and  $\text{HCO}_3^-$  to solution. Traces of calcite occur in the basin in joint planes in the quartz diorite, in veins, in occasional marble bands in the migmatite gneiss, and as superficial subglacial deposits associated with regelation processes under glacial ice. Although calcite makes up far less than 1 percent of the bedrock, it is the dominant source of solutes during weathering.

The abundance of vermiculite in the soil and the high relative concentration of  $\text{K}^+$  in the water suggest that weathering of phlogopite/biotite is an important source of solutes, and petrographic examination showed that amphiboles were also undergoing dissolution. Overall, the weathering of calcite, biotite, actinolite (amphibole), and pyrite to vermiculite and iron oxide could account for all the solutes (Table 12-11). Although the reactions chosen are not unique and the exact coefficients are subject to considerable uncertainty, there is no reasonable doubt that calcite and biotite are the main sources of solutes.

**TABLE 12-11** Weathering Reaction Calculated from Mean Composition of Waters Draining Quartz Diorite\* (after Drever and Hurcomb, 1988)



\*Corrected for atmospheric input. Coefficients represent micromoles per liter of runoff. Similar reactions can be written for the other lithologies.

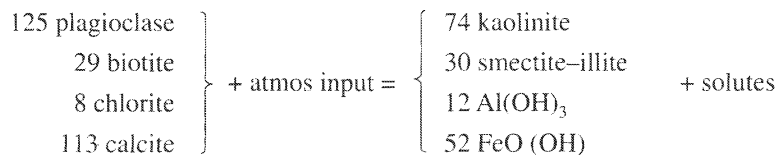
In summary, the study of weathering in the Cascade Mountains indicates that:

1. Even in a glacial environment chemical weathering can be rapid. Two important factors are a high rate of physical erosion to re-expose bedrock and a very high annual precipitation.
2. Some secondary products appear to be in chemical equilibrium with the waters in which they formed. Others, whose structure is inherited from minerals in the bedrock, do not.
3. Minerals do not contribute to the solutes in runoff in proportion to their abundance in the bedrock. Calcite, which is present only as a trace constituent, is the largest contributor to the solutes, whereas feldspars, the most abundant phases, make only a very minor contribution. This is only possible where a very high rate of physical erosion constantly re-exposes fresh rock. The South Cascade Glacier area represents an extreme example of a weathering-limited regime (see discussion of the Amazon basin earlier in this chapter).

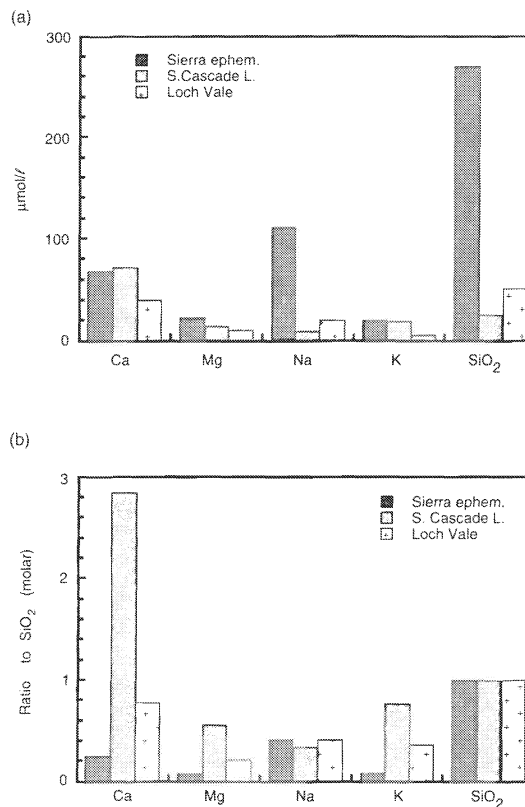
**Loch Vale, Colorado.** The Loch Vale catchment is an alpine-subalpine drainage basin located at an elevation of 3110 to 4010 m in Rocky Mountain National Park, Colorado. Over 80 percent of the basin consists of bare rock or active talus slopes; about 6 percent at the lowest elevations is covered by conifer forest. Average annual precipitation ranges from 75 to 100 cm, with more than 70 percent occurring as snow. The bedrock is granite and granite gneiss, with quartz, plagioclase ( $\text{An}_{27}$ ), K-feldspar, biotite, and sillimanite ( $\text{Al}_2\text{SiO}_5$ ) as major minerals. Biogeochemical budgets are presented and discussed by Baron (1992), detailed weathering budgets by Mast et al. (1990).

Chemically, the mean annual runoff composition is intermediate between South Cascade Lake and the Sierra Nevada ephemeral springs (Fig. 12-22). The  $\text{Ca}^{2+}/\text{Na}^+$  ratio is still too high to be explained by weathering of the common plagioclase in the basin, but the ratio is not as extreme as in the South Cascade area.

On the basis of the compositions of the minerals present in the catchment, Mast et al. came up with a mass-balance equation (moles/ha/y) for weathering:



**FIGURE 12-22** Comparison of water compositions from Sierra Nevada ephemeral springs, South Cascade and Loch Vale (a) in  $\mu\text{mol/l}$ , (b) as ratios to dissolved silica.



Mast et al. were unable to find any macroscopically visible calcite in the catchment, but demonstrated, using cathodoluminescence microscopy, that very fine-grained calcite was present in the bedrock in hydrothermally altered zones and in grain boundaries adjacent to plagioclase. They argued that deglaciation had occurred relatively recently, and rates of physical erosion were high, so that there was enough of this calcite in contact with meteoric waters to supply the observed excess of calcium. Over time, accessible calcite would be depleted and it would no longer serve as a significant source of calcium. One could use this argument, speculatively, to explain the excess calcium in the Sierra Nevada springs. The shallow, near-surface rocks (ephemeral springs) had been extensively flushed and no calcite remained. The deeper rocks (perennial springs) were less flushed and some calcite still remained.

Velbel (personal communication, 1994), on the other hand, explained the excess calcium in the runoff in Loch Vale on the basis of selective weathering of isolated regions of mafic amphibolite (amphibole and calcic plagioclase) in the bedrock. This alternative explanation cannot be ruled out on the basis of information that is presently available.

An excess calcium over what can be plausibly explained by weathering of bedrock plagioclase is almost universal in high-elevation lakes in North America (Stauffer, 1990; Turk and Spahr, 1991) and also in waters of many other regions. Understanding weathering reactions in these environments is an important part of predicting possible effects of acid deposition (Chapter 13), so the "problem" of excess calcium has received considerable attention.

Several mechanisms could give rise to it:

1. Weathering of calcite in the bedrock. It can be argued that, on the scale of a catchment, calcite will always be present initially in a granitic rock. It may be present in veins, in zones of hydrothermal alteration, or along grain boundaries as a result of deuteritic alteration or simply closed-system alteration in the presence of groundwater. (Petrologic descriptions of rocks are often misleading; petrologists systematically avoid sampling altered rocks, which are the ones most likely to contain calcite.) Although calcite may be present initially in a granitic rock, it will be rapidly depleted as the rock is exposed to meteoric water. Whether enough calcite remains at the present time to influence water chemistry will vary from catchment to catchment. It is most likely to occur in catchments that have recently been glaciated and that are undergoing rapid physical erosion.

2. Selective weathering of more calcic plagioclase in the bedrock. Clayton (1988) showed that zoned plagioclases in the bedrock of the Idaho Batholith did not weather uniformly: the calcic cores dissolved while the more sodic rims remained intact. He used this observation to explain why the  $\text{Ca}^{2+}/\text{Na}^+$  ratio in the water was higher than that of the average plagioclase in the rock. This is a plausible mechanism *provided the Ca/Na ratio in the water is not higher than the highest ratio present in the feldspar*. Some authors have claimed, on the basis of Clayton's results, that the albite and anorthite components of a feldspar could weather independently: the anorthite component could dissolve, leaving the albite component behind. I believe this is wrong: feldspars alter congruently, but different compositions alter at different rates.

3.  $\text{Ca}^{2+}$  comes from alteration of minor amounts of reactive Ca-containing silicates such as pyroxenes, amphiboles, or epidote. This is certainly the case in some catchments. Such reactions are often difficult to constrain by mass-balance equations because the secondary products are often smectites or vermiculites, whose compositions are poorly known. The overall plausibility of this mechanism must be assessed on a catchment by catchment analysis.

4. Ca comes from cation exchange sites. Calcium is greatly favored over sodium on the exchange sites of clays in dilute solutions. Thus the Ca/Na ratio of ions on exchange sites in a soil will be much higher than the Ca/Na ratio of plagioclase in the underlying bedrock. If exchangeable ions are displaced by, for example, an increased input of acidity from the atmosphere, the result will be an addition of Ca to runoff water. This is a plausible explanation for catchments affected by anthropogenic acidity. It is not a plausible explanation for the Rocky Mountain region of North America, where the input of anthropogenic acidity is minor so the cation-exchange system should be in steady state. Excess Ca could also be derived from a net decrease in biomass, but catchments showing a net decrease in biomass are relatively rare.

Documenting the source of calcium is an essential part of catchment mass-balance studies, particularly for modeling future responses to acid deposition. The predictions of mechanistic model will be quite different depending on which source for calcium is assumed.

### **Adirondack Mountains, New York**

The Adirondack Mountains in New York State have been the site of several intensive studies of processes controlling surface water chemistry, primarily because the area is receiving a large input of acidity from the atmosphere (see Chapter 13) and because the rocks there weather slowly, in some areas too slowly to neutralize the input of acidity. The most important

project there was called the Integrated Lake Water Acidification Project (ILWAS) (Electric Power Research Institute, 1984). April et al. (1986) discussed rates of weathering in two of the lake basins studied, Woods Lake and Panther Lake.

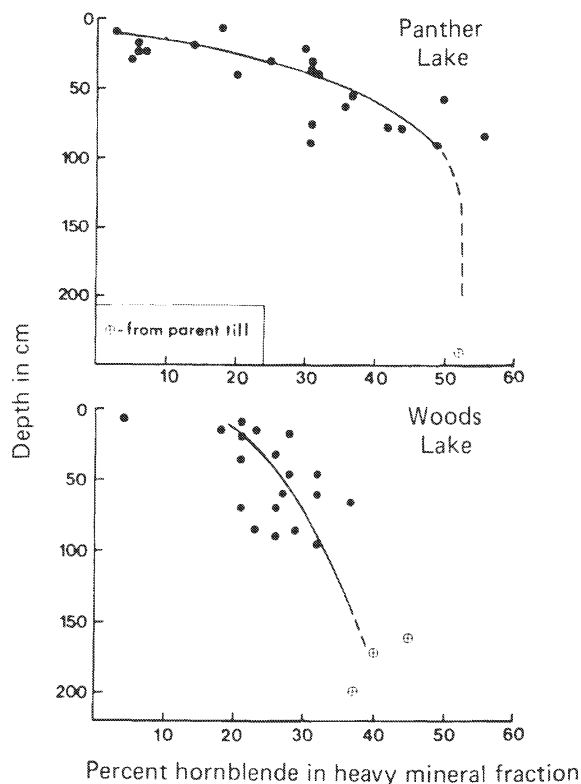
The lakes are within 30 km of each other, both receive essentially the same atmospheric input, and both are underlain by till, which is itself underlain by granitic gneiss. Despite these similarities, Woods Lake is "acidic," having a typical outlet pH between 4.5 and 5, whereas Panther Lake is "neutral," with a typical outlet pH near 7. The difference was attributed primarily to a difference in till thickness (Peters, 1984). In the Panther Lake basin, the mean till depth is 24.5 m, whereas in the Woods Lake basin it is only 2.3 m. It was hypothesized that where the till is thicker there is more contact between incoming water and weatherable minerals, and hence more neutralization by chemical weathering.

April et al. (1986) used three different mass-balance approaches to estimate weathering rates:

1. The present-day (1978–1980) flux of solutes leaving the basins, which reflects the present-day weathering rate  $\pm$  the effect of biomass changes  $\pm$  ion-exchange reactions. Since the input of ions from the atmosphere has changed in the relatively recent past, ion-exchange reactions cannot be ignored.

2. The depletion of weatherable minerals in soil profiles in the basins. The abundance of weatherable minerals such as hornblende and plagioclase feldspar increases with depth in the soil until it reaches a constant level in the underlying till (Fig. 12-23), presumably because they

**FIGURE 12-23** Abundance of hornblende (expressed as a percent of the heavy mineral fraction) as a function of depth in soils from Panther and Woods lake basins (from April et al., 1986).



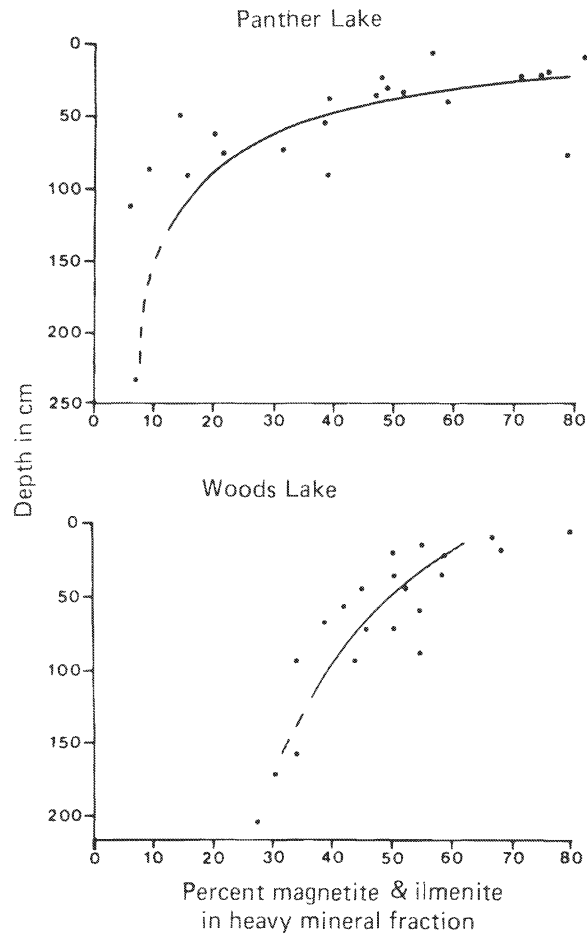


have been depleted in the upper horizons by weathering. If one assumes that there has been no physical erosion, mineral distribution curves can be used to calculate an average weathering rate since the onset of soil formation, assumed to coincide with the end of glaciation about 14,000 years ago. Soil formation is not an isovolumetric process, so some resistant mineral (here ilmenite and magnetite, Fig. 12-24) must be used to correct for volume losses (or gains) during weathering. If the stoichiometry of weathering of specific minerals is known and if it is assumed that weathering takes place only in the soil zone, the depletion curves for weatherable minerals can be used to calculate a mean flux of cations from weathering over the last 14,000 years. In principle, this represents a "true" weathering rate, unaffected by plant uptake or ion exchange.

3. The change in bulk chemistry of the soil with depth (Fig. 12-25). The principle here is the same as that for mineral-depletion curves, only the bulk chemistry of the soil is measured instead of the abundance of specific minerals. This method also yields an estimate of mean weathering rates over the last 14,000 years.

The cation fluxes calculated by methods 1 and 3 are shown in Table 12-12. A comparison of the mineral weathering rates computed from the present-day fluxes and from mineral

**FIGURE 12-24** Abundance of ilmenite plus magnetite (expressed as a percent of heavy mineral fraction) as a function of depth in soils from Panther and Woods lake basins (from April et al., 1986). The increase toward the surface is a consequence of removal of more soluble minerals by weathering.



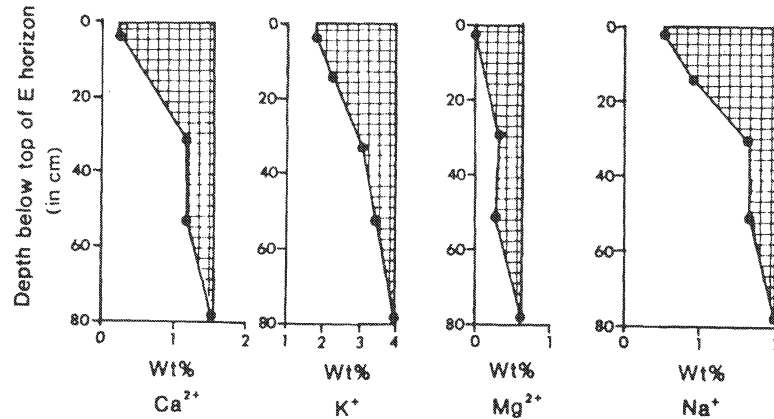


FIGURE 12-25 Depletion curves for major cations in soils in the Panther Lake basin (from April et al., 1986).

depletion curves is shown in Table 12-13. It is obvious that the results from the different methods are not mutually consistent. According to the soil chemistry profiles, the rates of weathering in the two basins are indistinguishable, whereas the measured present-day cation flux from Panther Lake is about eight times that from Woods Lake. The long-term rate at Woods Lake appears to be about three times the present rate, whereas the present rate at Panther Lake appears to be about three times the long-term rate. The rate of hornblende weathering calculated from the mineral depletion curves at Panther Lake is very much less than the rate calculated from the present-day cation flux.

The difference between the present and long-term rate at Woods Lake could be explained by a gradual decrease over time in the amount of weatherable minerals exposed to incoming precipitation. As reactive minerals were dissolved, the rate of weathering would decrease. There is no easy or unique explanation for the discrepancies at Panther Lake. One likely explanation is that solutes used to compute the depletion curves are derived from depths greater than 1 m. The big difference in outlet chemistry between Woods and Panther Lakes has been attributed to different thicknesses of till, which implies that reactions are taking place at depths greater than 1 m. It is impossible to say whether the immediate source is mineral

TABLE 12-12 Cation Fluxes (eq/ha/y) from Woods Lake and Panther Lake Basins in the Adirondack Mountains (data from April et al., 1986)

	Net present-day stream flux		Calculated from bulk composition of soil	
	Woods	Panther	Woods	Panther
Ca	167	1149	178	100
Mg	28	294	122	84
K	-21 <sup>a</sup>	32	129	150
Na	24	204	189	108
Total	198	1679	618	449

<sup>a</sup>K input from atmosphere was greater than stream output.

**TABLE 12-13** Mineral Weathering Rates (kg/ha/y) for Panther Lake Basin Calculated from Net Present-Day Stream Flux and from Mineral Depletion Curves in Soil (after April et al., 1986)

	<i>From net present-day stream flux</i>	<i>From mineral depletion curves</i>
Hornblende	312	8
Plagioclase	7	32
K-feldspar	-22	31

weathering or displacement of exchangeable cations as a result of the recent increase in the input of acidity, or even possibly biomass decrease.

The discrepancy between the present-day and long-term apparent weathering rates for hornblende suggests that ion exchange may be a significant present-day source of calcium. An alternative explanation would be that the weathering rate at Panther Lake has increased in response to the recent increase in acid deposition. However, it is hard to see why the rate of mineral weathering should increase at one lake and not at the other.

The study by April et al. illustrates again the importance of using the chemistry of solid phases as a check on the validity of a mass-balance calculation. Calculations based on solute compositions alone may not give a reliable estimate of the long-term weathering rate, particularly in areas where the rate of weathering is low and there has been a recent increase in the input of acidity from the atmosphere.

### **Waters from Ultramafic Rocks**

Ultramafic (or ultrabasic) rocks are those made up largely of the magnesium silicates forsterite ( $Mg_2SiO_4$ ) and enstatite ( $MgSiO_3$ ). Feldspars and quartz are minor or absent. The weathering of these rocks differs from that of other igneous rocks because of the different bulk chemistry and because forsterite and enstatite react particularly rapidly with water (see Table 11-2).

Barnes et al. (1972, 1978) and Barnes and O'Neil (1971) studied the chemistry of springs associated with ultramafic rocks in California and in other parts of the world. Isotopic analyses showed that the springs were all local meteoric water, so their unusual chemistry was a result of interaction with ultrabasic rock near the earth's surface. Most of the springs were magnesium-bicarbonate type water (Table 12-14, column 1). The high TDS is not surprising in view of the reactivity of the minerals involved, and the preponderance of magnesium is consistent with the chemistry and mineralogy of the rock.

Some of the springs were of a quite different chemical type (Table 12-14, column 2). The remarkable features of these waters are the very high pH (between 11 and 12), carbonate species below the detection limit, and low concentrations of magnesium and silica. The waters were essentially dilute solutions of calcium hydroxide. They were supersaturated with respect to brucite [ $Mg(OH)_2$ ], serpentine [ $Mg_3Si_2O_5(OH)_4$ ], and diopside [ $CaMgSi_2O_6$ ], but undersaturated with respect to forsterite and enstatite. Barnes and O'Neil showed that the Ca-OH waters could be derived by reaction of the Mg- $HCO_3$  waters with the ultramafic rock out of contact with the atmosphere. Dissolution of Mg silicates consumes  $H^+$ , driving the pH up. This

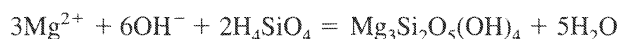
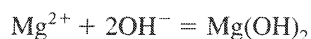
**TABLE 12-14** Mean Compositions (mg/l) of Springs from Ultramafic Rocks in the Western United States (average of analyses in Barnes and O'Neil, 1971)

	<i>Mg-HCO<sub>3</sub></i> <i>waters</i>	<i>Ca-OH</i> <i>waters</i>
pH	8.6	11.7
Ca <sup>2+</sup>	7.9	43
Mg <sup>2+</sup>	126	0.23
Na <sup>+</sup>	7.2	33
K <sup>+</sup>	0.7	1.3
Cl <sup>-</sup>	12	39
SO <sub>4</sub> <sup>2-</sup>	11	0.4
HCO <sub>3</sub> <sup>-</sup>	656	0
CO <sub>3</sub> <sup>2-</sup>	33	0
OH <sup>-</sup>	0.1	53
SiO <sub>2</sub> (total)	19	3.0

causes precipitation of calcium and magnesium carbonates until all carbonate species initially present are removed as solids, and free hydroxyl builds up in solution:



The solution becomes supersaturated with respect to brucite and serpentine, and these minerals precipitate:



Precipitation of brucite and serpentine keeps the concentrations of magnesium and silica at low values. The presence of  $\text{Mg}(\text{OH})_2$  rather than a silicate reflects the fact that the Mg:Si ratio is higher in forsterite than in any common secondary magnesium silicate (serpentine, talc, sepiolite). Small amounts of calcium present initially in enstatite are not precipitated as secondary phases (hydroxides and silicates of calcium are more soluble than their magnesium equivalents), so calcium is the major cation in solution.

The Ca-OH springs are an example of the  $\text{CO}_2$  in an infiltrating water being completely consumed and precipitated as a carbonate. In rocks such as granite, the primary minerals react much more slowly, and bicarbonate remains as the principal anion in the resulting water, at least in the water that is circulating relatively rapidly in fractures. However, the waters circulating in small pores of a granite may be quite similar to these ultramafic waters. It may have a high pH and low concentrations of carbonate species, indicating that precipitation of calcite has occurred. The occurrence of microscopic calcite crystals along grain boundaries mentioned in the discussion of sources of calcium in weathering may reflect reactions occurring in the intergranular porosity of igneous rocks.

### Rhine River

The Rhine flows through one of the most industrialized and densely populated areas of the world. Its principal headwaters are in the relatively unpopulated Swiss Alps, and where it

**TABLE 12-15** Composition (mg/l) of the Rhine River as it [A] Leaves the Swiss Alps and [B] Crosses the Border from Germany to Holland (data from Zobrist and Stumm, 1981)

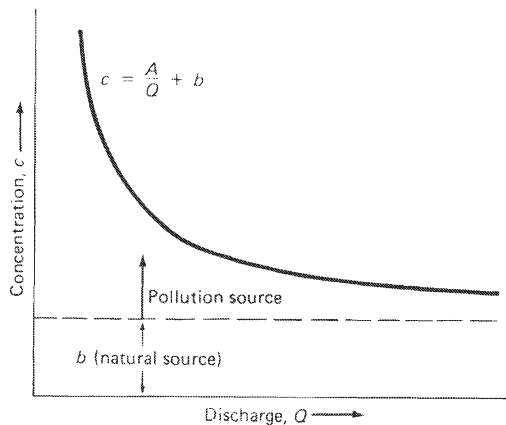
	A	B		A	B
Ca <sup>2+</sup>	40.7	83.6	DOC <sup>a</sup>	0.54	6.24
Mg <sup>2+</sup>	7.2	10.8	PO <sub>4</sub> <sup>3-</sup>	0.037	0.90
Na <sup>+</sup>	1.4	98.7	NH <sub>4</sub> <sup>+</sup>	0.042	1.53
K <sup>+</sup>	1.2	7.4	Zn <sub>total</sub>	0.012	0.19
HCO <sub>3</sub> <sup>-</sup>	113.5	152.5	Cu <sub>total</sub>	0.004	0.023
SO <sub>4</sub> <sup>2-</sup>	36.0	77.8	Pb <sub>total</sub>	0.003	0.025
Cl <sup>-</sup>	1.07	178.2	Cd <sub>total</sub>	<0.001	0.003
NO <sub>3</sub> <sup>-</sup>	1.9	14.3			
SiO <sub>2</sub>	3.7	5.5			

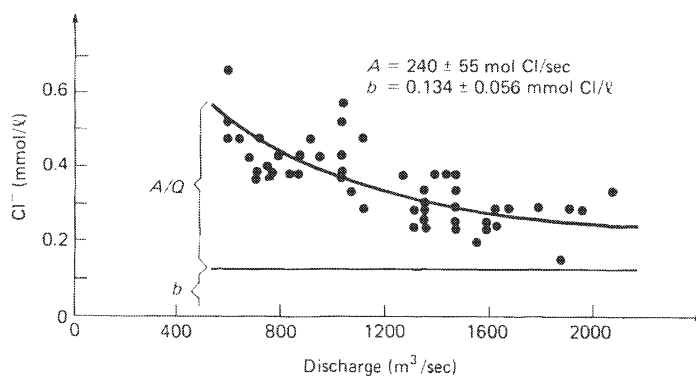
<sup>a</sup>Dissolved organic carbon reported as mg/lC.

leaves the Alps its composition (Table 12-15, column A) is typical for a ground- or surface water in a carbonate terrain (Chapter 3). The major ions are calcium and bicarbonate from limestone dissolution, with lesser amounts of magnesium (from dolomite) and sulfate (from gypsum–anhydrite). It is approximately in equilibrium with calcite and has an internal  $P_{\text{CO}_2}$  of about  $10^{-3.0}$  (the precise  $P_{\text{CO}_2}$  and degree of saturation vary seasonally). Where the Rhine crosses from Germany into Holland, concentrations of all solutes are higher, many much higher (Table 12-15, column B). Zobrist and Stumm (1981) attempted to calculate how much of the increase was anthropogenic by means of a statistical approach (Davis and Zobrist, 1978) and historical records. The statistical approach was to examine changes in solute concentrations as a function of discharge and to interpret the results on the assumption that:

1. Anthropogenic sources yield a fairly constant load per unit time (on a time-scale of months to years), independent of discharge.
2. Natural sources yield a fairly constant concentration, so the load transported per unit time increases as discharge increases. This assumption is reasonably valid for the Rhine because a large lake in its upper reaches (Lake Constance) serves as a reservoir of approximately constant composition.

**FIGURE 12-26** Predicted relationship between solute concentration and river discharge for a species whose concentration is strongly influenced by pollution. A represents the anthropogenic input per unit time (after Davis and Zobrist, 1978).





**FIGURE 12-27** Concentration of chloride in the Rhine at Basel (Switzerland) as a function of discharge, with the “best-fit” curve corresponding to the model discussed in the text (after Zobrist and Stumm, 1981).

If  $c$  is the concentration of a particular solute,  $b$  its natural (“background”) concentration,  $A$  its anthropogenic input per unit time, and  $Q$  is the river discharge per unit time, then ideally  $c$  should be given by the equation

$$c = \frac{A}{Q} + b$$

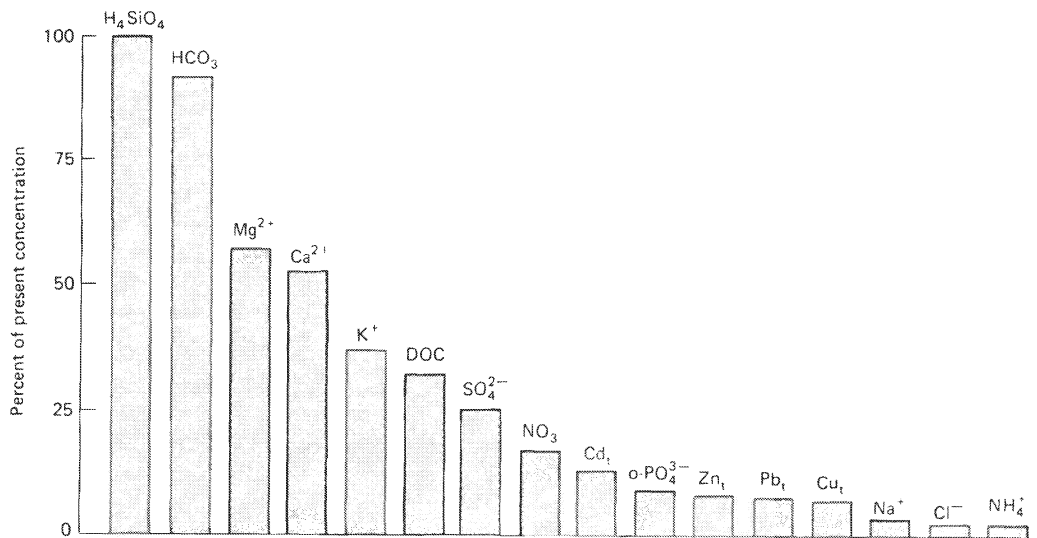
which is shown diagrammatically in Fig. 12-26. The data for several solutes fit this pattern reasonably well (Fig. 12-27), and an estimate of  $b$ , the background value, can be made from the parameters giving the best-fitting curve.

Chemical analyses of the Rhine date back to 1854, providing an independent estimate of the major-element composition of the Rhine prior to major industrial pollution. Both statistical and historical data indicate that more than 90 percent of the sodium and chloride in the lower Rhine are anthropogenic. Zobrist and Stumm concluded that the only solutes *not* strongly affected by human activities are silica and bicarbonate (Fig. 12-28).

## SUMMARY

### Thermodynamic Controls on Clay Mineral Formation

The formation of clay minerals during weathering is in general qualitative agreement with thermodynamic prediction. Gibbsite is formed where waters are extremely dilute, kaolinite is formed in dilute waters, and smectites are formed in more concentrated solutions. Water chemistry is closely tied to rainfall amount, so the distribution of soil clay minerals is also closely related to rainfall (Fig. 12-29). The apparent exceptions to this generalization are minerals such as vermiculite and illite, which are usually the result of slight alteration of pre-existing phases (micas) rather than completely new phases. Although general agreement is observed between clay mineral type, the agreement is only qualitative and no great importance should be attached to whether a water plots just to the left or just to the right of a particular boundary on a stability diagram. One reason is that the exact positions of the lines are not well defined because of uncertainties in the composition and degree of order in the natural minerals



**FIGURE 12-28** Estimated "natural" concentrations of solutes in the lower Rhine expressed as percentages of the concentrations now observed near the Germany-Holland border (Zobrist and Stumm, 1981). Note that very few species have not been influenced in a major way by human activities.

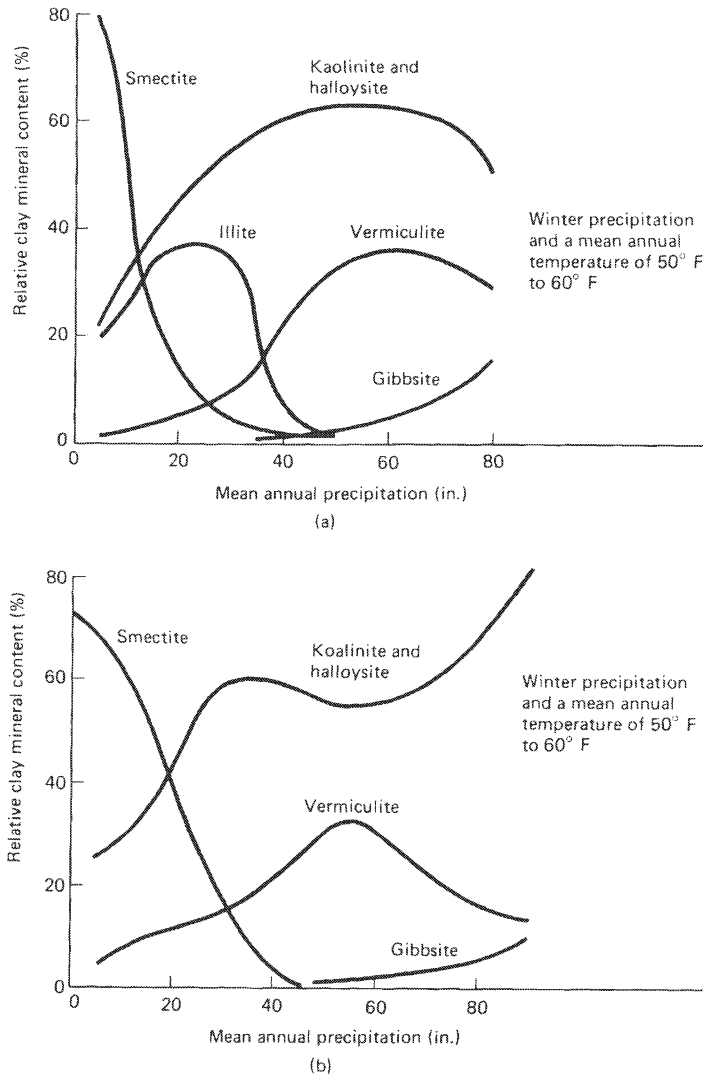
involved (Chapter 10). A second reason is that clay mineral formation commonly takes place in the soil zone. The chemistry of a stream draining a catchment is by no means identical to the chemistry of waters in the soils of the catchment. Finally, it is unlikely that secondary clay minerals, particularly smectite, form in true thermodynamic equilibrium with solution.

It is not clear at this time the extent to which natural water compositions are buffered by the coexistence of two clay minerals such as kaolinite and smectite. The concept that the identity of the secondary mineral formed during weathering changes in response to changes in solution chemistry is more generally useful than the idea of buffering by the coexistence of two solid phases.

### Environmental Factors and Water Chemistry

Here we try to make some generalizations about relationships among water chemistry and various environmental factors. As with most generalizations, there are many exceptions, and it is particularly difficult to generalize as to which of several factors will be most important in a specific situation.

**Rock Type.** Waters draining igneous and metamorphic rocks are relatively dilute (TDS generally less than 500 mg/l, often less than 100 mg/l), have bicarbonate as the major anion (unless there is an input of anthropogenic sulfate), and sodium and calcium as the major cations. Fine-grained and glassy rocks weather more rapidly and hence produce more concentrated waters than do coarse-grained rocks. Mafic rocks (basalt, gabbro, amphibolite) tend to produce more concentrated waters with higher Ca<sup>2+</sup>/Na<sup>+</sup> and Mg<sup>2+</sup>/Ca<sup>2+</sup> ratios than felsic rocks (granite, rhyolite). In very dilute waters from igneous rocks, the contribution of solutes from the atmosphere may be as large as the contribution from rock weathering. In such waters,



**FIGURE 12-29** Clay mineral composition of the surface layers of residual soils formed on (a) acid, and (b) basic igneous rocks in California (after Barshad, 1966).

the weathering of a volumetrically minor phase such as calcite or an amphibole may be the principal source of solutes.

Waters draining limestones and dolomites often have calcium, magnesium, and bicarbonate as the only significant solutes, although sulfate is commonly present from pyrite oxidation or associated gypsum. The TDS are limited by the solubility of the carbonate minerals in water that has been enriched in  $\text{CO}_2$  from the soil zone. TDS values are generally between 100 and 600 mg/l. Limestones weather more rapidly than igneous rocks, so, on average, waters draining limestones are more concentrated than those draining igneous rocks.



Among the siliciclastic (detrital) rocks, arkoses behave similarly to granites. Sandstones and, particularly, shales are more complex. The most abundant minerals in shales, illite and quartz, are relatively unreactive in the weathering environment and contribute relatively little to runoff chemistry. Shales commonly contain pyrite, which contributes sulfate to solution after oxidation, and calcite, which contributes calcium. Waters draining shales also often contain chloride and sodium. These are thought to originate from seawater trapped in the shale at the time of deposition, but the form in which these ions are stored in shales is not known. Thus waters draining shales are highly variable in composition. They usually have sulfate or chloride as major anions, and lower silica to total cation ratios than waters draining igneous rocks. The TDS values are highly variable.

Evaporites “weather” by simple dissolution and can give rise to waters of very high salinity. Typically, the principal anions are sulfate and/or chloride and the principal cations are sodium and calcium, although this may vary depending on the nature of the evaporite. In humid climates, evaporites generally do not survive for long near the surface and so do not usually cause high salinities in surface waters, although in tectonically active areas such as the Andes (Stallard and Edmond, 1983), evaporites may be present at the earth’s surface and be a significant source of solutes. In arid climates, saline waters resulting from solution of evaporites are quite common. High dissolved sulfate concentrations can also result from weathering of sulfide minerals in ore zones and in some igneous rocks.

Meybeck (1986, 1987) measured solute fluxes (the product of concentration and runoff) and calculated chemical denudation rates in more than 200 small, nonpolluted, monolithologic catchments in France. Amiotte-Suchet and Probst (1993) retabulated his results and calculated the weathering rate (determined as flux of  $\text{CO}_2$  from the atmosphere) for each rock type. The data was described well by the relationship:

$$F_{\text{CO}_2} = a \cdot Q_{\text{water}}$$

where  $F_{\text{CO}_2}$  represents the flux of  $\text{CO}_2$  consumed by weathering  $\text{mmol}/\text{km}^2/\text{s}$ ,  $Q_{\text{water}}$  is the runoff ( $\text{m}^3/\text{km}^2/\text{s}$ ), and  $a$  is a fitting parameter, which reflects the “weatherability” of the particular rock type. The constant  $a$  can be normalized to a value of 1 for plutonic and metamorphic rocks (Table 12-16). It then provides an index for the relative weathering rate of the minerals in different lithologies [in the climatic environment(s) of France].

**Climate.** White and Blum (1995) compiled input-output budgets from every gauged catchment on granitoid rocks in the world for which data were available. They restricted their study to granitoid rocks in order to minimize variability due to differences in lithology. They ignored biomass uptake and cation exchange, but focused their discussion on fluxes of sodium and silica, which are relatively unaffected by these processes. Their conclusions were:

1. Net sodium flux (corrected for atmospheric input) and silica flux could be described by an equation

$$Q_{i,w} = (a_i P) \exp \left[ -\frac{E_a}{R} \left( \frac{1}{T} - \frac{1}{T_0} \right) \right]$$

$Q_{i,w}$  is the flux of element  $i$  from weathering (moles/ha/y),  $a_i$  and  $E_a$  are constants (fitting parameters),  $P$  is annual precipitation (mm),  $R$  is the gas constant,  $T$  the mean annual temperature of the catchment (K), and  $T_0$  a “reference temperature,” taken to be 278°K or 5°C. Thus at a

**TABLE 12-16** Correlation Between CO<sub>2</sub> Consumption by Weathering and Runoff for Monolithologic Catchments in France [after Amiotte-Suchet and Probst, 1993]

Rock Type	N <sup>a</sup>	a (see text)	Correl. Coeff.	Relative Rate	
				CO <sub>2</sub> cons.	Solute flux <sup>b</sup>
Plutonic and metamorphic (granite, gneiss, schist)	41	0.095	0.92	1.0	1.0
Felsic volcanic rocks (rhyolite, andesite, trachite, etc.)	22	0.222	0.98	2.3	
Basalt	18	0.479	0.98	5.0	
Sandstone, arkose, graywacke	47	0.152	0.71	1.5	1.3
Argillaceous rocks (clays, shales, slate)	34	0.627	0.95	6.6	2.5
Carbonate rocks (limestone, dolomite, chalk, marl)	19	1.586	0.98	16.7	12.0
Evaporites	9	0.293	0.99	3.1	40-80

<sup>a</sup>Number of catchments; <sup>b</sup>Solute flux (from Meybeck, 1986, 1987) includes solutes (e.g. Cl<sup>-</sup>, SO<sub>4</sub><sup>2-</sup>) not directly related to CO<sub>2</sub> consumption.

given temperature, the flux from weathering was proportional to precipitation. At a given precipitation, the flux increased exponentially with increasing temperature.  $E_a$  is analogous to an activation energy for a single chemical reaction (Chapter 11). For dissolved SiO<sub>2</sub>,  $a$  had a value of 0.046 and  $E_a$  59.4 kJ/mol; for Na the values were 0.097 and 62.5 kJ/mol respectively.

2. Although silica and sodium fluxes could be related to precipitation and temperature, no such relationship could be established for Ca, Mg, and K. White and Blum implied that "noise" from variations in mineralogy, biomass uptake, and/or cation exchange was swamping the "signal" from precipitation and temperature. This lack of correlation is somewhat disturbing, because Ca is generally the most important cation in the total weathering flux.

In general, it is difficult to resolve the effect of temperature *per se* from that of other variables; relief, physical erosion rate, and vegetation type all tend to correlate with temperature.

**Relief.** The relationship between chemical weathering rate and relief is controversial. In the Amazon basin, there is a clear relationship: chemical weathering increases with increasing relief, such that most (about 86%) of the solutes delivered to the ocean by the Amazon come from the Andes mountains, which make up about 12 percent of the total basin area (Gibbs, 1967; Stallard and Edmond, 1983). The problem is that in the Amazon basin, lithology and relief are highly correlated. Outcrops of limestone and evaporites are present in the Andes, whereas the rest of the Amazon basin is underlain by silicate rocks (including alluvium). The question is thus whether the weathering rates of silicate rocks are a function of relief, or whether the high rate simply reflects the presence of easily weatherable rocks. Stallard (1985) presented a model in which weathering rate was limited by chemical processes where erosion was active (a weathering-limited system) and by the accumulation of secondary products where erosion is minimal (a transport-limited system). Weathering rate should thus reflect erosion rate, which should be a function of relief. Stallard (1985) and Edmond et al. (1995) imply that silicate weathering rate in the Andes does in fact increase with increasing relief. Probst et al. (1994) disagree, and contend that the apparent effect of elevation is simply an effect of lithology.

White and Blum (1995) saw no relationship between weathering rate and relief in the catchments they studied. This may be because their population of catchments did not include any areas of really low relief such as the Amazon basin, or it may be that any effect was lost in the "noise" of their data.

In any event, we would not expect weathering rate to increase as a simple monotonic function of relief. According to Stallard's (1985) model, weathering initially increases as soil thickness increases, only decreasing when a very thick layer of weathered material has accumulated. Thus at very high rates of erosion, weathering should be slow because of the absence of soil. It should go through a maximum at some intermediate erosion rate/soil thickness, and then decrease again at very low erosion rates. Even this discussion assumes that soil thickness represents some sort of steady state, which may be unrealistic. Drever and Zobrist (1992) showed a clear decrease in weathering rate with increasing elevation in the southern Swiss Alps. They attributed the higher rates at lower elevations to higher temperatures and greater soil thickness. The area was topographically steep; apparently soils had not become sufficiently thick for weathering to be inhibited. The presence of soil initially increases weathering rate because water is retained in the weathering environment, because fine-grained primary minerals are retained in the weathering environment increasing the mineral surface area exposed to solution, and because plants supply  $\text{CO}_2$  and organic acids to the weathering environment (Drever, 1994). Weathering rate will decrease only when primary minerals become depleted in the soil.

**Vegetation.** The effect of vegetation is complex, and vegetation is obviously not independent of climate, rock type, and relief. Vegetation supplies  $\text{CO}_2$  and organic acids to the soil, which increases the rate of chemical weathering. On the other hand, vegetation stabilizes the soil and prevents physical erosion. Fresh rock is then not exposed at the surface, there is less contact between rainwater and fresh rock, and the rate of chemical weathering is decreased. Deforestation of a forested area results in an increase in TDS in runoff waters, and colonization by plants of a previously unvegetated area, such as a lava flow, also causes an increase in TDS. The question is discussed in detail in Drever (1994).

**Time.** Time, in the sense of time of contact between rock and water, is probably the most important variable in determining the chemistry of runoff from igneous rocks, but contact time is itself a function of other environmental parameters. High rainfall leads to rapid fluxing of water and short contact time. Local drainage is also important; well-drained areas have short contact times and hence tend to have kaolinitic soils, whereas poorly drained areas have longer contact times and tend to have smectite as the soil clay mineral. The effect of rock permeability is not simple. If the permeability is high, contact time in the vadose zone may be short because the water drains rapidly, and may be short or long in the groundwater system, depending on local hydrology. If permeability is low, there may be little infiltration and hence little contact between water and bedrock.

By stabilizing the soil, vegetation has the effect of increasing the contact time of initial weathering products with incoming rainwater. Thus forested areas tend to have kaolinite (or gibbsite) in the soil. Even if a smectite was initially formed, the smectite will have been leached to kaolinite in the soil. (Vegetation also plays a more active role, of course, particularly in creating an acid microenvironment around rootlets.) In the absence of vegetation, an initially formed smectite would probably have been eroded before it could be weathered to kaolinite.

## REVIEW QUESTIONS

1. The following is a calculated composition for the average river draining North America (Garrels and Mackenzie, 1971). Draw up a plausible budget to account for the sources of the solutes. Units are milliequivalents per liter for ions, millimoles per liter for silica.

$\text{HCO}_3^-$	$\text{SO}_4^{2-}$	$\text{Cl}^-$	$\text{Ca}^{2+}$	$\text{Mg}^{2+}$	$\text{Na}^+$	$\text{K}^+$	$\text{SiO}_2$
1.26	0.42	0.22	1.05	0.42	0.39	0.04	0.15

2. Perform the same calculation using the computer code NETPATH or PHREEQC. What are the advantages and disadvantages of using this code compared to the manual calculations in question 1?
3. Repeat Garrels and Mackenzie's calculations for the mass balance of the Sierra Nevada Springs using NETPATH. What differences do you observe? (The NETPATH disk and manual contain an instructive discussion of this problem.)
4. Obtain chemical analyses of waters from your area. Try to evaluate the probable sources of the dissolved constituents, and assess the extent to which equilibria involving solid phases might be influencing the compositions of these waters.

## SUGGESTED READING

- BERNER, E. K., and R. A. BERNER. (1996). *Global Environment: Water, Air, and Geochemical Cycles*. Upper Saddle River, N.J.: Prentice-Hall. Chapters 4 and 5.
- GARRELS, R. M., and F. T. MACKENZIE. (1967). Origin of the chemical compositions of some springs and lakes. *Equilibrium Concepts in Natural Water Systems*. American Chemical Society Advances in Chemistry Series, 67, 222–242.
- GARRELS, R. M., and F. T. MACKENZIE. (1971). *Evolution of Sedimentary Rocks*. New York: W. W. Norton. Chapter 6.
- HOLLAND, H. D. (1978). *The Chemistry of the Atmosphere and Oceans*. New York: Wiley Interscience. Chapter 2.
- PLUMMER, L. N., and W. BACK. (1980). The mass-balance approach: Application to interpreting the chemical evolution of hydrologic systems. *American Journal of Science*, 280, 130–142.
- PLUMMER, L. N., E. C. PRESTOMON, and D. L. PARKHURST. (1994). An interactive code (NETPATH) for modeling *Net* geochemical reactions along a flow *Path*: Version 2.0. U.S. Geological Survey, Water-Resources Investigations Report 94–4169. This DOS/Windows version of NETPATH (and its successor PHREEQC) is available directly from the USGS and may be downloaded from the Internet. Macintosh versions are available commercially from GeoChem Software, Inc., P.O. Box 7252, Reston, VA 22091, USA.
- We strongly urge the reader to study the publications discussed in this chapter. The original papers contain much more information than the brief summaries presented here.

# 13

## Acid Waters

We introduced the concept of alkalinity in Chapter 3. Ignoring minor species,

$$\text{Alkalinity} = m_{\text{HCO}_3^-} + 2m_{\text{CO}_3^{2-}} + m_{\text{OH}^-} - m_{\text{H}^+}$$

For the common waters we have been discussing up to now, the dominant term in the equation has been  $m_{\text{HCO}_3^-}$  and alkalinity has been a positive quantity. In *acid* waters, as defined here, alkalinity is negative, which means

$$m_{\text{H}^+} > m_{\text{HCO}_3^-}$$

From the charge balance equation (Eq. 3-5), this means that some other anion must be present. The anion is most commonly sulfate, less commonly nitrate or an organic anion. Acid waters are an environmental concern because they are generally toxic to fish and other aquatic organisms and often contain high concentrations of heavy metals. The common causes of acidification are deposition of acidic compounds from the atmosphere ("acid rain"), and oxidation of sulfide minerals, commonly associated with mining activities (acid mine drainage). Acidification by organic acids may also occur naturally in cool, humid climates.

### ACIDITY AND ALKALINITY

Chapter 3 presented the concepts of alkalinity as the capacity of a system to neutralize acid and acidity as the capacity of a system to neutralize base. Here we will discuss the use of these terms in the context of acid waters.

In the simple carbonate system, the equivalence point where acidity and alkalinity are both zero is given by the condition:

$$m_{\text{H}^+} = m_{\text{HCO}_3^-} + 2m_{\text{CO}_3^{2-}} + m_{\text{OH}^-}$$

Since this will be at a pH below 7,  $m_{\text{CO}_3^{2-}}$  and  $m_{\text{OH}^-}$  will be negligible. The equivalence condition simplifies to:

$$m_{\text{H}^+} = m_{\text{HCO}_3^-}$$

From the expression for  $K_1$ , the first dissociation constant for carbonic acid (Eqs. 3-3 and 3-2), we can see that the equivalence point will vary as a function of  $P_{\text{CO}_2}$  (Fig. 13-1):

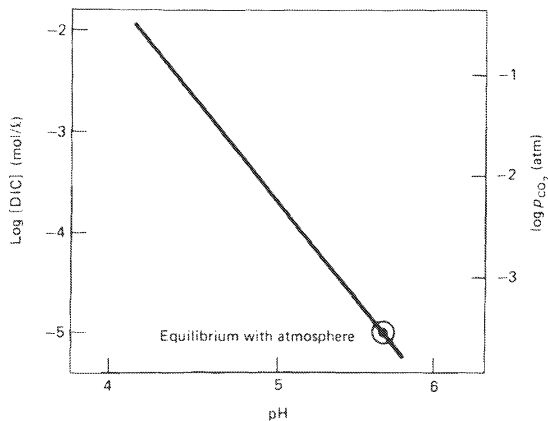
$$m_{\text{H}^+}^2 = K_1 K_{\text{CO}_2} P_{\text{CO}_2}$$

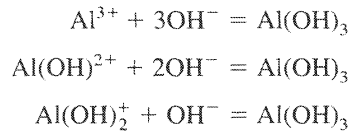
Thus the boundary between alkalinity and acidity does not occur at a fixed pH unless the  $P_{\text{CO}_2}$  (and temperature) is also fixed. If alkalinity and acidity are determined by titration, the equivalence point can be determined graphically by means of a Gran plot (Chapter 3). The  $P_{\text{CO}_2}$  at the equivalence will be determined by the  $\text{CO}_2$  produced during the titration, as well as the initial  $P_{\text{CO}_2}$  of the water. If anions of weak organic acids are important contributors to the alkalinity, there may be no clearly defined equivalence point. The definitions of alkalinity and acidity become conceptually difficult in such waters, and there is no definition that is both rigorous and convenient. The problem is that some organic acids are quite strong (oxalic acid has a  $\text{p}K_a$  value below 2), whereas others are quite weak. Probably the best practical approach is to define an *equivalence* or *reference* pH arbitrarily (say, pH 5.0); the acidity of a solution would then be the equivalents of base needed to raise the solution pH to 5.0, and the alkalinity would be the equivalents of acid needed to lower the pH to 5.0. The main disadvantage of this approach is that acidity and alkalinity defined in such a way are no longer strictly conservative. Alkalinity defined in this way includes those organic anions that are titrated to uncharged acids at pH 5 and above; anions of stronger organic acids are not included. The terms *acid-neutralizing capacity* (ANC) and *base-neutralizing capacity* (BNC) are more or less equivalent to alkalinity and acidity, respectively.

Pure water in equilibrium with atmospheric  $\text{CO}_2$  would have a pH of 5.66 at  $25^\circ\text{C}$  and 5.60 at  $0^\circ\text{C}$ . Thus, for waters in equilibrium with atmospheric  $\text{CO}_2$ , any water with a pH below 5.6 would properly be called "acid." For many purposes, 5.6 is not a particularly convenient point to define the onset of "acidification." Unpolluted rain commonly has a pH of around 5.0, and biological effects due to acidity are generally not noticeable until a pH of about 4.7. In common usage, a water is generally not considered acid unless it has a pH below 5.0. The terms *acidified* and *acidification* are used in different ways by different authors. The most common usage is "made acid" in the sense described above. Acidification is also sometimes used to describe any decrease in alkalinity from some previous value.

In acid waters, aluminum species often make a major contribution to acidity. If a solution containing  $\text{Al}^{3+}$  is titrated with strong base, the following reactions will occur:

**FIGURE 13-1** pH of the bicarbonate/ $\text{CO}_2$  equivalence point ( $25^\circ\text{C}$ ) as a function of dissolved  $\text{CO}_2$  (dissolved inorganic carbon, DIC) concentration or  $P_{\text{CO}_2}$ .





where the  $\text{Al}(\text{OH})_3$  represents a solid precipitate. (The concentration of the complex  $\text{Al}(\text{OH})_3^0$  is usually negligibly small.) The acidity (the negative alkalinity) thus becomes (ignoring organic anions,  $\text{CO}_3^{2-}$  and  $\text{OH}^-$ ):

$$\begin{aligned} \text{Acidity} &= m_{\text{H}^+} - m_{\text{HCO}_3^-} + 3m_{\text{Al}^{3+}} + 2m_{\text{Al}(\text{OH})^{2+}} + m_{\text{Al}(\text{OH})_2^+} \\ &\quad (\text{plus corresponding } \text{Fe}^{3+} \text{ species, usually minor}) \end{aligned}$$

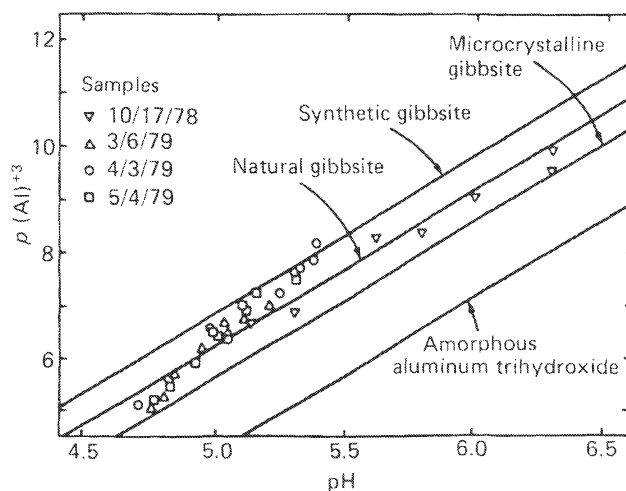
The contribution of Al species to the titration acidity is called the *aluminum acidity*.

## SOLUBILITY OF ALUMINUM HYDROXIDE

One characteristic of acid waters is the presence of elevated concentrations of dissolved aluminum. This would be expected on the basis of the solubility of aluminum hydroxides and aluminosilicates (Figs. 10-3 and 10-4), but it is remarkable how rapidly infiltrating water in soils acquires a dissolved Al concentration similar to that which would be expected for equilibrium with gibbsite (Figure 13-2; Johnson et al., 1981). Exact equilibrium is not attained (Hooper and Shoemaker, 1985; Neal et al., 1990), and the actual mineral source of the Al is not certain. Exchange sites on clays and hydroxy interlayers in vermiculite (Chapter 4) may both be important.

Calculations involving dissolved aluminum are complicated by the fact that aluminum forms strong complexes with fluoride ion and dissolved organic matter, and sulfate complexes can also be significant. Methodologies have been developed to distinguish organically complexed Al from inorganically complexed (e.g., Driscoll, 1984; Johnson et al., 1981; LaZerte, 1984; Seip et al., 1984), and accurate measurement of dissolved fluoride is necessary to evaluate complexing by fluoride. Fluoride concentrations well under 1 ppm are important for the

**FIGURE 13-2** Measured aluminum concentrations from Falls Brook, New Hampshire compared to solubilities of  $\text{Al}(\text{OH})_3$  phases. Reprinted from *Geochim. Cosmochim. Acta*, v. 45, Johnson et al., 1981, "Acid rain, dissolved aluminum and chemical weathering at the Hubbard Brook Experimental Forest, New Hampshire" (p. 1421-1437), with kind permission from Elsevier Science Ltd., The Boulevard, Langford Lane, Kidlington OX5 1GB, U.K.

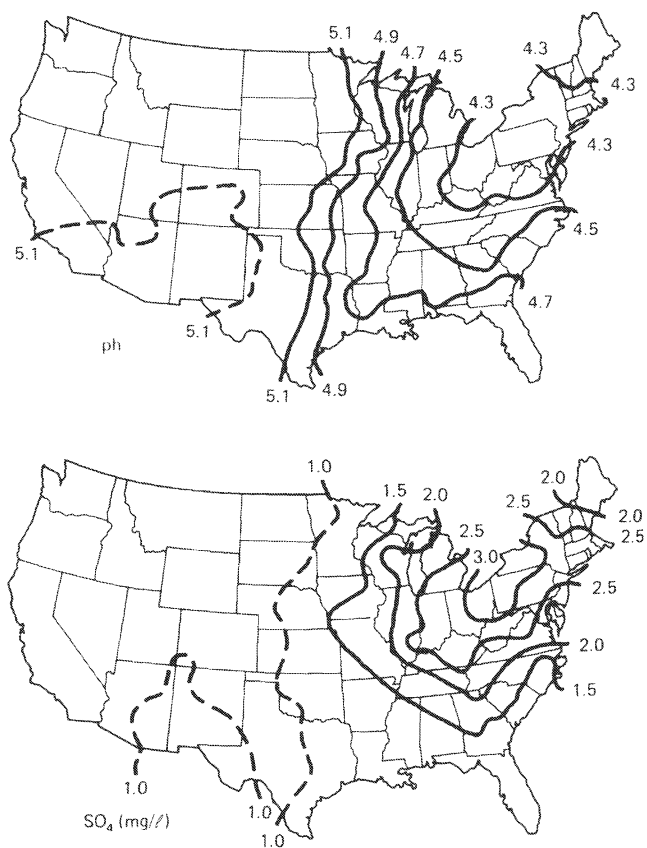


speciation of aluminum. Speciation of Al is important both for chemical calculations and for toxicity studies. Organically complexed Al is much less toxic to fish than free or inorganically complexed Al (e.g., Baker and Schofield, 1980, 1982).

## ACID DEPOSITION

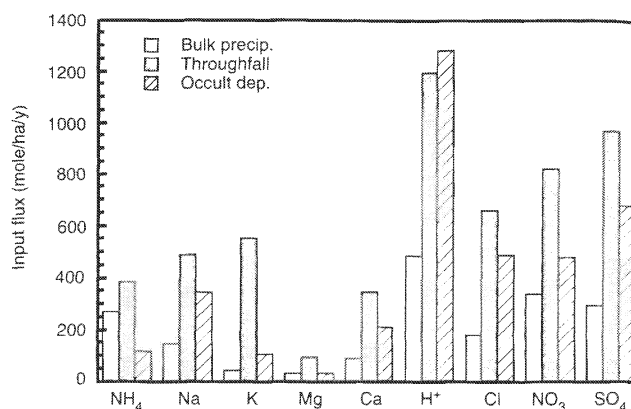
As we discussed in Chapter 1, large areas of eastern North America and northern Europe are receiving significant inputs of sulfuric and nitric acid as a result of fossil-fuel combustion and smelting of nonferrous metals (Fig. 13-3). The acid components can be dissolved in precipitation (wet deposition or "acid rain"), and they may be deposited as particles, or acid precursor gases such as  $\text{SO}_2$  and  $\text{NO}_x$  may be absorbed directly by plants and other surfaces as *dry* or *occult deposition* (Chapters 1 and 12). Occult deposition includes deposition from fog or clouds. Dry deposition is very difficult to measure quantitatively, but in many areas it is at least as important as wet deposition (Fig. 13-4). In areas receiving acid deposition, some, but by no means all, of the streams and lakes become acidified, implying a pH below 5. Acidified lakes generally contain elevated dissolved aluminum concentrations and cannot support fish populations. The loss of fish is generally attributed to the combined toxic effects of Al and acidity rather than the low pH alone (e.g., Baker and Schofield, 1980). The acidity of affected waters

**FIGURE 13-3** Annual weighted mean pH and sulfate concentration in precipitation in North America in 1985 (after NADP, 1987).





**FIGURE 13-4** Comparison of inputs from precipitation (Bulk precip.) collected in an open field with precipitation collected under the forest canopy (Throughfall) in a conifer forest in the Vosges mountains of France (data from Probst et al., 1990). The third column (Occult dep.) represents the difference between throughfall and precipitation, corrected for elements (most noticeably potassium) that are cycled through the trees. The hydrogen ion flux is also affected by this correction (after Drever and Clow, 1995).



often varies seasonally, with a “pulse” of acidity at the time of snowmelt as acid components deposited in snow are flushed into surface waters. This acid pulse may have a significant impact on aquatic organisms, particularly if they are in a sensitive life stage at the time of snowmelt.

As a consequence of the environmental effects of acid deposition, there has been a great deal of research on processes related to surface water acidification. This research is aimed partly at understanding why acidification occurs in one place and not another, partly at predicting where acidification will occur in the future, and partly at predicting the effectiveness of various mitigating measures. This research provides some excellent examples of the application of the principles discussed in previous chapters.

### Cation Exchange

As rain or snowmelt percolates through soil, the ions from the precipitation and any dissolved aluminum (see above) interact with exchangeable cations on clays, oxides, and organic matter in the soil. The cation ratios in the solution that exits from the soil will reflect the composition of the exchangeable cations, rather than the ratios in the incoming precipitation.

The exchangeable cations (often referred to as the *cation-exchange complex* or *cation-exchange pool*) in cool-temperate forest soils on granitic rocks are dominated by aluminum, with lesser amounts of calcium and other cations; that is, they have a low *base saturation*. The base saturation is the fraction of the exchange sites that are occupied by the *base cations*, Ca<sup>2+</sup>, Mg<sup>2+</sup>, Na<sup>+</sup>, and K<sup>+</sup>. The balance of the exchange sites are occupied by Al<sup>3+</sup> or H<sup>+</sup>. When a soil with low base saturation is made into a slurry with water, the pH of the water is generally low, commonly between 4 and 5, but sometimes below 4. The low pH is a consequence of exchangeable H<sup>+</sup>, hydrolysis of exchangeable Al, and sometimes dissociation of carboxylic acid groups on soil organic matter. Solid organic matter may be a major contributor to the cation exchange capacity of forest soils. A soil is referred to as acid when the pH of a slurry with water is below about 5.

The interaction of acid deposition with the exchange pool of soils has been modeled quantitatively by Reuss (1983). For simplicity, Al and Ca were regarded as the only exchangeable ions. The exchange equation (Eq. 4-7, Chapter 4) is

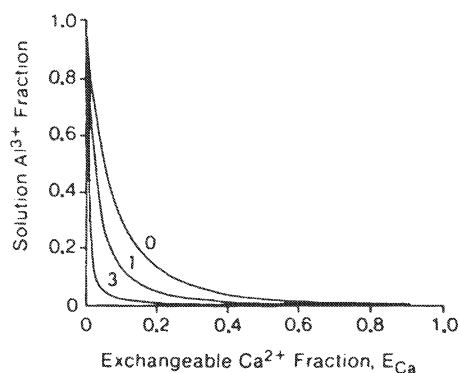
$$\frac{E_{\text{Al}}^2}{E_{\text{Ca}}^3} = K_{\text{ex}} \frac{C_{\text{Al}^{3+}}^2}{C_{\text{Ca}^{2+}}^3} \quad (13-1)$$

where  $E$  represents the equivalent fraction on the exchange sites ( $E_{Ca} = 1 - E_{Al}$ ),  $K_{ex}$  the exchange equilibrium constant, and  $\text{C}$  the activities in solution. If the sum of the cations in solution is constant (determined by the concentration of mobile anions, see below), the cation fraction of Al in solution ( $= 3m_{Al^{3+}}/[3m_{Al^{3+}} + 2m_{Ca^{2+}}]$ ) can be calculated as a function of the equivalent fraction of Ca on the exchange sites (Fig. 13-5).

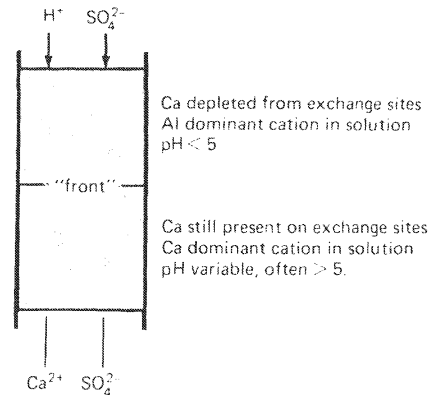
The behavior is similar for all reasonable values of  $K_{ex}$ : as long as the fraction of the exchange sites occupied by Ca is greater than about 0.15 to 0.2, calcium will be the dominant cation in solution. As the fraction of sites occupied by Ca drops below 0.2 or 0.15, there is a relatively abrupt change in solution composition from calcium dominance to aluminum dominance.

To understand the implications of this for acid deposition, let us consider what would happen if we poured dilute sulfuric acid onto a column of soil (Fig. 13-6) and monitored the composition of the outflow. Let us assume that the exchangeable Ca fraction was about 0.4 initially. When the hydrogen ion is added to the column, the  $H^+$  is consumed either by a cation-exchange reaction or by dissolution of an aluminum hydroxide to form  $Al^{3+}$  ions that interact with the exchange pool. Initially, the input of cations will be small compared to the amount of cations in the exchange pool, so the net effect will be that the input cations are adsorbed and are replaced in solution by an equivalent amount of cations from the exchange sites. With our initial exchangeable Ca fraction of about 0.4, essentially the only cation in solution will be  $Ca^{2+}$  (Fig. 13-5). Thus, as we add  $H_2SO_4$  to the top of the column, the solution coming out the bottom of the column will be  $CaSO_4$ , and the total concentration will be equivalent to the concentration of  $SO_4^{2-}$  in the input. It actually makes no difference initially which cation we add ( $H^+$ ,  $Na^+$ , or  $Ca^{2+}$ ) because the cation ratios in the output are determined by the exchange pool, not the input. This phenomenon is called the *salt effect*. If the soil is already acidified (exchange sites dominated by Al), we may see the reverse effect: the solution coming out will be acidic and dominated by Al regardless of whether the input is  $H^+$  or a base cation. Initially, then, as we add acid to the top of the column, the solution coming out the bottom is near-neutral and dominated by calcium. The only detectable effect of the acid is to increase the cation concentration in the output. As we continue to add acid, however, the supply of exchangeable calcium will become depleted, and a "front" will move down through the column. Above the front, exchangeable Ca will be depleted and the solution will be acidic and dominated by  $Al^{3+}$ ; below the front, exchangeable Ca will still be present, and the solution will be near-neutral and dominated by  $Ca^{2+}$ . As the front reaches the base of the column, there will be a relatively abrupt change in the composition of the output, and the output will have become "acidified."

**FIGURE 13-5** Relationship between ratio of Al to Al + Ca in solution and ratio of Ca to Al + Ca on exchange sites (both in units of equivalents of charge) for different values of the exchange constant,  $\log K_{ex}$  (after Reuss, 1983).



**FIGURE 13-6** Soil column affected by simulated acid deposition.



The column experiment could be regarded as an analog for the soils in a drainage basin. Considerable time could elapse before the input of acidity from the atmosphere showed up as acidification of streams; indeed, if thick soils with high cation-exchange capacity were present, the time lag could be centuries. The salt effect also has implications for the restoration of acid-affected systems. Once the base cations of a soil are depleted, the cations in water draining from the soil will be aluminum and hydrogen regardless of what the input cation is (over the short term). Thus, in a basin where the streams have become acidified, the streams will remain acidified for a considerable time even if the input of acidity from the atmosphere stops.

### Anion Mobility and Anion Exchange

In soil solutions, anions such as chloride and sulfate are generally less affected by chemical and biological interactions than the major cations. In areas affected by acid deposition, sulfate is generally the major anion in soil solutions, and it tends, with some notable exceptions discussed below, to be carried unchanged through the soil by percolating water. An anion that is transported conservatively is referred to as a *mobile anion*. Charge balance requires that the mobile anion be balanced by equivalent cations; the concentration of the mobile anion generally dictates the total concentration of ions in solution, and the requirement of charge balance influences the distribution of protons and hence acidity–alkalinity (Seip et al., 1980). If, for example, a tree extracts  $K^+$  from the soil solution, some complementary process must take place to maintain charge balance (see biological effects below). The complementary process is often, in effect, the excretion of a proton, adding to the acidity of the soil solution.

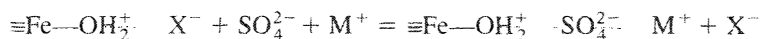
Nitrate is the other major anion associated with acid deposition. In areas where vegetation is active, nitrate is generally taken up by plants and does not behave as a mobile anion. Where plant growth is absent or where the input is so high that the vegetation's ability to take it up is swamped, nitrate behaves as a mobile anion, just as chloride would. This situation is referred to as *nitrogen saturation*. When nitrate is taken up by a plant, charge balance requires that either a proton (or a cation) be taken up with the nitrate or an anion (e.g.,  $OH^-$ ) be excreted. The net effect is a decrease in the acidity of the soil solution; the acidity associated with the nitrate in precipitation has effectively been neutralized.

Conversely, if there is a loss of nitrogen from the biomass due to nitrification, the release of nitrate will generate equivalent acidity.

### Processes Affecting Sulfate Mobility

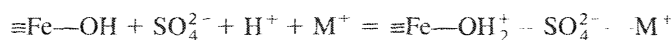
**Anion Exchange.** As discussed in Chapter 5, the surface charge on oxide surfaces is a function of pH. At low pH, aluminum and iron oxide surfaces tend to be positively charged and to exhibit anion exchange. The B-horizons of spodosols, the common type of soil in northern temperate forests, contain hydrated aluminum and iron oxides. As with cations, divalent anions are strongly favored on adsorption sites over monovalent anions in dilute solution, and sulfate is preferentially adsorbed over nitrate and chloride; adsorption of these two is negligible in the presence of sulfate. Phosphate species are much more strongly adsorbed than sulfate, but phosphate concentrations are generally too low to be of any significance in the overall anion balance. The stoichiometry of anion exchange can be regarded in several ways:

1. At a single preexisting positive site,



---represents association by electrostatic adsorption, and  $\text{M}^+$  represents a cation ( $\text{H}^+$ ,  $1/3\text{Al}^{3+}$ ,  $1/2\text{Ca}^{2+}$ ,  $\text{Na}^+$ , etc). Since the dominant adsorbed cation in acid soils is  $\text{Al}^{3+}$  and the dominant cations in solution are likely to be  $\text{H}^+$  and  $\text{Al}^{3+}$  adsorption of sulfate will result in a decrease in acidity. The net effect on acidity will depend on whether there is significant uptake of a nonacidic cation (i.e.,  $\text{Ca}^{2+}$ ) and the nature of  $\text{X}^-$ , the anion displaced. Assuming adsorption of  $\text{Ca}^{2+}$  is negligible, if  $\text{X}^-$  is a mobile anion, the loss of acidity will equal half the loss of sulfate; if  $\text{X}^-$  is bicarbonate or hydroxide, the loss in acidity will equal the loss of sulfate. If  $\text{X}^-$  is an organic anion, the net effect on acidity will depend on the subsequent fate of the anion. If it is adsorbed or decomposed, the corresponding acidity will be removed from solution. Experimental work by Wiklander (1980) with sulfate salts suggests that adsorption at a single preexisting positive site describes sulfate uptake by natural hydrous oxides.

2. Adsorption by generation of a new positively charged site:



Here it could be argued that new sites would be formed either by protonation of surface sites or specific adsorption of sulfate. If  $\text{M}^+$  represents  $\text{H}^+$  and/or  $1/3\text{Al}^{3+}$ , the net effect is removal of acidity from solution equal to the amount of sulfate removed.

Several other mechanisms can be postulated, but the net effect of any can be estimated from charge-balance considerations. If an anion is removed from solution, either equivalent cations (most probably protons or  $\text{Al}^{3+}$  and hence acidity in acid soils) are removed with it, or equivalent anions are released to solution. The only plausible anions are  $\text{OH}^-$  from the oxide surface (which is equivalent to an uptake of protons) or organic anions, as discussed above. Overall, adsorption of sulfate in acid soils results in a decrease in solution acidity, although there may not be a 1:1 relationship between sulfate loss and acidity loss.

**Biological Mechanisms.** Sulfate is an essential nutrient and is taken up by plants. Uptake of sulfate results in a corresponding loss of acidity, as discussed for nitrate above.

However, in areas affected by acid deposition, the input of sulfate from the atmosphere is far in excess of plant requirements, and so net uptake by plants is relatively unimportant.

Sulfate reduction to sulfide may also be an important process in anaerobic (gleyic) horizons in soils, swamps and bogs, and lake sediments. Here again, the net effect is removal of acidity (or generation of alkalinity) equal to the sulfate lost. Sulfate reduction is locally important, but probably does not have much effect on a regional scale.

The reverse process—oxidation of preexisting sulfides (commonly in bedrock)—may be a locally important source of sulfate and acidity.

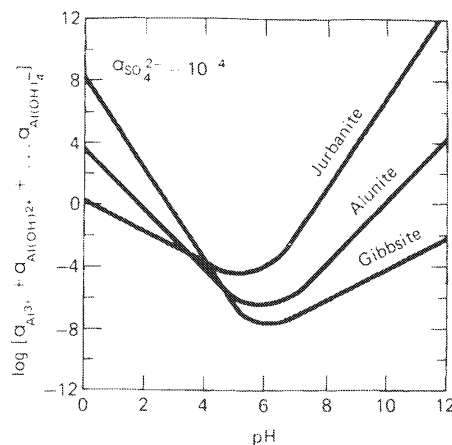
**Aluminum Sulfate Precipitation.** The minerals alunite  $[KAl_3(SO_4)_2(OH)_6]$  and jurbanite  $[Al(SO_4)(OH)]$  may be more stable than gibbsite in acidic sulfate-containing waters (Fig. 13-7). They are well known in waters acidified by oxidation of sulfide minerals, and it has been suspected that they may form in soils subject to acid deposition (Nordstrom, 1982). They have not been observed directly, and their presence was inferred from the compositions of soil solutions. It is very difficult in practice to distinguish the effect of aluminum sulfate precipitation from sulfate adsorption. Both cause removal of acidity equivalent to removal of sulfate from solution. The current consensus is that alunite and jurbanite are not important in soils affected by acid deposition, but are important in acid mine drainage (see below).

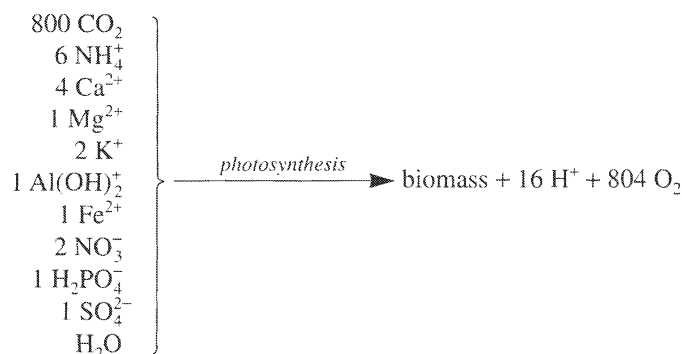
### Biological Processes

Biological processes affect the proton balance of soils and surface waters in a variety of ways, and there has been considerable confusion in the literature over the role of these processes in the acidification of surface waters.

**Biomass Changes.** The term *biomass* is used loosely here to include both living plants and nonliving organic matter in the soil. In terms of mass, there is much more organic carbon in the soil than in living plants. When a plant grows, it extracts both cations and anions as nutrients from the soil solution. As discussed in Chapter 12, the effects of biomass changes on ionic budgets can be quite large. In the context of acid deposition, Schnoor and Stumm (1985) described the synthesis of terrestrial biomass by the equation

**FIGURE 13-7** Solubility curves for gibbsite, alunite, and jurbanite at sulfate and potassium activities of  $10^{-4}$  (solubility of alunite is relatively insensitive to  $K^+$  activity, even though it contains K) (after Nordstrom, 1982).





According to this budget, plants take up more cations than anions and must thus “excrete” protons to maintain charge balance. There is some uncertainty as to the appropriate form of nitrogen to use in the balance (which has a large influence on the net production of protons), but there is no doubt that biomass aggradation depletes base cations and supplies acidity to soil solutions. If the biomass were in a steady state, removal of base cations by growth would be exactly balanced by the supply of base cations by decomposition. Biomass is rarely in a steady state, however (e.g., Vitousek and Reiners, 1975). Logging, particularly whole tree removal, removes base cations permanently from the system. Also, reforestation has taken place in many parts of the northeastern United States and northern Europe, and this may have contributed to the acidification of surface waters in these areas (Rosenqvist, 1978; Krug and Frink, 1983). Trees have a second major effect on acidification. As discussed in Chapter 12, trees, particularly conifers, greatly increase rates of dry deposition of sulfate and nitrate compared to grassland and heath. Thus planting conifers, which is a common practice, particularly in northern Europe, significantly increases the input of acidity into the ecosystem.

A decrease in biomass should have the reverse effect: it should contribute alkalinity to the soil solution. This effect is most noticeable following a fire; the potential anions (mostly nitrate) are lost to the atmosphere, while the base cations are returned to the soil and cause a corresponding increase in alkalinity. In the absence of fire, the process can be more complicated. Any cations released during decomposition will interact with the exchangeable cation pool in the soil (see discussion above). The cations that leave the soil will tend to be aluminum and calcium, so the net effect of a decrease in biomass may be release of acidity to surface waters, with a corresponding decrease in acidity in the soil. This is another example of the salt effect discussed above. Nitrification processes may also cause a short-term release of nitrate (acidity) unaccompanied by base cations.

In aquatic systems, mosses such as sphagnum extract cations very efficiently from the water and hence contribute to acidification (Clymo, 1967). The effect is most noticeable in waters associated with peat bogs and swamps, waters that are typically associated with high concentrations of organic acids.

**Production of Organic Acids.** Decomposition of organic matter produces organic acids, particularly humic/fulvic acids (see Chapter 6). These acids contribute protons to the soil solution and affect the acidity–alkalinity balance. The growth of forest on a previously unforested area is accompanied by a progressive decrease in soil pH (for a discussion, see Krug and Frink, 1983). The decrease is due to the related processes of humus buildup and removal of readily weathered minerals from the upper soil horizons. There is no question that

organic acids cause low pH values in soil solutions, but their overall effect on surface waters is less clear. Low-pH lakes and streams in which the principal solutes are organic (mostly fulvic) acids are quite common in association with swamps and peat bogs, but these waters normally support fish populations, and they are not typical of the waters thought to be acidified by atmospheric deposition. The distribution of organic acids in waters in the Adirondack Park region of New York State is probably typical of areas affected by acid deposition. Soil solutions there often contain more than 30 mg C/l of dissolved organic carbon, which corresponds to about 150  $\mu\text{eq/l}$  of organic acidity (Cronan and Aiken, 1985). The sulfate concentration in soil waters in areas receiving acid deposition is on the order of 200  $\mu\text{eq/l}$ , so organic acids are major contributors to the anion, and hence proton, balance. DOC concentrations in surface waters in the Adirondack Park area ranged from 2 to 8 mg C/l, much lower than in soil solutions (Cronan and Aiken, 1985). Values in Falls Brook in the Hubbard Brook Experimental Forest, New Hampshire, ranged from 2 to 4 mg C/l (Johnson et al., 1981). Organic anions thus represent about 10 to 40  $\mu\text{eq/l}$ , which is fairly small compared to the sulfate concentrations of about 150 to 200  $\mu\text{eq/l}$ . As a general statement, the input of organic acidity to surface waters in areas affected by acid deposition is commonly much smaller than the input of atmospherically derived sulfuric acid. The low pH values in soil solutions are more a consequence of organic acids and high  $P_{\text{CO}_2}$  values due to biological activity than of atmospherically derived pollutants, but the reverse is generally true in surface waters.

**Transport of Base Cations.** It has been observed at some localities (e.g., Likens et al., 1977) that acid rain becomes neutralized when it contacts the forest canopy; it picks up base cations from the leaves and is already neutralized by the time it reaches the ground. Assuming that the cations come from the plant and not dust on the leaf surfaces, can we say that trees have neutralized the incoming acidity and the problem is over? The answer has really been given under Biomass Changes, above. When a tree takes up a base cation from the soil, it "excretes" equivalent protons to the soil solution to maintain charge balance. Thus, for each cation that is used to neutralize atmospheric acidity, assuming constant biomass, a proton is released to the soil solution. The incoming acidity is not really neutralized; for each proton that is neutralized in the canopy, a proton is produced in the soil zone and the overall acidity of the system is unchanged.

Vegetation performs an important role in the distribution of base cations in the soil profile. Roots that go down into the C horizon or bedrock "mine" base cations and transfer them to the upper soil horizons in leaf fall (Schnoor and Stumm, 1985). This tends to counteract the depletion of base cations to the upper soil horizons and may accelerate chemical weathering of the bedrock by extracting cations from regions that would otherwise have relatively little contact with incoming precipitation.

## Chemical Weathering

Chemical weathering, which is defined here as the dissolution or chemical alteration of minerals, excluding simple ion exchange, is essentially the only process by which acidity from the atmosphere can be neutralized over long periods of time (e.g., Galloway et al., 1983). Cation exchange can cause neutralization, but unless the supply of base cations is replenished by weathering, exchangeable base cations will be depleted, and neutralization will no longer take place. Where easily weathered rocks such as limestones and basalts are present, acid deposition

does not result in acidification of surface waters. Such acidification occurs only in areas underlain by chemically resistant bedrock (e.g., granite, granite gneiss, quartzite), and even in such areas, acidification tends to occur only where there is relatively little infiltration and hence relatively little opportunity for chemical reaction between the bedrock and incoming precipitation.

Various aspects of chemical weathering have already been discussed in previous chapters. Here we shall confine our attention to two questions of great importance to the acid-deposition problem:

1. What is the present rate of chemical weathering in areas affected by acid deposition?
2. How, if at all, is the rate of chemical weathering likely to be affected by acid deposition?

Answers to these questions are essential for prediction of future effects of acid deposition and for evaluating the probable effects of future reductions in acid input.

The first approach to estimating a weathering rate would be to measure the output of solutes from a carefully monitored drainage basin, as was discussed in Chapter 12. The problem is that the output of solutes, or *cation denudation rate*, is not identical to the chemical weathering rate because biomass change and changes in the cation exchange pool may also affect the composition of runoff. In Chapter 12 we presented the general mass balance equation:

$$\begin{aligned} \text{solute in outflow} = & \text{solute from atmosphere} + \text{solute from weathering of minerals} \\ & \pm \text{solute from change in biomass} \pm \text{change in exchange pool} \end{aligned}$$

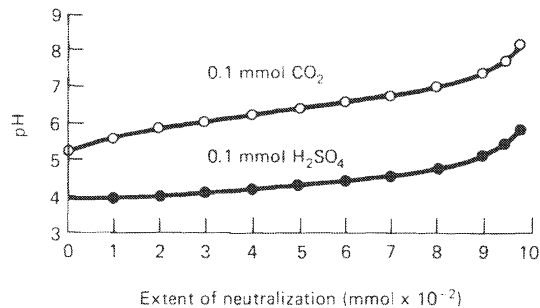
In areas where the effects of acid deposition are of concern, the rate of weathering is very low, and the change in the exchange pool is likely to be large as a result of a historically recent increased input of protons. The term [solute from weathering of minerals] thus tends to be small in comparison to the other terms in the equation and cannot be determined reliably. An alternative approach would be to choose one solute—for example,  $\text{Na}^+$  or  $\text{H}_4\text{SiO}_4$ —that is relatively unaffected by adsorption or biological uptake in soils, and use it to estimate a rate of chemical weathering. If the ratios of  $\text{Ca}^{2+}$ ,  $\text{Mg}^{2+}$ , and  $\text{K}^+$  to sodium and/or silica released during weathering were known, the rate of release of base cations and consumption of protons could then be calculated. Problems with this approach are that the ratio of cation release to silica release is not known (see discussion of “excess” calcium in Chapter 12), and silica can be affected by adsorption and biological uptake.

The quantitative models discussed below include estimates of chemical weathering rates, but the estimates are based on rather tenuous data (Wright, 1987). Commonly, weathering rate is a fitted parameter in the models.

The response of weathering rates to a change in the input of acidity from the atmosphere is also poorly known. The rates of dissolution of most silicates in the acid range are proportional to  $\alpha_{\text{H}^+}^n$ , where  $n$  lies between 0.4 and 1 depending on the mineral (Chapter 11). However, mineral dissolution rates are sensitive to the concentration of other solutes in addition to pH. On bare-rock areas, it is probably reasonable to use the laboratory dissolution rates to estimate the effect of a change in the pH of precipitation. In areas where vegetation and soil are present, however, the laboratory experiments are probably not directly applicable. The pH of soil solutions is largely determined by  $\text{CO}_2$  and organic acids from the biota (see discussions above) and is, over the short term at least, rather insensitive to inputs of acidity from the atmosphere. On the other hand, solution pH will not rise as rapidly during weathering when  $\text{H}_2\text{SO}_4$  is the source of acidity as when the source is  $\text{H}_2\text{CO}_3$  (Fig. 13-8). The best guess at the



**FIGURE 13-8** Change in pH as acidity from 0.1 mmol  $\text{CO}_2$  ( $P_{\text{CO}_2} = 10^{-2.7}$  atm.) and 0.1 mmol  $\text{H}_2\text{SO}_4$  are neutralized by weathering.



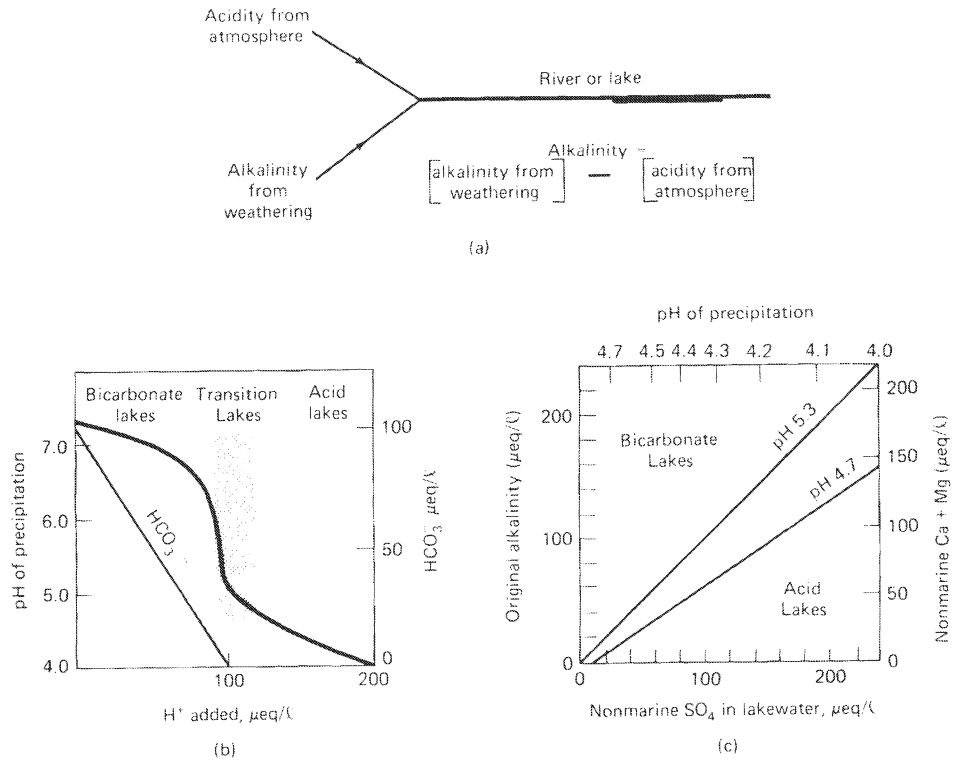
present time is that, at least on the short term, weathering rates in vegetated soils are more or less independent of the rate of input of acidity from the atmosphere.

The relationship between acid input and weathering rate has major practical importance. A reasonable environmental objective would be to decrease emissions to a level where input of acidity from the atmosphere was equal to the rate of chemical weathering in sensitive areas. If weathering rate decreased as acid input decreased, a greater reduction in emissions would be required to bring acid loading into balance with weathering.

### Integrated Models

Several quantitative models have been developed to relate the chemistry of runoff in specific localities to the input of acidity from the atmosphere. Such models are essential for policy making, as they allow quantitative prediction of the effect of a given level of emissions on the future chemistry of streams and lakes. The cost effectiveness of various emission-control strategies can thus be assessed. There is obviously uncertainty in the predictions of such models, but they represent the best available approach, and they are being continually improved. Source-receptor or atmospheric-transport models, which link deposition at locality A with emissions at locality B, have also been developed, but these are beyond the scope of this book.

The models differ greatly in the number of processes they consider and the extent to which they break a drainage basin down into sub-units. In general, the more complex a model is the more accurate its predictions should be, but the greater the amount of detailed information that must be supplied as input. The simplest model is that of Henriksen (1980), in which the acidity-alkalinity of a lake is regarded as being the result of a titration between acidity from the atmosphere (assumed equivalent to the sulfate content of the water) and alkalinity derived from chemical weathering (assumed independent of acid input and proportional to the sum of calcium and magnesium in the water). The pH is predicted from the titration curve for  $\text{HCO}_3^-$  with strong acid (Fig. 13-9). The effect of a change in acid input is calculated by moving up or down the titration curve to the new input value. The original model treated the drainage basin as an inert substrate whose only chemical function is to produce a constant supply of alkalinity from weathering. This model might be expected to provide a reasonable description of a bare-rock basin or of a more complex basin in the long term after transient effects such as ion exchange and adsorption are past, but it cannot be expected to provide an accurate description of short-term fluctuations or of basins in which soil is present and ion exchange-adsorption properties play a major role. To account for some of these processes, a factor  $f$  was introduced. This factor represents the fraction of the input of acidity that is neutralized by additional production of base

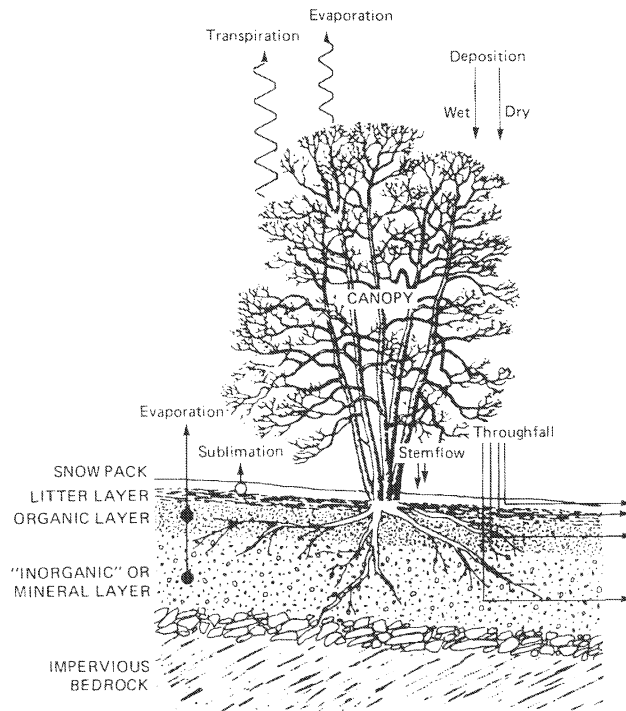


**FIGURE 13-9** The Henriksen model for acidification of surface waters: (a) the concept, (b) the titration curve for bicarbonate: note the abrupt change from pH > 6 (bicarbonate lakes) to pH < 5 (acid lakes), (c) nomograph to predict the pH of a lake as a function of the original alkalinity (proportional to the present nonmarine Ca + Mg concentration) and the nonmarine sulfate concentration of the lake or pH of precipitation. The relationships between precipitation pH and sulfate concentration, and between Ca + Mg and pH (i.e., the *f* factor), are empirical, based on a large number of lakes in southern Norway. The lines are in part empirical, and include the effect of dissolution of aluminum compounds on pH (after Henriksen, 1980).

cations (i.e., that which does not cause alkalinity loss or acidity gain). An *f* of 0 corresponds to the original model; an *f* of 1 would imply strong buffering against acidification. The choice of an *f* value for a particular catchment or lake is somewhat arbitrary.

At the other end of the spectrum of complexity is the ILWAS (Integrated Lake Watershed Acidification Study) model (Chen et al., 1983, 1984), which was based on studies in the Adirondack Mountains of New York State. The drainage basin to be modeled is subdivided (segmented) horizontally into subareas of approximately similar properties. Streams are regarded as a series of horizontal segments and lakes as a single horizontal segment. Each terrestrial horizontal segment is subdivided vertically into segments corresponding to canopy, snowpack, and three soil layers (Fig. 13-10). A hydrologic model calculates the flow of water through all the segments, and the hydrologic properties of each segment, vertical and horizontal, are necessary inputs to the model. Some of the processes modeled for the terrestrial segments are shown in Table 13-1. Equations are developed for each of the processes considered, and the model is calibrated by analysis of the change in composition of water as it flows

**FIGURE 13-10** Vertical segmentation of a watershed for the ILWAS model (after Chen et al., 1983).



through the various compartments. The ILWAS model represents the state of the art in modeling of this type, but it does have its drawbacks. Before it can be applied to a new area, an enormous amount of data must be collected for that area, which implies a considerable financial cost and a time delay while the data are collected. Also, any model such as this contains a large number of parameters (e.g., rate constants and exchange equilibrium constants) that are estimated from field data. With a large number of free parameters, it is usually possible to obtain a good match between model "predictions" and field data, even if the assumed mechanisms are grossly in error. This may limit the ability of the model to make accurate predictions in environments or under conditions that are outside the range of those used in the calibration.

A compromise between the extremes described above is the MAGIC (Model of Acidification of Groundwater in Catchments) model (Cosby et al., 1985). It is described by its authors as a lumped-parameter model. It treats the soil in a drainage basin as a single entity, and it restricts the number of physical processes modeled to equilibria in the carbonate system, aluminum hydroxide solubility, cation exchange, and sulfate adsorption. The model was quite successful in simulating the chemistry of White Oak Run, a small stream in Virginia. Ion-exchange parameters and soil-solution compositions calculated from the model were in good agreement with available field measurements, which supported the validity of the modeling approach. Much less data collection is needed to apply this model to other areas, and it is being widely used in Europe and North America.

A model of roughly similar complexity has been developed to simulate stream-water chemistry in the Birkenes catchment of Norway (Christophersen et al., 1982). This model is based on a two-layer soil system and incorporates considerably more hydrology than the

**TABLE 13-1** Some of the Biogeochemical Processes Considered in the ILWAS Model (after Chen et al., 1983)

Canopy	Inorganic layers
Dry deposition	Evapotranspiration
Oxidation	Decomposition
Nitrification	Nitrification
Foliar exudation	Nutrient uptake
Wet deposition	Weathering
Interception and evaporation	Anion sorption
pH equilibrium	Cation exchange
Wash-off	Aluminum dynamics
Snowpack	Chemical equilibrium
Accumulation	CO <sub>2</sub> exchange
Dry deposition	Stream segment
Nitrification	Advection
Leaching	Dilution
Litter layer	Evaporation
Accumulation	CO <sub>2</sub> exchange
Leaching	Heat budget
Break-down—decomposition	Chemical equilibrium
Evaporation	Lake layers
Organic layer	Advection
Evapotranspiration	Dilution
Decomposition	Evaporation
Nitrification	Diffusion
Nutrient uptake	CO <sub>2</sub> exchange
Root respiration	Heat budget
Aluminum dissolution	Algal uptake
CO <sub>2</sub> exchange	Aluminum precipitation
Cation exchange	Nitrification
Chemical equilibrium	Decomposition
	Chemical equilibrium

MAGIC model. The chemical processes modeled (sulfate adsorption, cation exchange, and aluminum hydroxide solubility) are similar. As Wright (1984) points out, the Henriksen and Birkenes models are in a sense complementary. The Henriksen model predicts long-term average trends, whereas the Birkenes model predicts short-term fluctuations, particularly seasonal changes, that may have a large effect on biological systems.

The Birkenes model actually points out some of the pitfalls in formulating a complex model. The model was originally set up and calibrated to simulate the behavior of discharge, pH, Al concentration, and sulfate concentration in the runoff from a catchment. It did this very well. However, when the model was used to predict the concentration of chloride, a conservative tracer, in the catchment output, the results were unsatisfactory: the model predicted rapid fluctuations in chloride concentrations corresponding to different amounts of seasalts in different rainstorms, whereas the observed streamwater concentration was remarkably constant. This implies that the fundamental hydrologic model was unrealistic, and needed to be revised (Christophersen and Neal, 1990; Hooper et al., 1988).

There has recently been something of a reaction against the integrated, mechanistic, modeling approach. An alternative is End-Member Mixing Analysis (EMMA) (Hooper et al., 1990; Neal et al., 1990) in which the outflow from a catchment is interpreted as a mixture of

different proportions of different "end-member" waters. Examples of end-member waters would be waters from the upper part of the soil profile (acidic, high-Al, low base cation), and base-flow waters from a deeper circulation path (near-neutral, low-Al, high base-cation). A hydrologic model is used to predict the proportions of the different water types as a function of precipitation.

A different modeling approach altogether is used by the PROFILE model (Altveg et al., 1993; Sverdrup and Warfvinge, 1988, 1995). This model computes concentrations of solutes in water infiltrating through a soil column on the basis of the dissolution kinetics of the primary minerals present in the profile. The mineralogy of each soil layer is input, as is an equation describing the dependence of dissolution rate for each mineral on pH and dissolved Al concentration. The only major "free parameter" is the specific surface area of the minerals in each soil layer, which must be supplied as an input. The model has been quite successful in describing the chemistry of surface waters in Scandinavia.

### Environmental Effects

Various environmental effects have been attributed to acid deposition, among which the most important are probably deterioration of building stones and monuments; the disappearance of fish from dilute, soft-water lakes; and injury and death to trees (*Waldsterben*, as it is called in German). The connection between acid deposition and deterioration of building stones and monuments is fairly direct and noncontroversial, although even here microbial processes may play an important role (Eckhardt, 1978). Increased acidity causes increased dissolution of carbonate minerals, so limestone and marble dissolve, and sandstone cemented by carbonate tends to disintegrate. Crystallization of gypsum (from atmospheric sulfate) within the pores of a sandstone may also cause disintegration.

Losses of fish populations associated with surface-water acidification have been well documented in Canada, downwind from the smelters at Sudbury, Ontario (Beamish, 1976), and in southern Norway (Wright and Snekvik, 1978). Losses have been observed in other areas affected by acid deposition, notably the Adirondack Mountains of New York and parts of Scotland, but the relationship to acid deposition is less clear-cut. The mechanistic connection between acid deposition and loss of fish population is complex and involves many ecosystem interactions. One simple mechanism involves dissolved inorganic aluminum, which is highly toxic to fish (Baker and Schofield, 1980, 1982). Acid deposition that is not neutralized in the soil zone causes mobilization of aluminum into surface waters, and hence, death of fish. It is striking that in Norway the lakes and streams with damaged or extinct fish populations are located only in areas in which the weighted-average pH is 4.7 or lower (Wright, 1983). Fish populations in areas of Norway receiving less acidic pH appear to be undamaged. Low pH may itself cause fish mortality, even in the absence of elevated aluminum concentrations. Acidification of surface waters is also influenced by land use practices, particularly afforestation as well as acid deposition.

The connection between acid deposition and damage to trees is much less clear. In West Germany, over 50 percent of the forest area showed evidence of damage in 1984, and the proportion was increasing rapidly (Blank, 1985). Since 1984, however, the condition of many forests has improved. Damage to forests in the eastern United States has also been reported, but not to nearly the same extent as in West Germany; the NAPAP (U.S. National Acid Precipitation Assessment Program)(1991) summary concluded that the vast majority of forests in the United States and Canada are *not* affected by decline. Several theories, including

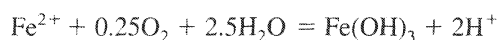
natural processes such as drought and disease, have been advanced to explain the forest dieback. In artificial experiments, trees can be damaged by both sulfuric acid and gaseous sulfur dioxide (Haines et al., 1980), and large-scale damage to trees is observed in areas receiving high inputs of sulfur dioxide (Freedman and Hutchinson, 1980). The concentrations required to cause damage are, however, well above those in areas such as the Black Forest of Germany, where damage is extensive. Alternative theories are that the input of acid depletes base cations, particularly magnesium, in the soil (and perhaps accelerates base cation leaching from the leaves; Rehfuess, 1981) so that the trees are deprived of essential nutrients, or that the concentrations of dissolved aluminum in acidified soils are toxic to roots or soil microbiota (Ulrich et al., 1980; Ulrich, 1983). Mists, which can be much more acidic than bulk precipitation, occur frequently in high-elevation forests and may be implicated in forest dieback in these areas (Lovett et al., 1982).

Ozone rather than acidity per se may also be a cause of forest decline (e.g., Arndt et al., 1982; Fuhrer, 1985; NAPAP, 1991; Prinz et al., 1982). Ozone is produced in the atmosphere by photochemical transformations involving oxides of nitrogen. It is known to cause damage to trees, and is present in remarkably high concentrations in the air of West Germany (Prinz et al., 1982). Ozone has been documented as a cause of forest decline in the Los Angeles Basin and Sierra Nevada mountains of California (NAPAP, 1991).

In a complex phenomenon such as damage to trees, it is probably a mistake to try to identify one single cause (Landolt and Keller, 1985; Schütt and Cowling, 1985). The condition of a forest ecosystem is the result of complex interactions between many environmental variables and external inputs. Anything that causes physiological stress to a plant (perhaps nutrient deprivation or acid input) may make it more susceptible to damage from another stress (perhaps ozone, disease, or drought). In such a scenario, there really is no single cause. While this may be a satisfactory conclusion for a scientist, it is not a satisfactory situation for a governmental policy maker. Should the emphasis be on reduction of sulfur emissions from power plants, the main source of acidity, or should it be on automobile emissions, the main source of nitrogen oxides and hence ozone?

## ACID MINE DRAINAGE

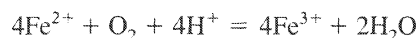
The waters draining from many coal mines in the eastern United States are strongly acidic as a consequence of oxidation of pyrite in the coal. Waters associated with mining of sulfide ores are also commonly acidic as a result of oxidation of sulfide minerals. There are many examples of such acid mine drainage in the Rocky Mountains. The stoichiometry of the oxidation can be represented by the equations



The overall mechanism by which pyrite is oxidized in natural acidic systems can be represented better by a two-step process in which pyrite is oxidized by ferric iron:



and ferric iron is (re)generated by microbial oxidation of ferrous iron:

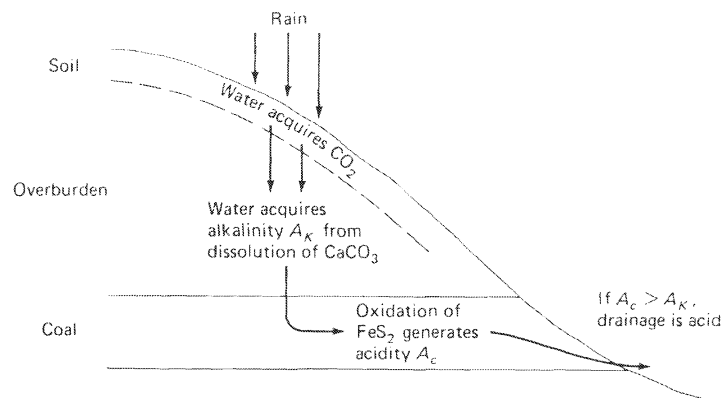


The rate-determining step in this sequence is commonly the microbial oxidation of  $\text{Fe}^{2+}$  to form  $\text{Fe}^{3+}$  (Singer and Stumm, 1970). Ferric iron that is not consumed in this catalytic cycle is ultimately precipitated as  $\text{Fe}(\text{OH})_3$ .

When streams become contaminated by acid mine drainage, adjacent vegetation dies and precipitation of ferric hydroxide occurs over long distances. Although the oxidation reactions are bacterially mediated and complex, the balance of acidity and alkalinity can be visualized in terms of a simple model (Fig. 13-11). Rain penetrates overburden and acquires a certain alkalinity, usually by dissolution of calcite (Caruccio and Geidel, 1978). The amount of alkalinity acquired is determined by the  $P_{\text{CO}_2}$  of the water and the solubility of calcite. As the water moves through the coal seam, oxidation of pyrite occurs, generating acidity, which at first is neutralized by the alkalinity in the groundwater. If the acidity generated is greater than the initial alkalinity of the water, all the alkalinity will be consumed and an acid water will result. If sufficient oxygen is present, the amount of acidity generated is determined by the amount of reactive pyrite in the coal. Only very fine-grained pyrite is reactive, so the total sulfur content of a coal may be a poor predictor of potential acidity problems (Caruccio, 1975). Usually, the underclay below the coal seam is impermeable, so water exits to the surface before interacting with any other rock type.

In the absence of mining, acid waters are uncommon because dissolved oxygen in the groundwater is insufficient to produce acidity greater than the alkalinity of the groundwater. Approximately 1 mol of  $\text{O}_2$  is required to generate 1 mol of acidity, and soil waters generally contain less than 0.6 mmol  $\text{O}_2$  per liter. When mining occurs, additional  $\text{O}_2$  is introduced, and water movement through the system is accelerated. Oxidation is no longer limited by groundwater transport of oxygen, and acidity may result. The bacteria that catalyze the acidity-producing reactions thrive only under acid conditions, so once acidity is initiated, acid production becomes more rapid and the acidity problem increases rapidly.

Acid waters associated with metal (e.g., Cu, Zn, Ag, Pb, Au) mining commonly contain high concentrations of heavy metals. Most of the metals are soluble under acid, oxidizing conditions (Chapter 9), and the metals are not adsorbed by oxyhydroxides at low pH (Chapter 5). Control of the generation of acidity is a significant aspect of mine design.



**FIGURE 13-11** Schematic balance between acidity and alkalinity in generation of acid mine drainage, as discussed by Caruccio and Geidel (1978).

### Prediction of Acid Generation

Two basic approaches are used to predict whether a particular rock is likely to cause acid generation: The so called *static test* or *acid-base accounting*, and *kinetic tests*, the most important of which is humidity-cell testing (Steffen, Robertson, and Kirsten, 1989).

**Static Test.** In the static test, the *acid-producing potential* or *acid-generating potential* of the rock is calculated from the analytical sulfide concentration using the equations for pyrite oxidation shown above. This represents the total acidity that could be generated by oxidation of all sulfides in the rock. The acidity will tend to react with (and be neutralized by) any carbonate minerals in the rock. The *acid-neutralizing potential* of the rock is calculated from its carbonate content, or measured by “titrating” the ground rock with acid.



The *net acid-producing potential* is the difference between these numbers

$$\text{Net acid-producing potential} = \text{Acid-producing potential} - \text{acid-neutralizing potential}$$

If the number is negative then, in principle, there is enough carbonate present in the rock to neutralize any acidity produced by sulfide oxidation. If the number is positive, then production of acid is likely.

One limitation of this approach is that it is based on total amounts of sulfur and carbonate without any consideration of relative rates of reaction or physical location in the rock. For example, if the sulfides were located in veins and the carbonate in the rock matrix, the sulfide might oxidize and produce acid out of contact with the carbonate. A second problem is that of sampling: both sulfides and carbonates are typically heterogeneously distributed (in veins, for example), and a large number of analyses may be required to characterize the rock adequately.

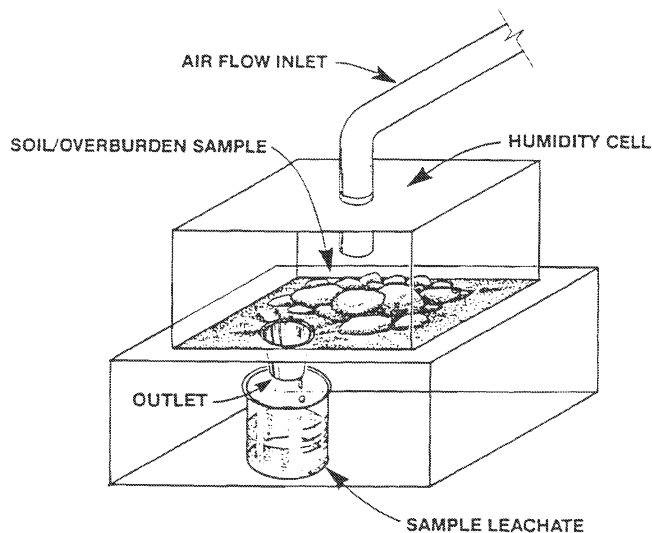
**Kinetic Tests.** The most commonly used kinetic test is the *humidity cell* (Fig. 13-12), which is intended to simulate the unsaturated environment of a spoil pile or pit wall. Crushed rock (less than 1/4 inch, 6.4 mm) is placed on a filter in a plastic chamber. It is exposed alternately to air at 100 percent relative humidity and ambient air, and is rinsed with distilled water once a week. The water is analyzed for pH, sulfate, and metals of interest. The test is conducted for ten to twenty weeks. Any acid formed by oxidation of sulfides and any metals released in the process show up in the leach solutions. This approach takes account of the possible different rates of reaction of different sulfide species. However, in the ten- to twenty-week testing period typically only about 10 percent of the sulfide in the rock oxidizes, so there is some question of its value for long-term prediction. Also, humidity cell tests are relatively expensive and time-consuming. It is not feasible to analyze a large number of samples, so the problem of heterogeneity remains.

### Prevention of Acid Generation

The main strategies to prevent acid generation are prevention (or minimization) of water circulation through acid-generating material by covering it with an impermeable cap (which may simply be a soil in relatively arid climates). Another approach is to dispose of materials under



FIGURE 13-12 A humidity cell.



water, for example in a flooded mine pit. The solubility of oxygen in water is quite low, so sulfide oxidation in the saturated zone is generally low, limited by the availability of oxygen. Treatment of acid mine drainage by placing limestone boulders in the affected streams has not been a particularly successful approach. The boulders tend to become armored by iron and aluminum oxyhydroxides that precipitate as the water is neutralized.

## REVIEW QUESTIONS

1. An unpolluted lake presently has an alkalinity of  $50 \mu\text{eq}/\ell$ . Use Fig. 13-9 to estimate the pH of rain that would cause the pH of the lake to drop to (a) 5.3, (b) 4.7. Are these values likely to occur in industrial areas (Fig. 13-3)?
2. What would the minimum alkalinity of an unpolluted lake have to be for its pH to remain above 5.3 even under the highest loadings shown on Fig. 13-3? (Use Fig. 13-9.)
3. A forest soil has an average cation exchange capacity of  $5 \text{ meq}/100 \text{ g}$ , a base saturation of 20 percent, a thickness of 1 m, and a bulk density of  $1.8 \text{ g}/\text{cm}^3$ . If 1 m/y of pH 4.0 acid rain fell on the soil, how many years would it take for the hydrogen ions added from the atmosphere to equal the exchangeable base cations present in the soil?

## SUGGESTED READING

Acidic Deposition: State of Science and Technology. Summary report of the U.S. National Acid Precipitation Assessment Program. (1991). Washington, D.C.: U.S. Government Printing Office. Summaries of the state of knowledge (in 1991) of most aspects of acid deposition.

REUSS, J. O., and D. W. JOHNSON. (1986). *Acid Deposition and the Acidification of Soils and Waters. Ecological Studies 59*. New York: Springer-Verlag.

SEIP, H. M., and A. TOLLAN. (1985). Acid deposition. In J. C. Rodda, (Ed.), *Facets of Hydrology* (pp. 69–98). New York: Wiley.



# 14

## Isotopes

Isotopes of a particular element have the same number of protons in the atomic nucleus but different numbers of neutrons. Thus they have the same atomic number but different atomic weights. Oxygen, for example, occurs as  $^{16}\text{O}$  with an atomic weight of 16 (99.76 percent of the total),  $^{18}\text{O}$  with an atomic weight of 18 (0.2 percent), and as  $^{17}\text{O}$  (0.04 percent) with an atomic weight of 17. Isotopes are called *stable* if they are not involved in any natural radioactive decay scheme, *radioactive* if they undergo radioactive decay, and *radiogenic* if they are formed by radioactive decay but do not themselves decay. Radioactive isotopes are used primarily to measure age. Stable isotopes are used to understand the sources of a water, or processes that have affected a water since it was “formed” (since it entered an aquifer, for example). Radiogenic isotopes are less widely used in water studies; they are used primarily for determining the source of specific elements, particularly strontium.

### STABLE ISOTOPES

The chemical properties of an element are determined by the atomic number, so that the chemical behavior of different isotopes of the same element is almost identical. There are, however, minor differences that result solely from the differences in mass. The differences are significant only among isotopes of the lighter elements, in which the difference in mass is a significant fraction of the total mass of the atom. The differences in mass cause isotopic fractionation in nature. *Fractionation* is any process that causes the isotopic ratios in particular phases or regions to differ from one another. For example, the ratio of  $^{16}\text{O}/^{18}\text{O}$  in rain is different from the ratio in the oceans, which is different again from the ratio in carbonate shells forming in the ocean.

The ratio of  $^{18}\text{O}$  to  $^{16}\text{O}$  in nature averages about 1:500. It is not particularly convenient to use (or easy to measure) absolute isotopic ratios, and the  $\delta$  (delta) notation is used instead. With oxygen, for example,  $\delta^{18}\text{O}$  is defined by

$$\delta^{18}\text{O} = \frac{\left(\frac{^{18}\text{O}}{^{16}\text{O}}\right)_{\text{sample}} - \left(\frac{^{18}\text{O}}{^{16}\text{O}}\right)_{\text{standard}}}{\left(\frac{^{18}\text{O}}{^{16}\text{O}}\right)_{\text{standard}}} \times 1000$$

$\delta^{18}\text{O}$  represents the relative difference in parts per thousand [called per mil (‰) by analogy with percent (%)] between the ratio in a sample and the ratio in some standard. For  $\delta^{18}\text{O}$ , the normal reference standard is V-SMOW, an acronym for “Vienna Standard Mean Ocean Water.” In practice, each laboratory has its own standard or set of standards which have been calibrated against the V-SMOW scale. During a measurement, the isotopic ratio of the sample is compared to that of the laboratory standard (by means of a mass spectrometer), and the result is recalculated to the SMOW scale. Oxygen isotopes in carbonates all used to be reported on the PDB scale, which has a marine calcite (a belemnite from the Pee Dee Formation of South Carolina) as its reference point rather than SMOW. The PDB (or V-PDB) scale for  $\delta^{18}\text{O}$  is now used only in paleoclimatic studies.  $^{13}\text{C}/^{12}\text{C}$  ratios are reported as  $\delta^{13}\text{C}$ , with the PDB calcite as the reference standard,  $^{34}\text{S}/^{32}\text{S}$  ratios are reported as  $\delta^{34}\text{S}$ , with the Canyon Diablo troilite (an iron sulfide in the Canyon Diablo meteorite) as the reference standard, and  $^{15}\text{N}/^{14}\text{N}$  ratios are reported as  $\delta^{15}\text{N}$ , with atmospheric  $\text{N}_2$  as the reference standard.

### Fractionation Processes

Fractionation may be caused by chemical processes, such as reaction between a solid and solution, or by physical processes such as evaporation and diffusion. Biological processes can be regarded as special cases of chemical and physical processes.

**Equilibrium Chemical Processes.** Consider the exchange of  $^{18}\text{O}$  between water and carbon monoxide (carbon monoxide was chosen for simplicity; the same principles apply for carbon dioxide and calcium carbonate):



$$K_{\text{equilib}} = \frac{\alpha_{\text{C}^{18}\text{O}} \alpha_{\text{H}_2^{16}\text{O}}}{\alpha_{\text{C}^{16}\text{O}} \alpha_{\text{H}_2^{18}\text{O}}}$$

The activity coefficients will be the same for each isotope, so,

$$K_{\text{equilib}} = \frac{\left(\frac{^{18}\text{O}}{^{16}\text{O}}\right)_{\text{CO}}}{\left(\frac{^{18}\text{O}}{^{16}\text{O}}\right)_{\text{H}_2\text{O}}} \quad (14-2)$$

$K_{\text{equilib}}$  here is called the *fractionation factor*, usually represented by the symbol  $\alpha$ . When reactants or products contain more than one oxygen atom ( $\text{CO}_2$ , for example),  $K_{\text{equilib}}$  can be written in more than one way. The fractionation factor  $\alpha$  is always simply the isotopic ratio in one compound divided by the ratio in the other compound.

If the chemical behavior of the two isotopes were identical, the  $\Delta G_R^\circ$  value for Eq. (14-1) would be zero, and  $\alpha$  would have a value of unity. Because of the way the vibrational energy of molecules is quantized, however, the energy of the C— $^{18}\text{O}$  bond is slightly different from the energy of the C— $^{16}\text{O}$  bond, and the energy of the H— $^{18}\text{O}$  bond is different from that of the

H—<sup>16</sup>O bond. The difference in bond energy for the C—O bond is slightly less than that for the H—O bond, and, as a consequence, the total free energy of the system is minimized when the ratio <sup>18</sup>O/<sup>16</sup>O is slightly higher in the CO than in the H<sub>2</sub>O. This means that the  $\Delta G_R^\circ$  value for Eq. (14-1) has a small negative value, and  $\alpha$  is slightly greater than 1 (for calcite-water,  $\alpha$  is 1.028 at 25°C). Thus when carbon monoxide (or calcite) is in isotopic equilibrium with water, the carbon monoxide (or calcite) will be slightly enriched in <sup>18</sup>O relative to the water, or, in the commonly used jargon, it will be isotopically heavier. The value of  $\alpha$  for all isotopic exchange reactions approaches unity as temperature increases; that is, fractionation increases as temperature decreases.

When the  $\delta$  notation is used, Eq. (14-2) becomes (since  $\alpha$  is close to 1)

$$\delta^{18}\text{O}_{\text{CO}} = \delta^{18}\text{O}_{\text{H}_2\text{O}} + \Delta \quad (14-3)$$

where  $\Delta$  is approximately  $1000 \ln \alpha$ , which is approximately equal to  $(1 - \alpha) \times 1000$ .  $\Delta$  values approach zero as temperature increases. Although  $\alpha$  and  $\Delta$  can in principle be calculated by statistical mechanics, uncertainties in the calculation make this approach impractical. The fractionation factors used in geochemistry are either measured experimentally or calculated from natural systems that are assumed to be in isotopic equilibrium. Eq. (14-3) is the basis of the use of isotopes to measure temperatures (discussed later in this chapter). If the isotopic compositions of two coexisting compounds are known,  $\Delta$  can be calculated, and one can look up (e.g., Friedman and O'Neil, 1977) the temperature at which the fractionation between the two compounds has the magnitude of the measured  $\Delta$ .

**Nonequilibrium Chemical Processes.** In the discussion above it was assumed that isotopic equilibrium existed between the compounds being considered. This is generally the case for precipitates growing from solution by inorganic processes, but is often not the case for reactions involving biological systems. When equilibrium is not maintained, the process causing fractionation is usually the *kinetic isotope effect*. The principle of this effect is as follows: the strength of a chemical bond—meaning the energy that must be supplied to break the bond—is different for different isotopes because of the way molecules vibrate. In CO<sub>2</sub>, for example, the <sup>12</sup>C—O bond is weaker than the <sup>13</sup>C—O bond (<sup>12</sup>C is the common isotope of carbon making up 98.89 percent of the total carbon in nature; <sup>13</sup>C is a stable isotope that makes up 1.11 percent of natural carbon). In a chemical reaction in which the C—O bond is broken—photosynthesis, for example—the activation energy (Chapter 11) for the reaction is largely determined by the energy needed to break the C—O bond. The activation energy is thus lower for <sup>12</sup>C—O bonds than for <sup>13</sup>C—O bonds. The reaction rate is related to activation energy by the Arrhenius equation [Eq. (11-3)]:

$$\text{Rate} = A \exp\left(-\frac{\text{activation energy}}{RT}\right)$$

Thus molecules with <sup>12</sup>C—O bonds will react more rapidly than molecules with <sup>13</sup>C—O bonds. The organic matter produced by photosynthesis is enriched in <sup>12</sup>C relative to (is isotopically lighter than) the CO<sub>2</sub> source. In the oceans, for example, dissolved CO<sub>2</sub> species have a  $\delta^{13}\text{C}$  of about zero per mil, whereas marine organic matter (mostly photosynthetic phytoplankton) has a  $\delta^{13}\text{C}$  of about -20 per mil. The kinetic isotope effect is most important in reactions involving isotopic fractionation of carbon and sulfur, whose low-temperature chemistry

in nature is dominated by biological processes. The direction of the effect is always to cause enrichment of the light isotope in the reaction product, and the magnitude of the effect may be variable. In an equilibrium process, the isotopic fractionation between two particular compounds is constant at a particular temperature, but in a nonequilibrium process the amount of fractionation may depend on reaction rate and environmental factors in addition to temperature.

**Physical Processes.** Isotopic fractionation can also be caused by physical processes. The most important such process in nature is vapor–liquid fractionation during evaporation and condensation. The vapor pressure of water containing the light isotopes ( $^1\text{H}$  and  $^{16}\text{O}$ ) is greater than that of water containing the heavier isotopes, deuterium (D) and  $^{18}\text{O}$ . When liquid water and water vapor are in equilibrium, the vapor is isotopically lighter with respect to both D/H and  $^{18}\text{O}/^{16}\text{O}$  than the liquid, and hence water vapor in the atmosphere is isotopically lighter than water in the ocean.

If evaporation is rapid, fractionation between liquid and vapor is greater than the equilibrium value. The reason for the kinetic effect is probably the different rates of diffusion of light and heavy isotopes to the surface of the liquid (Dansgaard, 1964).

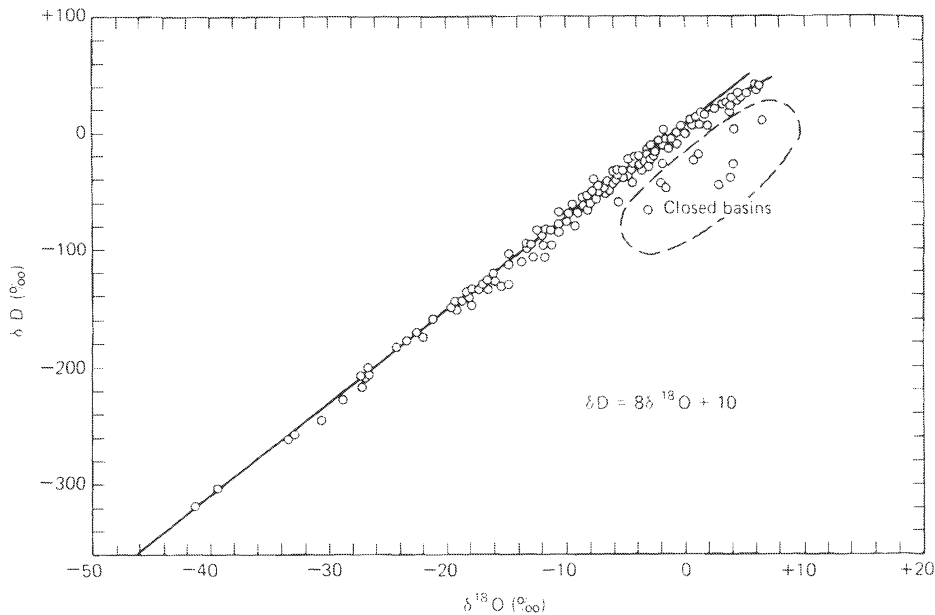
### $^{18}\text{O}/^{16}\text{O}$ and D/H

The important stable isotopes of oxygen are  $^{16}\text{O}$  and  $^{18}\text{O}$ , and the stable isotopes of hydrogen are  $^1\text{H}$  and  $^2\text{H}$ , the latter commonly written as D from the name deuterium. There is about one D atom per 6700 H atoms in the hydrosphere. Tritium ( $^3\text{H}$ ), the radioactive isotope of hydrogen, is discussed in a separate section.

The isotopic composition of seawater is, by the definition of the SMOW scale, zero per mil for both  $\delta^{18}\text{O}$  and  $\delta\text{D}$ . Variations from place to place in the oceans are relatively small, except where there is a large influx of fresh water.

**Source of Waters.** Water vapor in equilibrium with liquid water at  $20^\circ\text{C}$  would be depleted by about 80‰ in deuterium and about 10‰ in  $^{18}\text{O}$ . The water formed by evaporation at the ocean surface is not completely in equilibrium with seawater and has a  $\delta^{18}\text{O}$  value of about  $-13\text{‰}$  (Siegenthaler, 1979). When water vapor condenses to form rain, fractionation takes place in the reverse direction, with the liquid being isotopically heavier than the vapor. If the fraction during condensation is about 10‰, then the first rain to fall from water vapor over the ocean would have a  $\delta^{18}\text{O}$  value of about  $-3\text{‰}$ ; the fractionation during evaporation is largely reversed during condensation.

If a rain of  $\delta^{18}\text{O} = -3\text{‰}$  forms from a vapor of  $\delta^{18}\text{O} = -13\text{‰}$ ,  $^{18}\text{O}$  is being selectively removed from the vapor phase. As rain continues to fall, the  $\delta^{18}\text{O}$  of the vapor will become progressively more negative. The difference between vapor and liquid will remain about 10‰, and so the rain will become progressively lighter in  $\delta^{18}\text{O}$ . This process, in which material is progressively removed from a system without subsequent reequilibration, is called *Rayleigh fractionation*. Similar fractionation processes affect the hydrogen isotopes, so rain becomes progressively lighter in both  $\delta\text{D}$  and  $\delta^{18}\text{O}$  as it occurs farther from the ocean source. The  $\delta\text{D}$  and  $\delta^{18}\text{O}$  values in precipitation and hence in fresh waters generally plot close to a straight line,  $\delta\text{D} = 8\delta^{18}\text{O} + 10$  (Fig. 14-1). The position along this line (the *meteoric water line*) of a particular rainfall depends, in the simplest view, on the amount of precipitation that has occurred between the time the air mass left the ocean and the time of the particular rainfall. This is somewhat of an oversimplification, as we are ignoring the complexities of atmospheric processes and the



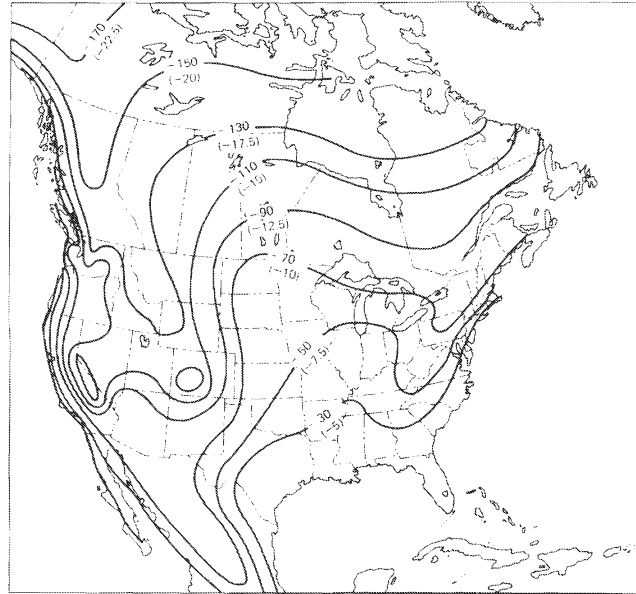
**FIGURE 14-1** Deuterium and  $\delta^{18}\text{O}$  variations in rivers, lakes, rain, and snow. (Craig, 1961. Copyright 1961 by the American Association of Science.)

effect of temperature on fractionation. In general, rain becomes progressively lighter in  $\delta\text{D}$  and  $\delta^{18}\text{O}$  from the equator toward the poles, from the coast inland, and from lower to higher elevations (Fig. 14-2). The isotopically lightest precipitation occurs at the poles both because of temperature effects and because almost all the water vapor originally present in the air has been removed as precipitation before the air reaches polar regions.

When water undergoes evaporation, the residual water becomes progressively enriched in the heavier isotopes,  $^{18}\text{O}$  and D. However, the composition of the residual water does not follow the meteoric water line. It evolves along a line that is less steep than the meteoric water line, the precise slope being determined by the temperature and relative humidity at which the evaporation takes place (Gonfiantini, 1986). The deviations of the points labeled "Closed basins" on Fig. 14-1 from the meteoric water line illustrate the effect of evaporation.

Analyses of  $\delta\text{D}$  and  $\delta^{18}\text{O}$  can be used in conjunction with Fig. 14-1 to identify the probable source of an underground water.  $\delta\text{D}$  is generally unaffected by reaction with aquifer materials at low temperatures.  $\delta^{18}\text{O}$  is generally unaffected by reaction with silicates at low temperatures for short periods of time (less than 1 million years or so), but exchange with  $\text{CaCO}_3$  in limestone aquifers may cause a significant shift toward heavier  $\delta^{18}\text{O}$  values (Clayton et al., 1966). Thus if the isotopic composition of an underground water plots close to the meteoric water line in a position similar to that of present-day precipitation in the same region, the water is almost certainly meteoric. If it has the same  $\delta\text{D}$  value as local precipitation but a slightly heavier  $\delta^{18}\text{O}$  value, the water is probably meteoric, but has been affected by exchange with calcite. If it plots close to the seawater value, and the seawater value is far from the local precipitation range, the water is not meteoric, and may perhaps be connate. Because of shifts in climatic patterns, precipitation during the Pleistocene (about 10,000 to 2,000,000 years ago) and the Tertiary (the time before the Pleistocene) differed cyclically in isotopic composition

**FIGURE 14-2** Distribution of  $\delta D$  and corresponding  $\delta^{18}O$  (in parentheses) in meteoric waters in North America (adapted from Sheppard et al., 1969).

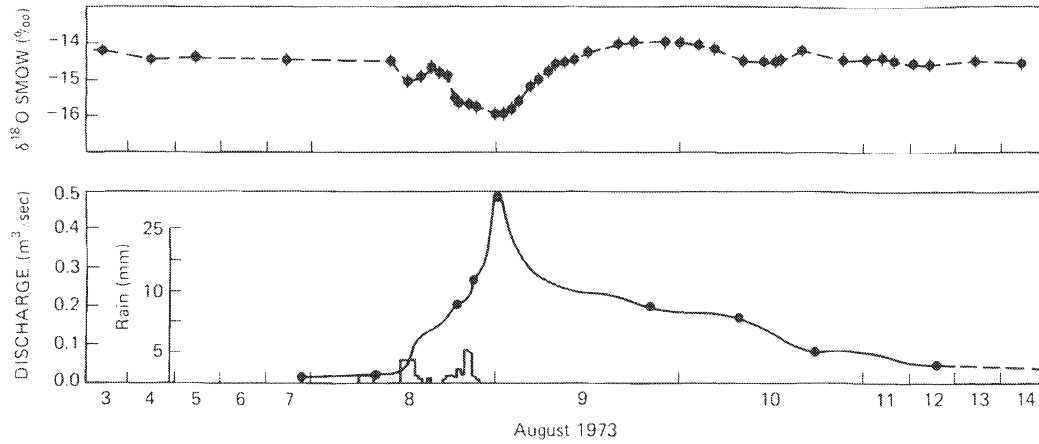


from present-day precipitation. Thus isotopes may indicate that a water is meteoric but was formed sometime in the geological past.

Although the isotopic composition of precipitation at a particular location is approximately constant, it varies from season to season and from one rainstorm to another. The reasons for the variations include different histories for individual air masses, different atmospheric temperatures, and different amounts of evaporation from raindrops as they fall through the atmosphere. The variations can be used to identify the season at which most recharge takes place, and they have been used to identify the source of runoff associated with individual storms.

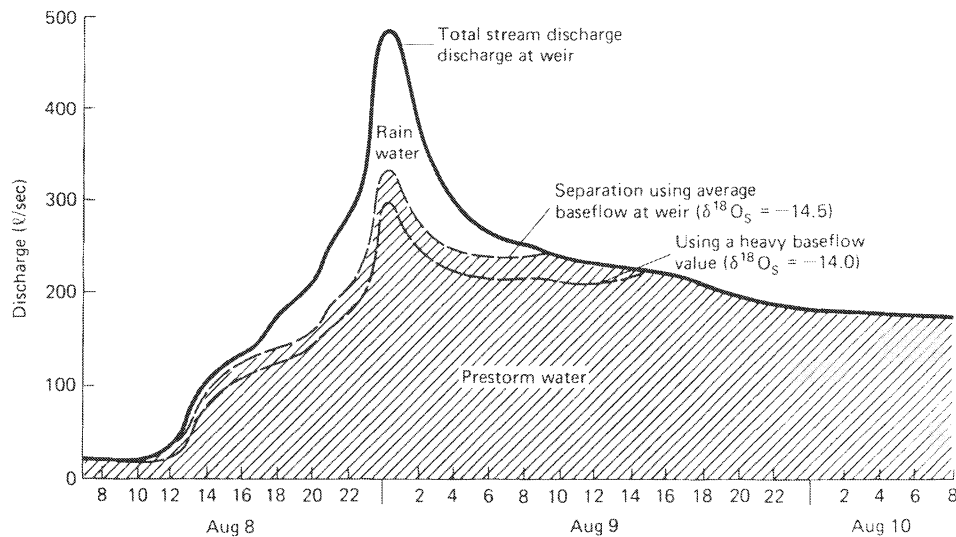
In a study of the Wilson Creek drainage basin in Manitoba, Canada, Fritz et al. (1976) found that the local groundwater and the base flow of the stream had a  $\delta^{18}O$  of about  $-14.5\text{‰}$ . A storm occurred during August 1973 in which the isotopic composition of the rain was about  $-19\text{‰}$ . The variation in the isotopic composition of the runoff during the storm is shown in Fig. 14-3. The isotopic composition of the runoff can be interpreted in terms of a mixing model, in which the runoff is regarded as a mixture of rainwater ( $\delta^{18}O = -19\text{‰}$ ) and water that was present in the basin prior to the storm ( $\delta^{18}O = -14.5\text{‰}$ ). On this assumption, the runoff from the storm is mostly pre-storm water (Fig. 14-4), not water that arrived as rain during the storm. Similar results were obtained for headwater catchments in New Zealand (Pearce et al., 1986; Sklash et al., 1986). There, only about 3 percent of storm runoff was water that had entered the catchment during the particular storm. This sort of information would be very difficult to obtain by physical measurements, and the  $\delta^{18}O$ , which is a property of the water itself, can be interpreted with less ambiguity than concentrations of individual solutes whose sources are not known with certainty. It is interesting that the conclusion of this study—that most storm runoff is not simply rainwater that has flowed over the ground surface—is similar to the conclusion reached by Kennedy and Malcolm (1977) on the basis of chemical arguments (Chapter 12). The process of assigning runoff to different sources is called *hydrograph separation*.



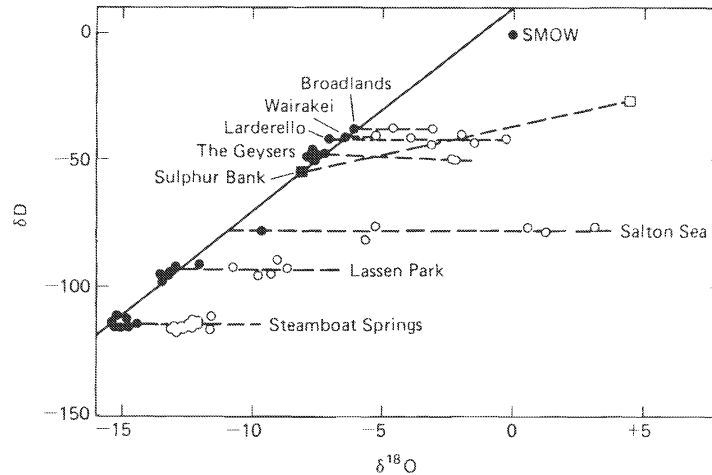


**FIGURE 14-3** Variation of rainfall (lowest curve), discharge, and  $\delta^{18}\text{O}$  of runoff during a storm on the Wilson Creek drainage (Fritz et al., 1976).

In many thermal (hot-spring) waters, the deuterium content of the water is the same as that of local precipitation, but the  $\delta^{18}\text{O}$  is heavier than that of local precipitation (Fig. 14-5). The interpretation of these results is that the waters are meteoric, and the  $\delta^{18}\text{O}$  has been shifted by isotopic exchange with rock. The reason that the  $\delta^{18}\text{O}$  value is shifted but not the  $\delta\text{D}$  value is that rock contains a large amount of oxygen, but very little hydrogen. In a water-saturated rock, 50 percent or more of the total oxygen in the system is in the rock, but almost all the hydrogen in the system is in the water. In an isotopic exchange reaction the total mass of each isotope remains constant. In a geothermal system, some  $^{18}\text{O}$  is transferred from the rock to the water,



**FIGURE 14-4** Discharge of Wilson Creek divided into rainwater and prestorm components on the basis of  $^{18}\text{O}$ . Dashed line shows effect of different assumed isotopic composition for prestorm water (Fritz et al., 1976).



**FIGURE 14-5** Values of  $\delta D$  and  $\delta^{18}O$  for samples of thermal (open circles) and local meteoric waters (solid circles) in several areas (after Ellis and Mahon, 1977).

and some  $^{16}O$  from the water to the rock. The rock becomes isotopically lighter and the water becomes isotopically heavier. There is so little hydrogen in the rock, however, that no change in the  $\delta D$  of the rock could be large enough to balance a significant change in the  $\delta D$  of the water. Thus alteration of rock in hydrothermal systems may cause a significant change in the  $\delta^{18}O$  of the water but usually no detectable change in the  $\delta D$  of the water. Clayton et al. (1966) concluded on the basis of similar arguments that the water in several oilfield brines was meteoric in origin. The  $\delta D$  values were similar to present-day (or in some cases Pleistocene) surface waters from the same area; the  $\delta^{18}O$  values were generally heavier than present-day local surface waters, which was interpreted as being a result of isotopic exchange with calcite in limestones.

**Water-Rock Interaction.** We mentioned above that interaction between meteoric water and limestone usually causes an increase in the  $\delta^{18}O$  of the water. Limestones were generally formed in approximate isotopic equilibrium with seawater at temperatures below  $20^{\circ}C$ . Meteoric waters have  $\delta^{18}O$  values lower than that of seawater, and aquifer temperatures are often higher than the original temperature of formation of the limestone. As a result of both the  $\delta^{18}O$  difference and the temperature difference, recrystallization of calcite in an aquifer generally results in a net transfer of  $^{16}O$  to the calcite and  $^{18}O$  to the water. The magnitude of the shift in the water value depends on the mass ratio of water to reacting calcite in addition to temperature and initial isotopic compositions. If a water is flowing rapidly through an aquifer, the effective ratio of water to reacting calcite is likely to be high, so the shift in the  $\delta^{18}O$  of the water is likely to be small. Conversely, if the water is almost stagnant, the effective water-rock ratio will be high, and larger isotopic shifts can be expected in the water.

When isotopic exchange occurs between silicates and water at low temperatures, the important reaction is conversion of one solid phase to another rather than recrystallization. Consider the water in the pores of a feldspar-containing rock. If the feldspar does not undergo alteration, the  $\delta^{18}O$  of the water will not change. If the feldspar alters to a clay mineral, the clay mineral will form in isotopic equilibrium with the water, and this will normally cause a shift in the  $\delta^{18}O$  of the water. The magnitude of the shift can sometimes be used to

estimate the amount of reaction that has taken place. In a sediment core taken by the Deep Sea Drilling Project from near Antarctica, for example, the  $\delta^{18}\text{O}$  of the interstitial water decreased with depth (Fig. 14-6). Lawrence et al. (1979) showed that the depletion was caused by conversion of volcanic material ( $\delta^{18}\text{O} = +6$  to  $+10$  per mil) to smectite ( $\delta^{18}\text{O} = +20$  to  $+25$  per mil), but that this reaction alone was inadequate to explain the shift; alteration of the volcanic basement was also contributing to the  $^{18}\text{O}$  depletion in the interstitial water.

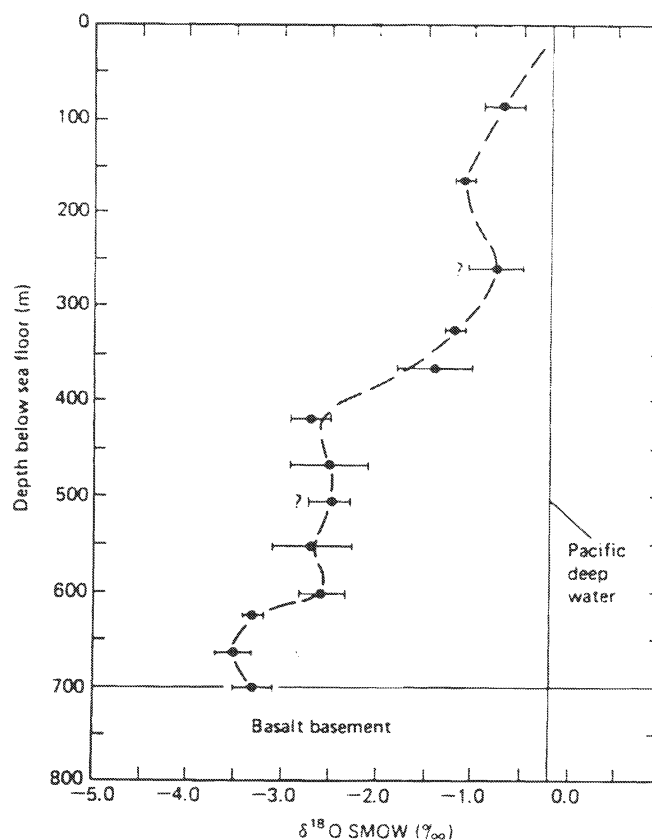
In weathering zones, the ratio of water to altered rock is normally high (water in this context means total water, integrated over time, that has flowed through the weathering zone during the alteration, not the amount present at any instant), and so clay minerals and hydroxides formed during weathering are normally in isotopic equilibrium with local meteoric water (Lawrence and Taylor, 1971; Savin, 1980).

**Isotopic Temperature Measurement.** When two oxygen-containing compounds are in isotopic equilibrium, the fractionation between them ( $\Delta$ ) is a function of temperature only:

$$\delta^{18}\text{O}_A = \delta^{18}\text{O}_B + \Delta$$

If A and B are two minerals that grew together in isotopic equilibrium, and neither mineral has undergone subsequent isotopic exchange, measurement of  $\delta^{18}\text{O}_A$  and  $\delta^{18}\text{O}_B$  allows the

**FIGURE 14-6**  $\delta^{18}\text{O}$  of pore fluids from Site 323 of the Deep Sea Drilling Project. The total depletion (the area between the curve and the Pacific deep water line) can be used to estimate the amount of reaction that has taken place (Lawrence et al., 1979).



equilibration temperature to be measured: it is not necessary to know anything about the fluid from which the minerals grew.

In low-temperature environments, such as soils, the oceans, and normal aquifers, it is rare for two minerals to form at the same time in isotopic equilibrium with each other. Calcite is the most common mineral to form. When calcite is precipitated inorganically, it is usually in isotopic equilibrium with the solution. When it is precipitated by an organism, sometimes it is in equilibrium with the solution and sometimes it is not, depending on the physiology of the organism involved. The carbonate that makes a shell is normally involved in physiological processes before it is deposited as calcite, and it is not surprising that these processes sometimes cause fractionation of their own.

When calcite is precipitated in the ocean, no other suitable mineral is precipitated at the same time in isotopic equilibrium with the same water (attempts to use silica and phosphate minerals have been unsuccessful). A large number of “paleotemperature” measurements have been made by measuring the  $\delta^{18}\text{O}$  of an ancient calcite shell (one phase) and assuming a value for seawater (the other phase). On this basis, curves have been published showing the variation in oceanic temperature over a time range of tens of millions of years. The main uncertainty in this approach is the isotopic composition of ancient seawater. We mentioned earlier in this chapter that precipitation in polar regions is isotopically very light (low  $\delta^{18}\text{O}$ ). The ice caps are simply accumulated precipitation, and so the ice caps represent a large mass of isotopically light water. The isotopic composition of the total hydrosphere is constant or changing only slowly with time, so that when large ice caps are present, seawater must be isotopically heavier than average. Isotopic measurement of shells shows that during glacial maxima,  $\delta^{18}\text{O}$  values are greater than during glacial minima. This could be explained by:

1. The isotopic composition of seawater being constant but temperatures lower (the absolute value of  $\Delta$  increases with decreasing temperature).
2. The temperature of seawater being constant, but its isotopic composition being different because of removal of  $^{16}\text{O}$  into ice caps.
3. Some combination of the two effects.

It is now generally agreed that both effects are important.

### $^{13}\text{C}/^{12}\text{C}$

The  $\delta^{13}\text{C}$  of dissolved carbonate species (mostly  $\text{HCO}_3^-$ ) in the ocean is about 0‰ and of atmospheric  $\text{CO}_2$  is about -7‰. Photosynthesis causes an enrichment of  $^{12}\text{C}$  in the photosynthetic product. The magnitude of the fractionation depends on the biochemical pathway used for photosynthesis, particularly the  $\text{C}_3$  versus the  $\text{C}_4$  pathway, and on other biological and environmental factors. Marine plankton has  $\delta^{13}\text{C}$  values around -20‰ in the tropical oceans and around -25 to -30‰ in the polar oceans (Deines, 1980). The values for land plants are variable, typically around -25‰. The  $\text{CO}_2$  in the soil atmosphere, which is largely biogenic, is typically about -20‰. The  $\delta^{13}\text{C}$  of meteoric waters is usually negative, but the specific values are variable. Carbonate minerals formed in the oceans have  $\delta^{13}\text{C}$  values close to zero.

The  $\delta^{13}\text{C}$  of a groundwater is determined by the  $\delta^{13}\text{C}$  of the inflow water and the supply of carbon to, and removal of carbon from, the water during its transit through the aquifer.

There are several possible sources of carbon:

1. Dissolution of calcite, aragonite, or dolomite from limestones, which introduces relatively heavy carbon.
2. Oxidation of organic matter, which introduces relatively light carbon.
3. Transport of CO<sub>2</sub> gas from a soil atmosphere, which also introduces relatively light carbon.

Redox reactions involving methane (Chapter 8) can also have a large effect on  $\delta^{13}\text{C}$ . Methanogenesis produces an isotopically very light methane and an isotopically heavy CO<sub>2</sub>, whereas oxidation of (typically light) methane produces light CO<sub>2</sub>.

Carbon may be lost from the water by precipitation of a carbonate mineral or by loss of CO<sub>2</sub> gas. The systematics of how these processes affect the  $\delta^{13}\text{C}$  of groundwater are discussed by Wigley et al. (1978). Plummer (1977) used a combination of chemical and isotopic arguments to identify the reactions involved in the chemical evolution of the water in the Floridan aquifer and showed specifically that soil zone CO<sub>2</sub> was being transported across the vadose zone into the groundwater.

In general, <sup>13</sup>C is used to identify sources of carbon and is particularly valuable for distinguishing between carbon derived from organic matter (isotopically light) and carbon derived from carbonate minerals (isotopically heavy). Carbon isotopes are very useful in understanding the origin of secondary carbonate minerals. Carbon isotopes are not used in low-temperature isotopic temperature determinations because there is no suitable equilibrium fractionation in nature.

### <sup>34</sup>S/<sup>32</sup>S

The most important natural fractionation is between oxidized sulfur (sulfate) and reduced sulfur (H<sub>2</sub>S, sulfide minerals). The fractionation is an example of the kinetic isotope effect in a complex, multistep biological process. The  $\Delta$  value varies, depending on the rate of sulfate reduction and on various biochemical factors (Kaplan and Rittenberg, 1964). The sulfate in modern seawater has a  $\delta^{34}\text{S}$  of about +20‰; the  $\delta^{34}\text{S}$  of pyrite in modern marine sediments varies over a wide range, from about +4 to -35‰ (Goldhaber and Kaplan, 1974). The variation is partly due to variations in the fractionation factor, and partly to the fact that pyrite does not grow from normal seawater. It grows from interstitial water in a sediment, and the  $\delta^{34}\text{S}$  of the sulfate in the interstitial water increases progressively as <sup>32</sup>S is preferentially transferred into solid phases—another example of Rayleigh fractionation.

In studies of modern waters,  $\delta^{34}\text{S}$  can be used to distinguish different sources of sulfur—sea salt versus atmospheric pollution in rain (Kellogg et al., 1972); recharge sources and pollution in groundwater (Holt et al., 1972; Krouse, 1980)—but the technique is not widely used in hydrologic studies.

### <sup>15</sup>N/<sup>14</sup>N

Atmospheric nitrogen contains about one atom of the stable isotope <sup>15</sup>N per 273 atoms of <sup>14</sup>N. During the various biochemical reactions involving nitrogen, fractionation occurs. The fractionation processes are complex and not completely understood (Létolle, 1980; Smith, 1975).

Nitrogen isotopes have been used to identify sources, particularly anthropogenic sources, of nitrate in natural waters (e.g., Kreitler and Jones, 1975). The interpretation of such results is often ambiguous as a consequence of the large number of biological processes that may affect nitrogen compounds. Analysis of the  $\delta^{18}\text{O}$  of nitrate as well as  $\delta^{15}\text{N}$  may greatly increase the value of the technique for determining sources of nitrate (Aravena et al., 1993).

## RADIOACTIVE ISOTOPES

The kinetics of radioactive decay and the concept of the half-life were discussed in Chapter 11.

### Tritium

Tritium ( $^3\text{H}$  or T) has a half-life of 12.3 years. It is produced naturally in the atmosphere by interaction of cosmic rays with nitrogen and oxygen in the atmosphere, but by far the most important source for modern studies is thermonuclear weapons testing which took place in the atmosphere between 1952 and 1969. The natural (prebomb) level in rainwater was about 5–10 TU [one TU (tritium unit) = one T atom per  $10^{18}$  H atoms]; the number is uncertain because few measurements were made before testing began, and the levels in old samples (notably wine) are now very low. During the 1960s, the levels in rainwater rose above  $10^3$  TU, and modern values are usually between 20 and 100 TU, varying considerably with time and location.

Tritium in groundwater is not significantly affected by chemical processes. Its most important use is in distinguishing between water that entered an aquifer prior to 1952 (prebomb water) and water that was in contact with the atmosphere after 1952. Prebomb water contains no tritium detectable by normal procedures; post-1952 water contains relatively high levels of tritium. Mazor (1991) summarized the interpretation of tritium values in groundwater as follows:

- Water with zero tritium (in practice  $<0.5$  TU) has a pre-1952 age.
- Water with tritium concentrations  $>10$  TU has a post-1952 age.
- Water with tritium concentrations between 0.5 and 10 TU represents a mixture of pre-1952 and post-1952 water.

Because of the variable source of tritium and uncertainties due to possible mixing, tritium is not used for age dating in the conventional way.

The properties of tritium make it useful in studies of mixing in the upper layers of the ocean (e.g., Rooth and Ostlund, 1972) and mixing in lakes (Imboden et al., 1977). For example, Imboden et al. found that the vertical distribution of tritium in Lake Tahoe was almost uniform, indicating that complete turnover and mixing had taken place not long before the time of sampling.

### $^{14}\text{C}$

Like tritium, radiocarbon is produced in the atmosphere by interaction of cosmic rays with nitrogen and was introduced in large amounts by nuclear weapons testing. Unlike tritium,  $^{14}\text{C}$  has a half-life of 5,730 years, making it a useful tool for dating waters as old as 50,000 years. Also, the amount of  $^{14}\text{C}$  introduced by bomb testing relative to the amount naturally present is much smaller than is the case with tritium, so the distribution of  $^{14}\text{C}$  in nature is not completely dominated by the bomb input. The  $^{14}\text{C}$  generated in the atmosphere is carried down to the earth's

surface by precipitation and becomes incorporated into the biomass or transported into water bodies such as lakes, the ocean, and groundwater.  $^{14}\text{C}$  undergoes radioactive decay (to  $^{14}\text{N}$ ), so once isolated from the atmosphere the amount of  $^{14}\text{C}$  decreases with time according to the equation:

$$(^{14}\text{C})_t = (^{14}\text{C})_0 e^{-kt}$$

where  $(^{14}\text{C})_t$  is the amount present at time  $t$ ,  $(^{14}\text{C})_0$  is the amount present at  $t = 0$ , and  $k$  is the decay constant, which is related to the half-life  $T_{1/2}$  by the equation:

$$t_{1/2} = \frac{\ln 2}{k}$$

To determine the time since a water was last in contact with the atmosphere, it is necessary to know  $(^{14}\text{C})_0$ . This is determined by tree rings for the most recent 7,000 years; there is no accurate way to determine it prior to 7,000 years, so it is generally assumed arbitrarily to have been constant. This gives rise to a time scale in “ $^{14}\text{C}$  years,” which may be different from astronomical years.

**Groundwater Flow Velocity.** There are some complications in the behavior of  $^{14}\text{C}$  during recharge, so the “absolute” age of a groundwater cannot be determined reliably. However, if the  $^{14}\text{C}$  concentration is measured at several points along a flow line within an aquifer, the differences in age between the points and hence the flow velocity can be determined. One complication is that dissolution of carbonate minerals or oxidation of organic matter within the aquifer may add “old” or “dead” (no detectable  $^{14}\text{C}$ ) carbon to the water, giving an erroneously old age. The contribution of carbon from these sources can be estimated from  $^{13}\text{C}/^{12}\text{C}$  measurements and chemical arguments (Wigley, 1976; Wigley et al., 1978). These calculations can be performed with the aid of the computer codes NETPATH and PHREEQC (see Chapter 16). Another complication is mixing. A low  $^{14}\text{C}$  concentration may mean that we are looking at a relatively “old” water, or it may mean that we are looking at a mixture of relatively “young” water and “dead” water.  $^{14}\text{C}$  measurements can be interpreted as ages only where mixing is insignificant.

### Chlorine-36

A large number of radioactive species in addition to tritium and  $^{14}\text{C}$  are produced by cosmic ray interactions in the atmosphere. One that may be particularly useful for dating very old groundwater is  $^{36}\text{Cl}$  (Bentley et al., 1986a, 1986b). Chloride serves as a good tracer for groundwater because it is not generally adsorbed or involved in chemical reaction, and  $^{36}\text{Cl}$  has a half-life of  $3.01 \times 10^5$  years, which is in the right range for very old groundwater. The disadvantage of the technique is that the abundance of  $^{36}\text{Cl}$  is extremely small, and the analytical techniques required (based on tandem accelerator mass spectrometry) are complex and expensive. Bentley et al. (1986b) and Phillips et al. (1986) give examples of use of the technique to date groundwaters more than 1 million years old. Interpretations of  $^{36}\text{Cl}$  concentrations in terms of water ages are not without controversy (Fontes and Andrews, 1993; Mazor, 1992, 1993a, 1993b; Phillips, 1993).

### Radon-222

The decay of uranium and thorium to lead is one of the most widely used dating techniques in geology, but it is not directly applicable to hydrology. Several intermediate products in the decay

scheme have been used in water studies, however, particularly in oceanographic studies. One example is the use of  $^{222}\text{Rn}$  to measure eddy diffusion in the ocean (e.g., Broecker et al., 1968) and in lakes (e.g., Imboden and Emerson, 1978).  $^{222}\text{Rn}$  is produced by decay of  $^{226}\text{Ra}$  (radium), which is itself a decay product of  $^{238}\text{U}$ .  $^{222}\text{Rn}$  is a gas, and when it is formed in sediment it diffuses into the overlying water. It has a half-life of 3.8 days, so that its concentration decreases with distance from the sediment. The profile of  $^{222}\text{Rn}$  above the sediment depends on the rate at which it is transported upward in the water by eddy diffusion. If the eddy diffusion rate is slow, the profile will be compressed close to the sediment; if it is fast, radon will be carried to greater distances from the sediment before it disappears by decay. Knowledge of transport rates near the sediment-water interface is important, because these rates determine the rate at which other species such as nutrients are transported from the sediment into the overlying water.

$^{222}\text{Rn}$  has also attracted a great deal of attention as a potential health hazard. It is generated in rocks and soil by decay of  $^{238}\text{U}$  and diffuses upward into the atmosphere. In the open air, rapid dilution by mixing, coupled with the short half-life of  $^{222}\text{Rn}$ , makes it insignificant as a health hazard. When it seeps into buildings from below, however, it may build up to dangerous concentrations. It is inhaled into the lungs, and the radiation emitted as it undergoes radioactive decay can cause cancer.

## RADIOGENIC ISOTOPES: STRONTIUM-87

$^{87}\text{Sr}$  is produced by the radioactive decay of  $^{87}\text{Rb}$ , which has a half-life of  $4.88 \times 10^{10}$  years. The ratio of the concentration of  $^{87}\text{Sr}$  to the stable, non-radiogenic  $^{86}\text{Sr}$  can be used to deduce the source of strontium in a water.  $^{87}\text{Sr}/^{86}\text{Sr}$  ratios can be measured with great precision (by mass spectrometry), which makes this a potentially sensitive technique. Since the geochemical behavior of calcium is very similar to that of strontium, strontium isotopes are often used to infer the source of calcium.

To a first approximation, rubidium behaves chemically like potassium, whereas strontium behaves like calcium. Old granitic rocks (high ratios of Rb to Sr, long time for the decay of  $^{87}\text{Rb}$  to form of  $^{87}\text{Sr}$ ) have high  $^{87}\text{Sr}/^{86}\text{Sr}$  ratios—commonly above 0.80—whereas young basalts typically have values of between 0.702 and 0.706. The present-day ratio in seawater is 0.709, reflecting a mixture of relatively radiogenic Sr derived from the continents and relatively non-radiogenic Sr derived from oceanic basalts. The value for seawater has varied in the past, increasing from about 0.7077 in the early Tertiary (50 my ago) to the present value. The exact mechanisms responsible for the changes are controversial.

The use of  $^{87}\text{Sr}/^{86}\text{Sr}$  ratios to elucidate weathering reactions is well illustrated by the study of Blum et al. (1994) of weathering in the Sierra Nevada of California, the same general area as was studied by Garrels and Mackenzie (1967), a paper discussed extensively in Chapter 12. The main observation was that the Sr in runoff, particularly from glaciated terrains, was more radiogenic than the calculations of Garrels and Mackenzie would predict. They predicted that the main source of solutes was weathering of plagioclase: plagioclase contains relatively non-radiogenic strontium because it contains little rubidium. The  $^{87}\text{Sr}/^{86}\text{Sr}$  of K-feldspar in the rock was not sufficiently high to explain the ratio in the water. The only mineral with a high enough ratio was biotite; the  $^{87}\text{Sr}/^{86}\text{Sr}$  ratios in the water indicated that biotite was weathering much more rapidly, at least in terms of strontium release, than would be predicted by the simple mass balance calculations involving the major elements (Chapter 12).



This is another indication that the results of such mass balance calculations should be treated with caution. Strontium isotopes systematics have been incorporated into the geochemical code KINDIS (Madé and Fritz, 1992), which is a kinetic and thermodynamic model for weathering reactions.

Other uses for Sr isotopes in water studies include distinguishing between atmospherically-derived Sr and bedrock-derived Sr (Aberg et al., 1989; Graustein and Armstrong, 1983), and distinguishing between Sr derived from exchange sites in soil and Sr derived from bedrock weathering (Miller et al., 1993). Distinguishing among these sources of strontium (and by implication calcium) is particularly important in studies of the effect of acid deposition on surface waters (Chapter 13).

## REVIEW QUESTIONS

1. Suppose you have a groundwater that contains free oxygen in the recharge area moving through a sandstone aquifer containing disseminated organic matter that causes the  $p_e$  of the water to become progressively lower. How would you expect the  $\delta^{13}\text{C}$  of bicarbonate and the  $\delta^{34}\text{S}$  of sulfate in the groundwater to change along the flow path? Would you expect the  $\delta^{13}\text{C}$  distribution to be any different if the aquifer was a marine limestone rather than a sandstone? Explain your reasoning.
2. It is fairly common to find water samples from groundwater wells that have radiocarbon ages greater than 1,000 y but detectable tritium concentrations. How might you explain the discrepancy?
3. Suppose you have meteoric water reacting progressively with a granite, as exemplified by the Sierra Nevada Springs discussed in Chapter 12. How would you expect the  $^{87}\text{Sr}/^{86}\text{Sr}$  ratio of the water to evolve as a function of contact time between water and rock?

## SUGGESTED READING

- FAURE, G. (1986). *Principles of Isotope Geology*, (2nd ed.). New York: Wiley.
- FRITZ, P., and J. C. FONTES, (Eds.). (1980). *Handbook of Environmental Isotope Geochemistry, Vol. 1, The Terrestrial Environment A*. New York: Elsevier.
- FRITZ, P., and J. C. FONTES, (Eds.). (1986). *Handbook of Environmental Isotope Geochemistry, Vol. 2, The Terrestrial Environment B*. New York: Elsevier.
- MAZOR, E. (1991). *Applied Chemical and Isotopic Groundwater Hydrology*. New York: Halstead Press.
- PHILLIPS, F. M. (1995). The use of isotopes and environmental tracers in subsurface hydrology. *Reviews of Geophysics, Supplement, U.S. National Report to International Union of Geodesy and Geophysics 1991–1994*, 1029–1033.



# 15

## Evaporation and Saline Waters

Evaporation is a major process in the hydrologic cycle. Of the rain that falls on the continents, more than half is returned to the atmosphere either by direct evaporation or by transpiration through plants. The net effect of evaporation is to remove pure H<sub>2</sub>O from solution, so the concentrations of all dissolved components tend to increase. Although evaporation takes place in all climates, it is only in relatively arid climates that the buildup of dissolved components through evaporation is a major control on water composition. The basic principles of the evolution of nonmarine brines were presented by Jones (1966). These principles were quantified and expanded by Garrels and Mackenzie (1967), Hardie and Eugster (1970), and Eugster and Jones (1979).

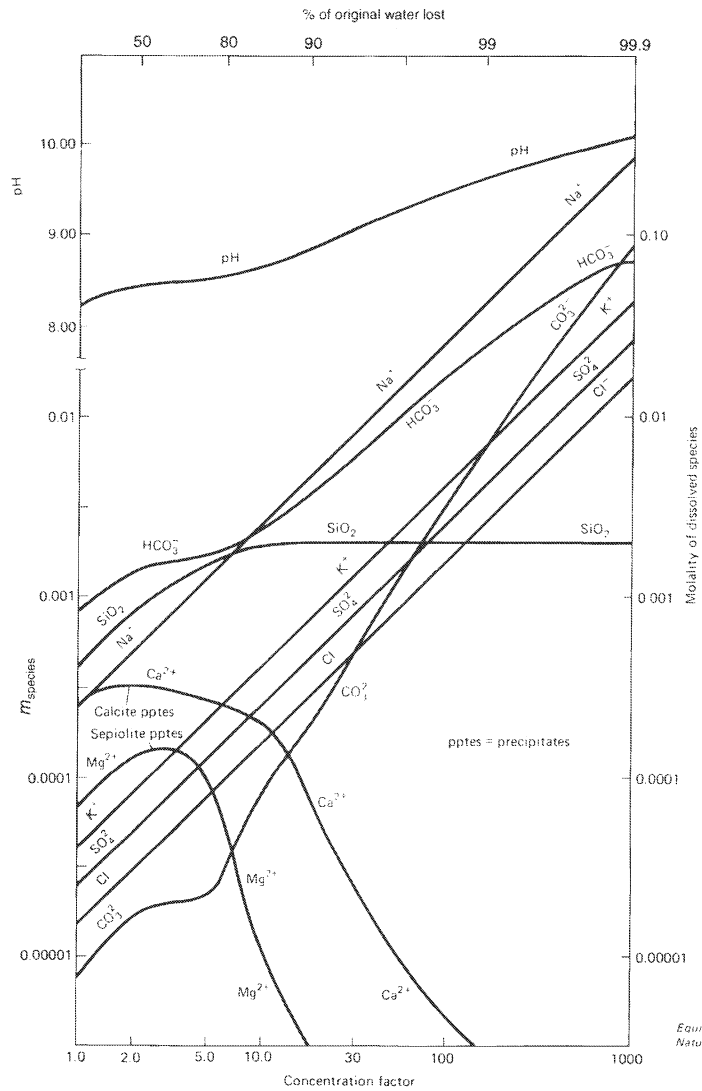
### EVAPORATION OF SIERRA NEVADA SPRING WATER

Garrels and Mackenzie (1967) calculated what should happen if water from the Sierra Nevada springs discussed in Chapter 12 was progressively evaporated. Their calculation assumed that:

1. A constant  $P_{\text{CO}_2}$  of  $10^{-3.5}$  atm and temperature of 25°C were maintained.
2. Whenever the water became saturated with respect to a solid phase, that phase would precipitate and the solution would remain in equilibrium with that phase.
3. There was no reaction between the water and any suspended sediment or between the water and its surroundings other than loss of CO<sub>2</sub> and H<sub>2</sub>O.

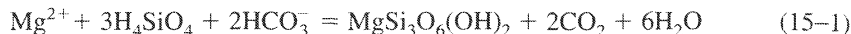
The calculation is thus a simulation of what might happen if streams from the Sierra Nevada flowed out into one of the arid basins of Nevada.

The results of the calculation are summarized in Fig. 15-1, which shows the concentrations of individual solutes on a logarithmic scale plotted against concentration factor, also on a logarithmic scale. Concentration factor is the ratio of the initial volume of water to the volume remaining after evaporation: a concentration factor of 3 means that  $\frac{1}{3}$  of the original water



**FIGURE 15-1** Calculated result of evaporating Sierra Nevada spring water at 25°C and  $P_{\text{CO}_2} = 10^{-3.5}$  atm [R. M. Garrels and F. T. Mackenzie, *Equilibrium Concepts in Natural Water Systems*, in *Advances in Chemistry Series*, no. 67, W. Stumm, ed. (Washington, D.C.: American Chemical Society, 1967)].

remains. On this plot, solutes that simply accumulate in the water plot as lines with a slope of +1. After only slight evaporation, calcite would start to precipitate. As evaporation proceeds, calcite would continue to precipitate until essentially all the calcium was removed from solution. In the calculation, the next mineral to precipitate would be sepiolite, represented by the formula  $\text{MgSi}_3\text{O}_6(\text{OH})_2$ . In theory, dolomite should precipitate before sepiolite, but because the rate of dolomite precipitation is so slow compared to that of sepiolite precipitation, Garrels and Mackenzie decided that sepiolite was a more realistic phase to use. Precipitation of sepiolite would remove  $\text{Mg}^{2+}$ ,  $\text{SiO}_2$ , and alkalinity (bicarbonate or carbonate ion) from solution:



and would continue until essentially all of the  $\text{Mg}^{2+}$  was consumed. Further evaporation would cause precipitation of amorphous silica but not, in the range considered, any salts of  $\text{Na}^+$  or  $\text{K}^+$ . The pH would remain relatively constant while  $\text{CaCO}_3$  and sepiolite were precipitating and would then increase steadily to a value of about 10. The end result, when the water had been concentrated by a factor of 1,000, would be a strongly alkaline sodium carbonate brine. The computed brine compositions showed the same general character as several natural saline lake waters from the western United States, suggesting that the chemistry of these lakes could be explained by simple evaporation of dilute spring waters whose chemistry was in turn controlled by reactions between rainwater and igneous rock.

### CHEMICAL DIVIDES AND THE HARDIE-EUGSTER MODEL

Hardie and Eugster (1970) generalized the calculation procedure of Garrels and Mackenzie to cover a wide range of starting compositions for the water to be evaporated. The most important concept in the model is that of a *chemical divide*. Consider a solution in equilibrium with gypsum, in which  $m_{\text{Ca}^{2+}} = m_{\text{SO}_4^{2-}}$ . As this solution is evaporated, gypsum will precipitate, but because the ratio of calcium to sulfate is the same in solution as in the solid, the ratio in solution will not change as evaporation progresses. Now consider a solution in which  $m_{\text{Ca}^{2+}} = 2m_{\text{SO}_4^{2-}}$ , also in equilibrium with gypsum. If we neglect activity coefficients and assume a solubility product for gypsum of  $10^{-4.54}$ , then

$$m_{\text{Ca}^{2+}} = 7.63 \times 10^{-3}$$

$$m_{\text{SO}_4^{2-}} = 3.81 \times 10^{-3}$$

Suppose that we evaporate this solution until the mass of water remaining is  $1/n$  of the original (i.e., a concentration factor of  $n$ ), precipitating  $y$  moles of gypsum per kilogram of original water in the process. The concentrations of calcium and sulfate will then be

$$m_{\text{Ca}^{2+}} = n(7.63 \times 10^{-3} - y) \quad (15-2)$$

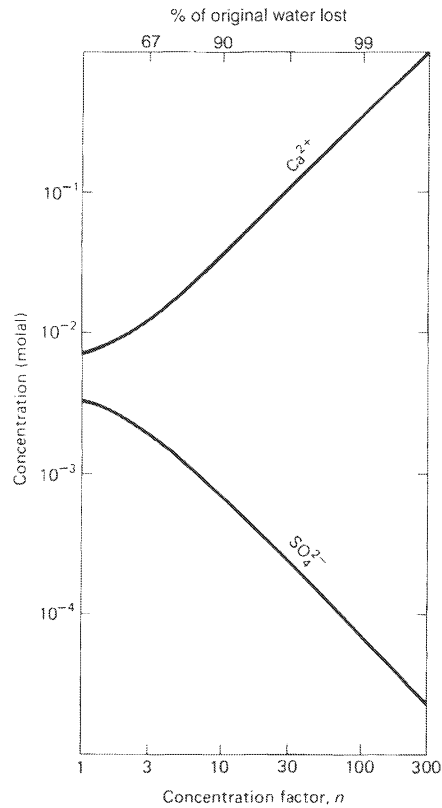
$$m_{\text{SO}_4^{2-}} = n(3.81 \times 10^{-3} - y) \quad (15-3)$$

If the solution is in equilibrium with gypsum, then

$$K_{\text{sp}} = 10^{-4.54} = n^2(7.63 \times 10^{-3} - y)(3.81 \times 10^{-3} - y)$$

For any value of  $n$ , the quadratic can be solved to give the corresponding value of  $y$ . This value can be substituted in Eqs. (15-2) and (15-3) to give the corresponding calcium and sulfate concentrations. The results of the calculation are shown in Fig. 15-2. The important conclusion is that calcium (the species present in higher relative concentration) builds up in solution, and sulfate (the species present in lower relative concentration) becomes progressively less concentrated in solution, its concentration ultimately becoming extremely small. If we had started instead with the condition  $m_{\text{SO}_4^{2-}} = 2m_{\text{Ca}^{2+}}$ , the calculation would be identical except that sulfate would build up in solution, while the concentration of calcium would become vanishingly small. The calculation above is an illustration of a general principle: *whenever a binary salt is precipitated during evaporation, and the effective ratio of the two ions in the salt is different from the ratio of the concentrations of these ions in solution, further evaporation*

**FIGURE 15-2** Concentrations of calcium and sulfate during evaporation of a solution in equilibrium with gypsum, assuming initial  $m_{\text{Ca}^{2+}} = 2m_{\text{SO}_4^{2-}}$  and neglecting activity corrections.



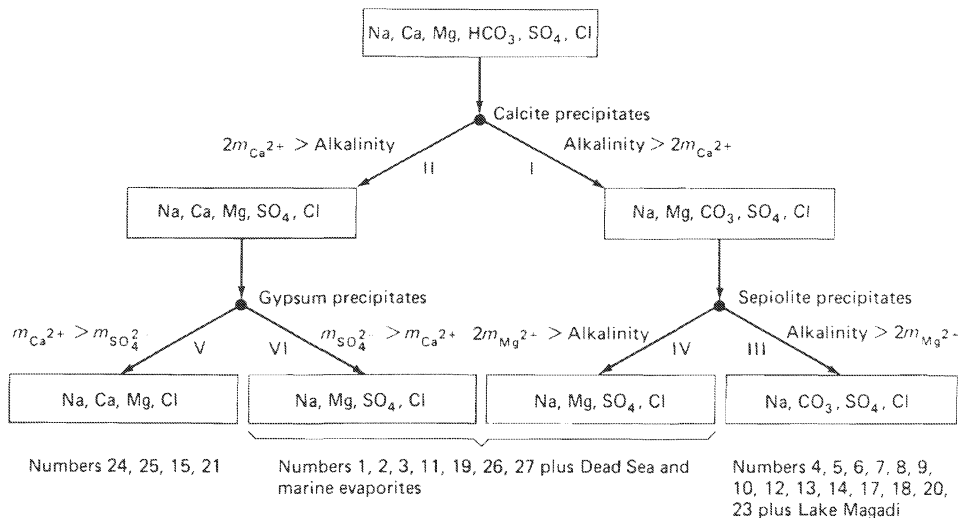
will result in an increase in the concentration of the ion present in greater relative concentration in solution and a decrease in the concentration of the ion present in lower relative concentration. (The term *effective ratio* is used rather than *ratio* to cover salts such as carbonates where the ion in the solid,  $\text{CO}_3^{2-}$ , may not be the same as the ion in solution,  $\text{HCO}_3^-$ ; see below.) This is the basic idea of a chemical divide: of the two ions involved in precipitation of a salt during evaporation, one will build up in solution while the concentration of the other will become very small.

The Hardie–Eugster model interprets the chemistry of waters undergoing evaporation in terms of a succession of chemical divides (Fig. 15-3). With almost all natural waters, the first mineral to precipitate, and hence to cause the first chemical divide, is calcite. The path taken by the solution then depends on whether the calcium concentration (in equivalents) is greater or less than the carbonate alkalinity (in equivalents), that is, whether  $2m_{\text{Ca}^{2+T}}$  is greater or less than  $(m_{\text{HCO}_3^-T} + 2m_{\text{CO}_3^{2-}T})$ , where  $T$  signifies total analytical concentration. In a water whose solutes are derived entirely from atmospheric  $\text{CO}_2$  and dissolution of calcite, the charge balance equation (Chapter 3) is

$$2m_{\text{Ca}^{2+}} + m_{\text{H}^+} = m_{\text{HCO}_3^-} + 2m_{\text{CO}_3^{2-}} + m_{\text{OH}^-}$$

If  $m_{\text{H}^+}$  and  $m_{\text{OH}^-}$  are negligible,

$$2m_{\text{Ca}^{2+}} = m_{\text{HCO}_3^-} + 2m_{\text{CO}_3^{2-}} \quad (15-4)$$



**FIGURE 15-3** Some possible paths for the model evaporation of natural waters (modified from Hardie and Eugster, 1970). The numbers correspond to analyses in Table 15-1, indicating how these analyses might be interpreted on the original Hardie–Eugster model. It is not implied that the actual processes at each lake correspond closely with the model.

Evaporation of such a water will result in precipitation of  $\text{CaCO}_3$ , but no buildup of  $\text{Ca}^{2+}$  relative to alkalinity or vice versa (if equilibrium with calcite and the atmosphere is maintained, the composition of the water will not change during evaporation). Eq. (15-4) thus defines the *balance point* of the chemical divide; if, in any solution, the criterion of Eq. (15-4) is not met, either  $\text{Ca}^{2+}$  or alkalinity will build up on evaporation.

If calcium concentration is less than alkalinity, essentially all the calcium will be removed from solution during evaporation, and the solution will tend toward an alkaline carbonate brine (path I, Fig. 15-3). Conversely, if calcium concentration is greater than alkalinity, essentially all carbonate species will be removed from solution, and the solution will tend toward a nearly neutral sulfate or chloride brine (path II, Fig. 15-3). Following path I, the next chemical divide is caused by sepiolite precipitation. In their original model, Hardie and Eugster followed Garrels and Mackenzie and used sepiolite as the magnesium-containing phase rather than dolomite. One reason for this choice was that their computer program could not handle a double salt such as dolomite. Precipitation of sepiolite (Eq. 15-1), and thus the chemical divide, involves three species— $\text{Mg}^{2+}$ ,  $\text{HCO}_3^-$ , and  $\text{H}_4\text{SiO}_4$ . In practice, the important criterion is whether  $2m_{\text{Mg}^{2+}}$  is greater or less than the carbonate alkalinity remaining after calcite precipitation. If magnesium concentration (in equivalents) is less than remaining alkalinity (path III), the water will become an alkali carbonate brine. Path I followed by path III is the sequence simulated by Garrels and Mackenzie (see above). If the magnesium concentration is greater than remaining alkalinity (path IV), the solution will tend toward a carbonate-free sulfate or chloride brine.

On path II, the next mineral that is likely to precipitate is gypsum, causing a chemical divide that has already been discussed. If the calcium concentration remaining after calcite precipitation is greater than the sulfate concentration (path V), the resulting brine will have

chlorides of Na, Ca, and Mg as the major solutes. If the concentration of sulfate is greater than that of remaining calcium, the resulting brine will have chloride and sulfate as major anions and sodium and magnesium as major cations. Examples of natural brines representing (approximately) the different paths of evolution are indicated in Fig. 15-3, and some chemical analyses are listed in Table 15-1. The most important conclusions that may be drawn from the Hardie–Eugster model are that brines should be chemically simple, containing relatively few ions as major species, and that the composition of the final brine is determined by the composition of the dilute water from which the brine was derived.

A more sophisticated model based on the principles of Hardie and Eugster (1970) has been presented by Droubi et al. (1976) and Al-Droubi et al. (1980). The solubilities of highly soluble evaporite salts can be predicted by the Pitzer model (Harvie et al., 1984; see Chapter 2).

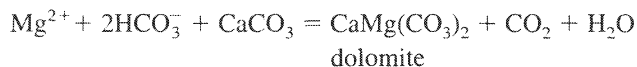
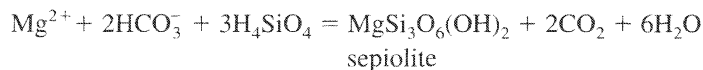
## MODIFICATIONS OF THE HARDIE–EUGSTER MODEL

The model presented above is obviously an oversimplification of the real world. We shall discuss here some important processes that were not included in the original model, and later we will examine some specific examples of natural systems.

### Magnesium Carbonate Formation

Both the calculation procedures discussed above invoked sepiolite formation as the primary control on magnesium concentration. Although sepiolite does fulfill this role in some places, the most common magnesium-containing phases to be formed in nature appear to be a magnesium-rich smectite (e.g., Gac et al., 1978; Jones and Van Denburgh, 1966), dolomite, or high-magnesium calcite. The stoichiometry of Mg-smectite formation should be similar to that of sepiolite formation.

If we consider the reactions



we can see that the net effects are very similar. In both cases precipitation is favored by an increase in alkalinity, and the ratio of  $\text{Mg}^{2+}$  to alkalinity removed is the same in both cases. Thus, in terms of chemical divides, it often does not make much difference whether  $\text{Mg}^{2+}$  is removed as a carbonate or as a silicate.

One situation where the distinction is important occurs when dolomitization takes place in the absence of excess alkalinity:



In this situation, the calcium may build up in solution or it may precipitate as gypsum. In either case, the end result is likely to be different from that predicted by the original Hardie–Eugster model. Eugster and Hardie (1978) have discussed in detail how the overall model should be adapted to include both high-magnesium calcite and dolomite.



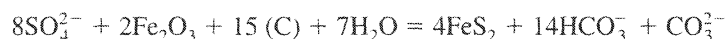
**TABLE 15-1 Analyses (mg/kg) of Brines from Saline Lakes in Western North America<sup>a,b</sup> [from Eugster and Hardie, 1978]**

	1	2	3	4	5	6	7	8	9	10	11	12	13	14	
		Basque Lake No. 1, B.C.		Hot Lake, Wash.	Lenore Lake, Wash.	Soap Lake, Wash.	Harney Lake, Ore.	Summer Lake, Ore.	Alkali Valley, Ore.	Abert Lake, Ore.	Surprise Valley, Calif.	Great Salt Lake, Utah	Honey Lake, Calif.	Pyramid Lake, Nev.	Winnemucca Lake, Nev.
Kamloops Lake No. 7, B.C.	—	—	—	22	101	31	103	542	645	36	48	55	1.4	11	
SiO <sub>2</sub>	tr	—	640	3	3.9	7	tr	—	—	11	241	—	10	4.2	
Ca	34,900	42,400	22,838	20	23	tr	tr	—	—	31	7,200	—	113	4.5	
Mg	10,900	13,660	7,337	5,360	12,500	8,826	6,567	117,000	119,000	4,090	83,600	18,300	1,630	4,350	
Na	—	1,570	891	c	—	336	264	8,850	3,890	11	4,070	1,630	134	c	
K	2,400	3,020	6,296	6,090	12,270	4,425	5,916	2,510	—	1,410	251	5,490	1,390	744	
HCO <sub>3</sub>	—	—	—	3,020	5,130	d	d	91,400	60,300	644	—	8,020	—	128	
CO <sub>3</sub>	160,800	195,710	103,680	2,180	6,020	1,929	695	46,300	9,230	900	16,400	12,100	264	918	
SO <sub>4</sub>	200	1,690	1,668	1,360	4,680	6,804	3,039	45,700	115,000	4,110	140,000	9,680	1,960	5,290	
Cl	209,000	258,000	143,000	18,000	40,700	22,383	16,633	314,000	309,000	10,600	254,000	52,900	5,510	11,100	
Total								10.1	9.8	9.2	7.4	9.7		8.7	
pH															
	15	16	17	18	19	20	21	22	23	24	25	26	27		
	Carson Sink, Nev.	Rhodes Marsh, Nev.	Monto Lake, Calif.	Deep Springs Lake, Calif.	Saline Valley, Calif.	Owens Lake, Calif.	Death Valley, Calif.	Searles Lake, Calif.	Soda Lake, Calif.	Bristol Dry Lake, Calif.	Cadiz Lake, Calif.	Danby Lake, Calif.	Salton Sea, Calif.		
SiO <sub>2</sub>	19	142	14	—	36	299	—	—	—	—	—	—	20.8		
Ca	261	17	4.5	3.1	286	43	—	—	—	43,296	4,504	325	505		
Mg	129	0.5	34	1.2	552	21	150	—	—	1,061	412	108	581		
Na	56,800	3,680	21,500	111,000	103,000	81,398	109,318	110,000	114,213	57,365	22,603	137,580	6,249		
K	3,240	102	1,170	19,500	4,830	3,462	4,043	26,000	tr	3,294	1,038	—	112		
HCO <sub>3</sub>	322	23	5,410	9,360	614	52,463	—	—	—	—	—	tr	232		
CO <sub>3</sub>	—	648	10,300	22,000	—	d	—	27,100	12,053	—	—	—	—		
SO <sub>4</sub>	786	2,590	7,380	57,100	22,900	21,220	44,356	46,000	52,026	223	280	13,397	4,139		
Cl	88,900	3,070	13,500	119,000	150,000	53,040	140,196	121,000	124,618	172,933	44,764	119,789	9,033		
Total	152,000	10,400	56,600	335,000	282,360	213,700	299,500	336,000	305,137	279,150	73,600	271,200	20,900		
pH	7.8	9.5	9.6	7.35											

<sup>a</sup>The compositions are related to the original Hardie-Eugster model in Fig. 15-13.  
<sup>b</sup>tr, trace.  
<sup>c</sup>Reported Na represents Na + K.  
<sup>d</sup>Reported HCO<sub>3</sub> represents HCO<sub>3</sub> + CO<sub>3</sub>.

### Sulfate Reduction and Sulfide Oxidation

Reduction of sulfate to sulfide species is an additional process that removes sulfate from natural waters. Anoxic conditions (Chapter 8) develop rather easily in brines, because the solubility of oxygen in water decreases as salinity increases. Sulfate reduction can be represented by the equation:



where (C) represents organic carbon and  $\text{Fe}_2\text{O}_3$  is the reactive iron-containing minerals in sediments with which the water is in contact. The net effect is to “convert” sulfate into an equivalent amount of alkalinity, which may precipitate as calcium or magnesium carbonate or may build up in solution. The result of the process is nicely illustrated by comparison of the water chemistry in two evaporitic ponds adjacent to Lake Chad in Africa (Eugster and Hardie, 1978; Eugster and Maglione, 1979). One of the ponds contained an alkaline Na– $\text{CO}_3$  brine, the other a nearly neutral Na–Cl– $\text{SO}_4$  brine. The source of water was essentially the same for each pond, but sulfate reduction had occurred during subsurface flow from the lake in the former case, but not in the latter.

Sulfate reduction accounts for unexpectedly low sulfate concentrations in some waters and also for the less-than-predicted amounts of sulfate minerals in many deposits from ancient saline lakes. Oxidation of sulfide minerals in soil or bedrock can cause the reverse effect—removal of alkalinity and introduction of sulfate. This may be a cause of acid saline waters that are fairly common in Australia (McArthur et al., 1991).

### Ion Exchange and Adsorption

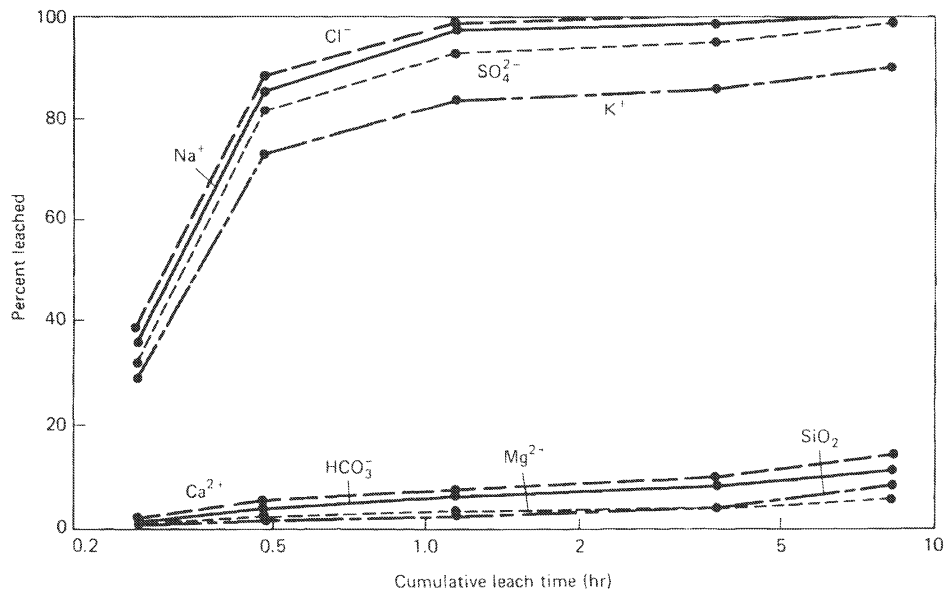
When water flows through a porous medium (sediment or rock), exchange reactions take place between ions in the water and ions adsorbed on the medium. Neutral species, notably  $\text{H}_4\text{SiO}_4$ , and even the sulfate anion may also be adsorbed on solid surfaces. The cation-exchange capacities of most media are sufficient to have a significant influence on the composition of waters flowing through them.

The major ion most affected by exchange reactions is potassium. Potassium does not form any salts, except at very high concentrations, and calculations such as those of Garrels and Mackenzie (1967) and Hardie and Eugster (1970) predict that potassium should, like sodium, simply build up in solution during evaporation. In practice, however, potassium is almost always found to be depleted relative to sodium in saline waters. Eugster and Jones (1979) showed that the removal took place only when the water was flowing underground (not in a lake, for example) and argued convincingly that the removal process for potassium was sorption on cryptocrystalline surfaces or ion exchange. If a sediment in which the exchange sites are largely occupied by  $\text{Ca}^{2+}$  is exposed to a relatively saline water, monovalent ions should displace the divalent calcium (Chapter 4). In ion-exchange reactions involving clay minerals or zeolites, potassium is greatly favored on the exchange sites over sodium, so potassium is removed from solution. The calcium released in exchange for sodium probably precipitates as a carbonate within the medium. The exchangeable cation is often initially calcium, because many regions that are now arid were much wetter during the late Pleistocene; waters were generally more dilute then, and ion exchangers in contact with these waters tended to have calcium as the major exchangeable cation. Biological uptake can also remove potassium from waters but appears to be less important than adsorption in regulating potassium concentrations in saline waters.

### Cyclic Wetting and Drying

The Hardie–Eugster model is based on the assumption that the dilute water entering an arid basin undergoes continuous evaporation until it becomes a concentrated brine. In nature, however, an important process is complete evaporation of a water and deposition of all the solutes in it during a dry period, followed by partial re-solution of these solutes during a wet period. The water undergoing evaporation often occurs in the pores of alluvium or as near-surface groundwater rather than as an open lake. If the initial water was already saline, the deposited salts tend to form efflorescent crusts on the ground surface. If it was relatively dilute, the salts may be deposited in the ground just below the surface, or they may form in the capillary fringe above the water table where the water table is near the surface.

During the evaporation stage, all the solutes in the water are deposited as solid phases, presumably in the order predicted by the Hardie–Eugster model. During the re-solution stage, very soluble minerals such as sodium salts dissolve rapidly, whereas less soluble compounds such as gypsum, calcite, and, especially, silica dissolve only slowly (Fig. 15-4). The end result of an evaporation–solution cycle is a water that contains all the ions that precipitate only as highly soluble salts, but has lost some of the ions that precipitate as less soluble compounds. The chemistry of the resultant solution is controlled by the kinetics of dissolution of the precipitated phases, and not strictly by their solubilities. Waters resulting from such cycles may be strongly undersaturated with respect to gypsum, amorphous silica, and sepiolite, even though the waters have clearly lost calcium, sulfate,



**FIGURE 15-4** Results of an experiment simulating an evaporation–solution cycle. A large volume of water with the composition of rain near Teels Marsh, Nevada, was evaporated on a bed of pure quartz sand. The sand was then leached with successive volumes of distilled water, and the solutes acquired by the distilled water were measured. The graph shows the percentage of the total amount of each species added in the rainwater that was leached after a particular time. Only a small fraction of the silica, calcium, magnesium, and alkalinity was dissolved after 8 hours' contact with distilled water (Drever and Smith, 1978).

silica, and magnesium relative to the input. The process is discussed further in one of the examples later in this chapter.

Cyclic wetting and drying will also affect the  $\delta D$  and  $\delta^{18}O$  of the water (Chapter 14). The chemistry of the water may indicate extensive evaporation (accumulation of chloride and sulfate), whereas its isotopic composition may indicate “fresh” precipitation. The isotopes in the water would show no record of the previous evaporation cycle.

## EXAMPLES

### Lake Magadi Basin, Kenya

Lake Magadi is a saline-alkaline lake in the East African Rift Valley. Most of the time, the “lake” is an expanse of solid trona ( $Na_2CO_3 \cdot NaHCO_3 \cdot 2H_2O$ ) with a few pools of open water near the margins where springs are discharging. Just below the surface, the trona contains interstitial brines, which are referred to as lake brines. The hydrochemistry of the Magadi basin has been studied in detail by Eugster (1970) and Jones et al. (1977).

The lake is situated in the lowest part of the Rift Valley, where temperatures are high and rainfall is very low as a consequence of the orographic shielding effect of the highlands on either side. Bedrock in the Rift Valley is predominately trachytic volcanics; in the adjacent highlands the bedrock is granitic. The principal source of water for the Lake Magadi system is rainfall on the highlands. There, perennial streams flow and the water is dilute, comparable in composition to the Sierra Nevada springs discussed in Chapter 12. As the water flows off the escarpment into the Rift Valley, it becomes progressively more concentrated through evaporation. Near the base of the escarpment, the streams disappear into alluvium; there is no continuous surface flow into Lake Magadi. As the water flows through the alluvium, it becomes further concentrated by evaporation. Some of it flows to sufficient depth to become heated (the geothermal gradient is very high in the Rift Valley). The water reappears as springs around the margin of the lake. The waters in the springs are already highly concentrated (Table 15-2), and the water undergoes further evaporative concentration as it moves out across the “lake” as an interstitial brine in the solid trona.

**TABLE 15-2** Water Compositions [mg/kg] from the Lake Magadi System  
(from Jones et. al., 1977)

	<i>Na</i>	<i>K</i>	<i>Ca</i>	<i>Mg</i>	<i>HCO<sub>3</sub></i>	<i>CO<sub>3</sub></i>	<i>SO<sub>4</sub></i>	<i>Cl</i>	<i>SiO<sub>2</sub></i>	<i>pH</i>
Rim (highland)										
streams (average)	19	5	9.6	4.7	74	—	11	8.8	30	7.6
Hot springs (greater than 50°C) (average)	11,400	204	<sup>a</sup>	<sup>a</sup>	12,800	4,180	171	5,430	87	9.3
Warm springs (less than 50°C) (average)	10,400	122	<sup>a</sup>	<sup>a</sup>	7,680	5,560	197	5,300	64	9.7
Main lake, surface brines (average)	106,000	1,580	<sup>a</sup>	<sup>a</sup>	5,000	83,600	1,680	64,500	819	10.5

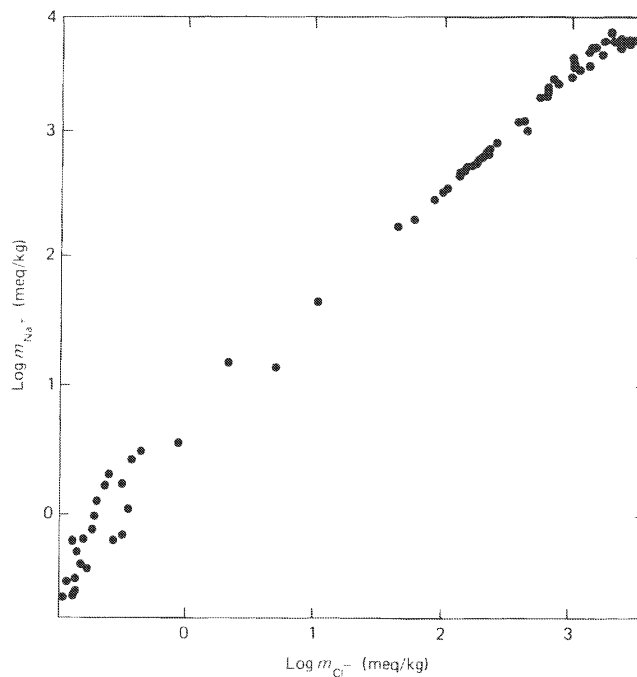
<sup>a</sup>Below detection limit.

In examining the chemistry of the waters, Eugster (1970) and Jones et al. (1977) chose chloride as a reference ion to demonstrate the effects of evaporation. The chloride in the system appeared to be derived entirely from rainfall. Because chloride is not removed or supplied significantly by interaction with rocks and is not precipitated as a salt until very high salinities are reached, the chloride concentration in the water indicates the amount of evaporation that has taken place since the water started out as rainfall. If the concentration of any other ion (e.g., sodium, Fig. 15-5) is plotted against chloride concentration, the extent to which the concentration of that ion is controlled by evaporation becomes apparent, and the degree to which other processes are influencing its concentration can be seen. On a log-log plot, progressive evaporation should cause points to lie on a line with a 1:1 slope, regardless of the initial ratio of the concentrations of the species being plotted.

The plot of sodium against chloride concentration (Fig. 15-5) shows that most of the points fall close to the 1:1 line over a concentration range of four orders of magnitude. In the relatively dilute waters of the highland streams, sodium increases more rapidly than chloride, indicating the effects of feldspar weathering, whereas at very high concentrations chloride increases faster than sodium because sodium is being precipitated as trona. Between the extremes, simple evaporative concentration appears to control sodium concentration.

Calcium and magnesium show the behavior predicted by the Hardie-Eugster model. In the dilute streams of the highlands they make up a major fraction (in some streams more than 50 percent) of the cations. As chloride concentration increases, the concentrations of both calcium and magnesium decrease; both are below the detection limit (approximately 1 mg/kg) in the spring waters around Lake Magadi. In the streams of the highlands,

**FIGURE 15-5** Sodium and chloride concentrations in waters from the Lake Magadi region (Eugster and Hardie, 1978).



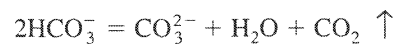
$$2m_{\text{Ca}^{2+}} < m_{\text{HCO}_3^-} + 2m_{\text{CO}_3^{2-}}$$

and

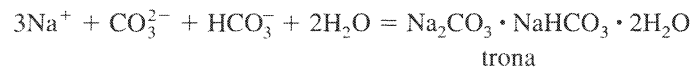
$$2m_{\text{Ca}^{2+}} + 2m_{\text{Mg}^{2+}} < m_{\text{HCO}_3^-} + 2m_{\text{CO}_3^{2-}}$$

so calcium is presumably precipitated as a carbonate and magnesium as a carbonate or silicate.

Carbonate species are removed from solution over the entire concentration range (Fig. 15-6). During the early stages, the main removal process is precipitation of calcium carbonate and magnesium carbonate or silicate. During the intermediate stages,  $\text{HCO}_3^-$  is converted to  $\text{CO}_3^{2-}$  in response to rising pH, and  $\text{CO}_2$  is lost:

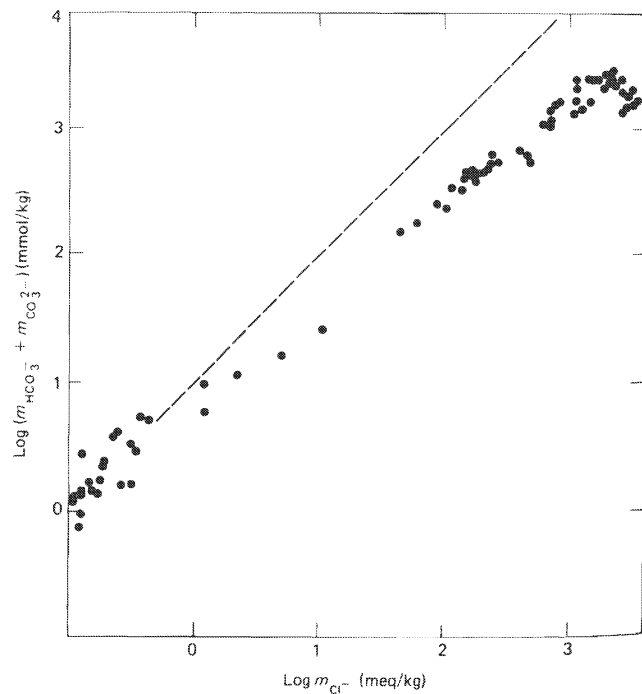


During the final stages, trona precipitation removes both  $\text{CO}_3^{2-}$  and  $\text{HCO}_3^-$  from solution:

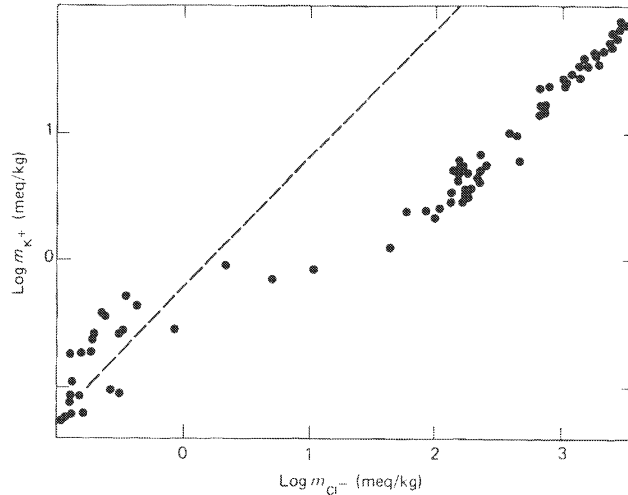


Potassium and silica show rather similar behavior (Figs. 15-7 and 15-8). Potassium is removed from solution, presumably by cation exchange, as the water moves underground and then increases in the expected manner in the lake brines. Silica concentrations are relatively uniform in the dilute waters of the highlands, remain approximately constant at 50 mg/kg during the underground evolution phase, and then increase slightly less rapidly than chloride in the lake brines. Silica loss underground could conceivably be due to precipitation of a silica glass, but adsorption and cyclic evaporation–dissolution are more probable

**FIGURE 15-6** Carbonate species and chloride in waters from the Lake Magadi region. The dashed line is the 1:1 slope expected from simple evaporation (Eugster and Hardie, 1978).



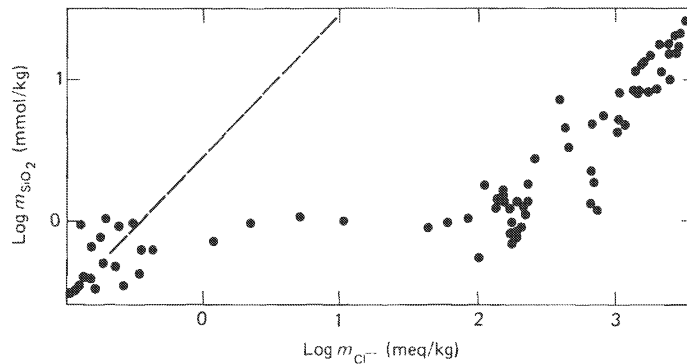
**FIGURE 15-7** Potassium and chloride in waters from the Lake Magadi region. The change in slope at about  $10^2$  meq/kg  $\text{Cl}^-$  corresponds to the change from subsurface brines to lake brines (Eugster and Hardie, 1978).



mechanisms. The loss of silica from the lake brines may be a result of formation of zeolites or magadiite [ $\text{NaSi}_7\text{O}_{13}(\text{OH})_3$ ], or it may be a result of adsorption. Note the very high silica concentrations that can exist in alkaline brines (compare Chapter 10).

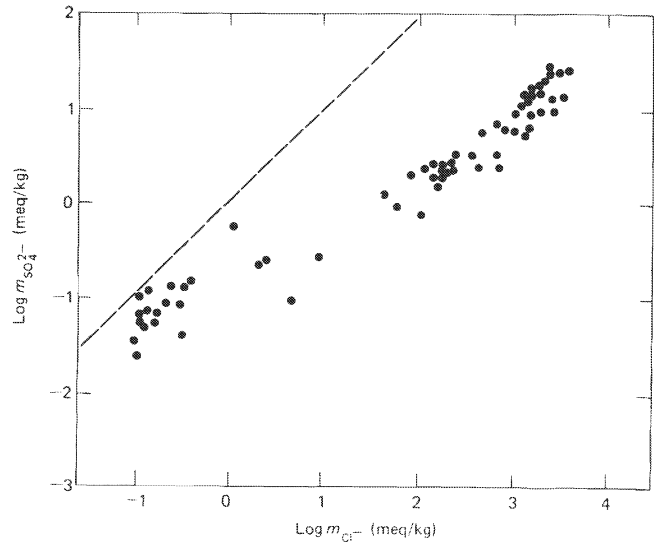
Sulfate is progressively removed from the water at all stages of brine evolution (Fig. 15-9). In the lake brines, the removal process is clearly sulfate reduction. In the more dilute waters, the removal process has not been documented; Jones et al. (1977) suggest both adsorption and reduction as possibilities.

The log-log plots used above give a somewhat misleading impression of the extent to which various ions are removed from solution during brine evolution. With the exception of sodium and chloride, the amounts of the major solutes present in the springs around Lake Magadi represent only a small fraction of the amounts present in the dilute streams of the highlands (Fig. 15-10).



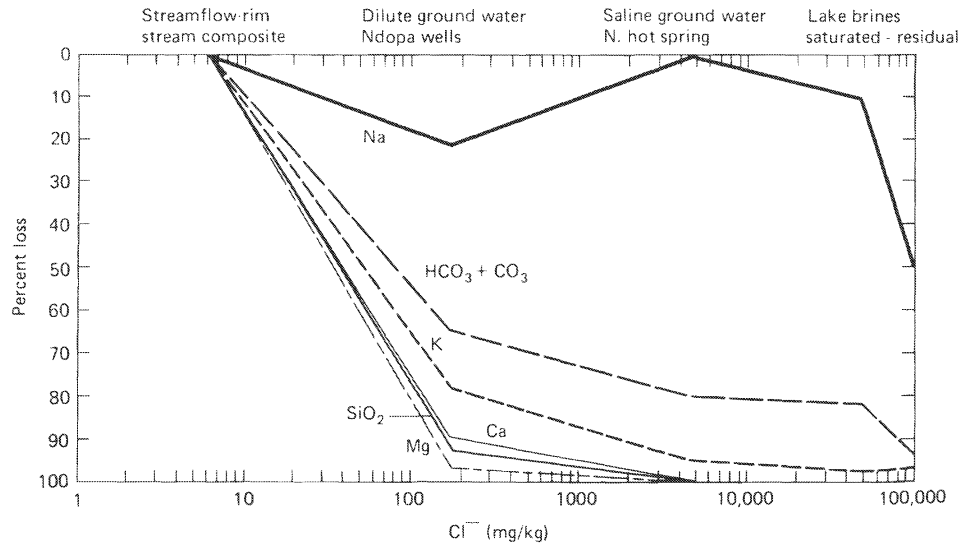
**FIGURE 15-8** Silica and chloride in waters from the Lake Magadi region. Note again the change in slope as subsurface brines become lake brines (Eugster and Hardie, 1978).

**FIGURE 15-9** Sulfate and chloride in waters from the Lake Magadi region. Dashed line is 1:1 slope expected from simple evaporation (modified from Jones et al., 1977).



### Teels Marsh, Nevada

Teels Marsh is a playa located in a closed basin in western Nevada. It resembles Lake Magadi in that it is in an area of intense evaporation and is underlain by igneous rocks, but differs in scale (Teels Marsh is much smaller) and, most important, in hydrology. In the case of Lake Magadi, dilute waters from a humid highland move into an arid lowland, whereas at Teels Marsh the entire drainage basin is arid; the source of water is rain and snowfall in the basin.



**FIGURE 15-10** Percentage of solutes in dilute inflow removed at various stages of evaporation in the Lake Magadi system (Jones et al., 1977).



Also, at Teels Marsh there is probably no deep circulation of groundwater and certainly no hot-spring activity. The chemistry of springs in the Teels Marsh basin cannot be explained by a simple progression from a single dilute source to a concentrated brine, as was the case at Lake Magadi.

The chemistry of springs in the Teels Marsh basin was studied by Smith and Drever (1976). They divided the springs into three groups on the basis of salinity and location:

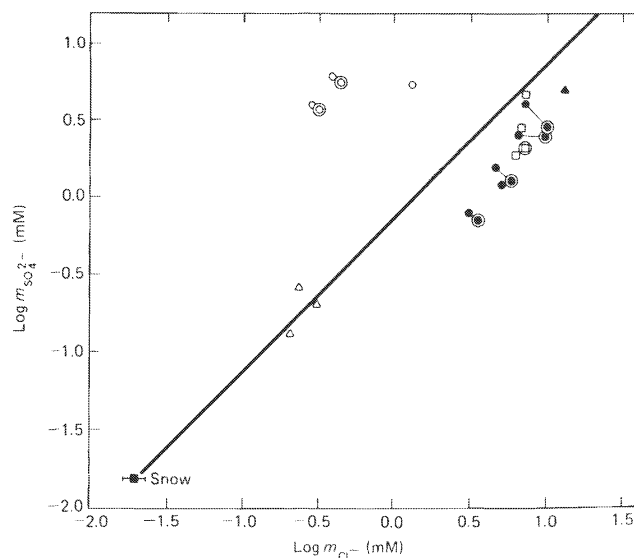
1. Dilute springs at relatively high elevations to the south of the playa (open triangles in Figs. 15-11 to 15-13).
2. Springs of intermediate salinity associated with sulfide mineralization north of the playa (open circles in the figures).
3. Relatively concentrated springs close to the playa itself (open squares in the figures) and at the edge of the alluvium around the playa (solid circles and triangles in the figures).

The relationship between sulfate and chloride concentrations in the springs and in the local precipitation is shown in Fig. 15-11. The sulfate content of the dilute springs is close to what would be expected from simple evaporation of snow or rainfall. The intermediate springs show clearly the effect of weathering of sulfides:



The concentrated springs actually contain less sulfate than would be expected from simple evaporation of snow or rainfall. The loss of sulfate might be explained according to the Hardie–Eugster model by precipitation of gypsum, but all the spring waters are highly undersaturated with respect to gypsum. Smith and Drever invoked cyclic wetting and drying to explain the apparent anomaly. When rain falls on an arid area such as the Teels Marsh basin, it normally wets the ground to a depth of less than 1 m. After the rainstorm, the water evaporates, leaving behind any dissolved salts from either the rain itself or from interaction between the rain and rock. Very occasionally, there will be a rainstorm of sufficient intensity for the

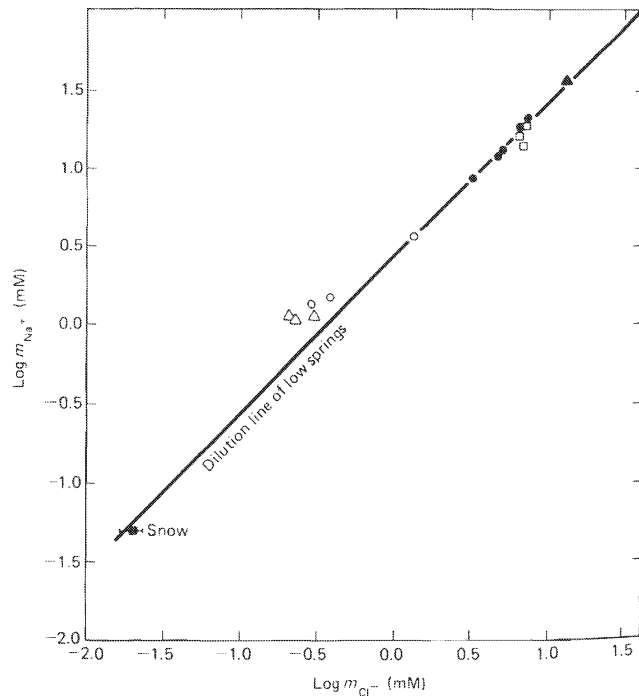
**FIGURE 15-11** Sulfate and chloride concentrations in springs from the Teels Marsh basin. Line is composition predicted from simple evaporation of snow. Lines connect the same springs sampled in summer (circled) and in winter. The black square represents the snow sample; open triangles represent dilute springs at relatively high elevation; filled circles represent springs discharging near the contact between bedrock and alluvium around the playa; open squares are springs near the edge of the playa; open circles represent high elevation associated with sulfide mineralization (Smith and Drever, 1976).



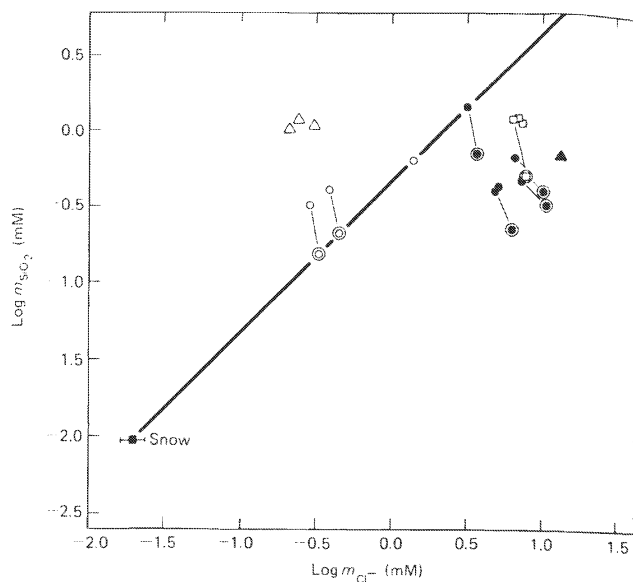
water to percolate through the soil zone and recharge the groundwater system. The percolating water will dissolve completely all highly soluble salts (such as NaCl), but only partially dissolve sparingly soluble salts such as gypsum. The water reaching the groundwater system will thus appear to have lost sulfate relative to chloride but will be undersaturated with respect to gypsum, because there was not sufficient contact time between gypsum and water for equilibrium to be established. The process was duplicated in the laboratory by Drever and Smith (1978) (Fig. 15-4). A very similar mechanism involves dissolution of salts deposited in the capillary fringe above the water table. When the water table is near the ground surface, water drawn up above the water table by capillarity will evaporate and deposit salts, even though the groundwater proper remains undersaturated with respect to these salts (Hellwig, 1974). If these salts are leached by percolating water, chlorides will dissolve rapidly, whereas gypsum will not, giving the result already discussed. Note that the wet-season samples (Fig. 15-11) contain less chloride and more sulfate than the dry-season samples, as would be expected on the basis of the evaporation–dissolution mechanism.

On the plot of sodium versus chloride concentration (Fig. 15-12), a 1:1 line through the points representing the concentrated springs passes through the point (or area, allowing for analytical uncertainty) representing snowfall. Thus the sodium in the concentrated springs could have been derived entirely from rain and snow, with no significant contribution from rock weathering. The points representing dilute springs, which occur at higher elevations where precipitation is greater, plot above the 1:1 line, indicating that feldspar weathering is providing some sodium. Over the basin as a whole, however, the contribution of sodium from rock weathering is minor compared to the contribution from the atmosphere. This is probably a consequence of the accumulation of salts near the ground surface. When rain falls, it will rapidly dissolve salts,

**FIGURE 15-12** Sodium and chloride concentrations in springs from the Teels Marsh basin. Straight line is best fit to data from concentrated springs and has 1:1 slope. Symbols as in Fig. 15-11 (after Smith and Drever, 1976).



**FIGURE 15-13** Silica and chloride concentrations in spring waters from the Teels Marsh basin. Straight line is 1:1 slope through snow point. Symbols as in Fig. 15-11 (Smith and Drever, 1976).



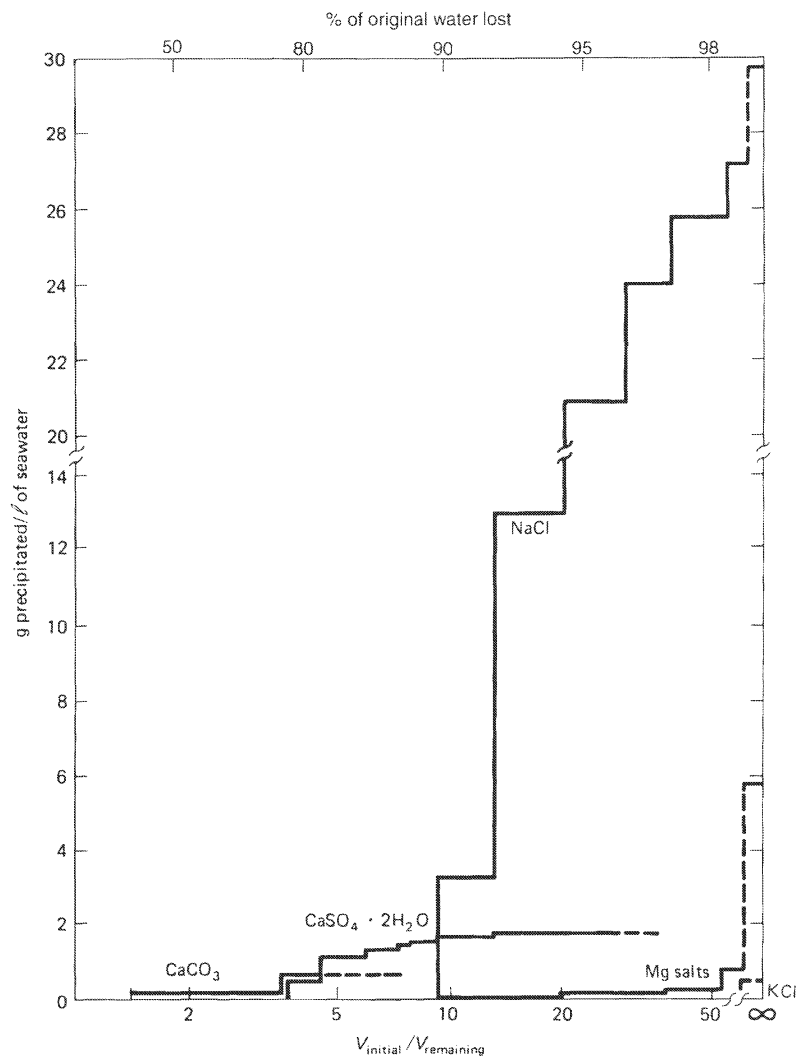
including some carbonates. The pH and cation content of the water will rise rapidly, so the waters become less “aggressive” and silicate weathering becomes very slow.

Silica shows a somewhat similar pattern to sodium (Fig. 15-13). In the dilute springs, silica concentrations are much higher than would be predicted from simple evaporation of rain and snow, showing the effect of rock weathering. In the concentrated springs, however, silica concentrations are generally much lower than would be predicted from simple evaporation of rain and snow. The waters are all strongly undersaturated with respect to amorphous silica, and almost all are undersaturated with respect to sepiolite. Presumably, silica deposited during evaporation is not redissolved on subsequent wetting (compare Fig. 15-4).

If all chloride in the springs is derived from the atmosphere, the concentrations of calcium, magnesium, potassium, and alkalinity are all lower in the concentrated springs than would be expected from simple evaporation of rain and snowfall. The influence of rock weathering on spring-water chemistry in the Teels Marsh basin is thus minimal; almost all the ions in the concentrated springs could have been derived from the atmosphere. The most important process controlling water chemistry there appears to be evaporation resulting in deposition of salts, followed by partial dissolution of these salts.

## EVAPORATION OF SEAWATER

Evaporation of seawater has been extensively studied by geologists and chemists, primarily to gain an understanding of the origin of ancient salt deposits. Brines resulting directly from evaporation of seawater are remarkably rare in the present-day world. The basic sequence of minerals deposited by evaporation of seawater was described by Usiglio in 1849 (Fig. 15-14). Usiglio’s experiments have been repeated many times with essentially similar results; and although precipitation does not occur exactly when saturation is reached, the “overshoot” appears to be significant only for carbonate minerals and gypsum. The path of solution com-



**FIGURE 15-14** Amounts of salts precipitated by evaporation of 1 l of seawater. Dashed values on right are calculated from what remained in solution at end of experiment. Data from Usiglio (1849), tabulated in Stewart (1963).

position and the sequence of minerals precipitated have been calculated theoretically by Harvie et al. (1980).

Surface seawater, except in polar regions, is supersaturated with respect to calcite and aragonite, and calcium carbonate starts to precipitate soon after evaporation commences. Since the calcium concentration (in equivalents) in seawater is much greater than the alkalinity (Table 15-3), precipitation of calcium carbonate removes essentially all the alkalinity, and calcium builds up in the residual solution. After 80 percent of the water has been removed by evaporation (and essentially all the carbonate has been precipitated), gypsum starts to precipitate. [The amount of evaporation required to cause gypsum precipitation does vary somewhat depending on experimental conditions; Posnjak (1940) found that gypsum precipitation

**TABLE 15-3** The Major-Element Composition of Sea Water (mg/kg)

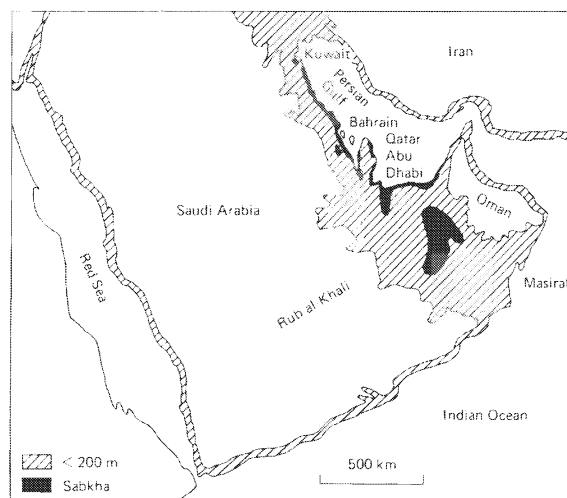
Chloride	19,350	Bromide	67
Sodium	10,760	Strontium	8
Sulfate	2,710	Boron	4.5
Magnesium	1,290	Fluoride	1.3
Calcium	411		
Potassium	399	Silica	0.5–10
Bicarbonate	142	Diss. Org. C	0.3–2

occurred after concentration by a factor of 3.35 rather than 5.] The concentration of sulfate in seawater is much greater than that of calcium, and so gypsum precipitation removes essentially all the calcium from solution while the concentration of sulfate builds up. After 90 percent of the water is removed (and most of the calcium is removed as gypsum), halite (NaCl) starts to precipitate, removing most of the sodium from solution. After an evaporation factor of about 20 (95 percent of the water removed), chlorides and sulfates of magnesium and potassium start to precipitate. A large number of different salts can form at this stage, depending on temperature and, most important, on the extent to which the brines can react with previously deposited minerals.

### Persian Gulf Sabkhas

Probably the best studied modern example of the natural evaporation of seawater is the coastal sabkha environment near Abu Dhabi on the Persian Gulf (Fig. 15-15). The coastal sabkhas are broad supratidal areas that have developed as a result of carbonate sedimentation and a relative fall in sea level. The surface elevation of the sabkha is controlled by the water table, which is never more than 1 to 1.5 m below the ground surface. When the water table lies at this depth, the surface has achieved a state of deflational equilibrium; capillary moisture prevents surface grains from being blown away by the prevailing onshore winds. The chemistry of groundwater

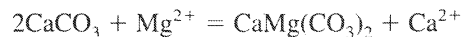
**FIGURE 15-15** Location of Persian Gulf sabkhas (Patterson and Kinsman, 1977).



in the sabkha and the development of diagenetic carbonate and evaporite minerals have been discussed by Kinsman (1966, 1969), Butler (1969), and Patterson and Kinsman (1977). The subsurface water beneath the sabkha may be derived from two sources (Fig. 15-16): seawater that is driven up over the sabkha by strong onshore winds, and groundwater that moves into the landward part of the sabkha from the continental area inland. Here we will discuss only the evolution of the seawater-derived brine in the sabkha environment.

Adjacent to the open marine lagoon is the intertidal zone, which is usually less than 1 km wide. Aragonite precipitation takes place in the lagoon and in the intertidal zone. The intertidal zone is regularly flooded by tide waters and is covered by mats of living cyanobacteria (blue-green algae). Gypsum crystals occur in the sediments and cyanobacterial mats toward the landward side of the intertidal zone. Inland from the intertidal zone, gypsum becomes abundant on the sediment surface, the sediment becomes dolomitized, and then anhydrite ( $\text{CaSO}_4$ ) progressively increases in abundance, while the abundance of gypsum decreases. Halite forms ephemerally on the ground surface, but there is no permanent accumulation of halite (or of the soluble potassium and magnesium salts).

These observations are consistent with simple ideas on the chemistry of evaporation of seawater. As we would expect, gypsum precipitates early in the evaporation sequence. Precipitation of gypsum removes calcium from the water, increasing the  $\text{Mg}^{2+}/\text{Ca}^{2+}$  ratio (Fig. 15-17). When this ratio exceeds about 6, calcium carbonate (as aragonite) in the sediment is converted to dolomite according to the equation



The calcium released by dolomitization precipitates as gypsum. The formation of anhydrite at the expense of gypsum is a consequence of the high salinities and temperatures of the brines in the landward part of the sabkha. Gypsum and anhydrite are related by the reaction

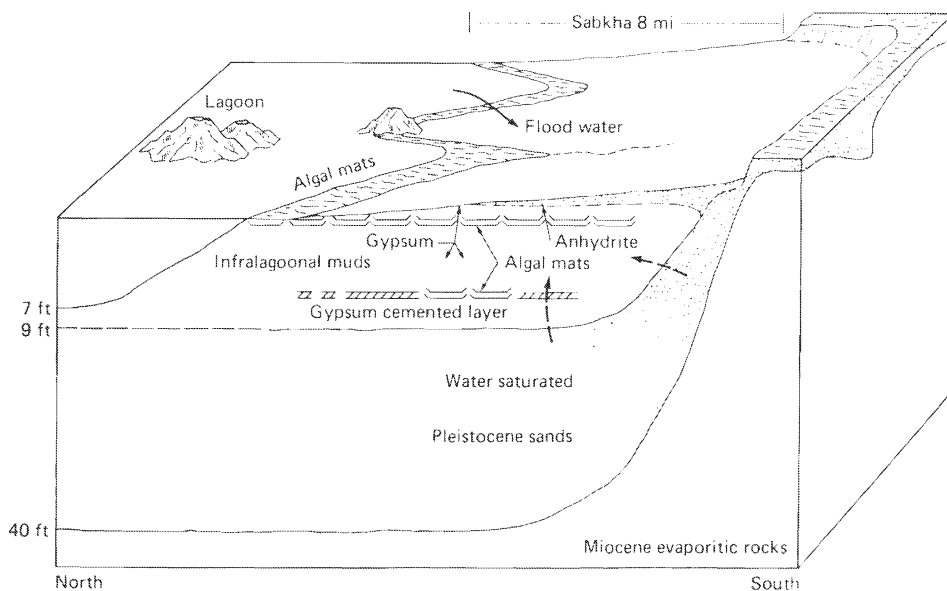


FIGURE 15-16 Schematic cross section of Persian Gulf sabkha near Abu Dhabi (Butler, 1969).

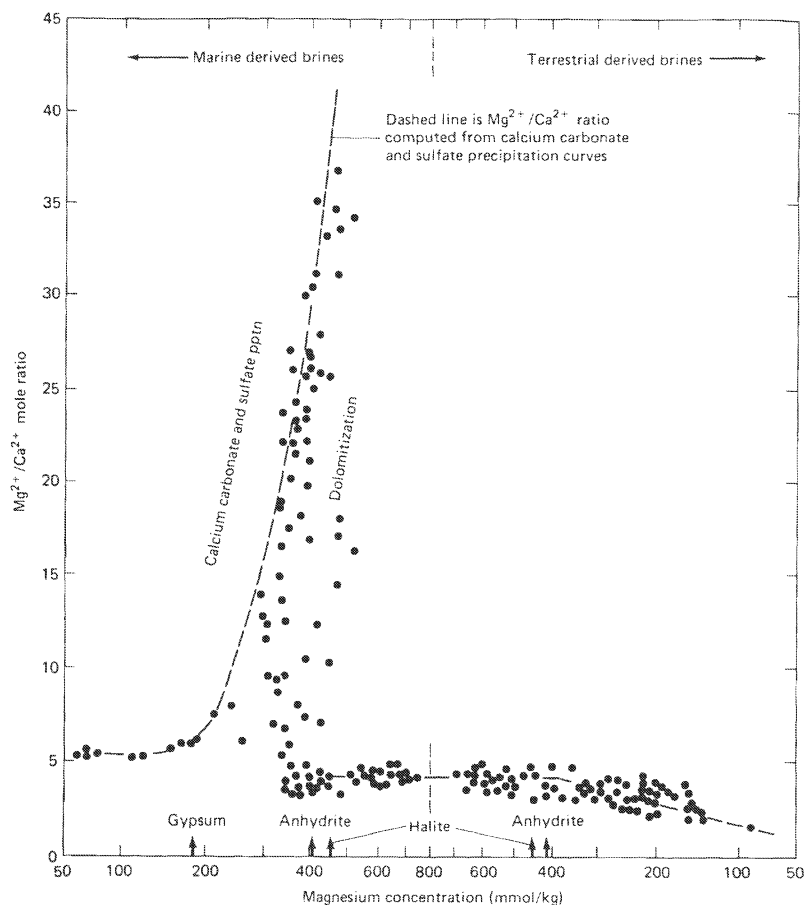
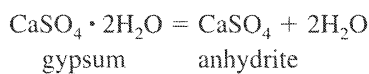


FIGURE 15-17  $Mg^{2+}/Ca^{2+}$  ratio as a function of Mg concentration for Abu Dhabi sabkha waters (Butler, 1969).

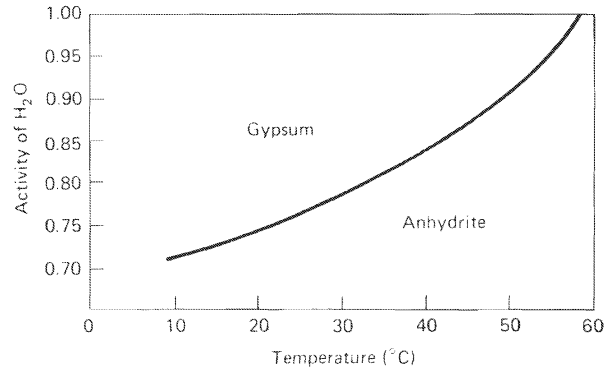


$$K_{\text{eq}} = a_{\text{H}_2\text{O}}^2$$

The activity of water for gypsum-anhydrite equilibrium is shown in Fig. 15-18. The brines from the inner part of the sabkha plot in the anhydrite stability field, in accord with the observed mineralogy. The activity of water in concentrated brines is significantly less than 1.

The lack of accumulation of halite and more soluble salts is at first surprising. The brines over a large part of the sabkha are saturated with respect to halite, so some accumulation would be expected. One possible explanation is that when the sabkha is flooded by seawater and/or rainwater during storms all halite is redissolved. Another explanation (Kinsman, 1976) is related to atmospheric humidity. As mentioned above, the activity of water in a brine decreases as its salinity increases. The activity of water in a brine is numerically equal to the relative humidity of the atmosphere that would be in equilibrium with the brine. For simple evaporation of seawater, the equilibrium relative humidity at the start of

**FIGURE 15-18** Gypsum–anhydrite stability relationships (after Hardie, 1967).



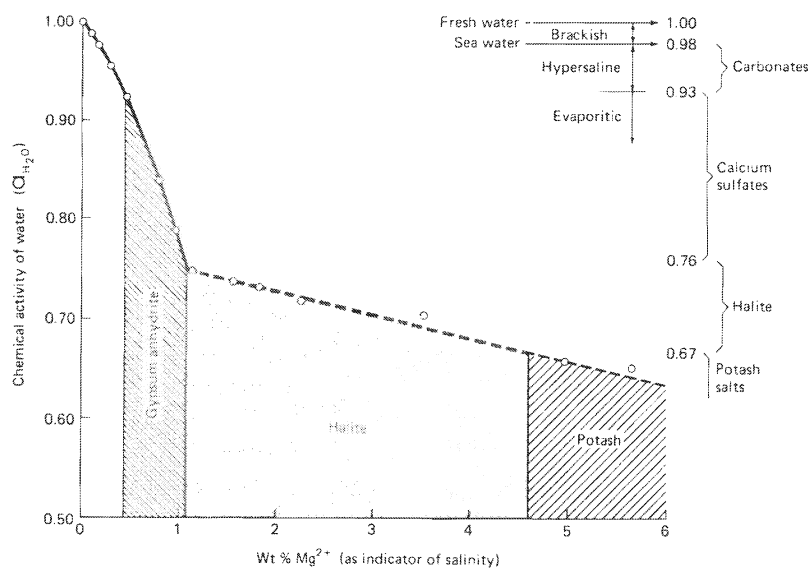
gypsum precipitation would be 93 percent; at the start of halite precipitation it would be 76 percent, and for potassium and magnesium salts, it would be 67 percent or less\* (Fig. 15-19). If the humidity of the atmosphere is greater than that which would be in equilibrium with a particular brine, evaporation cannot take place. Rather, water comes out of the atmosphere and dilutes the brine. The Persian Gulf sabkhas are next to the open waters of the Persian Gulf, and the wind direction is generally onshore. Typical daytime humidities are 34 to 45 percent, but nighttime humidities are generally greater than 90 percent, often reaching 100 percent (Kinsman, 1976). Thus, any halite (or more soluble salts) exposed at the surface during the night should draw water out of the atmosphere and dissolve. The humidity of the atmosphere should provide an upper limit to the salinity of brines in the sabkha. A corollary to this theory is that halite and the more soluble salts can accumulate only in an environment where the atmospheric humidity is relatively low.

## SALINE FORMATION WATERS

The waters in the pores of deeply buried sedimentary rocks are often saline. Such waters are most commonly encountered during exploration for petroleum, and they are often referred to as *oilfield brines*. The compositions and salinities of such waters are highly variable (White, 1965). Hitchon et al. (1971) showed that the volume-weighted mean composition of formation waters in the western Canada sedimentary basin was similar to seawater. The main differences were slightly higher  $\text{Na}^+$  and  $\text{Cl}^-$  concentrations, much higher  $\text{Ca}^{2+}$  and lower  $\text{Mg}^{2+}$  and  $\text{SO}_4^{2-}$  concentrations in the mean brine composition than in seawater. Deuterium and  $^{18}\text{O}$  analyses (Chapter 14) of the same brines indicated that they were mixtures of seawater and meteoric water in varying proportions (Hitchon and Friedman, 1969). Hitchon et al. postulated that the formation waters were originally seawater trapped at the time of deposition. Much of the original water had been displaced by later meteoric water, but the solutes in the water had been retained largely by membrane filtration (Chapter 4). They considered that the following processes might have been important in addition to membrane filtration:

\*The precise values are significant only if brine and atmosphere are at the same temperature (Walton, 1978).





**FIGURE 15-19** Chemical activity of water ( $a_{H_2O}$ ) in seawater brines undergoing evaporation. The relative humidity in the atmosphere in equilibrium with the brine is simply the activity of water expressed as a percentage (Kinsman, 1976).

1. *Dissolution of halite.* The increase in the proportions of  $Na^+$  and  $Cl^-$  relative to seawater was attributed to dissolution of halite from marine evaporites. The distribution of  $Na^+$  and  $Cl^-$  concentrations in the formation waters agreed well with the known distribution of evaporites. In general, dissolution of evaporites and membrane filtration appear to be the main causes of the high salinities in formation waters.

2. *Dolomitization.* High  $Ca^{2+}$  and low  $Mg^{2+}$  concentrations relative to seawater are general features of formation waters. Many authors have attributed this to dolomitization of pre-existing calcite (the  $Mg^{2+}/Ca^{2+}$  ratio for coexistence of calcite and dolomite decreases with increasing temperature), but Hitchon et al. (1971) showed that the statistical relationship between  $Ca^{2+}$  and  $Mg^{2+}$  concentrations was not simple, suggesting that dolomitization was not the only process occurring.

3. *Bacterial sulfate reduction.* The relatively low sulfate concentrations commonly observed in formation waters (there are also many exceptions) have generally been attributed to sulfate reduction (see Chapter 14). Hitchon et al. (1971) tended to reject this explanation because there was not sufficient  $H_2S$  present in the water and associated gas to match the missing (relative to seawater) sulfate. On the other hand, they did not consider the possibility that the missing sulfur might be present as pyrite rather than  $H_2S$ .

4. *Anhydrite precipitation.* The solubility of anhydrite ( $CaSO_4$ ) decreases with increasing temperature, and temperature, of course, increases with depth below the earth's surface. The combination of high calcium concentrations and elevated temperatures may result in precipitation of anhydrite. In general, it appears that both sulfate reduction and anhydrite precipitation are important in removing sulfate from solution.

5. *Diagenetic reactions of silicates.* The increased temperature associated with burial causes various diagenetic reactions, of which the most important are probably the conversion

of smectite-type clay minerals to illite and the formation of chlorite (Boles and Franks, 1979; Hower et al., 1976). These reactions undoubtedly affect the composition of associated waters and also release water that was present in smectite interlayers, but the overall effects on water chemistry are not well understood at present. Removal of Mg from solution has been attributed to formation of diagenetic chlorite.

6. *Cation exchange.* Changes in fluid composition and temperature will both cause a redistribution of ions between solution and exchange sites on clay minerals and oxides (Chapter 4). The increased Ca concentration in formation waters has been attributed in part to displacement of  $\text{Ca}^{2+}$  from exchange sites by  $\text{Na}^+$ .

7. *Reactions involving organic matter (other than sulfate reduction).* Hitchon et al. (1971) did not notice any effects that could be ascribed to reactions involving organic matter, but their study was not designed to evaluate this aspect. Oilfield brines often contain high concentrations of organic anions (Carothers and Kharaka, 1978; Willey et al., 1975) which result from thermal alteration of organic matter.

In summary, saline formation waters show a wide range of chemical compositions, the result of many different chemical processes. The main reasons for the high salinities are dissolution of evaporites and membrane filtration (the importance of which is somewhat disputed). Their occurrence in deep strata is also probably related to the fact that dense solutions tend to move downward and displace less dense solutions toward the surface. The topic is well reviewed by Hanor (1983).

## SUMMARY

The compositions of most saline brines at the earth's surface can be explained by evaporation of dilute inflow waters. The general trend is always for sodium to increase relative to the other cations, at least in the early stages of evaporation. The compositions of dilute waters (the potential precursors of brines) are discussed in Chapter 12. Brines of the sodium carbonate type are likely to be derived from waters draining areas underlain by igneous or high-grade metamorphic rocks. In such waters,

$$m_{\text{HCO}_3^-} \approx m_{\text{Na}^+} + m_{\text{K}^+} + 2m_{\text{Ca}^{2+}} + 2m_{\text{Mg}^{2+}}$$

and so,

$$m_{\text{HCO}_3^-} > 2m_{\text{Ca}^{2+}} + 2m_{\text{Mg}^{2+}}$$

which is the general condition necessary for an alkaline brine to be formed. Sulfate-rich brines generally result from waters draining areas underlain by sedimentary rocks or marine evaporites. Marine evaporites contribute sulfate from gypsum, and shales contribute sulfate from pyrite oxidation. Also, neither shales nor evaporites contribute much bicarbonate from silicate weathering. Saline lakes often occur in basins that contain evaporites from previous saline lakes; recycling of these older evaporites can be the major control on water chemistry, often resulting in a chloride-rich brine.

Use of water for irrigation always results in evaporation and usually results in an increase in both the absolute and relative concentration of sodium downstream. High concentrations of sodium, both absolutely and relative to other cations, make a water unsuitable for irrigation, so extensive irrigation in the upper part of a river system may make

irrigation difficult or impossible in the lower part of the system. The situation along the Colorado River is a good example of this problem.

Most of the water used for irrigation is evaporated rapidly into the atmosphere, causing deposition of salts in the soil and/or an increase in the salinity and sodium content of the soil moisture. The prolonged buildup of salinity by this process decreases soil fertility, and so sufficient irrigation water should be applied to wash the salts to a depth in the ground greater than root depth. Thus, combating salinity buildup demands large volumes of irrigation water and may cause salinity problems in shallow groundwater or nearby surface water.

### REVIEW QUESTIONS

The following table gives analyses (mg/l) of the major inflows to:

1. Great Salt Lake, Utah (after Spencer et al., 1985)
2. Pyramid Lake, Nevada (from Livingstone, 1963)
3. The ocean (from Meybeck, 1979)

<i>Inflow to:</i>	<i>Ca</i>	<i>Mg</i>	<i>Na</i>	<i>K</i>	<i>Cl</i>	<i>SO<sub>4</sub></i>	<i>HCO<sub>3</sub></i>	<i>SiO<sub>2</sub></i>
Gt. Salt L.	62	33	101	10	141	107	285	15
Pyramid L.	8.4	2.7	4.3	1.4	2.2	1.0	48	16
Ocean	13.4	4.44	3.56	1.25	3.09	7.82	51.6	10.4

Which path should each water follow on evaporation (Fig. 15-3)? Qualitatively, how do the actual waters (Tables 15-1 and 15-3) compare with the predictions from the simple model?

### SUGGESTED READING

- EUGSTER, H. P., and L. A. HARDIE. (1978). Saline lakes. In A. Lerman (Ed.), *Lakes: Chemistry, Geology, Physics* (pp. 237–293). New York: Springer-Verlag.
- EUGSTER, H. P., and B. F. JONES. (1979). Behavior of major solutes during closed-basin brine evolution. *American Journal of Science*, 279, 609–631.
- HANOR, J. S. (1983). Fifty years of development of thought on the origin and evolution of subsurface sedimentary brines. In S. J. Boardman (Ed.), *Revolution in the Earth Sciences* (pp. 99–111). Dubuque, IA: Kendall/Hunt.



# 16

## Transport and Reaction Modeling

There have recently been tremendous advances in quantitative modeling of chemical processes in the subsurface. A prime motivation for this is the need, for both regulatory and practical purposes, to predict the consequences of human activities such as waste disposal and mining. Such predictions are usually based on a *hydrologic model*, which describes the movement of water, and a *chemical model*, which describes the behavior of solutes in the water. An adequate hydrologic model is a prerequisite for chemical modeling. (Hydrologic modeling is a complex subject beyond the scope of this book; some references are suggested at the end of the chapter.)

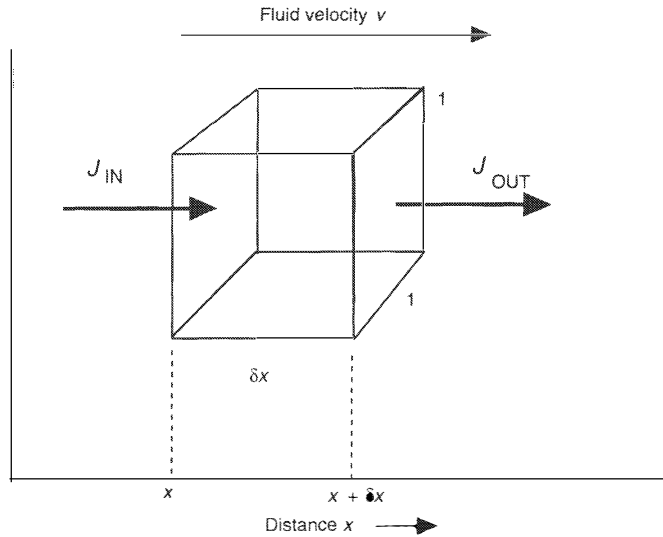
### THE ADVECTION-DIFFUSION EQUATION

As groundwater moves through a porous medium, the concentration of each solute is affected by both physical processes (fluid movement, diffusion, or dispersion) and chemical processes. The traditional starting point for modeling chemical transport in groundwater is the *advection-diffusion equation*. In its simplest one-dimensional form, it can be represented by:

$$\frac{\partial C_i}{\partial t} = D_i \frac{\partial^2 C_i}{\partial x^2} - v \frac{\partial C_i}{\partial x} \pm (\text{reaction terms}) \quad (16-1)$$

diffusion term      advection term

$C_i$  represents the concentration of a solute  $i$ ,  $x$  distance, and  $t$  time (the subscript  $i$  will be omitted for clarity in the following discussion).  $D$  represents a diffusion coefficient and  $v$  the velocity of the fluid; the definitions of  $D$  and  $v$  will be discussed in more detail below. The terms in Eq. (16-1) can be understood by reference to a hypothetical “elementary volume” (Fig. 16-1). First, the advection term says that if concentration varies spatially, moving the solution will bring solution with a different composition into our elementary volume (advection means physical movement of the fluid). The rate of change in composition with time ( $\partial C/\partial t$ ) will simply be the product of the rate of movement of the fluid ( $v$ ) and the rate at which



For advection:

$$J_{\text{IN}} = v C_{x=x}$$

$$J_{\text{OUT}} = v C_{x=x+\delta x}$$

For diffusion:

$$J_{\text{IN}} = -D \left( \frac{\partial C}{\partial x} \right)_{x=x}$$

$$J_{\text{OUT}} = -D \left( \frac{\partial C}{\partial x} \right)_{x=x+\delta x}$$

FIGURE 16-1 One-dimensional advection and diffusion on the scale of an elementary volume.

the composition varies with distance ( $\partial C/\partial x$ ). The diffusion term can be understood in a similar way: The rate of change of mass (and hence in concentration) with time in the elementary volume ( $\partial C/\partial t$ ) is equal to the difference between the amount that diffuses into the volume from the left and the amount that diffuses out on the right. Diffusion (see below) is governed by what are called *Fick's laws*. The first law is given by (in one dimension)

$$J = -D \frac{\partial C}{\partial x} \quad (16-2)$$

$J$  is the flux (the mass moving across a unit area in unit time),  $D$  is a diffusion coefficient, and  $\partial C/\partial x$  is the concentration gradient. The units of the diffusion coefficient can be deduced from dimensional analysis of Eq. (16-2).  $J$  has dimensions  $ML^{-2}T^{-1}$ ;  $\partial C/\partial x$  has dimensions  $ML^{-4}$ , which gives  $D$  dimensions  $L^2T^{-1}$ . The common units for diffusion coefficients are  $\text{cm}^2/\text{sec}$  or  $\text{m}^2/\text{sec}$ . Fick's first law simply states that the flux is proportional to the concentration gradient: the constant of proportionality is the diffusion coefficient. The  $-$  sign reflects the fact that the flux is in the opposite direction to the concentration gradient: solutes diffuse from regions of high concentration to regions of low concentration.

Returning to the elementary volume in Fig. 16-1, the diffusional flux into the volume from the left is given by

$$J_{\text{in}} = -D \left( \frac{\partial C}{\partial x} \right)_{x=x} \quad (16-3)$$

and the flux out of the volume from the right is given by

$$J_{\text{out}} = -D \left( \frac{\partial C}{\partial x} \right)_{x=x+\delta x} \quad (16-4)$$

The change in mass ( $\delta m$ ) in the  $1 \times 1 \times \delta x$  volume in time increment  $\delta t$ , is given by

$$\delta m = (J_{\text{in}} - J_{\text{out}}) \delta t \quad (16-5)$$

Also, since mass = concentration  $\times$  volume,

$$\delta m = \delta C \delta x \quad (16-6)$$

Combining Eqs. (16–3), (16–4), (16–5), and (16–6) gives

$$\frac{\partial C}{\partial t} = D \frac{\left( \frac{\partial C}{\partial x} \right)_{x+\delta x} - \left( \frac{\partial C}{\partial x} \right)_x}{\delta x}$$

or

$$\frac{\partial C}{\partial t} = D \frac{\partial^2 C}{\partial x^2} \quad (16-7)$$

Eq. (16–7) is the diffusional term in the advection-diffusion equation. It is also referred to as *Fick's second law*.

In summary, Eq. (16–1) simply states that the change in concentration with time at a point is equal to the sum of the change due to diffusion, the change due to advection, and the change due to chemical reaction. Note that the diffusion term is important only if the concentration gradient is non-linear, and advection is important only if the concentration gradient is non-zero. We shall discuss the chemical reaction term(s) later.

The discussion so far has been very general. We have treated our system as a uniform continuum, whereas we know that real aquifers are not continuous; they consist of grains and pores. The traditional approach in hydrology has been based on the concept of the *Representative Elementary Volume* (REV). Consider how the porosity of a sandstone will vary as a function of the volume over which the porosity is measured. If the volume is very small, much smaller than the grain-size of the rock, the porosity will be either 1 (if the volume is located in a pore) or zero (if it is located in a grain). If the size of the measuring volume is similar to the size of the grains, the porosity will still vary quite strongly depending on whether the volume is centered on a grain or a pore, however, as the size of the volume is increased to include many grains, the porosity will be independent of the exact location of the center of the volume. If the size of the volume is further increased, larger-scale heterogeneities in the rock (perhaps bedding) will become important, so the porosity will again depend on the location of the center of the measuring volume. Thus, conceptually, the REV represents a scale large enough to average out the effect of individual grains but not sufficiently large as to involve macroscopic heterogeneities in the rock. The rock is modeled as a continuum whose properties are averages on the scale of the REV. This discussion has focused on porosity, but an exactly analogous argument can be made for other properties such as permeability or cation

exchange capacity. Our discussion has also focused on a granular porous medium. The same concept is often applied to a fractured rock, in which the “pores” are the fractures and the intervening blocks are considered impermeable. The REV in this case would have to be large enough to include a population of fractures and blocks. There is considerable debate as to whether this is a realistic way to model transport in fractured rock.

Let us now consider advection and diffusion in more detail.

### Advection

Velocity can be defined in several ways. There is the *microscopic velocity*, the actual velocity of the fluid as it winds its way through the pores of the aquifer. This velocity is essentially unknowable and is probably important only for erosion and transport of particles within the aquifer. We will generally be concerned with velocities averaged on the scale of the REV (or greater).

At the REV scale, we can define the *specific discharge* or *Darcy velocity* by

$$v_{\text{Darcy}} = \frac{Q}{A}$$

$Q$  is the volumetric flux (volume/unit time),  $A$  is the cross-sectional area (*total*). On the other hand, if we recognize that only part of the cross-sectional area is available for flow (the areal porosity), we can define an *average linear velocity* as

$$v_{\text{av. linear}} = \frac{Q}{\phi A}$$

where  $\phi$  is the porosity (the ratio of the volume of the pores in a rock to the total volume of the rock; we shall ignore the possible difference between effective areal porosity and volumetric porosity). For solute migration purposes, the velocity of interest is the average linear velocity. It represents the average rate at which a *conservative tracer* would be transported through the aquifer. A conservative tracer is one that moves with the water and does not undergo any chemical reactions or adsorption. (The term *convection* is often used in place of advection, particularly in the engineering literature. We prefer to reserve the term *convection* for the case where fluid movement is driven by internal density differences. The term *advection* implies fluid movement but does not imply any specific cause.)

### Diffusion and Dispersion

The term  $D$  in the diffusion–advection equation may represent different things, depending on the environmental/physical system being described. For stationary or very slow-moving fluids,  $D$  represents the *coefficient of molecular diffusion*, or simply *diffusion coefficient*. Where fluid movement in a porous medium is not very slow (to be defined later), the process that causes mixing is hydrodynamic dispersion rather than diffusion, and  $D$  becomes the *dispersion coefficient*. In open bodies of water, flow is turbulent rather than laminar, and mixing is by turbulent transport rather than molecular diffusion.  $D$  then becomes the *eddy diffusivity*. Processes such as dispersion are called *fickian* if the equations describing them have the same form as Fick’s laws.



**Molecular Diffusion.** The concept of molecular diffusion is familiar. In a stationary medium, solutes tend to migrate from regions of high concentration to regions of low concentration as a consequence of thermal motion on the molecular scale. As discussed above, the movement is described by Fick's laws. From a theoretical perspective, molecular diffusion is driven by gradients in chemical potential (Chapter 2) rather than gradients in concentration *per se*. In most situations the distinction is unimportant. Diffusion coefficients of simple ions in solution are on the order of  $10^{-5}$  cm<sup>2</sup>/sec ( $10^{-9}$  m<sup>2</sup>/sec). Diffusion coefficients in solids are much lower.

**Charge Balance and Coupled Diffusion.** Conceptually, a single ion cannot diffuse in isolation. In order for charge balance to be maintained, either an ion of opposite charge must diffuse in the same direction at the same rate, or an ion of the same charge must diffuse in the opposite direction (e.g., Berner, 1980; Lerman, 1979). The mathematics of coupled diffusion is fairly complex and will not be presented here. The error introduced by ignoring it is generally small.

**Porosity and Tortuosity.** Diffusion coefficients are measured and tabulated for species in aqueous solution. Diffusion through a sediment is slower because:

1. Only part of the cross-sectional area of the sediment is occupied by solution. This is the *porosity* effect.
2. The path followed by a diffusing species is not straight; it has to wind its way around grains. This is the *tortuosity* effect. Tortuosity ( $\theta$ ) is defined as:

$$\theta = dl/dx$$

where  $dl$  is the length of the actual sinuous path in length interval  $dx$ .  $\theta$  is always greater than 1.

The combined effects of porosity and tortuosity on the diffusion coefficient can be represented by:

$$D_{\text{sediment}} = D_{\text{soln}} \frac{\phi}{\theta^2} \quad (16-8)$$

Tortuosity cannot be readily measured, but fortunately the effects of porosity and tortuosity on the diffusion coefficient are essentially the same as the effect on electrical conductivity or resistivity. The *Formation factor* ( $F$ ) is defined by:

$$F = R/R_0$$

where  $R$  is the electrical resistivity of the sediment and  $R_0$  is the electrical resistivity of the fluid in the sediment alone. As a good approximation,

$$D_{\text{sediment}} = \frac{D_{\text{soln}}}{F}$$

Another way to estimate  $F$  for sands and sandstones is the strictly empirical *Archie's law*:

$$F = \phi^{-2}$$

Diffusion in a sediment may also be affected by adsorption. We shall delay discussion of this until we discuss adsorption.

The presence of grains and porosity rather than a continuum affects Fick's second law in another way by affecting the volume of solution present in the elementary volume. Because the volume of solution in our elementary volume is  $\phi$  times the volume itself ( $1 \times 1 \times \delta x$ ), Eq. (16-6) becomes

$$\delta m = \phi D \delta C \delta x$$

and Fick's second law becomes

$$\frac{\partial C}{\partial t} = \frac{D_{\text{sediment}}}{\phi} \frac{\partial^2 C}{\partial x^2} \quad (16-9)$$

We can combine porosity term into the diffusion coefficient by defining an effective diffusion coefficient for non-steady-state diffusion ( $D_{\text{eff}}$ ) by:

$$D_{\text{eff}} = \frac{D_{\text{sediment}}}{\phi} = \frac{D_{\text{soln}}}{\theta^2} \quad (\text{from Eq. 16-8})$$

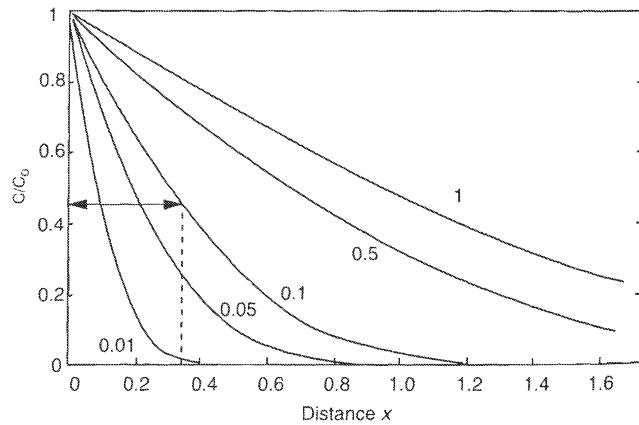
*In what situations is molecular diffusion important?* There are various ways to answer the question; it usually comes down to "important compared to advection" or "important compared to hydrodynamic dispersion." First, let us consider a simple analytical solution to the diffusion equation: suppose we have an infinite reservoir of constant concentration adjacent to an infinite porous medium in which the concentration of the species is initially zero (Fig. 16-2). The distribution of the solute in the porous medium as a function of time and space is given by the equation:

$$C_{(x,t)} = C_0 \operatorname{erfc} \left( \frac{x}{2(D_{\text{eff}} t)^{0.5}} \right) \quad (16-10)$$

where  $C_0$  is the concentration in the reservoir and  $\operatorname{erfc}$  is the complementary error function:

$$\operatorname{erfc} x = \frac{2}{\sqrt{\pi}} \int_x^{\infty} e^{-y^2} dy$$

**FIGURE 16-2** Non-steady state diffusion from a source of constant composition into an adjacent infinite porous medium with an initial concentration of zero: contours of concentration (as ratio to concentration in source) at different times (in units of  $D_{\text{eff}} t$ ). The arrow represents the "diffusion length" for the 0.1  $D_{\text{eff}} t$  contour.



Intuitively, an error function is a reasonable solution, since diffusion is essentially random motion. A simple solution to Eq. (16–10) can be obtained by defining (Freeze and Cherry, 1979) a “characteristic length” for diffusion:

$$L_{\text{diff}} = (D_{\text{eff}}t)^{0.5} \quad (16-11)$$

In Fig. 16-2,  $L_{\text{diff}}$  represents approximately the distance to which a solute will diffuse in time  $t$ . To be more precise, the distance at which  $C/C_o = 0.5$  is approximately  $0.95 L_{\text{diff}}$ ; the distance at which  $C/C_o = 0.01$  is about  $4 L_{\text{diff}}$ . Also, the total mass that has diffused into the porous medium is  $1.13 C_o L_{\text{diff}}$ . Some representative diffusion distances are shown in Table 16-1. They are on the order of 10 to 20 cm in 1 year, or 1 m in about a century.

We can compare this with a similar “scale length” for advection, which will simply be

$$L_{\text{advec}} = vt$$

The relative importance of the two processes in any situation can be evaluated from the ratio of the two scale lengths:

$$\frac{L_{\text{advec}}}{L_{\text{diff}}} = v \left( \frac{t}{D_{\text{eff}}} \right)^{0.5}$$

Squaring this and substituting  $L_{\text{advec}} = vt$ ,

$$\left( \frac{L_{\text{advec}}}{L_{\text{diff}}} \right)^2 = v^2 \frac{t}{D_{\text{eff}}} = \frac{vL}{D_{\text{eff}}}$$

The quantity  $\frac{vL}{D_{\text{eff}}}$  is the non-dimensional *Peclet number*. The Peclet number is a dimensionless number like the more familiar Reynolds number for laminar vs. turbulent flow. If it is much less than 1, diffusion dominates and advection is negligible. If it is much greater than 1, advection dominates and diffusion is negligible. The significance of the scale length,  $L$ , in the Peclet number depends on the exact process being considered. If we are comparing diffusion and advection, as here,  $L$  represents the scale length of diffusion or advection. If the comparison is between molecular diffusion and hydrodynamic dispersion (see below), the appropriate scale length is generally taken to be the grain diameter of the porous medium.

As an overall generalization, diffusion is the dominant transport process in Recent sediments (marine and lake), and in *unfractured* low-permeability rocks—claystones, igneous rocks, etc. In permeable rocks, molecular diffusion is generally negligible compared to advection/dispersion. In fractured rock, diffusion may be negligible *within* the fractures, but be the dominant process in the adjacent matrix.

**TABLE 16-1** Approximate Diffusion Length (see text for discussion) for Non-Steady State Diffusion of a Solute with a  $D_{\text{eff}}$  of  $5 \times 10^{-6}$  cm<sup>2</sup>/sec

Time (y)	Distance (m)
1	0.13
10	0.4
100	1.3
1000	4

**Example 1**

In a lake sediment the concentration of  $\text{Mn}^{2+}$  in the interstitial water increases linearly from 0.1 ppm at the sediment-water interface to 2 ppm at a depth of 50 cm. Assuming a sedimentation rate of zero and constant porosity, what is the flux of  $\text{Mn}^{2+}$  to the sediment-water interface (in units of  $\text{g}/\text{cm}^2/\text{y}$ )? Assume a diffusion coefficient for  $\text{Mn}^{2+}$  in water of  $5 \times 10^{-6} \text{ cm}^2/\text{sec}$ , a porosity of 0.7, a tortuosity of 1.3.

First, we need to convert the diffusion coefficient for pure water to a diffusion coefficient in the sediment. Substituting the numbers in Eq. (16-8) gives

$$D_{\text{sedim}} = 5 \times 10^{-6} \times \frac{0.7}{1.3^2} = 2.07 \times 10^{-6} \text{ cm}^2/\text{sec}$$

The concentration gradient needs to be expressed in appropriate units for the problem. The units we are using here are g and cm, so

$$\begin{aligned} \frac{\partial C}{\partial x} &= \frac{(2 - 0.1) \times 10^{-3} \times 10^{-3}}{50} \text{ g}/\text{cm}^3/\text{cm} \\ &= 3.8 \times 10^{-8} \text{ g}/\text{cm}^3/\text{cm} \end{aligned}$$

Substituting these numbers into Fick's first law (Eq. 16-2):

$$\begin{aligned} J &= -D_{\text{sedim}} \frac{\partial C}{\partial x} \\ &= -2.07 \times 10^{-6} \times 3.8 \times 10^{-8} \\ &= -7.87 \times 10^{-14} \text{ g}/\text{cm}^2/\text{sec} \\ &= -2.48 \times 10^{-6} \text{ g}/\text{cm}^2/\text{y} \end{aligned}$$

The minus sign simply indicates that the flux is upwards, the direction of decreasing  $x$ . Note that the flux is a rather small number. This reflects partly the fact that diffusional flux depends on the *absolute* concentration gradient and not the relative concentration gradient. Although the concentration gradient represents a 95 percent decrease over 50 cm, it is the absolute decrease, 1.9 ppm, that determines the flux.

**Example 2**

Suppose an organic pollutant species with the same diffusion coefficient as  $\text{Mn}^{2+}$  were introduced into the lake. How long would it take for the pollutant to reach a depth of 50 cm in the sediment, assuming no adsorption is taking place? Define what is meant by *reach*.

Fick's second law for a sediment is given by Eq. (16-9):

$$\frac{\partial C}{\partial t} = \frac{D_{\text{sedim}}}{\phi} \frac{\partial^2 C}{\partial x^2}$$

The value of  $D_{\text{sedim}}/\phi = D_{\text{eff}}$ , from the numbers given in Example 1, is  $2.96 \times 10^{-6} \text{ cm}^2/\text{s}$ .

If we define *reach* as the time it takes for a concentration of about 0.5 times the original to reach 50 cm:

$$\begin{aligned} 0.95 \left( \frac{D}{\phi} t \right)^{0.5} &= 50 \\ t &= 9.36 \times 10^8 \text{ sec} \\ &= 29.5 \text{ y} \end{aligned}$$

If we define *reach* as the time it takes for a concentration 0.01 times the original to reach 50 cm:

$$4 \left( \frac{D}{\phi t} \right)^{0.5} = 50$$

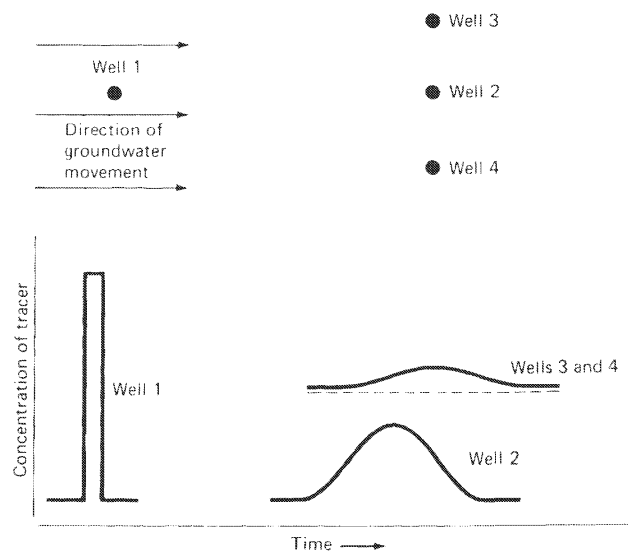
$$t = 5.28 \times 10^7 \text{ sec}$$

$$= 1.67 \text{ y}$$

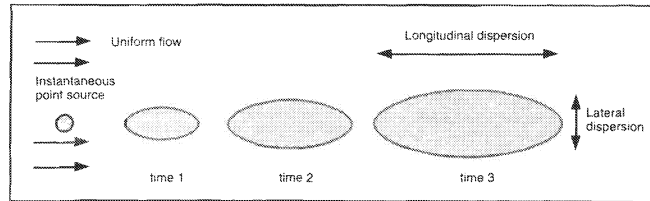
Note that the choice of definition of *reach* makes a big difference to the answer. For most contaminant problems, 1 percent of the original concentration is a much more realistic criterion than 50 percent. In many instances the criterion would be even lower than 1 percent.

**Hydrodynamic Dispersion.** Hydrodynamic dispersion, or more simply, dispersion, is a process of mixing that occurs when a fluid flows through a porous medium. If a conservative tracer is injected as a “spike” into well 1 (Fig. 16-3), and its concentration is monitored at wells 2, 3, and 4, the variation of concentration with time will be approximately as shown in Fig. 16-3 and 16-4. Two effects can be observed: The sharp spike at well 1 has become diffuse (and its maximum value lower), and the tracer is observed at wells that are not directly downstream from the injection well. The first effect is called *longitudinal dispersion* and the second *lateral dispersion*. Longitudinal dispersion can be explained by different water velocities in larger, compared to smaller, pores; different possible path lengths in the pore system; or different solution velocities in the center of a pore compared to the edges (Fig. 16-5). Lateral dispersion can be explained, even in the absence of turbulence, by the network of possible paths through the pores or fractures in an aquifer (Fig. 16-6). Spreading due to dispersion is analogous to spreading due to molecular diffusion, and it has been described by equations analogous to Fick’s laws. The coefficient *D* then becomes the *dispersion coefficient*. Since dispersion depends on pore or fracture geometry, it will generally not be uniform in all directions. The dispersion coefficient is thus a tensor rather than a

FIGURE 16-3 Schematic illustration of the effects of dispersion.



**FIGURE 16-4** Spreading due to dispersion of a tracer injected as a point source. The boundary would represent a contour such as  $C/C_0 = 0.1$ .



scalar quantity. There is some question (discussed below) as to whether it is really appropriate to use Fick's laws to describe dispersion at the field scale.

The effect of longitudinal dispersion can be illustrated by a simple column experiment (Fig. 16-7, p.364). For a step-function input, concentration profile is described by (Freeze and Cherry, 1979):

$$\frac{C}{C_0} = \frac{1}{2} \operatorname{erfc} \left( \frac{x - vt}{2(Dt)^{1/2}} \right)$$

where  $\operatorname{erfc}$  is again the complementary error function.

The net effect is that the concentration profile becomes smeared out, with its center ( $C/C_0 = 0.5$ ) at  $x = vt$ , i.e., at the position the front would have if dispersion were absent. Longitudinal dispersion coefficients can be measured by measuring the concentration profile in effluent from such columns, as represented by the *breakthrough curve* in Fig. 16-7. As one would expect, transport by dispersion (longitudinal and transverse) increases with  $v$ . The rate of spreading is proportional to the rate of fluid movement, that is to say, the amount of spreading down the cylinder in a given time is a function only of the distance moved. The distance moved is proportional to the velocity, so the dispersion coefficient is also proportional to the velocity. It is convenient to introduce the quantity *dispersivity*,  $\alpha$ , where

$$D_{\text{longit}} = \alpha_l v$$

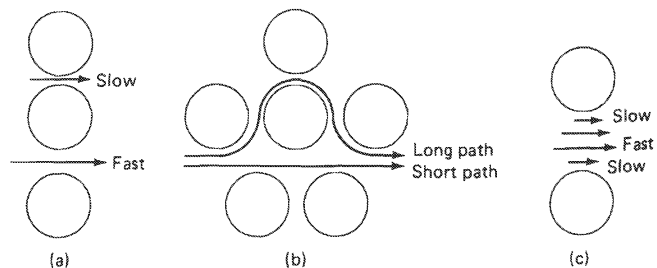
$$D_{\text{transv}} = \alpha_t v$$

$\alpha_l$  is the *longitudinal dispersivity* and  $\alpha_t$  is the *transverse dispersivity*. The dimensions of dispersivity are L; units are m or cm. The dispersivity is thus a property of the medium and independent of fluid velocity.

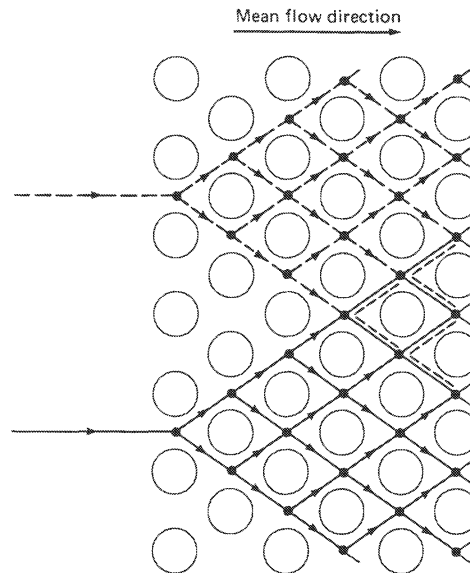
These equations are not strictly correct in that they imply that  $D$  becomes zero as  $v$  becomes zero. In fact, at low velocities, the dispersion coefficient becomes equal to the molecular diffusion coefficient:

$$D_{\text{longit}} = D_{\text{molec}} + \alpha_l v$$

**FIGURE 16-5** Causes of longitudinal dispersion: (a) different pore diameters; (b) different path lengths in the pore system; (c) different velocities in center compared to margins of pore.



**FIGURE 16-6** Simple model of lateral dispersion; at each point indicated by a heavy dot, the flow divides, with half going around each side of the grain in front.



$$D_{\text{transv}} = D_{\text{molec}} + \alpha_1 v$$

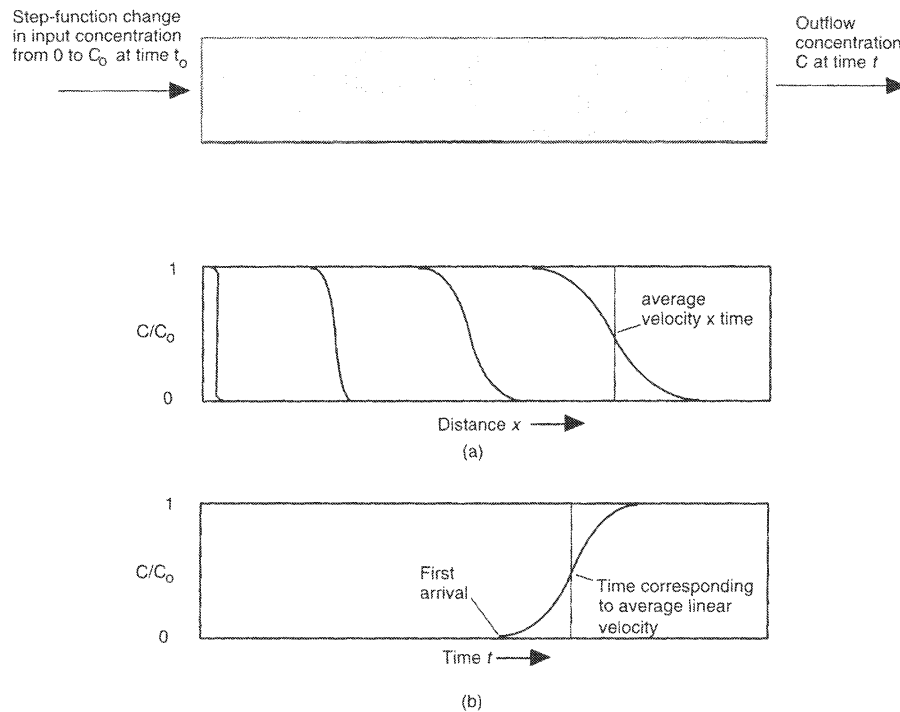
The molecular diffusion coefficient is commonly much smaller than  $\alpha_1 v$ , and is ignored.

As a general rule, longitudinal dispersivities are greater than transverse dispersivities. There are relatively few actual measurements of transverse dispersivities in the literature. Various authors have used  $\alpha_1 = 0.03 \alpha_L$ ,  $\alpha_1 = 0.1 \alpha_L$ , and  $\alpha_1 = 0.4 \alpha_L$  as rules of thumb (Anderson, 1979). The ratio of the width to the length of the elliptical plume in Fig. 16-4 is equal to the ratio of the transverse to the longitudinal dispersivity.

Dispersivities can be measured in the laboratory for permeable media such as sand: Values of less than 1 cm are typically obtained. Values obtained using tracer methods in the field are much greater than this, typically between 10 and 100 m (Anderson, 1979). Dispersivity generally increases with the scale over which it is measured. One reason for this is that measured dispersion is very sensitive to heterogeneities in an aquifer. Consider the experiment shown in Fig. 16-8, in which a tracer is injected into an aquifer that consists of layers of differing permeability, and the tracer is measured at a well that samples water from the entire thickness of the aquifer. The “breakthrough curve” (Fig. 16-9) for the tracer arriving at the second well will be smeared out because of the different travel times through the different layers, rather than because of dispersion within a single layer. The layering shown in Fig. 16-9 is obviously unrealistic, but the principle is quite general: any inhomogeneities in an aquifer will cause an increase in dispersivity.

The layering shown in Fig. 16-9 has another consequence. The time at which the contaminant first appears at well 2 will be much less than the average time for water to move from well 1 to well 2. “Fingering” (transport through high-permeability channels) allows contaminants to travel through an aquifer at a faster rate than the average groundwater velocity (e.g., Gillham and Cherry, 1982).

An extreme case of aquifer heterogeneity would be high-permeability fractures in a low-permeability rock. In this situation, water movement will be almost entirely within the



**FIGURE 16-7** (a) Concentration profiles at different times as a function of distance in a one-dimensional column experiment; and (b) concentration versus time curve (breakthrough curve) at the exit from the column. The tracer was input as a step function: the step becomes spread out as a result of longitudinal dispersion.

fractures, but transport of solutes between fractures and the blocks will occur by molecular diffusion. The phenomenon is called *matrix diffusion*. The best-documented examples of the effect of matrix diffusion on solute transport involve fractured rocks such as chalk (Foster, 1975) and glacial clay (Cherry et al., 1979) that have high porosities, but matrix diffusion is also important for igneous rocks, which typically have matrix porosities on the order of  $10^{-1}$  to  $10^{-2}$  (Norton and Knapp, 1977). It is a key aspect in the modeling of transport of radionuclides from a disposal site in igneous rock (e.g., Rasmuson and Neretnieks, 1986). The theory of matrix diffusion is discussed in detail by Grisak and Pickens (1980), Tang et al. (1981), Bradbury and Green (1985), and Chen (1986).

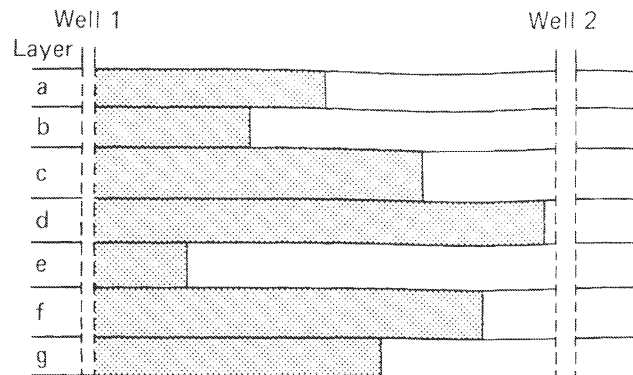
Overall, because dispersivity depends on the scale at which it is measured, Fick's laws are not a particularly good description of dispersion in the field. An alternative approach is to model the distribution of permeability explicitly; the problem is that the necessary field data generally do not exist, so some sort of statistical approach must be used.

### Chemical Reaction and Retardation

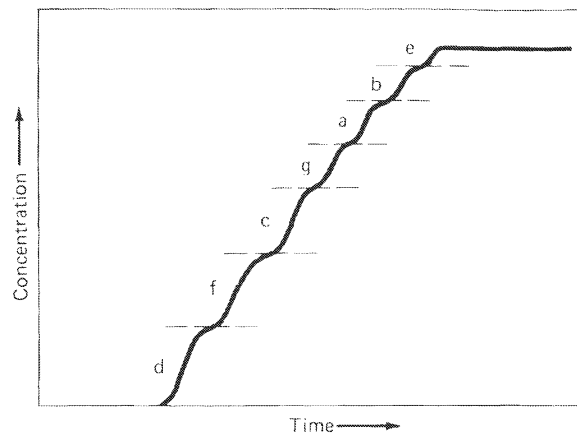
The mathematical form of the reaction term in Eq. (16-1) can take many different forms, depending on the process involved. This term must contain mathematical expressions for all processes causing removal of component  $i$  from, or addition of component  $i$  to, the water, and



**FIGURE 16-8** Movement of a conservative tracer through an aquifer consisting of layers of different permeability. Shaded areas indicate distance tracer has moved after some time  $t$ .



**FIGURE 16-9** Breakthrough curve for a conservative tracer arriving at well 2 (Fig. 16-8), assuming linear groundwater flow. The curve is a composite of the breakthrough curves from the individual layers, and the dispersion is thus much greater than would be observed from a single, uniform layer.



the expressions must be in such a form that the differential equation can be integrated in a reasonable amount of computer time.

There are several other processes for which satisfactory expressions can be formulated, for example:

1. Radioactive decay
2. Adsorption equilibria (discussed below), including ion exchange
3. Chemical equilibrium with simple solids (e.g., calcite or gypsum)
4. Simple kinetic expressions for the rate of precipitation or dissolution of a solid phase as a function of solution composition

For more complex chemical reactions, there is generally no single expression that can be used as a “reaction term.” A separate chemical model, or sub-model, is usually necessary. Such models are discussed below.

**Linear Adsorption and the Retardation Factor.** We discussed in Chapter 5 the use of a linear distribution coefficient to describe adsorption. The basic equation can be written

$$C_{\text{ads}} = K_d C$$

Where  $C_{\text{ads}}$  is the adsorbed concentration of a solute (moles/kg of solid),  $C$  is the concentration in solution (moles/l of solution), and  $K_d$  is the distribution coefficient, which here has the units l/kg.

Mathematically, the linear  $K_d$  can be very conveniently included in the diffusion–advection equation:

$$\frac{\partial C}{\partial t} = D \frac{\partial^2 C}{\partial x^2} - v \frac{\partial C}{\partial x} \pm (\text{reaction terms})$$

Rather than formulate a separate reaction term, let us see how adsorption affects the advection and diffusion terms.

*Advection:* Consider, referring back to Fig. 16-1, the change in mass ( $\delta m$ ) in an elementary volume (with unit dimensions, i.e.  $\delta x = 1$ ) in time  $\delta t$ :

$$\delta m = \phi v \frac{\partial C}{\partial x} \delta t$$

The change in mass is the sum of the change in the amount in solution and the change in the amount adsorbed:

$$\delta m = \phi \delta C + (1 - \phi) \rho_{\text{gr}} \delta C_{\text{ads}}$$

where  $\rho_{\text{gr}}$  is the grain density. But  $C_{\text{ads}} = K_d C$ , so

$$\delta m = \phi \delta C + (1 - \phi) \rho_{\text{gr}} K_d \delta C$$

$$\delta m = \phi \delta C \left( 1 + \frac{(1 - \phi)}{\phi} \rho_{\text{gr}} K_d \right)$$

or

$$\phi \delta C \left( 1 + \frac{(1 - \phi)}{\phi} \rho_{\text{gr}} K_d \right) = \phi v \frac{\partial C}{\partial x} \delta t$$

which rearranges (changing the finite time step to a differential) to:

$$\frac{\partial C}{\partial t} = \frac{v}{\left( 1 + \frac{(1 - \phi)}{\phi} \rho_{\text{gr}} K_d \right)} \frac{\partial C}{\partial x}$$

The velocity ( $v$ ) in the original equation has been replaced by a “velocity” equal to

$$\frac{v}{\left( 1 + \frac{(1 - \phi)}{\phi} \rho_{\text{gr}} K_d \right)}$$

The term  $\left( 1 + \frac{(1 - \phi)}{\phi} \rho_{\text{gr}} K_d \right)$  is called the *retardation factor* ( $R$ ), which is dimensionless. The significance of the retardation factor for advection is simply that an adsorbed species (*that is rapidly, reversibly, linearly adsorbed*) will migrate through an aquifer as an unadsorbed

species would, but with a velocity  $1/R$  times that of the unadsorbed species. The factor  $[(1 - \phi)/\phi]\rho_{gr}$  typically has a value between 4 and 10, so retardation will be highly significant for finite values of  $K_d$ . For many cations of interest for the disposal of radioactive waste,  $K_d$  values lie between 10 and 100, which means that the species are almost immobile.

The retardation factor is also commonly expressed in terms of the dry bulk density ( $\rho_{bulk}$ )

$$\rho_{bulk} = (1 - \phi)\rho_{gr}$$

and so

$$R = \left(1 + \frac{\rho_{bulk}}{\phi} K_d\right)$$

Occasionally one comes across the *dimensionless distribution coefficient* ( $K$ ), which is the ratio of the concentration on the solid to the concentration in solution *where both concentrations are expressed in units of mass per unit volume of solution*. In this case

$$K = \frac{(1 - \phi)}{\phi} \rho_{gr} K_d$$

and

$$R = (1 + K)$$

This dimensionless form is mathematically convenient for modeling.

*Diffusion:* Consider again our elementary volume. The change in mass ( $\delta m$ ) of the species of interest in the volume in time  $\delta t$  is equal to the flux in minus the flux out

$$\delta m = (\text{Flux in} - \text{Flux out}) = D \frac{\partial^2 C}{\partial x^2} \delta t \quad (16-10)$$

As in the case of advection, the change in mass in an elementary volume with unit dimensions is equal to the change of mass in solution plus the change of mass on the solid phase:

$$\delta m = \phi \delta C + (1 - \phi) \rho_{gr} \delta C_{ads}$$

where  $\rho_{gr}$  is the grain density. Again,  $C_{ads} = K_d C$ , so

$$\delta m = \phi \delta C + (1 - \phi) \rho_{gr} K_d \delta C$$

$$\delta m = \phi \delta C \left(1 + \frac{(1 - \phi)}{\phi} \rho_{gr} K_d\right)$$

Substituting this in the Eq. (16-10),

$$\phi \delta C \left(1 + \frac{(1 - \phi)}{\phi} \rho_{gr} K_d\right) = D \frac{\partial^2 C}{\partial x^2} \delta t \quad (16-12)$$

Substituting  $R$  (retardation factor) for the expression in parentheses, rearranging, and substituting differentials for the finite time-step gives

$$\frac{\partial C}{\partial t} = \frac{D}{\phi R} \frac{\partial^2 C}{\partial x^2}$$

This is exactly the expression we had for a non-adsorbed solute (Eq. 16–9), but with  $D/R$  substituted for  $D$  (which could be either a dispersion coefficient or a diffusion coefficient). Thus spreading by diffusion or dispersion is retarded in an analogous manner to advection. Provided dispersion is much greater than diffusion, the geometry of movement and spreading of an adsorbed solute as it moves through an aquifer will be exactly the same as that of an unadsorbed solute, but the time taken to reach a particular position and “width” will be a factor of  $R$  longer.

Adsorption affects only non-steady-state diffusion. At steady state (e.g., a constant concentration gradient between a constant source and a constant sink), there is no net uptake or release by adsorption, so adsorption has no effect on diffusion. The diffusional flux will be given by Fick’s first law with no correction for adsorption.

The above discussion applies only to the limiting case of rapid, reversible, linear adsorption. Because of its mathematical convenience, the retardation equation based on the linear  $K_d$  is often used as an approximation even where these conditions do not hold. It should also be remembered that, in general, the numerical value of  $K_d$  is specific to the solute, the substrate, and the composition of the groundwater. It is not readily transferred from one experiment or situation to another.

### Example 3

Suppose the pollutant in Example 2 above is adsorbed by the sediment, and the adsorption can be described by a constant  $K_d$  of 5 l/kg. How long will it now take for the pollutant to reach a depth of 50 cm?

If we assume a grain density of 2.6 g/cm<sup>3</sup>, the retardation factor,  $R$ , is

$$\left( 1 + \frac{0.3}{0.7} \times 2.6 \times 5 \right) = 6.57$$

The times calculated in Example 2 will be multiplied by this number. The time for 1 percent of the initial concentration to reach 50 cm will thus be 10.97 y rather than 1.67 y. Note that, for a given  $K_d$ , the retardation factor increases as the porosity decreases as a result of the factor  $(1 - \phi)/\phi$ . If, in this example, the porosity had been 10 percent rather than 70 percent, the retardation factor would have been 118 rather than 6.57.

## REACTION PATH MODELING

Reaction path calculations, or *mass-transfer* codes, give us the successive compositions of a solution as a mineral (or several minerals) reacts with a solution or as some other process, such as evaporation of the solution, proceeds. The mass of each solid phase or gas produced or consumed is calculated. Such codes do not, in general, contain any kinetic information: They calculate changes as a function of the amount of reaction that has taken place but do not say anything about how long the reaction should take. The most widely available and widely used codes are PHREEQE (Parkhurst et al., 1980), EQ3/6 (Wolery, 1979), SOLMINEQ.88 (Kharaka et al., 1988), and MINTQA2 (Allison et al., 1991). PHRQPITZ (Plummer et al., 1988) is a version of PHREEQE modified to include Pitzer’s equations for calculations at high ionic strength (see Chapter 2); PHREEQC (Parkhurst, 1995) is an updated version of PHREEQE that includes inverse modeling analogous to NETPATH (see Chapter 12 and later in this chapter). Each of these codes was developed for a slightly different purpose, which

gives them advantages and disadvantages for particular applications. PHREEQE is a relatively versatile code that can model many different types of reaction at a fixed temperature. However, the database supplied is fairly limited, particularly for trace elements, so the user may have to enter all the information for particular elements/reactions him/herself. It is not a particularly easy code for a beginner to use. MINTEQA2 is in a sense the reverse: it has an extensive database and is quite “user friendly,” but the range of calculations it can perform is more limited. EQ3/6 is a large, complex, and versatile program, currently geared towards simulations associated with radioactive waste disposal. It can simulate reactions with changing temperature as well as reactions at a fixed temperature. SOLMINEQ.88 was designed particularly to simulate processes associated with petroleum basins, which implies moderately elevated temperatures and the presence of several organic species.

As an example of a reaction path calculation, let us consider the case of a mineral reacting with water. The general approach is:

1. A small increment of the mineral is dissolved.
2. A speciation-saturation program (Chapter 2) tests if the solution is supersaturated with respect to any solid phase. (The speciation–saturation program is part of the mass-transfer code. Thus each of these codes can be used for speciation–saturation calculations.)
3. If the solution is supersaturated with respect to any phase (or to specific phases specified by the user), an amount of that phase is precipitated sufficient to bring the solution into equilibrium with that phase. If the solution becomes undersaturated with respect to a previously precipitated phase, that phase redissolves to establish equilibrium.
4. An iteration procedure ensures that the solution is in equilibrium with all solid reaction products before another increment of the original mineral is dissolved.

The procedure for simulating evaporation is the same, except that increments of water are removed instead of increments of mineral being added. The calculated composition of a solution reacting with K-feldspar is shown in Figs. 16-10 and 16-11.

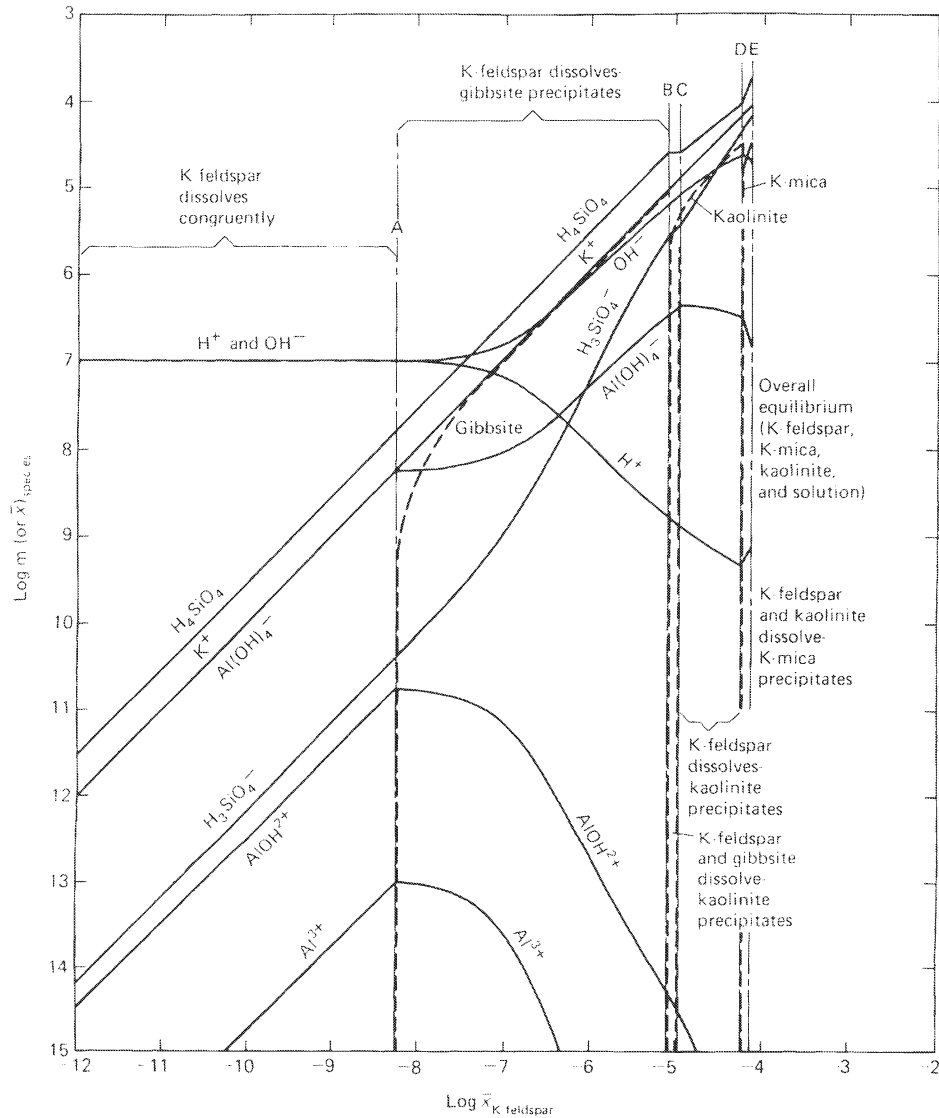
Although mass-transfer programs in the strict sense calculate only the path that the solution composition will follow and do not contain any rate expressions to relate reaction progress to time, it is possible to combine a mass-transfer model with a kinetic model to predict solution composition as a function of time. Examples include KINDIS (Madé et al., 1990) and PHREEQM (Appelo and Postma, 1993). There is some question as to whether our understanding of kinetics at low temperatures is sufficient for this approach to be realistic.

#### Example 4

A mining company proposes to dig a pit, which will be left to form a lake at the end of mining operations. The composition of the groundwater that will flow into the pit is shown in Table 16-2. The bedrock is altered granite containing calcite as the only reactive mineral. Use MINTEQA2 to predict the composition of the final lake.

In order to solve this problem, we need to make some simplifying assumptions. Some of these are:

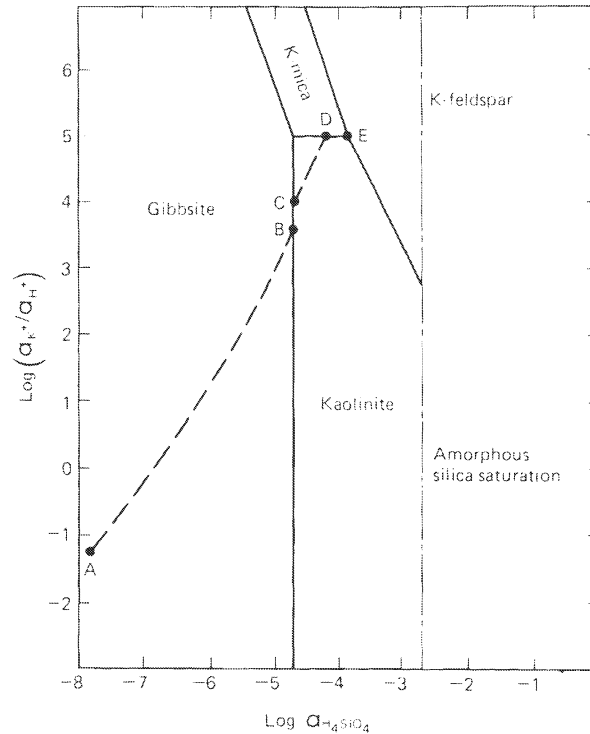
1. A chemical equilibrium model is a suitable approximation.
2. The final lake will be in equilibrium with atmospheric oxygen and CO<sub>2</sub>.



**FIGURE 16-10** Concentration (m) of species in the aqueous phase (solid lines) and amounts (mol/kg H<sub>2</sub>O) of minerals produced and destroyed (dashed lines) as K-feldspar reacts with water at 25°C and 1 atm pressure. The abscissa represents the number of moles of K-feldspar destroyed per kg H<sub>2</sub>O. The letters correspond to the points on the reaction path shown in Fig. 16-11 (Helgeson et al., 1969).

- Reactions involving silicates can be ignored. The justification for this assumption is that the groundwater has been in contact with the silicate minerals surrounding the pit for a long time and should be close to equilibrium or at least steady state.
- Our time span and flow rate are such that evaporation and dilution by rainfall can be neglected. In reality these would be incorporated into the model. They are omitted here for the sake of simplicity.

**FIGURE 16-11** Path of solution composition (ABCDE) as K-feldspar reacts with water, plotted on a mineral stability diagram (after Helgeson et al., 1969).



The first step is to use MINTQA2 as a speciation-saturation program only, with the water of Table 16-2 as the input. This has two purposes: (1) To see which phases are supersaturated and hence are likely to precipitate, and (2) To convert the alkalinity input into total concentration of carbonate species and concentration of the component  $H^+$ . MINTQA2 requires the input to be in this form for further calculations. At this stage we also have to decide on an oxidation state for the Fe in the analysis. We can either input it as  $Fe^{2+}$  (which is probably the actual form), or we can input it as the oxidized species,  $Fe^{3+}$ , with the justification that the final water will be in equilibrium with atmospheric oxygen. If iron is input as  $Fe^{3+}$ , MINTQA2 does not have to perform any redox calculations, as all the inputs are in their oxidized form. There are often advantages to minimizing the number of different reactions that the reaction path code has to consider simultaneously. The concentration of Fe is sufficiently low that the choice of oxidation state does not affect the cation-anion balance significantly. Part of the output from this first run is shown in Table 16-3.

**TABLE 16-2** Composition of Inflow Water for Example 4

Na	64.2	ppm	As	0.05	ppm
K	17	ppm	Cu	0.014	ppm
Ca	151.4	ppm	Zn	1.1	ppm
Mg	54.6	ppm			
Cl	23.8	ppm	pH	7.51	
SO <sub>4</sub>	104	ppm			
Alkalinity	12.54	meq/l	T	20°C	

**TABLE 16-3** Output from the MINTEQA2 Speciation-Saturation Calculation for Example 4  
 [The output file has been condensed for this table.]

PART 1 of OUTPUT FILE

---

Example 4: Speciation/saturation for input water

---

-----

Temperature (Celsius): 20.00  
 Units of concentration: MG/L  
 Ionic strength to be computed.  
 Carbonate concentration represents carbonate alkalinity.  
 Do not automatically terminate if charge imbalance exceeds 30%  
 Precipitation is allowed only for those solids specified as ALLOWED  
 in the input file (if any).  
 The maximum number of iterations is: 40  
 The method used to compute activity coefficients is: Davies equation  
 Intermediate output file

---

INPUT DATA BEFORE TYPE MODIFICATIONS

ID	NAME	ACTIVITY GUESS	LOG GUESS	ANAL TOTAL
330	H+1	3.090E-08	-7.510	0.000E-01
61	H3AsO4	3.548E-07	-6.450	5.000E-02
150	Ca+2	3.802E-03	-2.420	1.514E+02
180	Cl-1	6.761E-04	-3.170	2.380E+01
231	Cu+2	2.188E-07	-6.660	1.400E-02
281	Fe+3	2.291E-05	-4.640	1.270E+00
460	Mg+2	2.239E-03	-2.650	5.460E+01
410	K+1	4.365E-04	-3.360	1.700E+01
500	Na+1	2.818E-03	-2.550	6.420E+01
732	SO4-2	1.072E-03	-2.970	1.040E+02
950	Zn+2	1.698E-05	-4.770	1.100E+00
140	CO3-2	8.913E-06	-5.050	3.759E+02
2	H2O	1.000E+00	.000	0.000E-01

Charge Balance: UNSPECIATED  
 Sum of CATIONS= 1.539E-02 Sum of ANIONS = 1.538E-02  
 PERCENT DIFFERENCE = 3.739E-02 (ANIONS - CATIONS)/(ANIONS + CATIONS)

PART 3 of OUTPUT FILE

---

Type I - COMPONENTS AS SPECIES IN SOLUTION

ID	NAME	CALC MOL	ACTIVITY	LOG ACTVTY	GAMMA	NEW LOGK
330	H+1	3.475E-08	3.090E-08	-7.51000	.88929	.051
61	H3AsO4	1.668E-13	1.676E-13	-12.77578	1.00472	-.002
150	Ca+2	3.352E-03	2.007E-03	-2.69747	.59863	.223
180	Cl-1	6.718E-04	5.808E-04	-3.23596	.86453	.063
231	Cu+2	3.453E-09	2.051E-09	-8.68799	.59400	.226
281	Fe+3	1.760E-14	6.123E-15	-14.21304	.34783	.459
460	Mg+2	1.977E-03	1.196E-03	-2.92216	*.60526	.218
410	K+1	4.338E-04	3.751E-04	-3.42589	.86453	.063
500	Na+1	2.775E-03	2.420E-03	-2.61618	.87200	.059
732	SO4-2	8.043E-04	4.576E-04	-3.33950	.56899	.245
950	Zn+2	3.808E-06	2.262E-06	-5.64555	.59400	.226
140	CO3-2	2.426E-05	1.424E-05	-4.84648	.58709	.231

Type II - OTHER SPECIES IN SOLUTION OR ADSORBED

ID	NAME	CALC MOL	ACTIVITY	LOG ACTVTY	GAMMA	NEW LOGK
3301401	H2CO3 AQ	6.927E-04	6.960E-04	-3.15739	1.00472	16.707
3307320	HSO4 -	1.373E-09	1.196E-09	-8.92227	.87129	1.987
3300020	OH-	2.554E-07	2.213E-07	-6.65496	.86647	-14.103
4603300	MgOH +	4.641E-08	4.084E-08	-7.38892	.87996	-11.921



4601400	MgCO3 AQ	1.499E-05	1.506E-05	-4.82226	1.00472	2.944
4601401	MgHCO3 +	1.629E-04	1.415E-04	-3.84911	.86892	11.491
4607320	MgSO4 AQ	9.307E-05	9.351E-05	-4.02915	1.00472	2.230
1503300	CaOH +	1.228E-08	1.078E-08	-7.96731	.87790	-12.723
1501400	CaHCO3 +	2.129E-04	1.869E-04	-3.72829	.87790	11.382
1501401	CaCO3 AQ	3.640E-05	3.657E-05	-4.43686	1.00472	3.105
1507320	CaSO4 AQ	1.785E-04	1.793E-04	-3.74635	1.00472	2.289
5001400	NaCO3 -	5.646E-07	4.942E-07	-6.30606	.87534	1.214
5001401	NaHCO3 AQ	1.274E-05	1.280E-05	-4.89266	1.00472	10.078
5007320	NaSO4 -	6.140E-06	5.374E-06	-5.26968	.87534	.744
4107320	KSO4 -	1.261E-06	1.104E-06	-5.95711	.87534	.866
2813300	FeOH +2	1.628E-09	9.480E-10	-9.02317	.58236	-2.085
2813301	FeOH2 +	1.565E-05	1.370E-05	-4.86330	.87534	-5.612
2813302	FeOH3 AQ	5.182E-06	5.207E-06	-5.28343	1.00472	-13.602
2813303	FeOH4 -	1.924E-06	1.684E-06	-5.77356	.87534	-21.542
2311400	CuCO3 AQ	1.561E-07	1.569E-07	-6.80447	1.00472	6.728
2311401	Cu(CO3)2-2	4.928E-09	2.812E-09	-8.55094	.57063	10.074
2313301	Cu(OH)2 AQ	4.464E-08	4.485E-08	-7.34825	1.00472	-13.682
2311402	CuHCO3 +	1.039E-08	9.027E-09	-8.04447	.86914	13.061
9501800	ZnCl +	3.252E-09	2.826E-09	-8.54890	.86892	.394
9503300	ZnOH +	6.277E-08	5.455E-08	-7.26319	.86914	-9.067
9503301	Zn(OH)2 AQ	2.973E-08	2.987E-08	-7.52481	1.00472	-16.901
9501804	ZnOHCl AQ	1.401E-09	1.407E-09	-8.85164	1.00472	-7.482
9507320	ZnSO4 AQ	2.322E-07	2.333E-07	-6.63205	1.00472	2.351
9507321	Zn(SO4)2-2	1.582E-09	9.025E-10	-9.04455	.57063	3.524
9501400	ZnHCO3 +	2.877E-06	2.500E-06	-5.60203	.86914	12.461
9501401	ZnCO3 AQ	6.396E-06	6.426E-06	-5.19203	1.00472	5.298
9501402	Zn(CO3)2-2	3.429E-06	1.957E-06	-5.70851	.57063	9.874
3300611	H2AsO4 -	3.743E-08	3.253E-08	-7.48765	.86914	-2.161
3300612	HAsO4 -2	3.150E-07	1.798E-07	-6.74528	.57063	-8.746
3301400	HCO3 -	1.197E-02	1.048E-02	-1.97984	.87534	10.434

PART 6 of OUTPUT FILE

Saturation indices and stoichiometry of all minerals

ID #	NAME	Sat. Index	Stoichiometry in [brackets]			
6015000	ANHYDRITE	-1.447	[ 1.000]	150	[ 1.000]	732
5015000	ARAGONITE	.748	[ 1.000]	150	[ 1.000]	140
5015001	CALCITE	.902	[ 1.000]	150	[ 1.000]	140
5015002	DOLOMITE	1.584	[ 1.000]	150	[ 1.000]	460 [ 2.000] 140
2028100	FERRIHYDRITE	3.426	[ -3.000]	330	[ 1.000]	281 [ 3.000] 2
2028102	GOETHITE	7.636	[ -3.000]	330	[ 1.000]	281 [ 2.000] 2
6015001	GYPSUM	-1.186	[ 1.000]	150	[ 1.000]	732 [ 2.000] 2
3028100	HEMATITE	20.256	[ -6.000]	330	[ 2.000]	281 [ 3.000] 2
5015003	HUNTITE	-1.204	[ 3.000]	460	[ 1.000]	150 [ 4.000] 140
6041002	JAROSITE K	6.724	[ -6.000]	330	[ 1.000]	410 [ 3.000] 281
			[ 2.000]	732	[ 6.000]	2
3028101	MAGHEMITE	10.248	[ -6.000]	330	[ 2.000]	281 [ 3.000] 2
5046002	MAGNESITE	.183	[ 1.000]	460	[ 1.000]	140
5023100	CUCO3	-3.904	[ 1.000]	231	[ 1.000]	140
2023100	CU(OH)2	-2.499	[ -2.000]	330	[ 1.000]	231 [ 2.000] 2
2023101	TENORITE	-1.479	[ -2.000]	330	[ 1.000]	231 [ 1.000] 2
6023104	CUSO4	-15.264	[ 1.000]	231	[ 1.000]	732
5095000	SMITHSONITE	-.547	[ 1.000]	950	[ 1.000]	140
5095001	ZNCO3, 1H2O	-.232	[ 1.000]	950	[ 1.000]	140 [ 1.000] 2
2095005	ZNO(ACTIVE)	-1.936	[ -2.000]	330	[ 1.000]	950 [ 1.000] 2
2095006	ZINCITE	-2.039	[ -2.000]	330	[ 1.000]	950 [ 1.000] 2
5023101	MALACHITE	-2.218	[ 2.000]	231	[ 2.000]	2 [ 1.000] 140
			[ -2.000]	330		
3006100	AS2O5	-32.318	[ 2.000]	61	[ -3.000]	2
7215000	CA3(ASO4)26W	-10.884	[ 3.000]	150	[ 2.000]	61 [ 4.000] 2
			[ -6.000]	330		
7223100	CU3(ASO4)26W	-12.656	[ 3.000]	231	[ 2.000]	61 [ 2.000] 2
			[ -6.000]	330		
3028102	LEPIDOCROCIT	6.946	[ -3.000]	330	[ 1.000]	281 [ 2.000] 2

We can see from Table 16-3 that the water is supersaturated with respect to various phases, including calcite, dolomite, magnesite, and a range of compounds containing ferric iron (ferrihydrite, goethite, hematite, jarosite, etc.) the high saturation indices for these phases is a consequence of our decision to specify the total Fe as  $\text{Fe}^{3+}$ . The next step is to choose which phases will precipitate. We shall choose ferrihydrite as the iron compound, as it is the phase most likely to precipitate. We shall also choose calcite as a phase likely to precipitate in a natural system, but we shall not allow dolomite (or other Mg-carbonate phases) to precipitate because the kinetics of precipitation of these phases are generally slow (Chapter 3). Note that no phases containing the trace elements Cu, Zn, or As are supersaturated.

With these choices, we can now perform a second MINTEQA2 run in which we:

1. Do not specify the input pH, instead allowing MINTEQA2 to calculate the pH.
2. Specify equilibrium with a  $\text{CO}_2$  gas phase at a pressure of  $3.16 \times 10^{-4}$  atm (atmospheric  $\text{CO}_2$  pressure). We could also list  $\text{O}_2$  at a fixed pressure of 0.2 atm, but this is unnecessary if our input does not contain any reduced species.
3. Specify calcite and ferrihydrite as *possible solids*. A possible solid is one that is allowed to precipitate if the solution is supersaturated with respect to it. Phases that are not listed in this way (or in an analogous way) will not be considered in the calculations.

Part of the output from this run is shown in Table 16-4. The solution is in equilibrium with calcite and ferrihydrite, and has a final pH of 8.88. This output would constitute our prediction for the major ions in solution. Note that the solution is still supersaturated with respect to ferric (hydr)oxides more stable than ferrihydrite (Chapter 7), and with respect to Mg-containing carbonates. 99.9 percent of the iron has been precipitated as ferrihydrite, and 98.6 percent of the calcium as calcite. The presence or absence of calcite in the bedrock would make no difference to the calculation, as calcite is precipitating and not dissolving. The main reason why so much calcite precipitated is the drop in  $P_{\text{CO}_2}$  from a value of  $10^{-1.7}$  in the inflow water to  $10^{-3.5}$  in the equilibrated pit lake.

So far, the only process we have considered is precipitation of supersaturated phases. Adsorption is also likely to be a significant control on trace element concentrations, particularly As, Cu, and Zn in our example (Table 16-2). As discussed in Chapter 5, adsorption can also be modeled by use of MINTEQA2. This calculation is performed after the major element chemistry has been calculated. It is necessary to specify the amount and properties of the adsorption substrate, which requires further assumptions. The details of these calculations are not presented here. A reasonable set of assumptions would be that ferrihydrite is the adsorbing phase, the amount present is equal to the amount precipitated in the previous modeling step, and its properties are the same as those of ferrihydrite used in laboratory experiments by Dzombak and Morel (1990). The Dzombak and Morel numbers are supplied as a data file with MINTEQA2. Calculations based on these assumptions indicate that adsorption should greatly reduce the concentrations of arsenic, copper, and zinc.

### Application to Contaminant Transport in Groundwater

It has become recognized in recent years that human activities are introducing contaminants into groundwater systems on an enormous scale. Examples include leaching from municipal landfills, hazardous waste burial sites, mine tailings, and various spills, both deliberate and accidental. Agriculture itself often causes contamination of groundwater by fertilizers (notably nitrate) and pesticides. A great deal of effort is currently being put into modeling the

**TABLE 16-4** Output from the MINTEQA2 Equilibration Calculation for Example 4 (The output file has been greatly condensed.)

----- PART 1 of OUTPUT FILE -----  
 Example 4: Equilibration with atmosphere and solid phases

-----  
 Temperature (Celsius): 20.00  
 Units of concentration: MG/L  
 Ionic strength to be computed.  
 If specified, carbonate concentration represents total inorganic carbon.  
 Do not automatically terminate if charge imbalance exceeds 30%  
 Precipitation is allowed only for those solids specified as ALLOWED  
 in the input file (if any).  
 The maximum number of iterations is: 40  
 The method used to compute activity coefficients is: Davies equation  
 Intermediate output file

-----  
 INPUT DATA BEFORE TYPE MODIFICATIONS

ID	NAME	ACTIVITY GUESS	LOG GUESS	ANAL TOTAL
330	H+1	1.000E-07	-7.000	1.370E+01
61	H3AsO4	3.548E-07	-6.450	5.000E-02
150	Ca+2	3.802E-03	-2.420	1.514E+02
180	Cl-1	6.761E-04	-3.170	2.380E+01
231	Cu+2	2.188E-07	-6.660	1.400E-02
281	Fe+3	2.291E-05	-4.640	1.270E+00
460	Mg+2	2.239E-03	-2.650	5.460E+01
410	K+1	4.365E-04	-3.360	1.700E+01
500	Na+1	2.818E-03	-2.550	6.420E+01
732	SO4-2	1.072E-03	-2.970	1.040E+02
950	Zn+2	1.698E-05	-4.770	1.100E+00
140	CO3-2	9.333E-05	-4.030	7.859E+02
2	H2O	1.000E+00	.000	0.000E-01

Charge Balance: UNSPECIATED  
 Sum of CATIONS= 2.900E-02 Sum of ANIONS = 2.906E-02  
 PERCENT DIFFERENCE = 1.065E-01 (ANIONS - CATIONS)/(ANIONS + CATIONS)

Type V - POSSIBLE SOLIDS

ID	NAME	CALC MOL	LOG MOL	NEW LOGK	DH
5015001	CALCITE	1.937E+02	2.287	8.446	2.585
2028100	FERRIHYDRITE	6.817E+02	2.834	-4.891	.000

----- PART 5 of OUTPUT FILE -----

-----EQUILIBRATED MASS DISTRIBUTION-----

IDX	NAME	DISSOLVED		SORBED		PRECIPITATED	
		MOL/KG	PERCENT	MOL/KG	PERCENT	MOL/KG	PER-
CENT							
330	H+1	4.365E-03	100.0	0.000E-01	.0	0.000E-01	.0
61	H3AsO4	3.527E-07	100.0	0.000E-01	.0	0.000E-01	.0
950	Zn+2	1.685E-05	100.0	0.000E-01	.0	0.000E-01	.0
180	Cl-1	6.721E-04	100.0	0.000E-01	.0	0.000E-01	.0
231	Cu+2	2.206E-07	100.0	0.000E-01	.0	0.000E-01	.0
732	SO4-2	1.084E-03	100.0	0.000E-01	.0	0.000E-01	.0
460	Mg+2	2.248E-03	100.0	0.000E-01	.0	0.000E-01	.0

(Continued)

410	K+1	4.353E-04	100.0	0.000E-01	.0	0.000E-01	.0
500	Na+1	2.796E-03	100.0	0.000E-01	.0	0.000E-01	.0
281	Fe+3	1.853E-08	.1	0.000E-01	.0	2.275E-05	99.9
150	Ca+2	5.213E-05	1.4	0.000E-01	.0	3.730E-03	98.6
140	CO3-2	4.727E-03	55.9	0.000E-01	.0	3.730E-03	44.1
2	H2O	9.297E-06	100.0	0.000E-01	.0	0.000E-01	.0

Charge Balance: SPECIATED

Sum of CATIONS = 7.178E-03 Sum of ANIONS 7.239E-03

PERCENT DIFFERENCE = 4.291E-01 (ANIONS - CATIONS)/(ANIONS + CATIONS)

EQUILIBRIUM IONIC STRENGTH (m) = 1.029E-02

EQUILIBRIUM pH = 8.879

PART 6 of OUTPUT FILE

Saturation indices and stoichiometry of all minerals

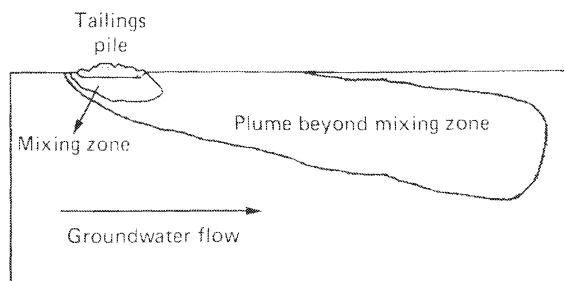
ID #	NAME	Sat. Index	Stoichiometry in [brackets]				
5015000	ARAGONITE	-.154	[ 1.000]	150	[ 1.000]	140	
5015001	CALCITE	.000	[ 1.000]	150	[ 1.000]	140	
5015002	DOLOMITE	1.654	[ 1.000]	150	[ 1.000]	460	[ 2.000] 140
2028100	FERRIHYDRITE	0.000	[ -3.000]	330	[ 1.000]	281	[ 3.000] 2
2028102	GOETHITE	4.210	[ -3.000]	330	[ 1.000]	281	[ 2.000] 2
6015001	GYP SUM	-2.897	[ 1.000]	150	[ 1.000]	732	[ 2.000] 2
3028100	HEMATITE	13.405	[ -6.000]	330	[ 2.000]	281	[ 3.000] 2
5015003	HUNTITE	.812	[ 3.000]	460	[ 1.000]	150	[ 4.000] 140
6041002	JAROSITE K	-7.386	[ -6.000]	330	[ 1.000]	410	[ 3.000] 281
			[ 2.000]	732	[ 6.000]	2	
3028101	MAGHEMITE	3.397	[ -6.000]	330	[ 2.000]	281	[ 3.000] 2
5046002	MAGNESITE	1.156	[ 1.000]	460	[ 1.000]	140	
2023101	TENORITE	-.815	[ -2.000]	330	[ 1.000]	231	[ 1.000] 2
5095000	SMITHSONITE	-.861	[ 1.000]	950	[ 1.000]	140	
5095001	ZNCO3, 1H2O	-.546	[ 1.000]	950	[ 1.000]	140	[ 1.000] 2
2095005	ZNO (ACTIVE)	-.449	[ -2.000]	330	[ 1.000]	950	[ 1.000] 2
2095006	ZINCITE	-.552	[ -2.000]	330	[ 1.000]	950	[ 1.000] 2
5023101	MALACHITE	-2.691	[ 2.000]	231	[ 2.000]	2	[ 1.000] 140
			[ -2.000]	330			
3028102	LEPIDOCROCIT	3.520	[ -3.000]	330	[ 1.000]	281	[ 2.000] 2

behavior of contaminants in the subsurface, both for predicting the fate of and designing remediation strategies for existing contaminants and for designing and locating disposal sites for future waste, particularly high-level radioactive waste.

Before any detailed geochemical modeling can be attempted, the hydrology of the area in question, particularly groundwater flow paths and velocities, must be established. This is by no means a trivial requirement; the information required for an adequate hydrologic model may be greater than that required for a chemical model, and the mathematical formulation of the hydrologic model may be extremely complex.

For modeling purposes, it is often convenient to divide the region to be studied into a source, a mixing zone (*near field*, in the terminology of radioactive waste disposal), and a relatively undisturbed aquifer or aquifers (*far field*). This is illustrated conceptually in Fig. 16-12 for a mill tailings pile. A real example of modeling applied to a uranium mill tailings pile is given by White et al. (1984) and Narasimhan et al. (1986). The source is the downward movement of solutions from the tailings pile. These solutions are oxygenated and highly acidic from the processing used in the mill and contain high concentrations of iron and several trace elements such as uranium, molybdenum, and selenium.

**FIGURE 16-12** Schematic illustration of migration of contaminants from a uranium mill tailings pile.



Groundwaters are typically mildly alkaline and may be oxidizing or reducing. When the acid tailings solution enters the aquifer, it reacts chemically with the groundwater and with the minerals of the aquifer. Calcite dissolves, gypsum may precipitate, and iron and aluminum hydroxides precipitate, coprecipitating trace metals with them. Chemical reactions such as these can be modeled successfully by a program such as PHREEQE, MINTEQA, or EQ3/6. The mixing zone, where the major chemical reactions take place, is commonly a relatively small volume, and the hydrology of such a small volume can be modeled in a relatively simple way.

Beyond the mixing zone, the groundwater is more or less in equilibrium with the minerals of the aquifer. Dissolution and precipitation are no longer major processes, and modeling focuses on hydrology/water movement plus hydrodynamic dispersion and on relatively simple chemical processes such as adsorption, radioactive decay, and, for some organic compounds, biodegradation.

An additional problem with modeling of contaminant transport is the question of how to treat uncertainty. One can never know with certainty the porosity, permeability, and dispersivity, for example, at all points in an aquifer. One can make estimates for the regions in which data are missing and, using them, calculate, for example, a travel time for a particular solute between two locations. For problems such as disposal of high-level radioactive waste, it is important to know the uncertainty associated with the travel time as well as the “best estimate.” Increasingly, *stochastic modeling* is being used to assess uncertainty. Instead of single values being assigned to the properties of each location in the aquifer, a statistical distribution of properties is assigned, and the model generates a statistical distribution of travel times or whatever other output is required.

## CHEMICAL EVOLUTION OF GROUNDWATER

The reaction path modeling discussed above has been “forward” modeling in that we posed the problem in the form: “Suppose we have water A and allow it to react with minerals B and C, what will be the final composition of the water?” For understanding the chemical composition of groundwater, we are generally presented by the “inverse” problem (Plummer, 1992): we know the composition of the final water, the problem is to deduce the reactions that gave rise to it. One approach is simply to solve the forward problem repeatedly, changing the identity and amount of the minerals reacting until a “match” is achieved. Alternatively, one can use the code NETPATH (Plummer et al., 1991) or PHREEQC (Parkhurst, 1995) to solve the inverse problem directly. The use of NETPATH to solve a mass balance problem was discussed in Chapter 12. The input is an initial water composition, a final water composition, and

a list of phases that may dissolve, precipitate, or both. The output is a list of all the possible reactions involving the listed minerals that satisfy the mass balance constraints. NETPATH also considers isotopic balance for  $^{13}\text{C}$ ,  $^{14}\text{C}$ ,  $^{34}\text{S}$ , D, T,  $^{18}\text{O}$  and  $^{87}\text{Sr}$ , and includes WATEQ4F as a subroutine to test whether the reactions deduced from mass balance are chemically reasonable. It would not be reasonable, for example, to postulate that gypsum precipitates from a solution that is undersaturated with respect to gypsum.

An excellent example of this type of modeling is the study by Plummer et al. (1990) of the chemical evolution of groundwater in the Madison aquifer as it moves several hundred km eastward from recharge areas in Montana and Wyoming. The chemical evolution of the water was consistent with dissolution of gypsum and dolomite, precipitation of calcite, and oxidation of organic matter. That set of reactions explained not only the major element chemistry, but also the isotopes of carbon and sulfur.

A major problem with NETPATH-type modeling, particularly of silicate weathering reactions, is that solutions are rarely unique. Several different sets of minerals can usually be found that satisfy the constraints. Also, depending on the number of solid phases chosen, there may be no solution or an indeterminately large number of solutions. The code is thus a tool to be used in conjunction with geologic insight and judgment: it does not provide simple, unique answers. The inclusion of isotopes may greatly constrain the number of possible answers, provided sufficient isotopic data are available.

## REVIEW QUESTIONS

- Suppose you had a 1 mm wide fracture in an igneous rock, and the concentration of a contaminant in the fracture were kept at a constant value (say by rapid flushing). How long would it take for a mass of contaminant equal to the mass present in the fracture at any instant to diffuse into the rock matrix? Assume a porosity for the matrix of 0.01 and an effective diffusion coefficient of  $1 \times 10^{-7} \text{cm}^2 \text{s}^{-1}$ .
- Suppose you assume instead (Problem 1) that the fluid in the fracture were not moving. Estimate how long it would take for half the material in the fracture to diffuse into the rock matrix. How long would it take if the fracture width were 0.1 mm?  
*Note:* The analytical solution to this problem is by no means simple. You could (a) make an educated guess based on example 1 above; (b) construct a simple numerical model; or (c) (if you have the background) construct a finite difference model.
- The following analyses (from Plummer et al., 1990) represent two wells from the Madison aquifer in Montana that lie approximately along a flowline. The aquifer contains limestone, dolomite, and occasional evaporites. Use NETPATH to come up with a set (or more than one set) of reactions that could account for the difference. Do you think the reactions are plausible?

	$T(^{\circ}\text{C})$	$pH$	$Ca$	$Mg$	$Na$	$K$	$Cl$	$SO_4$	$\Sigma CO_2$
Well 1	11	7.58	1.87	1.15	0.10	0.02	0.05	1.46	3.31
Well 2	32	7.08	6.50	3.96	3.44	0.31	1.89	10.32	3.72

- In Example 4 above, suppose the pit lake were to stratify, forming an anoxic hypolimnion (Chapter 8). Predict the chemical composition of the anoxic waters. Make your assumptions clear, and discuss how reasonable these assumptions are.

## SUGGESTED READING

- ALABARÈDE, F. (1995). *Introduction to Geochemical Modeling*. Cambridge, England: Cambridge University Press.
- ANDERSON, M. P. (1979). Using models to simulate the movement of contaminants through groundwater flow systems. *CREC Critical Reviews in Environmental Control* (pp. 97–156). Boca Raton, FL: CREC Press.
- ANDERSON, M. P., and W. W. WOESSNER. (1992). *Applied Groundwater Modeling: Simulation of Flow and Advective Transport*. San Diego, CA: Academic Press, Inc.
- APPELO, C. A. J., and D. POSTMA. (1993). *Geochemistry, Groundwater, and Pollution*. Rotterdam, Germany: Balkema.
- FETTER, C. W. (1994). *Applied Hydrogeology*. (3rd ed.). New York: Macmillan.
- FREEZE, R. A., and J. A. CHERRY. (1979). *Groundwater*. Englewood Cliffs, NJ: Prentice-Hall. Chapters 7 (Chemical Evolution of Natural Groundwater) and 9 (Groundwater Contamination).
- LICHTNER, P. C.; C. I. STEEFEL; and E. H. OELKERS, (Eds.) (1996). Reactive transport in porous media. *Reviews in Mineralogy*, (v. 34). Washington, DC: Mineralogical Society of America.





## References

- AAGAARD, P. and H. C. HELGESON. (1982). Thermodynamic and kinetic constraints on reaction rates among minerals and aqueous solutions, I. Theoretical considerations. *Amer. J. Sci.* 282, 237–285.
- ABERG, G.; G. JACKS; and P. J. HAMILTON. (1989). Weathering rates and  $^{87}\text{Sr}/^{86}\text{Sr}$  ratios: an isotopic approach. *J. Hydrol.* 109, 65–78.
- AIKEN, G. R.; P. A. BROWN; T. I. NOYES; and D. J. PINCKNEY. (1994). Molecular size and weight of humic acids from the Suwannee River. In R. C. Averett, J. A. Leenher, D. M. McKnight and K. A. Thorn (Eds.), *Humic Substances in the Suwannee River, Georgia: Interactions, Properties, and Proposed Structures*, (pp. 89–97). U.S. Geological Survey Water-Supply Paper 2373.
- AIKEN, G. R., and A. H. GILLAM. (1989). Determination of molecular weights of humic substances by colligative property measurements. In M. B. Hayes, P. MacCarthy, R. L. Malcolm, and R. S. Swift (Eds.), *Humic Substances II: In Search of Structure* (pp. 515–544). Chichester, England: John Wiley.
- AIKEN, G. R.; D. M. MCKNIGHT; R. L. WERSHAW; and P. MACCARTHY. (1985). *Humic Substances in Soil, Sediment, and Water*. New York: Wiley-Interscience.
- AL-DROUBI, A.; B. FRITZ; J.-Y. GAC; and Y. TARDY. (1980). Generalized residual alkalinity concept: application to prediction of natural waters by evaporation. *Am. J. Sci.*, 280; 560–572.
- ALBARÈDE, F. (1995). *Introduction to Geochemical Modeling*. Cambridge, England: Cambridge University Press.
- ALI, M. A., and D. A. DZOMBAK. (1996). Effects of simple organic acids on sorption of  $\text{Cu}^{2+}$  and  $\text{Ca}^{2+}$  on goethite. *Geochim. Cosmochim. Acta*, 60, 291–304.
- ALLISON, J. D.; D. S. BROWN; and K. J. NOVO-GRADAC. (1991). *MINTEQA2/PRODEFA2, A Geochemical Assessment Model for Environmental Systems: Version 3.0 User's Manual*. Washington, DC: U.S. Environmental Protection Agency.
- ALPERS, C. H., and D. W. BLOWES. (Ed.). (1994). *Environmental Geochemistry of Sulfide Oxidation*. American Chemical Society Symposium Series 550. Washington, DC: American Chemical Society.
- ALTVEG, M.; P. WARFVINGE; and H. SVERDRUP. (1993). Profile 3.2: User's guidance for the Apple Macintosh version. Unpublished manuscript. Dept. of Chemical Engineering II, Chemical Center, P.O. Box 124, S-221 00 Lund, Sweden.
- AMIOTTE-SUCHET, P., and J.-L. PROBST. (1993). Flux de  $\text{CO}_2$  consommé par altération chimique continentale: Influences du drainage et de la lithologie. *C.R. Acad. Sci. Paris*, 317(II), 615–622.
- AMRHEIN, C., and D. L. SUAREZ. (1988). The use of a surface complexation model to describe the kinetics of ligand-promoted dissolution of anorthite. *Geochim. Cosmochim. Acta*, 52, 2785–2793.
- ANBEEK, C. (1992a). The dependence of dissolution rates on grain size for some fresh and weathered

- feldspars. *Geochim. Cosmochim. Acta*, 56, 3957–3970.
- ANBEEK, C. (1992b). Surface roughness of minerals and implications for dissolution studies. *Geochim. Cosmochim. Acta*, 56, 1461–1469.
- ANDERSON, M. P. (1979). Using models to simulate the movement of contaminants through groundwater flow systems. *CRC Critical Reviews in Environmental Control* (97–156). Boca Raton, FL: CRC Press.
- ANDERSON, M. P., and W. W. WOESSNER. (1992). *Applied Groundwater Modeling: Simulation of Flow and Advective Transport*. San Diego, CA: Academic Press, Inc.
- ANOVITZ, L. M.; D. PERKINS; and E. J. ESSENE. (1991). Metastability in near-surface rocks of minerals in the system  $\text{Al}_2\text{O}_3\text{-SiO}_2\text{-H}_2\text{O}$ . *Clays and Clay Minerals*, 39, 225–233.
- ANTWEILER, R. C., and J. I. DREVER. (1983). The weathering of a late Tertiary volcanic ash: Importance of organic solutes. *Geochim. Cosmochim. Acta*, 47, 623–629.
- APPELO, C. A. J., and D. POSTMA. (1993). *Geochemistry, Groundwater, and Pollution*. Rotterdam, Netherlands: Balkema.
- APRIL, R.; R. NEWTON; and L. T. COLES. (1986). Chemical weathering in two Adirondack watersheds: Past and present-day rates. *Geol. Soc. Amer. Bull.*, 97, 1232–1238.
- ARAVENA, R.; M. L. EVANS; and J. A. CHERRY. (1993). Stable isotopes of oxygen and nitrogen in source identification of nitrate from septic systems. *Ground Water*, 31, 180–186.
- ARNDT, U.; G. SEUFFERT; and W. NOBEL. (1982). Staub-Reinhalt. *Luft*, 42, 243–247.
- AVERETT, R. C.; J. A. LEENHEER; D. M. MCKNIGHT; and K. A. THORN. (Eds.). (1994). *Humic Substances in the Suwannee River, Georgia: Interactions, Properties, and Proposed Structures*. U.S. Geological Survey Water-Supply Paper 2373.
- AXTMANN, E. V., and R. F. STALLARD. (1995). Chemical weathering in the South Cascade Glacier basin, comparison of subglacial and extra-glacial weathering. In K. A. Tonnessen, M. W. Williams, and M. Tranter (Eds.), *Biogeochemistry of Seasonally Snow-Covered Catchments*. IAHS Publ. no. 228 (pp. 431–439). Wallingford, Oxfordshire, England: International Association of Hydrologic Sciences.
- BACK, W. (1966). *Hydrochemical Facies and Groundwater Flow Patterns in Northern Part of Atlantic Coastal Plain*. U.S. Geological Survey Professional Paper 498–A.
- BACK, W., and B. B. HANSHAW. (1970). Comparison of chemical hydrology of Florida and Yucatan. *J. Hydrol.* 10, 360–368.
- BACK, W., and B. B. HANSHAW. (1971). Rates of physical and chemical processes in a carbonate aquifer. *Nonequilibrium Systems in Natural Water Chemistry* (pp. 77–93). *Am. Chem. Soc. Adv. Chem. Ser.*, 106. Washington, DC: American Chemical Society.
- BAILEY, S. W. (Ed.). (1988). *Hydrous Phyllosilicates*. Reviews in Mineralogy (Vol. 19). Washington, DC: Mineralogical Society of America.
- BAILEY, S. W.; G. W. BRINDLEY; D. S. FANNING; H. KODAMA; and R. T. MARTIN. (1984). Report of the Clay Minerals Society Nomenclature Committee for 1982 and 1983. *Clays and Clay Minerals*, 32, 239–240.
- BAKER, J. P., and C. L. SCHOFIELD. (1980). Aluminum toxicity to fish as related to acid precipitation and Adirondack surface water quality. In D. Trablø and A. Tollan (Eds.), (pp. 292–293). *Ecological Impact of Acid Precipitation*. Oslo-Ås. SNSF Project.
- BAKER, J. P., and C. L. SCHOFIELD. (1982). Aluminum toxicity to fish in acidic waters. *Water, Air, Soil Pollution*, 18, 289–309.
- BAKER, P. A., and M. KASTNER. (1981). Constraints on the formation of sedimentary dolomites. *Science*, 213, 214–216.
- BALL, J. W., and D. K. NORDSTROM. (1991). User's manual for WATEQ4F, with revised thermodynamic database and test cases for calculating speciation of major, trace, and redox elements in natural waters. *U.S. Geological Survey Open-File Report 91–183*. Menlo Park, CA.
- BARNES, I. (1970). Metamorphic waters from the Pacific Tectonic Belt of the west coast of the United States. *Science*, 168, 973–975.
- BARNES, I., and J. D. HEM. (1973). Chemistry of subsurface waters. *Ann. Rev. Earth Planet. Sci.*, 1, 157–301.
- BARNES, I., and J. R. O'NEIL. (1971). The relationship between fluids in some fresh alpine-type ultramafics and possible modern serpentization, western United States. *Geol. Soc. Am. Bull.*, 80, 1947–1960.

- BARNES, I.; J. R. O'NEIL; and J. J. TRESKASES. (1978). Present-day serpentinization in New Caledonia, Oman and Yugoslavia. *Geochim. Cosmochim. Acta*, 42, 144–145.
- BARNES, I., J. B. RAPP; J. R. O'NEIL; R. A. SHEPPARD; and A. J. GUDE III. (1972) Metamorphic assemblages and the direction of flow of metamorphic fluids in four instances of serpentinization. *Contrib. Mineral. Petrol.*, 35, 263–276.
- BARON, J. (1992). *Biogeochemistry of a Subalpine Ecosystem: Loch Vale Watershed. Ecological Studies*, v. 90. New York: Springer-Verlag.
- BARSHAD, I. (1966). The effect of variation in precipitation on the nature of clay mineral formation in soils from acid and basic igneous rocks. *Proc. Int. Clay Conf., Jerusalem*, 1, 167–173.
- BEAMISH, R. J. (1976). Acidification of lakes in Canada by acid precipitation and the resulting effects on fishes. *Water, Air, Soil Pollution*, 6, 501–514.
- BECK, K. C.; J. H. REUTER; and E. M. PERDUE. (1974). Organic and inorganic geochemistry of some coastal plain rivers of the southeastern United States. *Geochim. Cosmochim. Acta*, 38, 341–364.
- BENTLEY, H. W., et al. (1986a). Chlorine-36 dating of very old groundwater 1. The Great Artesian Basin, Australia. *Water Resources Research*, 22, 1991–2001.
- BENTLEY, H. W.; F. M. PHILLIPS; and S. N. DAVIS. (1986). Chlorine-36 in the terrestrial environment. In P. Fritz and J. C. Fontes (Eds.), *Handbook of Environmental Isotope Geochemistry* (pp. 422–475). New York: Elsevier.
- BERNER, E. K., and R. A. BERNER. (1996). *Global Environment: Water, Air, and Geochemical Cycles*. Upper Saddle River, NJ: Prentice-Hall.
- BERNER, R. A. (1964). Iron sulfides formed from aqueous solution at low temperatures and atmospheric pressure. *J. Geol.*, 72, 293–306.
- BERNER, R. A. (1969). Chemical changes affecting dissolved calcium during the bacterial decomposition of fish and clams in sea water. *Marine Geology*, 7, 253–274.
- BERNER, R. A. (1970). Sedimentary pyrite formation. *Am. J. Sci.*, 268, 1–23.
- BERNER, R. A. (1971). *Principles of Chemical Sedimentology*. New York: McGraw-Hill.
- BERNER, R. A. (1974). Kinetic models for the early diagenesis of nitrogen, sulfur, phosphorus, and silicon in anoxic marine sediments. In E. D. Goldberg (Ed.), *The Sea. Vol. 5*, (pp. 427–450). New York: Wiley-Interscience.
- BERNER, R. A. (1975). The role of magnesium in the crystal growth of calcite and aragonite from sea water. *Geochim. Cosmochim. Acta*, 39, 489–504.
- BERNER, R. A. (1978). Rate control of mineral dissolution under earth surface conditions. *Am. J. Sci.*, 278, 1235–1252.
- BERNER, R. A. (1980). *Early Diagenesis: A Theoretical Approach*. Princeton, NJ: Princeton University Press.
- BERNER, R. A., and G. R. HOLDREN, JR. (1979). Mechanism of feldspar weathering II. Observations of feldspars from soils. *Geochim. Cosmochim. Acta*, 43, 1173–1186.
- BERNER, R. A., and G. R. HOLDREN, JR. (1977). Mechanism of feldspar weathering: Some observational evidence. *Geology*, 5, 369–372.
- BERNER, R. A., and J. W. MORSE. (1974). Dissolution kinetics of calcium carbonate in sea water: IV. Theory of calcite dissolution. *Am. J. Sci.*, 274, 108–134.
- BISCHOFF, W. D.; F. T. MACKENZIE; and F. C. BISHOP. (1987). Stabilities of synthetic magnesian calcites in aqueous solution: Comparison with biogenic materials. *Geochim. Cosmochim. Acta*, 51, 1413–1424.
- BLANK, L. W. (1985). A new type of forest decline in Germany. *Nature*, 314, 311–314.
- BLUM, A. E. (1994). Feldspars in weathering. In I. Parsons (Ed.), *Feldspars and Their Reactions. NATO Advanced Study Workshop, Series C* (pp. 595–629). Dordrecht, Netherlands: Kluwer.
- BLUM, A. E., and A. C. LASAGA. (1988). Role of surface speciation in the low-temperature dissolution of minerals. *Nature*, 331, 431–433.
- BLUM, A. E.; R. A. YUND; and A. C. LASAGA. (1990). The effect of dislocation density on the dissolution rate of quartz. *Geochim. Cosmochim. Acta*, 54, 283–297.
- BLUM, J. D.; Y. EREL; and K. BROWN. (1994).  $^{87}\text{Sr}/^{86}\text{Sr}$  ratios of Sierra Nevada stream waters: implications for relative mineral weathering rates. *Geochim. Cosmochim. Acta*, 58, 5019–5025.
- BOLES, J. R., and S. G. FRANKS. (1979). Clay diagenesis in Wilcox sandstones of southwest Texas: Implications of smectite diagenesis on sandstone cementation. *J. Sedim. Petrol.*, 49, 55–70.

- BOLT, G. H. (Ed.) (1982). *Soil Chemistry*. Amsterdam, Netherlands: Elsevier.
- BONSANG, B., et al. (1980). Sulfate enrichment in marine aerosols owing to biogenic gaseous sulfur compounds. *J. Geophys. Res.*, *85*, 7410–7416.
- BOWERS, T. S.; K. J. JACKSON; and H. C. HELGESON. (1984). *Equilibrium Activity Diagrams*. New York: Springer-Verlag.
- BOWSER, C. J., and B. F. JONES. (1993). Mass balances of natural waters: Silicate dissolution, clays, and the calcium problem. *BioGEOmon* (pp. 30–31). Prague, Czech Republic: Czech Geological Survey.
- BRADBURY, M. H., and A. GREEN. (1985). Measurement of important parameters determining aqueous phase diffusion rates through crystalline rock matrices. *J. Hydrol.*, *82*, 39–55.
- BRADY, P. V., and J. V. WALTHER. (1989). Controls on silicate dissolution rates in neutral and basic pH solutions at 25°C. *Geochim. Cosmochim. Acta*, *53*, 2823–2830.
- BRECK, W. G. (1974). Redox levels in the sea. In E. D. Goldberg (Ed.), *The Sea, Vol. 5*. (pp. 153–179). New York: Wiley-Interscience.
- BRICKER, O. P. (1965). Some stability relations in the system Mn–O<sub>2</sub>–H<sub>2</sub>O at 25°C and one atmosphere total pressure. *Am. Mineralogist*, *50*, 1296–1354.
- BRICKER, O. P. (1969). Stability constants and Gibbs free energies of formation of magadiite and kenyaite. *Am. Mineralogist*, *54*, 1026–1033.
- BRICKER, O. P.; H. W. NESBITT; and W. D. GUNTER. (1973). The stability of talc. *Am. Mineralogist*, *58*, 64–72.
- BROECKER, W. S.; J. CROMWELL; and Y. H. LI. (1968). Rates of vertical eddy diffusion near the ocean floor based on measurements of the distribution of excess <sup>222</sup>Rn. *Earth Planet. Sci. Lett.*, *5*, 101–105.
- BROOKINS, D. G. (1988). *Eh–pH Diagrams for Geochemistry*. New York: Springer-Verlag.
- BRUNAUER, S.; P. H. EMMETT; and E. TELLER. (1938). Adsorption of gases in multimolecular layers. *J. Amer. Chem. Soc.*, *60*, 309–319.
- BUOL, S. W.; F. D. HOLE; and R. J. McCracken. (1980). *Soil Genesis and Classification*. Ames, IA: Iowa State University Press.
- BURCH, T. E.; K. L. NAGY; and A. C. LASAGA. (1993). Free energy dependence of albite dissolution kinetics at 80°C and pH 8.8. *Chem. Geol.*, *105*, 137–162.
- BUSENBERG, E., and C. V. CLEMENCY. (1976). The dissolution kinetics of feldspars at 25°C and 1 atm CO<sub>2</sub> partial pressure. *Geochimica et Cosmochimica Acta*, *40*, 41–49.
- BUSENBERG, E., and L. N. PLUMMER. (1986). The solubility of BaCO<sub>3</sub>(cr) (witherite) in CO<sub>2</sub>–H<sub>2</sub>O solutions between 0 and 90°C, evaluation of the association constants of BaHCO<sub>3</sub><sup>+</sup>(aq) and BaCO<sub>3</sub><sup>0</sup>(aq) between 5 and 80°C, and a preliminary evaluation of the thermodynamic properties of Ba<sup>2+</sup>(aq). *Geochim. Cosmochim. Acta*, *50*, 2225–2234.
- BUSENBERG, E.; L. N. PLUMMER; and V. B. PARKER. (1984). The solubility of strontianite (SrCO<sub>3</sub>) in CO<sub>2</sub>–H<sub>2</sub>O solutions between 2 and 91°C, the association constants of SrHCO<sub>3</sub><sup>+</sup>(aq) and SrCO<sub>3</sub><sup>0</sup>(aq) between 5 and 80°C, and an evaluation of the thermodynamic properties of Sr<sup>2+</sup>(aq) and SrCO<sub>3</sub>(cr) at 25°C and 1 atm total pressure. *Geochim. Cosmochim. Acta*, *48*, 2021–2036.
- BUTLER, G. P. (1969). Modern evaporite deposition and geochemistry of coexisting brines, the sabkha, Trucial Coast, Arabian Gulf. *J. Sediment. Petrology*, *39*, 70–89.
- BUTLER, J. N. (1982). *Carbon Dioxide Equilibria and Their Applications*. Reading, MA: Addison-Wesley.
- CAROTHERS, W. W., and Y. K. KHARAKA. (1978). Aliphatic acid anions in oil-field water—Implications for origin of natural gas. *Am. Assoc. Petroleum Geologists Bull.*, *62*, 2441–2453.
- CARSON, M. A., and M. J. KIRKBY. (1972). *Hillslope Form and Process*. New York: Cambridge University Press.
- CARUCCIO, F. T. (1975). Estimating the acid potential of coal mine refuse. *The Ecology of Resource Degradation and Renewal*, (pp. 197–205). Oxford, England: Blackwell.
- CARUCCIO, F. T., and G. GEIDEL. (1978). Geochemical factors affecting coal mine drainage quality. *Reclamation of Drastically Disturbed Lands* (pp. 129–147). Madison, WI: ASA-CSSA-SSSA.
- CASEY, W. H., and B. BUNKER. (1990). Leaching of mineral and glass surfaces during dissolution. In M. F. Hochella and A. F. White (Eds.), *Mineral-Water Interface Geochemistry; Reviews in Mineralogy, Vol. 23* (pp. 397–426).

- CASEY, W. H.; H. R. WESTRICH; T. MASSIS; J. F. BANFIELD; and G. W. ARNOLD. (1989). The surface of labradorite feldspar after acid hydrolysis. *Chemical Geology*, 78, 205–218.
- CHAPELLE, F. H. (1993). *Ground-Water Microbiology and Geochemistry*. New York: Wiley.
- CHEN, C. S. (1986). Solutions for radionuclide transport from an injection well into a single fracture in a porous formation. *Water Resources Res.*, 22, 508–518.
- CHEN, C. W.; S. A. GHERINI; J. D. DEAN; R. J. M. HUDSON; and R. A. GOLDSTEIN. (1984). Development and calibration of the Integrated Lake-Watershed Acidification study model. In J. L. Schnoor (Ed.), *Modeling of Total Acid Precipitation Impacts* (pp. 175–203). Ann Arbor, MI: Ann Arbor Science.
- CHEN, C. W.; S. A. GHERINI; R. J. M. HUDSON; and J. D. DEAN. (1983). *The Intergrated Lake-Watershed Acidification Study, Vol. 1: Model Principles and Application Procedures*. Palo Alto, CA: Electric Power Research Institute.
- CHERRY, J. A.; D. E. DESAULNIERS; E. O. FRIND; P. FRITZ; R. W. GILLHAM; and B. LELIVRE. (1979a). Hydrogeologic properties and porewater origin and age: Clayey till and clay in south-central Canada. *Workshop on Low-Flow, Low-Permeability Measurements in Largely Impermeable Rocks*, Paris, France: OECD/Nuclear Energy Agency.
- CHERRY, J. A.; A. U. SHAIKH; D. E. TALLMAN; and R. V. NICHOLSON. (1979b). Arsenic species as an indicator of redox conditions in groundwater. *J. Hydrol.*, 43, 373–392.
- CHOU, L., and R. WOLLAST. (1984). Study of the weathering of albite at room temperature and pressure with a fluidized bed reactor. *Geochim. Cosmochim. Acta*, 48, 2205–2218.
- CHRIST, C. L.; P. B. HOSTETLER; and R. M. SIEBERT. (1973). Studies in the system  $MgO-SiO_2-CO_2-H_2O$  (III): The activity-product constant of sepiolite. *Am. J. Sci.*, 273, 507–525.
- CHRISTOPHERSEN, N., and C. NEAL. (1990). Linking hydrological, geochemical, and soil chemical processes on the catchment scale: an interplay between modelling and field work. *Water Resources Res.*, 26, 3077–3086.
- CHRISTOPHERSEN, N.; H. M. SEIP; and R. F. WRIGHT. (1982). A model for streamwater chemistry at Birkenes, Norway. *Water Resources Res.* 18, 977–996.
- CLAYTON, J. L. (1988). Some observations on the stoichiometry of feldspar hydrolysis in granitic soils. *J. Environmental Quality*, 17, 153–157.
- CLAYTON, R. N., et al. (1966). The origin of saline formation waters: I. Isotopic composition. *J. Geophys. Res.*, 71, 3869–3882.
- CLEAVES, E. T.; A. E. GODFREY; and O. P. BRICKER. (1970). Geochemical balance of a small watershed and its geomorphic implications. *Geol. Soc. Am. Bull.*, 81, 3015–3032.
- CLOW, D. W. (1992). Weathering rates from field and laboratory experiments on naturally weathered soils. Unpublished Ph.D. Dissertation, University of Wyoming.
- CLOW, D. W., and J. I. DREVER. (1996). Weathering rates as a function of flow through an alpine soil. *Chemical Geology*, 132, 131–141.
- CLOW, D. W., and A. M. MAST. (1995). Composition of precipitation, bulk deposition, and runoff at a granitic bedrock catchment in the Loch Vale Watershed, Colorado, USA. In K. A. Tonnessen, M. W. Williams, and M. Tranter (Eds.), *Biogeochemistry of Seasonally Snow-Covered Catchments*. IAHS Publ. no. 228 (235–242). Wallingford, Oxfordshire, England: International Association of Hydrologic Science.
- CLYMO, R. S. (1967). Control of cation concentrations and in particular of pH in Sphagnum dominated communities. In H. L. Golterman and R. S. Clymo (Eds.), *Chemical Environment in the Aquatic Habitat* (pp. 273–284). Amsterdam, Netherlands: Noord-Hollandsche Uitgevers Maatschappij.
- COSBY, B. J.; G. M. HORNBERGER; J. N. GALLOWAY; and R. F. WRIGHT. (1985). Modeling the effects of acid deposition: Assessment of a lumped parameter model of soil water and streamwater chemistry. *Water Resources Res.*, 21, 51–63.
- COSTON, J. A.; C. C. FULLER; and J. A. DAVIS. (1995).  $Pb^{2+}$  and  $Zn^{2+}$  adsorption by a natural aluminum- and iron-bearing surface coating on an aquifer sand. *Geochim. Cosmochim. Acta*, 59, 3535–3547.
- COWAN, D. C. (1988). *Review of Selenium Thermodynamic Data*. Report EA-5655. Palo Alto, CA: Electric Power Research Institute.
- COX, J. D.; D. D. WAGMAN; and V. A. MEDVEDEV. (1989). *CODATA Key Values for Thermodynamics*. Washington, DC: Hemisphere.

- CRAIG, H. (1961). Isotopic variations in meteoric waters. *Science*, *133*, 1702–1703.
- CRONAN, C. S., and G. R. AIKEN. (1985). Chemistry and transport of soluble humic substances in forested watersheds of the Adirondack Park, New York. *Geochim. Cosmochim. Acta*, *49*, 1697–1705.
- DANSGAARD, W. (1964). Stable isotopes in precipitation. *Tellus*, *16*, 436–468.
- DAVIES, C. W. (1962). *Ion Association*. Washington, DC: Butterworth.
- DAVIS, J. A. (1984). Complexation of trace metals by adsorbed natural organic matter. *Geochim. Cosmochim. Acta*, *46*, 2381–2393.
- DAVIS, J. A.; C. C. FULLER; and A. D. COOK. (1987). Mechanisms of trace metal sorption by calcite: adsorption of Cd<sup>2+</sup> and subsequent solid solution formation. *Geochim. Cosmochim. Acta*, *51*, 1477–1490.
- DAVIS, J. A.; R. O. JAMES; and J. O. LECKIE. (1978). Surface ionization and complexation at the oxide/water interface. I. Computation of electrical double layer properties in simple electrolytes. *J. Colloid and Interface Sci.*, *63*, 480–499.
- DAVIS, J. A., and D. B. KENT. (1990). Surface complexation modeling in aqueous geochemistry. In M. F. Hochella and A. F. White (Eds.), *Mineral-Water Interface Geochemistry* (pp. 177–260). Washington, DC: Mineralogical Society of America.
- DAVIS, J. S., and J. ZOBRIST. (1978). The interrelationships among chemical parameters in rivers—Analyzing the effect of natural and anthropogenic sources. *Prog. Water Technol.*, *10*, 65–78.
- DEGENS, E. T. (Ed.). (1982). Transport of carbon and minerals in major world rivers. *SCOPE/UNEP Sonderband, Mitteilungen aus dem Geologisch-Paläontologischen Institut der Universität Hamburg*. Hamburg, Germany: University of Hamburg.
- DEINES, P. (1980). The carbon isotopic composition of reduced organic carbon. In P. Fritz and J. C. Fontes (Eds.), *Handbook of Environmental Isotope Geochemistry* (pp. 329–406). Amsterdam, Netherlands: Elsevier.
- DETHIER, D. P. (1979). Atmospheric Contributions to stream water chemistry in the North Cascade Range, Washington. *Water Resources Research*, *15*, 787–794.
- DIXON, J. B., and S. B. WEED (Eds.). (1977). *Minerals in Soil Environments*. Madison, WI: Soil Science Society of America.
- DOMENICO, P. A., and F. W. SCHWARTZ. (1990). *Physical and Chemical Hydrogeology*. New York: Wiley.
- DREVER, J. I. (1972). Relations among pH, carbon dioxide pressure, alkalinity, and calcium concentration in waters saturated with respect to calcite at 25°C and one atmosphere total pressure. *Contrib. Geol.*, *11*, 41–43.
- DREVER, J. I. (1994). The effect of land plants on weathering rates of silicate minerals. *Geochim. Cosmochim. Acta*, *58*, 2325–2332.
- DREVER, J. I., and D. W. CLOW. (1995). Weathering rates in catchments. In A. F. White and S. L. Brantley (Eds.), *Chemical Weathering Rates of Silicate Minerals* (pp. 463–483). Washington, DC: Mineralogical Society of America.
- DREVER, J. I., and D. R. HURCOMB. (1986). Neutralization of atmospheric acidity by chemical weathering in an alpine drainage basin in the North Cascade Mountains. *Geology*, *14*, 221–224.
- DREVER, J. I.; J. W. MURPHY; and R. C. SURDAM. (1977). The distribution of As, Be, Cd, Cu, Hg, Mo, Pb, and U associated with the Wyodak coal seam, Powder River Basin, Wyoming. *Contrib. Geol.*, *15*, 93–101.
- DREVER, J. I.; K. M. MURPHY; and D. W. CLOW. (1994). Field weathering rates versus laboratory dissolution rates: an update. *Mineralogical Magazine*, *58A*, 239–240.
- DREVER, J. I., and C. L. SMITH. (1978). Cyclic wetting and drying of the soil zone as an influence on the chemistry of ground water in arid terrains. *Am. J. Sci.*, *278*, 1448–1454.
- DREVER, J. I., and J. ZOBRIST. (1992). Chemical weathering of silicate rocks as a function of elevation in the southern Swiss Alps. *Geochim. Cosmochim. Acta*, *56*, 3209–3216.
- Driscoll, C. T. (1984). A procedure for fractionation of aqueous aluminum in dilute acidic waters. *Int. J. Environ. Anal. Chem.*, *16*, 267–284.
- DROUBI, A.; C. CHEVERRY; B. FRITZ; and Y. TARDY. (1976). Géochemie des eaux et des sels dans les sols des polders du Lac Tchad: Application d'un modèle thermodynamique de simulation de l'évaporation. *Chem. Geol.*, *17*, 165–177.

- DZOMBAK, D. A., and F. M. M. MOREL. (1990). *Surface Complexation Modeling: Hydrous Ferric Oxide*. New York: Wiley-Interscience.
- ECKHARDT, F. E. W. (1978). Microorganisms and weathering of a sandstone monument. In W. E. Krumbein (Ed.), *Environmental Biogeochemistry and Geomicrobiology* (pp. 675–686). Ann Arbor, MI: Ann Arbor Science.
- EDMOND, J. M. (1970). High precision determination of titration alkalinity and total carbon dioxide content of sea water. *Deep-Sea Research*, 17, 737–750.
- EDMOND, J. M., and J. M. GIESKES. (1970). On the calculation of the degree of saturation of sea water with respect to calcium carbonate under in situ conditions. *Geochim. Cosmochim. Acta*, 34, 1261–1291.
- EDMOND, J. M.; M. R. PALMER; C. I. MEASURES; B. GRANT; and R. F. STALLARD. (1995). The fluvial geochemistry and denudation rate of the Guayana Shield in Venezuela, Colombia, and Brazil. *Geochim. Cosmochim. Acta*, 59, 3301–3326.
- ELECTRIC POWER RESEARCH INSTITUTE. (1984). *The Integrated Lake-Watershed Acidification Study 4. Summary of Major Results*. Report EA-3221. Palo Alto, CA: Electric Power Research Institute.
- ELLIS, A. J., and W. A. J. MAHON. (1977). *Geochemistry and Geothermal Systems*. New York: Academic Press, Inc.
- EMERSON, S. M. (1976). Early diagenesis in anaerobic lake sediments: chemical equilibria in interstitial waters. *Geochim. Cosmochim. Acta*, 40, 925–934.
- EMERSON, S. M., and G. WIDMER. (1978). Early diagenesis in anaerobic lake sediments: II. Thermodynamic and kinetic factors controlling the formation of iron phosphate. *Geochim. Cosmochim. Acta*, 42, 1307–1316.
- EPHRAIM, J.; S. ALEGRET; A. MATHUTHU; M. BICKING; R. L. MALCOLM; and J. A. MARINSKY. (1986). A unified physicochemical description of the protonation and metal ion complexation equilibria of natural organic acids (humic and fulvic acids). 2. Influence of polyelectrolyte properties and functional group heterogeneity on the protonation equilibria of fulvic acid. *Environ. Sci. & Technol.*, 20, 354–366.
- EUGSTER, H. P. (1970). Chemistry and origin of the brines of Lake Magadi, Kenya. *Mineral. Soc. Am. Spec. Paper* 3, 213–235.
- EUGSTER, H. P., and L. A. HARDIE. (1978). Saline Lakes. In A. Lerman (Ed.), *Lakes—Chemistry, Geology, Physics* (pp. 237–293). New York: Springer-Verlag.
- EUGSTER, H. P.; C. E. HARVIE; and J. H. WEARE. (1980). Mineral equilibria in the six-component seawater system, Na–K–Mg–Ca–Cl–SO<sub>4</sub>–H<sub>2</sub>O at 25°C. *Geochim. Cosmochim. Acta*, 44, 1335–1347.
- EUGSTER, H. P., and B. F. JONES. (1979). Behavior of major solutes during closed-basin brine evolution. *Am. J. Sci.*, 279, 609–631.
- EUGSTER, H. P., and G. MAGLIONE. (1979). Brines and evaporites of the Lake Chad basin, Africa. *Geochim. Cosmochim. Acta*, 43, 973–982.
- FAHEY, T. J.; J. B. YAVITT; A. E. BLUM; and J. I. DREVER. (1985). Controls of soil-solution chemistry in lodgepole pine forest ecosystems, Wyoming. In D. E. Caldwell, J. A. Brierly and C. L. Brierly (Eds.), *Planetary Ecology* (pp. 473–484). New York, Van Nostrand Reinhold.
- FAURE, G. (1986). *Principles of Isotope Geology*. (2nd ed.). New York: Wiley.
- FETH, J. H.; C. E. ROBERSON; and W. L. POLZER. (1964). Sources of mineral constituents in water from granitic rocks, Sierra Nevada, California and Nevada. *U.S. Geological Survey Water-Supply Paper* 1535–I.
- FETTER, C. W. (1993). *Contaminant Hydrogeology*. New York: Macmillan.
- FETTER, C. W. (1994). *Applied Hydrogeology*. New York: Macmillan.
- FINLEY, J. B., and J. I. DREVER. (in press). Chemical mass balance and rates of mineral weathering in a high-elevation catchment, West Glacier Lake, Wyoming. In O. P. Bricker (Ed.), *The Use of Mass Balance Studies in Watershed Research*.
- FONTES, J. C., and J. N. ANDREWS. (1993). Comment on “Reinterpretation of <sup>36</sup>Cl data: Physical processes, hydraulic interconnections and age estimates in groundwater systems” by E. Mazor. *Applied Geochemistry*, 8, 663–666.
- FOSTER, S. S. D. (1975). The Chalk groundwater tritium anomaly: A possible explanation. *J. Hydrology*, 25, 159–165.
- FOWLER, D. (1980). Removal of sulfur and nitrogen compounds from the atmosphere in rain and by dry deposition. In D. Drabløs and A. Tollan (Eds.), *Ecological Impact of Acid Precipitation* (pp. 22–32). Oslo, Norway: SNSF.

- FREEDMAN, B., and T. C. HUTCHINSON. (1980). Long-term effects of smelter pollution at Sudbury, Ontario, on forest community composition. *Canad. J. Botany*, 58, 2123–2140.
- FREEZE, R. A., and J. A. CHERRY. (1979). *Groundwater*. Englewood Cliffs, NJ: Prentice-Hall.
- FRIEDMAN, I., and J. R. O'NEIL. (1977). Compilation of stable isotope fractionation factors of geochemical interest. In M. Fleischer (Ed.), *U.S. Geol. Surv. Prof. Paper 440-KK*.
- FRITZ, P.; J. A. CHERRY; K. U. WEYER; and M. SKLASH. (1976). Storm runoff analysis using environmental isotopes and major ions. *Interpretation of Environmental Isotope and Hydrochemical Data in Groundwater Hydrology* (pp. 111–130). Vienna, Austria: International Atomic Energy Agency.
- FRITZ, P., and J. C. FONTES. (Eds.). (1980). *Handbook of Environmental Isotope Geochemistry, Vol. 1, The Terrestrial Environment A*. New York: Elsevier.
- FRITZ, P., and J. C. FONTES (Eds.). (1986). *Handbook of Environmental Isotope Geochemistry, Vol. 2, The Terrestrial Environment B*. New York: Elsevier.
- FROELICH, P. N., et al. (1979). Early oxidation of organic matter in pelagic sediments of the eastern equatorial Atlantic: suboxic diagenesis. *Geochim. Cosmochim. Acta*, 43, 1075–1090.
- FUHRER, H. (1985). Formation of secondary air pollutants and their occurrence in Europe. *Experientia*, 41, 286–301.
- GAC, J.; D. BADAUT; A. AL-DROUBI; and Y. TARDY. (1978). Comportement du calcium, du magnésium et de la silice en solution. Précipitation de calcite magnésienne, de silice amorphe et de silicates magnésiens au cours de l'évaporation des eaux du Chari (Tchad). *Sci. Géol. Bull. Strasbg.*, 31, 185–193.
- GÄCHTER, R., and J. S. MEYER. (1993). The role of microorganisms in mobilization and fixation of phosphorus in sediments. *Hydrobiologia*, 253, 103–121.
- GALLOWAY, J. N. (1979). Alteration of trace metal geochemical cycles due to the marine discharge of wastewater. *Geochim. Cosmochim. Acta*, 43, 207–218.
- GALLOWAY, J. N.; S. A. NORTON; and M. R. CHURCH. (1983). Freshwater acidification from atmospheric deposition of sulfuric acid: A conceptual model. *Environ. Sci. Technol.*, 17, 541A–545A.
- GARRELS, R. M. (1967). Genesis of some groundwaters from igneous rocks. In P. H. Abelson (Ed.), *Researches in Geochemistry, Vol. 2* (pp. 405–420). New York: Wiley.
- GARRELS, R. M., and C. L. CHRIST. (1965). *Solutions, Minerals, and Equilibria*. New York: Harper & Row.
- GARRELS, R. M., and F. T. MACKENZIE. (1967). Origin of the chemical compositions of some springs and lakes. In R. F. Gould (Ed.), *Equilibrium Concepts in Natural Water Systems* (pp. 222–242). Advances in Chemistry Series 67. Washington, DC: American Chemical Society.
- GARRELS, R. M., and F. T. MACKENZIE. (1971). *Evolution of Sedimentary Rocks*. New York: W. W. Norton.
- GARRELS, R. M.; F. T. MACKENZIE; and C. HUNT. (1975). *Chemical Cycles and the Global Environment: Assessing Human Influences*. Los Altos, CA: William Kaufmann.
- GARRELS, R. M., and E. A. PERRY. (1974). Cycling of carbon, sulfur, and oxygen through geologic time. In E. D. Goldberg (Ed.), *The Sea, Vol. 5* (pp. 303–336). New York: Wiley-Interscience.
- GARVIN, D.; V. B. PARKER; and H. J. WHITE. (1987). *CODATA Thermodynamic Tables—Selections for Some Compounds of Calcium and Related Mixtures: a Prototype Set of Tables*. Washington, DC: Hemisphere.
- GIBBS, R. J. (1967). The geochemistry of the Amazon River system: I. The factors that control the salinity and the composition and concentration of the suspended solids. *Geol. Soc. Amer. Bull.*, 78, 1203–1232.
- GIBBS, R. J. (1970). Mechanisms controlling world water chemistry. *Science*, 170, 1088–1090.
- GIBBS, R. J. (1972). Water chemistry of the Amazon river. *Geochim. Cosmochim. Acta*, 36, 1061–1066.
- GILLHAM, R. W., and J. A. CHERRY. (1982). Contaminant migration in saturated unconsolidated geologic deposits. In T. A. Narasimhan (Ed.), *Recent Trends in Hydrogeology. Geol. Soc. Amer. Special Paper 189* (pp. 31–62). Boulder, CO: Geological Society of America.
- GOLDHABER, M. B., and I. R. KAPLAN. (1974). The sulfur cycle. In E. D. Goldberg (Ed.), *The Sea, Vol. 5* (pp. 569–655). New York: Wiley-Interscience.



- GONFIANTINI, R. (1986). Environmental isotopes in lake studies. In P. Fritz and J. Ch. Fontes (Eds.), *Handbook of Environmental Isotope Geochemistry* (pp. 113–168). Amsterdam, Netherlands: Elsevier.
- GRAF, D. (1982). Chemical osmosis, reverse chemical osmosis, and the origin of subsurface brines. *Geochim. Cosmochim. Acta*, 46, 1431–1448.
- GRANDSTAFF, D. E. (1986). The dissolution rate of forsteritic olivine from Hawaiian beach sand. In S. M. Coleman and D. P. Dethier (Eds.), *Rates of Chemical Weathering of Rocks and Minerals* (pp. 41–59). Orlando, FL: Academic Press, Inc.
- GRAUSTEIN, W. C., and R. L. ARMSTRONG. (1983). The use of strontium-87/strontium-86 ratios to measure atmospheric transport into forested watersheds. *Science*, 219, 289–292.
- GRAUSTEIN, W. C.; K. CROMACK; and P. SOLLINS. (1977). Calcium oxalate: occurrence in soils and effect on nutrient and geochemical cycles. *Science*, 198, 1252–1254.
- GRIM, R. E.; R. H. BRAY; and W. F. BRADLEY. (1937). The mica in argillaceous sediments. *Am. Mineralogist*, 22, 813–829.
- GRISAK, G. E., and J. F. PICKENS. (1980). Solute transport through fractured media 1. The effect of matrix diffusion. *Water Resources Res.*, 16, 719–730.
- HAINES, B.; M. STEFANI; and F. HENDRICKS. (1980). Acid rain: Threshold of leaf damage in eight plant species from a southern Appalachian forest succession. *Water, Air, and Soil Pollution*, 14, 403–407.
- HANOR, J. S. (1983). Fifty years of development of thought on the origin and evolution of subsurface sedimentary brines. In S. J. Boardman (Ed.), *Revolution in the Earth Sciences: Advances in the Past Half-Century* (pp. 99–111). Dubuque, IA: Kendall/Hunt.
- HANSEN, T. A. (1993). Carbon metabolism of sulfate-reducing bacteria. In J. M. Odom and R. Singleton, Jr. (Eds.), *The Sulfate-Reducing Bacteria: Contemporary Perspectives* (pp. 21–40). New York: Springer-Verlag.
- HANSHAW, B. B., and T. B. COPLEN. (1973). Ultrafiltration by a compacted clay membrane: II. Sodium ion exclusion at various ionic strengths. *Geochim. Cosmochim. Acta*, 37, 2311–2327.
- HARDIE, L. A. (1967). The gypsum-anhydrite equilibrium at one atmosphere pressure. *Am. Mineralogist*, 52, 171–200.
- HARDIE, L. A., and H. P. EUGSTER. (1970). The evolution of closed-basin brines. *Mineralogical Soc. Am. Spec. Publ.* 3, 273–290.
- HARVEY, G. R., and D. A. BORAN. (1985). Geochemistry of humic substances in seawater. In G. R. Aiken et al. (Eds.), *Humic Substances in Soil, Sediment, and Water* (pp. 233–247). New York: Wiley-Interscience.
- HARVIE, C. E.; H. P. EUGSTER; and J. H. WEARE. (1982). Mineral equilibria in the six-component seawater system, Na–K–Mg–Ca–Cl–SO<sub>4</sub>–H<sub>2</sub>O at 25°C. II: Compositions of the saturated solutions. *Geochim. Cosmochim. Acta*, 46, 1603–1618.
- HARVIE, C. E.; N. MOLLER; and J. H. WEARE. (1984). The prediction of mineral solubilities in natural waters: The Na–K–Mg–Ca–H–Cl–SO<sub>4</sub>–OH–HCO<sub>3</sub>–CO<sub>3</sub>–CO<sub>2</sub>–H<sub>2</sub>O system to high ionic strengths at 25°C. *Geochim. Cosmochim. Acta*, 48, 723–752.
- HARVIE, C. E., and J. H. WEARE. (1980). The prediction of mineral solubilities in natural waters: The Na–K–Mg–Ca–Cl–SO<sub>4</sub>–H<sub>2</sub>O system from zero to high concentrations at 25°C. *Geochim. Cosmochim. Acta*, 44, 981–997.
- HARVIE, C. E.; J. H. WEARE; L. A. HARDIE; and H. P. EUGSTER. (1980). Evaporation of seawater: Calculated mineral sequences. *Science*, 208, 498–500.
- HAYES, K. F.; G. REDDEN; W. ELA; and J. O. LECKIE. (1991). Surface complexation models: an evaluation of model parameter estimation using FITEQL and oxide mineral titration data. *J. Colloid Interface Sci.*, 142, 448–469.
- HAYES, M. B. H.; P. MACCARTHY; R. L. MALCOLM; and R. S. SWIFT (Eds.). (1989). *Humic Substances II: In search of structure*. New York: Wiley.
- HELGESON, H. C.; J. M. DELANEY; H. W. NESBITT; and D. K. BIRD. (1978). Summary and critique of the thermodynamic properties of rock-forming minerals. *Am. J. Sci.*, 278–A, 1–229.
- HELGESON, H. C.; R. M. GARRELS; and F. T. MACKENZIE. (1969). Evaluation of irreversible reactions in geochemical processes involving minerals and aqueous solutions: II. Applications. *Geochim. Cosmochim. Acta*, 33, 455–481.
- HELLWIG, D. H. R. (1974). Evaporation of water from sand: V. The effect of evaporation on the concentration of salts dissolved in water stored in sand. *J. Hydrology*, 21, 101–110.

- HEM, J. D. (1978). Redox processes at surfaces of manganese oxide and their effects on aqueous metal ions. *Chem. Geol.*, 21, 199–218.
- HEM, J. D. (1985). *Study and interpretation of the chemical characteristics of natural water*. U.S. Geological Survey Water-Supply Paper 2254.
- HEMINGWAY, B. S., and G. SPOSITO. (1989). Inorganic aluminum bearing solid phases. In G. Sposito (Ed.), *The Environmental Chemistry of Aluminum* (pp. 55–85). Boca Raton, FL: CRC Press.
- HENRIKSEN, A. (1980). Acidification of fresh waters—a large scale titration. In D. Drabløs and A. Tollan (Eds.), *Ecological Impact of Acid Precipitation* (pp. 68–74). Oslo-Ås: SNSF Project.
- HITCHON, B.; G. K. BILLINGS; and J. E. KLOVAN. (1971). Geochemistry and origin of formation waters in the western Canada sedimentary basin: III. Factors controlling chemical composition. *Geochim. Cosmochim. Acta*, 35, 567–598.
- HITCHON, B., and I. FRIEDMAN. (1969). Geochemistry and origin of formation waters in the western Canada sedimentary basin: I. Stable isotopes of hydrogen and oxygen. *Geochim. Cosmochim. Acta*, 33, 1321–1349.
- HOFFMAN, W. A.; S. E. LINDBERG; and R. R. TURNER. (1980). Some observations of organic constituents in rain above and below a forest canopy. *Environ. Sci. & Technol.*, 14, 999–1002.
- HOLDREN, G. R., JR., and R. A. BERNER. (1979). Mechanism of feldspar weathering I. Experimental studies. *Geochim. Cosmochim. Acta*, 43, 1161–1171.
- HOLLAND, H. D. (1978). *The Chemistry of the Atmosphere and Oceans*. New York: Wiley-Interscience.
- HOLLAND, H. D.; T. V. KIRSIPU; J. S. HUEBNER; and U. M. OXBURGH. (1964). On some aspects of the chemical evolution of cave waters. *J. Geol.*, 72, 36–67.
- HOLT, B. D.; A. G. ENGELKEMEIR; and A. VENTERS. (1972). Variations in sulfur isotope ratios in samples of water and air near Chicago. *Environ. Sci. & Technol.*, 6, 338–341.
- HOOPER, R. P.; N. CHRISTOPHERSEN; and N. E. PETERS. (1990). Modelling streamwater chemistry as a mixture of soilwater end-members—An application to the Panola Mountain catchment, Georgia, USA. *J. Hydrol.*, 116, 321–343.
- HOOPER, R. P., and C. A. SHOEMAKER. (1985). Aluminum mobilization in an acidic headwater stream: Temporal variation and mineral dissolution equilibria. *Science*, 229, 463–465.
- HOOPER, R. P.; A. STONE; N. CHRISTOPHERSEN; E. DE GROSBOIS; and H. M. SEIP. (1988). Assessing the Birkenes model of stream acidification using a multisignal calibration methodology. *Water Resources Res.*, 24, 1308–1316.
- HOSTETTLER, P. B., and R. M. GARRELS. (1962). Transportation and precipitation of uranium and vanadium at low temperatures, with special reference to sandstone type uranium deposits. *Econ. Geol.*, 57, 137–167.
- HOSTETTLER, J. D. (1984). Electode electrons, aqueous electrons, and redox potentials in natural waters. *Am. J. Sci.*, 284, 734–759.
- HOSTETTLER, J. D. (1985). Reply: On the importance of distinguishing Eh from pe. *Am. J. Sci.*, 285, 859–863.
- HOWER, J.; E. V. ESLINGER; M. E. HOWER; and E. A. PERRY. (1976). Mechanism of burial metamorphism of argillaceous sediment: I. Mineralogical and chemical evidence. *Geol. Soc. Am. Bull.*, 87, 725–737.
- HOWER, J., and T. C. MOWATT. (1966). The mineralogy of illites and mixed-layer illite/montmorillonites. *Am. Mineralogist*, 51, 825–854.
- HSÜ, K. J. (1967). Chemistry of dolomite formation. In G. V. Chilingar, H. J. Bissel, and R. W. Fairbridge (Eds.), *Carbonate Rocks* (pp. 169–191). Amsterdam, Netherlands: Elsevier.
- HUANG, C. P., and W. STUMM. (1973). Specific adsorption of cations on hydrous  $\alpha$ -Al<sub>2</sub>O<sub>3</sub>. *J. Colloid Interface Sci.*, 22, 231–259.
- HUFFMAN, E. D. W., and H. A. STUBER. (1985). Analytical methodology for elemental analysis of humic substances. In G. R. Aiken et al. (Eds.), *Humic Substances in Soil, Sediment, and Water*, (pp. 433–455). New York: Wiley-Interscience.
- IMBODEN, D. M., and S. EMERSON. (1978). Natural radon and phosphorus as limnological tracers: horizontal and vertical eddy diffusion in Greifensee. *Limnol. Oceanogr.*, 23, 77–90.
- IMBODEN, D. M.; R. F. WEISS; H. CRAIG; R. L. MICHEL; and C. R. GOLDMAN. (1977). Lake Tahoe geochemical study: I. Lake chemistry and tritium mixing study. *Limnol. Oceanogr.*, 22, 1039–1051.
- JAMES, R. O., and M. G. MACNAUGHTON. (1977). The adsorption of aqueous heavy metals on inorganic

- minerals. *Geochim. Cosmochim. Acta*, 41, 1549–1555.
- JENNE, E. A. (1977). Trace element sorption by sediments and soils—sites and processes. In W. Chappel and K. Petersen (Eds.), *Symposium on Molybdenum in the Environment, Vol. 2* (pp. 425–553). New York: Marcel Dekker.
- JOHNSON, N. M.; C. T. DRISCOLL; J. S. EATON; G. E. LIKENS; and W. H. McDOWELL. (1981). "Acid rain," dissolved aluminum and chemical weathering at the Hubbard Brook Experimental Forest, New Hampshire. *Geochim. Cosmochim. Acta*, 45, 1421–1437.
- JONES, B. F. (1966). Geochemical evolution of closed basin water in the western Great Basin. *Second Symp. Salt, North. Ohio Geol. Soc.*, 1, 181–200.
- JONES, B. F., and A. S. VAN DENBURGH. (1966). Geochemical influences on the chemical character of closed lakes. *Hydrology of Lakes and Reservoirs. Proc. Int. Assoc. Sci. Hydrol. Publ.*, 70, 435–446.
- JONES, B. F.; H. P. EUGSTER; and S. L. RETTIG. (1977). Hydrochemistry of the Lake Magadi basin, Kenya. *Geochim. Cosmochim. Acta*, 41, 53–72.
- JONES, B. F.; V. C. KENNEDY; and G. W. ZELLWEGER. (1974). Comparison of observed and calculated concentrations of dissolved Al and Fe in stream water. *Water Resources Res.*, 10, 91–793.
- JÖRESKOG, K. G.; J. E. KLOVAN; and R. A. REYMENT. (1976). *Geological Factor Analysis*. Amsterdam, Netherlands: Elsevier.
- JUNGE, C. E., and R. T. WERBY. (1958). The concentration of chloride, sodium, potassium, calcium, and sulfate in rain water over the United States. *J. Meteorol.*, 15, 417–425.
- KAPLAN, I. R., and S. C. RITTENBERG. (1964). Microbiological fractionation of sulfur isotopes. *J. Gen. Microbiol.*, 34, 195–212.
- KARICKHOFF, S. W. (1984). Organic pollutant sorption in aquatic systems. *Journal of Hydraulic Engineering*, 110, 707–735.
- KEENE, W. C., and J. N. GALLOWAY. (1984). Organic acidity in precipitation of North America. *Atmos. Environment*, 18, 2491–2497.
- KELLOGG, W. W.; R. D. CADLE; E. R. ALLEN; A. LAZRUS; and E. A. MARTELL. (1972). The sulfur cycle. *Science*, 175, 587–596.
- KENNEDY, V. C. (1971). Silica variation in stream water with time and discharge. *Nonequilibrium Systems in Natural Water Chemistry* (pp. 94–130). *Adv. Chem. Ser. 106*. Washington, DC: American Chemical Society.
- KENNEDY, V. C., and R. L. MALCOLM. (1977). Geochemistry of the Mattole River of Northern California. *U.S. Geological Survey Open-File Report 78–205*.
- KENT, D. B.; J. A. DAVIS; L. C. D. ANDERSON; B. A. REA; and T. D. WAITE. (1994). Transport of chromium and selenium in the suboxic zone of a shallow aquifer: Influence of redox and adsorption reactions. *Water Resources Research*, 30, 1099–1114.
- KHARAKA, Y. K., and F. A. W. BERRY. (1973). Simultaneous flow of water and solutes through geological membranes: I. Experimental investigation. *Geochim. Cosmochim. Acta*, 37, 2577–2603.
- KHARAKA, Y. K.; W. D. GUNTER; P. K. AGGARWAL; E. H. PERKINS; and J. D. DEBRAAL. (1988). SOLMINEQ.88: A computer program for geochemical modeling of water-rock interactions. *U.S. Geological Survey Investigations Report 88–4277*.
- KINSMAN, D. J. J. (1966). Gypsum and anhydrite of Recent age, Trucial Coast, Persian Gulf. *Proc. Second Symp. Salt, North. Ohio Geol. Soc.*, 1, 302–326.
- KINSMAN, D. J. J. (1969). Modes of formation, sedimentary associations and diagnostic features of shallow-water and supratidal evaporites. *Am. Assoc. Pet. Geol. Bull.*, 53, 830–840.
- KINSMAN, D. J. J. (1976). Evaporites: Relative humidity control of primary mineral facies. *J. Sediment. Petrol.*, 46, 273–279.
- KLOVAN, J. E. (1975). R- and Q-mode factor analysis. In R. B. McCammon (Ed.), *Concepts in Geostatistics*, (pp. 21–69). New York: Springer-Verlag.
- KREITLER, C. W., and D. C. JONES (1975). Natural soil nitrate: the cause of the nitrate contamination of ground water in Runnels County, Texas. *Ground Water*, 13, 53–61.
- KROUSE, H. R. (1980). Sulfur isotopes in our environment. In P. Fritz and J. C. Fontes (Eds.), *Environmental Isotope Geochemistry* (pp. 437–471). New York: Elsevier.
- KRUG, E. C., and C. R. FRINK. (1983). Acid rain on acid soil: A new perspective. *Science*, 221, 520–525.
- LANDOLT, W., and T. KELLER. (1985). Uptake and effects of air pollutants on woody plants. *Experientia*, 41, 301–310.

- LANGMUIR, D. (1971). The geochemistry of some carbonate groundwaters in central Pennsylvania. *Geochim. Cosmochim. Acta*, 35, 1023–1045.
- LANGMUIR, D. (1978). Uranium solution-mineral equilibria at low temperatures with applications to sedimentary ore deposits. *Geochim. Cosmochim. Acta*, 42, 547–579.
- LASAGA, A. C.; J. M. SOLER; J. GANOR; T. E. BURCH; and K. L. NAGY. (1994). Chemical weathering rate laws and global geochemical cycles. *Geochim. Cosmochim. Acta*, 58, 2361–2386.
- LAWRENCE, J. R.; J. I. DREVER; T. F. ANDERSON; and H. K. BRUECKNER. (1979). Importance of alteration of volcanic material in the sediments of Deep Sea Drilling Site 323: Chemistry,  $^{18}\text{O}/^{16}\text{O}$  and  $^{87}\text{Sr}/^{86}\text{Sr}$ . *Geochim. Cosmochim. Acta*, 43, 573–588.
- LAWRENCE, J. R., and H. P. TAYLOR. (1971). Deuterium and oxygen-18 correlation: Clay minerals and hydroxides in Quaternary soils compared to meteoric waters. *Geochim. Cosmochim. Acta*, 35, 993–1003.
- LAZERTE, B. D. (1984). Forms of aqueous aluminium in acidified catchments of central Ontario: A methodological analysis. *Can. J. Fisheries Aquatic Sci.*, 41, 766–776.
- LECKIE, J. O., and R. O. JAMES. (1974). Control mechanisms for trace metals in natural waters. In A. J. Rubin (Ed.), *Aqueous-Environmental Chemistry of Metals* (pp. 1–76). Ann Arbor, MI: Ann Arbor Science Publishers.
- LEENHEER, J. A.; R. L. MALCOLM; P. W. MCKINLEY; and L. A. ECCLES. (1974). Occurrence of dissolved organic carbon in selected groundwater samples in the United States. *U.S. Geol. Surv. Journal of Research*, 2, 361–369.
- LEENHEER, J. A.; D. M. MCKNIGHT; E. M. THURMAN; and P. MACCARTHY. (1994). Structural components and proposed structural models of fulvic acid from the Suwannee River. In R. C. Averett, J. A. Leenheer, D. M. McKnight, and K. A. Thorn (Eds.), *Humic Substances in the Suwannee River, Georgia: Interactions, Properties, and Proposed Structures*, (pp. 195–211). U.S. Geological Survey Water-Supply Paper 2373.
- LERMAN, A. (1979). *Geochemical Processes*. New York: Wiley-Interscience.
- LÉTOLLE, R. (1980). Nitrogen-15 in the natural environment. In P. Fritz and J. C. Fontes (Eds.), *Handbook of Environmental Isotope Geochemistry* (pp. 407–433). New York: Elsevier.
- LI, Y. H.; J. L. BISCHOFF; and G. MATHIEU. (1969). The migration of manganese in the Arctic Basin sediment. *Earth Planet. Sci. Lett.*, 7, 265270.
- LIKENS, G. E.; F. H. BORMANN; R. S. PIERCE; J. S. EATON; and N. M. JOHNSON. (1977). *Biogeochemistry of a Forested Ecosystem*. New York: Springer-Verlag.
- LIKENS, G. E., and F. H. BORMANN. (1995). *Biogeochemistry of a Forested Ecosystem* (2nd ed.) New York: Springer-Verlag.
- LINDBERG, R. D., and D. D. RUNNELLS. (1984). Ground water redox reactions: An analysis of equilibrium state applied to Eh measurements and geochemical modeling. *Science*, 225, 925–927.
- LIVINGSTONE, D. A. (1963). *Chemical composition of rivers and lakes. U.S. Geological Survey Professional Paper 440G*.
- LOVETT, G. M.; W. A. REINERS; and R. K. OLSON. (1982). Cloud droplet deposition in subalpine balsam fir forests: Hydrological and chemical inputs. *Science*, 218, 1303–1305.
- LUNDEGARD, P. D., and Y. K. KHARAKA. (1994). Distribution and occurrence of organic acids in subsurface waters. In E. D. Pittman and M. D. Lewan (Eds.), *Organic Acids in Geological Processes* (pp. 40–69). New York: Springer-Verlag.
- MACKAY, D.; W. Y. SHIU; and K. C. MA. (1992). *Illustrated Handbook of Physical-Chemical Properties and Environmental Fate for Organic Chemicals*. Boca Raton, FL: Lewis Publishers.
- MADÉ, B.; A. CLEMENT; and B. FRITZ. (1990). Modélisation cinétique et thermodynamique de l'altération: le modèle géochimique KINDIS. *C.R. Acad. Sci. Paris*, 310, II, 31–36.
- MADÉ, B., and B. FRITZ. (1992). Theoretical approach and modelling of the dissolution and precipitation of minerals under kinetic control. In Y. K. Kharaka and A. S. Maest (Eds.), *Water-Rock Interaction* (pp. 101–105). Rotterdam, Netherlands: Balkema.
- MALCOLM, R. L. (1985). Geochemistry of stream fulvic and humic substances. In G. R. Aiken et al. (Eds.), *Humic Substances in Soil, Sediment, and Water* (pp. 181–209). New York: Wiley-Interscience.
- MALCOLM, R. L.; D. M. MCKNIGHT; and R. C. AVERETT. (1994). History and description of the Okefenokee Swamp. In R. C. Averett, J. A. Leenheer, D. M.

- McKnight, and K. A. Thorn (Eds.), *Humic Substances in the Suwannee River, Georgia: Interactions, Properties, and Proposed Structures* (pp. 1–12). U.S. Geological Survey Water-Supply Paper 2373.
- MARINSKY, J. A., and J. EPHRAIM. (1986). A unified physicochemical description of the protonation and metal ion complexation equilibria of natural organic acids (humic and fulvic acids). I. Analysis of the influence of polyelectrolyte properties on protonation equilibria in ionic media: Fundamental concepts. *Environ. Sci. Technol.*, 20, 349–354.
- MARTENS, C. S., and M. B. GOLDBERGER. (1978). Early diagenesis in transitional sedimentary environments of the White Oak River Estuary, North Carolina. *Limnol. Oceanogr.*, 23, 428–441.
- MARTIN, J., and M. MEYBECK. (1979). Elemental mass-balance of material carried by major world rivers. *Mar. Chem.*, 7, 173–206.
- MASON, R. P.; W. F. FITZGERALD; and F. M. M. MOREL. (1994). The biogeochemical cycling of elemental mercury: Anthropogenic influences. *Geochim. Cosmochim. Acta*, 58, 3191–3198.
- MAST, M. A., and J. I. DREVER. (1987). The effect of oxalate on the dissolution rates of oligoclase and tremolite. *Geochim. Cosmochim. Acta*, 51, 2559–2568.
- MAST, M. A.; J. I. DREVER; and J. BARON. (1990). Chemical weathering in the Loch Vale Watershed, Rocky Mountain National Park, Colorado. *Water Resources Research*, 26, 2971–2978.
- MATZNER, E. (1986). Deposition/canopy interactions in two forest ecosystems of Northwest Germany. In H. W. Georgii (Ed.), *Atmospheric Pollution in Forested Areas* (pp. 247–462). Dordrecht, Netherlands: Reidel.
- MAZOR, E. (1991). *Applied Chemical and Isotopic Groundwater Hydrogeology*. New York: Halstead Press.
- MAZOR, E. (1992). Reinterpretation of  $^{36}\text{Cl}$  data: Physical processes, hydraulic interconnections and age estimates in groundwater systems. *Applied Geochemistry*, 7, 351–360.
- MAZOR, E. (1993). Chlorine-36 data and basic concepts of hydrology—Comment on F. M. Phillips' comment with special reference to the Great Artesian Basin. *Applied Geochemistry*, 8, 649–651.
- MAZOR, E. (1993). Some basic principles of  $^{36}\text{Cl}$  hydrology: a reply to the discussion by Kellett, Evans, Allan, and Fifield. *Applied Geochemistry*, 8, 659–662.
- MCCARTHER, J. M.; J. V. TURNER; W. B. LYONS; A. O. OSBORN; and M. F. THIRWALL. (1991). Hydrochemistry on the Yilgarn Block, Western Australia: Ferrololysis and mineralisation in acidic brines. *Geochim. Cosmochim. Acta*, 55, 1273–1288.
- MCKNIGHT, D. M., and K. E. BENCALA. (1990). The chemistry of iron, aluminum, and dissolved organic material in three acidic, metal-enriched, mountain streams, as controlled by watershed and in-stream processes. *Water Resources Res.*, 26, 3087–3100.
- MCKNIGHT, D. M.; E. M. THURMAN; R. L. WERSHAW; and H. HEMOND. (1985). Biogeochemistry of aquatic humic substances in Thoreau's Bog, Concord, Massachusetts. *Ecology*, 66, 1339–1352.
- MEANS, J. L.; D. A. CRERAR; M. P. BORCSIK; and J. O. DUGUID. (1978). Adsorption of Co and selected actinides by Mn and Fe oxides in soils and sediments. *Geochim. Cosmochim. Acta*, 42, 1763–1774.
- MELCHIOR, D. C., and R. L. BASSETT, (Eds.). (1990). *Chemical Modeling of Aqueous Systems II*. American Chemical Society Symposium Series 416. Washington, DC: American Chemical Society.
- MEYBECK, M. (1979). Concentrations des eaux fluviales en éléments majeurs et apports en solution aux océans. *Rev. Géol. Dyn. Géogr. Phys.*, 21, 215–246.
- MEYBECK, M. (1986). Composition chimique des ruisseaux non pollués de France. *Sci. Géol. Bull.*, 39, 3–77.
- MEYBECK, M. (1987). Global chemical weathering of surficial rocks estimated from river dissolved load. *Am. J. Sci.*, 287, 401–428.
- MILLER, E. K.; J. D. BLUM; and A. J. FRIEDLAND. (1993). Determination of soil exchangeable-cation loss and weathering rates using Sr isotopes. *Nature*, 362, 438–441.
- MILLER, W. R., and J. I. DREVER. (1977a). Chemical weathering and related controls on surface water chemistry in the Absaroka Mountains, Wyoming. *Geochim. Cosmochim. Acta*, 41, 1693–1702.
- MILLER, W. R., and J. I. DREVER. (1977b). Water chemistry of a stream following a storm, Absaroka Mountains, Wyoming. *Geol. Soc. Amer. Bull.*, 88, 286–290.

- MOHN, W. W., and J. M. TIEDJE. (1992). Microbial reductive dehalogenation. *Microbiological Reviews*, 56, 482–507.
- MONNIN, C., and J. SCHOTT. (1984). Determination of the solubility products of sodium carbonate minerals and an application to trona deposition in Lake Magadi (Kenya). *Geochim. Cosmochim. Acta*, 48, 571–581.
- MOREL, F., and J. G. HERING. (1993). *Principles and Applications of Aquatic Chemistry*. New York: Wiley.
- MORSE, J. W. (1974a). Dissolution kinetics of calcium carbonate in sea water: III. A new method for the study of reaction kinetics. *Am. J. Sci.*, 274, 97–101.
- MORSE, J. W. (1974b). Dissolution kinetics of calcium carbonate in seawater: V. Effects of natural inhibitors and the position of the lysocline. *Am. J. Sci.*, 274, 638–647.
- MORSE, J. W., and R. A. BERNER. (1972). Dissolution kinetics of calcium carbonate in seawater: II. A kinetic origin for the lysocline. *Am. J. Sci.*, 272, 840–851.
- MORSE, J. W., and F. T. MACKENZIE. (1990). *Geochemistry of Sedimentary Carbonates*. Amsterdam, Netherlands: Elsevier.
- MUCCI, A.; J. W. MORSE; and M. S. KAMINSKY. (1985). Auger spectroscopy analysis of magnesian calcite overgrowths precipitated from seawater and solutions of similar composition. *Am. J. Sci.*, 285, 289–305.
- MURPHY, K. M. (1993). *Kinetics of albite dissolution: The effect of grain size*. Unpublished M.S. Thesis, Laramie, WY: University of Wyoming.
- MURRAY, J. W. (1975). The interaction of metal ions at the manganese dioxide-solution interface. *Geochim. Cosmochim. Acta*, 39, 505–520.
- NADP. (1987). *NADP Annual Data Summary: Precipitation Chemistry in the United States, 1985*. Washington, DC: National Atmospheric Deposition Program.
- NAPAP. (1991). *Acidic Deposition: State of Science and Technology. Summary of the U.S. National Acid Precipitation Assessment Program*. Washington, DC: U.S. Government Printing Office.
- NAPAP. (1991). *National Acid Precipitation Assessment Program: 1990 Integrated Assessment Report*. Washington DC: NAPAP Office of the Director.
- NARASIMHAN, T. N.; A. F. WHITE; and T. TOKUNGA. (1986). Groundwater contamination from an inactive uranium mill tailings pile 2. Application of a dynamic mixing model. *Water Resources Res.*, 22, 1820–1834.
- NATIONAL RESEARCH COUNCIL. (1994). *Alternatives for Ground Water Cleanup*. Washington, DC: National Academy Press.
- NEAL, C. (1988a). Aluminium solubility in acid waters. *Earth & Planetary Sci. Lett.*, 86, 105–112.
- NEAL, C. (1988b). Aluminium solubility relationships in acid waters; a practical example of the need for a radical reappraisal. *J. Hydrol.*, 104, 141–159.
- NEAL, C., and D. M. COOPER. (1983). Extended version of Gouy-Chapman electrostatic theory as applied to the exchange behavior of clay in natural waters. *Clays & Clay Minerals*, 31, 367–376.
- NEAL, C.; J. MULDER; N. CHRISTOPHERSEN; M. NEAL; D. WATERS; and R. C. FERRIER. (1990). Limitations to the understanding of ion exchange and solubility controls for acidic Welsh, Scottish, and Norwegian sites. *J. Hydrol.*, 116, 11–23.
- NEAL, C.; C. J. SMITH; J. WALLS; P. BILLINGHAM; S. HILL; and M. NEAL. (1990). Hydrogeochemical variations in Hafren forest stream waters, mid-Wales. *J. Hydrol.*, 116, 185–200.
- NELSON, W. H., and W. G. PIERCE. (1968). Wapiti formation and Trout Peak trachyandesite, northern Wyoming, U.S.A. *Schweiz. Mineral. Petrogr. Mitt.*, 49, 47–64.
- NORDSTROM, D. K. (1982). The effect of sulfate on aluminum concentrations in natural waters: Some stability relations in the system  $Al_2O_3$ - $SO_3$ - $H_2O$  at 298K. *Geochim. Cosmochim. Acta*, 46, 681–692.
- NORDSTROM, D. K. and J. L. MUNOZ. (1994). *Geochemical Thermodynamics (2nd ed.)*. Boston: Blackwell Scientific Publications.
- NORTON, D., and R. KNAPP (1977). Transport phenomena in hydrothermal systems: The nature of porosity. *Am. J. Sci.*, 277, 913–936.
- NRIAGU, J. O. (1972). Stability of vivianite and ion pair formation in the system  $Fe_3(PO_4)_2$ - $H_3PO_4$ - $H_2O$ . *Geochim. Cosmochim. Acta*, 36, 454–470.
- NRIAGU, J. O.; A. L. W. KEMP; H. T. K. WONG; and N. HARPER. (1979). Sedimentary record of heavy metal pollution in Lake Erie. *Geochim. Cosmochim. Acta*, 43, 247–258.

- O'NEIL, J. R. (1979). Stable isotope geochemistry of rocks and minerals. In E. Jäger and J. C. Hunziker (Eds.), *Lectures in Isotope Geology* (pp. 236–263). New York: Springer-Verlag.
- OELKERS, E. H.; J. SCHOTT; and J.-L. DEVIDAL. (1994). The effect of aluminum, pH, and chemical affinity on the rates of aluminosilicate dissolution reactions. *Geochim. Cosmochim. Acta*, 58, 2011–2024.
- OXBURGH, R.; J. I. DREVER; and Y. SUN. (1994). Mechanism of plagioclase dissolution in acid solution at 25°C. *Geochim. Cosmochim. Acta*, 58, 661–669.
- PAČES, T. (1972). Chemical characteristics and equilibrium in natural water-felsic rock-CO<sub>2</sub> system. *Geochim. Cosmochim. Acta*, 36, 217–240.
- PAČES, T. (1973). Steady-state kinetics and equilibrium between ground water and granitic rock. *Geochim. Cosmochim. Acta*, 37, 2641–2663.
- PAČES, T. (1976). Kinetics of natural water systems. *Interpretation of Environmental Isotope and Hydrochemical Data in Groundwater Hydrology* (pp. 85–108). Vienna, Austria: International Atomic Energy Agency.
- PAČES, T. (1983). Rate constants of dissolution derived from the measurements of mass balance in hydrological catchments. *Geochim. Cosmochim. Acta*, 47, 1855–1864.
- PARKHURST, D. L. (1990). Ion association models and mean activity coefficients of various salts. In D. C. Melchior and R. L. Bassett (Eds.), *Chemical Modeling of Aqueous Systems II. American Chemical Society Symposium Series 416*, (pp. 30–43). Washington, DC: American Chemical Society.
- PARKHURST, D. L. (1995). User's Guide to PHREEQC—A Computer Program for Speciation, Reaction-Path, Advective-Transport, and Inverse Geochemical Calculations. *U.S. Geological Survey Water-Resources Investigations Report 95–4227*.
- PARKHURST, D. L.; L. N. PLUMMER; and D. C. THORSTENSON. (1982). BALANCE—A computer program for calculating mass transfer for geochemical reactions in ground water. *U.S. Geological Survey Water-Resources Investigations 82–14*.
- PARKHURST, D. L.; D. C. THORSTENSON; and L. N. PLUMMER. (1980). PHREEQE—A computer program for geochemical calculations. *U.S. Geological Survey Water-Resources Investigations 80–96*.
- PARKS, G. A. (1965). The isoelectric points of solid oxides, solid hydroxides, and aqueous hydroxo complex systems. *Chem. Rev.*, 65, 177–198.
- PATTERSON, R. J., and D. J. J. KINSMAN. (1977). Marine and continental groundwater sources in a Persian Gulf coastal sabkha. *Am. Assoc. Pet. Geol. Stud. Geol.*, 4, 381–397.
- PEARCE, A. J.; M. K. STEWART; and M. G. SKLASH. (1986). Storm runoff generation in humid headwater catchments 1. Where does the water come from? *Water Resources Research*, 22, 1263–1272.
- PERDUE, E. M. (1985). Acidic functional groups of humic substances. In G. R. Aiken et al. (Eds.), *Humic Substances in Soil, Sediment, and Water* (pp. 493–526). New York: Wiley-Interscience.
- PETERS, N. E. (1984). Hydrologic analysis of Woods and Panther Lake basins in the west-central Adirondack Mountains, New York. *The Integrated Lake-Watershed Acidification Study 4. Summary of Major Results*. Palo Alto, CA: Electric Power Research Institute.
- PETERS, N. E. (1989). Atmospheric deposition of sulfur to a granite outcrop in the piedmont of Georgia, U.S.A. *International Association of Hydrologic Sciences*, 179, 173–180.
- PETROVIC, R.; R. A. BERNER; and M. B. GOLDBABER. (1976). Rate control in dissolution of alkali feldspars. I. Study of residual feldspar grains by X-ray photoelectron spectroscopy. *Geochim. Cosmochim. Acta*, 45, 2123–2135.
- PHILLIPS, F. M. (1993). Comment on "Reinterpretation of <sup>36</sup>Cl data: physical processes, hydraulic interconnections and age estimates in groundwater systems" by E. Mazor. *Applied Geochemistry*, 8, 643–647.
- PHILLIPS, F. M. (1995). The use of isotopes and environmental tracers in subsurface hydrology. *Reviews of Geophysics, Supplement, U.S. National Report to International Union of Geodesy and Geophysics 1991–1994* (pp.1029–1033).
- PHILLIPS, F. M.; H. W. BENTLEY; S. N. DAVIS; D. ELMORE; and G. B. SWANICK. (1986). Chlorine 36 dating of very old groundwater 2. Milk River Aquifer, Alberta, Canada. *Water Resources Res.*, 22, 2003–2016.
- PIPER, A. M. (1944). A graphic procedure in the geochemical interpretation of water analyses. *Am. Geophys. Union Trans.*, 25, 914–923.

- PITTMAN, E. D., and M. D. LEWAN. (Eds.). (1994). *Organic Acids in Geological Processes*. New York: Springer-Verlag.
- PITZER, K. S. (1973). Thermodynamics of electrolytes I: Theoretical basis and general equations. *J. Phys. Chem.*, 77, 268–277.
- PITZER, K. S. (1979). Theory: Ion interaction approach. In R. M. Pytkowicz (Ed.), *Activity Coefficients in Electrolyte Solutions, Vol. 1* (pp. 157–208). Boca Raton, FL: CRC Press.
- PITZER, K. S. (1980). Electrolytes. From dilute solutions to fused salts. *J. Am. Chem. Soc.*, 102, 2902–2906.
- PITZER, K. S. (1987). Electrolyte theory—improvements since Debye-Hückel. *Acc. Chem. Res.* 10, 371–377.
- PLUMMER, L. N. (1977). Defining reactions and mass transfer in part of the Floridan Aquifer. *Water Resources Res.*, 13, 801–812.
- PLUMMER, L. N. (1992). Geochemical modeling of water-rock interaction: Past, present, future. In Y. K. Kharaka and A. S. Maest (Eds.), *Water-Rock Interaction* (pp. 23–33). Rotterdam, Netherlands: Balkema.
- PLUMMER, L. N., and W. BACK. (1980). The mass balance approach: application to interpreting the chemical evolution of hydrologic systems. *Am. J. Sci.*, 280, 130–142.
- PLUMMER, L. N.; J. F. BUSBY; R. W. LEE; and B. B. HANSHAW. (1990). Geochemical modeling of the Madison aquifer in parts of Montana, Wyoming, and South Dakota. *Water Resources Research*, 26, 1981–2014.
- PLUMMER, L. N., and E. BUSENBERG. (1982). The solubilities of calcite, aragonite and vaterite in CO<sub>2</sub>-H<sub>2</sub>O solutions between 0 and 90°C, and an evaluation of the aqueous model for the system CaCO<sub>3</sub>-CO<sub>2</sub>-H<sub>2</sub>O. *Geochim. Cosmochim. Acta*, 46, 1011–1040.
- PLUMMER, L. N., and F. T. MACKENZIE. (1974). Predicting mineral solubility from rate data: application to the dissolution of magnesian calcites. *Am. J. Sci.*, 274, 61–83.
- PLUMMER, L. N.; D. L. PARKHURST; G. W. FLEMING; and S. A. DUNKLE. (1988). A Computer Program Incorporating Pitzer's Equations for Calculation of Geochemical Reactions in Brines. *U.S. Geological Survey Water-Resources Investigations Report* 88–4153.
- PLUMMER, L. N.; E. C. PRESTEMON; and D. L. PARKHURST. (1991). An Interactive Code (NET-PATH) for Modeling *Net* Geochemical Reactions along a Flow Path. U.S. Geological Survey Water-Resources Investigations Report 91–4078.
- PLUMMER, L. N.; E. C. PRESTEMON; and D. L. PARKHURST. (1994). An Interactive Code (NET-PATH) for Modeling *Net* Geochemical Reactions along a Flow Path. Version 2.0. U.S. Geological Survey Water-Resources Investigations Report 94–4169.
- PLUMMER, L. N., and T. M. L. WIGLEY. (1976). The dissolution of calcite in CO<sub>2</sub>-saturated solutions at 25°C and 1 atmosphere total pressure. *Geochim. Cosmochim. Acta*, 40, 191–202.
- POSJNAK, E. (1940). Deposition of calcium sulfate from sea water. *Am. J. Sci.*, 238, 559–568.
- PRINZ, B.; G. M. H. KRAUSE; and H. STRATMANN. (1982). *Forest damage in the Federal Republic of Germany*. Essen, Germany: Land Institute for Pollution Control of the Land North-Rhine Westphalia.
- PROBST, A.; E. DAMBRINE; D. VIVELLE; and B. FRITZ. (1990). Influence of acid atmospheric inputs on surface water chemistry and mineral fluxes in a declining spruce stand within a small granitic catchment (Vosges Massif, France). *J. Hydrology*, 116, 101–124.
- PROBST, J. L.; J. MORTATTI; and Y. TARDY. (1994). Carbon river fluxes and weathering CO<sub>2</sub> consumption in the Congo and Amazon river basins. *Applied Geochem.*, 9, 1–13.
- RASMUSON, A., and I. NERETNIEKS. (1986). Radionuclide transport in fast channels in crystalline rock. *Water Resources Res.*, 22, 1247–1256.
- REDFIELD, A. C.; B. J. KETCHUM; and F. A. RICHARDS. (1963). The influence of organisms on the composition of sea water. In M. N. Hill (Ed.), *The Sea (Vol. 2)*, (pp. 26–77). New York: Wiley-Interscience.
- REEDER, R. J., (Ed.). (1983). *Carbonates: Mineralogy and Chemistry*. Reviews in Mineralogy (Vol. 11). Washington, DC: Mineralogical Society of America.
- REEDER, S. W.; B. HITCHON; and A. A. LEVINSON. (1972). Hydrogeochemistry of the surface waters of the Mackenzie River drainage basin, Canada: I.



- Factors controlling inorganic composition. *Geochim. Cosmochim. Acta*, 36, 825–865.
- REHFUESS, K. E. (1981). Über die Wirkungen der säuren Niederschläge in Waldökosystemen. *Forstwissenschaftliches Zentralblatt*, 100, 363–381.
- REUSS, J. O. (1983). Implications of the calcium-aluminum exchange system for the effect of acid precipitation on soils. *J. Environ. Qual.*, 12, 591–595.
- REUSS, J. O., and D. W. JOHNSON. (1986). *Acid Deposition and the Acidification of Soils and Waters. Ecological Studies 59*. New York: Springer-Verlag.
- REYNOLDS, R. C. (1971). Clay mineral formation in an alpine environment. *Clays and Clay Minerals*, 19, 361–374.
- REYNOLDS, R. C. (1980). Interstratified clay minerals. In G. W. Brindley and G. Brown (Eds.), *Crystal Structures of Clay Minerals and their X-Ray Identification*, (pp. 249–303). London, England: The Mineralogical Society.
- REYNOLDS, R. C. (1985). *NEWMOD© a Computer Program for the Calculation of One-Dimensional Diffraction Patterns of Mixed-Layer Clays*. Hanover, NH: R. C. Reynolds.
- REYNOLDS, R. C. (1988). Mixed layer chlorite minerals. In S. W. Bailey (Ed.), *Hydrous Phyllosilicates* (pp. 601–629). Washington, DC: Mineralogical Society of America.
- REYNOLDS, R. C., and J. HOWER. (1970). The nature of interlayering in mixed-layer illite/montmorillonites. *Clays & Clay Miner.*, 18, 25–36.
- REYNOLDS, R. C., and N. M. JOHNSON. (1972). Chemical weathering in the temperate glacial environment of the Northern Cascade Mountains. *Geochim. Cosmochim. Acta*, 36, 537–544.
- ROBERTS, W. M. B.; A. L. WALKER; and A. S. BUCHANAN. (1969). The chemistry of pyrite formation in aqueous solution and its relation to the depositional environment. *Miner. Deposita*, 4, 18–29.
- ROBIE, R. A.; B. S. HEMINGWAY; and J. R. FISHER. (1978). *Thermodynamic properties of minerals and related substances at 298.15 K and 1 bar (10<sup>5</sup> pascals) pressure and at higher temperatures*. U.S. Geol. Surv. Bull. 1452.
- ROOTH, C. G., and H. G. OSTLUND. (1972). Penetration of tritium into the Atlantic thermocline. *Deep-Sea Res.*, 19, 481–492.
- ROSENQVIST, I. T. (1978). Alternative sources for acidification of river water in Norway. *Sci. Total Environment*, 10, 39–49.
- RUNNELLS, D. D. (1969). Diagenesis, chemical sediments, and the mixing of natural waters. *J. Sedim. Petrol.*, 39, 1188–1201.
- RUNNELLS, D. D., and R. D. LINDBERG. (1990). Selenium in aqueous solutions: The impossibility of obtaining a meaningful Eh using a platinum electrode, with implications for modeling of natural waters. *Geology*, 18, 212–215.
- RUNNELLS, D. D., and R. E. SKODA. (1990). Redox modeling of arsenic in the presence of iron: Applications to equilibrium computer modeling. *Environmental Research Conference on Groundwater Quality and Waste Disposal*. EPRI EN-6749. Palo Alto, CA: Electric Power Research Institute.
- RUSSELL, K. L. (1970). Geochemistry and halmyrolysis of clay minerals, Rio Ameca, Mexico. *Geochim. Cosmochim. Acta*, 34, 893–907.
- SANGSTER, J. (1989). Octanol-water partition coefficients of simple organic compounds. *J. Phys. Chem. Ref. Data*, 18, 1111–1229.
- SAVIN, S. M. (1980). Oxygen and hydrogen isotope effects in low-temperature mineral-water interactions. In P. Fritz and J. C. Fontes (Eds.), *Handbook of Environmental Isotope Geochemistry* (pp. 283–327). New York: Elsevier.
- SAYLES, F. L., and P. C. MANGELSDORF. (1977). The equilibration of clay minerals with sea water: Exchange reactions. *Geochim. Cosmochim. Acta*, 41, 951–960.
- SAYLES, F. L., and P. C. MANGELSDORF. (1979). Cation-exchange characteristics of Amazon River suspended sediment and its reaction with seawater. *Geochim. Cosmochim. Acta*, 43, 757–779.
- SCHINDLER, P. W. (1981). Surface complexes at oxide-water interfaces. In M. A. Anderson and A. J. Rubin (Eds.), *Adsorption of Inorganics at Solid-Liquid Interfaces* (pp. 1–49). Ann Arbor, MI: Ann Arbor Science.
- SCHNOOR, J. L. (1990). Kinetics of chemical weathering: a comparison of laboratory and field weathering rates. In W. Stumm (Ed.), *Aquatic Chemical Kinetics* (pp. 475–504). New York: Wiley.

- SCHNOOR, J. L., and W. STUMM. (1985). Acidification of aquatic and terrestrial systems. In W. Stumm (Ed.), *Chemical Processes in Lakes* (pp. 311–338). New York: Wiley-Interscience.
- SCHOTT, J.; R. A. BERNER; and E. L. SJÖBERG. (1981). Mechanism of pyroxene and amphibole weathering—I. Experimental studies of iron-free minerals. *Geochim. Cosmochim. Acta*, 45, 2123–2135.
- SCHÜTT, P., and E. B. COWLING. (1985). Waldsterben—A general decline of forests in central Europe: Symptoms, development, and possible causes of a beginning breakdown of forest ecosystems. *Plant Disease*, 69, 548–558.
- SCHWARZENBACH, R. P.; P. M. GSCHWEND; and D. M. IMBODEN. (1993). *Environmental Organic Chemistry*. New York: Wiley-Interscience.
- SCHWEDA, P. (1990). *Kinetics and Mechanisms of Alkali Feldspar Dissolution at Low Temperatures*. Ph.D. Dissertation. Stockholm, Sweden: Stockholm University.
- SEDLAK, D. L., and J. HOIGNÉ. (1993). The role of copper and oxalate in the redox cycling of iron in atmospheric waters. *Atmospheric Environment*, 27A, 2173–2185.
- SEIP, H. M.; D. DRABLØS; I. SEVALDRUD; and J. A. TIMBERLID. (1980). Acidification of freshwater—sources and mechanisms. In D. Drabløs and A. Tollan (Eds.), *Ecological Impact of Acid Precipitation* (pp. 358–366). Oslo-Ås: SNSF Project.
- SEIP, H. M.; L. MÜLLER; and A. NAAS. (1984). Aluminum speciation: Comparison of two spectrophotometric analytical methods and observed concentrations in some acidic aquatic systems in southern Norway. *Water, Air, and Soil Pollution*, 23, 81–98.
- SEIP, H. M., and A. TOLLAN. (1985). Acid Deposition. In J. C. Rodda (Ed.), *Facets of Hydrology II* (pp. 69–98). New York: Wiley.
- SHEPPARD, S. F. M.; R. L. NIELSEN; and H. P. TAYLOR. (1969). Oxygen and hydrogen isotope ratios of clay minerals from porphyry copper deposits. *Econ. Geol.*, 64, 755–777.
- SIEGENTHALER, U. (1979). Stable hydrogen and oxygen isotopes in the water cycle. In E. Jäger and J. C. Hunziger (Eds.), *Lectures in Isotope Geology* (pp. 264–273). New York: Springer-Verlag.
- SILLÉN, L. G., and A. E. MARTELL. (1971). *Stability Constants of Metal-Ion Complexes. Supplement 1*. Special Publication no. 25. London, England: The Chemical Society.
- SINGER, P. C., and W. STUMM. (1970). Acidic mine drainage: the rate determining step. *Science*, 167, 1121–1123.
- SJÖBERG, E. L., and D. T. RICKARD. (1985). The effect of added dissolved calcium on calcite dissolution kinetics in aqueous solutions at 25°C. *Chem. Geol.*, 49, 405–413.
- SKLASH, M. G.; M. K. STEWART; and A. J. PEARCE. (1986). Storm runoff generation in humid headwater catchments 2. A case study of hillslope and low-order stream response. *Water Resources Res.*, 22, 1263–1272.
- SMITH, C. L., and J. I. DREVER. (1976). Controls on the chemistry of springs at Teels Marsh, Mineral County, Nevada. *Geochim. Cosmochim. Acta*, 40, 1081–1093.
- SMITH, J. W. (1975). Stable isotope studies and biological element cycling. *Environ. Chem.*, 1, 1–21.
- SOIL SURVEY STAFF. (1992). *Keys to Soil Taxonomy*. SMSS Technical Monograph No. 19. Blacksburg, VA: Pocahontas Press, Inc.
- SOLLEY, W. B.; C. F. MERK; and R. R. PIERCE. (1988). Estimated use of water in the United States in 1985. *U.S. Geological Survey Circular 1004*.
- SPENCER, R. J.; H. P. EUGSTER; B. F. JONES; and S. L. RETTIG. (1985). Geochemistry of Great Salt Lake, Utah I: Hydrochemistry since 1850. *Geochim. Cosmochim. Acta*, 49, 727–738.
- SPOSITO, G. (1984). *The Surface Chemistry of Soils*. Oxford, England: Oxford University Press.
- SPOSITO, G. (1985). Chemical models of weathering in soils. In J. I. Drever (Ed.), *The Chemistry of Weathering* (pp. 1–18). Dordrecht, Netherlands: Reidel.
- SRODON, J.; D. J. MORGAN; E. V. ESLINGER; D. D. EBERL; and M. R. KARLINGER. (1986). Chemistry of illite/smectite and end-member illite. *Clays & Clay Minerals*, 34, 368–378.
- STALLARD, R. F. (1985). River chemistry, geology, geomorphology, and soils in the Amazon and Orinoco Basins. In J. I. Drever (Ed.), *The Chemistry of Weathering*, (pp. 293–316). Dordrecht, Netherlands: Reidel.
- STALLARD, R. F., and J. M. EDMOND. (1981). Geochemistry of the Amazon: I. Precipitation chemistry and the marine contribution to the dissolved

- load at the time of peak discharge. *J. Geophys. Res.*, *86*, 9844–9858.
- STALLARD, R. F., and J. M. EDMOND. (1983). Geochemistry of the Amazon: 2. The influence of the geology and weathering environment on the dissolved load. *J. Geophys. Res.*, *88*, 9671–9688.
- STALLARD, R. F., and J. M. EDMOND. (1987). Geochemistry of the Amazon: 3. Weathering chemistry and limits to dissolved inputs. *J. Geophys. Res.*, *92*, 8293–8302.
- STAUFFER, R. E. (1990). Granite weathering and the sensitivity of alpine lakes to acid deposition. *Limnology and Oceanography*, *35*, 1112–1134.
- STEELINK, C. (1985). Implications of elemental characteristics of humic substances. In G. R. Aiken et al. (Eds.), *Humic Substances in Soil, Sediment, and Water* (pp. 457–476). New York: Wiley-Interscience.
- STEFFEN, ROBERTSON, and KIRSTEN (BC), INC. (1989). Draft Acid Rock Drainage Technical Guide. Vancouver, British Columbia, Canada: British Columbia Acid Mine Drainage Task Force.
- STEVENS, F. J. (1985). Geochemistry of soil humic substances. In G. R. Aiken et al. (Eds.), *Humic Substances in Soil, Sediment, and Water*. (pp. 13–52). New York: Wiley-Interscience.
- STEVENS, F. J. (1994). *Humus Chemistry: Genesis, Composition, Reactions*. New York: Wiley.
- STEWART, F. H. (1963). Marine evaporites. *Data of Geochemistry* (6th ed.). U. S. Geological Survey Professional Paper 440Y.
- STILLINGS, L. L.; J. I. DREVER; S. L. BRANTLEY; Y. SUN; and R. OXBURGH. (1996). Rates of feldspar dissolution at pH 3–5 with 0–8 mM oxalic acid. *Chem. Geol.*, *132*, 79–89.
- STUMM, W. (1978). What is the  $p_e$  of the sea? *Thalassia Jugosl.*, *14*, 197–208.
- STUMM, W., (Ed.). (1990). *Aquatic Chemical Kinetics*. New York: Wiley.
- STUMM, W. (1992). *Chemistry of the Solid-Water Interface*. New York: Wiley-Interscience.
- STUMM, W., and P. BACCINI. (1978). Man-made perturbation of lakes. In A. Lerman (Ed.), *Lakes—Chemistry, Geology, Physics* (pp. 91–126). New York: Springer-Verlag.
- STUMM, W., and J. J. MORGAN. (1985). Comment on the conceptual significance of  $p_e$ . *Am. J. Sci.*, *285*, 856–859.
- STUMM, W., and J. J. MORGAN. (1996). *Aquatic Chemistry* (3rd ed.). New York: Wiley-Interscience.
- STUMM, W., and E. WIELAND. (1990). Dissolution of oxide and silicate minerals: Rates depend on surface speciation. In W. Stumm (Ed.), *Aquatic Chemical Kinetics* (pp. 367–400). New York: Wiley-Interscience.
- SUAREZ, D. L., and D. LANGMUIR. (1976). Heavy metal relationships in a Pennsylvania soil. *Geochim. Cosmochim. Acta*, *40*, 589–598.
- SULZBERGER, B. (1990). Photoredox reactions at hydrous metal oxide surfaces: A surface coordination chemistry approach. In W. Stumm (Ed.), *Aquatic Chemical Kinetics* (pp. 401–429). New York: Wiley-Interscience.
- SULZBERGER, B., and S. I. HUG. (1994). Light-induced processes in the aquatic environment. In G. Bidoglio and W. Stumm (Eds.), *Chemistry of Aquatic Systems: Local and Global Perspectives* (pp. 183–212). Dordrecht, Netherlands: Kluwer.
- SUNDA, W. G.; S. A. HUNTSMAN; and G. R. HARVEY. (1983). Photoreduction of manganese oxides in seawater and its geochemical and biological implications. *Nature*, *301*, 234–236.
- SVERDUP, H., and P. WARFVINGE. (1995). Estimating field weathering rates using laboratory kinetics. In A. F. White and S. L. Brantley (Eds.) *Chemical Weathering Rates of Silicate Minerals*. (pp. 485–541). Washington, DC: Mineralogical Society of America.
- SVERDRUP, H., and P. WARFVINGE. (1988). Weathering of primary silicate minerals in the natural soil environment in relation to a chemical weathering model. *Water, Air, and Soil Pollution*, *38*, 387–408.
- SVERDRUP, H. U. (1990). *The Kinetics of Base Cation Release due to Chemical Weathering*. Lund, Sweden: Lund University Press.
- SWOBODA-COLBERG, N. G.; and J. I. DREVER. (1993). Mineral dissolution rates in plot-scale field and laboratory experiments. *Chem. Geol.*, *105*, 51–69.
- TANG, D. H.; E. O. FRIND; and E. A. SUDICKY. (1981). Contaminant transport in fractured porous media: analytical solution for a single fracture. *Water Resources Res.*, *17*, 555–564.
- TESSENOW, U. (1974). Lösungs-, Diffusions-, und Sorptions-Prozesse in der Oberschicht von Seesedimenten. *Arch. Hydrobiol. Suppl.*, *47*, 1–79.

- TESSIER, A.; D. FORTIN; N. BELZILE; R. R. DEVITRE; and G. G. LEPPARD. (1996). Metal sorption to diagenetic iron and manganese oxyhydroxides and associated organic matter: Narrowing the gap between field and laboratory measurements. *Geochim. Cosmochim. Acta*, 60, 387–404.
- THOMPSON, J. B., JR. (1955). The thermodynamic basis for the mineral facies concept. *Am. J. Sci.*, 53, 65–103.
- THURMAN, E. M. (1985). *Organic Geochemistry of Natural Waters*. Dordrecht, Netherlands: Martinus Nijhoff/Dr W. Junk.
- TIPPING, E., and M. A. HURLEY. (1992). A unifying model of cation binding by humic substances. *Geochim. Cosmochim. Acta*, 56, 3627–3642.
- TRIPATHI, V. S. (1979). Comments on "Uranium solution-mineral equilibria at low temperatures with applications to sedimentary ore deposits." *Geochim. Cosmochim. Acta*, 43, 1989–1990.
- TRUESDALE, G. A.; A. L. DOWNING; and G. F. LOWDEN. (1955). The solubility of oxygen in pure water and in sea water. *J. Appl. Chem.*, 5, 53–62.
- TRUESDELL, A. H., and B. F. JONES. (1974). WATEQ, a computer program for calculating chemical equilibria of natural waters. *J. Res. U.S. Geol. Surv.*, 2, 233–274.
- TUREKIAN, K. K. (1971). Elements, geochemical distribution of. *Encyclopedia of Science and Technology*, Vol. 4. McGraw-Hill, New York, pp. 627–630.
- TURK, J. T., and N. E. SPAHR. (1991). Rocky Mountains. In D. Charles and S. Christie (Eds.), *Acid Deposition and Aquatic Ecosystems: Regional Case Studies* (pp. 471–501). New York: Springer-Verlag.
- ULRICH, B. (1983). An ecosystem oriented hypothesis on the effect of air pollution on forest ecosystems. *Ecological Effects of Acid Deposition*, Stockholm, Sweden: Swedish Environment Protection Board Report PM 1636, 221–231.
- ULRICH, B.; R. MAYER, and T. K. KHANNA. (1980). Chemical changes due to acid precipitation in a loess-derived soil in central Europe. *Soil Sci.*, 130, 193–199.
- U.S. ENVIRONMENTAL PROTECTION AGENCY. (1971). Inorganic Sulfur Oxidation by Iron-Oxidizing Bacteria. Water Pollution Control Research Series 14010-DAY-06/71. Washington, DC: U. S. Government Publications Office.
- U.S. NATIONAL ACID PRECIPITATION ASSESSMENT PROGRAM. (1991). *Acid Deposition: State of Science and Technology*. Washington, DC: U. S. Government Printing Office.
- USIGLIO, M. J. (1849). Etudes sur la composition de l'eau de la Méditerranée et sur l'exploitation des sels qu'elle contient. *Ann. Chim. Phys.*, 27, 172–191.
- VAN CAPPELLEN, P., and Y. WANG. (1996). Cycling of iron and manganese in surface sediments: A general theory for the coupled transport and reaction of carbon, oxygen, nitrogen, sulfur, iron, and manganese. *Am. J. Sci.*, 296, 197–243.
- VAN OLPHEN, H. (1963). *An Introduction to Clay Colloid Chemistry*. New York: Wiley-Interscience.
- VELBEL, M. A. (1985). Geochemical mass balances and weathering rates in forested watersheds of the southern Blue Ridge. *Am. J. Sci.*, 285, 904–930.
- VELBEL, M. A. (1986). The mathematical basis for determining rates of geochemical and geomorphic processes in small forested watersheds by mass balance: Examples and implications. In S. M. Coleman and D. P. Delthier (Eds.), *Rates of Chemical Weathering of Rocks and Minerals* (pp. 439–451). New York: Academic Press, Inc.
- VELBEL, M. A. (1989). Effect of chemical affinity on feldspar hydrolysis rates in two natural weathering systems. *Chem. Geol.*, 78, 245–253.
- VITOUSEK, P. M., and W. A. REINERS. (1975). Ecosystem succession and nutrient retention: A hypothesis. *Bioscience*, 25, 376–381.
- WAGMAN, D. D.; W. H. EVANS; V. B. PARKER; R. H. SCHUMM; I. HARLOW; S. M. BAILEY; K. L. CHURNEY; and R. L. NUTTALL. (1982). The NBS tables of chemical thermodynamic properties: Selected values for inorganic and C1 and C2 Organic substances in SI units. *J. Phys. Chem. Ref. Data*, 11 (Suppl. 2); 1–392.
- WALTON, A. W. (1978). Evaporites: Relative humidity control of primary mineral facies: a discussion. *J. Sedim. Petrol.*, 48, 1357–1359.
- WEARE, J. H. (1987). Models of mineral solubility in concentrated brines with application to field observations. *Thermodynamic Modeling of Geological Materials: Minerals, Fluids, and Melts* (pp. 143–176). Reviews in Mineralogy v. 17, Washington DC: Mineralogical Society of America.
- WEAVER, C. E. (1989). *Clays, Muds, and Shales. Developments in Sedimentology 44*. New York, Elsevier.

- WELCH, S. A., and W. J. ULLMAN (1993). The effect of organic acids on plagioclase dissolution rates and stoichiometry. *Geochim. Cosmochim. Acta*, 57, 2725–2736.
- WERSHAW, R. L. (1985). Application of nuclear magnetic resonance spectroscopy for determining functionality in humic substances. In G. R. Aiken et al. (Eds.), *Humic Substances in Soil, Sediment, and Water* (pp. 561–582). New York: Wiley-Interscience.
- WERSHAW, R. L., and G. R. AIKEN. (1985). Molecular size and weight measurements of humic substances. In G. R. Aiken et al. (Eds.), *Humic Substances in Soil, Sediment, and Water* (pp. 477–492). New York: Wiley-Interscience.
- WESOLOWSKI, D. J. (1992). Aluminum speciation and equilibria in aqueous solution: I. The solubility of gibbsite in the system Na–K–Cl–OH–Al(OH)<sub>3</sub> from 0 to 100°C. *Geochim. Cosmochim. Acta*, 56, 1065–1092.
- WESOLOWSKI, D. J., and D. A. PALMER. (1994). Aluminum speciation and equilibria in aqueous solution: V. Gibbsite solubility at 50°C and pH 3–9 in 0.1 molal NaCl solutions. *Geochim. Cosmochim. Acta*, 58, 2947–2970.
- WESTALL, J. C. (1987). Adsorption mechanisms in aquatic surface chemistry. In W. Stumm (Ed.), *Aquatic Surface Chemistry* (pp. 3–32). New York: Wiley.
- WESTALL, J. C., and H. HOHL (1980). A comparison of electrostatic models for the oxide/solution interface. *Adv. Colloid Interface Sci.*, 12, 265–294.
- WETZEL, R. G. (1983). *Limnology* (2nd ed.). Philadelphia, PA: Saunders.
- WHITE, A. F. (1983). Surface chemistry and dissolution kinetics of glassy rocks at 25°C. *Geochim. Cosmochim. Acta*, 47, 805–816.
- WHITE, A. F., and A. BLUM. (1995). Effects of climate on chemical weathering in watersheds. *Geochim. Cosmochim. Acta*, 59, 1729–1748.
- WHITE, A. F., and S. L. BRANTLEY, (Eds.). (1995). *Chemical Weathering Rates of Silicate Minerals*. Reviews in Mineralogy (Vol. 31). Washington, DC: Mineralogical Society of America.
- WHITE, A. F.; J. M. DELANEY; T. N. NARASIMHAN; and A. SMITH. (1984). Groundwater contamination from an inactive uranium mill tailings pile I. Application of a chemical mixing model. *Water Resources Res.*, 20, 1743–1752.
- WHITE, D. E., (1965). Saline waters of sedimentary rocks. Fluids in subsurface environments—A symposium., *Am. Assoc. Pet. Geol. Mem.*, 4, 342–366.
- WIEDER, R. K. (1993). Ion input/output budgets for five wetlands constructed for acid coal mine drainage treatment. *Water, Air, and Soil Pollution*, 71, 231–270.
- WIELAND, E., and W. STUMM. (1992). Dissolution kinetics of kaolinite in acidic aqueous solutions at 25°C. *Geochim. Cosmochim. Acta*, 56, 3339–3355.
- WIGLEY, T. M. L. (1976). Effect of mineral precipitation on isotopic composition and <sup>14</sup>C dating of ground water. *Nature*, 263, 219–221.
- WIGLEY, T. M. L., and L. N. PLUMMER. (1976). Mixing of carbonate waters. *Geochim. Cosmochim. Acta*, 40, 989–995.
- WIGLEY, T. M. L.; L. N. PLUMMER; and F. J. PEARSON. (1978). Mass transfer and carbon isotope evolution in natural water systems. *Geochim. Cosmochim. Acta*, 42, 1117–1139.
- WIKLANDER, L. (1980). Interaction between cations and anions influencing adsorption and leaching. In T. C. Hutchinson and M. Havas (Eds.), *Effects of Acid Precipitation on Terrestrial Ecosystems* (pp. 239–254). New York: Plenum.
- WILLEY, L. M.; Y. K. KHARAKA; T. S. PRESSER; J. B. RAPP; and I. BARNES. (1975). Short chain aliphatic acid anions in oil field waters and their contribution to the measured alkalinity. *Geochim. Cosmochim. Acta*, 39, 1707–1711.
- WILLIAMS, J. D. H.; J.-M. JAQUET; and R. L. THOMAS. (1976). Forms of phosphorus in the surficial sediments of Lake Erie. *J. Fish. Res. Can.*, 33, 413–429.
- WILLIAMS, P. M. (1971). The distribution and cycling of organic matter in the ocean. In S. D. Faust and J. V. Hunter (Eds.), *Organic compounds in aquatic environments* (pp. 145–164). New York: Marcel Dekker.
- WILSON, M. J., and P. H. NADEAU. (1985). Interstratified clay minerals and weathering processes. In J. I. Drever (Ed.), *The Chemistry of Weathering* (pp. 97–118). NATO ASI Series, Dordrecht, Netherlands: Reidel.
- WOLERY, T. J. (1979). Calculation of Chemical Equilibria Between Aqueous Solution and Minerals. the

- EQ3/6 Software Package. Lawrence Livermore Laboratory Report UCCR-52658.
- WOLLAST, R. (1967). Kinetics of the alteration of K-feldspar in buffered solutions at low temperature. *Geochim. Cosmochim. Acta*, 31, 635-648.
- WOLLAST, R. (1990). Rate and mechanism of dissolution of carbonates in the system  $\text{CaCO}_3$ - $\text{MgCO}_3$ . In W. Stumm (Ed.), *Aquatic Chemical Kinetics* (pp. 431-445). New York: Wiley.
- WRIGHT, R. F. (1983). Letter in *Science*, 225, 1426-1427.
- WRIGHT, R. F. (1984). Norwegian models for surface water chemistry: An overview. In J. L. Schnoor (Ed.), *Modeling of Total Acid Precipitation Impacts* (pp. 73-87). Ann Arbor, MI: Ann Arbor Science.
- WRIGHT, R. F. (1987). Influence of acid rain on weathering rates. In A. Lerman and M. Meybeck (Eds.), *Physical and Chemical Weathering in Geochemical Cycles* (pp. 181-196). NATO ASI Series, Dordrecht, Netherlands: Reidel.
- WRIGHT, R. F., and E. SNEKVIK. (1978). Acid precipitation: Chemistry and fish populations in 700 lakes in southernmost Norway. *Verhandlung der Internationalen Vereinigung für Theoretische und Angewandte Limnologie*, 20, 765-775.
- YAVITT, J. B., and T. J. FAHEY. (1985). Organic chemistry of the soil solution during snowmelt leaching in *Pinus contorta* forest ecosystems, Wyoming. In D. E. Caldwell, J. A. Brierly, and C. L. Brierly (Eds.), *Planetary Ecology* (pp. 485-496). New York: Van Nostrand Reinhold.
- ZHANG, J. W., and G. H. NANCOLLAS. (1990). Mechanisms of growth and dissolution of sparingly soluble salts. In M. F. Hochella, Jr., and A. F. White (Eds.), *Mineral-Water Interface Geochemistry* (pp. 365-396). Reviews in Mineralogy Vol. 23. Washington, DC: Mineralogical Society of America.
- ZOBRIST, J., and W. STUMM. (1981). Chemical dynamics of the Rhine catchment area in Switzerland: Extrapolation to the "pristine" Rhine river input into the ocean. *Proceedings of the Review and Workshop on River Inputs to Ocean Systems*. Rome, Italy: Food and Agriculture Organization.

# Glossary of Geological Terms

**Actinolite** A member of the amphibole group with an approximate formula  $\text{Ca}_2(\text{Fe,Mg})_5\text{Si}_8\text{O}_{22}(\text{OH})_2$ . Common in metamorphic rocks.

**Albite** The sodium end member of the feldspar series, formula  $\text{NaAlSi}_3\text{O}_8$ . A very common mineral in granitic and metamorphic rocks.

**Amphibole** Ferromagnesian mineral group common in intermediate igneous rocks such as diorite and andesite, and in metamorphic rocks. The chemical formula is  $\text{A}_{2-3}\text{B}_5(\text{Si,Al})_8\text{O}_{22}(\text{OH})_2$  where A is mainly Mg,  $\text{Fe}^{2+}$ , Ca or Na; B is mainly Mg,  $\text{Fe}^{2+}$ ,  $\text{Fe}^{3+}$ , and Al. Many individual names have been given to members of the group; probably the most familiar is *hornblende*.

**Amphibolite** (Commonly) a high-grade metamorphic rock containing a high percentage of amphibole, usually hornblende. Amphibolites often represent metamorphosed basalts.

**Analcite or Analcime** A member of the zeolite group of minerals, approximate formula  $\text{NaAlSi}_2\text{O}_6 \cdot \text{H}_2\text{O}$ . Analcite contains only Na as a cation and, compared to other zeolites, has a low Si/Al ratio, a low  $\text{H}_2\text{O}$  content, and a high thermal stability.

**Andesine** An intermediate member of the plagioclase feldspar series, with a composition range 70 to 50 percent albite, 30 to 50 percent anorthite.

**Andesite** An intermediate volcanic rock (chemically intermediate between rhyolite and basalt), normally consisting of plagioclase feldspar (andesine) and either hornblende, biotite, or pyroxene. Andesite is the fine-grained equivalent of diorite.

**Anhydrite** Anhydrous calcium sulfate,  $\text{CaSO}_4$ .

**Anorthite** The calcium end member of the plagioclase feldspar series, formula  $\text{CaAl}_2\text{Si}_2\text{O}_8$ .

**Apatite** A mineral group that is essentially calcium phosphate plus some other anion, formula  $\text{Ca}_5(\text{PO}_4)_3(\text{F, Cl, OH, } \frac{1}{2}\text{CO}_3)$ . Apatite is a common accessory mineral in granitic rocks, and is the common mineral of bones and teeth. It often contains large cations such as uranyl as impurities.

- Arkose** A sandstone containing 25 percent or more feldspar, commonly derived from erosion of a granitic rock.
- Basalt** A volcanic (fine-grained igneous) rock consisting of calcic plagioclase feldspar and pyroxene. Basalt is the common dark-colored volcanic rock and is almost the only volcanic rock formed in ocean basins.
- Bauxite** A rock or soil containing a high proportion of aluminum hydroxide.
- Beidellite** A member of the smectite clay mineral group with an idealized formula (Exch. Cation)<sub>0.33</sub>Al<sub>2.33</sub>Si<sub>3.67</sub>O<sub>10</sub>(OH)<sub>2</sub> · nH<sub>2</sub>O (see Chapter 4).
- Biotite** The common dark mica, formula K(Mg,Fe<sup>2+</sup>)<sub>3</sub>AlSi<sub>3</sub>O<sub>10</sub>(OH)<sub>2</sub> (see Chapter 4).
- Calcrete or Caliche** Calcium carbonate deposited in a soil; occurs in relatively dry climates.
- Chernozem** Black-colored (from organic matter) soil containing CaCO<sub>3</sub>, formed under cool to temperate semiarid conditions.
- Chert** A compact, siliceous rock made up of microcrystalline silica (usually quartz). Cherts are commonly formed by diagenesis of biogenic silica, less commonly from magadiite, hot springs, or, in the Precambrian, inorganic precipitation of silica.
- Chlorite** A group of minerals occurring in soils, sedimentary and metamorphic rocks, with an approximate general formula (Mg, Fe, Al)<sub>6</sub>(Si, Al)<sub>4</sub>O<sub>10</sub>(OH)<sub>8</sub> (see Chapter 4).
- Connate Water** Water trapped in a sedimentary rock at the time it was deposited (see Chapter 1).
- Detrital** Minerals/sediments/rocks derived from transport of solid grains from preexisting rocks. In contrast to chemical or biological precipitates.
- Diagenesis** Processes (physical and chemical) affecting a sediment/sedimentary rock after it is deposited, excluding those processes occurring at sufficiently high temperature to be considered metamorphic.
- Dike or Dyke** A tabular body of igneous rock that cuts across the structure of adjacent rocks or cuts massive rocks. Dikes usually appear to have resulted from intrusion of molten rock into a crack.
- Diorite** A coarse-grained (plutonic) igneous rock consisting largely of plagioclase feldspar (andesine) plus hornblende, biotite, or pyroxene. Diorite is chemically intermediate between granite and gabbro. If significant quartz is present, the rock is called a *quartz diorite*.
- Dolomite** A mineral CaMg(CO<sub>3</sub>)<sub>2</sub> or a rock composed dominantly of that mineral.
- Evaporite** Sedimentary rock formed of minerals precipitated by evaporation of water. Most evaporites were formed by evaporation of seawater and have gypsum and halite as the main minerals (see Chapter 15).
- Feldspar** The most abundant mineral group in the earth's crust. Commonly divided into the alkali feldspars KAlSi<sub>3</sub>O<sub>8</sub> (orthoclase, microcline) and NaAlSi<sub>3</sub>O<sub>8</sub> (albite), and the plagioclase feldspars, a solid solution series between albite (NaAlSi<sub>3</sub>O<sub>8</sub>) and anorthite



( $\text{CaAl}_2\text{Si}_2\text{O}_8$ ). Solid solution also occurs in the alkali feldspar series at high temperatures (volcanic rocks), giving the minerals sanidine (mostly K) and anorthoclase (Na + K).

**Felsic Rock** General term for light-colored rock consisting (usually) of feldspars and/or quartz.

**Ferrihydrite** A poorly-ordered hydrous ferric oxide, of approximate formula  $\text{Fe}(\text{OH})_3$ . The common ferric oxyhydroxide initially precipitated under earth-surface conditions (see Chapter 7); very important as a substrate for adsorption of heavy metals.

**Ferromagnesian Mineral** General term for dark-colored minerals containing high proportions of Fe and Mg. The common ferromagnesian minerals are pyroxenes, hornblende, olivine, and biotite.

**Forsterite** The Mg end-member olivine,  $\text{Mg}_2\text{SiO}_4$ .

**Gabbro** A coarse-grained igneous (plutonic) rock consisting largely of calcic plagioclase and pyroxene. The coarse-grained equivalent of basalt.

**Geothermal Gradient** The rate at which temperature increases with depth in the earth. Typical near-surface values are 2 to 3°C per 100 m.

**Gibbsite** Aluminum hydroxide,  $\text{Al}(\text{OH})_3$ .

**Glauconite** An iron-rich illitic clay mineral commonly formed as green pellets on the sea floor.

**Gneiss** A coarse-grained metamorphic rock in which the different minerals are, to a greater or lesser extent, segregated into bands. In mineralogy and chemistry, gneisses are often similar to granites.

**Granite** A coarse-grained igneous (plutonic) rock consisting principally of K-feldspar and quartz. Also used as a general term for any light-colored, coarse-grained igneous rock. Chemically, granites have high proportions of silica and potassium and low proportions of iron, magnesium, and calcium.

**Graywacke or Greywacke** A type of sandstone characterized by sand-size grains of quartz, feldspar, and rock fragments set in a matrix of clay.

**Gypsum** Hydrated calcium sulfate,  $\text{CaSO}_4 \cdot 2\text{H}_2\text{O}$ .

**Hematite** Ferric oxide,  $\text{Fe}_2\text{O}_3$ .

**Hornblende** The most common member of the amphibole group in igneous and high-grade metamorphic rocks. The approximate formula is  $(\text{Ca}, \text{Na})_{2-3}(\text{Mg}, \text{Fe}, \text{Al}, \text{Ti})_5(\text{Si}, \text{Al})_8\text{O}_{22}(\text{OH}, \text{F})_2$ .

**Igneous Rock** Rock formed by solidification of a silicate melt.

**Illite** A general term for clay minerals belonging to the mica group. Also used by some authors in a more restricted sense (see Chapter 4). Illite is the major mineral in ancient shales.

**Ilmenite** An iron-titanium oxide with ideal formula  $\text{FeTiO}_3$ .

**Kaolinite** A clay mineral, formula  $\text{Al}_2\text{Si}_2\text{O}_5(\text{OH})_4$  (see Chapter 4).

- Lamprophyre** An igneous rock with a characteristic texture, which occurs as dikes. The  $K_2O$  content is usually high, and biotite, hornblende, or pyroxene is usually the most abundant mineral.
- Laumontite** A calcium-rich zeolite, with an idealized formula  $CaAl_2Si_4O_{12} \cdot 4H_2O$  (the Si/Al ratio is quite variable in natural laumontites). Used as an example of a calcic zeolite in Chapter 10 because free-energy data happen to be available.
- Lepidocrocite** A common hydrated ferric oxide mineral, formula  $FeO(OH)$ .
- Mafic Rock** Rock (usually dark-colored) containing a high proportion of ferromagnesian minerals.
- Magadiite** A sodium silicate mineral,  $NaSi_7O_{13}(OH)_3 \cdot nH_2O$ , formed in saline-alkaline lakes. On diagenesis, magadiite converts to a chert with a characteristic surface texture.
- Magnetite** An iron oxide containing both ferrous and ferric iron, formula  $Fe_3O_4$ .
- Metadiorite** A metamorphosed diorite (or rock of similar composition that has been metamorphosed to such a degree that the original source cannot be distinguished from diorite).
- Metamorphic Rock** A rock that has been transformed from some other rock (sedimentary, igneous, or metamorphic) by the effects of heat, pressure, and commonly, deformation. The grade of a metamorphic rock corresponds approximately to the temperature of metamorphism. Low-grade rocks contain hydrous minerals such as mica and chlorite; high-grade metamorphic rocks often have mineralogy similar to that of igneous rocks.
- Meteoric Water** Water derived from the atmosphere (usually in geologically recent time).
- Microcline** A variety of K-feldspar ( $KAlSi_3O_8$ ) with a highly ordered structure.
- Migmatite** Rock consisting of thin alternating layers of granite-type and metamorphic-type rock. Could be a metamorphic rock that has been partially melted, or one into which granitic liquid has been injected.
- Monazite** A phosphate mineral containing high concentrations of the rare earth elements and thorium,  $(Ce, La, Th)PO_4$ . A fairly common accessory mineral in granitic rocks and in detrital sediments derived from them.
- Montmorillonite** A member of the smectite clay mineral group with idealized formula  $(Exch. \text{Cations})_{0.33}Mg_{0.33}Al_{1.67}Si_4O_{10}(OH)_2 \cdot nH_2O$ . The term is also used for the smectite group in general (see Chapter 4).
- Monzonite** A coarse-grained igneous (plutonic) rock containing approximately equal amounts of K-feldspar and plagioclase plus minor hornblende or biotite. Intermediate between a diorite and a syenite. If significant quartz is present, the term *quartz monzonite* is used.
- Muscovite** The common white mica, formula  $KAl_3Si_3O_{10}(OH)_2$ .
- Olivine** Mineral of composition  $(Mg, Fe)_2SiO_4$  common in mafic and ultramafic rocks. The pure Mg end-member is called *forsterite*.
- Pelitic Schist** A schist (strongly foliated micaceous metamorphic rock) formed by metamorphism of a fine-grained sedimentary rock (shale or mudstone).

- Phillipsite** A zeolite mineral of variable Si/Al ratio, commonly with K and Na as the major cations. Phillipsite is formed in oceanic sediments by alteration of volcanic material.
- Phlogopite** Mg end-member mica, formula  $\text{KMg}_3\text{AlSi}_3\text{O}_{10}(\text{OH})_2$ .
- Phreatic** Below the water table (see Chapter 1).
- Plagioclase Feldspar** A mineral group consisting of a solid-solution series between albite (Ab,  $\text{NaAlSi}_3\text{O}_8$ ) and anorthite (An,  $\text{CaAl}_2\text{Si}_2\text{O}_8$ ). Individual names (albite, Ab100–90; oligoclase, Ab90–70; andesine, Ab70–50; labradorite, Ab50–30; bytownite, Ab30–10; anorthite, Ab10–0, with numbers representing percent of albite component in the solid solution) are given to compositional ranges within the series. Calcic varieties (An greater than 50 percent) occur in mafic igneous rocks; sodic varieties (Ab greater than 50 percent) are common in granitic and metamorphic rocks.
- Pleistocene** The time period before the most recent (Holocene), corresponding roughly to the ice ages, 10,000 to 2 million years before present.
- Plutonic** Igneous rock that formed at depth, well below the surface of the earth. Because such rocks cooled slowly, they are normally coarse grained.
- Podsol or Podzol** A soil formed in cool, humid climates, in which iron and aluminum are leached from the upper part of the soil profile. Roughly equivalent to Spodosol.
- Pyroxene** Mineral group of the general formula  $\text{ABSi}_2\text{O}_6$ . In the orthopyroxenes (enstatite, hypersthene), A and B are both mostly Mg plus Fe. In the common clinopyroxenes (diopside, augite), A is mostly Ca, and B is (Mg, Fe, Al, Ti). Many other less common varieties exist. Pyroxenes are most common in mafic igneous rocks.
- Quartz Diorite** A diorite (see entry for diorite in this glossary) containing significant quartz. A granitic (in the loose sense) rock with plagioclase as the main feldspar mineral.
- Quartz Microcline Gneiss** A gneiss (banded high-grade metamorphic rock) with quartz and microcline (K-feldspar) as the most abundant minerals.
- Quartz Monzonite** A monzonite containing significant quartz. A granitic (loose sense) rock with K-feldspar and plagioclase in approximately equal abundance.
- Quartzite** A metamorphic or sedimentary rock consisting largely of quartz.
- Rhyolite** The fine-grained (volcanic) rock chemically equivalent to granite.
- Sandstone** A detrital sedimentary rock, most of whose grains are in the sand size class (0.06 to 2 mm in diameter). The main detrital mineral is usually quartz; variable amounts of feldspar are also commonly present. Sandstones are often cemented by calcite or silica.
- Saponite** A member of the smectite clay mineral group with idealized formula (Exch. Cations) $_{0.33}\text{Mg}_3\text{Al}_{0.33}\text{Si}_{3.67}\text{O}_{10}(\text{OH})_2 \cdot n\text{H}_2\text{O}$ .
- Saprolite** A residual layer or mass of weathered rock, commonly composed of clay minerals and/or oxides of Al and Fe plus resistant minerals from the primary rock.

- Sepiolite** A fibrous magnesium-rich clay mineral (see Chapter 4).
- Shale** A laminated sedimentary rock in which the grains are predominantly in the clay size class (less than 2 or 4  $\mu\text{m}$ ). The term is used loosely for any rock or sediment containing a high proportion of clay-size grains; it is often implied that the grains are clay minerals rather than fine-grained carbonates. Oil shale is generally a fine-grained laminated carbonate rock containing a high proportion of organic matter.
- Siltstone** A consolidated rock, most of whose constituent grains are in the silt size class (0.002 or 0.004 to 0.06 mm).
- Smectite** Any expandable 2:1 clay mineral (see Chapter 4).
- Syenite** A coarse-grained igneous (plutonic) rock consisting chiefly of K-feldspar plus hornblende or biotite.
- Till** Unsorted, unstratified sediment that has been transported or deposited by a glacier.
- Trachyte** A fine-grained igneous (volcanic) rock composed chiefly of alkali (K-rich) feldspar plus hornblende or biotite. The fine-grained equivalent of syenite.
- Ultramafic or Ultrabasic Rocks** Igneous rocks containing less than 45 percent total  $\text{SiO}_2$ . They consist essentially of ferromagnesian minerals (olivine, pyroxene), and contain little or no feldspar or quartz.
- Vadose** Above the water table (see Chapter 1).
- Vermiculite** A group of 2:1 clay minerals distinguished from the smectites by an absence of swelling with ethylene glycol (see Chapter 4).
- Volcanic Rocks** Igneous rocks that have solidified at or near the earth's surface. They are normally fine-grained (in part, at least) because they have cooled rapidly.
- Zeolite** Group of hydrated aluminosilicate minerals corresponding chemically to feldspars plus water plus or minus silica. Some zeolites have high cation-exchange capacities, and some are used in industry as molecular sieves.
- Zircon** A mineral,  $\text{ZrSiO}_4$ , commonly occurring as an accessory in granitic rocks and in sediments derived from them.

# Appendix I: Piper and Stiff Diagrams

Piper and Stiff diagrams are convenient ways of displaying water chemistry data. They are widely used by hydrogeologists.

## PIPER DIAGRAMS

*Piper diagrams*, also called *trilinear diagrams* (Piper, 1944; Back, 1966), are drawn by plotting the proportions (in equivalents) of the major cations [Ca, Mg, (Na + K)] on one triangular diagram, the proportions of the major anions (alkalinity, chloride, sulfate) on another, and combining the information from the two triangles on a quadrilateral (Fig 1). Let us go through an example in detail by plotting the composition of the following:

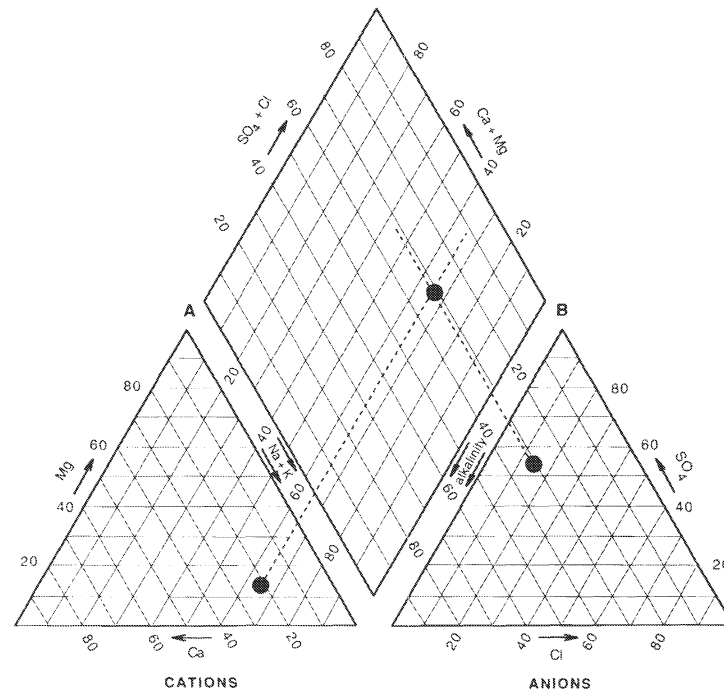
Ca	40 ppm	Alkalinity	2.8 meq/kg
Mg	15 ppm	Sulfate	234 ppm
Na	120 ppm	Chloride	45 ppm
K	20 ppm		

First, convert these numbers to equivalents:

Ca	$1.996 \times 10^{-3}$	Alkalinity	$2.8 \times 10^{-3}$
Mg	$1.234 \times 10^{-3}$	Sulfate	$4.88 \times 10^{-3}$
Na	$5.22 \times 10^{-3}$	Chloride	$1.27 \times 10^{-3}$
K	$0.51 \times 10^{-3}$		

Then normalize the numbers (combining Na and K) so that the concentrations of the cations and of the anions each separately sum to 100 percent.

Ca	22.3	Alkalinity	31.3
Mg	13.7	Sulfate	54.5
Na + K	64.0	Chloride	14.2
	<u>100</u>		<u>100</u>



**FIGURE 1** Illustration of a Piper (trilinear) diagram, with the composition discussed in the text plotted. The corner A corresponds to 100 percent Mg in the cation triangle, 100 percent (Ca + Mg), 0 percent (Na + K); 100 percent alkalinity, 0 percent (SO<sub>4</sub> + Cl) in the quadrilateral. The corner B is 100 percent SO<sub>4</sub> in the anion triangle, 100 percent (Na + K), 0 percent (Ca + Mg); 100 percent (SO<sub>4</sub> + Cl), 0 percent alkalinity in the quadrilateral. Alkalinity is often written HCO<sub>3</sub><sup>-</sup> + CO<sub>3</sub><sup>2-</sup> (after Piper, 1944).

These proportions can now be plotted on the triangular graphs. The scales on triangular graphs are set up such that the proportions of the three variables add up to 100 percent (or 1.00). The graphs thus show the relative proportions of the major ions, but not their absolute concentrations. Sometimes the points are plotted as circles whose size corresponds to the TDS of the samples.

The information on the two triangles are transferred to the quadrilateral by drawing a line through the point on the cation triangle parallel to the Mg axis up into the quadrilateral, and a line through the point in the anion triangle up into the quadrilateral parallel to the SO<sub>4</sub> axis. The intersection of the two lines is the location of the point to be plotted on the quadrilateral. The quadrilateral thus combines information on cations and anions. In the transfer, some information is lost: Mg is combined with Ca, and Cl is combined with SO<sub>4</sub>. Thus the SE to NW axis represents cations, with the SE margin representing 100 percent (Na + K) and the NW margin representing 100 percent (Ca + Mg). The NE to SW axis represents the anions, with the NE boundary representing 100 percent (Cl + SO<sub>4</sub>) and the SW boundary 100 percent alkalinity.

Piper diagrams have two main uses:

1. As a visual way of displaying a water analysis, often in the context of classifying a water into a "type" or "hydrochemical facies" (Fig. 2). The idea is to classify a water on the

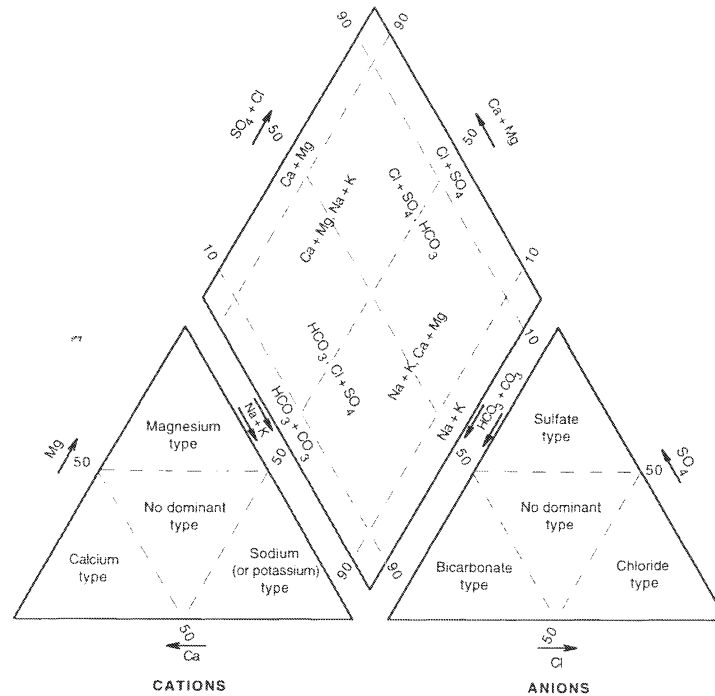


FIGURE 2 Hydrochemical facies based on percent of total equivalents of each ion (after Back, 1966).

basis of the relative proportions of the major ions. One can see at a glance the main features of the water chemistry, especially if different-sized circles are used to display TDS values. One can also see if the analyses fall into distinct clusters.

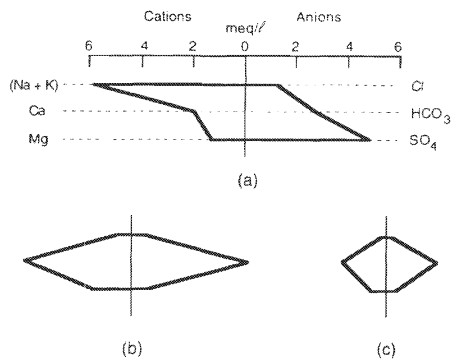
2. As a quick test as to whether a series of water compositions can be explained by mixing between two end-members. If the waters are mixtures of two end-members, the compositions will all plot along a straight line in each of the fields of the diagram. Conversely, if the water compositions do *not* plot along straight lines in each of the fields, their compositions are not controlled by simple mixing. The fact that waters plot along straight lines does not prove that mixing is the controlling mechanism, but it strongly suggests it.

## STIFF DIAGRAMS

*Stiff diagrams* are a way of plotting the major-ion composition of a water to produce a symbol whose shape indicates the relative proportions of the different ions, and whose size indicates total concentrations. It is particularly useful for plotting on maps, as it allows similarities and differences between different waters to be seen at a glance.

The diagram is illustrated in Fig. 3 by plotting the same analysis as was plotted in the Piper diagram above. The three major anions are plotted as points to the right of the center axis, and the three major cations to the left. The points are connected to form the figure. The

**FIGURE 3** Illustration of a Stiff diagram: (a) Method of construction using the example in the text; (b) and (c) Groundwaters from carbonate aquifers in Pennsylvania and Florida (Table 3-2, Chapter 3). Note that the two waters from the carbonate aquifers have the same general shape but have different dimensions reflecting the different concentrations in the two aquifers.



waters from Table 3-2 (Chapter 3) are also plotted to illustrate how different waters result in different "shapes." The diagrams are not used in any further calculation procedures.



## Appendix II: Standard-State\* Thermodynamic Data for Some Common Species

These data have been compiled from various sources and their reliability varies from species to species. They have generally been adjusted to be consistent with CODATA values (Cox et al., 1989; Garvin et al., 1987) and the equilibrium constants in Appendix III, but have not been checked completely for consistency (see discussion at the end of Chapter 10). The reader should evaluate the original source before using the data for serious calculations. The units used are based on the joule and on a standard state of 100 kPa (0.9869 atm) and 298.15 K (25°C). Original data in calorie-based units were converted to joule-based units by multiplying by 4.1840. The difference between 100 kPa and 1 atm is insignificant for solids and liquids and small for gases. Rules for converting from one standard-state pressure to another are explained in Wagman et al. (1982).

The superscript <sup>0</sup> denotes an uncharged species in solution.

Species	$\Delta G_f^0$ (kJ/mol)	$\Delta H_f^0$ (kJ/mol)	$S^0$ (J/mol/K)	Source
Al <sup>3+</sup>	-487.65	-540	-340	1
Al(OH) <sup>2+</sup>	-696.54	-778	-204	1
Al(OH) <sub>2</sub> <sup>+</sup>	-901.7	-1000	-16	1
Al(OH) <sub>3</sub> <sup>0</sup>	-1100.6	-1230	108	1
Al(OH) <sub>4</sub> <sup>-</sup>	-1305.8	-1487	160	1
Al(OH) <sub>3</sub> gibbsite	-1154.86	-1293.1	68.4	1
AlOOH boehmite	-913	-994		2
Al <sub>2</sub> Si <sub>2</sub> O <sub>5</sub> (OH) <sub>4</sub> kaolinite	-3785.8	-4133		3
Al <sub>2</sub> Si <sub>2</sub> O <sub>5</sub> (OH) <sub>4</sub> halloysite	-3769.4	-4114		3
Al <sub>2</sub> Si <sub>4</sub> O <sub>10</sub> (OH) <sub>2</sub> pyrophyllite	-5273.3			3

(Continued)

\*(298.15 K, 25°C; 100 kPa, 0.9869 atm)

Species	$\Delta G_f^0$ (kJ/mol)	$\Delta H_f^0$ (kJ/mol)	$S^0$ (J/mol/K)	Source
Ba <sup>2+</sup>	-555.36	-532.5	8.4	4
BaCO <sub>3</sub> witherite	-1132.21	-1210.85	112.1	4
BaSO <sub>4</sub> barite	-1362.2	-1473.2	132.2	5
C graphite	0	0	5.74	6
CH <sub>4</sub> (g)	-50.72	-74.81	186.3	5
CO (g)	-137.17	-110.53	197.6	6
CO <sub>2</sub> (g)	-394.37	-393.51	213.7	6
H <sub>2</sub> CO <sub>3</sub> <sup>0</sup>	-623.14	-699.09	189.31	consistent with 6
HCO <sub>3</sub> <sup>-</sup>	-586.8	-689.9	98.4	6
CO <sub>3</sub> <sup>2-</sup>	-527.9	-675.2	-50.0	6
Ca <sup>2+</sup>	-552.8	-543.0	-56.2	6
Ca(OH) <sub>2</sub> portlandite	-897.5	-985.2	83.4	7
CaCO <sub>3</sub> calcite	-1129.07	-1207.6	91.7	7
CaCO <sub>3</sub> aragonite	-1128.3	-1206.4	93.9	7
CaMg(CO <sub>3</sub> ) <sub>2</sub> dolomite	-2161.7	-2324.5	155.2	3
CaSO <sub>4</sub> anhydrite	-1321.98	-1435.5	106.5	7
CaSO <sub>4</sub> · 2H <sub>2</sub> O gypsum	-1797.36	-2022.92	193.9	7
Ca <sub>5</sub> (PO <sub>4</sub> ) <sub>3</sub> OH hydroxyapatite	-6338.3	-6721.6	390.4	8
CaAl <sub>2</sub> Si <sub>2</sub> O <sub>8</sub> anorthite	-4002.2	-4227.8	199.3	5
CaAl <sub>2</sub> Si <sub>4</sub> O <sub>12</sub> · 4H <sub>2</sub> O laumontite	-6682.0	-7233.6	485.8	9
Ca <sub>2</sub> Mg <sub>5</sub> Si <sub>8</sub> O <sub>22</sub> (OH) <sub>2</sub> tremolite	-11592.6	-12319.7	548.9	9
Ca <sub>0.167</sub> Al <sub>2.33</sub> Si <sub>3.67</sub> O <sub>10</sub> (OH) <sub>2</sub> Ca-beidellite	-5346			3
Cl <sup>-</sup>	-131.2	-167.1	56.6	6
F <sup>-</sup>	-281.5	-335.35	-13.8	6
Fe metal	0	0	27.3	5
Fe <sup>3+</sup>	-8.56	-48.85		11
Fe <sup>2+</sup>	-82.88	-89.0		10
Fe(OH) <sup>2+</sup>	-233.20	-291.2		3
Fe(OH) <sub>2</sub> <sup>+</sup>	-450.5	-548.9		3
Fe(OH) <sub>3</sub> <sup>0</sup>	-648.3	-802.5		3
Fe(OH) <sub>4</sub> <sup>-</sup>	-833.83	-1058.7		3
Fe(OH) <sub>2</sub> (s)	-486.5	-569.0	88	5
FeOOH goethite	-488.55	-559.3	60.4	8
Fe <sub>2</sub> O <sub>3</sub> hematite	-742.8	-824.7	87.7	12
Fe(OH) <sub>3</sub> ferrihydrite	-692.07			10
Fe <sub>3</sub> O <sub>4</sub> magnetite	-1012.9	-1116.1	146.1	12/
FeCO <sub>3</sub> siderite	-673.05	-753.8		10
FePO <sub>4</sub> · 2H <sub>2</sub> O strengite	-1662.9	-1888.2	171.1	8
Fe <sub>2</sub> SiO <sub>4</sub> fayalite	-1379.0	-1479.9	145.2	5
FeS <sub>2</sub> pyrite	-166.9	-178.2	52.9	5
FeS pyrrhotite	-100.4	-100.0	60.3	{ 10

Species	$\Delta G_f^0$ (kJ/mol)	$\Delta H_f^0$ (kJ/mol)	$S^0$ (J/mol/K)	Source
FeS <sub>mackinawite</sub>	-93.0			10
Fe <sub>3</sub> S <sub>4</sub> <sub>greigite</sub>	-290			10
H <sub>2</sub> (g)	0	0	130.57	6
H <sub>2</sub> O (liquid)	-237.14	-285.83	69.95	6
H <sub>2</sub> O (gas)	-228.58	-241.83	188.73	6
H <sup>+</sup>	0	0	0	
OH <sup>-</sup>	-157.2	-230.0	-10.9	6
K <sup>+</sup>	-282.5	-252.14	101.2	6
KCl <sub>sylvite</sub>	-408.6	-436.5	82.6	8
KAlSi <sub>3</sub> O <sub>8</sub> <sub>microcline, K-feldspar</sub>	-3742.9	-3681.1	214.2	5
KAl <sub>3</sub> Si <sub>3</sub> O <sub>10</sub> (OH) <sub>2</sub> <sub>muscovite</sub>	-5608.4	-5984.4	305.3	5
Mg <sup>2+</sup>	-455.4	-467.0	-237	6
MgO <sub>periclase</sub>	-569.3	-601.6	26.95	7
Mg(OH) <sub>2</sub> <sub>brucite</sub>	-833.51	-924.54	63.18	5
MgCO <sub>3</sub> <sub>magnesite</sub>	-1012.1	-1095.8	65.7	5
Mg <sub>2</sub> SiO <sub>4</sub> <sub>forsterite, olivine</sub>	-2056.7	-2175.7	95.2	9
MgSiO <sub>3</sub> <sub>enstatite</sub>	-1459.9	-1546.8	67.8	9
Mg <sub>3</sub> Si <sub>2</sub> O <sub>5</sub> (OH) <sub>4</sub> <sub>chrysotile, serpentine</sub>	-4035.4			3
Mg <sub>3</sub> Si <sub>4</sub> O <sub>10</sub> (OH) <sub>2</sub> <sub>talc</sub>	-5527.1	-5893	260.7	3
Mg <sub>5</sub> Al <sub>2</sub> Si <sub>3</sub> O <sub>10</sub> (OH) <sub>8</sub> <sub>chlorite</sub>	-8207.8	-8857.4	465.3	9
Mg <sub>4</sub> Si <sub>6</sub> O <sub>15</sub> (OH) <sub>2</sub> • 6H <sub>2</sub> O <sub>sepiolite</sub>	-9251.6	-10116.9	613.4	9
Mn <sub>metal</sub>	0	0	32.0	5
Mn <sup>2+</sup>	-228.1	-220.79	-73.6	5
Mn(OH) <sub>2</sub> <sub>pyrochroite</sub>	-616.5			13
MnOOH <sub>manganite</sub>	-133.3			13
Mn <sub>3</sub> O <sub>4</sub> <sub>hausmannite</sub>	-1283.2	-1387.8	155.6	5
Mn <sub>2</sub> O <sub>3</sub> <sub>bixbyite</sub>	-881.1	-959.0	110.5	5
MnO <sub>2</sub> <sub>pyrolusite</sub>	-465.14	-520.3	53.1	5
MnO <sub>2</sub> <sub>birnessite</sub>	-453.1			13
MnCO <sub>3</sub> <sub>rhodochrosite</sub>	-816.7	-894.1	85.8	5
MnS <sub>alabandite</sub>	-218.0	-213.8	78.2	5
MnSiO <sub>3</sub> <sub>rhodonite</sub>	-1243.1	-1319.2	102.5	5
N <sub>2</sub> (g)	0	0	191.5	6
NH <sub>3</sub> (g)	-16.45	-46.11	192.5	5
NH <sub>3</sub> (aq)	-26.5	-80.29	111.3	5
NH <sub>4</sub> <sup>+</sup>	-79.31	-132.51	113.4	5
NO <sub>3</sub> <sup>-</sup>	-108.74	-205	146.4	5
Na <sup>+</sup>	-262.0	-240.34	58.45	6
NaCl <sub>halite</sub>	-384.14	-411.15	72.1	5
NaHCO <sub>3</sub> <sub>nahcolite</sub>	-851.9	-947.7	102.1	14
NaHCO <sub>3</sub> • Na <sub>2</sub> CO <sub>3</sub> • 2H <sub>2</sub> O <sub>trona</sub>	-2386.6			14
Na <sub>2</sub> SO <sub>4</sub> <sub>thenardite</sub>	-1269.8	-1387.8	149.6	8

(Continued)

<i>Species</i>	$\Delta G_f^0$ (kJ/mol)	$\Delta H_f^0$ (kJ/mol)	$S^0$ (J/mol/K)	<i>Source</i>
Na <sub>2</sub> SO <sub>4</sub> · 10H <sub>2</sub> O mirabilite	-3646.4	-4327.1	592.0	8
NaSi <sub>7</sub> O <sub>13</sub> (OH) <sub>3</sub> magadiite	-6651.9	-241.83	188.73	15
NaAlSi <sub>3</sub> O <sub>8</sub> albite	-3711.5	-3935.1	207.4	5
NaAlSi <sub>2</sub> O <sub>6</sub> · H <sub>2</sub> O analcite	-3082.6	-3300.8	234.3	5
Na <sub>0.33</sub> Al <sub>2.33</sub> Si <sub>3.67</sub> O <sub>10</sub> (OH) <sub>2</sub> Na-beidellite	-5343			3
O <sub>2</sub> (g)	0	0	205.0	5
S <sub>solid, rhombic</sub>	0	0	32.05	5
H <sub>2</sub> S <sub>(g)</sub>	-33.4	-20.6	205.7	5
H <sub>2</sub> S <sub>(aq)</sub>	-27.7	-38.6	126	3, 5
HS <sup>-</sup>	12.2	-16.3	67	5
S <sup>2-</sup>	85.9	34		consistent with 3, 5
SO <sub>2</sub> (g)	-300.1	-296.8	248.1	5
HSO <sub>4</sub> <sup>-</sup>	-755.3	-886.9	131.7	5
SO <sub>4</sub> <sup>2-</sup>	-744.0	-909.34	18.5	5
SiO <sub>2</sub> quartz	-856.3	-910.7	41.5	3
SiO <sub>2</sub> amorph	-849.1	-899.7		10
H <sub>4</sub> SiO <sub>4</sub> <sup>0</sup>	-1307.9	-1457.3		3
H <sub>3</sub> SiO <sub>4</sub> <sup>-</sup>	-1251.8	-1431.7		3
H <sub>2</sub> SiO <sub>4</sub> <sup>2-</sup>	-1176.6	-1383.7		10
Sr <sup>2+</sup>	-563.83	-550.90	-35.1	16
SrCO <sub>3</sub> strontianite	-1144.73	-1225.8	97.2	16
SrSO <sub>4</sub> celestite	-1345.7	-1456.9		3

### Sources

1. Adjusted to be consistent with Wesolowski and Palmer (1994).
2. Adjusted from Wagman et al. (1982) to be consistent with Source 1.
3. Consistent with Ball and Nordstrom (1991).
4. Busenberg and Plummer (1986).
5. Wagman et al. (1982).
6. Cox et al. (1989).
7. Garvin et al. (1987).
8. Robie et al. (1978).
9. Helgeson et al. (1978).
10. Adjusted by the author to be consistent with other values.
11. Adjusted to be consistent with Garvin et al. (1987) and Ball and Nordstrom (1991).
12. Hemingway and Sposito (1990).

13. Bricker (1965).
14. Garrels and Christ (1965).
15. Calculated from Bricker (1969).
16. Busenberg et al. (1984).



# Appendix III: Equilibrium Constants at 25°C and Enthalpies of Reaction for Selected Reactions

The notations (c) and (d) indicate well-crystallized and disordered materials respectively. The superscript <sup>0</sup> denotes an uncharged complex in solution. Where two values are given, the subscript (c) refers to well-crystallized material, and the subscript (d) to disordered material. The values are taken largely from the WATEQ4F data base (Ball and Nordstrom, 1991). Data on Al species from Wesolowski and Palmer (1994) is indicated by (W&P94).

Reaction	log $K_{25}$	$\Delta H_R^0$ (kJ/mol)
$\text{Al}(\text{OH})_3 \text{ gibbsite} + 3\text{H}^+ = \text{Al}^{3+} + 3\text{H}_2\text{O}$ (W&P94)	7.74	-105.3
$\text{Al}(\text{OH})_3 \text{ gibbsite(c)} + 3\text{H}^+ = \text{Al}^{3+} + 3\text{H}_2\text{O}$	8.11	-95.4
$\text{Al}(\text{OH})_3 \text{ amorphous} + 3\text{H}^+ = \text{Al}^{3+} + 3\text{H}_2\text{O}$	10.8	-110.9
$\text{AlOOH boehmite} + 3\text{H}^+ = \text{Al}^{3+} + 2\text{H}_2\text{O}$	8.58	-117.9
$\text{KAl}_3(\text{SO}_4)_2(\text{OH})_6 \text{ alunite} = \text{K}^+ + 3\text{Al}^{3+} + 2\text{SO}_4^{2-} + 6\text{OH}^-$	-1.4	-210
$\text{AlOHSO}_4 \text{ jarbanite} + \text{H}^+ = \text{Al}^{3+} + \text{SO}_4^{2-} + \text{H}_2\text{O}$	-3.23	
$\text{Al}_4(\text{OH})_{10}\text{SO}_4 \text{ bassaluminite} + 10\text{H}^+ = 4\text{Al}^{3+} + \text{SO}_4^{2-} + 10\text{H}_2\text{O}$	22.7	
$\text{Al}_2\text{Si}_2\text{O}_5(\text{OH})_4 \text{ kaolinite} + 6\text{H}^+ = 2\text{Al}^{3+} + 2\text{H}_4\text{SiO}_4^0 + \text{H}_2\text{O}$	7.435	-147.7
$\text{Al}_2\text{Si}_2\text{O}_5(\text{OH})_4 \text{ halloysite} + 6\text{H}^+ = 2\text{Al}^{3+} + 2\text{H}_4\text{SiO}_4^0 + \text{H}_2\text{O}$	12.50	-166.6
$\text{Al}_2\text{Si}_4\text{O}_{10}(\text{OH})_2 + 6\text{H}^+ + 4\text{H}_2\text{O} = 2\text{Al}^{3+} + 4\text{H}_4\text{SiO}_4^0$ pyrophyllite	-2.9	
$\text{Al}^{3+} + \text{H}_2\text{O} = \text{Al}(\text{OH})^{2+} + \text{H}^+$ (W&P94)	-4.95	
$\text{Al}(\text{OH})^{2+} + \text{H}_2\text{O} = \text{Al}(\text{OH})_2^+ + \text{H}^+$ (W&P94)	-5.6	
$\text{Al}(\text{OH})_2^+ + \text{H}_2\text{O} = \text{Al}(\text{OH})_3^0 + \text{H}^+$ (W&P94)	-6.7	
$\text{Al}(\text{OH})_3^0 + \text{H}_2\text{O} = \text{Al}(\text{OH})_4^- + \text{H}^+$ (W&P94)	-5.6	
$\text{Al}^{3+} + \text{H}_2\text{O} = \text{Al}(\text{OH})^{2+} + \text{H}^+$	-5.00	48.07
$\text{Al}^{3+} + 2\text{H}_2\text{O} = \text{Al}(\text{OH})_2^+ + 2\text{H}^+$	-10.1	125.1
$\text{Al}^{3+} + 4\text{H}_2\text{O} = \text{Al}(\text{OH})_4^- + 4\text{H}^+$	-22.7	177.0
$\text{Al}^{3+} + \text{F}^- = \text{AlF}^{2+}$	7.0	4.44
$\text{Al}^{3+} + 2\text{F}^- = \text{AlF}_2^+$	12.7	8.28
$\text{Al}^{3+} + 3\text{F}^- = \text{AlF}_3^0$	16.8	9.04
$\text{Al}^{3+} + 4\text{F}^- = \text{AlF}_4^-$	19.4	9.20
$\text{Al}^{3+} + \text{SO}_4^{2-} = \text{Al}(\text{SO}_4)^+$	3.5	9.58
$\text{Al}^{3+} + 2\text{SO}_4^{2-} = \text{Al}(\text{SO}_4)_2^-$	5.0	13.01
$\text{BaCO}_3 \text{ witherite} = \text{Ba}^{2+} + \text{CO}_3^{2-}$	-8.56	2.94

(Continued)

Reaction	log $K_{25}$	$\Delta H_R^0$ (kJ/mol)
$\text{BaSO}_4 \text{ barite} = \text{Ba}^{2+} + \text{SO}_4^{2-}$	-9.97	26.6
$\text{CaCO}_3 \text{ calcite} = \text{Ca}^{2+} + \text{CO}_3^{2-}$	-8.48	-9.61
$\text{CaCO}_3 \text{ aragonite} = \text{Ca}^{2+} + \text{CO}_3^{2-}$	-8.34	-10.83
$\text{CaMg}(\text{CO}_3)_2 \text{ dolomite(c)} = \text{Ca}^{2+} + \text{Mg}^{2+} + 2\text{CO}_3^{2-}$	-17.09	-39.48
$\text{CaMg}(\text{CO}_3)_2 \text{ dolomite(d)} = \text{Ca}^{2+} + \text{Mg}^{2+} + 2\text{CO}_3^{2-}$	-16.54	-46.40
$\text{CaSO}_4 \cdot 2\text{H}_2\text{O} \text{ gypsum} = \text{Ca}^{2+} + \text{SO}_4^{2-} + 2\text{H}_2\text{O}$	-4.58	-0.46
$\text{CaSO}_4 \text{ anhydrite} = \text{Ca}^{2+} + \text{SO}_4^{2-}$	-4.36	-7.15
$\text{CaF}_2 \text{ fluorite} = \text{Ca}^{2+} + 2\text{F}^-$	-10.6	19.62
$\text{CaAl}_2\text{Si}_2\text{O}_8 \text{ anorthite} + 8\text{H}^+ = \text{Ca}^{2+} + 2\text{Al}^{3+} + 2\text{H}_4\text{SiO}_4^0$	25.7	-306
$\text{Ca}_{0.17}\text{Al}_{2.33}\text{Si}_{3.67}\text{O}_{10}(\text{OH})_2 \text{ Ca-bendellite} + 7.33\text{H}^+ + 2.33\text{H}_2\text{O}$ $= 0.17\text{Ca}^{2+} + 2.33\text{Al}^{3+} + 3.67\text{H}_4\text{SiO}_4^0$	7.94	-169
$\text{Ca}^{2+} + \text{HCO}_3^- = \text{CaHCO}_3^+$	1.11	22.64
$\text{Ca}^{2+} + \text{CO}_3^{2-} = \text{CaCO}_3^0$	3.22	16.86
$\text{Ca}^{2+} + \text{SO}_4^{2-} = \text{CaSO}_4^0$	2.30	6.90
$\text{Ca}^{2+} + \text{F}^- = \text{CaF}^+$	0.94	17.24
$\text{CO}_2(\text{g}) + \text{H}_2\text{O} = \text{H}_2\text{CO}_3^0$	-1.47	-19.98
$\text{H}_2\text{CO}_3^0 = \text{HCO}_3^- + \text{H}^+$	-6.35	9.40
$\text{HCO}_3^- = \text{CO}_3^{2-} + \text{H}^+$	-10.33	13.25
$\text{HF}^0 = \text{H}^+ + \text{F}^-$	-3.18	-13.31
$\text{HF}_2^- = \text{H}^+ + 2\text{F}^-$	-3.76	-19.04
$\text{Fe}_2\text{O}_3 \text{ hematite} + 6\text{H}^+ = 2\text{Fe}^{3+} + 3\text{H}_2\text{O}$	-4.01	-129.06
$\text{FeOOH} \text{ goethite} + 3\text{H}^+ = \text{Fe}^{3+} + 2\text{H}_2\text{O}$	-1.0	-60.58
$\text{Fe}(\text{OH})_3 \text{ ferrihydrite} + 3\text{H}^+ = \text{Fe}^{3+} + 3\text{H}_2\text{O}$	4.89	
$\text{KFe}_3(\text{SO}_4)_2(\text{OH})_6 + 6\text{H}^+ = \text{K}^+ + 3\text{Fe}^{3+} + 2\text{SO}_4^{2-} + 6\text{H}_2\text{O}$ jarosite	-14.8	-131
$\text{Fe}_3\text{O}_4 \text{ magnetite} + 8\text{H}^+ = 2\text{Fe}^{3+} + \text{Fe}^{2+} + 4\text{H}_2\text{O}$	3.737	-211.12
$\text{FeCO}_3 \text{ siderite(c)} = \text{Fe}^{2+} + \text{CO}_3^{2-}$	-10.89	-10.38
$\text{FeCO}_3 \text{ siderite(d)} = \text{Fe}^{2+} + \text{CO}_3^{2-}$	-10.45	
$\text{Fe}_3(\text{PO}_4)_2 \cdot 8\text{H}_2\text{O} \text{ vivianite} = 3\text{Fe}^{2+} + 2\text{PO}_4^{3-} + 8\text{H}_2\text{O}$	-36.0	
$\text{FeS}_2 \text{ pyrite} + 2\text{H}^+ + 2e^- = \text{Fe}^{2+} + 2\text{HS}^-$	-18.48	47.3
$\text{FeS} \text{ amorphous} + \text{H}^+ = \text{Fe}^{2+} + \text{HS}^-$	-3.915	
$\text{Fe}_3\text{S}_4 \text{ greigite} + 4\text{H}^+ = 2\text{Fe}^{3+} + \text{Fe}^{2+} + 4\text{HS}^-$	-45.04	
$\text{Fe}^{3+} + \text{H}_2\text{O} = \text{FeOH}^{2+} + \text{H}^+$	-2.19	43.5
$\text{Fe}^{3+} + 2\text{H}_2\text{O} = \text{Fe}(\text{OH})_2^+ + 2\text{H}^+$	-5.67	71.6
$\text{Fe}^{3+} + 3\text{H}_2\text{O} = \text{Fe}(\text{OH})_3^0 + 3\text{H}^+$	-12.56	103.8
$\text{Fe}^{3+} + 4\text{H}_2\text{O} = \text{Fe}(\text{OH})_4^- + 4\text{H}^+$	-21.6	133.5
$\text{Fe}^{3+} + \text{SO}_4^{2-} = \text{FeSO}_4^+$	4.04	16.36
$\text{Fe}^{3+} + \text{Cl}^- = \text{FeCl}^{2+}$	1.48	23.4
$\text{Fe}^{3+} + 2\text{Cl}^- = \text{FeCl}_2^+$	2.13	
$\text{Fe}^{3+} + 3\text{Cl}^- = \text{FeCl}_3^0$	1.13	
$\text{Fe}^{2+} = \text{Fe}^{3+} + e^-$	-13.02	40.5
$\text{Fe}^{2+} + \text{H}_2\text{O} = \text{FeOH}^+ + \text{H}^+$	-9.5	55.2
$\text{Fe}^{2+} + \text{SO}_4^{2-} = \text{FeSO}_4^0$	2.25	13.51
$\text{KAlSi}_3\text{O}_8 \text{ adularia} + 4\text{H}_2\text{O} + 4\text{H}^+ = \text{K}^+ + \text{Al}^{3+} + 3\text{H}_4\text{SiO}_4^0$	2.13	-48
$\text{KAl}_3\text{Si}_3\text{O}_{10}(\text{OH})_2 \text{ muscovite} + 10\text{H}^+ = \text{K}^+ + 3\text{Al}^{3+} + 3\text{H}_4\text{SiO}_4^0$	12.70	-248.4
$\text{KMg}_3\text{AlSi}_3\text{O}_{10}(\text{OH})_2 + 10\text{H}^+ = \text{K}^+ + 3\text{Mg}^{2+} + \text{Al}^{3+} + 3\text{H}_4\text{SiO}_4^0$ phlogopite	43.3	177
$\text{K}^+ + \text{SO}_4^{2-} = \text{KSO}_4^-$	0.85	9.4
$\text{Mg}(\text{OH})_2 \text{ brucite} + 2\text{H}^+ = \text{Mg}^{2+} + 2\text{H}_2\text{O}$	16.84	-113.4
$\text{MgCO}_3 \text{ magnesite} = \text{Mg}^{2+} + \text{CO}_3^{2-}$	-8.03	-25.81
$\text{Mg}_3(\text{CO}_3)_4(\text{OH})_2 \cdot 4\text{H}_2\text{O} + 2\text{H}^+ = 5\text{Mg}^{2+} + 4\text{CO}_3^{2-} + 6\text{H}_2\text{O}$ hydromagnesite	-8.76	-218.59



Reaction	log $K_{25}$	$\Delta H_R^0$ (kJ/mol)
$\text{Mg}_3\text{Si}_2\text{O}_5(\text{OH})_4$ chrysotile + $6\text{H}^+ = 3\text{Mg}^{2+} + 2\text{H}_4\text{SiO}_4^0 + \text{H}_2\text{O}$	32.20	-195.8
$\text{Mg}_3\text{Si}_4\text{O}_{10}(\text{OH})_2$ talc + $4\text{H}_2\text{O} + 6\text{H}^+ = 3\text{Mg}^{2+} + 4\text{H}_4\text{SiO}_4^0$	21.40	-193.94
$\text{Mg}_2\text{Si}_3\text{O}_7\text{OH} \cdot 3\text{H}_2\text{O} + 0.5\text{H}_2\text{O} + 4\text{H}^+ = 2\text{Mg}^{2+} + 3\text{H}_4\text{SiO}_4^0$ sepiolite(c)	15.76	
$\text{Mg}_2\text{Si}_3\text{O}_7\text{OH} \cdot 3\text{H}_2\text{O} + 0.5\text{H}_2\text{O} + 4\text{H}^+ = 2\text{Mg}^{2+} + 3\text{H}_4\text{SiO}_4^0$ sepiolite(d)	18.66	
$\text{Mg}_3\text{SiO}_4$ forsterite + $4\text{H}^+ = 2\text{Mg}^{2+} + \text{H}_4\text{SiO}_4^0$	28.31	-203.25
$\text{MgSiO}_3$ clinostatite + $\text{H}_2\text{O} + 2\text{H}^+ = \text{Mg}^{2+} + \text{H}_4\text{SiO}_4^0$	11.342	-83.9
$\text{Fe}_3\text{Si}_2\text{O}_5(\text{OH})_4$ granaulite + $6\text{H}^+ = 3\text{Fe}^{2+} + 2\text{H}_4\text{SiO}_4^0 + \text{H}_2\text{O}$	20.81	
$\text{Mg}^{2+} + \text{HCO}_3^- = \text{MgHCO}_3^+$	1.07	3.31
$\text{Mg}^{2+} + \text{CO}_3^{2-} = \text{MgCO}_3^0$	2.98	11.35
$\text{Mg}^{2+} + \text{SO}_4^{2-} = \text{MgSO}_4^0$	2.37	19.04
$\text{MnCO}_3$ rhodochrosite(c) = $\text{Mn}^{2+} + \text{CO}_3^{2-}$	-11.43	-5.98
$\text{MnCO}_3$ rhodochrosite(d) = $\text{Mn}^{2+} + \text{CO}_3^{2-}$	-10.39	
$\text{Mn}(\text{OH})_2$ pyrochroite + $2\text{H}^+ = \text{Mn}^{2+} + 2\text{H}_2\text{O}$	15.2	
$\text{Mn}_3\text{O}_4$ hausmannite + $8\text{H}^+ + 2e^- = 3\text{Mn}^{2+} + 4\text{H}_2\text{O}$	61.03	-421.1
$\text{MnOOH}$ manganite + $3\text{H}^+ + e^- = \text{Mn}^{2+} + 2\text{H}_2\text{O}$	25.34	
$\text{MnO}_2$ pyrolusite + $4\text{H}^+ + 2e^- = \text{Mn}^{2+} + 2\text{H}_2\text{O}$	41.38	-272.4
$\text{MnO}_2$ bixessite + $4\text{H}^+ + 2e^- = \text{Mn}^{2+} + 2\text{H}_2\text{O}$	43.60	
$\text{Mn}^{2+} = \text{Mn}^{3+} + e^-$	-25.51	108
$\text{Mn}^{2+} + 4\text{H}_2\text{O} = \text{MnO}_4^{2-} + 8\text{H}^+ + 4e^-$	-127.82	739
$\text{MnS}_{\text{green}} + \text{H}^+ = \text{Mn}^{2+} + \text{HS}^-$	3.8	-24.23
$\text{NaHCO}_3$ nahcolite = $\text{Na}^+ + \text{HCO}_3^-$	-0.548	15.56
$\text{NaHCO}_3 \cdot \text{Na}_2\text{CO}_3 \cdot 2\text{H}_2\text{O} = 3\text{Na}^+ + \text{CO}_3^{2-} + \text{HCO}_3^- + 2\text{H}_2\text{O}$ trona	-0.795	75.3
$\text{NaCl}_{\text{halite}} = \text{Na}^+ + \text{Cl}^-$	1.582	3.84
$\text{NaAlSi}_3\text{O}_8$ albite + $4\text{H}_2\text{O} + 4\text{H}^+ = \text{Na}^+ + \text{Al}^{3+} + 3\text{H}_4\text{SiO}_4^0$	4.70	-68.7
$\text{NaAlSi}_2\text{O}_6 \cdot \text{H}_2\text{O}$ analcite + $4\text{H}^+ + \text{H}_2\text{O} = \text{Na}^+ + \text{Al}^{3+} + 2\text{H}_4\text{SiO}_4^0$	10.0	-100.8
$\text{NaSi}_7\text{O}_{13}(\text{OH})_3 \cdot 3\text{H}_2\text{O} + \text{H}^+ + 9\text{H}_2\text{O} = \text{Na}^+ + 7\text{H}_4\text{SiO}_4^0$ magadiite	14.30	
$\text{Na}_{0.33}\text{Al}_{2.33}\text{Si}_{3.67}\text{O}_{10}(\text{OH})_2$ Na-bedeellite + $7.33\text{H}^+ + 2.68\text{H}_2\text{O}$ = $0.33\text{Na}^+ + 2.33\text{Al}^{3+} + 3.67\text{H}_4\text{SiO}_4^0$	7.7	-160.5
$\text{Na}^+ + \text{CO}_3^{2-} = \text{NaCO}_3^+$	1.27	37.3
$\text{Na}^+ + \text{HCO}_3^- = \text{NaHCO}_3^0$	-0.25	
$\text{Na}^+ + \text{SO}_4^{2-} = \text{NaSO}_4^-$	0.70	4.69
$\text{SiO}_2$ quartz + $2\text{H}_2\text{O} = \text{H}_4\text{SiO}_4^0$	-3.98	25.06
$\text{SiO}_2$ amorphous + $2\text{H}_2\text{O} = \text{H}_4\text{SiO}_4^0$	-2.71	14.0
$\text{H}_4\text{SiO}_4^0 = \text{H}^+ + \text{H}_3\text{SiO}_4^-$	-9.83	25.61
$\text{H}_4\text{SiO}_4^0 = 2\text{H}^+ + \text{H}_2\text{SiO}_4^{2-}$	-23.0	73.6
$\text{H}_3\text{SiO}_4^- = \text{H}^+ + \text{H}_2\text{SiO}_4^{2-}$	-13.17	
$\text{SrCO}_3$ strontianite = $\text{Sr}^{2+} + \text{CO}_3^{2-}$	-9.27	-1.68
$\text{SrSO}_4$ celestite = $\text{Sr}^{2+} + \text{SO}_4^{2-}$	-6.63	-4.34
$\text{HSO}_4^- = \text{SO}_4^{2-} + \text{H}^+$	-1.988	-16.11
$\text{SO}_4^{2-} + 10\text{H}^+ + 8e^- = \text{H}_2\text{S}^0 + 4\text{H}_2\text{O}$	40.644	273.8
$\text{S}_{\text{solid}} + 2\text{H}^+ + 2e^- = \text{H}_2\text{S}^0$	4.88	-39.75
$\text{H}_2\text{S}^0 = \text{H}^+ + \text{HS}^-$	-6.994	22.18
$\text{HS}^- = \text{H}^+ + \text{S}^{2-}$	-12.92	50.6
$\text{As}_2\text{O}_3$ arsenolite + $3\text{H}_2\text{O} = 2\text{H}_3\text{AsO}_3^0$	-1.40	30.0
$\text{As}_2\text{S}_3$ orpiment + $6\text{H}_2\text{O} = 2\text{H}_3\text{AsO}_3^0 + 3\text{HS}^- + 3\text{H}^+$	-60.97	346.8
$\text{AsS}_{\text{realgar}} + 3\text{H}_2\text{O} = \text{H}_3\text{AsO}_3^0 + \text{HS}^- + 2\text{H}^+ + e^- \text{FeAsO}_4 \cdot$	-19.75	127.8
$2\text{H}_2\text{O}$ scorodite = $\text{Fe}^{3+} + \text{AsO}_4^{3-} + 2\text{H}_2\text{O}$	-20.25	
$\text{As}_{\text{solid}} + 3\text{H}_2\text{O} = \text{H}_3\text{AsO}_3^0 + 3\text{H}^+ + 3e^-$	-12.17	

(Continued)

Reaction	log $K_{25}$	$\Delta H_R^0$ (kJ/mol)
$H_3AsO_4^0 = H_2AsO_4^- + H^+$	-2.24	-7.07
$H_2AsO_4^- = HAsO_4^{2-} + H^+$	-6.76	
$HAsO_4^{2-} = AsO_4^{3-} + H^+$	-11.60	
$H_3AsO_3^0 = H_2AsO_3^- + H^+$	-9.23	27.45
$H_2AsO_3^- = HAsO_3^{2-} + H^+$	-12.10	
$HAsO_3^{2-} = AsO_3^{3-} + H^+$	-13.41	
$CdCO_3 \text{ oravite} = Cd^{2+} + CO_3^{2-}$	-12.1	-0.08
$CdO \text{ monteponite} + 2H^+ = Cd^{2+} + H_2O$	13.77	-103.6
$CdS \text{ greenockite} + H^+ = Cd^{2+} + HS^-$	-15.93	68.45
$Cd^{2+} + H_2O = CdOH^+ + H^+$	-10.1	54.8
$Cd^{2+} + Cl^- = CdCl^+$	1.98	2.47
$CuO \text{ tenorite} + 2H^+ = Cu^{2+} + H_2O$	7.62	-63.76
$Cu_2O \text{ cuprite} + 2H^+ = 2Cu^+ + H_2O$	-1.55	26.13
$Cu \text{ metal} = Cu^+ + e^-$	-8.76	71.7
$Cu_2(OH)_2CO_3 \text{ malachite} + 3H^+ = 2Cu^{2+} + 2H_2O + HCO_3^-$	5.15	-81.42
$Cu_3(OH)_2(CO_3)_2 \text{ azurite} + 4H^+ = 3Cu^{2+} + 2H_2O + 2HCO_3^-$	3.75	-128.8
$CuS \text{ covellite} + H^+ = Cu^{2+} + HS^-$	-22.27	100.5
$Cu_2S \text{ chalcocite} + H^+ = 2Cu^+ + HS^-$	-34.62	206.5
$Cu^+ = Cu^{2+} + e^-$	-2.72	-6.90
$Cu^{2+} + H_2O = CuOH^+ + H^+$	-8.0	
$Cu^{2+} + 2H_2O = Cu(OH)_2^0 + 2H^+$	-13.68	
$Cu^{2+} + 3H_2O = Cu(OH)_3^- + 3H^+$	-26.9	
$Cu^{2+} + 4H_2O = Cu(OH)_4^{2-} + 4H^+$	-39.6	
$Cu^{2+} + CO_3^{2-} = CuCO_3^0$	6.73	
$Cu^{2+} + Cl^- = CuCl^+$	0.43	36.2
$Cu^{2+} + 2Cl^- = CuCl_2^0$	0.16	44.18
$PbCO_3 \text{ cerussite} = Pb^{2+} + CO_3^{2-}$	-13.13	20.3
$PbO \text{ litharge} + 2H^+ = Pb^{2+} + H_2O$	12.72	-65.53
$PbSO_4 \text{ anglesite} = Pb^{2+} + SO_4^{2-}$	-7.79	9.00
$PbS \text{ galena} + H^+ = Pb^{2+} + HS^-$	-12.78	81.2
$Pb \text{ metal} = Pb^{2+} + 2e^-$	4.27	1.7
$Pb^{2+} + H_2O = PbOH^+ + H^+$	-7.71	
$Pb^{2+} + Cl^- = PbCl^+$	1.60	18.33
$Pb^{2+} + 2Cl^- = PbCl_2^0$	1.80	4.52
$Pb^{2+} + 2HS^- = Pb(HS)_2^0$	15.27	
$Fe_3(SeO_3)_3 \text{ solid} = 2Fe^{2+} + 3SeO_3^{2-}$	-35.43	
$FeSe_2 \text{ solid} + 2H^+ + 2e^- = Fe^{2+} + 2HSe^-$	-18.58	
$CaSeO_3 \text{ solid} = Ca^{2+} + SeO_3^{2-}$	-5.6	
$HSeO_4^- = SeO_4^{2-} + H^+$	-1.66	20.5
$H_2SeO_3 = HSeO_3^- + H^+$	2.75	
$HSeO_3^- = SeO_3^{2-} + H^+$	-8.5	
$H_2Se = H^+ + HSe^-$	-3.8	22.2
$SeO_3^{2-} + H_2O = SeO_4^{2-} + 2H^+ + 2e^-$	-30.26	
$SeO_3^{2-} + 7H^+ + 6e^- = HSe^- + 3H_2O$	42.51	
$Se \text{ solid} + H^+ + 2e^- = HSe^-$	-17.32	
$ZnCO_3 \text{ smithsonite} = Zn^{2+} + CO_3^{2-}$	-10.00	-18.24
$ZnO \text{ zincite} + 2H^+ = Zn^{2+} + H_2O$	11.14	-91.5
$ZnO \text{ amorphous} + 2H^+ = Zn^{2+} + H_2O$	11.31	
$ZnS \text{ sphalerite} + H^+ = Zn^{2+} + HS^-$	-11.62	34.52
$Zn \text{ metal} = Zn^{2+} + 2e^-$	25.76	-153.89
$Zn^{2+} + H_2O = ZnOH^+ + H^+$	-8.96	56.1
$Zn^{2+} + Cl^- = ZnCl^+$	0.43	32.6
$Zn^{2+} + 2HS^- = Zn(HS)_2^0$	14.94	

# Answers to Problems

## Chapter 2

1. Gypsum, by 1.1 kJ/mole. The simplest way is to calculate the  $\Delta G_R^0$  of the reaction  $\text{CaSO}_4 \cdot 2\text{H}_2\text{O} = \text{CaSO}_4 + 2 \text{H}_2\text{O}$ . An alternative way is to compare the solubility products of gypsum and anhydrite. The more soluble (anhydrite) is the less stable in contact with water.
2.  $10^{-34.27}$ . Note that the solubility product is written in terms of  $\text{OH}^-$ , whereas the corresponding equilibrium constant in Appendix III is written in terms of  $\text{H}^+$ . The difference between the two constants is a factor of  $(K_w)^3$ .
3. From the data in Appendix II, for this reaction  $\log K_{25} = 7.75$ ,  $\Delta H_R^0 = -104.4$  kJ/mole, and  $\log K_5 = 9.06$ . At pH 4, this gives  $\alpha_{\text{Al}^{3+}} = 10^{-2.94}$ .  
Appendix III gives values for  $\log K_{25}$  of 7.74,  $\Delta H_R^0 = -105.3$  kJ/mol and  $\log K_{25} = 8.11$ ,  $\Delta H_R^0 = -95.4$  kJ/mole (from two different data sources). This gives  $\log K_5 = 9.07$  or 9.31, which gives  $\alpha_{\text{Al}^{3+}} = 10^{-2.93}$  or  $10^{-2.69}$  at pH 4 and 5°C. The values derived from the different data sources are slightly different; the question of data consistency is discussed in more detail in Chapter 10.  
The solubility of gibbsite at pH 4 *increases* with decreasing temperature; this is a consequence of the value of  $\Delta H_R^0$  being negative.
4. With the numbers given, the activity of the complex is almost exactly equal to the activity of the free ion, so the total concentration (assuming  $\alpha = m$ ) is almost exactly double that of the free ion. The values are 3.1 or 3.0 ppm, depending on which data set is used.
5. The activity of the  $\text{Al}(\text{SO}_4)_2^-$  complex is  $10^{-5.36}$ , which is 8% of the concentration of the free ion or 4 percent of the concentration of the free ion plus  $\text{AlSO}_4^+$  complex. That is, it increases the solubility by about 4 percent.  
At a sulfate activity of  $10^{-1}$ , the activity of the  $\text{Al}(\text{SO}_4)_2^-$  is a factor of 794 times that of the free ion, and the activity of the  $\text{AlSO}_4^+$  complex is a factor of 100 greater than that of

the free ion. These numbers illustrate that the complexes become more important as the concentration of the ligand increases, and that as the concentration of the ligand increases, the concentrations of complexes containing two (or more) ligands become progressively more important compared to the complex containing only one ligand.

6. Appendix II:  $K_{sp} = 10^{-11.01}$ , Solubility ( $C = m$ ) =  $10^{-5.50}$  m = 0.73 mg BaSO<sub>4</sub>/ℓ  
The activity correction increases the solubility by 1.6 percent.  
Appendix III:  $K_{sp} = 10^{-9.97}$ , Solubility ( $C = m$ ) =  $10^{-4.99}$  m = 2.42 mg BaSO<sub>4</sub>/ℓ  
The activity correction increases the solubility by 3.0 percent.
7. Total cations = 26.39 meq/kg, total anions = 26.10 meq/kg; charge balance error [ $100 \times (\sum \text{cations} - \sum \text{anions}) / (\sum \text{cations} + \sum \text{anions})$ ] = 0.6 percent. This represents good balance between cations and anions, considering analytical uncertainty.  
The activity coefficients are both 0.469.  
Using  $K_{SrSO_4} = 10^{-6.63}$  (Appendix III),  $\log (IAP/K) = -1.00$ ,  $IAP/K = 0.10$ , Saturation ratio = 0.32.

### Chapter 3

1. 3.91
2. 5.93,  $6.45 \times 10^{-3}$  ( $10^{-2.19}$ ) m
3.  $1.31 \times 10^{-3}$  ( $10^{-2.88}$ ) m
4. (a)  $0.36 \times 10^{-3}$  mol/kg; (b)  $0.052 \times 10^{-3}$  mol/kg, 7.35.  $10^{-2.13}$  atm. Note that much less calcite is precipitated in the closed system case, and the final  $P_{CO_2}$  is a factor of 2.3 higher in the closed system.
5. 32 ppm, pH 6.88
6. pH 7.58,  $m_{HCO_3^-} = 0.18 \times 10^{-3}$
7. pH 8.32
8. 1.63 mm/100 y
9. 1.75 mm/100 y (Note how little difference the "acid" makes in this calculation.)
10.  $P_{CO_2} = 5.31 \times 10^{-4}$  ( $10^{-3.27}$ ) atm;  $IAP/K = 0.58$  (SR = 0.76),  $\log (IAP/K) = -0.23$ .

### Chapter 4

1. Smectite, dioctahedral
3. 18 meq/100 g (based on structural formula)
4. 50.2 to 100 meq/100 g
5. Na<sup>+</sup> = 15.7 ppm; K<sup>+</sup> = 0.33 ppm

### Chapter 6

1. (a)  $5 \times 10^{-2}$ ; (b) 1.0 ppm; (c) 1.0 ppm
2. 1.20, 10 to 30 for porosity 25 to 10 percent
3. 63 ℓ

**Chapter 7**

1. (a) 12.41; (b) 10.41; (c) -5.05

**Chapter 8**

1. 4.0 y
2. 6.75 moles/m<sup>2</sup>
3. 9.8 μmol/l

**Chapter 10**

1. 6.8, 13.7, 97 ppm (using dissociation constants from the chapter)
2.  $1.46 \times 10^{-3}$  ( $10^{-2.84}$ )
3.  $10^{-5.40}$
4. 6.91 (Appendix II); 6.90 (c), 7.63 (d) (Appendix III)
5. 2.27 ppm (Appendix II); 2.21 ppm (c), 20.5 ppm (d) (Appendix III)
6.  $10^{-8.15}$  (Appendix II);  $10^{-8.01}$  (Appendix III)
7.  $10^{-7.03}$  (Appendix II);  $10^{-4.51}$  (Appendix III) kaolinite (less soluble)

**Chapter 11**

4.  $3.44 \times 10^7$  y,  $9.55 \times 10^5$  y,  $5.83 \times 10^5$  y, 107 y
5. A factor of 2.85. This suggests a strong temperature dependence.

**Chapter 12**

1. Garrels and Mackenzie (1971, pp. 170–173) suggested the atmosphere, halite, gypsum, limestone/dolomite, Na and K feldspars altering to smectite.

**Chapter 13**

1. (a) 4.5 to 4.6; (b) 4.4. Yes.
2. About 140 μeq/l (based on a pH of 4.2)
3. 180 y

**Chapter 16**

1. 23 days.
2. This can be rationalized in various ways. You could say the mass to be diffused is only half as much as in the previous example, but the mean concentration gradient will be a bit less, so the required time will be a bit more than half that calculated in problem 1. A reasonable guess would be anything between 0.5 and 1 times the value in example 1 (12 to 30 days). A numerical model gives  $1.48 \times 10^6$  sec = 17.1 days. Time scales as (crack thickness)<sup>2</sup>, so decreasing the crack by a factor of 10 decreases the time by a factor of 100, to about 4 hours.

# Author Index

## A

Aagaard, P., 231, 381  
 Aberg, G., 325, 381  
 Aggarwal, P. K., 391  
 Aiken, G. R., 113, 114, 115, 118, 127, 299, 381, 386, 401  
 Albarède, F., 379, 381  
 Al-Droubi, A., 332, 381, 388  
 Alegret, S., 387  
 Ali, M. A., 179, 381  
 Allen, E. R., 391  
 Allison, J. D., 37, 195, 368, 381  
 Alpers, C. H., 177, 196, 381  
 Altveg, M., 305, 381  
 Amiotte-Suchet, P., 285, 286, 381  
 Amrhein, C., 230, 381  
 Anbeek, C., 227, 381, 382  
 Anderson, L. C., D. 391  
 Anderson, M. P., 363, 382  
 Anderson, T. F., 392  
 Andrews, J. N., 323, 387  
 Anovitz, L. M., 207, 382  
 Antweiler, R., C., 8, 107, 118, 382  
 Appelo, C. A., J. 369, 379, 382  
 April, R., 276, 277, 278, 279, 382  
 Aravena, R., 322, 382  
 Armstrong, R., L. 325, 389  
 Arndt, U., 30, 382  
 Arnold, G.W., 385  
 Averett, R. C., 116, 127, 382, 393  
 Axtmann, E. V., 270, 382

## B

Baccini, P., 174, 177, 399  
 Back, W., 10, 62, 64, 288, 382, 396, 410, 411

Badaut, D., 388  
 Bailey, S. M., 400  
 Bailey, S. W., 77, 86, 382  
 Baker, J. P., 292, 305, 382  
 Baker, P. A., 59, 382  
 Ball, J. W., 28, 36, 382, 416, 419  
 Banfied, J. F., 385  
 Barnes, I., 12, 13, 164, 279, 280, 382, 383, 401  
 Baron, J., 239, 273, 383, 393  
 Bartlett, R. W.,  
 Bashad, I., 284, 383  
 Bassett, R. L., 40, 393  
 Beamish, R. J., 305, 383  
 Beck, K. C., 118, 188, 383  
 Belzile, N., 400  
 Bencala, K. E., 187, 393  
 Bentley, H. W., 323, 383, 396  
 Berner, E. K., 1, 13, 288, 383  
 Berner, R. A., 1, 13, 161, 171, 174, 183, 219, 220, 221, 222, 223, 224, 226, 227, 288, 357, 383, 390, 394, 395, 398  
 Berry, F. A., W. 82, 391  
 Bicking, M., 387  
 Billingham, P., 394  
 Billings, G. K., 390  
 Bird, D. K., 389  
 Bischoff, J. L., 392  
 Bischoff, W. D., 60, 383  
 Bishop, F. C., 383  
 Blank, L. W., 305, 383  
 Blowes, D. W., 177, 196, 381.  
 Blum, A. E., 227, 230, 234, 285, 286, 383, 387, 401  
 Blum, J. D., 324, 383, 393  
 Boles, J. R., 350, 383

Bolt, G. H., 101, 384  
 Bonsang, B., 5, 384  
 Boran, D. A., 115, 389  
 Borcsik, M. P., 393  
 Bormann, F. H., 392  
 Bowers, T. S., 213, 384  
 Bowser, C. J., 244, 384  
 Bradbury M. H., 364, 384  
 Bradley, W. F., 389  
 Brady, P. V., 228, 384  
 Brantley, S. L., 234, 399, 401  
 Bray, R. H., 389  
 Breck, W. G., 163, 174, 384  
 Bricker, O. P., 201, 384, 385, 417  
 Brindley, G. W., 382  
 Broecker, W. S., 324, 384  
 Brookins D. G., 157, 183, 194, 196, 384  
 Brown, D. S., 381  
 Brown, K. 383  
 Brown, P. A., 381  
 Brueckner, H. K., 392  
 Brunauer, S., 27, 384  
 Buchanan, A., S., 397  
 Bunker, B., 227, 384  
 Buol, S. W., 235, 384  
 Burch, T. E., 231, 232, 234, 384, 392  
 Busby, J. F., 396  
 Busenberg, E. 32, 384, 396, 416, 417  
 Butler, G. P. 346, 347, 384  
 Butler, J. N., 68, 384

## C

Cadle, R. D., 391  
 Carothers, W. W., 350, 384  
 Carson, M. A., 260, 384

- Caruccio, F. T., 307, 384  
Casey, W. H., 227, 384, 385  
Chapelle, F. H., 127, 161, 174, 385  
Chen, C. S., 364, 385  
Chen, C. W., 302, 303, 304, 385  
Cherry, J. A., 13, 136, 359, 362, 363, 364, 379, 382, 385, 388  
Cheverry, C., 386  
Chou, L., 227, 385  
Christ, C. L., 40, 52, 139, 153, 157, 183, 201, 385, 388, 417  
Christophersen, N., 303, 304, 385, 390, 394  
Church, M. R., 388  
Churney, K. L., 400  
Clayton, J. L., 275, 385  
Clayton, R. N., 315, 318, 385  
Cleaves, E. T., 266, 385  
Clement, A., 392  
Clow, D. W., 6, 229, 233, 237, 238, 293, 385, 386  
Clymo, R. S., 298, 385  
Coles, L. T., 382  
Cook, A. D., 386  
Cooper, D. M., 394  
Coplen, T. B., 81, 389  
Cosby, B. J., 303, 385  
Coston, J. A., 188, 385  
Cowan, D. C., 193, 385  
Cowling, E. B., 306, 398  
Cox, J. D., 385, 413, 416  
Craig, H., 315, 386, 390  
Crerar, D. A., 393  
Cromack, K., 389  
Cromwell, J., 384  
Cronan, C. S., 118, 299, 386
- D**  
Dambrine, E., 396  
Dansgaard, W., 314, 386  
Davies, C. W., 28, 386  
Davis, J. A., 91, 97, 101, 102, 105, 179, 188, 385, 386, 391  
Davis, J. S., 281, 386  
Davis, S. N., 383, 396  
Dean, J. D., 385  
DeBraul, J. D., 391  
Degens, E. T., 118, 386  
Deines, P., 320, 386  
Delaney, J. M., 389, 401  
Desaulniers, D. E., 385  
Devidal, J.-L., 395  
Devitre, R. R., 400
- Dixon, J. B., 86, 386  
Domenico, P. A., 13, 386  
Downing, A. L., 400  
Drablos, D., 398  
Drever, J. I., 6, 8, 107, 118, 181, 188, 229, 230, 231, 233, 237, 244, 262, 263, 264, 265, 266, 267, 268, 270, 271, 272, 273, 286, 287, 293, 335, 341, 342, 382, 385, 386, 392, 393, 394, 395, 398, 399  
Driscoll, C. T., 291, 386, 391  
Droubi, A., 332, 386  
Duguid, J. O., 393  
Dunkle, S. A., 396  
Dzombak, D. A., 91, 97, 99, 101, 102, 104, 105, 179, 192, 194, 374, 381, 386, 387
- E**  
Eaton, J. S., 391, 392  
Eberl, D. D., 398  
Eccles, L. A., 392  
Eckhardt, F. E. W., 305, 387  
Edmond, J. M., 5, 36, 50, 257, 260, 261, 262, 285, 286, 387, 399  
Ela, W., 389  
Electric Power Research Institute, 276, 387  
Ellis, A. J., 12, 318, 387  
Elmore, D., 396  
Emerson, S. M., 180, 324, 387, 390  
Emmett, P. H., 227, 390  
Engelkemeir, A. G., 390  
Ephraim, J., 115, 387, 393  
Erel, Y., 383  
Eslinger, E. V., 390, 398  
Essene, E. J., 382  
Eugster, H. P., 33, 327, 329, 330, 331, 332, 333, 333, 334, 335, 336, 337, 338, 339, 340, 351, 387, 389, 391, 398  
Evans, M. L., 382  
Evans, W. H., 400
- F**  
Fahey, T. J., 118, 387, 402  
Fanning, D. S., 382  
Faure, G., 325, 387  
Ferrier, R. C., 394  
Feth, J. H., 249, 387  
Fetter, C. W., 121, 123, 127, 379, 387  
Finley, J. B., 244, 387
- Fisher, J. R., 397  
Fitzgerald, W. F., 393  
Fleming, G. W., 396  
Fontes, J.-C., 323, 325, 387, 388  
Foster, S. D. D., 364, 387  
Fowler, D. D., 387  
Franks, S. G., 350, 383  
Freedman, B., 306, 388  
Freeze, R. A., 13, 359, 362, 379, 388  
Friedland, A. J., 393  
Friedman, I., 313, 348, 388, 390  
Frind, E. O., 385, 399  
Frink, C. R., 298, 391  
Fritz, B., 325, 381, 386, 392, 396  
Fritz, P., 316, 317, 325, 385, 388  
Froelich, P. N., 164, 165, 388  
Fuhrer, H., 306, 388  
Fuller, C. C., 385, 386
- G**  
Gac, J.-Y., 332, 381, 388  
Gächter, R., 169, 388  
Galloway, J. N., 6, 107, 177, 299, 385, 388, 391  
Ganor, J. W., 234, 392  
Garrels, R. M., 2, 13, 40, 52, 139, 153, 157, 159, 177, 183, 184, 213, 241, 242, 243, 244, 245, 249, 250, 264, 287, 288, 324, 327, 328, 329, 331, 334, 388, 389, 390, 417  
Garvin, D., 388, 413, 416  
Geidel, G., 307, 384  
Gherini, S. A., 385  
Gibbs, R. J., 257, 259, 260, 286?, 388  
Gieskes, J. M., 36, 387  
Gillam, A. H., 381, 114  
Gillham, R. W., 363, 385, 388  
Godfrey, A. E., 385  
Goldhaber, M. B., 164, 165, 321, 388, 393, 395  
Goldman, C. R., 390  
Goldstein, R. A., 385  
Gonfiantini, R., 315, 389  
Graf, D., 82, 389  
Grandstaff, D. E., 227, 389  
Grant, B., 387  
Graustein, W. C., 118, 325, 389  
Green, A., 364, 384  
Grim, R. E., 77, 389  
Grisak, G. E., 364, 389  
de Grosbois, E., 390  
Gschwend, P. M., 127, 398

- Gude, A. J., III 383  
 Gunter, W. D., 384, 391
- H**
- Haines, B., 306, 389  
 Hamilton, P. J., 381  
 Hanor, J. S., 350, 351, 389  
 Hansen, T. A., 161, 389  
 Hanshaw, B. B., 10, 62, 64, 81, 382, 389, 396  
 Hardie, L. A., 27, 329, 330, 331, 332, 333, 333, 334, 335, 337, 338, 339, 348, 351, 387, 389  
 Harlow, L. 400  
 Harper, N., 395  
 Harvey, G. R., 119, 389, 399  
 Harvie, C. E., 33, 332, 344, 387, 389  
 Hayes, K. F., 100, 101, 389  
 Hayes, M. B. H., 114, 127, 389  
 Helgeson, H. C., 231, 246, 248, 370, 371, 381, 384, 389, 416  
 Hellwig, D. H. R., 342, 389  
 Hem, J. D., 13, 187, 196, 382, 390  
 Hemingway, B. S., 390, 397, 416  
 Hemond, H., 393  
 Hendricks, E., 389  
 Henriksen, A., 301, 302, 390  
 Hering, J. G., 40, 68, 394  
 Hill, S., 394  
 Hitchon, B., 348, 349, 350, 390, 397  
 Hoffman, W. A., 107, 390  
 Hohl, H., 80, 102, 401  
 Hoigné, J., 107, 398  
 Holdren, G. R., Jr., 226, 227, 383, 390  
 Hole, F. D., 284  
 Holland, H.D., 62, 63, 68, 159, 288, 390  
 Holt, B. D., 321, 390  
 Hooper, R. P., 291, 304, 390  
 Hornberger, G. M., 385  
 Hostetler, P. B., 177, 184, 385, 390  
 Hostetler, J. D., 130, 390  
 Hower, J., 77, 78, 350, 390, 397  
 Hower, M. E., 390  
 Hsü, K. J., 59, 390  
 Huang, C. P., 96, 101, 390  
 Hudson, R. J. M., 385  
 Huebner, J. S., 390  
 Huffman, E. D. W., 114, 390  
 Hug, S. I., 119, 399  
 Hunt, C., 13, 388  
 Huntsman, S. A., 399  
 Hurcomb, D. R., 270, 271, 272, 273, 386  
 Hurley, M. A., 191, 400  
 Hutchinson, T. C., 306, 388
- I**
- Imboden, D. M., 127, 322, 324, 390, 398
- J**
- Jacks, G., 381  
 Jackson, K. J., 384  
 James, R. O., 94, 196, 386, 390, 392  
 Jaquet, J.-M., 401  
 Jenne, E. A., 83, 187, 196, 391  
 Johnson, D. W., 240, 309, 397  
 Johnson, N. M., 270, 271, 291, 299, 391, 392, 397  
 Jones, B. F., 28, 36, 179, 244, 327, 332, 334, 336, 337, 339, 340, 351, 384, 387, 391, 398, 400  
 Jones, D. C., 391, 322  
 Jöreskog, K. G., 253, 391  
 Junge, C. E., 4, 391
- K**
- Kaminsky, M. S., 394  
 Kaplan, I. R., 321, 388, 391  
 Karickhoff, S. W., 124, 391  
 Karlinger, M. R., 398  
 Kastner, M., 59, 382  
 Keene, W. C., 6, 107, 391  
 Keller, T., 306, 391  
 Kenlogg, W. W., 321, 391  
 Kemp, A. L. W., 395  
 Kennedy, V. C., 269, 270, 316, 391  
 Kent, D. B., 91, 97, 102, 105, 181, 193, 386, 391  
 Ketchum, B. J., 396  
 Khanna, T. K., 400  
 Kharaka, Y. K., 82, 118, 350, 368, 384, 391, 392, 401  
 Kinsman, D. J. J., 345, 346, 347, 348, 349, 391, 395  
 Kirkby, M. J., 260, 384  
 Kirsipu, T. V., 390  
 Klovan, J. E., 253, 390, 391  
 Knapp, R., 364, 394  
 Kodama, H., 382  
 Krause, G. M., H., 396  
 Kreitler, C. W., 322, 391  
 Krouse, H. R., 321, 391  
 Krug, E. C., 298, 391
- L**
- Landolt, W., 306, 391  
 Langmuir, D., 63, 64, 177, 178, 184, 185, 186, 187, 392, 399
- Lasaga, A. C., 230, 232, 233, 234, 383, 384, 392  
 Lawrence, J. R., 319, 392  
 LaZerte, B. D., 291, 392  
 Lazrus, A., 391  
 Leckie, J. O., 94, 196, 386, 389, 392  
 Lee, R. W., 396  
 Leenheer, J. A., 113, 116, 117, 118, 127, 382, 392  
 Lelivre, B., 385  
 Leppard, G. G., 400  
 Lerman, A., 357, 392  
 Létolle, R., 321, 392  
 Levinson, A. A., 397  
 Lewan, M. D., 127, 396  
 Li, Y.-H., 179, 384, 392  
 Lichtner, P. C., 379  
 Likens, G. E., 8, 238, 239, 266, 299, 391, 392  
 Lindberg, R. D., 181, 182, 193, 392, 397  
 Lindberg, S. E., 390  
 Livingstone, D. A., 351, 392  
 Lovett, G. M., 392  
 Lowden, G. F., 400  
 Lundegard, P. D., 118, 392  
 Lyons, W. B., 393
- M**
- Ma, K. C., 392  
 MacCarthy, P., 381, 389, 392  
 Mackay, D., 122, 392  
 Mackenzie, F. T., 2, 13, 60, 68, 213, 241, 242, 243, 244, 245, 249, 250, 264, 287, 288, 324, 327, 328, 329, 331, 334, 383, 388, 389, 394, 396  
 MacNaughton, M. G., 94, 390  
 Madé, B., 325, 369, 392  
 Maglione, G., 334, 387  
 Mahon, W. A., J., 12, 318, 387  
 Malcolm, R. L., 116, 119, 269, 270, 316, 387, 389, 391, 392, 393  
 Mangelsdorf, P. C., 83, 85, 397  
 Marinsky, J. A., 115, 387, 393  
 Martell, A. E., 398  
 Martell, E. A., 391  
 Martens, C. S., 164, 165, 393  
 Martin, J., 176, 393  
 Martin, R. T., 382  
 Mason, R. P., 195, 393  
 Massis, T., 385  
 Mast, M. A., 230, 231, 238, 273, 274, 385, 393  
 Mathieu, G., 392



- Mathuthu, A., 387  
 Matzner, E., 238, 393  
 Mayer, R., 400  
 Mazor, E., 322, 323, 325, 393  
 McArthur, J. M., 334, 393  
 McCracken, R. J., 384  
 McDowell, W. H., 391  
 McKinley, P. W., 392  
 McKnight, D. M., 110, 127, 187, 381, 382, 392, 393  
 Means, J. L., 187, 393  
 Measures, C. I., 387  
 Medvedev, V. A., 385  
 Melchior, D. C., 40, 393  
 Merk, C. F., 398  
 Meybeck, M., 176, 285, 286, 351, 393  
 Meyer, J. S., 164, 388  
 Michel, R. L., 390  
 Miller, E. K., 325, 393  
 Miller, W. R., 8, 262, 263, 264, 265, 266, 267, 268, 394  
 Mohn, W. W., 126, 394  
 Moller, N., 389  
 Monin, C., 33, 394  
 Morel, F. M. M., 40, 68, 91, 97, 99, 101, 102, 104, 105, 192, 194, 374, 386, 393, 394  
 Morgan, D. J., 398  
 Morgan, J. J., 40, 50, 68, 130, 136, 157, 174, 196, 213  
 Morse, J. W., 68, 220, 221, 222, 223, 383, 394, 399  
 Mortatti, J., 396  
 Mowatt, T. C., 77, 390  
 Mucci, A., 224, 394  
 Mulder, J., 394  
 Müller, L., 398  
 Munoz, J. L., 22, 40, 157, 213, 394  
 Murphy, J. W., 386  
 Murphy, K. M., 227, 386, 394  
 Murray, J. W., 187, 394
- N**
- Naas, A., 398  
 Nadeau, P. H., 78, 401  
 NADP, 5, 292, 309, 394  
 Nagy, K. L., 234, 384, 392  
 Nancollas, G. H., 25, 402  
 NAPAP, 305, 306, 394  
 Narasimhan, T. N., 376, 394, 401  
 National Research Council, 122, 126, 127, 394  
 Neal, C., 83, 180, 291, 304, 385, 394  
 Neal, M., 394  
 Neretnieks, I., 364, 396
- Nesbitt, H. W., 384, 389  
 Newton, R., 382  
 Nicholson, R. V., 385  
 Nielsen, R. L., 398  
 Nobel, W., 382  
 Nordstrom, D. K., 22, 28, 36, 40, 157, 213, 297, 382, 394, 416, 419  
 Norton, D., 364, 394  
 Norton, S. A., 388  
 Novo-Gradac, K. J., 381  
 Noyes, T. I., 381  
 Nriagu, J. O., 177, 180, 395  
 Nuttall, R. L., 400
- O**
- Oelkers, E. H., 231, 379, 395  
 Olson, R. K., 392  
 O'Neil, J. R., 279, 280, 313, 382, 383, 388, 395  
 Osborn, A. O., 393  
 Ostlund, H. G., 322, 397  
 Oxburgh, R., 230, 395  
 Oxburgh, U. M., 390
- P**
- Pačes, T., 209, 232, 250, 251, 263, 395  
 Palmer, D. A., 202, 203, 401, 416, 419  
 Palmer, M. R., 387  
 Parker, V. B., 384, 388, 400  
 Parkhurst, D. L., 29, 37, 244, 245, 288, 368, 377, 395, 396  
 Parks, G. A., 94, 395  
 Patterson, R. J., 345, 346, 395  
 Pearce, A. J., 316, 395, 398  
 Pearson, F. J., 401  
 Perdue, E. M., 112, 113, 115, 383, 395  
 Perkins, D., 382  
 Perkins, E. H., 391  
 Perry, E. A., 159, 388, 390  
 Peters, N. E., 238, 276, 390, 395  
 Petrovic, R., 226, 395  
 Phillips, F. M., 323, 325, 383, 395, 396  
 Pickens, J. F., 364, 389  
 Pierce, R. R., 398  
 Pierce, R. S., 392  
 Pinckney, D. J., 381  
 Piper, A. M., 396, 409, 410  
 Pittman, E. D., 127, 396  
 Pitzer, K. S., 33, 396  
 Plummer, L. N., 37, 42, 56, 60, 63, 64, 68, 222, 244, 245, 288, 321, 368, 377, 378, 384, 395, 396, 401, 416  
 Polzer, W. L., 387
- Posnjak, E., 344, 396  
 Postma, D., 369, 379, 382  
 Presser, T. S., 401  
 Prestemon, E. C., 288, 396  
 Prinz, B., 306, 396  
 Probst, A., 293, 396  
 Probst, J.-L., 285, 286, 381, 396
- R**
- Rapp, J. B., 401  
 Rasmuson, A., 364, 396  
 Rea, B. A., 391  
 Redden, G., 389  
 Redfield, A. C., 159, 396  
 Reeder, R. J., 68, 397  
 Reeder, S. W., 255, 256, 257, 258, 259, 397  
 Rehfuss, K. E., 306, 397  
 Reiners, W. A., 238, 298, 392, 400  
 Rettig, S. L., 391, 398  
 Reuss, J. O., 240, 293, 294, 309, 397  
 Reuter, J. H., 383  
 Reymont, R. A., 391  
 Reynolds, R. C., 78, 270, 271, 397  
 Richards, F. A., 396  
 Rickard, D. T., 222, 398  
 Rittenberg, S. C., 321, 391  
 Roberson, C. E., 387  
 Roberts, W. M. B., 183, 397  
 Robie, R. A., 397, 416  
 Rooth, C. G., 322, 397  
 Rosenqvist, I. T., 298, 397  
 Runnells, D. D., 56, 181, 182, 193, 392, 397  
 Russell, K. L., 83, 397
- S**
- Sangster, J., 122, 397  
 Savin, S. M., 319, 397  
 Sayles, F. L., 83, 85, 397  
 Schindler, P. W., 91, 93, 397  
 Schnoor, J. L., 238, 297, 299, 398  
 Schofield, C. L., 292, 305, 382  
 Schott, J., 33, 234, 394, 395, 398  
 Schumm, R. H., 400  
 Schütt, 306, 398  
 Schwartz, F. W., 13, 386  
 Schwarzenbach, R. P., 110, 124, 125, 127, 398  
 Schweda, P., 230, 397  
 Sedlak, D. L., 107, 398  
 Seip, H. M., 291, 295, 309, 385, 390, 398  
 Seuffert, G., 382

- Sevaldrud, I., 398  
 Shaikh, A. U., 385  
 Sheppard, R. A., 383  
 Sheppard, S. F. M., 316, 398  
 Shiu, W. Y., 392  
 Shoemaker, C. A., 291, 390  
 Siebert, R. M., 385  
 Siegenthaler, U., 314, 398  
 Sillén, L. G., 97, 398  
 Singer, P. C., 307, 398  
 Sjöberg, 222, 398  
 Sklash, M., 316, 388, 395, 398  
 Skoda, R. E., 181, 397  
 Smith, A., 401  
 Smith, C. J., 394  
 Smith, C. L., 335, 341, 342, 386, 398  
 Smith, J. W., 321, 398  
 Snekvik, E., 305, 402  
 Soil Survey Staff, 235, 398  
 Soler, J., 234, 392  
 Solley, W., B., 12, 398  
 Sollins, P., 389  
 Spahr, N. E., 274, 400  
 Spencer, R. J., 351, 398  
 Spósito, G., 101, 105, 212, 390, 398, 416  
 Srodon, J., 77, 398  
 Stallard, R. F., 5, 257, 260, 261, 262, 270, 285, 286, 382, 387, 398, 399  
 Stauffer, R. E., 274, 399  
 Steefel, C. I., 379  
 Steelink, C., 114, 399  
 Stefani, M., 389  
 Steffen, Robertson and Kirsten, 308, 399  
 Stevenson, F. J., 118, 124, 127, 399  
 Stewart, F. H., 344, 399  
 Stewart, M. K., 395, 398  
 Stillings, L. L., 231, 399  
 Stone, N., 390  
 Stratmann, H., 396  
 Stuber, H. A., 114, 390  
 Stumm, W., 40, 50, 68, 89, 90, 91, 94, 96, 98, 101, 105, 130, 136, 157, 163, 174, 177, 196, 213, 228, 229, 230, 232, 234, 238, 281, 282, 283, 297, 299, 307, 390, 398, 399, 401, 402  
 Suarez, D. L., 187, 230, 381, 399  
 Sudicky, E. A., 399  
 Sulzberger, B., 119, 187, 399  
 Sun, Y., 395, 399  
 Sunda, W. G., 187, 399  
 Surdam, R. C., 386  
 Sverdrup, H., 230, 232, 305, 381, 399  
 Swanick, G. B., 396  
 Swift, R. S., 389  
 Swoboda-Colberg, N. G., 181, 233, 399
- T**
- Tallman, D. E., 385  
 Tang, D. H., 364, 399  
 Tardy, Y., 381, 386, 388, 396  
 Taylor, H. P., 319, 392, 398  
 Teller, E., 227, 384  
 Tessenow, U., 180, 399  
 Tessier, A., 179, 400  
 Thirwall, M. F., 393  
 Thomas, R. L., 401  
 Thompson, J. B., Jr., 204, 400  
 Thorn, K. A., 382  
 Thorstenson, D. C., 395  
 Thurman, E. M., 107, 108, 112, 118, 119, 127, 392, 393, 400  
 Tiedje, J., M., 126, 394  
 Timberlid, J. A., 398  
 Tipping, E., 191, 400  
 Tokunga, T., 394  
 Tollan, A., 309, 398  
 Trescases, J. J., 383  
 Tripathi, V. S., 179, 400  
 Truesdale, G. A., 167, 400  
 Truesdell, A. H., 28, 36, 400  
 Turekian, K. K., 176, 400  
 Turk, J. T., 274, 400  
 Turner, J. V., 393  
 Turner, R. R., 390
- U**
- Ullman, W. J., 231, 400  
 Ulrich, B., 306, 400  
 U.S. Environmental Protection Agency, 400  
 U.S., NAPAP, 305, 306, 309, 400  
 Usiglio, M. J., 343, 344, 400
- V**
- Van Cappellen, P., 164, 400  
 Van Denburgh, A. S., 332, 391  
 van Olphen, H., 86, 400  
 Velbel, M. A., 231, 232, 243, 274, 400  
 Venters, A., 390  
 Vitousek, P. M., 238, 298, 400  
 Vivelle, D., 396
- W**
- Wagman, D. D., 385, 400, 413, 416  
 Waite, T. D., 391  
 Walker, A. L., 397  
 Walls, J., 394  
 Walther, J. V., 228, 384  
 Walton, A. W., 348, 400  
 Wang, Y., 164, 400  
 Warfvinge, P., 305, 381, 399  
 Waters, D., 394  
 Weare, J. H., 33, 387, 389, 400  
 Weaver, C. E., 86, 400  
 Weed, S. B., 86, 386  
 Weiss, R. F., 390  
 Welch, S. A., 231, 400  
 Werby, R. T., 4, 391  
 Wershaw, R. L., 115, 381, 393, 401  
 Wesolowski, D. J., 202, 203, 212, 401, 416, 419  
 Westfall, J. C., 80, 102, 105, 401  
 Westrich, H. R., 385  
 Wetzell, R. G., 119, 168, 174, 401  
 Weyer, K. U., 388  
 White, A. F., 227, 234, 285, 286?, 376, 394, 401  
 White, D. E., 348, 401  
 White, H. J., 388  
 Widmer, G., 180, 387  
 Wieder, R. K., 189, 401  
 Wieland, E., 228, 229, 230, 234, 399, 401  
 Wigley, T. M. L., 56, 222, 321, 323, 396, 401  
 Wiklander, L., 296, 401  
 Willey, L. M., 350, 401  
 Williams, J. D., 169, 401  
 Williams, P. M., 119, 401  
 Wilson, M. J., 78, 401  
 Woessner, W. W., 379, 382  
 Wolery, T. J., 368, 401  
 Wollast, R., 225, 227, 234, 385, 401, 402  
 Wong, H. T. K., 395  
 Wright, R. F., 300, 304, 305, 385, 402
- Y**
- Yavitt, J. B., 118, 387, 402  
 Yund, R. A., 383
- Z**
- Zellweger, G. W., 391  
 Zhang, J.-W., 25, 402  
 Zobrist, J., 281, 282, 283, 286, 386, 402

# Subject Index

## A

- Absaroka Mountains, 262–268  
Abu Dhabi, 345  
Acid  
  -base accounting, 308  
  deposition, 240, 279, 289, 292–306  
  -generating potential, 308  
  mine drainage, 306–309  
  -neutralizing potential, 308  
  pulse, 6, 293  
Acidification, 290  
Acidity  
  aluminum, 52  
  definition, 51, 289  
Activated complex, 229  
Activation energy, 216–217  
Activity, 18–19  
  coefficient, 19, 26–33  
  of electrons, 130  
  product, 25  
  stoichiometric activity coefficient, 36  
  of water, 19, 41, 347–349  
Adirondack Mountains  
  DOC, 118  
  ILWAS, 302  
  weathering, 275–279  
Adsorption  
  of anions, 98–99, 194  
  by carbonates, 188  
  as control on metals, 185–188, 192  
  definition, 87  
  edge, 97–99, 192  
  and evaporation, 334  
  and MINTEQA2, 102–105, 374  
  of organic compounds, 122–125  
  and organic ligands, 179  
  by oxyhydroxides, 186–187, 192, 196  
  and retardation, 364–368  
  and silicate dissolution rate, 228–230  
  by silicates, 188  
Advection, 356, 366–367  
Advection–diffusion equation, 353–364  
Aerobic metabolism, 160  
Affinity of reaction, 229–232  
Aging of surfaces, 232–233  
Albite  
  alteration reactions, 248  
  dissolution rate, 231–232  
Alfisol, 235  
Algae, 159  
Aliphatic hydrocarbons, 120–121  
Alkalinity  
  carbonate, 46  
  definition, 46, 289  
  organic anions, 51  
  titration, 45–52  
Allophane, 225  
Aluminosilicate solubility, 203–205  
Aluminum  
  acidity, 290–291  
  effect on silicate dissolution, 231  
  hydrolysis, 200–203  
  hydroxide solubility, 180–181, 200–204, 291–292  
  speciation, 291–292  
  toxicity, 179, 292  
Alunite, 297  
Amazon  
  cation exchange, 85  
  geochemistry, 257–262  
  precipitation composition, 5  
Amines, 112  
Amino acids, 112  
Ammonia, 161  
Ammonium in precipitation, 5–6  
Amorphous  $\text{Fe}(\text{OH})_3$  (*See* ferrihydrite)  
Amorphous phases, 225  
Amorphous silica, 209  
  solubility, 197–199  
Anaerobic basins, 170–171  
ANC, 290  
Andes, 259–262  
Anhydrite, 346–349  
Anion adsorption, 194, 296  
Anion exclusion, 81–82  
Annite, 75  
Anthropogenic inputs, 281, 283  
Apatite, 175  
Aquifer, 10  
Aquitard, 10  
Aragonite, 52  
  growth in seawater, 223–225  
Archie's law, 357  
Aridisol, 236  
Aromatic hydrocarbons, 119–124  
Arrhenius equation, 216–217, 313  
Arsenic, 99, 177, 181, 185, 192–194  
Artesian aquifer, 10  
Attapulgite, 79  
Average linear velocity, 356

## B

- BALANCE, 244  
Bank storage, 7  
Basalt, 164, 176  
Base cations, 293  
Base flow, 7  
Base saturation, 293–295

- Batch reactor, 225  
 Bauxite, 270  
 Beidellite, 75–76, 249  
   stability, 209–211  
 Berthierine, 74  
 BET, 94, 227  
 Biological uptake, 188–189  
 Biomass changes, 238–239, 296–298  
   and acidification, 298  
 Bioremediation, 122, 125–126  
 Biotite, 75, 77  
   weathering, 241–243  
 Birkenes, 303–304  
 Bjerrum plot, 43–44, 49, 143  
 Black Sea, 170  
 Black waters, 107, 109, 115  
 BNC, 290  
 BOD, 168–169  
 Bohemian Massif, 251–252  
 Box model, 2–3  
 Brackish water, 13  
 Breakthrough curve, 363–364  
 Brine, 13, 33  
 Brucite, 69–71  
   solubility, 198–199, 201  
 Buffering  
   pH, 51  
   redox, 162–165
- C**
- Cadmium, 177, 188–192  
 Calcite  
   adsorption on, 188  
   dissolution kinetics, 221–223  
   growth in sea water, 223–225  
   high–magnesium, 58–60  
   solubility, 52–58, 60–63  
   source of Ca in weathering, 243,  
   272–275  
 Calcium  
   in precipitation, 5, 6  
 Calcrete/caliche, 235  
 Calorie, 15  
 Calorimetry, 211  
 Ca–OH waters, 280  
 Capillary fringe, 9  
 Carbon–13, 320–321  
 Carbon–14, 322–323  
 Carbonic acid, 41  
 Carboxylic acids, 109–112, 115  
 Cariaco Basin, 170  
 Cascade Mountains, 269–273  
 Catchment processes, 236–240  
 Cation denudation rate, 300  
 Cation exchange, 82–85, 87, 90, 104,  
   188  
   and acid deposition, 240, 293–295  
   capacity, 82  
   and catchment budgets, 239–240,  
   275  
   and evaporation, 334  
   and groundwater composition, 245,  
   350  
 Charge balance, 44, 45, 53–55, 58  
 Chelate, 35, 111  
 Chemical affinity, 230–232  
 Chemical divide, 329–332  
 Chemical potential, 18–20  
 Chemical weathering and acid deposi-  
   tion, 299–301  
 Chloride  
   in evaporation, 337  
   in precipitation, 4–5  
 Chlorinated hydrocarbons, 120  
 Chlorine-36, 323  
 Chlorite, 77–79  
 Chlorite, (7 Å) 73  
 Chromium, 194  
 Clay minerals  
   in California soils, 284  
   definition, 69  
   formation, 282–284  
 Climate and weathering, 285–286  
 Closed system, 61–63  
 CO<sub>2</sub>  
   in groundwater, 62–63  
   pressure and alkalinity, 46  
   in soil gas, 60  
   solubility, 41–42  
   system, equilibrium constants, 42  
 Coal, 171–172, 188  
 Coatings, 83, 122  
 COD, 168–169  
 Colligative properties, 114–115  
 Colloid, 79–81  
 Colorado  
   precipitation composition, 5  
 Cometabolism, 126  
 Communalities, 255  
 Complex formation, 34, 110  
 Component, 17  
 Conductance, 13  
 Confined aquifer, 10  
 Connate water, 12, 315  
 Conservative species, 46, 356  
 Consortium, 126  
 Constant capacitance model, 100–102  
 Contaminant transport, 374, 376–377  
 Convection, 356  
 Coordination compound, 34  
 Copper, 177, 179, 189–192  
 Coprecipitation, 186–187  
 Correlation analysis, 253  
 Coulombic effect, 94  
 Coupled, diffusion, 357  
 Cyclic wetting and drying, 335–336,  
   341–342
- D**
- Darcy velocity, 356  
 Davies equation, 28  
 DDT, 121  
 Debye–Hückel, 27–31  
 Delayed-return flow, 269–270  
 Denitrification, 160, 164  
 Density of water, 166  
 Detergents, 125  
 Deuterium, 314–319, 348  
   exchange, 94, 96  
 Diaspore, 207  
 Diatoms, 9  
 Dickite, 71  
 Diffuse double-layer model, 100–102  
 Diffusion, 218–219, 221–222,  
   353–361, 367–368  
 Dimethyl sulfide, 5  
 Dimictic lakes, 166  
 Dioctahedral clays, 70  
 Discharge area, 10  
 Disequilibrium  
   indices, 209, 250–252  
   measures of, 24–25  
 Dislocations, 220–221, 227, 232  
 Dispersion, hydrodynamic, 356,  
   361–365  
   lateral, 361–363  
   longitudinal, 361–364  
 Dispersivity, 362–363  
 Dissolved organic carbon (DOC) 6,  
   107  
   in groundwater, 107–108, 118  
   in the oceans, 119  
   in rainwater, 107–108  
   in soil solutions, 118  
   in surface water, 107–108, 118  
   in swamps and wetlands, 118–119  
 Distribution coefficient, 84, 88  
   activity, 88, 103  
   nonpolar organics, 124  
 DNAPLs, 121, 123

- Dolomite, 58–59, 63–64, 216, 331–332, 346  
 Double layer, 79–82, 99–102  
 Dry deposition, 6, 237–238, 292–293
- E**
- EDTA, 35  
 Eh, 132–134,  
   definition by redox pairs, 135–136  
   in groundwaters, 181–182  
   measurement, 136  
 Eh–pH diagrams, 137–154, 152–154, 182–186, 189–195  
   sulfur species, 148–152,  
   stability of water, 137–138  
   system As–S–O–H<sub>2</sub>O, 193  
   system Cd–CO<sub>2</sub>–S–O–H<sub>2</sub>O, 190  
   system Cr–O–H<sub>2</sub>O, 194  
   system Cu–CO<sub>2</sub>–O–H<sub>2</sub>O, 191  
   system Cu–S–O–H<sub>2</sub>O, 190  
   system Fe–O–H<sub>2</sub>O, 137–144  
   system Fe–O–H<sub>2</sub>O–CO<sub>2</sub>, 144–148, 184  
   system Fe–O–H<sub>2</sub>O–S, 148–153, 183  
   system Hg–O–S–H<sub>2</sub>O, 195  
   system Pb–CO<sub>2</sub>–S–O–H<sub>2</sub>O, 190  
   system Se–O–H<sub>2</sub>O, 193  
   system Zn–CO<sub>2</sub>–S–O–H<sub>2</sub>O, 190  
 Electrostatic effect, 94, 103  
 EMMA, 304–305  
 Enthalpy, 17, 21, 22  
   tables, 413–422  
 Entropy, 17, 18, 21, 22  
   table, 413–416  
 Ephemeral springs, 241–243  
 Epilimnion, 166–169  
 EQ3/6, 368–369, 377  
 Equilibrium constant, 19–24  
   apparent, 35  
   as function of temperature, 22–24  
   table of, 419–422  
 Equilibrium control in weathering, 249–251, 263, 282–283  
 Equivalence pH, 290  
 Etch pits, 221, 227  
 Ethylenediamine, 34  
 Eutrophic lake, 168  
 Evaporation  
   effect on D/H and δ<sup>18</sup>O, 315  
   effect on solutes, 327–351  
 Evaporite weathering, 261, 285  
 Evapotranspiration, 6–7  
 Exchangeable cations, 76
- F**
- Factor analysis, 253–259, 265–268  
 Faraday's constant, 132  
 Fermentation, 162  
 Fe(OH)<sub>2</sub>, 142  
 Ferrihydrite stability, 141–147  
 Fertilizers, 168  
 Fick's laws, 354–355  
 Field weathering rates, 232–233  
 Fine particles, 212, 226  
 Fingering, 363, 365  
 First-order reaction, 216–217  
 Fish populations, 305  
 Fjords, 170–171  
 Flocculation, 80–81  
 Florida, 10, 63–64  
 Flow-through reactors, 227–228  
 Flux, 1, 354  
 Forest damage, 305–306  
 Formation factor, 357  
 Formation water, 12, 348–350  
 Forsterite, 279–280  
 Fossil fuels, 5–6  
 France, weathering rates, 285–286  
 Fresh water, 13  
 Freundlich isotherm, 89, 104  
 Fuels as contaminants, 120–123  
 Fugacity, 18–19  
   –fugacity diagrams, 154–156  
 Fulvic acid, 114–119  
 Functional groups, 109
- G**
- Gaines–Thomas equation, 85, 104  
 Gapon equation, 85  
 Gasoline, 120–126  
 Geochemical prospecting, 177  
 Geysers, 12  
 Gibbs free energy, 17–27  
   table, 413–416  
 Gibbsite, 69–71, 270  
   solubility, 200–204, 291–292  
   stability, 204–213  
 Glauconite, 77  
 Gouy–Chapman, 101  
 Gouy layer, 80–82  
 Gran plot, 50, 290  
 Granite, trace elements, 176  
 Greifensee, 180  
 Groundwater  
   in carbonate terrains, 60–64  
   chemical evolution, 377–378  
   contamination, 11, 63
- DOC, 107, 118  
 redox conditions, 171–174  
 usage, 11–12  
 Güntelberg equation, 28  
 Gypsum  
   precipitation in evaporation, 329–330, 346–348  
   solubility product, 22, 25, 30–31  
   source of sulfate, 240, 252–253
- H**
- Half-life, 216–217  
 Halite, in sabkhas, 347–349  
 Halloysite, 73  
 Hardie–Eugster model, 329–333  
 Hardness, 13  
 Hawaii beach sand, 227  
 Heavy metals, 175, 177  
 Hematite, 21, 138–147, 154–156  
 Henriksen model, 301–302  
 Henry's law, 42  
 Heterogeneous reaction, 215  
 Homogeneous reaction, 215  
 Hot springs, 12, 317–318  
 Hubbard Brook, 238–239, 299  
 Humic acid, 113–119  
 Humic substances, 112–119  
   elemental analysis, 114  
   metal binding constants, 192  
   molecular weight and size, 114–118  
 Humidity and evaporites, 347–349  
 Humidity cell, 308–309  
 Humin, 113  
 Hydrogen, 162, 164  
 Hydrograph separation, 316–317  
 Hydrologic cycle, 1–3  
 Hydrologic model, 353  
 Hydrolysis and hydroxide complexes  
   Al, 200–203  
   Fe, 142–144  
 Hydrophilic properties, 110  
 Hydrophobic  
   partitioning, 124  
   properties, 110, 124  
 Hydroxy interlayers, 78, 291  
 Hypolimnion, 166–169  
 Hyporheic zone, 8
- I**
- Illite, 77  
 ILWAS model, 302–304  
 Incongruent dissolution, 204

- Inconsistency in thermodynamic data, 212
- Infinite dilution convention, 19
- Inhibitors, 220
- Inner-sphere complex, 34, 97–98
- Interlayer water, 76
- Intrinsic constants, 93–95
- Inverse modeling, 377
- Ion activity product, 25
- Ion exchange, 82–85, 104
- Ion pairs, 31, 32
- Ionic radii, 70
- Ionic strength, 27
- Iron
  - in groundwater, 173
  - microbial reduction, 160, 164–165
  - monosulfide, 152
  - oxyhydroxide, 87, 186–187, 192  
(*See also* Ferrihydrite)
  - speciation, 177, 182
  - solubility, 183–184
- Irreducible saturation, 121
- Irrigation, 350–351
- Isoelectric point, 93–94
- Isotherm, 88
- Isotopic
  - fractionation, 311–314
  - temperature measurement, 319–320
- J**
- Jurbanite, 297
- Juvenile water, 12
- K**
- Kaolinite, 71–73,
  - formation, 241–243
  - solubility, 203–205
  - stability, 204–213
- K-feldspar
  - dissolution, 225–226, 246–247
  - reaction path, 369–371
  - stability, 205–213
  - in weathering, 242
- KINDIS, 325, 369
- Kinetic isotope effect, 313–314
- Kinetics, 215–234
  - carbonate dissolution & growth, 221–225
- Kinetic test, 308
- Kinks, 220, 223
- L**
- Lakes
  - DOC in, 118–119
  - redox processes, 159, 166–169
- Langmuir isotherm, 89–90, 102–103
- Laumontite, 209–211
- Leached layer, 226–227
- Lead, 176, 189–192
- Ligand, 34–35, 92
- Limestone, (*See also* calcite) trace elements, 176
- Linear distribution coefficient, 88
- Linear rate law, 226
- LNAPLs, 121, 123
- Loch Vale, CO, 239, 273–275
- M**
- Mackenzie river, 255–259
- Mackinawite, 183
- Madison Aquifer, 378
- Magadi, Lake, 336–340
- Magadiite, 339
- MAGIC model, 303–304
- Magnesium
  - effect on carbonate growth, 223–225
  - silicate solubility, 199–201
- Magnetite, 21, 138–140, 142, 152, 154–156
- Manganese, 164, 173, 179–180, 182
- oxyhydroxides, 186–187, 192
- Marcasite, 152
- Mass balance, 236–246, 264–265, 272–273, 276–279, 324
- Mass transfer, 246, 368–378
- Matrix diffusion, 364
- Matrix equations, mass balance, 243–245
- Mattole River, 269–270
- Membrane filtration, 81–82, 348
- Mercury, 177, 195
- Meromictic, 169
- Metalimnion, 166–169
- Metalloids, 175
- Metamorphic water, 12
- Meteoric water line, 314–315
- Methane, 148, 149
- Methanogenesis, 162
- Mica, 77, 79
- Mine pit lake, 369–376
- Mineral depletion curves, 276–279
- Mineral weathering reactions, 240–251
- MINTEQ, MINTEQA2, 36–37, 88, 91, 101–104, 177, 187, 368–377
- Mixed kinetics, 219
- Mixed-layer clays, 78, 270
- Mixed potential, 136
- Mixing and calcite solubility, 56
- Mobile anion, 295
- Molal units, 15
- Molar units, 15
- Molecular diffusion (*See* diffusion)
- Mole fraction, 15
- Mollisol, 236
- Molybdenum, 175, 177, 185
- Monazite, 175
- Monomictic lake, 166
- Montmorillonite, 75–76, 209, 242
- Multiple regression, 253, 259
- Muscovite, 75, 77
  - stability, 205–213
- N**
- Nacrite, 71
- NAPLs, 121, 123, 125
- NETPATH, 244–246, 287, 323, 368, 377–378
- Nevada (*See* Teels Marsh)
- Nitrate
  - in anaerobic sediment, 164–165
  - as limiting nutrient, 159, 168
  - as mobile anion, 295
  - in precipitation, 5–6
  - reduction, 160
- Nitrogen
  - isotopes, 321–322
  - oxides, 5–6
  - saturation, 295
- Nontronite, 85
- North Carolina, 164–165
- North Fork, Shoshone River, 262–268
- Nuclear magnetic resonance (NMR), 115
- Nucleation, 217–218
- Nutrients, 9, 159, 164–165, 239
- O**
- Occult deposition, 6, 237–238, 292–293
- Ocean
  - redox conditions, 169–171
  - residence time of water, 1
  - trace elements, 176
- Octanol–water partition coefficient, 121–122
- Oilfield brines, 118, 348–350
- Okefenokee Swamp, 115
- Oligotrophic lake, 168
- Olivine, 227
- Olympic Peninsula, precipitation, 5
- Order/disorder, 212
- Order of reaction, 215–216

- Organic acids and anions  
 and acidification, 298–299  
 and adsorption of metals, 179  
 in alkalinity titration, 51  
 complexing metals, 177–179,  
 188–189, 191  
 dissociation constants, 111–112  
 in oilfield brines, 118  
 in precipitation, 6, 107  
 and silicate dissolution, 229–231  
 in soil solutions, 118, 299  
 in sulfate reduction, 161
- Organic matter, adsorption on, 188
- Organic pollutants, 119–126
- Orinoco River, 257–262
- Outer-sphere complex, 34, 97–98
- Oxalate, 34, 230–231
- Oxygen  
 fugacity, 129  
 isotopes, 311–320, 348  
 minimum zone, 170–171  
 solubility, 126, 167
- Ozone, 306
- P**
- Palygorskite, 79
- Panther Lake, 276–279
- Parabolic rate law, 225–227
- Partial pressure diagrams, 154–156
- PDB scale, 312
- pe, 130, 134–137  
 in aerobic waters, 163  
 definition by redox pairs, 135  
 in groundwaters, 181–182
- pe–pH diagrams, 137–154, 182–186,  
 189–195  
 stability of water, 137–138  
 system As–S–O–H<sub>2</sub>O, 193  
 system Cd–CO<sub>2</sub>–S–O–H<sub>2</sub>O, 190  
 system Cr–O–H<sub>2</sub>O, 194  
 system Cu–CO<sub>2</sub>–O–H<sub>2</sub>O, 191  
 system Cu–S–O–H<sub>2</sub>O, 190  
 system Fe–O–H<sub>2</sub>O, 137–144  
 system Fe–O–H<sub>2</sub>O–CO<sub>2</sub>, 144–148,  
 184  
 system Fe–O–H<sub>2</sub>O–S, 148–153,  
 183  
 system Hg–O–S–H<sub>2</sub>O, 195  
 system Pb–CO<sub>2</sub>–S–O–H<sub>2</sub>O, 190  
 system Se–O–H<sub>2</sub>O, 193  
 system Zn–CO<sub>2</sub>–S–O–H<sub>2</sub>O, 190
- Peclet number, 359
- Pennsylvania  
 groundwater, 63–64  
 precipitation composition, 5–6
- Peptides, 112
- Perennial springs, 241–243
- Permeability, 9
- Persian Gulf, 345–349
- Pesticides, 121
- Phenols, 110–111, 113
- Phlogopite, 75, 77, 270
- pH of bicarbonate end-point, 290
- Phosphate, 159–160, 168–169, 180,  
 206  
 as surface poison, 222
- Photochemistry, 107, 119
- Photoreduction, 187
- Photosynthesis  
 C-isotopes, 320  
 calcite solubility, 54–55  
 redox conditions, 159
- Phreatic zone, 9
- PHREEQC, 244–245, 287, 323, 368,  
 377
- PHREEQE, 368–369, 377
- PHREEQM, 369
- PHRQPTZ, 37, 368
- Physical erosion, 242, 259–261, 287
- Piezometric surface, 10
- Piper diagrams, 409–411
- Pitzer model, 33, 37, 332
- Plagioclase weathering, 241–243,  
 271–272, 275
- Platinum electrode, 130, 136, 181
- Polar functional groups, 109
- Polynuclear aromatic hydrocarbons  
 (PAH), 120–121
- Porosity, 9, 357–358
- Ppm, ppb units, 16
- Precipitation  
 composition of, 3–6, 237, 292  
 pH of, 45, 292
- PROFILE model, 305
- Pump and treat, 121–122
- Pyrite, 151–153, 171, 183, 240
- Pyrophyllite, 74–75  
 solubility, 203–205  
 stability, 205–213
- Q**
- Quartz solubility, 197–199
- Quick-return flow, 269–270
- R**
- Radioactive decay, 216–217, 311,  
 322–324
- Radiogenic isotopes, 311, 324–325
- Radium, 187
- Radon-222, 323–324
- Rain (*See* precipitation)
- Rayleigh fractionation, 314
- Reaction path modeling, 368–378
- Recharge area, 10
- Redfield ratios, 159–160
- Redox pairs, 135
- Redox reactions, 129–156  
 and solubility, 180
- Reference pH, 290
- Relative humidity, 347–349
- Relief, 257, 259–262, 286
- Representative elementary volume,  
 355–356
- Reservoir, 1
- Residence time, 1
- Residual saturation, 121
- Respiration, 160
- Response time, 1–2
- Retardation, 364–368  
 factor, 366
- Rhine River, 280–283
- Rhodochrosite, 179
- Rift Valley (*See* Magadi, Lake)
- Rio Ameca, 83
- Rio Grande, 28
- Road salt, 63
- Rock type and water chemistry,  
 283–285
- Rotation (factor), 254
- Rounding of grains, 221
- Runoff, 8
- S**
- Sabkhas, 345–349
- Saline lakes (table), 333
- Saline water, 13
- Salt bridge, 130–131
- Salt effect, 294–295
- Sandstone  
 trace elements, 176  
 weathering, 285
- Saponite, 75–76, 270–271
- Saturation index, 25, 33
- Saturation ratio, 25–26, 33
- Screw dislocation, 220–221
- Seawater  
 evaporation of, 343–349  
 major elements, 345  
 trace elements, 176
- Selectivity coefficient, 83
- Selenium, 175, 177, 181, 185, 192–194
- Sepiolite, 79, 224–225, 328–329  
 solubility, 200–201

- Serpentine, 73  
 solubility, 199–201
- Sewage, 168
- Shale  
 trace elements, 176  
 weathering, 285
- SI units, 15
- Siderite, 144–148, 154–156
- Sierra Nevada springs, 241–245,  
 249–250  
 evaporation, 327–329
- Silicate dissolution kinetics, 225–233  
 effect of pH, 228–229
- Silver, 176
- Smectite, 75–76, 79, 242, 332  
 stability, 209–213
- SMOW, 312
- Sodium  
 in precipitation, 3–5,
- Soil  
 formation, 235–236  
 horizons, 235–236  
 mineral depletion, 276–279
- SOLMINEQ.88, 368–369
- Solubility  
 as control on metals, 179–183  
 of organic pollutants, 121–122  
 product, 22, 198  
 quartz and amorphous silica,  
 197–199
- Solution model, 27, 212
- South Cascade glacier, 270–273
- Speciation, 177
- Species, 17
- Sphagnum, 298
- Spodosol, 118, 235
- Stability diagrams (silicate), 204–213
- Stable isotopes, 311–322
- Standard electrode potential, 133
- Standard free energy, 20–21  
 of formation, table, 413–417
- Standard hydrogen electrode, 130–132,  
 135
- Standard state, 19
- Static test, 308
- Statistical association, 251–253
- Stem flow, 237
- Steps, 220
- Stern layer, 80
- Stiff diagrams, 411–412
- Stochastic modeling, 377
- Stoichiometric saturation, 60
- Storm runoff, 265–268
- Streams, trace elements, 176
- Strontium–87, 324–325
- Sulfate  
 adsorption, 240, 296  
 mobility, 296–297  
 in precipitation, 5, 6, 292  
 reduction, 55, 160–162, 164–165,  
 297, 334, 349
- Sulfide  
 deposits, 177  
 oxidation, 297, 306–309, 350
- Sulfur  
 elemental, 149–151  
 isotopes, 321  
 in organic compounds, 113
- Surface  
 charge, 92–94  
 complexation, 90–102, 228–230  
 layer, 226  
 poisons, 220  
 reaction mechanisms, 220–221  
 titration, 95–97
- Surfactants, 125
- Suwannee River, 115–117
- Swelling clays, 76
- System, defined, 17
- T**
- Talc, 74–75  
 solubility, 199–201
- Teels Marsh, 340–343
- Terminal electron acceptor, 126,  
 160–162
- Thermal waters, 317–318
- Thermocline, 166–169
- Throughfall, 6, 8
- Time, and weathering, 287
- Tortuosity, 357
- Total dissolved solids, 13
- Total organic carbon (TOC), 107
- Toxicity, 179
- Trace elements (table), 176
- Transition state theory, 228, 231
- Transport-limited regime, 260–262
- Transport processes, 215, 218–219,  
 353–364
- Trioctahedral clays, 70
- Triple layer model, 100–102
- Tritium, 322
- Trona, 336–337
- Turnover, 166–169
- U**
- Ultisol, 235
- Ultramafic rocks, 279–280
- Uncertainty, 210–213
- Unstable phases, 224–225
- Uranium, 175, 177–179, 184–186  
 roll-front deposits, 184–186  
 tailings, 376–377
- V**
- Vadose zone, 9
- Vanadium, 184
- Van der Waals force, 70
- Van't Hoff equation, 23
- Vapor extraction, 122
- Vegetation and weathering, 287
- Vermiculite, 75–77, 270
- Vinyl chloride, 126
- Vivianite, 180
- Vosges Mountains, 293
- V-SMOW, 312
- W**
- Waldsterben*, 305–306
- WATEQ, WATEQ4F, 36–39, 64–67,  
 102, 136–137, 177, 378, 419
- Water table, 9
- Water usage, 12
- Weathering and acid deposition,  
 299–301
- Weathering-limited regime, 260–262,  
 273
- Weathering reactions, 240–251
- Wetlands, 118–119, 189
- Wetting and drying, 335–336, 341–342
- Wilson Creek, 316–317
- Woods Lake, 276–279
- Wyoming, 8, 262–268
- X**
- Xenobiotics, 125
- XPS, 226
- Z**
- Zeolites, 187, 209–211
- Zero point of charge, 93, 95, 97
- Zinc, 177, 189–192
- Zircon, 175



# THE GEOCHEMISTRY OF NATURAL WATERS

Surface and Groundwater Environments

THIRD EDITION

JAMES I. DREVER

Now in its third edition, James I. Drever's **The Geochemistry of Natural Waters** remains a comprehensive presentation of the processes controlling the chemistry of unpolluted and polluted natural waters. While keeping the chemical and mathematical formulations simple, Drever offers both theoretical and practical approaches to understanding the geochemistry of rivers, lakes, and groundwater.

The new edition features greatly expanded coverage of pollutants in natural waters. There is a new discussion of **organic contaminants**. There are also new chapters on **adsorption, heavy metals and metalloids**, and **transport and reaction modeling**. The use of U.S. Environmental Agency (MINTEQA2) and U.S. Geological Survey (WATEQ4F, NETPATH, PHREEQC) **computer codes** has been integrated into many of the chapters and review questions. Drever has updated and greatly expanded tables of thermodynamic data, using, where possible, data that are consistent with the U.S.G.S. and E.P.A. computer codes. The technical level of the book remains unchanged, which makes it accessible to students from a wide range of disciplines. Students studying environmental science and ecology, as well as hydrologists and geologists, will benefit from **numerous examples, illustrations, diagrams, review questions and answers**, and **lists of suggested reading**.

PRENTICE HALL  
Upper Saddle River, NJ 07458  
<http://www.prenhall.com>

ISBN 0-13-272790-0

